ANTICANCER PROPERTIES OF *SARACA ASOCA* (ROXB.) DE WILDE AND ITS ALLIED SPECIES *KINGIODENDRON PINNATUM* (ROXB. EX DC.) HARMS WITH SPECIAL EMPHASIS ON BREAST CANCER

Thesis submitted to

UNIVERSITY OF CALICUT

For the Degree of

Doctor of Philosophy in Biotechnology

(Faculty of Science)

By

PAREETH C M, M.Sc.

Under the co-guidance of

Dr. T. D. BABU, Ph.D., Associate Professor, Department of Biochemistry,

Amala Cancer Research Centre, Thrissur &

Dr. THARA, K. M., Ph.D., Technical Assistant, Department of Biotechnology,

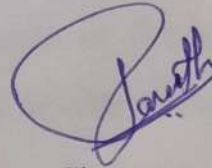**University of Calicut, Malappuram**

at

AMALA CANCER RESEARCH CENTRE, THRISSUR

April 2024

DECLARATION

I hereby declare that the work presented in the thesis entitled 'ANTICANCER PROPERTIES OF *SARACA ASOCA* (ROXB.) DE WILDE AND ITS ALLIED SPECIES *KINGIODENDRON PINNATUM* (ROXB. EX DC.) HARMS WITH SPECIAL EMPHASIS ON BREAST CANCER' is based on the original work done by me under the guidance of Dr. T. D. Babu, Associate Professor, Department of Biochemistry, Amala Cancer Research Centre and Dr. Thara K. M., Technical Assistant, Department of Biotechnology, University of Calicut and has not been included in any other thesis submitted previously for the award of any degree. The contents of the thesis are undergone plagiarism check using iThenticate software at C.H.M.K. Library, University of Calicut, and the similarity index found within the permissible limit. I also declare that the thesis is free from AI generated contents.
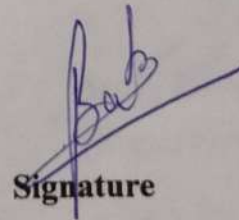
Signature

Name of the scholar

Thrissur

18/04/2024

Signature

Name of the supervising teacher

Dr. T. D. Babu, Ph.D
Asso. Professor, Dept. of Biochemistry
Amala Cancer Research Centre
Amala Nagar P.O., Thrissur-680 555
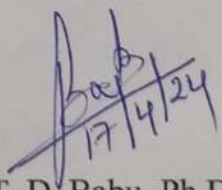Kerala, India

Ref.No. ACRC/REG(b1)/127/2024   Date: 17.04.2024

CERTIFICATE

This is to certify that the thesis entitled **"ANTICANCER PROPERTIES OF SARACA ASOCA (ROXB.) DE WILDE AND ITS ALLIED SPECIES KINGIODENDRON PINNATUM (ROXB. EX DC.) HARMS WITH SPECIAL EMPHASIS ON BREAST CANCER"** is a bonafide record of research work carried out by Mr. Pareeth C. M., under my guidance and supervision at Department of Biochemistry, Amala Cancer Research Centre, Thrissur, Kerala and no part thereof has been presented for the award of any other degree, diploma or other similar titles. The contents of the thesis have been subjected to plagiarism check and the percentage of similar content was found to be within the acceptable maximum limit.

Thrissur

Dr. T. D. Babu, Ph.D
(Supervising guide)

Dr. T. D. Babu, Ph.D
Asso. Professor, Dept. of Biochemistry
Amala Cancer Research Centre
Amala Nagar P.O., Thrissur-680 555
Kerala, India

CERTIFICATE

This is to certify that the thesis entitled **"ANTICANCER PROPERTIES OF *SARACA ASOCA* (ROXB.) DE WILDE AND ITS ALLIED SPECIES *KINGIODENDRON PINNATUM* (ROXB. EX DC.) HARMS WITH SPECIAL EMPHASIS ON BREAST CANCER"** is a bonafide record of research work carried out by Mr. Pareeth C. M., under my guidance and supervision at Department of Biochemistry, Amala Cancer Research Centre, Thrissur, Kerala and no part thereof has been presented for the award of any other degree, diploma or other similar titles. The contents of the thesis have been subjected to plagiarism check and the percentage of similar content was found to be within the acceptable maximum limit.

Thenhipalam

17/04/2024

Dr. Thara K. M., Ph.D.

(Supervising co-guide)

Dr. K.M. THARA
Technical Assistant
Department of Biotechnology
University of Calicut
Thenhipalam, Pin : 673635

Ref.No. ACRC/REG(b1)/284/2024

Date: 19.07.2024

CERTIFICATE

This is to certify that all the corrections/suggestions recommended by the adjudicators in the Ph D thesis of Mr Pareeth C M (Reg. no. U.O.No. 14364/2017/Admn dt: 15.11.2017) entitled 'ANTICANCER PROPERTIES OF *SARACA ASOCA* (ROXB.) DE WILDE AND ITS ALLIED SPECIES *KINGIODENDRON PINNATUM* (ROXB. EX DC.) HARMS WITH SPECIAL EMPHASIS ON BREAST CANCER' have been duly incorporated and the contents in the thesis and the soft copy are one and the same.

19/7/24

Dr. T D Babu

Supervising Guide

Dr. T. D. Babu, Ph.D
Asso. Professor, Dept. of Biochemistry
Amala Cancer Research Centre
Amala Nagar P.O., Thrissur-680 555
Kerala, India

DEPARTMENT OF BIOTECHNOLOGY
UNIVERSITY OF CALICUT
THENHIPALAM PO
MALAPPURAM KERALA- 673 635 INDIA
PHONE: 9446342696

Dr. THARA, K. M., Ph.D.   **Date: 20-07-2024**
Technical Assistant

CERTIFICATE

This is to certify that all the corrections/suggestions recommended by the adjudicators in the Ph D thesis of Mr Pareeth C M (Reg. no. U.O.No. 14364/2017/Admn dt: 15.11.2017) entitled 'ANTICANCER PROPERTIES OF *SARACA ASOCA* (ROXB.) DE WILDE AND ITS ALLIED SPECIES *KINGIODENDRON PINNATUM* (ROXB. EX DC.) HARMS WITH SPECIAL EMPHASIS ON BREAST CANCER' have been duly incorporated and the contents in the thesis and the soft copy are one and the same.

Thenhipalam   Dr. Thara K. M., Ph.D.
20/07/2024   (Supervising co-guide)

Dr. K.M. THARA
Technical Assistant
Department of Biotechnology
University of Calicut
Thenhipalam, Pin : 673635

Institutional Animal Ethical Committee

(Reg. No. 149/PO/Rc/S/1999/CPCSEA)

Amala Cancer Research Centre

RESEARCH DIRECTOR &   AMALANAGAR - 680 555, THRISSUR
CHAIRMAN, IAEC   : **DR. RAMADASAN KUTTAN, Ph.D.**   KERALA, INDIA

Ref :   Approval No: ACRC/IAEC/17(1)/P-05   Date: 22.12.2017

Certificate

This is to certify that the project title Anticancer properties of *Saraca asoca* (Roxb.) De Wilde

and its allied species *Kingiodendron pinnatum* (Roxb. Ex DC.) Harms with special emphasis

on breast cancer has been approved by the Institutional Animal Ethical Committee.

Name of Chairman/Member Secretary IAEC   Name of CPCSEA nominee:

Dr.Ramadasan Kuttan, Ph D.   Prof. (Dr.) E Vijayan, Ph D.

Signature with date

Chairman/Member Secretary of IAEC   **CPCSEA nominee**

(Kindly make sure that minutes of the meeting duly signed by all the participants are
maintained by Office)

UNIVERSITY OF CALICUT
CERTIFICATE ON PLAGIARISM CHECK

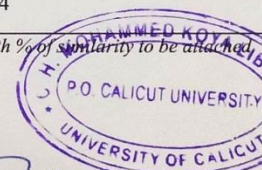| 1.	Name of the Research Scholar	PAREETH C. M.	
2.	Title of thesis / dissertation	ANTICANCER PROPERTIES OF SARACA ASOCA (ROXB.) DE WILDE AND ITS ALLIED SPECIES KINGIODENDRON PINNATUM (ROXB. EX DC.) HARMS WITH SPECIAL EMPHASIS ON BREAST CANCER	
3.	Name of the Supervisor	Dr. T. D. BABU and Dr. THARA K. M.	
4.	Department/Institution	AMALA CANCER RESEARCH CENTRE, THRISSUR	
5.	Similar content (%) identified	**Non Core** Introduction/ Theoretical overview/Review of literature/ Materials & Methods/ Methodology	**Core** Analysis/Result/Discussion/ Summary/Conclusion / Recommendations
		4 %	4 %
	Acceptable maximum limit (%)	10	10
6.	Software used	iThenticate	
7.	Date of verification	15/04/2024	

*Report on plagiarism check, specifying included/excluded items with % of similarity to be attached.

Checked by (with name, designation & signature)

JAMSHEER N. P.
Assistant Librarian
University of Calicut
Malappuram - 673 635

Name and signature of the Researcher: PAREETH C. M.

Name and signature of the Supervisor: Dr. T. D. BABU

Dr. T. D. Babu, Ph.D
Asso. Professor, Dept. of Biochemistry
Amala Cancer Research Centre
Amala Nagar P.O., Thrissur-680 555

Dr. THARA K. M.

Dr. K.M. THARA
Technical Assistant
Department of Biotechnology

The Doctoral Committee* has verified the report on plagiarism check with the contents of the thesis, as summarized above and appropriate measures have been taken to ensure originality of the Research accomplished herein.

Dr. V. RAMAN KUTTY
RESEARCH DIRECTOR

Name & Signature of the HoD/HoI (Chairperson of the Doctoral Committee)

*In case of languages like Malayalam, Tamil etc..on which no software is available for plagiarism checks a manual check shall be made by the Doctoral Committee, for which an additional certificate has to be attached.

ACKNOWLEDGEMENT

My first and most important prayer is to my creator, the Almighty, for providing me with the resilience and perseverance that have enabled me to successfully complete my research work.

*I extend my heartfelt gratitude to my guide and mentor **Dr. T. D. Babu**, Associate Professor, Department of Biochemistry, Amala Cancer Research Centre, Thrissur, whose profound understanding, invaluable guidance, and unwavering support have been instrumental in enabling me to successfully complete my work within the stipulated time. I consider myself extremely fortunate to have him as my guiding light, not only in my professional endeavours but also in my personal journey. His encouraging words have helped me live a more focused life and I will always be thankful for everything I acquired while working under his guidance. Thank you sir for everything!*

*I express sincere thanks to my co-research supervisor, **Dr. Thara K. M**., Technical Assistant, Department of Biotechnology, University of Calicut, for accepting me as a student and for her unwavering support, prompt guidance and insightful recommendations throughout my research. It would not have been possible to complete this Ph.D. without her direction and feedback.*

*I owe a debt of gratitude to **Dr. V. Ramankutty**, Research Director, Amala Cancer Research Centre, for his assistance and support in making this research work proceed smoothly. Additionally, I sincerely appreciate the valuable suggestions and assistance provided by **Dr. Ramadasan Kuttan**, Former director, Amala Cancer Research Centre.*

*I am grateful for the valuable research discussions and recommendations provided **by Dr. Achuthan C. Raghavamenon**, Associate Professor in the Department of Biochemistry, Amala Cancer Research Centre. I am thankful to **Dr. Suraj K**, Associate Professor in the*

DEDICATED TO PARENTS, TEACHERS AND FRIENDS

Abstract

Saraca asoca, commonly known as Asoka is the primary component in *Asokarishta*, an Ayurvedic polyherbal preparation for treating gynecological conditions in women. Various pharmacological and biological properties including antioxidant, antibacterial, anti-inflammatory, anti-keratinization and others have been reported in this plant. *Kingiodendron pinnatum*, known as Malabar mahogany is used as an alternative for *S. asoca* in *Asokarishta*, has shown similar phytochemical composition and efficacy. While, *K. pinnatum* has been shown to possess antioxidant and anti-inflammatory qualities, its other biological properties remain underexplored. Therefore, the present study sought to investigate the anticancer potential of *S. asoca* and *K. pinnatum* with a special emphasis on breast cancer.

The crude methanol extracts of *S. asoca* and *K. pinnatum* bark demonstrated cytotoxic effect on murine DLA and EAC tumour cells and exhibited significant antitumour properties on mouse solid and ascites tumour models. In MTT assay, the extract shows potent antiproliferative effect on cell lines of breast cancer expressing ERβ, including MDA-MB-231, MDA-MB-468 and SK-BR-3. Similar results were observed on prostate, colorectal and cervical cancer cell lines, which also express ERβ. However, despite at high concentrations, the extracts didn't exhibit anti-proliferative effects on the ERα expressing cell line, MCF-7. Given the low efficacy of conventional chemotherapy in treating triple-negative breast cancer, this particular cytotoxicity against ERβ expressing breast cell lines is noteworthy. Phytochemical study of both plant extracts revealed the existence of several compounds like phenols, alkaloids, saponins, flavonoids, terpenoids, phytosterols and tannins. Numerous functional groups, including aldehydes, alkenes, amines, aromatics, carboxylic acids, esters, phenols, and others, were identified by FT-IR analysis. Chromatographic techniques, such as HPTLC, HPLC, and LC-MS, disclosed the existence of phytoestrogenic compounds like β-sitosterol, quercetin, kaempferol, and others. This raises the possibility that the phytoestrogens identified in the plants may have an agonistic effect on cells expressing ERβ. Consequently molecular docking of phytoestrogens with targeted estrogen receptors were done and results shows that phytoestrogens such as quercetin and kaempferol bind to the ERβ more deeply than the ERα.

The *in vitro* anti-inflammatory capabilities of plant extracts was demonstrated through the

inhibition of 5-lipoxygenase enzyme activity and scavenging of NO radicals in LPS-activated RAW 264.7 cells. The extracts effectively decreased inflammation in acute and chronic paw edemas in mice induced by carrageenan and formalin, respectively. The antiestrogenic ability of extracts was evaluated using the estrogen screen assay revealing proliferative effect of extracts on ERα-expressing cells and modest antiproliferative effect on ERβ-expressing breast cancer cell lines. Furthermore, the *in vivo* rodent uterotropic assay shows suppressed growth of the endometrial lining and reduced serum estrogen levels indicating the antiestrogenic effects of extracts. The antioxidant potency of the plants was assessed through *in vitro* and *in vivo* models. The extracts effectively inhibited or scavenged free radicals such as ABTS, DPPH, superoxide and hydroxyl, in a concentration-dependent manner. Additionally, the plant extracts considerably hindered AAPH-induced lipid peroxidation and hemolysis in human erythrocytes. Significant augmentation of the endogenous antioxidant system has been seen in the *in vivo* sodium fluoride intoxication model, as demonstrated by increased levels of SOD, catalase, and GSH, coupled with a reduction in lipid peroxidation. Both plant extracts substantially mitigated the structural changes in the liver tissue exposed to NaF.

Considerable protective effects were shown by the extracts against DMBA induced mammary carcinogenesis *in vivo*. The elevation in liver marker enzymes by DMBA was mitigated by the extracts, and the histology of the mammary gland exhibited fewer invasive cancer cells and reduced cell proliferation. The extracts decreased the mRNA expression of oncogenes *ER-α1, BCL2* and *c-MYC*, which were elevated by DMBA except for *PIN1* expression. The extract also demonstrated potent inhibition of both tumour growth and metastasis in 4T1 cell induced breast cancer in mice. Histological analysis of the mammary glands exhibited a marked reduction in malignant cell proliferation, thereby effectively preventing metastasis in the group administered with the plant extract.

The possible mechanism of action of *S. asoca* and *K. pinnatum* extracts on TNBC cells was analysed *in vitro* by assessing cell death patterns and the results point to apoptotic-mediated cell death. Fluorescent staining with EB/AO reveals structural alterations with dispersed chromatin and perforated cells, which are indications of apoptosis. In the FRET-based caspase-3 activation assay, treatment of MDA-MB-231 cells with plant extracts activates

executioner caspases like caspase 3, and flow cytometry-based cell cycle analysis demonstrates arrest in the G0/G1 phase, reflected by percentage of MDA-MB-231 cells in the sub-G0/G1 phase, indicating apoptosis. In conclusion, morphological and biochemical assays indicate that the cytotoxicity exerted by *S. asoca* and *K. pinnatum* extracts, particularly against TNBCs, is through an apoptotic mechanism.

The results suggest that the activation of caspase 3 likely played a significant role in the anticancer ability of both plant extracts on triple-negative breast cancer cells, by inducing apoptosis. This opens a promising avenue for further research addressing TNBCs, and additional exploration is warranted to understand the influence of phytoestrogens on cancers expressing ERβ. Compounds capable of binding to ERβ have the potential to prevent or treat malignancies such as TNBCs. Consequently, the development of antiestrogenic drugs is crucial for impeding the growth of this subtype of cancer.

Key words: *Saraca asoca*, *Kingiodendron pinnatum,* phytoestrogens, TNBC, antiestrogenic, anti-inflammatory, anticancer

സറാക്ക അശോക എന്ന അശോകം സ്ത്രീകളിലെ പ്രത്യുൽപ്പാദനവുമായി ബന്ധപ്പെട്ട അവസ്ഥകൾ ചികിത്സിക്കുന്നതിനുള്ള ആയുർവേദ രൂപീകരണമായ അശോകാരിഷ്ടത്തിലെ പ്രാഥമിക ഘടകമാണ്. ആന്റിഓക്സിഡന്റ്, ആന്റി ബാക്ടീരിയൽ, ആന്റി-ഇൻഫ്ലമേറ്ററി, ആന്റി-കെരാറ്റിനൈസേഷൻ തുടങ്ങി വിവിധ ഫാർമക്കോളജിക്കൽ ഗുണങ്ങൾ ഈ ചെടിയിൽ റിപ്പോർട്ട് ചെയ്യപ്പെട്ടിട്ടുണ്ട്. കിങ്ങിയോഡെൻഡ്രോൺ പിന്നാറ്റം എന്ന മലബാർ മഹാഗണി അശോകാരിഷ്ടത്തിലെ അശോകത്തിന് സമാനമായ ഫൈറ്റോകെമിക്കൽ ഘടനയും ഫലപ്രാപ്തിയും കാണിച്ചിട്ടുണ്ട്. മലബാർ മഹാഗണിക്ക് ആന്റിഓക്സിഡന്റ്, ആന്റി-ഇൻഫ്ലമേറ്ററി ഗുണങ്ങൾ ഉണ്ടെന്ന് തെളിയിക്കപ്പെട്ടിട്ടുണ്ടെങ്കിലും, അതിന്റെ മറ്റ് ജൈവ ഗുണങ്ങൾ പര്യവേക്ഷണം ചെയ്യപ്പെടാതെ തുടരുന്നു. അതിനാൽ, സ്തനാർബുദത്തിന് പ്രത്യേക ഊന്നൽ നൽകിക്കൊണ്ട് അശോകം, മലബാർ മഹാഗണി എന്നിവയുടെ അർബുദ വിരുദ്ധ സാധ്യതകൾ അന്വേഷിക്കുവാൻ ഈ പഠനത്തിലൂടെ ശ്രമിച്ചു.

അശോകം, മലബാർ മഹാഗണി എന്നിവയുടെ പുറംതൊലിയുടെ അസംസ്കൃത മെഥനോളിക് സത്തിന് എലികളുടെ അർബുദകോശങ്ങളായ ഡിഎൽഎ, ഇഎസി ക്കെതിരെ സൈറ്റോടോക്സിക് പ്രഭാവം പ്രകടമാക്കുകയും എലികളുടെ സോളിഡ്, അസൈറ്റ്സ് ട്യൂമർ മോഡലുകളിൽ ഗണ്യമായ ആന്റിട്യൂമർ ഗുണങ്ങൾ പ്രദർശിപ്പിക്കുകയും ചെയ്തു. എംടിടി പരിശോധനയിൽ, എംഡിഎ-എംബി-231, എംഡിഎ-എംബി-468, എസ്കെ-ബിആർ-3 എന്നിവയുൾപ്പെടെ ഇആർബീറ്റ പ്രകടിപ്പിക്കുന്ന സ്തനാർബുദത്തിന്റെ സെൽ ലൈനുകളിൽ ഈ സത്തുകളുടെ ശക്തമായ ആന്റിപ്രോലിഫെറേറ്റീവ് പ്രഭാവം കാണിക്കുന്നു. ഇആർബീറ്റ പ്രകടിപ്പിക്കുന്ന പ്രോസ്റ്റേറ്റ്, വൻകുടൽ, സെർവിക്കൽ അർബുദ സെൽ ലൈനുകളിലും സമാനമായ ഫലങ്ങൾ നിരീക്ഷിക്കപ്പെട്ടു. എന്നിരുന്നാലും, ഉയർന്ന ഗാഢത ഉണ്ടായിരുന്നിട്ടും, ചെടികളുടെ സത്തുകൾക്ക് ഇആർആൽഫ പ്രകടിപ്പിക്കുന്ന സെൽ ലൈൻ ആയ എം.സി.എഫ്-7 ൽ ആന്റി-പ്രൊലിഫറേറ്റീവ് ഫലം പ്രകടിപ്പിക്കാനായില്ല. ട്രിപ്പിൾ നെഗറ്റീവ് സ്തനാർബുദം ചികിത്സിക്കുന്നതിൽ പരമ്പരാഗത കീമോതെറാപ്പിയുടെ കുറഞ്ഞ ഫലപ്രാപ്തി കണക്കിലെടുക്കുമ്പോൾ, ഇആർബീറ്റ പ്രകടിപ്പിക്കുന്ന സ്തനാർബുദകോശങ്ങൾക്ക് എതിരെയുള്ള ഈ പ്രത്യേക സൈറ്റോടോക്സിസിറ്റി ശ്രദ്ധേയമാണ്. രണ്ട് സസ്യ സത്തിൻറെയും ഫൈറ്റോകെമിക്കൽ പഠനം ഫിനോളുകൾ, ആൽക്കലോയിഡുകൾ, സാപ്പോണിനുകൾ, ഫ്ലേവനോയിഡുകൾ, ടെർപെനോയിഡുകൾ, ഫൈറ്റോസ്റ്റെറോളുകൾ, ടാനിൻസ് തുടങ്ങിയ നിരവധി സംയുക്തങ്ങളുടെ സാന്നിധ്യം വെളിപ്പെടുത്തി. ആൽഡിഹൈഡുകൾ, ആൽക്കീനുകൾ, അമീനുകൾ, ആരോമാറ്റിക്സ്, കാർബോക്സിലിക് ആസിഡുകൾ, എസ്റ്ററുകൾ, ഫിനോളുകൾ തുടങ്ങി നിരവധി പ്രവർത്തന ഗ്രൂപ്പുകൾ എഫ്ടി-ഐആർ വിശകലനത്തിലൂടെ തിരിച്ചറിഞ്ഞു. എച്ച്പിടിഎൽസി, എച്ച്പിഎൽസി, എൽസി-എംഎസ് തുടങ്ങിയ ക്രോമാറ്റോഗ്രാഫിക് സാങ്കേതികവിദ്യകൾ ബീറ്റ-സൈറ്റോസ്റ്റെറോൾ, കൊർസെറ്റിൻ, കെംപ്ഫെറോൾ തുടങ്ങിയ ഫൈറ്റോ ഈസ്ട്രജനിക് സംയുക്തങ്ങളുടെ സാന്നിധ്യം വെളിപ്പെടുത്തി. സസ്യങ്ങളിൽ കാണപ്പെടുന്ന ഫൈറ്റോ ഈസ്ട്രജനുകൾക്ക് ഇആർബീറ്റ പ്രകടിപ്പിക്കുന്ന കോശങ്ങളുമായി അനുകൂലമായി ഇടപെഴകാൻ കഴിഞ്ഞേക്കുമെന്ന് ഇത് സൂചിപ്പിക്കുന്നു. തൽഫലമായി ഫൈറ്റോ ഈസ്ട്രജനുകളെ ഈസ്ട്രജൻ റിസപ്റ്ററുകളുമായി മോളിക്യുലർ ഡോക്കിംഗ് നടത്തുകയും, അതിന്റെ ഫലങ്ങൾ കാണിക്കുന്നത് കൊർസെറ്റിൻ, കെംപ്ഫെറോൾ തുടങ്ങിയ ഫൈറ്റോ ഈസ്ട്രജനുകൾ ഇആർആൽഫ യേക്കാൾ ആഴത്തിൽ ഇആർബീറ്റ യുമായി ബന്ധിപ്പിക്കുന്നുവെന്നാണ്.

5-ലിപ്പോക്സിജനേസ് എൻസൈം പ്രവർത്തനത്തെ തടയുന്നതിലൂടെയും എൽപിഎസ്-ആക്റ്റിവേറ്റഡ് റോ 264.7 കോശങ്ങളിൽ നൈട്രിക് ഓക്സൈഡ് റാഡിക്കലുകളുടെ സ്കാവെഞ്ചിംഗിലൂടെയും പ്ലാന്റ് എക്സ്ട്രാക്റ്റുകളുടെ ഇൻ വിട്രോ ആന്റി-ഇൻഫ്ലമേറ്ററി

കഴിവുകൾ പ്രകടമാക്കി. യഥാക്രമം കാരജീനൻ, ഫോർമാലിൻ എന്നിവ കുത്തിവെച്ച എലികളുടെ പാദങ്ങളിലെ അക്യൂട്ട്, ക്രോണിക് വീക്കം ഈ സത്തുകൾ ഫലപ്രദമായി കുറച്ചു. ഈസ്ട്രജൻ സ്ക്രീൻ വിലയിരുത്തലിൽ ഇആർആൽഫ പ്രകടിപ്പിക്കുന്ന സ്തനാർബുദ കോശങ്ങളിൽ സത്തുകളുടെ പ്രൊലിഫെറേറ്റീവ് പ്രഭാവവും ഇആർബീറ്റ പ്രകടിപ്പിക്കുന്ന സ്തനാർബുദ സെൽ ലൈനുകളിൽ മിതമായ ആന്റിപ്രൊലിഫെറേറ്റീവ് പ്രഭാവവും വെളിപ്പെടുത്തുകയും അത് സത്തുകളുടെ ആന്റിഈസ്ട്രോജെനിക് കഴിവിനെ സൂചിപ്പിക്കുകയും ചെയ്യുന്നു. കൂടാതെ, റോഡെന്റ് യൂട്ടറോട്രോപിക് പരിശോധനയിൽ എൻഡോമെട്രിയൽ ലൈനിംഗിന്റെ കനത്തെ കുറയ്ക്കുകയും സെറം ഈസ്ട്രജന്റെ അളവ് കുറയുന്നതും സത്തുകളുടെ ആന്റിഈസ്ട്രജനിക് ഫലങ്ങളെ സൂചിപ്പിക്കുന്നു. ഇൻ വിട്രോ, ഇൻ വിവോ മോഡലുകളുടെ സഹായത്താലാണ് ചെടികളുടെ ആന്റിഓക്സിഡന്റ് കഴിവ് വിലയിരുത്തിയത്. ഫ്രീ റാഡിക്കലുകളായ എബിടിഎസ്, ഡിപിപിഎച്ച്, സൂപ്പർഓക്സൈഡ്, ഹൈഡ്രോക്സിൽ എന്നിവയെ രണ്ട് ചെടികളുടെ സത്തുകളും ഫലപ്രദമായി തടയുന്നതായും കണ്ടു. മനുഷ്യന്റെ എറിത്രോസൈറ്റുകളിൽ എഎപിഎച്ച് മൂലമുണ്ടാക്കിയ ലിപിഡ് പെറോക്സിഡേഷനും ഹീമോളിസിസും ചെടിയുടെ സത്തുകൾ ഗണ്യമായി കുറച്ചു. സോഡിയം ഫ്ലൂറൈഡ് കൊടുക്കപ്പെട്ട എലികളിൽ അവരുടെ എൻഡോജെനസ് ആന്റിഓക്സിഡന്റ് അളവുകളിൽ ക്രമാതീതമായ മാറ്റം കാണപ്പെട്ടു. ആന്റിഓക്സിഡന്റുകളായ എസ്ഒഡി, കാറ്റലേസ്, ജിഎസ്എച്ച് എന്നിവയുടെ അളവ് സത്തുകൾ നല്കപ്പെട്ട എലികളിൽ വർദ്ധിച്ചതായും ലിപിഡ് പെറോക്സിഡേഷൻ കുറയ്ക്കുന്നതായും കാണപ്പെട്ടു. സോഡിയം ഫ്ലൂറൈഡ് നല്കപ്പെട്ട എലികളിലെ കരൾ കോശങ്ങളിലുണ്ടായ ഘടനാപരമായ മാറ്റങ്ങൾ രണ്ട് സസ്യങ്ങളുടെ സത്തുകളും ഗണ്യമായി ലഘൂകരിച്ചു.

ഡിഎംബിഎ ഉപയോഗിച്ചുണ്ടാകിയ സ്തനാർബുദങ്ങൾക്കെതിരെ രണ്ട് സസ്യങ്ങളുടെ സത്തുകളും ഗണ്യമായ സംരക്ഷണ ഫലങ്ങൾ കാണിച്ചു. ഡിഎംബിഎ മൂലമുണ്ടായ കരൾ മാർക്കർ എൻസൈമുകളുടെ ഉയർന്ന അളവുകൾ സത്തുകൾ ലഘൂകരികുകയും സ്തനഗ്രന്ഥിയുടെ ഹിസ്റ്റോളജിയിൽ അർബുദകോശങ്ങളുടെ വ്യാപനം കുറക്കുന്നതായും കാണപ്പെട്ടു. പിൻ 1 എക്സ്പ്രഷൻ ഒഴികെ ഡിഎംബിഎ ഉയർത്തിയ ഓങ്കോജീനുകളായ ഇആർ-α1, ബിസിഎൽ-2, സി-എംവൈസി എന്നിവയുടെ എംആർഎൻഎ എക്സ്പ്രഷൻ ഈ സത്തുകൾ കുറച്ചു. എലികളിൽ 4ടി1 കോശം കുത്തിവെച്ചുണ്ടാക്കിയ സ്തനാർബുദത്തിന്റെ വളർച്ചയെ കുറക്കുകയും മറ്റൊരു അവയവത്തിലേക്ക് മാരകാം വിധം അർബുദം പകരുന്നത് കുറക്കുകയും ചെയ്തു. സ്തനഗ്രന്ഥിയുടെ ഹിസ്റ്റോളജിയിൽ മാരകമായ കോശവ്യാപനത്തില് ഗണ്യമായ കുറവ് കാണിക്കുകയും അങ്ങനെ സത്തുകൾ നല്കിയ ഗ്രൂപ്പിലെ മെറ്റാസ്റ്റാസിസ് ഫലപ്രദമായി തടയുന്നതായും കണ്ടു.

ടിഎൻബിസി കോശങ്ങളെ അശോകത്തിന്റെയും മലബാർ മഹാഗണിയുടെയും സത്തുകൾ നശിപ്പിക്കുന്നത് പ്രോഗ്രാം ചെയ്ത കോശമരണത്തിലൂടെയാണെന്ന് ഫലങ്ങൾ കാണിച്ചു. ഇബി/എഒ ഫ്ലൂറസെന്റ് സ്റ്റയിനിങ്ങിൽ ഘടനാപരമായ മാറ്റങ്ങളായ ചിതറിക്കിടക്കുന്ന ക്രോമാറ്റിൻ, സുഷിരങ്ങളുള്ള കോശങ്ങൾ എന്നിവയെ വെളിപ്പെടുത്തുകയും അവ അപ്പോപ്റ്റോസിസിനെ സൂചിപ്പിക്കുകയും ചെയ്യുന്നു. ഫ്രെറ്റ് അടിസ്ഥാനമാക്കിയുള്ള കാസ്പേസ്-3 ആക്റ്റിവേഷൻ വിലയിരുത്തലിൽ എംഡിഎ-എംബി-231 കോശങ്ങളിൽ സത്തുകൾ ഉപയോഗിക്കുമ്പോൾ കാസ്പേസ് 3 പോലുള്ള എക്സിക്യൂഷൻ കാസ്പേസുകൾ സജീവമാകുന്നതായും കണ്ടു. കൂടാതെ ഫ്ലോ സൈറ്റോമെട്രി അടിസ്ഥാനമാക്കിയുള്ള സെൽ സൈക്കിൾ വിശകലനം G0/G1 ഘട്ടത്തിൽ എംഡിഎ-എംബി-231 കോശങ്ങളെ അറസ്റ്റ് ചെയ്യുന്നതായും, അത് അപ്പോപ്റ്റോസിസിനെ സൂചിപ്പിക്കുകയും ചെയ്യുന്നു.

ഉപസംഹാരമായി, ഘടനാപരമായ പരിശോധനകളും ബയോകെമിക്കൽ പരിശോധനകളും സൂചിപ്പിക്കുന്നത് അശോകയുടെയും മലബാർ മഹാഗണിയുടെയും സത്തുകൾക്ക് ടിഎൻബിസി അർബുദത്തിനെതിരെ ചെലുത്തുന്ന സൈറ്റോടോക്സിസിറ്റി ഒരു അപ്പോപ്റ്റോട്ടിക് സംവിധാനത്തിലൂടെയാണ് എന്നാണ്.

അപ്പോപ്റ്റോസിസ് ഉണ്ടാകുന്നതിലൂടെ ട്രിപ്പിൾ നെഗറ്റീവ് ബ്രെസ്റ്റ് കാൻസർ സെല്ലുകളിൽ രണ്ട് സസ്യ സത്തുകളുടെയും ആൻറി കാൻസർ കഴിവിൽ കാസ്പേസ്-3 സജീവമാകുന്നത് ഒരു പ്രധാന പങ്ക് വഹിച്ചുവെന്ന് ഫലങ്ങൾ സൂചിപ്പിക്കുന്നു. ടിഎൻബിസികളെ അഭിസംബോധന ചെയ്യുന്ന കൂടുതൽ ഗവേഷണങ്ങൾക്ക് ഇത് ഒരു നല്ല വഴി തുറക്കുന്നു, കൂടാതെ ഇആർബിറ്റ പ്രകടിപ്പിക്കുന്ന അർബുദങ്ങളിൽ ഫൈറ്റോ ഈസ്ട്രജനുകളുടെ സ്വാധീനം മനസിലാക്കുവാൻ കൂടുതൽ പര്യവേക്ഷണം ആവശ്യമാണ്. ഇആർബിറ്റയുമായി ബന്ധിപ്പിക്കാൻ കഴിവുള്ള സംയുക്തങ്ങൾക്ക് ടിഎൻബിസികൾ പോലുള്ള മാരക അർബുദങ്ങളെ തടയാനോ ചികിത്സിക്കാനോ കഴിയും. തൽഫലമായി, ഈ ഉപവിഭാഗത്തിലെ അർബുദത്തിന്റെ വളർച്ചയെ തടയുന്നതിന് ഈസ്ട്രജനിക് വിരുദ്ധ മരുന്നുകളുടെ വികസനം നിർണായകമാണ്.

പ്രധാന വാക്കുകൾ: സറാക്ക അശോക, കിങ്ങിയോഡെൻഡ്രോൺ പിന്നാറ്റം, ഫൈറ്റോ ഈസ്ട്രജൻസ്, ടിഎൻബിസി, ആന്റി ഈസ്ട്രോജെനിക്, ആൻറി-ഇൻഫ്ലമേറ്ററി, ആൻറി കാൻസർ

TABLE OF CONTENTS

LIST OF TABLES

LIST OF FIGURES

chloroform: methanol in the ratio 8:3:1, on pre-coated silica gel plate. The plates scanned at 366 nm (A) and derivatized plate sprayed with reagent (B). Lane 1 – Crude extract of *S. asoca*, Lane 2 - Methanol fraction of *S. asoca*, Lane 3 - Crude extract of *K. pinnatum*, Lane 4 – Methanol fraction of *K. pinnatum,* Lane 5 – *β*-sitosterol

ABBREVIATIONS

μg	Microgram
μL	Microliter
AAPH	2, 2′ azobis (2-amidinopropane)
ALP	Alkaline phosphate
b.wt.	Body weight
DLA	Dalton's Lymphoma Ascites
DMBA	7, 12- Dimethyl benz[a]anthracene
DPPH	2, 2-Diphenyl-1-picrylhydrazyl
DTNB	5-5'Dithiobis (2-nitrobenzoic acid)
EAC	Ehrlich ascites carcinoma
ERα	Estrogen receptor alpha
ERβ	Estrogen receptor beta
EDTA	Ethylene diamine tetra acetic acid
FBS	Fetal bovine serum
FCR	Folin–Ciocalteau colorimetric reagent
FRAP	Ferric reducing antioxidant power assay
FTIR	Fourier Transform Infrared Spectrophotometer
GAE	Gallic acid equivalents
g	Gram
GLU	Glutamic acid
GLY	Glycine
HeLa	Henrietta Lacks Cervical Cancer Cells
HepG2	Hepatoma G2 Liver Carcinoma cells
IEC-6	Intestinal Epithelial Cell Line-6
IARC	International agency for Research on Cancer
ICMR	Indian Council of Medical Research
IC$_{50}$	Half maximal inhibitory concentration
KP	*Kingiodendron pinnatum*

KPLD	*Kingiodendron pinnatum* low dose
KPHD	*Kingiodendron pinnatum* high dose
LC-MS	Liquid chromatography
LEU	Leucine
MET	Methionine
MCF-7	Michigan Cancer Foundation-7
MDA	Malondialdehyde
MDAMB	M. D. Anderson Metastasis Breast cancer
mg	Milligram
min	Minutes
mL	Millilitre
NaF	Sodium fluoride
OECD	Organization for Economic Cooperation and Development
PBS	Phosphate buffered saline
RIA	Radioimmunoassay
RPMI	Rosewell Park Memorial Institute medium
SA	*Saraca asoca*
SALD	*Saraca asoca* low dose
SAHD	*Saraca asoca* high dose
SD	Standard deviation
SERM	Selective Estrogen Receptor Modulator
SGOT	Serum glutamate oxaloacetic transaminase
SGPT	Serum glutamate pyruvate transaminase
SOD	Superoxide dismutase
TBA	Thiobarbituric acid
TLC	Thin Layer Chromatography
TPTZ	2, 4, 6 – Tris (2-pyridyl)-*s*-triazine
TNBC	Triple negative breast cancer
WBC	White blood cells
WHO	World Health Organization

Introduction

Cancer is a multi-step process whereby uncontrollably dividing cells swiftly produce abnormal cells that invade neighbouring areas of the body and destroy normal tissue by crossing unusual boundaries. Immune system damage, and other potentially fatal impairments are the possible outcomes. Cancer is the second most common cause of mortality worldwide. Despite this, improvements in cancer identification and therapy are raising survival rates for a wide range of cancer types. Breast cancer is the most prevalent form among women worldwide. Due to its heterogeneity, breast cancer can vary significantly in terms of its behaviour, aggressiveness, and response to treatment. Genetic and environmental factors, such as age, family history, reproductive history, hormones, lifestyle choices, radiation and chemical exposure, are certain risk factors for breast cancer. Thus, the treatment may change depending on the patient's health, the type of cancer, and its stage. Most common treatments include hormone therapy, immunotherapy, radiation, chemotherapy, and surgery. There are many variables that affect the prognosis for breast cancer, including the stage at diagnosis, the presence of hormone receptors or other molecular markers, and the patient's overall health.

Breast cancer is divided into several categories based on tumour grade, lymph node status, histology, and the existence of markers like estrogen receptor (ER), progesterone receptor (PR), epidermal growth factor receptor 2 (HER2) (Amin *et al*., 2017). Depending on whether receptors are present, it can be further divided into five subtypes: Luminal A (ER+, PR+/-, HER2-), Claudin low (ER-, PR-, HER2-), Luminal B (ER+, PR+/-, HER2+), HER2 (ER-, PR-, HER2+) and Basal (ER-, PR-, HER2-). This categorization aids in predicting the prognosis for each subtype and customizing treatment strategies. The presence of hormone receptors in certain breast cancer subtypes makes them susceptible to hormone therapy. However, estrogen, progesterone and HER2 receptors are absent in triple negative breast cancer (TNBC), making it less responsive to traditional hormone therapies. Compared to Western nations, a comparatively larger percentage of breast cancer cases in India are reported to be TNBC. It accounts for 20–30% of all incidences of breast cancer in India (Sandhu *et al*., 2016). Numerous factors, including variations in genetic predisposition, lifestyle choices, environmental exposures and access to healthcare services, may be responsible for this increased occurrence.

Currently, the trials are being conducted throughout the world to discover new medicinal compounds derived from plants. Several specialized metabolites are found in plants,

many of which have medicinal properties. More than half of the top prescribed drugs contain a component derived from plants and approximately 80% of these drugs depend on plants or plant extracts to provide their health benefits (Ekor, 2014). According to the World Health Organization (WHO), almost 20,000 medicinal plants are distributed across 91 countries, particularly in 12 countries known for their high biodiversity. It is generally accepted that medicinal plants are safe, but they can have side effects due to their constituents, which can have adverse effects if they are misused (Anywar *et al.*, 2021). In this regard it is necessary to implement various steps when attempting to isolate a biologically active compound from plant resources. The extracted compounds should be screened pharmacologically, isolated, identified, characterized and evaluated toxicologically and clinically (Sasidharan *et al.*, 2011). The discovery of new drugs with therapeutic benefits can be made possible through the use of effective studies. *Saraca asoca* (Asoka) is a revered tree employed in Ayurveda for addressing a range of health conditions. Every component of this tree, including flowers, leaves, root, seed, and bark, is considered pharmacologically valuable. The bark, in particular, plays a significant role as a key ingredient in *Asokarishta*, an Ayurvedic polyherbal formulation utilized for diverse gynecological issues in women. *S. asoca* serves as a prolific reservoir of biologically important phytoconstituents, including *β*-sitosterol, catechin, gallic acid, quercetin, kaempferol, and numerous others, many of which are recognized as phytoestrogens. Occasionally, *Kingiodendron pinnatum*, a member of the same family as that of Asoka is used as an alternative in preparation of Ayurvedic formulations. The full extent of the biological properties of this plant has not been completely explored. In a prior investigation carried out by the Kerala Forest Research Institute (KFRI), *S. asoca* demonstrated anti-estrogenic and anti-inflammatory activities. Additionally, *K. pinnatum* was observed to be similarly effective as Asoka, potentially due to the anti-estrogenic properties of *K. pinnatum* as well. The phytoestrogens present in these plants have shown to have anti-angiogenesis, anti-metastasis, and other effects in addition to their vital role in cell cycle arrest. Furthermore, anti-estrogens have proven successful in breast cancer treatment. The preliminary investigation of *S. asoca* and *K. pinnatum* crude methanol extracts in our lab has revealed considerable cytotoxic activity especially targeting TNBCs. Therefore, the current study aims to delve into the biological properties, particularly the anticancer activity, of extracts from *Saraca asoca* and *Kingiodendron pinnatum* against breast cancer, with a special focus on triple-negative breast cancers.

Consequently, this dissertation is a combination of thorough analysis and experimental results of the biological characteristics of *Saraca asoca* and *Kingiodendron pinnatum* with the focus particularly on their relevance to breast cancers. The studies are organized into seven chapters: Chapter 1-Review of literature, Chapter 2- Materials and methods, Chapter 3- Anti-proliferative, anti-tumour activity analysis and phytochemical profiling of *S. asoca* and *K. pinnatum*, Chapter 4- Anti-inflammatory and anti-estrogenic properties of extracts of *S. asoca* and *K. pinnatum*, Chapter 5- Protective effect of *S. asoca* and *K. pinnatum* on sodium fluoride induced oxidative stress, Chapter 6- Evaluation of the effect of *S. asoca* and *K. pinnatum* extracts on DMBA induced mammary carcinogenesis and 4T1 induced TNBC model, Chapter 7- Elucidation of possible mechanism of action of *S. asoca* and *K. pinnatum* extracts on TNBC cells by cell death pattern analysis.

Chapter 1
Review of literature

1.1. Cancer

Cancer is a devastating disease characterized by uncontrolled cellular proliferation and insufficient apoptotic turnover caused by alterations in gene expression. Initiated by a single transformed cell, it multiplies rapidly, leading to invasion and ultimately metastasis from its location of origin. Various carcinogens, inflammatory agents and tumour promoters play an important role in triggering this dynamic process. A wide range of molecular targets are involved in the regulation of the entire process, including transcription factors, pro-apoptotic proteins, anti-apoptotic proteins, protein kinases, cell cycle proteins, cell adhesion molecules and other molecular targets (Aggarwal and Shishodia, 2006). The development of lead candidates derived from phytochemicals to block these targets is in progress.

1.2. Global statistics of cancer

Cancer is associated with a significant mortality rate, which is evident from the disease statistics reported by world health organization during the years. Among the top causes of mortality globally, cancer is surpassed only by cardiovascular disorders. Globally, cancer caused nearly 10 million deaths in 2020, or almost one death in six. Approximately 19.3 million cases of cancer were newly diagnosed worldwide in 2020 according to recent data released by the World Health Organization (WHO) through its cancer research agency, the International Agency for Research on Cancer (IARC) (Sung *et al*., 2021). Female breast cancer is estimated to be the most frequently diagnosed cancer by GLOBOCAN 2020, an IARC initiative that provides data on global cancer statistics, including mortality and incidence rates for 36 distinct forms of cancer across 185 countries. It accounts for an estimated 2.3 million new cases, constituting approximately 11.7% of all cancers. The next most common cancers are lung cancer (11.4%), colorectal cancer (10.0%), prostate cancer (7.3%), and stomach cancer (5.6%) (Figure 1.1) (Sung *et al*., 2021). The primary cause of cancer death remains lung cancer, which accounts for approximately 1.8 million deaths annually (18%). This was followed by colorectal cancer (9.4%), liver (8.3%), stomach (7.7%), and female breast cancer (9.4%) (Ferlay *et al*., 2021, Sung *et al*., 2021). The global cancer burden is projected to rise to 28.4 million cases by 2040, a 46% surge from 2020, as a result of increased risk factors brought on by economic growth and globalization.

Considering the Indian scenario the number of deaths attributed to non-communicable diseases in India was estimated to be 63%, with cancer accounting for 9 percent. India

ranked second in Asia in 2020 with 1.3 million new cases and 9.3 lakh deaths, and this number is anticipated to rise. It is estimated that more than 40% of the total cancer burden is due breast cancer (13.5%), oral cancer (10.3%), cervix and uteri cancer (9.4%), lung cancer (5.5%) and colorectal
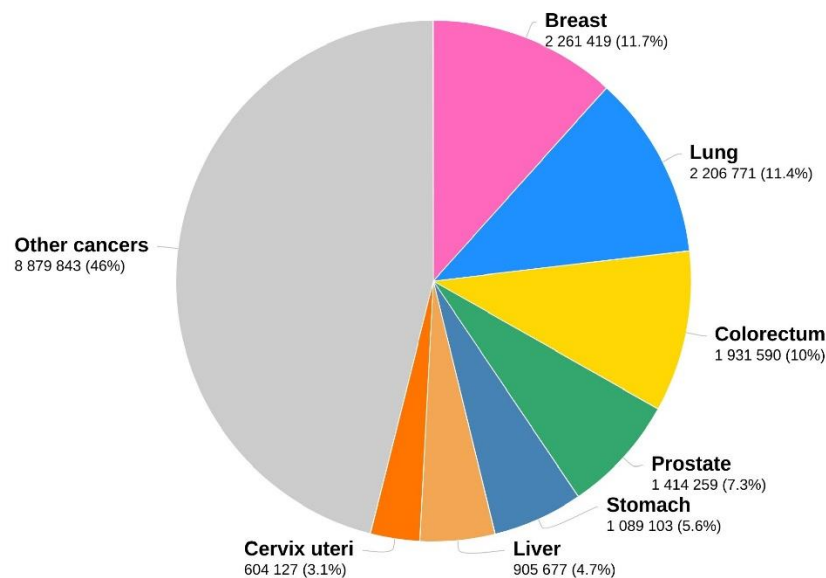
Figure 1.1. Pie chart representing distribution of estimated number of new cases of different cancer in 2020 (Data source: Globocan 2020, International Agency for Research on Cancer)

cancer (4.9%). The most common cancer sites among males were the lung, mouth, oesophagus, and stomach. In females, the most prevalent cancer sites were the breast, cervix, uterus, and ovary. The cancer statistics report, 2020 projects a mortality rate for men of 94.1 per 100,000 individuals and a mortality rate for women of 103.6 per 100,000 individuals for 2020 (Mathur *et al*., 2020). In India the number of new cancer patients registering, obtaining outpatient services, and undergoing major surgeries has decreased due to current pandemics of novel Coronavirus diseases (COVID-19) (Ranganathan *et al*., 2021).

Despite contributing immense dimensions of work to the field of cancer research, the above reports are few of the adoptions from the large body of cancer statistical data available to researchers worldwide. Building a sustainable infrastructure for cancer prevention and cancer care is imperative to the control of global cancer.

1.3. Worldwide breast cancer statistics

Breast cancer stands as the leading cause of cancer-related deaths globally, with its incidence rising steadily over recent decades. Surpassing lung cancer, breast cancer now ranks as the most commonly diagnosed cancer in the world, representing one in every eight cancer diagnoses. In 2020, there were over 2.3 million new cases of breast cancer and 685,000 deaths associated with the disease (Arnold *et al*., 2022). A large geographical variation in invasive breast cancer incidence exists across countries and world regions. According to GLOBOCAN 2020, the estimated global burden of breast cancer varies widely, ranging from fewer than 40 cases per 100,000 females in certain African and Asian countries to 80 cases per 100,000 females in northern America, New Zealand/Australia, and certain parts of Europe. According to the 2020 report from the National Cancer Registry Programme in India, the annual incidence rate of breast cancer witnessed a notable increase of 3% and along with cervical cancer, they represent 39.4% of all cancer cases among Indian women (Bengaluru, 2020). It was estimated that over 2 lakh women across the nation received a diagnosis of breast cancer, with over 76,000 casualties attributed to the disease. Breast cancer mortality exhibits relatively mild geographic variation. Nevertheless, in contrast to developed countries, breast cancer fatalities remain notably more prevalent in transitioning nations. Due to increasing population and ageing, the burden of breast cancer is expected to rise to about 3 million new cases and 1 million deaths annually by 2040 (Arnold *et al*., 2022).

1.4. Different types of cancers

Cancer is not a singular disease, but rather a group of diseases characterized by the uncontrolled growth and alteration of cells in the body. Cancers are classified either by the type of tissue or fluid from which they originate, or by their initial location in the body. Some cancers are also a mix of different types and there are more than 200 identified types of cancer that afflict people (Song *et al*., 2015). Not all lumps or tumours are cancerous; benign tumours, which do not spread to other bodily areas, are not categorized as cancer (Institute, 2007). Premalignant tumours have non-cancerous cells that have the potential to develop into malignant tumours, whereas malignant tumours have cancerous cells that can multiply and spread to other body areas. For increased precision, malignancies are further categorized based on the specific type of cell from

which the tumour cells originated, as certain body parts consist of diverse tissue types. Accordingly, there are six primary types of cancer based on cell type.

- Carcinomas: The majority of cancers, between 80% and 90%, are carcinomas, the most prevalent kind of cancer cell. These malignancies arise from epithelial cells, encompassing skin cells as well as cells that line body cavities and organs. Most carcinomas target organs or glands capable of secretion, such as the breasts, prostate, lungs, colon and bladder. There are specific terms for carcinomas originating in various types of epithelial cells. Adenocarcinoma arises from fluid or mucus producing epithelial cells. Most cases of prostate, colon and breast cancer are of this kind of malignancy. A basal cell carcinoma develops in the basal layer of the epidermis, the skin's outer layer. Squamous cell carcinoma develops from squamous cells, which are epithelial cells located just beneath the skin's surface. Squamous cells line several organs, including the bladder, kidneys, intestines, stomach, and lungs. Transitional cell carcinoma develops in the epithelial tissue known as the transitional epithelium, which lines the ureters, parts of the kidneys, bladder and some additional organs. This tissue, which is made up of many layers of epithelial cells can change in size.

- Sarcomas: These malignancies affect the body's bones and soft tissues, consisting of mesenchymal cells. Cartilage, blood vessels, Bone, fatty tissues, ligaments, muscles (both skeletal and smooth), nerves, synovial tissues (joint tissues) and tendons are all impacted by this type of cancer (Xiao *et al*., 2013). There are several types of sarcomas, including angiosarcoma (affect blood vessel), chondrosarcoma (affect cartilage), fibrosarcoma (fibrous tissue cancer), glioma (connective tissue cancer), Liposarcoma (affect fatty tissue), Osteosarcoma (bone cancer), rhabdomyosarcoma (skeletal muscle cancer) etc.

- Lymphomas: Cancer originating in lymphocytes like T cells/B cells is known as lymphoma. These white blood cells, integral to the immune system, combat various diseases. In lymphoma, abnormal cells accumulate in the lymphatic vessels, lymph nodes and some organs such as the brain, stomach or breast of the body. The primary types of lymphoma are Non-Hodgkin lymphoma and Hodgkin lymphoma. Non-Hodgkin lymphomas are sizable range of malignancies originating in B or T cell lymphocytes that can spread swiftly or slowly. Hodgkin

lymphomas are characterized by the presence of Reed-Sternberg cells which are abnormal lymphocytes typically derived from B cells.

- Leukemias: These are hematologic malignancies originating in the bone marrow. Termed as "liquid cancers" among blood related cancers, they are distinct from lymphomas and myeloma. These malignancies are often treated as solid tumours that have metastasized because of blood circulating cells. Examples include lymphocytic leukemias, which are malignancies of white blood cells and myelocytic leukemias, which are cancers of mature or immature myelocytes. Acute and chronic variants of lymphocytic and myelocytic leukemia both exist. With about 30% of cases, acute lymphoblastic leukemia is the most prevalent type of cancer in kids (Varricchio, 2004). On the other hand, leukemia strikes adults much more frequently than kids.

- Myelomas: Myeloma is a cancer originating in the plasma cells of the bone marrow, responsible for antibody production. Occasionally, myeloma cells accumulate in a single bone, forming a solitary tumour called a plasmacytoma. In other cases, these cells cluster in multiple bones, resulting in many bone tumours known as multiple myeloma. Multiple myeloma is also referred to as plasma cell myeloma or Kahler disease.

- Mixed types: The majority of tumours are heterogeneous. As a result, cells in one area of a tumour may differ significantly from those in another area of the tumour in terms of morphology. For example, lung cancer may contain cells resembling both adenocarcinoma and squamous cell carcinoma. In such cases, it may be classified as adenosquamous carcinoma. Blastomas are another type that is sometimes distinguished from others. These malignancies influence embryonic cells that have not yet differentiated into epithelial or mesenchymal cells.

1.5. Causes of cancers

Cancer can have many different causes and is triggered by a number of factors interacting together. Environmental or genetic variables may be at play. Stem cells are a common site or point of origin for childhood malignancies. These cells have the capacity to

produce several other specialized cell types that the body requires. Childhood cancer is frequently brought on by a random cell alteration or mutation that occurs by chance. In adulthood, the type of cell that typically matures into cancer is often an epithelial cell. Body cavities and the exterior of the body are lined with epithelial cells. Environmental exposure to these types of cells over time might end up in cancer (Parsa, 2012). Due to this, adult cancers are sometimes labelled as acquired.

1.5.1. Cancer risk factors

Various exposures or risk factors have been connected to some malignancies, notably in adults. Anything that could raise an individual's likelihood of contracting a health problem is a risk factor (World Health, 2002). While a risk factor doesn't invariably result in the disease, it can compromise the body's defenses. Cancer risk factors include the both intrinsic and non-intrinsic risk factors

1.5.5.1. Intrinsic risk factors

Intrinsic risk is the term used to describe inevitable spontaneous mutations that occur due to spontaneous errors in DNA replication processing and these errors occur at varying rates in different organisms. Randomly developed mutations such as single nucleotide errors, insertions and deletions must survive and divide in order to spread in a tissue. In contrast to "passenger mutations" that do not affect cancer formation yet are frequently seen in malignancies, randomly acquired mutations may result in "driver mutations" necessary for the development of cancer. The difficulty of developing cancer by intrinsic processes alone is increased by the requirement for many driver mutations to start cancer (Wu *et al*., 2018). According to one study, up to 64% of the chance of developing cancer may be attributable to uncontrollable random errors in DNA synthesis (Tomasetti and Vogelstein, 2015). Furthermore, tissues with more cell divisions are particularly susceptible to both intrinsic mutations and higher mutations brought on by environmental influences (Nowak and Waclaw, 2017).

1.5.5.2. Non-intrinsic risk factors

There are many different ways that non-intrinsic risk factors are thought to cause cancer. Some are members of the chemical family that cause new mutations, while others, like viruses, also cause cancer by activating oncogenes or blocking tumour suppressor genes.

Non-intrinsic risk factors are those that are not caused by intrinsic replication error. These include endogenous risk factors like inflammation, immune reactions, growth factors, hormones, metabolic impacts, reactive oxygen species, etc. as well as exogenous risk factors like ultraviolet radiation, HPV, tobacco, and drugs. The majority of the data supporting non-intrinsic risk factors comes from research on cancer epidemiology and cancer biology (Visvader, 2011).

1.5.5.2.1. Exogenous risk factors

Exogenous cancer risk factors have been established by a number of important epidemiologic and scientific investigations. These include UV radiation for skin cancer, viruses for hepatic and cervical cancer and tobacco use for lung cancer. In more recent times, a number of research groups have indicated that the number of cases and fatalities of colorectal cancer are rising in Asia and nearing those in Western nations (Sung *et al*., 2005). The geographic patterns of cancer incidence rates are diverse, with estimates in areas with a high incidence rate are often one or two orders of magnitude higher than those in areas with a low incidence rate. Early industrialized nations have shown greater rates of lifestyle-associated cancers, such as breast, colorectal, prostate and lung cancers. On the other hand, less developed locations and places where endemic infectious agents are prevalent have been found to have greater occurrences of infection-related cancers like cervical, stomach, liver, and cancers (Hemminki *et al*., 2014). Different exogenous factors contributing to the prevalence of cancers are as follows.

- Lifestyle influences: Some adult malignancies may be predisposed by cigarette smoking, alcohol, eating poorly, being sedentary, being exposed to the sun, and exposure to hazardous substances. However, most cancer patients are usually too young to have been exposed to these lifestyle risks over an extended period of time.
- Interaction with particular viruses: Some pediatric cancers are more likely to develop when the Epstein-Barr virus and HIV are involved. Hodgkin and non-Hodgkin lymphomas are examples of this. A cell may be modified by the virus in one or more ways, eventually changing the cell entirely. These alterations ultimately end up in a cancer cell that leads to additional cancer cells.
- Environmental exposures: Research has been conducted on fertilizers, pesticides, and transmission lines for a potential link to childhood malignancies. Evidence

suggests that specific areas and localities have reported cases of cancer among unrelated children. It remains unclear whether exposure to these substances during pregnancy or infancy leads to cancer or if it is merely coincidental.

- Excessive doses of chemotherapy and radiation: If exposed to these substances as a youngster, they may occasionally go on to acquire a secondary cancer. These effective anticancer drugs might alter cells or the immune system. A cancer that develops after therapy for another cancer is referred to as a secondary malignancy.

1.5.5.2.2. Endogenous risk factors

The risk for developing cancer may be influenced by endogenous factors as well as genetic factors. One of the most researched examples of an endogenous cancer risk factor is the relationship between individual levels of sex steroid hormones and breast cancer risk (Brown and Hankinson, 2015). The steroid sex hormones, which are endogenous determinants of cancer risk, vary throughout the course of a person's life and among individuals. Other exogenous elements that impact them include diet, hormone therapy, consistent physical activity, and other endogenous aspects including genetic background. The following are many endogenous factors influencing the incidence of cancer.

- Genetics, inheritance, and family history: These might be crucial in some childhood malignancies. It is possible for a family to have multiple instances of cancer in different types. Many times, it is difficult to determine if the disease is the result of a chemical exposure near a family's home, genetic mutation, a combination of these factors, or pure coincidence.

- Some genetic disorders: Our body's intricate immune systems protect us from disease and infection. The bone marrow produces immature immune system cells that subsequently develop and perform their functions. One hypothesis is that the stem cells in the bone marrow become harmed or dysfunctional. Therefore, when they proliferate in order to produce new cells, they form aberrant or cancerous cells. The deficiency in the stem cells could have resulted from contact with toxic substances, viruses or an inherited genetic defect. For instance, it is well-recognized that Wiskott-Aldrich syndrome alters the immune system.

- Inflammation and cancer: Nowadays, it is acknowledged that inflammation has a role in carcinogenesis, acting as a catalyst for tumorigenesis in a range of cancer forms. The enormous amount of evidence from animal and human studies has led

to this inclusion (Hanahan and Weinberg, 2011). In the area of chemoprevention, it has been demonstrated how crucial inflammation is to the cancer development. Anti-inflammatory drugs like aspirin along with different nonsteroidal anti-inflammatory medications have shown their ability to prevent cancer by inhibiting pro-inflammatory agents like prostaglandin E2 for a variety of cancers (Todoric *et al.*, 2016). In fact, the US Prevention Services Task Force advocated for the use of low-dose aspirin to prevent colorectal cancer in people at high risk (Chubak *et al.*, 2015).

- Ageing: It can be categorized biologically or chronologically and is one of the major risk factors for cancer (De Magalhães, 2013). Chronological ageing provides ample time for intrinsic risk and non-intrinsic risk factors to manifest their effects. Whereas, physiological aging events are more challenging to characterize or measure because of the incomplete understanding of their whole range. The association between ageing and cancer is widely regarded as the result of a decline in the cellular and molecular functions of the body.

1.6. Hallmarks of cancer

The multiple stages of carcinogenesis involve the progressive transition of normal cells into neoplastic cells, during which they develop certain abilities that make them tumourigenic. In the work, the hallmarks of cancer, published in 2000, Douglas Hanahan and Robert Weinberg proposed six fundamental principles that govern the multistep process by which normal cells become cancerous (Hanahan and Weinberg, 2000). These six initial hallmarks have increased to 14 in the third update, "Hallmarks of cancer: new dimensions," published more than 20 years later (Figure 1.2). These hallmarks define a set of parameters that explain how malignant tumours might form from normal cells by highlighting particular traits and outlining how they relate to one another (Hanahan, 2022). When these hallmarks come together, cancer cells are able to bypass the usual restrictions that limit cell growth and division. As a result, they can keep dividing and multiplying, developing tumours that can infiltrate neighbouring tissues and spread to different parts of the body. The respective hallmarks are summarized below.

1.6.1. Maintaining proliferative signaling

The most crucial feature of cancer cells is their capacity to continue proliferating. The cancerous cells stimulate signaling pathways leading to the proliferation and division of

cells. These pathways are generally highly regulated, but in cancer cells they are always active, allowing the cells to undergo division and multiply regardless of the lack of normal growth signals. This may be brought on by mutations in the genes encoding the signaling pathway-related proteins, which activate signaling molecules downstream and stimulate cell proliferation.

1.6.2. Evading growth suppressors

The ability to avoid growth suppression is a highly advantageous characteristic skill for maintaining proliferative signals in cancer cells. Normal purpose of growth suppressor genes is to prevent cell division and expansion. Numerous tumour-suppressing protein-coding genes that prevent cellular proliferation and development through a variety of mechanisms have been identified. The human tumour suppressor p53 and the retinoblastoma protein (RB) are two notable examples (Sherr, 2004, Rahman and Scott, 2007). Genes involved in cell cycle regulation, inducing apoptosis or repairing damaged DNA are expressed differently depending on the transcription factor. These genes are frequently rendered inactive in cancer cells, either because of mutations that render them inoperable or because of processes that hinder them from being expressed. As a result, cancer cells are able to circumvent the limitations imposed on cell development and division and can continue to multiply unregulated.
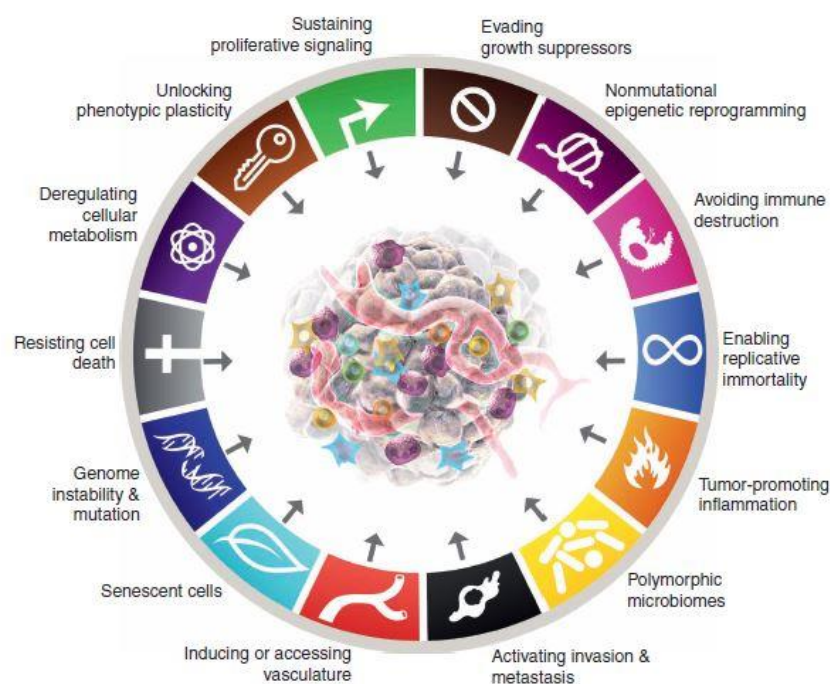
Figure 1.2. The hallmarks of cancer (Hanahan, 2022)

1.6.3. Resisting cell death

In addition to being resistant to growth inhibitors, cancer cells also show a significant degree of resistance to cell death. Apoptosis, also known as programmed cell death, is the normal process that cells undergo when they become damaged or cease to be needed. Cancer cells may alter their systems to identify abnormalities or defects which would prevent the right signals from being sent out and trigger apoptosis. Cancer cells might also cause errors in the proteins involved or the downstream signaling system, which could hinder normal apoptosis. It can be a consequence of mutations in genes that are involved in the apoptotic pathway, or it may result from activation of signaling pathways that encourage cell survival.

1.6.4. Tumour promoting inflammation

Inflammation favours all phases of cancer development and contributes to the development of cancer. Tumours displace pathways that are developed to facilitate resistance against infection and enhance tissue homeostasis. An inflammatory tumour microenvironment (TME) is made up of nearby stromal and inflammatory cells along with cancer cells. Inflammation also triggers the production of growth factors that promote tumour growth. The early inflammatory reactions may be initiated by a number of mechanisms. Microorganisms that cause cancer, environmental toxins, and obesity-related low-grade inflammation, as well as the deterioration of epithelial barriers caused by commensal microorganisms, are examples. Additionally, cancer-associated inflammation occurs at different times. Infections, malignant cells, and auto immunities are pertinent causes and stimuli. Even the anti-cancer treatment itself has been known to cause inflammation.

1.6.5. Enabling replicative immortality

Another essential element of the growth of tumours, which is often acknowledged as a characteristic of cancer, is their capacity for unrestricted replication. Cancer cells, in contrast to human body cells, can surpass the "Hayflick Limit" and divide endlessly without passing through the usual cellular aging process. Replication often comes to an end when a cell reaches the senescence or cellular death stage. This is mostly because of telomeres, a type of DNA present at the end of chromosomes. The telomeric DNA shrinks with each division until it reaches a point where senescence sets in, stopping the cell from

proliferating. Cancer cells overcome this barrier by altering the telomerase enzyme to prolong telomeres. They can divide indefinitely without surrendering to senescence.

1.6.6. Senescent cells

Senescence can be brought on in cells by a number of factors, including as abnormalities in cellular signaling networks, organelle damage, and microenvironmental stresses like nutritional depletion and damaged DNA (Huang *et al*., 2022). Cellular senescence, which is the process of inducing senescence in malignant cells, has long been thought of as a defense mechanism against cancers. The bulk of stimuli indicated above are linked to malignancy, especially DNA damage which results from uncontrolled hyperproliferation, also known as oncogene-induced senescence due to hyperactivated signalling (Liu *et al*., 2018). Recent papers, nevertheless, raise doubt on this linear connection. Senescent cells can in some circumstances encourage the growth of tumours and the spread of cancer. Senescence-associated secretory phenotypes (SASP) are regarded to be the main mechanism by which senescent cells enhance tumour phenotypes (Lopes-Paciencia *et al*., 2019).

1.6.7. Deregulating cellular metabolism

The tumours benefit from uncontrolled regulation of cell proliferation, as well as related modifications to the consumption of energy that facilitate cell proliferation and division. They have the ability to alter or modify the metabolism of cells to effectively promote the proliferation of cancer. Under aerobic conditions, glucose is first converted by normal cells to pyruvate in the cytosol by glycolysis, and subsequently to CO_2 in the mitochondria. Under anaerobic conditions, glycolysis is preferred and a small amount of pyruvate is delivered to the O_2 consuming mitochondria. The first person to notice an unusual aspect of malignant cell energy metabolism was Otto Warburg (Liberti and Locasale, 2016).

1.6.8. Avoiding immune destruction

Some cancer cells build defenses against immune system attacks and surveillance by the host's immune system. By seizing control of immunological checkpoint control mechanisms, cells can achieve this. The internal regulatory mechanisms known as immunological checkpoints maintain the immune system's self-tolerance and help to avert damage that might result from a physiological immune system reaction. It is

necessary to discriminate between the target cell's survival and the tumour cell's destruction by T lymphocytes that are specific to the tumour. Proteins on the T-cell and the target cell are essential for the decision-making process. The T lymphocytes are suppressed when tumour cells exhibit molecules that cause apoptosis or inhibit them, such as PD-L1 on their surface (Han *et al*., 2020). FasL, on the contrary, might cause T lymphocytes to undergo apoptosis (O'Connell, 2002). Certain types of cancer cells also endeavour to acquire resistance against cytotoxic CD8+ T cells, which play a pivotal role in the immune system's capability to combat tumours. To make themselves invisible to cytotoxic T cells, they downregulate the expression of MHC I. For the tumour to effectively elude the immune system, it is also imperative that the molecules involved in the apoptotic signal pathway are perturbed. Important targets include caspase 8, IAP, and BCL2.

1.6.9. Inducing or accessing vasculature

A growing tumour requires more nutrients to support its progression and spread. For the cancer cells to receive enough oxygen, the tumour needs new blood vessels. The cancer cells must acquire the ability to participate in angiogenesis, or the creation of new blood vessels, in order to achieve this. The process of angiogenesis is activated by signaling molecules released by cancer cells, which then control the growth of new blood vessels (Nishida *et al*., 2006). Non-cancerous cells that are present in the tumour are encouraged to create blood vessels by exploiting the process of angiogenesis.

1.6.10. Activating invasion and metastasis

Cancer is a deadly disease because it is capable of infecting nearby tissues and it determines whether a tumour is benign or malignant. Treatment becomes considerably more difficult when they spread throughout the body due to metastasis. Cancer cells must go through a number of alterations before they can potentially spread. The intricate process known as the metastatic cascade consists of the local tumour cell migration, infiltration of blood arteries, and acquisition of new tissue after the carcinoma cells leave the circulation. Primary cancer adjusts to the secondary location of tumour colonization via the tumour-stroma crosstalk after the early stage of effective cancer cell spreading (van Zijl *et al*., 2011).

1.6.11. Unlocking phenotypic plasticity

Mammalian cells typically have a limited potential for differentiation compared to the enormous differentiation and development that occurs during organogenesis, assuring that they stay organized and functional in their specific tissues. Cellular plasticity, which allows cells to adopt various phenotypic identities over a phenotypic range, occurs in cancer cells as a result of genetic and phenotypic alterations (Yuan *et al*., 2019). Developmental regulatory systems that resemble transdifferentiation include epithelial-to-mesenchymal transitions (EMT) and mesenchymal-to-epithelial transitions (MET). Because they can promote the development of tumours and metastasis, immune infiltration, chemoresistance, and many other features of tumour development, modifications to the cellular phenotype are essential to the progression of cancer.

1.6.12. Genome instability and mutation

Cancer cells are forced to have genetic changes as a result of genomic instability and mutability, which promote tumour growth. The subclones of cells with certain advantages can spread and finally take over a particular tissue environment due to specific mutant genotypes. Mammalian's genome repair mechanisms find and fix DNA errors and make sure that rates of spontaneous mutation are minimal after each cell generation. Cancer cells seek to accelerate the rates of mutation with the objective of increasing the amount of mutant genes required to coordinate cancer formation. The failure of the genomic maintenance machinery in various components and higher sensitivity to mutagenic agents are the main causes of the mutability rise (Hoeijmakers, 2001). The emergence of human cancer is strongly correlated with errors in the DNA maintenance machinery, which is frequently referred to as the caretakers of the genome. Along with telomerase, the infamous "guardian of the genome," p53, serves an essential role in the system.

1.6.13. Nonmutational epigenetic reprogramming

It has been recognized as an emerging characteristic in the overall framework of cancer hallmarks. It is a presumably independent method of genome reprogramming that only affects changes in gene expression that are controlled by the epigenome. Gene and histone alterations, structure of chromatin, and the activation of gene expression are a number of instances of epigenetic alterations that are persistent throughout time and are maintained via both positive and negative feedback cycles (Handy *et al*., 2011). They control how genes are expressed in both developing and mature cells. The notion that identical

epigenetic changes may aid in the formation of distinctive capacities during tumour development and malignant progression is supported by emerging data. The distinctive ability of phenotypic plasticity is made possible by nonmutational epigenetic reprogramming. Dynamic transcriptome heterogeneity, a characteristic of cancer cells, is the result of epigenetic reprogramming. A notable illustration of epigenetic reprogramming without mutation is ZEB1, the main regulator of the epithelial-mesenchymal transition (EMT). In order to maintain the EMT regulatory state, ZEB1 induces SETD1B, a histone methyltransferase that consequently maintains the expression of ZEB1 in a positive feedback loop (Lindner *et al*., 2020). Similar to this, the chromatin landscape changes due to the transcription factor SNAIL1 upregulation that causes EMT build-up (Wang *et al*., 2013). It is clear that the maintenance of the altered phenotypic state requires the chromatin modifiers that caused the changes.

1.6.14. Polymorphic microbiomes

There is growing evidence from research indicating the microbiomes, ecosystems made by local bacteria and fungi, have a significant impact on health and disease. As different tissues and organs have linked microbiomes with unique features in terms of population dynamics and range of microbial species, the gut microbiome has been at the center of this novel field of study. There is mounting proof that polymorphism variation in a population's microbiome among individuals might affect the cancer phenotype (Dzutsev *et al*., 2017, Helmink *et al*., 2019). Cancer may be caused directly by microorganisms, primarily bacteria, but not exclusively. They may also play a significant role in determining the effectiveness of anticancer therapy because they influence host immunological responses that support malignancy. The modification of the microbiome offers hope for influencing the outcome of cancer. One particular bacterial species that promotes cancer is butyrate-producing bacteria. The studies have shown that butyrate-producing bacteria in cancers of the colon patients and animal models resulted in the development of more tumours (Okumura *et al*., 2021). The synthesis of butyrate has multifaceted physiological impacts which include the generation of senescent epithelium and fibroblastic cells.

1.7. Development of cancer

Carcinogenesis, or oncogenesis, is the intricate progression through which healthy cells metamorphose into malignant or cancerous cells. Despite extensive research spanning

decades, our comprehension of cancer's development remains incomplete. It is widely accepted that cancer doesn't typically originate from a single isolated event, but rather emerges as a result of a series of intricate processes that lead ordinary cells down the path toward malignancy. The majority of healthy cells adhere to an intrinsic schedule, known as the cell cycle, wherein they undergo distinct life stages. This cycle initiates when a solitary cell divides into two offspring cells. The advancement of the cell cycle is meticulously governed by signals originating both externally and internally to the cells (Chow, 2010). Disrupting or modifying these signals has the potential to induce alterations within the cells. One of the prevailing explanations for cancer development is the widely accepted three-stage theory of carcinogenesis. This theory categorizes the process of cancer evolution into three distinct phases: initiation, promotion, and progression. Primarily employed for educational purposes, this theory is constrained by the absence of definitive biological markers that distinctly delineate each of these stages.

1.7.1. Initiation

Initiation, the inaugural stage, marks the point at which the initial cell mutation takes place. This mutation may encompass one or multiple cellular alterations, which can arise spontaneously or be triggered by exposure to carcinogenic agents. These alterations bestow upon the affected cell and its progeny the potential to evolve into cancerous cells. An interference with the cell's growth cycle can result from the activation of oncogenes, specific segments of DNA that oversee regular cell growth and repair processes (Cooper and Adams, 2023). On the flip side, inactivation refers to the process in which cellular genes, known as tumour suppressor genes, disrupt the regular cell cycle. These genes, integral components of DNA, play a pivotal role in halting, restraining, or suppressing cell division. Mutations in both oncogenes and tumour suppressor genes grant cells the ability to proliferate beyond the body's typical requirements. The progeny of these altered cells often gain a competitive edge over the original cells, showcasing unbridled growth and a reduction in apoptosis, which is the controlled death of cells regulated by apoptotic genes, another critical component of DNA. Mutations in apoptotic genes enable cancer cells to evade programmed cell death (Fan and Guo, 2001).

1.7.2. Promotion

The second stage, known as promotion, comes into play when the altered cells (or those that have undergone initiation) are induced to multiply. The conditions both within the

cell (intracellular) and in its external surroundings (extracellular) play a crucial role in shaping the course of cancer development. The process of malignant transformation may encompass multiple steps and necessitate recurrent encounters with promoting factors. As an illustration, estrogen, a naturally occurring hormone, serves as one such tumour promoter. On its own, estrogen doesn't have the capability to initiate cancer, but it can stimulate the proliferation of mutated breast cells (Russo and Russo, 2006).

1.7.3. Progression

Progression represents the third and final phase in the three-stage theory of cancer development. In this stage, tumour cells engage in a fierce struggle for survival, intensifying the process of accumulating additional mutations that enhance their aggressiveness. As the tumour expands in size, the cells undergo further genetic changes, resulting in heightened diversity within the tumour. This diversity, referred to as heterogeneity, encompasses various genetic variations among the mutated or transformed cells. The increased heterogeneity leads to a scenario in which the cancer cells within a single lump or mass can exhibit distinct appearances and behaviours, thereby complicating both diagnosis and treatment efforts (Marusyk and Polyak, 2010).

1.8. Cancer metastasis

Cancer cells exhibit a striking departure from the characteristics of normal cells, and one of the most significant distinctions is the loss of adhesiveness. In the world of normal cells, the surface of each cell is adorned with molecules that serve as a kind of molecular glue, allowing them to tightly bind to other cells bearing similar molecules. This adhesive property ensures that normal cells literally stick together and remain in their designated positions within the body, contributing to the harmony of bodily functions. However, cancer cells undergo a transformative process that leads to the depletion of these adhesive molecules. Consequently, they shed their ability to cling to neighbouring cells. This drastic loss of adhesiveness is pivotal in enabling cancer cells to break free from their cellular neighbours, embarking on a journey that can have profound consequences. They become remarkably mobile, capable of invading nearby tissues, a phenomenon known as metastasis (Seyfried and Huysentruyt, 2013). The main process by which cancer spreads to other organs and distant locales inside the body is this invasion into the surrounding tissues. Furthermore, these rogue cancer cells can exhibit another alarming talent. They may infiltrate the circulatory system, slipping into the bloodstream and lymphatic vessels.

Once on board, they embark on a journey throughout the body, potentially reaching far-flung destinations. This method of dissemination through the bloodstream and lymphatic system is a key contributor to the spread of cancer to distant sites, a process that significantly complicates the diagnosis and treatment of the disease.

Three basic steps can be used to categorize the metastatic cascade: invasion, intravasation and extravasation. Malignant tumour cells first lose their ability to adhere to other tumour cells, which allows them to separate from the main tumour mass. Concurrently, these cells are enabled by changes in the contacts between the cell and the matrix to invade the surrounding stromal tissues. Substances that weaken the extracellular matrix and basement membrane are secreted throughout this complex process. Additionally, it entails the modulation of proteins associated with the control of cellular motility and migration (Martin *et al*., 2013). In the quest for survival and growth, the tumour must also kick-start angiogenesis, a pivotal process without which tumour development would be hindered. Tumours up to 2 mm in diameter can rely on local diffusion for the exchange of nutrients and waste removal (Brooks, 1996). However, once angiogenesis is initiated, blood vessels within the tumour's vicinity provide a conduit for detached cells to enter the circulatory system, facilitating their metastasis to distant sites-a phenomenon referred to as intravasation (Folkman, 1992). The interaction between the tumour cell and its surrounding stroma plays a pivotal role in tumour angiogenesis (Ono *et al*., 1999). The tumour cell interacts with endothelial cells biochemically when it gets to a possible intravasation site. This interaction is mediated by carbohydrate-locking reactions, which are both weak and rapid. As a result, stronger bonds are formed between the tumour cell and endothelial cells, allowing the tumour cell to infiltrate the basement membrane and endothelium, signifying the extravasation process. Once established at this secondary site, the newly arrived tumour can commence proliferation, marking the beginning of a metastatic focus.

1.9. Breast cancer

Cancers of the breast are among the most common forms of cancer in women. It primarily affects women but can occur in men as well. According to the reports from the World Health Organization (WHO), female breast cancer takes the lead as the most frequently diagnosed cancer on a global scale, with approximately 2.3 million new cases documented in 2020 (Sung *et al*., 2021). These statistics encompass both incidence and

mortality rates. Breast cancer is characterized as a heterogeneous disease due to its remarkable diversity in terms of morphological features, clinical outcomes, and responses to different therapeutic approaches. This heterogeneity is evident in the wide spectrum of breast cancer subtypes, each displaying unique characteristics and behaviours (Russnes *et al*., 2017). These variations not only encompass the appearance of cancer cells under a microscope but also extend to the genetic and molecular profiles of the tumours. Furthermore, the clinical course of breast cancer can vary significantly from one individual to another, with some cases being more aggressive and others more indolent. The diversity in therapeutic responses is another facet of this heterogeneity, as treatments that prove effective for one subtype or stage of breast cancer may have limited impact on another. This intricate interplay of factors underscores the complexity of breast cancer and necessitates personalized and tailored treatment strategies for each patient.

1.9.1. Risk factors of breast cancer

The majority of breast cancers are classified as sporadic, signifying that they emerge due to random genetic alterations that occur after an individual's birth (Yang *et al*., 2010). Sporadic breast cancer carries no risk of transmitting the mutated gene to one's offspring. The origins of sporadic breast cancer are multifaceted, resulting from a combination of factors including internal hormonal influences, lifestyle choices, environmental exposures, and routine physiological processes, such as DNA replication. Less prevalent than sporadic cases, inherited breast cancers account for roughly 10% of all breast cancers (Lynch *et al*., 2008). Inherited breast cancer arises when genetic alterations, known as mutations or changes, are transmitted from one generation to the next within a family. Many of these mutations affect tumour suppressor genes, including well-known ones like BRCA1, BRCA2, and PALB2. These genes typically play a role in preventing abnormal cell growth and the development of cancer. However, when a mutation occurs within these genes, it can disrupt this control and lead to uncontrolled cell growth.

Several factors can increase an individual's susceptibility to breast cancer:

- Age: Breast cancer risk escalates with age, with the majority of cases emerging after reaching 50 years of age. The median age for breast cancer diagnosis typically hovers around 63.
- Previous breast cancer diagnosis: People who have had breast cancer in one breast are more likely to get cancer in the other breast in the future.

- Family breast cancer history: A family's history can influence the risk of breast cancer. This risk is increased if one or more women receive a breast cancer diagnosis at age 45 or under, or if several women in the family receive a breast cancer diagnosis prior to age 50. This risk is further increased if there is a family history of related cancers such as ovarian, metastatic prostate, or pancreatic cancer. Additionally, a significant family history could include multiple generations of breast and/or ovarian cancer on one side of the family, for example, having a grandmother and an aunt on the father's side who were both diagnosed with these malignancies. If a woman in the family has been diagnosed with both breast and ovarian cancer, or has had a second breast cancer in either breast, the risk increases even more. The presence of male breast cancer in the family is also a notable factor. It's essential to discuss these situations with a doctor, as they could indicate the presence of an inherited breast cancer genetic mutation, such as BRCA1, BRCA2, or PALB2 (Shuen and Foulkes, 2011). When evaluating family history, considering the father's side is equally important in assessing personal risk for breast cancer.

- Genetic predisposition or inherited risk: An elevated risk of breast cancer and other kinds of cancer is linked to several inherited genetic abnormalities. BRCA1 and BRCA2 are the most well-known genes associated with the risk of breast cancer. Mutations in these genes significantly increase the chances of developing breast and ovarian cancers, along with several other cancer types. Furthermore, a mutation in any one of them can increase a person's risk of developing prostate, breast and various other cancers. While BRCA1 and BRCA2 mutations are the most common, other gene mutations and hereditary conditions can also contribute to an individual's breast cancer risk. These mutations are less frequent and generally do not raise the risk of breast cancer to the same extent. Some of these genes and syndromes include Cowden syndrome (CS) associated with the PTEN gene (Lynch *et al*., 1997), Peutz-Jeghers syndrome (PJS) linked to the STK11 gene (Nakanishi *et al*., 2005), Li-Fraumeni syndrome (LFS) connected to the TP53 gene (Masciari *et al*., 2012), Lynch syndrome related to the MLH1, MSH2, MSH6, and PMS2 genes (Roberts *et al*., 2018), hereditary diffuse gastric cancer linked with the CDH1 gene (Pharoah *et al*., 2001), Ataxia telangiectasia associated with the ATM gene (Hall, 2005) and other genes like PALB2 and

CHEK2 (Weitzel *et al*., 2019). There are additional genes that might contribute to an elevated risk of breast cancer, although further research is required to fully comprehend how these genes influence an individual's risk. It's important to note that inheriting a gene mutation doesn't necessarily guarantee the development of breast cancer. Some individuals may carry gene mutations but never develop the disease. Ongoing research is actively seeking to identify and understand other genes that could impact breast cancer risk.

- Previous ovarian cancer diagnosis: Mutations in the BRCA1 and BRCA2 genes substantially heighten the chances of both breast and ovarian cancer. As a result, a person who has a genetic mutation in the BRCA gene that causes ovarian cancer is also more likely to develop breast cancer. Additionally, mutations in additional genes, like PALB2, RAD51C, and RAD51D, are associated with an elevated risk of both breast and ovarian cancer (Angeli *et al*., 2020). However, ovarian cancer does not usually affect women with breast cancer who do not have a mutation in such genes more frequently.

- Premature menstruation and delayed menopause: Women who started menstruating before the age of eleven or twelve or who went through menopause after the age of 55 are more likely to get breast cancer. This heightened risk is attributed to prolonged exposure of breast cells to estrogen and progesterone, which are hormones influencing secondary sex characteristics like pregnancy and breast development (Trabert *et al*., 2020). During menopause, estrogen and progesterone production decrease significantly, particularly as an individual ages. The extended exposure to these hormones contributes to an increased risk of breast cancer.

- Preparing for conception: Delaying the first pregnancy until after the age of 35 or never experiencing a full-term pregnancy increases the risk of developing breast cancer (Kobayashi *et al*., 2012). Pregnancy may offer a protective effect against breast cancer by promoting the maturation of breast cells.

- Postmenopausal hormone replacement therapy: The use of combined hormone therapy involving both estrogen and progestin following menopause, commonly known as hormone replacement therapy, either within the last five years or for an extended duration, raises the risk of breast cancer (Holmberg *et al*., 2008). Notably, the incidence of new breast cancer cases has significantly decreased due

to reduced postmenopausal hormone therapy usage. However, women who only took estrogen for up to five years typically due to a prior hysterectomy and who have never taken progestin, seem to face a slightly lower breast cancer risk.

- Birth control or contraceptive pills: Several studies indicate that oral contraceptives used for pregnancy prevention may marginally raise the likelihood of breast cancer (Marchbanks *et al*., 2002), whereas others have found no association between oral contraceptive use and the onset of breast cancer (Ursin *et al*., 1998). Ongoing research continues to explore this subject.

- Racial and ethnic background: Irrespective of racial background, breast cancer is the most prevalent malignancy among women, excluding skin cancer. White women exhibit a higher likelihood of developing breast cancer compared to Black women (Chlebowski *et al*., 2005). However, when considering women under the age of 45, breast cancer is more prevalent among Black women than their White counterparts. Additionally, Black women face a greater risk of mortality due to this disease (Palmer *et al*., 2003). Disparities in survival rates may be attributed to variations in biological factors, socioeconomic situations and other underlying health issues that influence obtaining medical attention. Women descended from Jews in Eastern Europe or Ashkenazi, face an elevated risk of breast cancer due to a higher likelihood of inheriting a mutation in BRCA1 gene. Conversely, breast cancer is less frequently diagnosed in American Indian or Alaska native women, Hispanic, Asian or Pacific Islander women. Compared to White women, Hispanic and Black women are more likely to be diagnosed with larger malignancies and later stage cancers. Nevertheless, compared to their White counterparts, Hispanic women often exhibit higher survival rates. Breast cancer incidence has been increasing among second-generation Hispanic women and Asian or Pacific Islander women (Solanki *et al*., 2016). And while the exact causes are not yet fully understood, changes in dietary and lifestyle patterns are probably related to it.

- Breast hyperplasia with atypical characteristics: Receiving a diagnosis of atypical hyperplasia of the breast increases the probability of getting breast cancer later on. This condition is defined by the presence of irregular, though non-cancerous, cells observed in a breast biopsy (Tomlinson-Hansen *et al*., 2023). These abnormal cells can serve as precursors to malignant changes within the breast tissue, underscoring the need for vigilant monitoring and potential preventive

measures to mitigate the increased risk of breast cancer in the future. Regular screenings and consultations with healthcare professionals are often recommended to closely monitor and manage this elevated risk.

- Lobular carcinoma *in situ* (LCIS): This condition relates to the existence of irregular cells located within the lobules or breast glands and it's critical to remember that these cells are not categorized as cancerous. Nevertheless, when LCIS is detected in one breast, it heightens the likelihood of developing invasive type of breast cancer on either breast. If a biopsy identifies LCIS, more testing could be conducted to explore the associated alterations or changes.

- Density of breast: Dense breast tissue indicates the presence of a higher concentration of milk glands, milk ducts, and supportive tissue within the breast, as opposed to predominantly fatty tissue. It's important to note that breast density is a characteristic used to describe mammographic images and does not relate to the tactile feel of the breast. Typically, breast density tends to decrease as individuals age. Having dense breast tissue elevates the risk of developing breast cancer (Boyd *et al*., 1998). Moreover, it can pose challenges in detecting tumours through conventional imaging methods like mammography. In certain states, there is a requirement to include information about breast density in mammogram reports for individuals with thick breast tissue. Nevertheless, there aren't any screening recommendations specifically tailored to individuals with thick breast tissue at the moment.

- Lifestyle aspects: As with other cancer types, ongoing research indicates that various lifestyle conditions can contribute to breast cancer development. Recent studies have highlighted that being overweight or obese and postmenopausal status is associated with an increased risk of breast cancer (Gravena *et al*., 2018). Furthermore, lower levels of physical activity are linked to a higher likelihood of both developing breast cancer and experiencing its recurrence after treatment (Bernstein *et al*., 1994). According to recent studies, drinking more than one or two glasses of alcohol every day encompassing spirits, wine and beer, heightens the risk of breast cancer. In general, recommendations advise limiting alcohol intake to 3 to 4 servings per week (Hendriks, 2020). However, there is currently no conclusive evidence supporting claims that specific dietary choices, either consumption or avoidance of particular foods, substantially increase the risk of

developing breast cancer or the risk of its recurrence post-treatment. Nonetheless, it's important to highlight that embracing a diet abundant in fruits and vegetables while minimizing the intake of animal fats offers various health advantages, and this dietary approach is linked to a modest decrease in the risk of breast cancer (Williams and Hord, 2005).

- Economic and social influences: Women of higher socioeconomic status within all racial and ethnic categories face an elevated risk of breast cancer when compared to their counterparts of lower socioeconomic status within the same groups. These disparities could be attributed to differences in dietary choices, pregnancy-related factors such as the frequency of pregnancies and the age of the initial pregnancy, as well as other variables that increase the risk. Conversely, women living in poverty are at a greater likelihood of receiving a breast cancer diagnosis at an advanced stage, and their chances of survival are diminished in comparison to more financially well-off women (Lobb *et al*., 2010). This discrepancy is likely influenced by a multitude of factors, encompassing lifestyle choices, underlying health conditions like obesity and the biological characteristics of tumours. Additionally, the accessibility of healthcare and the availability of treatment options also contribute to these disparities.

- Exposure to radiation during early life: Being exposed to ionizing radiation during childhood can potentially raise the likelihood of developing breast cancer in women. For instance, therapeutic radiation directed at the chest area as a treatment for Hodgkin lymphoma may elevate the risk of breast cancer in both breasts (Candela, 2016). In contrast, there is no evidence suggesting that the minimal amount of radiation received through mammography is associated with a higher risk of breast cancer.

1.9.2. Breast cancer types

Breast cancer exists in two primary forms: non-invasive and invasive. Non-invasive breast cancer is limited to the breast's lobules or milk ducts, whereas invasive breast cancer spreads to nearby tissues and, in some cases, to organs that are distant. Twenty percent of cases of breast cancer are non-invasive, while the remaining eighty percent are invasive.

- Invasive breast cancer: As its name implies, is characterized by its ability to spread from the initial site of origin, which is usually within the milk ducts or lobules of the breast (Sarkar and Mandal, 2011). This aggressive form of breast cancer can infiltrate neighbouring tissues, including the surrounding breast tissue, lymph nodes, and even distant organs through the bloodstream. As a result, it poses a heightened risk to the patient.

- Non-invasive breast cancer: It is often referred to as *in situ* breast cancer, is a state in which cancer cells are restricted to the milk ducts or lobules and have not extended into adjacent tissues or disseminated to other regions of the body (Sharma *et al.*, 2010). While it falls within the category of cancer, non-invasive breast cancer is characterized by its lower aggressiveness and an exceptionally high survival rate.

Breast cancer is a diverse disease encompassing various subtypes, which are distinguished by their microscopic characteristics and molecular features. Among the numerous subtypes of breast cancer, each is characterized by unique traits. These subtypes include:

- Ductal carcinoma *in situ* (DCIS): The cancer cells are limited to the milk ducts and have not infiltrated into the surrounding tissues or other parts of the body, making this type of breast cancer non-invasive (Muggerud *et al.*, 2010). It is often referred to as stage 0 breast cancer and is highly treatable with a very high survival rate.

- Lobular carcinoma *in situ* (LCIS): This is another subtype of breast cancer that is non-invasive. Similar to DCIS, it is confined to the breast lobules and will not invade neighboring tissues. LCIS is usually regarded as a marker for a higher chance of acquiring invasive breast cancer in later years rather than as a real malignancy (Śrutek *et al.*, 2017).

- Invasive ductal carcinoma (IDC): It is the most common form of breast cancer that is invasive. It starts in the breast's milk ducts and has the potential to spread beyond its initial site, invading nearby breast tissues and, in some cases, distant organs through the bloodstream. IDC is the most aggressive breast cancer form and poses a higher risk to the patient compared to non-invasive subtypes (Feng *et al.*, 2018).

- Invasive lobular carcinoma (ILC): It is a less frequent kind of breast cancer that is invasive. It originates in the breast lobules and, similar to IDC, has the potential to spread beyond its initial location, affecting surrounding breast tissues and possibly distant organs. ILC tends to have a distinct pattern of growth and may be harder to detect through imaging techniques (Mathew *et al*., 2017).

- HER2-positive breast cancer: It is characterized by the overexpression of a protein called HER2. About 20 percent of incidences of breast cancer are related to this subtype. HER2-positive breast cancer tends to be more aggressive, but targeted therapies have significantly improved treatment outcomes by specifically targeting the HER2 protein, inhibiting its activity and slowing the growth of cancer cells (Wang and Xu, 2019).

- Inflammatory breast cancer (IBC): It is an uncommon and severe form of breast cancer. It usually does not present as a distinct lump or tumour but rather as a rapidly developing, swollen, and reddened breast. The hallmark of IBC is the presence of cancer cells obstructing the lymphatic capillaries in the breast skin, leading to inflammation. This type of breast cancer is often at an advanced stage at the time of diagnosis (Menta *et al*., 2018).

- Metastatic breast cancer: It is also referred to as advanced or stage IV breast cancer which take place when cancer cells from the breast migrate to other areas of the body, such as bones, lungs, liver, and brain. This is the most advanced stage of breast cancer and is generally not considered curable (Bafford *et al*., 2009). However, it can often be managed with various treatments to control the cancer's growth, alleviate symptoms, and extend the patient's life.

- Triple-positive breast cancer: It is a subtype of breast cancer characterized by the presence of three specific receptors on the surface of cancer cells: estrogen receptor (ER), progesterone receptor (PR) and human epidermal growth factor receptor 2 (HER2) (Zeng *et al*., 2021). Triple-positive breast cancer tends to be more aggressive than other subtypes but is also more responsive to targeted therapies.

- Triple-negative breast cancer (TNBC): This subtype of breast cancer is identified by the absence of three particular receptors on the cancer cells surface such as the human epidermal growth factor receptor 2 (HER2), the progesterone receptor (PR), and the estrogen receptor (ER). As a result, hormone therapies, which target

these receptors, are not effective in treating TNBC. Also the other prominent target, the HER2 protein, is not overexpressed in TNBC. Triple-negative breast cancer is known for its aggressiveness and the limited range of targeted therapies available (Bosch *et al*., 2010). Radiation therapy, chemotherapy, and surgery are common TNBC treatment choices. Since therapies target the receptors are not effective, TNBC is often treated with more aggressive chemotherapy regimens. Research is ongoing to identify new treatment strategies, and clinical trials are exploring novel therapies and combinations to improve outcomes for individuals with TNBC. Due to its aggressive nature, early diagnosis and personalized treatment plans are crucial in managing triple-negative breast cancer.

1.9.3. Molecular classification of breast cancer

Breast cancer is categorized using molecular classification methods, based on molecular and genetic features. This classification assists oncologists in customizing treatment approaches and predicting patient outcomes. Breast cancer has various molecular subtypes, each characterized by unique genetic and biological traits (Holliday and Speirs, 2011). The primary molecular classifications of breast cancer are as follows:

- Luminal A: This type of breast cancer is identified by hormone receptor presence (ER+ and/or PR+), low Ki-67 levels (indicating low cell proliferation), and a lack of HER2 overexpression. This subtype typically exhibits slow growth and is associated with a positive prognosis. Hormone therapy is a common treatment approach for Luminal A breast cancer (Higgins and Stearns, 2009).

- Luminal B: This particular kind of breast cancer, is also hormone receptor-positive (ER+ and/or PR+) and usually exhibits higher Ki-67 levels and may show HER2 overexpression. This subtype is more aggressive than Luminal A and often necessitates additional treatments, including chemotherapy and targeted therapies (Lafcı *et al*., 2023).

- HER2-enriched: This subtype is marked by the overexpression of the HER2 protein, leading to rapid and aggressive growth. Treatment for this subtype typically involves HER2-targeted therapies, chemotherapy, and occasionally hormone therapy (Figueroa-Magalhães *et al*., 2014).

- Basal-like: Basal-like breast cancer is commonly characterized as triple-negative (ER-, PR-, and HER2-). It exhibits molecular similarities to the basal cells in the

breast and is frequently linked to a less favourable prognosis (Rakha and Ellis, 2009). Treatment approaches for this subtype often encompass chemotherapy and surgical interventions.

- Normal-like: This type exhibits similarities with normal breast tissue and is typically linked to a more positive prognosis. This subtype is characterized as hormone receptor-positive and HER2-negative (Yersal and Barutca, 2014).

- Claudin-low: This subtype of triple-negative breast cancer, is identified by low expression of tight junction proteins known as claudins. It is frequently correlated with a less favourable prognosis (Dias *et al*., 2017).

These molecular classifications play a crucial role in shaping treatment strategies, offering the potential for more personalized and efficient therapies for individuals with breast cancer. Typically, oncologists consider a blend of clinical, histological, and molecular data to categorize and manage breast cancer. The precise classification can influence decisions regarding surgical procedures, chemotherapy, radiation therapy, hormone therapy, targeted therapy, or immunotherapy.

1.9.4. Breast cancer risk-reducing drugs

Drugs that may help prevent breast cancer are taken into account if there is a higher than normal risk of breast cancer development and this approach as known as chemoprevention. This is the method of reducing the chance of breast cancer by using hormone-blocking drugs.

- Tamoxifen: It's a selective estrogen receptor modulator or SERM, which is commonly utilized in breast cancer therapy. It functions by obstructing the impact of estrogen on tumour growth. Tamoxifen can be considered to lower the chance of ER-positive breast cancer in women above 35 years of age or higher. Studies indicate that it might also be useful in lowering the risk of breast cancer for people with precancerous diseases (LCIS or atypical breast hyperplasia) or non-invasive breast cancer (DCIS), with few adverse effects. It is not suggested for people who have experienced a stroke, blood clot, or extended immobility. It should be avoided when trying to conceive, breastfeeding or while pregnant. Hot flashes, vaginal discharge, sexual side effects, mood swings, increased risk of uterine cancer, blood clots, and other adverse effects are possible.

- Raloxifene: Another selective estrogen receptor modulator (SERM), raloxifene, is frequently utilized as postmenopausal osteoporosis (bone weakening) prevention therapy. For people who have a higher risk of breast cancer beyond the age of 35, it may also be taken into consideration as an alternative. Long-term usage of raloxifene is appropriate as it not only lowers the risk of breast cancer but also helps prevent bone loss. Premenopausal women and those with a history of blood clots, stroke, or extended immobilization shouldn't consume it. Possible negative impacts include vaginal dryness, blood clots, leg cramps, a gain of weight, hot flashes, stroke, edema in arms and legs, and uncomfortable sexual experiences. Compared to individuals using tamoxifen, raloxifene users are less likely to experience cataracts, uterine issues, and clots in the blood.

- Aromatase inhibitors: Medication known as aromatase inhibitors (AIs) reduces estrogen levels by preventing the body from producing it. In postmenopausal women who are at higher risk, three AIs are thought to be viable means of lowering their chance of developing breast cancer: letrozole (Femara), anastrozole (Arimidex), and exemestane (Aromasin). Clinical trials have proven their efficacy in reducing risk, even though the FDA has approved them for breast cancer treatment. Therefore aromatase inhibitors have the potential to replace tamoxifen. They are generally not advised for people with osteoporosis and are not meant for premenopausal women. Hot flashes, exhaustion, trouble sleeping, diarrhoea, pain in the joints and muscles, dry vagina, and bone loss are the side effects.

1.10. Existing approaches to cancer treatment

Cancer treatment approaches vary widely, with the choice of therapy determined by factors like stage and type of cancer as well as the patient's general condition. The primary methods of cancer treatment encompass:

1.10.1. Surgery

Surgical procedures are a fundamental component of cancer treatment, involving the physical removal of cancerous tumours and, in some cases, nearby lymph nodes or adjacent tissues. This treatment modality is most commonly employed when dealing with solid tumours that are confined to a specific location in the body. The objective of surgery in cancer treatment is to completely excise the tumour, thus eliminating the primary source of cancer cells. The process typically involves the following steps:

- Initial evaluation before surgery: Prior to the surgical procedure, comprehensive evaluations are carried out to ascertain the tumour's dimensions, position, and stage. This critical information is instrumental in shaping the surgical approach and gaining insights into the cancer's scope.

- Surgical removal: In the course of the surgical procedure, the surgeon creates an opening to reach the tumour. The tumour, along with a surrounding area of healthy tissue, is subsequently excised. In certain instances, nearby lymph nodes may also be removed to assess the possible presence of cancer cell spread.

- Less invasive methods: Over recent years, less invasive surgical approaches, like laparoscopy or robotic-assisted surgery, have gained widespread popularity. These techniques involve smaller incisions, leading to shorter recovery periods and decreased post-operative discomfort.

- Pathological analysis: The excised tissue is dispatched to a pathology laboratory for a comprehensive analysis. This process enables pathologists to verify the complete removal of cancerous cells and assess the cancer's stage.

- Reconstructive procedures: When tissue or organs are excised, the surgical team may carry out reconstructive techniques to recover functionality and appearance.

- Complementary or preparatory therapy: Surgery can be complemented with additional treatments, including chemotherapy or radiation therapy, administered either before (neoadjuvant) or after (adjuvant) the surgical intervention. These supplementary therapies assist in eliminating residual cancer cells, reducing tumour size before surgery, or preventing cancer recurrence following the procedure.

The suitability of surgical treatment is contingent on multiple factors, encompassing the tumour's type, stage, location, and the patient's general health. In certain scenarios, surgery may stand alone as the primary treatment approach, whereas in others, it is integrated with complementary therapies to ensure comprehensive cancer care. It is noteworthy that the continual advancement of surgical techniques and technologies has notably enhanced the precision and results of cancer surgeries. This progress facilitates the more effective preservation of healthy tissue and fosters improved patient recovery.

1.10.2. Radiation therapy

Radiation therapy, often referred to as radiotherapy, is a medical procedure designed to

utilize high-energy X-rays or alternative forms of radiation with the specific purpose of targeting and eradicating malignant cells. The central objective of radiation treatment is to inflict damage to cancer cells' DNA, effectively impeding their ability to proliferate and divide. The choice of how radiation therapy is administered depends on the cancer's type, its location, and its stage, and it primarily falls into two categories:

- External radiation therapy: In this method, a radiation machine located outside the patient's body delivers highly precise radiation doses directly to the tumour. Patients typically undergo a series of treatment sessions spanning several weeks, during which the radiation beams are meticulously directed at the specific cancerous region. To ensure accuracy, radiation oncologists employ advanced imaging techniques, including CT scans, to pinpoint the exact location and shape of the tumour. This approach effectively minimizes radiation exposure to nearby healthy tissues while precisely targeting the cancer cells.

- Brachytherapy or internal radiation therapy: This treatment involves placing a radioactive source either inside the tumor or in close proximity to it. This approach is frequently employed for cancers affecting areas like the cervix, prostate and select other locations. Brachytherapy facilitates the precise delivery of a concentrated radiation dose to the tumour, effectively minimizing exposure to adjacent healthy tissues. The radioactive sources used can be either temporary or permanent, depending on the specific treatment strategy.

Radiation therapy is frequently selected as the primary treatment modality for various cancer types, or it is integrated into a comprehensive, multi-faceted approach that may involve surgical procedures, chemotherapy, or immunotherapy. The treatment decision hinges on factors such as the kind and stage of cancer, the overall health of the patient and the intended treatment objectives. Radiation therapy can be applied with the aim of achieving a curative outcome, completely eradicating the cancer, or it can serve to reduce tumour size before surgery (neoadjuvant therapy). Additionally, it can be employed in advanced or metastatic cases to enhance the life quality of patients and reduce symptoms, a practice known as palliative care. Technological advancements, including techniques like intensity-modulated radiation therapy (IMRT) and stereotactic radiosurgery, have significantly enhanced the precision of radiation therapy (Gürsel, 2018). These innovations enable a more focused and effective treatment approach while

simultaneously reducing the occurrence of side effects. This progress has elevated the role of radiation therapy as an increasingly vital component in the overall management of cancer.

1.10.3. Chemotherapy

Chemotherapy is a systemic treatment that employs powerful medications, often called cytotoxic drugs, to either eliminate or hinder the growth and division of cancer cells within the body. Unlike localized treatments such as surgery or radiation therapy, which target a specific tumour or region, chemotherapy is designed to travel throughout the circulation and target cancer cells located in different body areas. Chemotherapy drugs can be administered through different methods. Some chemotherapy drugs are available in pill or liquid form and can be taken by the patient at home. Many chemotherapy drugs are given as intravenous (IV) infusion, usually in an outpatient clinic or hospital setting. IV chemotherapy allows for precise dosing and monitoring. In some cases, chemotherapy may be given as an intramuscular injection. Often, multiple chemotherapy drugs are used in combination. This approach can be more effective in targeting cancer cells from different angles and minimizing the development of drug resistance. Chemotherapy can be employed in conjunction with different cancer treatments like immunotherapy, radiation therapy, and surgery to achieve the best treatment outcome. The choice of combination therapy depends on the specific cancer and its characteristics. Chemotherapy can be performed as a neoadjuvant prior to surgery in order to reduce tumour size and improve surgical manageability. In order to eliminate any cancer cells that may still be present and lower the chance of recurrence, it can also be used as an adjuvant following surgery. Chemotherapy is usually given in cycles, with a rest interval in between each cycle to let the body to heal from any side effects. The exact form of cancer and each patient's reaction determine the treatment plan and number of cycles.

Commonly used chemotherapy drugs constitute a crucial arsenal in the fight against cancer. They encompass a diverse range of medications, each carefully selected to combat different types and stages of cancer. Platinum-based drugs, including cisplatin and carboplatin, are renowned for their ability to disrupt DNA replication in cancer cells, hindering their growth (Dasari and Tchounwou, 2014). Antimetabolites like methotrexate and 5-fluorouracil imitate essential cellular components, deceiving cancer cells and interfering with their replication process (Cao *et al*., 2022). Anthracyclines such as

doxorubicin are potent drugs that target DNA and block the enzymes necessary for cell division (Binaschi *et al*., 2001). Taxanes like paclitaxel stabilize microtubules in the cell, preventing cell division and leading to cancer cell death (Wang *et al*., 2000). Alkylating agents, such as cyclophosphamide, attach alkyl groups to DNA strands, impeding their ability to replicate (Ralhan and Kaur, 2007). These drugs collectively aim to disrupt the uncontrolled growth and division of cancer cells. Antitumour antibiotics, such as bleomycin, mitomycin, and etoposide, work by altering the genetic material within cancer cells, thus impeding their ability to grow and proliferate (Nobili *et al*., 2009). Topoisomerase inhibitors like doxorubicin, and etoposide and irinotecan, find frequent application in the management of colorectal, haematological, ovarian and lung cancers (Martin, 2016).

The ongoing development of chemotherapy drugs and personalized treatment regimens reflects the ever-evolving field of oncology, with the goal of enhancing cancer patients' treatment results and minimizing negative effects. Advancements in cancer research continue to lead to the development of new chemotherapy drugs and treatment strategies, improving the effectiveness and reducing the side effects of these therapies.

1.10.4. Immunotherapy

Immunotherapy represents a cutting-edge approach to cancer treatment, with the primary goal of harnessing the body's immune system to identify and fight cancer cells. This innovative strategy employs various methods to activate, strengthen, and direct the immune response against cancer. Three key components of immunotherapy are checkpoint inhibitors, monoclonal antibodies, and cancer vaccines, each with its unique mechanism:

- Checkpoint Inhibitors: These drugs target immune checkpoint proteins that function as immune system brakes, like CTLA-4 and PD-1. By blocking these checkpoints, checkpoint inhibitors like pembrolizumab (Keytruda) and nivolumab (Opdivo) unleash the immune response, enabling T cells to identify and attack cancer cells (Shiravand *et al*., 2022). Checkpoint inhibitors have been particularly effective in the treatment of melanoma, lung cancer, and certain other malignancies.

- Monoclonal Antibodies: Proteins created specifically to bind to certain antigens on the surface of cancer cells are known as monoclonal antibodies. By attaching

to these antigens, monoclonal antibodies can trigger a variety of immune responses, including the recruitment of immune cells to attack the cancer. Trastuzumab (Herceptin) is a well-known monoclonal antibody used to treat HER2-positive breast cancer (Dean-Colomb and Esteva, 2008). Rituximab (Rituxan) is another example effective against B-cell lymphomas.

- Cancer Vaccines: Cancer vaccines like the hepatitis B and HPV vaccines can aid in the prevention of cancer by targeting viruses known to cause certain types of cancer. Additionally, therapeutic cancer vaccines are under development. The goal of these vaccines is to increase the immune system's capacity to identify and combat cancer cells. Sipuleucel-T (Provenge) is a vaccine used to treat advanced prostate cancer, providing a personalized immunotherapy approach (Gardner *et al*., 2012).

Immunotherapy has shown remarkable success in various cancers and is transforming the landscape of cancer treatment. It offers the potential for long-lasting responses, reduced side effects compared to traditional treatments, and an expanding array of options to tailor therapy to an individual patient's unique profile. As ongoing research unveils new immunotherapeutic agents and further understanding of the immune response, immunotherapy continues to gain importance as a promising weapon in the fight against cancer.

1.10.5. Targeted therapy

Targeted therapies represent a pivotal advancement in cancer treatment, with a focus on precision and effectiveness. These drugs are designed to specifically target cancer cells based on their unique molecular characteristics, including genetic mutations, proteins, or other specific features that distinguish them from normal cells. Targeted therapies can address various molecular targets, including growth factor receptors, signaling pathways, or specific enzymes. For instance, tyrosine kinase inhibitors, like imatinib (Gleevec), target specific proteins that drive the growth of chronic myeloid leukemia (Walz and Sattler, 2006). Similarly, drugs such as trastuzumab (Herceptin) target the HER2 protein in breast cancer.

1.10.6. Hormone therapy

Hormone therapy, also known as endocrine therapy, is a specialized approach to cancer treatment primarily employed in cases where hormones, specifically estrogen and

progesterone in breast cancer or testosterone in prostate cancer, play a crucial role in fueling the growth of cancer cells. This therapy seeks to block or interfere with the hormonal signals that encourage the proliferation of cancer cells. Types of hormone therapy include selective estrogen receptor modulators (SERMs), like tamoxifen, act by blocking estrogen receptors in breast cancer cells, preventing estrogen from binding to them (Eisen *et al*., 2008). Aromatase inhibitors (e.g., letrozole and anastrozole) reduce the body's production of estrogen and are often used in postmenopausal women with hormone receptor-positive breast cancer (Behan *et al*., 2015). Gonadotropin-releasing hormone (GnRH) agonists lower testosterone levels in men with prostate cancer (Labrie *et al*., 1986). Anti-androgens, such as bicalutamide, block the effects of testosterone on prostate cancer cells (Chen *et al*., 2009).

1.10.7. Stem cell transplantation

Stem cell transplantation, often referred to as bone marrow or hematopoietic stem cell transplant, is a sophisticated medical procedure employed in the treatment of specific blood cancers and disorders. It involves transplanting normal stem cells into damaged or malignant bone marrow, which results in the regeneration of the blood and immune systems. It is typically utilized for conditions such as leukemia, lymphoma, multiple myeloma, and certain non-malignant blood disorders like sickle cell anemia, aplastic anemia, and thalassemia (Barriga *et al*., 2012). It serves as a potential curative treatment for these diseases, especially when other treatments have proven inadequate.

Among the transplant varieties are autologous transplants, in which the patient has their own stem cells extracted and preserved prior to receiving intense radiation or chemotherapy. These stored stem cells are subsequently reinfused into the patient to rebuild their blood and immune systems. Allogeneic transplantation involves obtaining stem cells from a matched donor typically a family member or distant donor whose immune system closely matches the recipient's. This is often referred to as a "stem cell or bone marrow transplant" and it has the potential to have a graft-versus-tumour effect, in which the immune cells of the donor target any cancer cells that may still be present. Even though stem cell transplantation is associated with challenges and potential side effects, it offers the promise of renewed hope and improved outcomes for patients facing these conditions. Ongoing research and advances in transplant techniques continue to enhance the safety and efficacy of this treatment.

1.10.8. Precision medicine

Precision medicine, often referred to as personalized medicine, represents a transformative approach to cancer treatment that focuses on tailoring therapies to match the distinct genetic or molecular features of each patient's cancer. This approach leverages advanced technologies and a deep understanding of the specific genetic mutations or alterations driving the cancer. To initiate precision medicine, the first step is to conduct comprehensive genetic and molecular profiling of the patient's cancer. This is typically achieved through techniques like DNA sequencing and gene expression analysis. These analyses provide detailed information about the specific genetic mutations, altered pathways, or molecular markers that are responsible for the cancer's growth and progression (Naithani *et al*., 2021). Once the genetic and molecular profile of the cancer is elucidated, treatment plans are then customized to target these specific features. This may involve the use of targeted therapies, which are drugs designed to precisely interfere with the identified genetic mutations or molecular pathways responsible for the cancer.

Targeted therapies used in precision medicine include small molecule inhibitors, monoclonal antibodies and immunotherapies. These therapies are designed to block specific cellular processes or proteins that fuel cancer growth. For instance, imatinib (Gleevec) is highly effective in treating chronic myeloid leukemia (CML) by targeting the BCR-ABL fusion gene, which is the hallmark of CML (Pray, 2008). Precision medicine embodies a patient-centric approach, recognizing the individuality of each patient's cancer. It places a strong emphasis on shared decision-making, involving patients in treatment choices, and considering their unique genetic and clinical characteristics.

1.10.9. Palliative care

Palliative care is a specialized medical approach that places a primary emphasis on enhancing the quality of life and providing relief from the symptoms and suffering experienced by patients who are dealing with advanced or incurable cancer. This form of care goes far beyond pain management and extends to addressing a wide range of physical, emotional, social, and spiritual needs. Palliative care is not mutually exclusive with curative treatments. It can be provided alongside other cancer therapies, improving the patient's overall experience and well-being. It plays a vital role in the care continuum,

ensuring that individuals with advanced or incurable cancer receive holistic and patient-centered support as they navigate the challenges of their illness.

1.10.10. Complementary and alternative therapies

In addition to conventional cancer treatments, some patients choose to explore alternative or complementary therapies, which may include practices like acupuncture, herbal remedies, dietary modifications, meditation, or yoga. These complementary approaches aim to enhance overall well-being and alleviate treatment-related side effects. However, it is paramount for patients to engage in open and informed discussions with their healthcare providers regarding the integration of these therapies into their treatment plans. The communication between patients and medical staff helps to promote a comprehensive and patient-focused strategy of care by ensuring that the chosen therapies are secure, appropriate, and in harmony with the primary cancer treatment.

The selection of a treatment modality, or the decision to employ a combination of treatments, is contingent upon a range of variables, such as the specific kind and stage of cancer, the patient's general health, and the desired treatment objectives, whether they are curative or palliative. Treatment plans are frequently developed through a multidisciplinary approach, engaging the expertise of a diverse team that may include oncologists, surgeons, radiologists, and other specialized professionals. This collaborative effort ensures that each patient receives the most comprehensive and individualized care available, considering their unique medical condition and treatment goals.

1.11. Natural products' role in cancer treatment and research

Plants are a fascinating source of compounds known as secondary metabolites, which they produce as part of their natural defense mechanisms. These secondary metabolites, often referred to as natural products, possess a wide range of pharmacological activities, some of which hold great promise in the field of cancer research and treatment. For instance, sulforaphane found in broccoli and resveratrol in grapes have been meticulously studied for their potential to reduce the risk of cancer development (González-Vallinas *et al*., 2013). These compounds exhibit anti-cancer effects by influencing various cellular processes. Many plant-based compounds also act as antioxidants, which play a crucial role in protecting cells from oxidative damage. This is particularly significant because oxidative damage plays a role in the emergence of cancer. These antioxidants help

mitigate the cellular stress that can lead to DNA mutations and, ultimately, cancer. Furthermore, plant-derived compounds are now the focus of intensive research as potential targeted therapies for specific types of cancer. Paclitaxel from the Pacific yew tree and vinblastine from the Madagascar periwinkle, for instance, have become indispensable components of chemotherapy regimens (Cragg and Pezzuto, 2016). Also numerous compounds, including combretastatin and noscapine, are currently undergoing various phases of clinical trials (Lakshmi, 2020). These compounds interfere with the cell division process, preventing the uncontrolled growth of cancer cells.

A compelling development in this field is the concept of adjuvant therapy, where various plant-based compounds are combined with conventional cancer treatments. This approach aims to enhance the effectiveness of standard treatments while reducing their associated side effects. Adjuvant therapy is an actively explored area of research and holds significant potential in improving patient outcomes (Lin *et al*., 2020). Looking back in history, the reliance on specific plants in traditional medicines to treat various ailments, including cancer, has provided a wealth of knowledge for modern researchers. Systems like Ayurveda, Traditional Chinese Medicine, and indigenous practices have offered a rich source of information to identify potential anticancer agents. Collaboration with and respect for indigenous communities and traditional healers is crucial to preserving and utilizing this invaluable wisdom. Researchers are continually delving into new plant species, isolating their bioactive compounds, and evaluating their potential in the realm of cancer treatment. Innovative research methods, such as high-throughput screening, have expanded the possibilities of identifying novel leads, providing exciting avenues for exploration. In summary, the world of plants remains a profound source of inspiration and innovation in cancer research and treatment. Their diverse array of compounds, coupled with their long history of use in traditional medicine, underscores the promising avenue for developing innovative strategies to combat cancer. Researchers continue to explore, harness, and integrate the potential of these natural resources in the ongoing battle against this devastating disease.

Saraca asoca and *Kingiodendron pinnatum* both of which are part of the traditional Ayurveda system was explored for its anticancer activities in our study. Plant specimens were gathered from the Wayanad district of Kerala, India, and their authenticity was confirmed by Dr. N. Sasidharan, a taxonomist at the Kerala Forest Research Institute (KFRI) in Peechi, Thrissur, Kerala. Voucher specimens, assigned the specimen number

KFRI 4849 for *Saraca asoca* and KFRI 4725 for *Kingiodendron pinnatum*, and were deposited in the Herbarium of KFRI.

1.12.1. *Saraca asoca* (Roxb.) De Wilde: The all-encompassing remedy in Ayurveda

Saraca asoca, commonly known as the Asoka tree or Asoka, is a prominent and culturally significant species of flowering tree native to the Indian subcontinent. It holds a revered place in traditional medicine and is also deemed sacred in diverse Indian cultures. Its name, "Asoka," carries the meaning of "sorrow-less" or "without grief," embodying its positive and comforting symbolism. The bark, seeds and flowers are among the parts of the tree that are employed for their curative properties. Asoka is believed to have uterine tonic and astringent qualities and is commonly used to address gynecological issues, particularly as a remedy for menstrual problems and to support women's reproductive health. The bark of the Asoka tree is renowned for its capacity to harmonize menstrual cycles and alleviate symptoms associated with conditions like menorrhagia (excessive menstrual bleeding), dysmenorrhea (painful menstruation), and various female reproductive disorders (Kamat *et al*., 2015). Furthermore, it is recognized for its potential to enhance the overall well-being of women, earning it the endearing nickname "women's friend." Compounds such apigenin, catechin, caffeic acid, β-sitosterol, kaempferol, quercetin, gallic acid, tannic acid, vanillin, and rutin have been reported to be present in the bark methanolic extract of *Saraca asoca* (Mittal *et al*., 2013a, Ghatak *et al*., 2015a).

1.12.1.1. Nomenclature

1.12.1.1.1. Taxonomic classification

Scientific name: *Saraca asoca* (Roxb.) De Wilde

Kingdom : Plantae

Divison : Magnoliophyta

Class : Magnoliopsida

Order : Fabales

Family : Fabaceae

Genus : *Saraca*

Species : *asoca*

1.12.1.1.2. Common names

Saraca asoca goes by several vernacular names, some of them are as follows:-

Ashoka tree: English

Ashokam, Hemapushpam: Malayalam

Ashoka : Sanskrit

Ashok, Sita Ashok: Hindi

Ashokam : Tamil

Figure 1.3. *Saraca asoca* (Roxb.) De Wilde *(Saraca asoca*, 2023)

1.12.1.2. General characteristics
1.12.1.2.1. Description

Saraca asoca, is known for its exceptional botanical characteristics. Its evergreen foliage maintains a lush appearance even in dry seasons. This tree can reach an impressive height of up to 20 meters and features a straight, slender trunk with smooth, greyish bark, lending it an elegant and visually appealing aspect. Its compound, pinnate leaves, arranged in a feather-like pattern, further enhance its distinctive look. What truly captivates admirers are the Asoka tree's vibrant and fragrant flowers, which come in shades ranging from

bright orange to red, forming dense clusters that create a visually striking display. The delightful fragrance of these blossoms not only pleases the eye but also tantalizes the senses.

1.12.1.2.2. Habitat

The Asoka tree, native to the Indian subcontinent, can be found in diverse regions spanning India, Nepal, and Sri Lanka. It thrives in a variety of habitats within these countries, primarily favouring tropical and subtropical regions. These trees are frequently sighted in deciduous forests and are adaptable to hilly and mountainous terrain. Moreover, Asoka trees are widely cultivated in urban and rural areas, adorning gardens, parks, and lining streets. Their presence is owed to their cultural significance, ornamental appeal, and medicinal attributes. Consequently, one can encounter Asoka trees in a wide array of environments, both natural and cultivated, across their native range.

1.12.1.3. Pharmacological properties

1.12.1.3.1. Traditional uses

Saraca asoca has a rich history of traditional usage across different cultures, with a particular emphasis in India. In traditional Ayurvedic and Unani medicine, the bark of the Asoka tree is highly regarded for its potential medicinal properties. It is thought to provide therapeutic advantages for a variety of health issues, such as skin diseases, digestive disorders, infections and irregular menstruation (Sumangala *et al*., 2017). Notably, Asoka is renowned for its pivotal role in enhancing women's well-being, with its reputed capacity to regulate menstrual cycles, alleviate menstrual discomfort, and bolster overall reproductive health.

Asoka is one of the traditional medicinal plants that have been recorded for thousands of years in Indian writings. Asoka is praised in the 1000 BC Charaka Samhita for its analgesic and astringent qualities as well as its effectiveness in healing skin diseases like leprosy (Biswas and Debnath, 1972). Its many uses are described in the 500 BC treatise Susruta, which covers everything from womb abnormalities to fever, neurological problems, snake bites, eye conditions, and wounds (Singh *et al*., 2015). Asoka seeds are notably mentioned in Vaghbatta's sixth-century AD account of cough treatment. Asoka is described as a cooling agent, fragrant material, and heart tonic with healing powers for wounds, ulcers, hemorrhoids, and bone fractures in the 9th-century AD Dhanvantari

Nighantu (Biswas and Debnath, 1972). The 11th-century Chakradatta recommends the use of Asoka bark to treat severe bleeding and advocates consuming seeds to treat kidney stone-induced restriction of urine flow (Singh *et al*., 2015). Raj Nighantu, an Ayurvedic literature from the 14th century, mentions Asoka as a heart tonic and suggests it for treating tumours and stomach distress. Similar to this, Asoka bark and flowers are used to cure menorrhagia, bleeding piles, diarrhoea, and to prevent abortions, according to the 15th-century Ayurvedic treatise Kayadeva Nighantu. In the 18th century, Asokarista is introduced by the Ayurvedic treatise Bhaisajya Ratnavali. It is well-known for its effectiveness in treating a variety of conditions, including anemia, uterine pain, edema, hemorrhages, and edema (Begum *et al*., 2014).

Ashokarishta, also known as *Asokarishta* is one of the significant formulations that utilizes the benefits of the Asoka tree. This traditional Ayurvedic herbal elixir features the bark of the Asoka tree as its principal ingredient, complemented by other fourteen herbs such as Dhataki (*Woodfordia fruticosa*), Musta (*Cyperus rotundus*), and various additional components, which may vary by the specific formulation (Gahlaut *et al*., 2013a). Traditionally, *Asokaristha* has been employed to alleviate menstrual disorders, catering to women who grapple with irregular menstrual cycles, excessive menstrual bleeding (menorrhagia), or menstrual pain (dysmenorrhea) (Sweet *et al*., 2012). It is believed to contribute to the overall health of the uterus and is considered a potential remedy for uterine discomfort and related issues. Additionally, in some traditional practices, *Asokaristha* is utilized to nurture fertility and support women's reproductive health (Lans, 2007). It also finds application during the postpartum period to facilitate the recovery of women after childbirth (Jain *et al*., 2011). Moreover, the versatile attributes of the Asoka tree extend beyond gynecological applications. In certain traditional customs, a paste made from Asoka bark is topically applied to wounds to expedite the healing process (Varghese *et al*., 1993). Women often drink a decoction prepared from Asoka bark in water and milk, with the water drained, to treat leucorrhoea. To stop irregular vaginal secretions, Ksheerapaka preparation of Asoka bark is employed (Pradhan *et al*., 2009). Furthermore, there is evidence that applying a paste made from Asoka bark can relieve uterine pain (Beena and Radhakrishnan, 2010). This underscores the diverse utility of the Asoka tree's components. In addition to its medicinal significance, the Asoka tree holds a sacred place in the religious and cultural tapestry of various regions in India. It frequently plays a central role in festivals, rituals, and

ceremonies, symbolizing notions of fertility, purity, and the divine feminine energy. These cultural associations reflect the profound and holistic understanding of nature and wellness within these traditions, emphasizing the interconnectedness of human health and spiritual significance.

1.12.1.3.2. Biological activities

Saraca asoca has drawn attention due to its diverse biological activities, making it a focal point in both traditional medicine and scientific research. Some of the prominent biological activities linked to *S. asoca* include:

- Uterotonic effects: The dried bark from *Saraca asoca* is widely recognized in India to address uterine abnormalities, including menorrhagia, amenorrhea, painful periods, endometriosis, and menstrual cycle disorders. Experimental studies have unveiled the bark's extract's capacity to both stimulate and relax the intestinal muscle, extend uterine contractions, and act as a uterine sedative. The application of the bark as a uterine tonic is attributed to its influence on the endometrium and ovaries, acting as an estrogenic stimulant (Sulaiman *et al*., 2020, Deka *et al*., 2012).

- Anti-inflammatory properties: *Saraca asoca* is thought to possess anti-inflammatory properties, possibly attributed to the bioactive compounds and phytochemicals present in its bark and other components (Ahmad *et al*., 2016b, Sharif *et al*., 2011). These compounds are presumed to engage with pathways associated with inflammation, influencing the release of inflammatory mediators and cytokines such as TNFα and IL6 (Cibin *et al*., 2012). Consequently, the tree has been traditionally employed to alleviate conditions characterized by inflammation, including joint pain, rheumatism, and various other inflammatory disorders.

- Antioxidant activity: Asoka tree is recognized for its reported antioxidant activity, a quality that contributes to neutralizing harmful free radicals within the body and potentially enhancing overall health. Numerous reports have outlined the presence of diverse antioxidant compounds in the bark, flowers, and leaves of the Asoka tree. Among these compounds are flavonoids, catechin, β-sitosterol lignin glycosides, gallic acid etc (Jain *et al*., 2013, Kumar *et al*., 2012, Yadav *et al*., 2015). These antioxidants play a vital role in mitigating oxidative stress and are

implicated in the protection of cells and tissues from potential damage caused by free radicals.

- Antimicrobial effects: Research indicates that extracts derived from the bark of *Saraca asoca* exhibit antibacterial effects, potentially effective against a spectrum of bacteria. The action of these properties is believed to be associated with disrupting bacterial cell membranes, inhibiting enzyme activity, or interfering with essential bacterial processes (Rajan *et al*., 2008, Seetharam *et al*., 2003). Moreover, Asoka has demonstrated antifungal effects against specific fungi. The bioactive compounds within the tree are thought to interfere with fungal cell structures or processes, suggesting its potential as a natural remedy for fungal infections (Shirolkar *et al*., 2013, Dabur *et al*., 2007).

- Anticancer properties: Ethnobotanical investigations have unveiled that the flowers of Saraca asoca possess preventive properties against two-stage skin carcinogenesis and exhibit a preference for inhibiting Dalton's lymphoma ascites and Sarcoma-180 tumour cells (Cibin *et al*., 2012, Varghese *et al*., 1992). Extracts from Asoka have demonstrated inhibitory effects on breast, lung and prostate cancer (Yadav *et al*., 2015, Dharshini *et al*., 2021, Choudhary *et al*., 2021). Additionally, *in vitro* tests have shown that the lectin "saracin," which was separated from the seed integument, can cause human T cells to undergo apoptosis (Ghosh *et al*., 1999).

- Wound healing: In traditional usages pastes or solutions made from various Asoka tree parts, like the bark, are applied topically to wounds (Deepti *et al*., 2012, Bandarupalli *et al*., 2014). By fostering an environment that is both protective and possibly antibacterial at the wound site, this technique is believed to accelerate the healing process.

Additional biological and pharmacological attributes associated with *S. asoca* comprise, anti-diabetic (Thilagam *et al*., 2021), anti-ulcer (Panchawat *et al*., 2022), larvicidal (Mathew *et al*., 2009), anti-helminthic (Singh *et al*., 2014), anti-pyretic properties (Varaprasad *et al*., 2011).

1.12.2. *Kingiodendron pinnatum* **(Roxb. ex DC.) Harms**

Kingiodendron pinnatum, known by most as Malabar mahogany, is a sizable tree in the Fabaceae family that grows mostly in the tropical forests of Western Ghats, India.

Classified as an endangered species, the scientific and pharmacological profile of this tree has yet to be fully established, despite its traditional use by indigenous tribes. Within traditional medicine, this plant plays a role in addressing menstrual problems and serves as a substitute for Asoka in various Ayurvedic formulations (Shahid *et al*., 2018). The oleo-gum-resin extracted from *Kingiodendron pinnatum* is employed in treating conditions such as gonorrhea and healing elephant sores. Tribes also utilize it to address catarrhal conditions of the genito-urinary and respiratory tracts and to alleviate joint pains (Kumar *et al*., 2011). While some studies have explored its antioxidant, antimicrobial, anticancer, antidiabetic and antiobesity properties, further research is necessary to comprehensively understand its potential benefits. *Kingiodendron pinnatum* comprises a diverse array of organic compounds, including saponins, phenolic compounds such as flavonoids and phenolic acids, tannins, phospholipids, glycosides, enzymes, amino acids, and polyunsaturated fatty acids (Sheik and Chandrashekar, 2014).

1.12.2.1. Nomenclature

1.12.2.1.1. Taxonomic classification

Scientific name: *Kingiodendron pinnatum* (Roxb. ex DC.) Harms

Kingdom : Plantae

Divison : Magnoliophyta

Class : Magnoliopsida

Order : Fabales

Family : Fabaceae

Genus : *Kingiodendron*

Species : *pinnatum*

1.12.2.1.2. Common names

There are various colloquial names for *Kingiodendron pinnatum*, a few of them are as follows:-

Kodapalla: Malayalam

Enne mara: Kannada

Kodapalai: Tamil

Malabar mahogany: English

Figure 1.4. *Kingiodendron pinnatum* (Roxb. ex DC.) Harms (portal, 2021)

1.12.2.2. General characteristics

1.12.2.2.1. Description

Kingiodendron pinnatum are tall evergreen trees, reaching heights of up to 20 meters and characterized by thick bark. The bark surface displays a greyish-brown hue with green blotches that are rough to the touch, emitting a reddish sticky resin. The leaves are arranged alternately, and they are odd-pinnate. The small, numerous flowers are white, arranged in axillary and terminal dense racemes that form panicles. The fruit is in the form of a pod, obovate in shape, and each pod typically contains a solitary, compressed seed. The period of flowering and fruiting spans from February to December. Despite its relatively small population in the wild, this species is extensively utilized as a substitute for Asoka in various Ayurvedic preparations because of its substantial size and the potential for obtaining a larger volume of bark compared to an Asoka tree.

1.12.2.2.2. Habitat

Endemic to the Western Ghats, specifically the South Sahyadri and Central Sahyadri regions extending up to the Coorg region, *Kingiodendron pinnatum* thrives in evergreen hill forests and deciduous forests. This tree is commonly found at elevations of up to

1,000 meters in southern India, including the states of Kerala, Karnataka and Tamil Nadu. In Kerala, it is distributed across various districts such as Thiruvananthapuram, Kollam, Thrissur, Idukki, Palakkad, Kozhikode and Wayanad. The tree engages in a symbiotic relationship with specific soil bacteria. These bacteria create nodules on the roots, facilitating the fixation of atmospheric nitrogen. While a portion of this nitrogen benefits the growth of the plant itself, some is also accessible for utilization by neighbouring plants in close proximity.

1.12.2.3. Pharmacological properties

1.12.2.3.1. Traditional uses

Kingiodendron pinnatum holds diverse traditional uses within local communities. While ongoing scientific exploration delves into its properties, traditional knowledge underscores its multifaceted applications. Harvested from the wild for both local medicinal purposes and as a source of materials, the tree is notably employed as a substitute for Asoka in various Ayurvedic formulations, indicating parallel roles in traditional remedies (Shahid *et al.*, 2018). This includes addressing menstrual problems and alleviating related issues in the menstrual cycle. The trunk produces a balsam used historically in treating gonorrhoea and catarrhal conditions affecting the genito-urinary and respiratory tracts, showcasing its historical efficacy in managing specific infections (Kumar *et al.*, 2011). Among the Kanikkar tribe in the Kalakad-Mundanthurai region of the Western Ghats in Tirunelveli, Tamil Nadu, India, a resin obtained by piercing the trunk is utilized traditionally for rheumatism treatment. This practice involves applying the resin on affected joints before bedtime with gentle circular massaging, followed by pouring lukewarm water over the joints in the morning (Sutha *et al.*, 2010). Additionally, this resin finds application in the traditional treatment of sores in elephants, reflecting its historical use in veterinary care for animals (Sheik and Chandrashekar, 2014).

1.12.2.3.2. Biological activities

Kingiodendron pinnatum is currently under investigation for its potential biological activities, and while research on this species is ongoing, some reported activities include

- Anti-inflammatory properties: The plant is believed to exhibit anti-inflammatory effects, potentially impacting processes associated with inflammation. A study involving a polyherbal formulation containing *K. pinnatum* indicated a reduction

in chronic/acute inflammations in mice (Shahid *et al.*, 2018). Furthermore, the formulation improved the antioxidant status in experimental animals treated with the extracts (Suhail *et al.*, 2019).

- Antioxidant activity: *Kingiodendron pinnatum* has been researched for its antioxidative characteristics, with antioxidants playing a pivotal role in counteracting detrimental free radicals within the body. In one study, the methanol stem extract of *K. pinnatum* demonstrated substantial antioxidant activity (Sheik and Chandrashekar, 2014). Another investigation revealed elevated levels of superoxide dismutase, catalase glutathione peroxidase and glutathione enzymes in animals treated with *K. pinnatum* extract (Suhail, 2019).

- Antimicrobial effects: Traditional applications, particularly in addressing gonorrhea and catarrhal conditions, hint at potential antimicrobial properties of *Kingiodendron pinnatum* against specific infections (Kumar *et al.*, 2011). In a study, methanolic extracts of *K. pinnatum* demonstrated inhibitory effects on the growth of *Pseudomonas aeruginosa*, *Proteus vulgaris*, *Klebsiella pneumonia*, gram-positive bacteria, including *Staphylococcus aureus* and *Bacillus subtilis*, gram-negative bacteria such as *Escherichia coli*, as well as the fungal strain *Candida albicans* (Sheik and Chandrashekar, 2014).

- Anti- tubular activity: One of the biggest health issues in developing nations, like India, has been tuberculosis. The need to find novel, side-effect-free anti-mycobacterial drugs is important since drug-resistant forms of *Mycobacterium tuberculosis* are on the rise. A study using a proportion assay revealed the antitubercular activity of *Kingiodendron pinnatum* extract against *M. tuberculosis* (Kumar *et al.*, 2014). This test assesses the extract's capacity to stop M. *tuberculosis* from growing and provides an opportunity for the creation of antitubercular medications.

1.13. Phytoestrogens

Phytoestrogens are natural compounds found in certain plants, possessing a structure akin to the hormone estrogen. While not identical to the body's endogenous estrogen, phytoestrogens can mimic or modulate estrogen activity. They bind to estrogen receptors, exerting estrogen-like effects (Moutsatsou, 2007). Phytoestrogens comprise a diverse range of compounds organized into various classes. These classes include anthocyanins, water-soluble pigments that give the vibrant blue, purple and red tones in numerous

flowers, vegetables and fruits; proanthocyanidins, also known as condensed tannins, found in beverages like red wine and tea, vegetables and fruits; hydroxycinnamic acid, encompassing compounds such as caffeic acid and ferulic acid, distributed across various plants and foods; hydroxybenzoic acid, represented by substances like gallic acid and ellagic acid, present in fruits, nuts, and select beverages; flavonols group, housing quercetin, kaempferol, and myricetin, commonly encountered in fruits, vegetables, and beverages like tea; flavones, which include luteolin and apigenin, found in specific herbs, vegetables, and fruits; flavanones, containing hesperetin and naringenin, prevalent in citrus fruits; isoflavones such as genistein and daidzein in soybeans, soy products, and other legumes (Clair, 1998); lignans, polyphenolic compounds present in seeds, particularly flaxseeds, sesame seeds, and whole grains; stilbenes like resveratrol identified in red grapes, red wine, and peanuts (Welch *et al*., 2008). Each of these classes encompasses unique compounds with distinct chemical structures, contributing to the wide array of health-promoting phytoestrogens found in various plant-based foods.

Phytoestrogens, sharing structural similarities with the hormone estrogen, have the ability to interact with estrogen receptors (ERs) in the human body (Xu *et al*.). The two primary types of estrogen receptors are estrogen receptor α and β (Estrogen Receptor Beta). These receptors, central to diverse physiological processes and gene regulation, play crucial roles in both cancer biology and therapeutic interventions (Ikeda *et al*., 2015). The affinity for binding can differ among various phytoestrogens, with certain ones displaying a preference for ERα, while others exhibit a heightened affinity for ERβ. The nature of the binding, whether agonistic (mimicking estrogen) or antagonistic (blocking estrogen), depends on both the cellular context and the specific phytoestrogen involved. When exposed to estrogen, ERα forms a complex with the hormone and binds to estrogen response elements (EREs) in DNA, thereby activating the transcription of specific genes and influencing various cellular processes (Abdel-Magid, 2017). Similarly, ERβ, while binding to estrogen like ERα, regulates gene expression with variations in the specific genes it influences. ERβ is instrumental in modulating estrogen-mediated effects in diverse tissues. The ERβ activation is linked to the suppression of cellular proliferation, especially in relation to specific cancers (Williams *et al*., 2008). In cancers influenced by hormonal factors, such as breast and prostate cancers, ERβ is often considered to have a

protective or anti-tumour role, suppressing the growth of cancer cells (Omoto and Iwase, 2015), while in bone tissue, they may emulate estrogen-like effects (Katzenellenbogen, 2011). Notably, certain phytoestrogens, such as genistein found in soy, have been reported to exhibit a higher affinity for ERβ. The ERα receptor, particularly prominent in hormone-sensitive tissues such as the breast and uterus, has the capacity to stimulate cellular proliferation under the influence of estrogen. Gaining insights into the distinct roles of both ERα and ERβ is essential for deciphering the intricacies of estrogen signaling and customizing therapeutic strategies in conditions where estrogen receptors wield substantial influence (Chen *et al.*, 2022).

Phytoestrogens have been investigated for their potential ability to lower the chance of developing some malignancies, like prostate and breast cancer. The connection between phytoestrogens and breast cancer risk is intricate, with findings lacking universal consistency (Low *et al.*, 2005). Individual responses can differ, and the influence of phytoestrogens on breast cancer risk may be shaped by factors like genetics, overall diet, and lifestyle (Barnes, 1998). It is noteworthy that eating foods high in phytoestrogens is a prevalent dietary practice in many cultures, especially in areas where legumes and soy are commonly consumed (Reinli and Block, 1996). However considering phytoestrogens have a complicated effect on health, moderation and balance are essential when including them in the diet for optimum wellness (Patisaul and Jefferson, 2010). As ongoing research delves deeper into this field, acquiring a nuanced understanding of the role of phytoestrogens in cancer prevention becomes indispensable.

1.14. Scope of the current research

Breast cancer treatment presents a number of challenges that affect patient outcomes and care. It is a diverse disease with distinct subtypes, each responding differently to treatment. Customizing treatments for specific subtypes is essential but presents a challenge in devising personalized therapies (Zardavas *et al.*, 2013). Hormone-positive breast cancers typically exhibit favourable responses to hormone therapies like tamoxifen or aromatase inhibitors, although some tumours may develop resistance over time (AlFakeeh and Brezden-Masley, 2018). Determining the optimal duration of hormone therapy remains a challenge, necessitating a delicate balance between extended treatment benefits for preventing recurrence and potential side effects, requiring ongoing research.

The development of effective sequential therapy strategies for managing hormone-positive breast cancer, especially in cases of recurrent or metastatic disease, is challenging (Haddad *et al*., 2023). Identifying the most suitable sequence of hormonal and targeted therapies is crucial for optimal outcomes. Hormone therapies may induce side effects, including bone density loss, hot flashes, and musculoskeletal symptoms, posing a challenge in balancing side effect management with treatment efficacy, particularly during long-term therapy (Cella and Fallowfield, 2008).

Hormone-negative breast cancers, particularly triple-negative breast cancer, do not express receptors such as estrogen and progesterone, as well as HER2 receptors. This absence restricts the availability of targeted therapies, as hormone or HER2-targeted treatments are ineffective (Peddi *et al*., 2012). TNBCs tend to be more aggressive, with an increased risk of recurrence and metastasis. Developing targeted therapies tailored to the unique biology of these cancers poses a considerable challenge. Given their aggressive nature, clinical trials becomes pivotal for exploring innovative treatment approaches (Huynh *et al*., 2020). Encouraging and streamlining patient enrolment in relevant trials present logistical challenges. While immunotherapy has demonstrated promise in some cancers, its efficacy in hormone-negative breast cancer remains an active area of investigation. Overcoming challenges associated with immune evasion and refining patient selection for immunotherapy are ongoing priorities (Jia *et al*., 2017). Consequently, chemotherapy remains a primary treatment option for hormone-negative breast cancers (Miller *et al*., 2007). The ongoing challenge lies in identifying novel and more targeted agents to augment the effectiveness of chemotherapy while minimizing side effects. In individuals with advanced cancers, the toxic effects of chemotherapy may be lessened by combining natural products with chemotherapy medications (Sak, 2012). Plant-derived products are being used more often in modern medicine as complementary and alternative treatments as a result of this trend. Numerous plant species can be found in India's Western Ghats, which are well-known for their rich biodiversity. However, many of these species are still unknown and unexplored (Kumar and Jnanesha, 2017).

In a prior investigation conducted by the Kerala Forest Research Institute (KFRI), as documented in research report no. 424, the quest for suitable substitutes for *Saraca asoca* in *Asokarishta* led to the discovery that *Kingiodendron pinnatum*, belonging to the same botanical family as Asoka, exhibited a more or less similar phytochemical profile (Sasidharan and Padikkala, 2012). It was identified as a potential occasional substitute in

Asokarishta. The study further demonstrated that the polyherbal formulation incorporating *K. pinnatum* was as effective as *S. asoca* in reducing estradiol-induced keratinization in young immature rats. Another study underscored the pharmacological efficacy of *K. pinnatum* as a viable alternative to *S. asoca* by validating its inhibitory effect on estrogen-induced uterine endometrial thickening in immature female rats (Shahid *et al*., 2018). This scientific validation supports its inclusion in polyherbal formulations. The observed activity of both these plants may be attributed to their anti-estrogenic properties. While *Kingiodendron pinnatum* remains relatively unexplored, some reported biological properties, including anti-inflammatory activities are reported. In one research investigation, the formulation demonstrated enhanced antioxidant status in experimental animals subjected to *K. pinnatum* extracts (Suhail, 2019). Another study, involving a polyherbal formulation with *K. pinnatum*, revealed a decrease in chronic/acute inflammations in mice (Shahid *et al*., 2018). In addition to showing strong antibacterial and antiviral properties against several bacterial and fungal species, the methanol stem extract of *K. pinnatum* also showed significant antioxidant activity (Sheik and Chandrashekar, 2014, Suhail, 2019). A different investigation that employed a proportion assay demonstrated the antitubercular properties of *Kingiodendron pinnatum* extract against *Mycobacterium tuberculosis* (Kumar *et al*., 2014).

Saraca asoca is reported to exhibit anticancer properties, but there is a dearth of corresponding reports on *Kingiodendron pinnatum*. Consequently, the current study sought to investigate the anticancer properties of *K. pinnatum* along with *S. asoca*, particularly on breast cancers, focusing on triple-negative breast cancers due to their limited treatment options and high aggressiveness. Additionally, various other biological properties of the plant, such as anti-inflammatory, antioxidant, anti-tumour and anticancer potential, were assessed using different *in vitro* assays and *in vivo* mouse models in this study.

Chapter 2
Materials and Methods

2.1. Materials

2.1.1. Collection of plant sample

The stem barks of *Saraca asoca* and *Kingiodendron pinnatum* were gathered from the Wayanad area of the Western Ghats in Kerala, India. The plant specimens were authenticated by Dr. N. Sasidharan, Taxonomist at the Kerala Forest Research Institute in Thrissur, Kerala. The voucher specimen of *S. asoca* (No. KFRI 4849) and *K. pinnatum* (No. KFRI 4725) were deposited in the Herbarium of KFRI.

2.1.2. Chemicals

An overview of the chemicals used in the study, as well as the details of the distributors, are presented in table 2.1. Analytical grade chemicals were used in this study.

Table 2.1. List of chemicals

S. No	Chemicals	Distributors
1	2,2'-azobis(2-amidinopropane) dihydrochloride (AAPH)	Sigma Aldrich Inc., St. Louis, USA
2	2,2-azinobis (3-ethylbenzothiazoline-6-sulfonic acid) (ABTS)	Sigma Aldrich Inc., St. Louis, USA
3	7, 12 - Dimethylbenz(a)anthracene (DMBA)	Sigma Aldrich Inc., St Louis, USA
4	5-5'dithiobis (2-nitrobenzoic acid) (DTNB)	Sisco Research Laboratories (SRL) Pvt. Ltd., Mumbai, India
5	2,2-diphenyl-1-picrylhydrazyl (DPPH)	Sisco Research Laboratories (SRL) Pvt. Ltd., Mumbai, India
6	3-(4,5-Dimethylthiazol-2-yl)-2,5-Diphenyltetrazolium Bromide (MTT)	Sisco Research Laboratories (SRL) Pvt. Ltd.,Mumbai, India
7	17 β-estradiol	Himedia Laboratories Pvt. Ltd, India
8	Acetic acid	Merck India Pvt. Ltd., Mumbai, India

9	Acetonitrile	Merck India Pvt. Ltd., Mumbai, India
10	Acetone	Merck India Pvt. Ltd., Mumbai, India
11	Acridine orange	Merck India Pvt. Ltd., Mumbai, India
12	Ammonium molybdate	Sisco Research Laboratories (SRL) Pvt. Ltd., Mumbai, India
13	Agarose	Sisco Research Laboratories (SRL) Pvt. Ltd., Mumbai, India
14	L-Ascorbic acid	Sisco Research Laboratories (SRL) Pvt. Ltd., Mumbai, India
15	Bovine Serum Albumin	Sisco Research Laboratories (SRL) Pvt. Ltd., Mumbai, India
16	Carrageenan	Sigma Aldrich Inc., St Louis, USA
17	Charcoal stripped Fetal Bovine Serum	Gibco, Thermo Fisher Scientific, USA
18	Chloroform	Merck India Pvt. Ltd., Mumbai, India
19	Cyclophosphamide	Neon Laboratories Ltd, India
20	Copper (II) sulphate pentahydrate	E-Merck India Pvt LtD, Mumbai, India
21	Deoxy ribose	Sisco Research Laboratories (SRL) Pvt. Ltd., Mumbai, India
22	Dextran	Himedia Laboratories Pvt. Ltd, India
23	Dextrose	Sisco Research Laboratories (SRL) Pvt. Ltd., Mumbai, India
24	Diclofenac	Sigma Aldrich Inc., St. Louis, USA
25	Dimethyl sulfoxide (DMSO)	Merck India Pvt. Ltd., Mumbai, India

26	Di-potassium hydrogen phosphate	Merck India Pvt. Ltd., Mumbai, India
27	Dulbecco's Modified Eagle Medium (DMEM)	Gibco, Thermo Fisher Scientific, USA
28	Ethidium Bromide	Sisco Research Laboratories (SRL) Pvt. Ltd., Mumbai, India
29	Ethyl acetate	Merck India Pvt. Ltd., Mumbai, India
30	Ethylene diamine tetra acetic acid disodium salt (EDTA)	Sisco Research Laboratories (SRL) Pvt. Ltd., Mumbai, India
31	Ferrous ammonium sulphate	Merck India Pvt. Ltd., Mumbai, India
32	Ferric chloride	Merck India Pvt. Ltd., Mumbai, India
33	Fetal Bovine Serum	Gibco, Thermo Fisher Scientific, USA
34	Folin–Ciocalteu reagent (FCR)	Sisco Research Laboratories (SRL) Pvt. Ltd., Mumbai, India
35	Formaldehyde	Merck India Pvt. Ltd., Mumbai, India
36	Giemsa	Merck India Pvt. Ltd., Mumbai, India
37	Glutathione reduced (GSH)	Sisco Research Laboratories (SRL) Pvt. Ltd., Mumbai, India
38	Glucose-6-phosphate	Sisco Research Laboratories (SRL) Pvt. Ltd., Mumbai, India
39	HEPES buffer	Himedia Laboratories Pvt. Ltd, India
40	Hydrochloric acid	Merck India Pvt. Ltd., Mumbai, India
41	Hydrogen peroxide	Merck India Pvt. Ltd., Mumbai, India
42	Isopropanol	Merck India Pvt. Ltd., Mumbai, India

43	Kaempferol	Sigma Aldrich Inc., St Louis, USA
44	L-Glutamine	Sigma Aldrich Inc., St Louis, USA
45	L-Histidine	Sisco Research Laboratories (SRL) Pvt. Ltd., Mumbai, India
46	Methanol	Merck India Pvt. Ltd., Mumbai, India
47	Naphthylethylene diamine dihydrochloride (NEDD)	Spectrochem Pvt. Ltd, Mumbai, India
48	Nitro blue tetrazolium (NBT)	Sisco Research Laboratories (SRL) Pvt. Ltd., Mumbai, India
49	Petroleum benzene	Merck India Pvt. Ltd., Mumbai, India
50	Phenol-red free DMEM	Gibco, Thermo Fisher Scientific, USA
51	Potassium hydroxide	Merck India Pvt. Ltd., Mumbai, India
52	Pottasium chloride	Merck India Pvt. Ltd., Mumbai, India
53	Propidium iodide	Sigma Aldrich Inc., St Louis, USA
54	Propylene glycol	Nice Chemicals (P) Ltd., Cochin, India
55	Quercetin	Sigma Aldrich Inc., St Louis, USA
56	Riboflavin	Sisco Research Laboratories (SRL) Pvt. Ltd., Mumbai, India
57	Rosewell Park Memorial Institute medium (RPMI-1640)	Gibco, Thermo Fisher Scientific, USA
58	Sodium acetate	Merck India Pvt. Ltd., Mumbai, India
59	Sodium azide	Sisco Research Laboratories (SRL) Pvt. Ltd., Mumbai, India

60	Sodium caseinate	Sisco Research Laboratories (SRL) Pvt. Ltd., Mumbai, India
61	Sodium dihydrogen phosphate dihydrate	Sisco Research Laboratories (SRL) Pvt. Ltd., Mumbai, India
62	Sodium potassium tartrate	Merck India Pvt. Ltd., Mumbai, India
63	Sodium carbonate	Merck India Pvt. Ltd., Mumbai, India
64	Sodium bicarbonate	Merck India Pvt. Ltd., Mumbai, India
65	Sodium fluoride	Sisco Research Laboratories (SRL) Pvt. Ltd., Mumbai, India
66	Sodium hydroxide	Merck India Pvt. Ltd., Mumbai, India
67	Sodium nitroprusside	Merck India Pvt. Ltd., Mumbai, India
68	Sulfuric acid	Merck India Pvt. Ltd., Mumbai, India
69	Streptomycin	Himedia Laboratories Pvt. Ltd, India
70	Sulphanilamide	Spectrochem Pvt. Ltd, Mumbai, India
71	Thiobarbituric acid	Himedia Laboratories Pvt. Ltd, India
72	Toluene	Merck India Pvt. Ltd., Mumbai, India
73	Trichloroacetic acid	Merck India Pvt. Ltd., Mumbai, India
74	Tripyridyltriazine (TPTZ)	Sigma Aldrich Inc., St Louis, USA
75	Tris buffer	Merck India Pvt. Ltd., Mumbai, India
76	Tris-Hydrochloride	Merck India Pvt. Ltd., Mumbai, India

77	Triton-X 100	Merck India Pvt. Ltd., Mumbai, India
78	Trypan blue	Spectrum Pvt Ltd, Cochin, India
79	Trypsin	Sigma Aldrich Inc., St Louis, USA

2.1.3. Instruments

Table 2.2 outlines the instruments utilized in the study and their respective providers.

Table 2.2. List of instruments

S. No	Instrument	Company
1	Agarose gel electrophoresis unit	Bio-Rad Laboratories (India) Pvt Ltd
2	Autoclave	Kemi Lab Equipment, Kochi, India
3	Centrifuge	Rotek Laboratory Instruments, Kochi, India
4	Deep freezer (-20ºC)	Remi Laboratory Instruments, Mumbai, India
5	Deep freezer (-80 ºC)	Eppendorf, Germany
6	Electronic weighing balance	Shimadzu, Japan
7	Flow cytometer	BD Biosciences, USA
8	Fluorescent microscope	Leica Microsystems, Germany
9	FT-IR spectrophotometer	Shimadzu, Japan
10	GC-MS	Shimadzu, Japan
11	Gel documentation system	UVItec, Cambridge
12	High speed cooling centrifuge	Remi Laboratory Instruments, Mumbai, India
13	Horizontal Laminar flow hood	Rotek Laboratory Instruments, Kochi, India
14	Hot air oven	Kemi Lab Equipment, Kochi, India
15	Incubator	Rotek Laboratory Instruments, Kochi, India
16	Inverted microscope	Meiji, Japan; Labex, Labovision

17	LCMS	Agilent technologies, Inc., USA
18	Micro-centrifuge	Tarsons Products Private Ltd., Kolkata
19	NanoDrop ND-1000 spectrophotometer	ThermoFisher Scientific, India
20	PCR	ThermoFisher Scientific, India
21	pH meter	Elico Ltd., Hyderabad, India
22	Phase contrast microscope	Magnus, INVI, New Delhi, India
23	Real time-PCR	StepOnePlus^{TM}, ThermoFisher Scientific, India
24	UV/Visible spectrophotometer	PG Instruments, UK
25	Vacuum concentrator	Eppendorf, Germany
26	Vortex	Rotek Laboratory Instruments, Kochi, India

2.1.4. Animals

The animals utilized in the study were acquired from the Small Animal Breeding Station (SABS), College of Veterinary and Animal Sciences at Kerala Veterinary and Animal Sciences University (KVASU), Thrissur, Kerala. Female Swiss albino and female BALB/c mice, both weighing 25-30 grams and aged 7-8 weeks, as well as male Wistar rats (150-200 g, aged 7-8 weeks), and pregnant female Wistar rats, were used for the study. All of the animals were housed in the Amala Cancer Research Centre's animal house facilities, with typical parameters being 60-70% humidity, 24-28 °C temperature and 12-hour light/dark cycles. The animals were given regular rat feed, which was bought from Sai Durga Feeds in Bangalore, India and water was provided on an *ad libitum* basis. A prior approval (Approval No: ACRC/IAEC/17(1)/P-05, 22-12-2017) was obtained from the Institutional Animal Ethics Committee (IAEC) for all animal experiments. The guidelines set forth by the Committee for the Control and Supervision of Experiments on Animals (CCSEA), established by the Ministry of Environment and Forests, Government of India, were strictly followed during the animal studies.

2.1.5. Cell lines

Murine tumour cell lines including Ehrlich's Ascites Carcinoma (EAC) and Daltons Lymphoma Ascites (DLA), sourced from Adayar Cancer Institute, Tamil Nadu, were cultivated in the peritoneal cavity of Swiss albino mice as transplantable tumours within the Amala Cancer Research Center's animal house facility. These cells were collected from the inoculated mice's peritoneal cavity and thoroughly washed in phosphate-buffered saline (PBS) to maintain the stock. A total of 1×10^6 cells were counted and adjusted before being injected into the peritoneal cavity of healthy mice at intervals of 14 days. A variety of cell lines have been used for cell culture studies including HEK293T (human embryonic kidney cells), IEC-6 (rat intestinal epithelium cells), Vero (African monkey kidney cells), RAW 264.7 (murine macrophage), Hep G2 (human hepatocellular carcinoma), HCT-15 (human colorectal adenocarcinoma), HeLa (human cervical adenocarcinoma) and PC-3 (human prostate adenocarcinoma). The human mammary adenocarcinoma breast cancer cell lines MDA-MB-231, SK-BR-3, MDA-MB-468, MCF-7 and human mammary ductal carcinoma cell line, T-47D were used for the study. The National Center for Cell Science (NCCS), located in Pune, India, supplied the cell lines. The cells were cultured as recommended by the supplier in Dulbecco's Modified Eagle Medium (DMEM) or Roswell Park Memorial Institute (RPMI-1640) medium supplemented with 10% Fetal bovine serum (FBS), streptomycin (100 μg/ mL) and penicillin (100 U/mL). A 37 °C temperature, 100% relative humidity, 95% air and 5% CO_2 were maintained throughout the experiment.

2.2. Methods

2.2.1. Plant extract preparation

The plant material was manually cleaned in order to remove coarse impurities. For the purpose of removing moisture, stem barks were air-dried for one week in shade in a well-ventilated place followed by a further drying process at 40 °C in the incubator. An electric mixer-grinder was used to crush and grind the dried stem bark into fine powder (Odey *et al*., 2012). Approximately 20 grams of each plant's powder was extracted using 250 mL of methanol in a foil-covered flask. After being stirred at room temperature overnight, the extracts were filtered through Whatman No. 1 filter paper. The extraction process was repeated 2-3 times and the collected extracts were evaporated until dry (Sharma *et al*., 1971). Based on the weight of the dry extracts and the initial powder weight taken for

extraction, the percentage yield was determined using the formula: % Yield = (dry extract weight/weight used for extraction) $\times$ 100. For future use, each extract was assigned a unique label and kept in airtight containers at around 4°C in a cool, dark place.

2.2.2. Sequential extraction of the crude powder

An extraction was performed on 20 g of powdered bark from *S. asoca* and *K. pinnatum* using 250 mL of solvents with varying polarities (petroleum ether, ethyl acetate, methanol and water). The extracts were passed through Whatman No. 1 filter paper and dried by evaporating at a temperature of 40°C until they were dry. *In vitro* antioxidant radical scavenging assays and trypan blue dye cytotoxicity studies were used as preliminary screening methods for determining the biological efficacies of the residues obtained. As a result, the crude methanolic extract was found to exhibit greater activity than fractions which was therefore selected for evaluating the biological properties of both plants.

2.2.3. Phytochemical analysis

2.2.3.1. Initial phytochemical screening

In order to determine the presence of different phytochemicals, the crude methanolic extract obtained from both plants was dissolved in methanol and subjected to various analysis according to standard procedures (Das *et al*., 1964, Harborne, 1998).

2.2.3.1.1. Test for alkaloids

The extracts (0.5 g each) were mixed with 8 mL of HCl (1%), heated, and subsequently filtered. After treating around 2 mL of the filtrate separately with Dragendorff's reagent, the turbidity that developed during the precipitation process was thought to be an indication that alkaloids were present.

2.2.3.1.2. Test for flavonoids

After dissolving the extracts (1 mL) in 5 mL of 95% ethanol, a couple of drops of diluted sodium hydroxide solution were added. The test tube developed a yellowish hue that subsided after several drops of diluted HCl were added, indicating the presence of flavonoids.

2.2.3.1.3. Test for phenols

Five millilitre of distilled water was mixed with 0.5 g of dry extracts, followed by a few drops of 5% ferric chloride. The precipitation that appears bluish-black shows presence of phenols.

2.2.3.1.4. Test for phytosterols

In order to test for sterols (Salkowski reaction), 1 gram of extracts were dissolved in 2 mL of chloroform. Following this, concentrated sulphuric acid (2 mL) were poured into the tube's side. After a few minutes of shaking the tube, the chloroform layer developed a red colour, while the lower layer developed fluoresced greenish yellow, suggesting the presence of sterol.

2.2.3.1.5. Test for saponins

Small amounts of extract were dissolved in alcohol and distilled water was added to it drop by drop. A positive test for resin was confirmed by the appearance of turbidity.

2.2.3.1.6. Test for tannins

The extracts were mixed with methanol, heated and filtered using Whatman No. 1 filter paper. A precipitate formed after treating the filtrate obtained with 2-3 drops of lead acetate solution suggested the existence of tannins.

2.2.3.1.7. Test for terpenoids

The extracts (0.5 g) was boiled and cooled with a few drops of acetic anhydride. A lower layer was formed in the test tube by adding a few drops of concentrated sulphuric acid along its walls. Terpenoids are detected by the appearance of a brown ring at the junction of two layers (Liebermann- Burchard's test).

2.2.3.1.8. Total phenolic content determination

The Folin-Ciocalteau colorimetric reagent (FCR) method was used to assess the total phenolic content of *S. asoca* and *K. pinnatum* (Kaur and Kapoor, 2002). 1 mL of the plant extract was combined with 2.5 mL of the tenfold-diluted Folin-Ciocalteau phenol reagent. Following 5 min, 2.5 mL of a 75 g/L sodium carbonate solution was added and the resultant solution was left at room temperature for 30 min. A UV-Vis spectrophotometer (Systronics 119, Chennai, India) was used to measure the absorbance of the mixture at 765 nm. The calibration curve for gallic acid was also prepared in a similar manner, ranging from 20 to 80 μg/mL. The results are represented in mg gallic acid equivalent (GAE) per gram of extract.

2.2.3.1.9 Total flavonoid content determination

Aluminium chloride colorimetric method was used to determine the total flavonoid content of the two plant extracts (Chang *et al*., 2002). The calibration curve for quercetin

was prepared within the range of 20-80 μg/mL. The plant extracts were combined with 0.2 mL of 10% aluminium chloride, 3 mL of 80% methanol, 0.2 mL of 1 M potassium acetate and the volume was made up to 10 mL using distilled water. The standard (1mg/mL) and blank was prepared in the same manner but instead of the sample distilled water was added. All tubes were incubated for 30 minutes at room temperature, and the absorbance of each tube was measured at 415 nm. The total flavonoid content was shown as milligrams of quercetin equivalents (QTE) per gram of extract.

2.2.3.2 Ultraviolet-visible spectroscopy (UV-Vis)

The plants extracts were filtered using Whatman No. 1 filter paper after being centrifuged for 10 minutes at 3000 rpm. The extracts were diluted with methanol which was used for extraction and a solution of 1 mg/mL as final concentration was prepared. With a UV-Vis spectrophotometer (PG Instruments, UK), the extracts were scanned at a wavelength range from 200 to 900 nm, and distinctive peaks were detected.

2.2.3.3. FT-IR analysis

To determine the functional groups present in the plant extract, Fourier transform infrared spectroscopy was performed on the crude extract and methanolic fractions of *S. asoca* and *K. pinnatum*. A translucent sample disc was prepared by encapsulating 10 mg of sample powders in 100 mg of potassium bromide (KBr) pellets. The FTIR spectroscopy was conducted with a RF-5301 PC fluorescent spectrometer in the range of 4000 and 500 cm^{-1}. A chart which indicates the characteristic infrared absorption frequencies of organic and carbonyl functional groups was used for the analysis and interpretation of the spectra (Coates, 2000).

2.2.3.4. TLC and HPTLC profiling

For thin layer chromatography (TLC) analysis, a small amount of crude extract and methanolic fractions of both plant extracts were dissolved in a minimum quantity of methanol and spotted on TLC silica gel 60 F 254 plate (10×10 cm) using capillary tube along with authentic sample, kaempferol. The solvent system of toluene, ethyl acetate, and formic acid in the ratio 7: 3: 0.3 was used to develop the chromatogram. The plate was observed under UV (365 nm) for visualising the band formed. The presence of kaempferol was determined by comparing the Rf values (Athiralakshmy *et al*., 2016).

HPTLC system (CAMAG) consisting of a Linomat 5 sample injector with the nitrogen flow, delivering samples from the syringe at a rate of 150 nl/s, a twin trough chamber (20x10 cm), Camag TLC scanner detector and winCATS software were used for the high-performance thin-layer chromatography (HPTLC) analysis. An appropriate volume of standards, quercetin and β-sitosterol (5 μL) and samples of known concentrations (10 μL) were spotted as 10 mm band length on separate precoated silica gel 60 F 254 HPTLC plates (8.0 x 10.0 cm) (Merck, Mumbai, India). The plate was kept in twin trough developing chamber and was developed up to 70 mm with the mobile phase, toluene: chloroform: methanol in the ratio 8:3:1 for β-sitosterol and toluene: ethyl acetate: methanol in the ratio 6:3:1. Hot air was used to dry the developed plate to evaporate solvents. The plate was observed using CAMAG visualizer and the images were taken in 254 and 366 nm for quercetin. For the standard, β-sitosterol images were taken in 366 nm and the developed plate was sprayed with anisaldehyde sulphuric acid spray reagent which was then dried at 100 °C in a hot air oven (Saha *et al*., 2012).

2.2.3.5. HPLC analysis

The Shimadzu Prominent HPLC was used for the high-performance liquid chromatography (HPLC) technique. A Zorbax 300SB reverse phase column having a measurement of 4.5 mm $\times$ 250 mm, C18 column and 5 μm particle size was used for the analysis. It is complemented by a guard column of a similar diameter and pore size. The injection amount was 20 μL and a 0.2 mL/min flow rate was maintained. A temperature of 40°C was kept as the column temperature. An authentic sample of β-sitosterol (Sigma Aldrich Co.) was prepared by dissolving it in chloroform at a concentration of 1 mg/mL. At a concentration of 2 mg/mL*, S. asoca* and *K. pinnatum* extracts were dissolved in methanol. All samples were filtered as required before injecting into HPLC. The mobile phase used was 0.8 % acetonitrile in water in the isocratic elution method and all the reagents used were of HPLC grade. UV detection was conducted at 254 nm with a run time of 6.0 min (Mittal *et al*., 2013a).

2.2.3.6. GCMS analysis

A QP2010S Shimadzu system with an MS Shimadzu detector and a Rxi-5Sil MS column with a 30 m length, 0.25 μm thickness and 0.25 mm ID was used to perform the GCMS analysis. The carrier gas used was helium gas (99.99%), flowing at a steady rate of 3 mL/min and 1 μL injection volume was utilized in a splitless mode at an inlet pressure of

173 Pascals. The MS column has an injection temperature of 260 ℃; the GC column oven temperature of 80 ℃, and with an increment rate of 5 °C/min. The detector was maintained at a temperature of 280 °C and the temperature of ion source was fixed at 200 °C. The mass spectrum of compounds in the extracts were taken at 70 eV with a scan mode range of 50-500 amu. The total GC running time was 45 min. The software used to handle mass spectra and chromatograms was GCMS solutions with the libraries used being NIST 11 and WILEY 8 (Mukhopadhyay *et al.*, 2017).

2.2.3.7. HR-LCMS

The chemical profiling of crude and methanol fraction were subjected to High Resolution-Liquid chromatography/mass spectrometry. An Agilent 6550 iFunnel Q-TOF LC/MS system (G6550A) was used for the analysis with an Agilent 1200 series thermostatted column compartment, an Agilent 1290 Infinity's Autosampler (G4226A) and binary pump VL (G4220B). For the separation, a reverse phase analytical column (Zorbax SB-C18, 100 x 2.1 mm i.d., 1.8 μm particle size) was employed with a flow rate of 0.3 mL/min for a total of 30 min. For analysis, a volume of 5 μL of the sample was injected. The mobile phases used were aqueous 0.1% formic acid (A) and 90% acetonitrile in 0.1% aqueous formic acid (B). A dual ion source system with full scan mode was used for the mass spectroscopy, covering a mass range between 50 and 500 m/z. In order to analyze the acquired data, the mass hunter qualitative analysis software program was used.

2.2.4. Acute toxicity studies of plant extracts

Three female Swiss albino mice (25-30 g) was given single oral doses of the crude extract of *Saraca asoca* and *Kingiodendron pinnatum* at 2500 mg/kg b. wt, respectively, in accordance with the Organization for Economic Co-operation and Development's (OECD) guidelines for testing chemicals (Oecd, 2008). The animals' behaviour, body weight, water and food consumption, hair loss, mortality and other obvious changes were observed over the course of 14 consecutive days. At the end of the study period, the animals were sacrificed, and a necropsy was performed to look for any signs of change in the internal organs. With a different group of animals, the experiment was repeated.

2.2.5. *In vitro* antioxidant assays

2.2.5.1. ABTS radical scavenging assay

71

In this study, 2,2'-azino-bis(3-ethylbenzothiazoline-6-sulphonic acid (ABTS) radical cation decolorization was used to determine the scavenging activity of different fractions and extracts (Re *et al*., 1999). The ABTS•+ cation radicals were generated by a 1:1 reaction between 2.45 mM potassium persulfate and 7 mM ABTS. Before being used, the solution was mixed with an equal volume of methanol and was incubated for 12 to 16 hours in the dark at room temperature. Following this, methanol was added to the ABTS•+ solution to dilute it until the absorbance at 734 nm was between 0.700 and 0.800. Upon adding the samples, the reaction system was adjusted to 4 mL with diluted ABTS•+ solution, and the mixture's absorbance was measured within 30 min of mixing. All measurements were performed at least three times, with a solvent blank run in each assay. In order to calculate the percentage inhibition of absorbance at 734 nm, the following formula was used:

$$\% \text{ Inhibition} = \frac{\text{Absorbance of Control} - \text{Absorbance of test}}{\text{Absorbance of control}} \times 100$$

2.2.5.2. DPPH radical scavenging assay

The extracts were tested for their ability to scavenge free radicals by using the 2,2-diphenyl-1-picrylhydrazyl (DPPH) method (Aquino *et al*., 2001). A mixture of different concentrations of extracts was added to 187 μL of freshly prepared DPPH solution and methanol was added to make this mixture into 1000 μL. Following a 20 minutes dark incubation, the reaction mixture's absorbance was measured at 517 nm. The results were assessed using the formula, percentage DPPH scavenging = Abs. of control - Abs. of test/ Abs. of control x 100). A graph was plotted and the IC_{50} value for extracts was calculated (the concentration of sample at which DPPH absorbance decreased by 50% as compared to control absorbance).

2.2.5.3. Superoxide radical scavenging assay

A nitro blue tetrazolium (NBT) reduction method was used to determine the extracts' ability to scavenge superoxide radicals (McCord and Fridovich, 1969). The process relies on the production of superoxide by riboflavin and the light-induced reduction of NBT. Different concentrations of the plant extracts were added to the reaction mixture that contained 0.1 M EDTA, 1.5 mM NBT, 0.3 mM NaCN, 0.067 M phosphate buffer and 0.12 mM riboflavin. The tubes were illuminated for 15 min with an incandescent lamp, and measurements of the optical density at 560 nm were taken both before and following

the exposure to light. By comparing the absorbance readings of the experimental and control tubes, the following formula was used to calculate the percentage inhibition of superoxide generation, % scavenging of superoxide radical = Abs. of control - Abs. of test/ Abs. of control x 100. The graph was plotted as a result of the analysis.

2.2.5.4. Ferric reducing antioxidant power activity

The extracts were tested against the stable free radical FRAP reagent in order to determine their scavenging activity (Benzie and Strain, 1999). Antioxidants work as reductants in the FRAP assay, which is based on a redox-linked calorimetric technique that uses the readily reduced oxidant Fe (III). By determining the absorbance at 595 nm, the reduction of the colourless ferric tripyridyltriazine complex (ferric (III)) to blue ferrous-(2, 4, 6-tripyridyl-s-triazine)2 (ferrous (II)) can be assessed. Test compounds contain electron-donating antioxidants that act as electron donors, which are reflected in the absorption readings. The plant extracts at various concentrations were added to the FRAP reagent, with acetate buffer being used to make up the volume to 1000 mL. After 15 minutes of incubation at 37°C, the optical density was measured at 595 nm. A comparison of control and experimental absorbance values was used to determine the percentage inhibition of FRAP (% scavenging of FRAP = Absorbance of control - Absorbance of test/ Absorbance of control x 100). The graph was plotted to demonstrate the percentage increase in the extracts' ferric ion reducing power activity.

2.2.5.5. Hydroxyl radical scavenging assay

The thiobarbituric acid reacting substances (TBARS) were used to measure the scavenging activity of extracts on hydroxyl radicals (Kunchandy and Rao, 1990). The scavenging activity was assessed by examining the competition for generated hydroxyl radicals between deoxyribose and test compounds using the $Fe3+$/ascorbate/EDTA/H2O2 system (Fenton reaction). The KH_2PO_4KOH buffer, 20 mM (pH 7.4), $FeCl_3$ (0.1 mM), deoxyribose (2.8 mM) and 10 to 100 μg/mL of the test sample were prepared in a 1 mL volume to set up the reaction system. After incubating for one hr at 37°C, the reaction mixture was cooled to room temperature. Deoxyribose is attacked by the hydroxyl radical resulting in the formation of thiobarbituric acid substances, which is measured at 530 nm using a spectrophotometer. The degradation of deoxyribose was measured as TBARS, and the % inhibition was computed (% scavenging

= Absorbance of control - Absorbance of test/ Absorbance of control x 100). The inhibitory concentration (IC$_{50}$) was determined and plotted on the graph.

2.2.5.6. AAPH induced erythrocyte haemolysis

2.2.5.6.1. Red blood cell suspension preparation

The blood was obtained from the Amala Institute of Medical Sciences, Thrissur that has been treated with acid-citrate-dextrose (ACD). Red blood cells (RBCs) were separated by centrifugation at 2000 rpm for 10 min. It was then rinsed three times in isotonic phosphate buffer saline (pH-7.4). After each wash, the buffy coat and plasma were eliminated by aspiration.

2.2.5.6.2. Erythrocyte haemolysis inhibition assay

In this assay, hemolysis is caused by oxidizing the membrane proteins and lipids when 2, 2′-Azobis (2-methylpropionamidine) dihydrochloride (AAPH), a peroxyl radical initiator, is introduced to an erythrocyte solution. The blood erythrocytes were isolated by centrifuging at 2000 rpm for ten min. The erythrocytes were resuspended in PBS after being washed three times with PBS to achieve a haematocrit level of 20 %. The plant extracts at different concentrations were mixed in to erythrocyte suspensions and the mixture was incubated for 15 min at 37°C. To stimulate the oxidation of free radical chains in the RBC lipids, a concentration of 200 mM AAPH was introduced to each tube, and the suspension was then incubated for three hours at 37°C. Erythrocyte suspension with AAPH was used as the control. After diluting the supernatant with 1.5 mL of PBS and centrifuged at 1,500 rpm for 10 min, the optical density of the supernatant was measured at 540 nm (Ajila and Rao, 2008). Based on the following formula, the concentration of extracts required to prevent 50% hemolysis was determined

$$\% \text{ Inhibition} = \frac{\text{Absorbance of Control} - \text{Absorbance of extracts}}{\text{Absorbance of control}} \times 100$$

2.2.5.6.3. AAPH induced lipid peroxidation

The extracts of varying concentrations were added to erythrocyte suspension in 1 mL and membrane damage was initiated with 200 mM AAPH. The reaction was stopped with the addition of 0.25 M HCl (2 mL) having 0.375% thiobarbituric acid (TBA) and 15% trichloroacetic acid (TCA) after it had been incubated at 37°C for one hour. The reaction mixture was boiled for 15 min, cooled, and centrifuged, and the absorbance of the

supernatant at 532 nm was measured (Ajila and Rao, 2008). The formula as follows was utilized to determine the lipid peroxidation inhibition percentage.

Percentage inhibition = (Abs. of control - Abs. of test/ Abs. of control) x 100

2.2.6. *In vivo* antioxidant activity of extracts

The *in vivo* antioxidant activity of extracts were evaluated using sodium fluoride (NaF) induced oxidative stress model. The animals utilized in the study were acquired from the Small Animal Breeding Station (SABS), College of Veterinary and Animal Sciences at Kerala Veterinary and Animal Sciences University (KVASU), Thrissur, Kerala. All of the animals were housed in the Amala Cancer Research Centre's animal house facilities, with typical parameters being 60-70% humidity, 24-28 °C temperature and 12-hour light/dark cycles. The animals were given regular rat feed, which was bought from Sai Durga Feeds in Bangalore, India and water was provided on an *ad libitum* basis. A prior approval (Approval No: ACRC/IAEC/17(1)/P-05, 22-12-2017) was obtained from the Institutional Animal Ethics Committee (IAEC) for all animal experiments. The guidelines set forth by the Committee for Control and Supervision of Experiments on Animals (CCSEA), established by the Ministry of Environment and Forests, Government of India, were strictly followed during the animal studies. To conduct this study, 42 male Wistar rats weighing 200–250 g were split up into seven groups, each including six animals. Following is a breakdown of the animal groupings;

Group I: normal (without any treatment); group II: control (NaF alone, 600 ppm/L/day); Group III: vehicle control- propylene glycol, Group IV: standard (Vitamin C-15 mg/kg b.wt.); Group V: SALD- *Saraca asoca* (SA) low dose (250 mg/kg b.wt., p.o); Group VI: SAHD- SA high dose (500 mg/kg b.wt., p.o); Group VII: KPLD- *Kingiodendron pinnatum* (KP) low dose (250 mg/kg b.wt., p.o), Group VIII: KPHD- KP high dose (500 mg/kg b.wt., p.o).

The treatment with plant extracts began one week prior to NaF administration and continued throughout the experiment. From the 8th day onwards, sodium fluoride (NaF, 600 ppm/L/day) was administered to all animals through their drinking water except group I, for inducing oxidative stress. In total, the plant extracts were administered orally for 14 days, seven days prior to NaF treatment and seven days following NaF treatment. Vitamin C was administered as a positive control to animals in the same manner (Nabavi *et al*., 2013). Upon completion of the experiment, all animals were euthanized and their

livers were dissected for further analysis. For histological analysis, a part of the tissue was preserved in 10% buffered formalin solution prior to the preparation of the liver homogenate for the determination of antioxidant parameters (section 2.2.8 of chapter 2). Direct cardiac puncture method was used to collect the blood, which was then preserved in vials coated with EDTA.

2.2.6.1. Hemolysate preparation from blood

In order to prepare the hemolysate, packed RBC were collected from heparinized blood by centrifugation at 2,500 rpm. After collecting the packed RBCs, they were washed with normal saline. According to section 2.2.7.1, hemoglobin concentrations of packed RBCs were determined. Hemolysis was achieved by mixing 0.1 mL of packed RBCs with 0.9 mL of cold water, 0.5 mL of ethanol, and 0.25 mL of chloroform, followed by vigorous shaking of the samples. Hemolysate was prepared by centrifuging for 60 min at 10,000 rpm. The levels of catalase, SOD and GSH in the hemolysate were estimated using the collected supernatant.

2.2.6.2. Tissue homogenate preparation

Following the sacrifice, the organs were collected and ice-cold saline was used to properly wash them. The filter paper was used to gently blot the organs and weighed using an analytical balance. With the assistance of a homogenizer, the tissue was homogenized in 0.1M tris buffer (pH 7). Homogenates were directly used to determine total protein and tissue lipid peroxidation. The supernatant obtained by centrifuging the homogenate was used to determine the concentration of superoxide dismutase (SOD), catalase (CAT), glutathione (GSH) and lipid peroxidation (TBARS). A cooling centrifuge was used to remove unbroken cells, nuclei, cell debris and mitochondria by centrifuging at 10,000 rpm for 60 min.

2.2.6.3. Histopathological evaluation

A sterilized scissors/surgical blade was used to excise the vital organs after sacrifice, and were rinsed with normal saline (0.9% NaCl) to remove any remaining blood. In order to preserve and protect the tissue from subsequent processing and staining, neutral buffered formalin (10%) was used as the fixative. As part of the dehydration process, tissue was immersed in increasing concentrations of ethanol (alcohol) solutions (from 0 to 100 %). By using xylene, the ethanol in the tissue was displaced by molten paraffin wax which,

in turn, was displaced by xylene. The tissue was embedded in paraffin after it had been dehydrated and cleared. Microtomy of embedded tissue was employed to obtain sections measuring approximately 3-4 μm in thickness. Deparaffinization was performed in xylene, followed by rehydration in decreasing alcohol concentrations (100-0 %). Following rehydration, nuclear staining with hematoxylin was performed, followed by counterstaining with cytoplasmic stain, eosin. In order to remove the excess stain, water was used. DPX was used to mount the stained sections, which were then observed under a light microscope and photographed.

2.2.7. Estimation of haematological parameters

2.2.7.1. Determination of haemoglobin (Hb) content

The estimation of haemoglobin content was performed using following method (Drabkin and Austin, 1935).

Principle

Potassium cyanide and potassium ferricyanide, which are included in the cyanmeth reagent, combine with hemoglobin to generate cyanmethemoglobin. The amount of hemoglobin in the blood is closely correlated with the absorbance of cyanmethemoglobin.

Procedure

Cyanmeth reagent was added to 20 μL of fresh heparinized blood after mixing and incubated at room temperature for 5 min. The wavelength at which the absorbance measured was 546 nm. In addition, absorbance of the standard solution corresponding to 60 mg/dl hemoglobin was determined. In order to calculate the hemoglobin content of blood, the following formula was used:

Hemoglobin (g/dL) = (Absorbance of the sample/Absorbance of Standard) $\times$ 60 $\times$ 0.251

2.2.7.2. Determination of total WBC count

Based on the following method, the total number of WBCs was estimated (Chesbrough and Arthur, 1972)

Principle

The acetic acid in Turk's fluid causes enucleated red blood cells to lyse, while the nucleated cells remain intact and stained with crystal violet.

Procedure

An amount of 20 μL of heparinized blood was diluted with 380 μL of Turk's fluid. A Neubauer counting chamber was used to dispense the blood mixture. By counting the white blood cells in the corner squares, the total number of white blood cells was calculated based on the formula below

Total WBC (cells/mm^3) = Number of cells counted $\times$ 50

2.2.7.3. Determination of total RBC count

The total number of RBC was estimated using following method (Chesbrough and Arthur, 1972)

Principle

A diluted solution of anticoagulated blood was prepared (1: 200) using Hayem's fluid (composed of sodium chloride, sodium sulfate, mercuric chloride, and distilled water). Isotonicity of fluids is maintained by combining sodium chloride and sodium sulphate. Mercuric chloride serves as a preservative as well as a fixative for the cells. In this way, the diluting fluid prevents hemolysis, coagulation of the blood, and the growth of bacteria and fungi.

Procedure

A small volume of blood diluted with RBC diluting fluid was introduced into the counting chamber coverslip in order to determine RBC count. Cells were allowed to settle for 2 to 3 min. Red blood cells were counted in the four corners and the central square of the counting chamber under the high power objective (40X) of a microscope, and the total count was calculated as follows:

RBC count (millions/mm^3) = [(No. of RBC counted x Dilution factor x Depth factor)/

(Number of chambers counted)]

2.2.7.4. Determination of platelet count

A manual counting of the platelets in the blood sample was conducted according to the method described (Chesbrough and Arthur, 1972).

Principle

The platelet count refers to the number of tiny cells in the blood that clot the blood. Platelets are smaller than RBC, which help to clot the blood. Sodium citrate which is an anticoagulant is used as dilution fluid for platelet counting.

Procedure

Sodium citrate was used to dilute the blood (1:20), followed by 5 min of incubation to lyse the erythrocytes in order to determine the platelet count. An appropriate volume of suspension was discharged into the counting chamber after it had been mixed gently. A moist environment was left in the chamber for 15-20 min in order to allow the platelets to settle. In a similar manner to counting RBCs, the cells were counted. Using the formula below the total number of platelets was determined.

Total platelet count (cells/ mm^3) = No. of platelet counted x 500

(where, 500 = 5 times to convert area to 1 square mm x 10 times for depth of chamber x 10 times for dilution factor).

2.2.7.5. Differential leukocyte count determination

A differential count of leucocytes is a method for determining the proportions of various types of leucocytes in the blood (Wintrobe *et al*., 2009).

Principle

Blood smears are stained with a polychromatic stain that contains methylene blue and eosin to determine the differential count. An acidic dye is used to stain the basic components of WBC (e.g. cytoplasm) while a basic dye is used to stain the acidic components (e.g. nucleus). Both dyes stain neutral components.

Procedure

Initially, a thin smear was prepared by spreading a drop of blood evenly on a glass slide using another slide, which was positioned at a 45 degree angle and moved in the opposite direction. After the blood smear dried, the sample was allowed to stand for 3 to 5 min, and then a few drops of Leishman's stain were applied to cover the smear. Following this, a few drops of distilled water were added to the slide, and it was left undisturbed for 10 min. After washing the slides under running water, they were allowed to dry. As part of

the count, various types of cells were examined, including polymorphonuclear neutrophils (nucleus dark blue, cytoplasm paler pink, granules reddish lilac), eosinophils (nucleus blue, cytoplasm blue, granules red-orange), basophils (nucleus purple or dark blue, granules dark purple, nearly black), non-granular monocytes (nucleus violet, cytoplasm sky blue), lymphocytes (nucleus violet, cytoplasm dark blue).

2.2.8. Measurement of antioxidants parameters

2.2.8.1. Determination of superoxide dismutase (SOD) activity

The activity of the SOD enzyme in blood and tissue was determined based on the method described by (McCord and Fridovich, 1969).

Principle

It is based on the fact that SOD inhibits the reduction of nitro blue tetrazolium (NBT) by superoxide radicals generated during photoreduction of riboflavin with oxygen.

Procedure

The sample was mixed with 200 μL of 0.0015 KCN in 0.1 M EDTA, 100 μL of 1.5 mM NBT, and 2950 μL of K-Na Phosphate buffer (pH 7.8) in a volume of 100 μL of the test sample (hemolysate or tissue sample). As a control, a reaction mixture was prepared without the test sample. An initial reading was taken at 560 nm after adding 50 μL of 0.12 mM riboflavin to the reaction mixture and measuring the absorbance of the mixture. An incandescent lamp was used to illuminate the tubes uniformly for 15 min. A final reading of the absorbance was taken and recorded. A percentage inhibition was calculated by comparing the absorbance of the test to that of the control. For the blood sample and the tissue sample, respectively, the concentration of the sample required to scavenge 50% of the generated superoxide anion was calculated as one unit of enzyme activity, which is expressed as U/g Hb for the blood sample and U/mg protein for the tissue sample.

2.2.8.2. Determination of catalase activity

The catalase activity in the blood (Aebi, 1984) and the tissue (Beers and Sizer, 1952) was determined according to respective methods.

Principle

A measure of catalase activity in a sample (blood or tissue) is obtained by measuring the decrease in the concentration of hydrogen peroxide (H_2O_2) observed after the sample has been incubated with standard H_2O_2 solutions.

Procedure

Estimation of blood catalase levels: The hemoglobin content was estimated to be between 4-5 g/dL in the lysate of packed erythrocytes prepared in ice water. A 1:1500 dilution of the concentrated hemolysate in sodium-potassium phosphate buffer (50 mM, pH 7) was performed prior to testing. There were 2 mL of diluted hemolysate in the test cuvette while 1 mL buffer and 2 mL of diluted hemolysate contained in the reference cuvette. The reaction was started by adding 1 mL of H_2O_2 (30 mM in buffer, freshly prepared) to the test cuvette, stirring gently, and recording the absorbance at 240 nm for 1 min with intervals of 15 sec. Based on the formula below, the catalase activity was estimated

Catalase (U/g Hb) = [(2.303 x (log A1/logA4) x dilution factor) / (15 x Hb)]

Where, the absorbance at time zero is A1 and the absorbance at time 60 is A4.

Estimation of tissue catalase levels: The reference cuvette contained 100 μL of tissue homogenate and 2.9 mL of phosphate buffer, which made up to a total of 3 mL. The test cuvettes contained 100 μL of tissue homogenate mixed with 1.9 mL of phosphate buffer. The reaction was initiated by adding 1 mL of H_2O_2 solution in buffer, followed by monitoring the decrease in extinction at 240 nm for 3 min at intervals of 1 min. A specific activity at 25 °C is defined as the amount of H_2O_2 consumed per min per mg of protein.

Catalase (U/mg protein) = [(ΔA/min x 1000 x 3) / (43.6 x mg protein in tissue)]

In this case, 43.6 represents the molar coefficient of H_2O_2.

2.2.8.3. Determination of glutathione (GSH) content

In this study, glutathione was determined in accordance with the method described by (Moron *et al*., 1979).

Principle

A yellow complex is produced by the reaction of reduced glutathione (GSH) with Ellman's reagent (DTNB), which can be quantified spectrophotometrically at 412 nm.

Procedure

Approximately 0.5 mL of the sample (tissue or hemolysate) was mixed with 125 μL of TCA (25%) and cooled on ice for 5 min. After shaking the reaction mixture gently, 600 μL of 5% TCA was added and the mixture was centrifuged for 10 min at 2000 rpm. In order to perform this experiment, 700 μL sodium phosphate buffer (0.2 M, pH 8.0) and freshly prepared 2 mL of DTNB (0.6 mM in 0.2 M phosphate buffer) was mixed with approximately 300 μL of the supernatant. An absorbance measurement at 412 nm was conducted on the reaction mixture. Based on the standard graph plotting GSH concentrations from 10 to 50 nmoles, the GSH content of the sample was estimated. The concentration of GSH in blood was expressed as nmol/g of hemoglobin and as nmol/mg protein in tissues.

2.2.8.4. Determination of lipid peroxidation

A method of (Ohkawa *et al.*, 1979) was used in order to determine the level of lipid peroxidation in tissue as determined by thiobarbituric acid reacting substances (TBARS).

Principle

This assay produces spectrophotometrically detectable pink coloured complex, thiobarbituric acid reactive substances (TBARS) based on the reaction between malondialdehyde (MDA), the product of lipid peroxidation, and TBA.

Procedure

There were approximately 400 μL of tissue homogenate added to the reaction mixture containing 0.2 mL of 8% SDS, 1.5 mL of acetic acid (20%, pH 3.5) and 0.8% TBA, making up the final volume to 4 mL using distilled water. After boiling for 1 hr at 95°C, the reaction mixture was cooled under running water. Upon cooling, 5 mL of pyridine: butanol (15:1) was added, mixed well, and centrifuged at 3000 rpm for 10 min. A measurement of the absorbance of the supernatant was made at 532 nm. Using the standard graph plotted for different MDA concentrations (1-10 nmoles), the concentration of MDA in the tissue was estimated and expressed in nmol of MDA/mg protein.

2.2.9. Estimation of serum markers

2.2.9.1. Estimation of serum glutamate pyruvate transaminase (SGPT)

An IFCC (International Federation of Clinical Chemistry) kinetic method was used to determine the activity of the SGPT or alanine aminotransferase (ALT) (Thefeld *et al.*, 1974).

Principle

An enzyme known as ALT catalyzes the transfer of amino groups from alanine to α-ketoglutarate, resulting in the formation of pyruvate and L-glutamate. L-lactate and NAD are then formed by the reaction between pyruvate and NADH in the presence of LDH. Due to the fact that NADH absorbs light at 340 nm while NAD does not, the rate at which the absorbance decreases is correlated with the ALT activity in the sample.

Procedure

To prepare the working reagent, 4 mL of tris, L-alanine, and lactate dehydrogenase were mixed with 1 mL of 2-oxaloglutarate and NADH. One mL of working reagent was mixed with a volume of 100 μL of the serum. After mixing for 1 min, the initial absorbance was measured at 340 nm, and subsequent measurements were recorded at 1-min intervals for the next 3 min.. An estimation of ALT was made using the following formula:

$$ALT/GPT \ (U/L) = \Delta A/min \ x \ 1746$$

where, ($\Delta A/min$) represents the average change in absorbance/min obtained through the subtraction of each reading from the previous one, followed by taking the average of the values.

2.2.9.2. Estimation of serum glutamate oxaloacetate transaminase (SGOT)

SGOT or aspartate aminotransferase (AST) activity was determined by the method presented by (Reitman and Frankel, 1957).

Principle

The Aspartate aminotransferase (AST), also known as Glutamate Oxaloacetate Transaminase (GOT) catalyses the conversion of L-aspartate and α-ketoglutarate into oxaloacetate and L-glutamate by the transamination reaction. A corresponding hydrazine will be formed when the unstable oxaloacetate formed combines with 2,4-dinitrophenylhydrazine (2, 4-DNPH) colour reagent. Under alkaline conditions, the absorbance of the resulting brown coloured complex can be determined spectrophotometrically at 505 nm.

Procedure

The following four reaction systems were maintained: blank, standard, test (for each serum sample) and control (for each serum sample). Each test tube was added with 250 μL of buffered aspartate - α- ketoglutarate substrate (pH 7.4). The test and standard were mixed well by adding 50 μL of serum and 50 μL of working pyruvate standard (8 mM). Following incubation at 37°C for 60 min, 250 μL of 2,4-DNPH colour reagent were added to all tubes. The blank and control serum samples were then mixed with 50 μL of distilled water and 50 μL of each serum sample, respectively, and incubated for 20 min at room temperature. In the following 15 min, 2.5 mL of NaOH solution (0.4 N) was added to all tubes, mixed thoroughly, and the absorbance was determined spectrophotometrically against distilled water as a blank. The calculation of enzyme activity was conducted using the following formula:

AST (GOT) activity (IU/L) = [(Absorbance of Test - Absorbance of Control)/ (Absorbance of Standard - Absorbance of Blank)] × Conc. of Standard

2.2.9.3. Estimation of alkaline phosphatase (ALP) activity

An estimate of the ALP activity was made using the method developed by (Kind and King, 1954).

Principle

Phenyl phosphate is converted to inorganic phosphate and phenol in serum by alkaline phosphatase at pH 10.0. The phenol thus formed reacts with 4-aminoantipyrine in the presence of potassium ferricyanide in an alkaline medium. The measurement of the resulting orange-red colored complex absorbance was done at 510 nm. The intensity of the colour formed is proportional to the activity of the enzyme.

Procedure

During this study, four reaction systems were maintained -- blanks, standards, test samples (for each serum sample), and control samples (for each serum sample). The test tubes were filled with 0.5 mL of working buffered substrate and 1.5 mL of distilled water, mixed well, and incubated at 37 °C for 3 min. The test and standard were dispensed with 50 μL serum and 50 μL of phenol, respectively, mixed thoroughly, and incubated under 37 ºC for 15 min. All tubes were then filled with 1 mL of chromogen reagent. To the

corresponding control tubes, serum was added in a volume of 0.05 mL each and mixed well. An absorbance measurement of 510 nm was taken within 15 min in a spectrophotometer with distilled water as the reference. In order to calculate enzyme activity, we used the following formula:

ALP activity (KA/dL) = [(Absorbance of Test-Absorbance of Control)/(Absorbance of Standard-Absorbance of Blank)] × 10

The activity (KA/dL) is expressed in IU/L by multiplying the value by 7.1.

2.2.9.4. Estimation of lactate dehydrogenase (LDH) activity

In this study, the LDH activity was determined using the method described in (McQueen, 1975).

Principle

The lactate dehydrogenase catalyses the reduction of pyruvate with NADH to produce NAD. As NADH is oxidized into NAD, absorbance decreases proportionally to LDH activity in the serum.

Procedure

A 4:1 mixture of Tris buffer (pH 7.4, 80 mM), pyruvate (1.6 mM), sodium chloride (200 mM), with NADH (240 mM) was prepared as a working reagent. To a volume of 1 mL of the working reagent, 10 μL of serum was added, well mixed, and incubated at 37 °C for 1 min. A change in absorbance at 340 nm was measured every min for 3 min. Based on the following formula, enzyme activity was calculated:

$$\text{LDH activity (U/L)} = (\Delta \text{ OD / min}) \times 16030$$

2.2.9.5. Estimation of total bilirubin

A spectrophotometric determination of bilirubin level was carried out using (Walters and Gerarde, 1970) method.

Principle

The reaction between sulfanilic acid and sodium nitrite produces diazotized sulfanilic acid. An azobilirubin complex is formed when bilirubin reacts with diazotized sulfanilic acid in the presence of diazo reagent (TAB). The complex is measured using a spectrophotometer at a wavelength of 546 nm.

Procedure

The total bilirubin reagent (28.9 mmol/L of sulfanilic acid and 9 mmol/L of TAB) was pipetted into test tubes in a volume of 1 mL. A total of 20 μL of activator and 50 μL of serum were added to this, and it was incubated at room temperature for 5 min. At 546 nm, the absorbance of this reaction mixture was measured. The reagent blanks without serum were also prepared simultaneously. According to the following formula, the concentration of bilirubin in the sample was calculated:

Total bilirubin concentration (mg/dL) = OD of the test – OD of blank × 25

2.2.9.6. Estimation of total protein

The protein concentration was determined using the method developed by (Lowry *et al*., 1951).

Principle

Folin-Ciocalteau reagent consists of sodium tungstate, molybdate and phosphate, and reacts with phenolic groups on tyrosine and tryptophan residues in a protein to form a blue coloured complex. The intensity of the colour depends on the amount of aromatic amino acids present and therefore differs for different proteins.

Procedure

Using distilled water, one mL of the test sample (10 μL) was prepared and incubated at room temperature for 10 min, with 5 mL of alkaline copper sulphate reagent (containing 0.5% copper sulphate in 1% sodium potassium tartarate and 2% sodium carbonate in 0.1 N NaOH in the ratio of 1:50). The folin-ciocalteau reagent diluted to 1:1 with distilled water (0.5 mL) was added and incubated for 30 min. At 660 nm, the reaction mixture's absorbance was measured. By using different concentrations of bovine serum albumin (BSA), the standard graph was plotted to determine the protein content.

2.2.9.7. Estimation of serum urea

An enzymatic UV method was used to determine the amount of urea present in serum (Young *et al*., 1975).

Principle

The urease enzyme converts urea in a sample into ammonia and carbon dioxide. Using

this modified method, glutamate and NAD are generated via a reaction between ammonium ions, α-ketoglutarate and NADH. In fixed time intervals, the rate of oxidation of NADH to NAD is proportional to the urea concentration, which can be determined by monitoring the decrease in absorbance at 340 nm.

Procedure

In order to prepare the working reagent, 4 volumes of BUN reagent were mixed with 1 volume of urease enzyme. A mixture of working reagent (1 mL) and serum (10 μL) was mixed well at 37 °C. A1 and A2 are the absorbance values at 340 nm after 30 and 60 sec, respectively. By subtracting A2 from A1, the change in absorbance (ΔA) was calculated. Also the same experiment was conducted with the standard. The serum concentration of urea was calculated by using the following formula:

$$\text{Urea (mg/dL)} = (\Delta A_T / \Delta A_S) \times 50$$

Where ΔA_T = change in absorbance of the test; ΔA_S = change in absorbance of the standard and 50 = concentration of the standard.

2.2.9.8. Estimation of serum creatinine

A modified version of Jaffe's two-point kinetic method was used to estimate serum creatinine concentration (Bones and Tausky, 1945, Toro and Ackermann, 1975).

Principle

A creatinine picrate complex is formed when sodium picrate (derived from picric acid present in reagent) reacts with creatinine in a sample under alkaline conditions. This orange coloured complex shows maximum absorbance at 520 nm. At 520 nm the orange coloured complex exhibits maximum absorption.

Procedure

Picric acid reagent (contains 8 mmol/L picric acid, 475 mmol/L sodium hydroxide, and 2 mmol/L EDTA) and alkaline buffer are two reagents used for creatinine estimation. For the preparation of working reagent equal volume of both these reagents are mixed. The working reagent (1 mL) and serum (50 μL) were mixed well and the absorbance of this mixture was measured at 520 nm after 30 sec (A0) and 90 sec (A1) respectively. The same experiments were also conducted with creatinine aqueous standard (2 mg/dL) and the amount of creatinine was calculated in accordance with the formula below

Serum creatinine (mg/dL) = (ΔA_T/ ΔA_S)×50

Where ΔA_T = change in absorbance of the test; ΔA_S = change in absorbance of the standard and 50 = concentration of the standard.

2.2.10. DMBA-induced mammary tumourigenesis

Using a DMBA-induced breast cancer model, the chemopreventive activity of *Saraca asoca* and *Kingiodendron pinnatum* crude extract was assessed. Each group of six female Swiss albino mice weighing between 25 and 30 g was divided into 8 groups.

Group I: Normal (without any treatment)

Group II: Control (DMBA-20 mg/mL),

Group III – Vehicle control (20 mg/mL DMBA + propylene glycol)

Group IV – Standard (20 mg/mL of DMBA + tamoxifen 10 mg/kg b.wt)

Group V – SALD- *Saraca asoca* (SA) low dose (20 mg/mL of DMBA + 250 mg/kg b.wt.)

Group VI – SAHD- *S. asoca* (SA) high dose (20 mg/mL of DMBA + 500 mg/kg b.wt.)

Group VII – KPLD- *Kingiodendron pinnatum* (KP) low dose (20 mg/mL of DMBA + 250 mg/kg b.wt.)

Group VIII – KPHD- *K. pinnatum* (KP) high dose (20 mg/mL of DMBA + 500 mg/kg b.wt.)

The DMBA (20 mg/mL) was dissolved in sesame oil and administered once a week for six consecutive weeks to all groups except group I. Propylene glycol was used to dissolve plant extracts, which were administered daily for six weeks. The standard was given orally in the aforementioned doses for the same duration every day. With the aid of a cannula attached to a feeding needle, all were administered intragastrically. Every day, the experimental and control animals underwent thorough examination. During the experiment, each pair of mouse mammary glands (6 pairs) was subjected to inspection, touching and palpitation to detect any abnormal mass that develops. At the end of the sixth week, mice were sacrificed. A cardiac puncture was used to collect the blood. Haematological analysis was done on non-coagulated blood that had been obtained in heparinized vials (Chapter 2, section 2.2.7). After centrifuging the remaining coagulated blood for 10 min at 3000 rpm, serum was separated for use in serum marker estimation,

renal function test and LDH level determination (Chapter 2, section 2.2.9).

The breast and liver tissues were removed from animals and fixed in 10% formal saline. Breast tissues for gene expression analysis was promptly added to RNAlater stabilization solution and kept at -80 °C deep freezer (section 2.2.11 of chapter 2). According to the method outlined in section 2.2.6.2 of chapter 2, tissue homogenate (10%) of breast tissue was prepared in 0.1 M tris-HCl buffer (pH- 7). Lowry's method (described in Chapter 2's section 2.2.9.6) was used to calculate the tissue's total protein content. In the homogenate, antioxidants such as superoxide dismutase, catalase and reduced glutathione were measured (section 2.2.8 of Chapter 2). Malondialdehyde (MDA) levels in the breast tissue were measured to estimate the degree of lipid peroxidation (section 2.2.8.4 of Chapter 2). A small portion of liver and breast tissues were sliced off for histopathological analysis (section 2.2.6.3 of chapter 2). A paraffin embedding was undertaken for the breast and liver tissues, which were then sectioned at 4-5 μm and subsequently stained with hematoxylin and eosin. All slides were examined under a light microscope at a magnification of 400 X and photographed (Minari *et al*., 2016). The mammary gland whole mount preparation and analysis were done by starting with dissecting the mammary pad and stretching it out on a slide. After a brief period of air drying, it was overnight fixed in Carnoy's fixative. The slides were put into a Carmine alum solution and left there for the entire night. In order to dehydrate the tissues, 70, 80, 95, and 100 % ethanol was used and the tissues were then placed in xylene for at least two days until the fats were thoroughly removed from the glands (Tolg *et al*., 2018). Images were taken of stained mammary glands mounted on slides.

2.2.11. Gene expression studies

TRIZOL was used to isolate the total RNA from the breast tissue of all the animal groups. A RevertAid cDNA first strand synthesis kit (ThermoFisher, India) was used to prepare cDNA from the isolated RNA.

2.2.11.1. RNA isolation

Tissue samples were homogenised using mortar and pestle in 1 mL TRIZOL reagent and the homogenates were transferred to tubes. The samples were incubated for five minutes at room temperature. Chloroform (0.2 mL) per mL of TRIZOL reagent was added to the homogenised sample, vigorously mixed for 15 sec, and then incubated for 2-3 min at

room temperature. The tubes were centrifuged for 15 min at 2-8 °C at 12000 x g. After carefully transferring the upper aqueous phase into a new tube, the solution was precipitated using 0.5 mL of isopropyl alcohol per utilised mL of TRIZOL reagent. The samples were centrifuged at 12000 x g for 10 min at 2 to 4 °C after being incubated for 10 min at room temperature. The supernatant was totally removed and the pellet was mixed by washing it once with 1 mL of 75% ethanol per mL of TRIZOL reagent. The sample was mixed and centrifuged for 5 min at 2-4 °C at 7500 x g. The RNA pellet was air dried for 5 to 10 min after all the remaining ethanol had been drained from it. Under -20 °C, the RNA was kept after being dissolved in 30 μL of DEPC-treated water. Electrophoresis on a 1 % gel was used to verify the integrity of the extracted RNA. Using a NanoDrop ND-1000 spectrophotometer, the amount of RNA was measured.

2.2.11.2. First strand cDNA synthesis

The RNA obtained from the mammary tissues was used to synthesise the cDNA. In a PCR tube, four μL of template DNA, one μL of OligodT primers, and seven μL of nuclease-free water were pipetted. For 5 min, tubes were incubated at 65 °C. After the incubation the mixture was frozen on ice and 4 μL of 5X reaction buffer, 1 μL of RiboLock RNase inhibitor, 2 μL of 10 mM dNTP mix, and 1 μL of Revert Aid M- MulV RT were added. After being quickly spun, the solution was incubated for 60 min at 42 °C and 5 min at 70 °C. Following incubation, the cDNA was kept at -80 °C for storage.

2.2.11.3. Quantitative Real-Time PCR (qRT-PCR)

Using qRT-PCR, the gene expression profile of four genes-ER-α1, BCL2, c-MYC and Pin 1-was investigated. In order to reduce quantification mistakes and improve the accuracy of qRT-PCR, β-actin was used as a house-keeping gene in the analysis. The table 2.3 lists the primers used for qRTPCR.

The PCR amplification was performed in a reaction mixture of 20 μL containing

    a)   SsoAdvancedTM Universal SYBR® Green Supermix – 10 μL

    b)   Forward primer   - 1 μL

    c)   Reverse primer   - 1 μL

    d)   DNA Template   - 5 μL

    e)   Nuclease free water   - 3 μL

        Total volume   - 20 μL

Table 2.3. Primers used in qRT-PCR analysis

Sl. No.	Gene	Primer Sequences (5'-3')	Reference
1	ER-α1	F: GGCACATGAGTAACAAAGGCA R: GGCATGAAGACGATGAGCAT	(Zeweil *et al.*, 2019)
2	BCL2	F: GTATGATAACCGGGAGATCG R: AGCCAGGAGAAATCAAACAG	(Zeweil *et al.*, 2019)
3	c-MYC	F: CTCCACTCACCAGCACAACT R: CGTTCCTCCTCTGACGTTCC	(Karimi *et al.*, 2020)
4	PIN1	F: TGATCAACGCTACATCCAG R: CAAACGAGGCGTCTTCAAAT	(Wang *et al.*, 2016)
5	β-actin	F: TCTTCCAGCCTTCCTTCCTG R: CACACAGAGTACTTGCGCTC	(Zeweil *et al.*, 2019)

Amplification was performed using the following programme

Stage	Temperature (ºC)	Time (Sec.)
1. Polymerase Activation and DNA Denaturation	95	30
2. Denaturation	95	15
3. Annealing/Extension	60	30

A total of 45 cycles were performed for steps 2 and 3

2.2.11.4. Calculation of fold change

The resulting Ct values were then used to calculate the ΔCt and $\Delta\Delta$Ct of the target genes in comparison to the house-keeping gene using the formula (Schmittgen and Livak, 2008),

ΔCt = Ct gene of interest **-** Ct internal control

where, internal control refers to the reference gene

$\Delta\Delta$Ct = ΔCt (Sample A) - ΔCt (Sample B) = [(Ct gene of interest – Ct internal control)   Sample A – (Ct gene of interest – Ct internal control) Sample B]

where, Sample A represents the treated sample and Sample B represents the untreated sample

Fold change = $2^{-\Delta\Delta Ct}$

2.2.12. 4T1 induced TNBC mouse model

A mouse model for triple-negative breast cancer using murine 4T1 was developed to analyse the effect of plant extracts against TNBC cancers. The female BALB/c mice weighing about 25-30 g were split into eight groups with six animals in each group.

Group I- Normal (without any treatment)

Group II- Control

Group III- Vehicle control (propylene glycol)

Group IV- Standard (Doxorubicin - 10 mg/kg b.wt)

Group V- SALD- *Saraca asoca* (SA) low dose (250 mg/kg b.wt.)

Group VI- SAHD- *S. asoca* (SA) high dose (500 mg/kg b.wt.)

Group VII- KPLD- *Kingiodendron pinnatum* (KP) low dose (250 mg/kg b.wt.)

Group VIII- KPHD- *K. pinnatum* (KP) high dose (500 mg/kg b.wt.)

As a pre-treatment, the plant extract was dissolved in propylene glycol and administered intragastrically by gavage over the course of ten days using a cannula attached to a feeding needle. Before counting, the 4T1 cells underwent trypsinization and washed thrice with phosphate buffer saline. The female BALB/c mice (5 weeks old) had their fourth mammary fat pads injected with 75 μL of PBS containing 2×10^6 cells. From the day after the injection to the 20th day, the plant extract was administered. Every day, the experimental and control animals underwent thorough inspection. The mammary glands of the mouse were examined, touched, and palpated. Every other day, the primary tumour was measured with a vernier calliper while the tumour-bearing mice were weighed. According to the following equation, the tumour volume was determined: V= 4/3 r_1^2 r_2, where r_1 denotes the minor radius and r_2 the major radius (Ma *et al*., 1991). All animals were sacrificed after 20 days following an overnight fast. Heart punctures were used to collect the blood and the hematopoietic parameters were analysed and relative organ

weight of the treated and untreated animals were compared. The breast and lung tissues from animals were cut out and preserved in 10% formal saline. The tissues were encased in paraffin, sliced into 4-5 μm sections and then dyed with hematoxylin/eosin stain. Slides underwent 400 X magnification light microscopy analysis and photography.

2.2.13. Anti-inflammatory activities

2.2.13.1. *In-vitro* anti-inflammatory activities

2.2.13.1.1. Nitric oxide scavenging assay

The Griess reagent, which was prepared by mixing 1% sulphanilamide with 2.5% phosphoric acid and 0.1% naphthyl ethylene diamine dihydrochloride with 2.5% phosphoric acid immediately prior to use, was used in nitric oxide scavenging experiments (Ebrahimzadeh *et al*., 2010). The mixture of sodium nitroprusside in PBS (0.5 mL) and 1 mL of each of the various concentrations of crude extract was incubated for three hours at 25 °C. A similar volume of freshly prepared Griess reagent was mixed with the extract. In the same way as the test sample, a control sample without extracts was prepared using the exact same amount of buffer. After the reaction mixture (150 μL) was placed into a 24-well plate, a UV/VIS spectrophotometer was employed to determine its absorbance at 546 nm. An analysis of the percentage inhibition of the extract was performed (% scavenging of NO = Abs. of control - Abs. of test/ Abs. of control x 100) and a graph was plotted.

2.2.13.1.2. 5-Lipoxygenase inhibition assay

This assay is based on a reaction between oxygen and linoleic acid mediated by 15-lipoxidase (15-LD). By using a UV-visible spectrophotometer, the conversion of linoleic acid to 13-hydroperoxylinoleic acid is spectrophotometrically measured by the appearance of conjugated dienes which have a maximum absorption at 234 nm. A reaction mixture (1 mL) containing 100 μM linoleic acid (in methanol) and 50 U of lipoxygenase enzyme in PBS was prepared by adding varying concentration of extracts to the reaction mixture. A UV-visible spectrophotometer was employed to determine the absorbance at 234 nm after incubating the reaction mixture for 1 hour at room temperature. The equation that follows was used to calculate the percentage inhibition.

Inhibition = (A control – A test) /A control) x100

Where A control represents the absorbance of the control sample, whereas A test represents the absorbance when the extract samples are present (Ben-Nasr *et al*., 2015).

2.2.13.1.3. Prevention of nitric oxide generation in LPS-stimulated RAW 264.7 cells by extracts

The incubation of murine macrophage, RAW 264.7 cells with different concentrations (0 to 100 μg/mL) of *S. asoca* and *K. pinnatum* crude methanolic extracts was conducted at 37 °C in the presence of lipopolysaccharide (LPS, 1.0 μg/mL) for 24 hr (Hong *et al*., 2015). Following the transfer of the cell supernatant onto a fresh well plate, 100 μL of each well's supernatant was combined with a similar amount of Griess reagent (5% phosphoric acid, 0.1% N-(1-naphathyl)-ethylenediamine dihydrochloride and 1% sulfanilamide) and allowed to sit for 10 min at room temperature. The concentration of nitrite was determined by measuring the absorbance at 540 nm and inhibition percentage was calculated. The MTT test was used to measure cell viability under similar experimental conditions to determine the cytotoxicity of extracts towards RAW 264.7 cells. Briefly, 100 μL of medium were transferred and each well received an addition of MTT dissolved in PBS. The cells had been incubated for four hours at 37 °C. The formazan crystals in the bottom of the wells were solubilized in 100 % DMSO after the supernatant from the cells was removed. The optical density (OD) was measured at 540 nm utilizing a microplate reader.

2.2.13.2. *In-vivo* anti-inflammatory activities

The anti-inflammatory efficacy of *S. asoca* and *K. pinnatum* extracts was assessed utilizing acute and chronic mouse models of inflammation induced by carrageenan and formalin, respectively.

2.2.13.2.1. Carrageenan induced acute paw edema

The female Swiss albino mice (25 to 30 g) were split into 7 groups of 6 mice each, and the following procedures were followed during treatment:

Group I - Control

Group II - Vehicle control (Propylene glycol)

Group III- Standard- Diclofenac (10 mg/kg b. wt)

Group IV - *S. asoca* low dose (SALD - 250 mg/kg b. wt)

Group V - *S. asoca* high dose (SAHD - 500 mg/kg b. wt)

Group VI - *K. pinnatum* low dose (KPLD - 250 mg/kg b. wt)

Group VII - *K. pinnatum* high dose (KPHD - 500 mg/kg b. wt)

The animals received pre-treatment for four days, with plant extracts or a dose of diclofenac. The inflammation was induced in the right hind paw of all animals on the fifth day, 1 hr after the extract or diclofenac administration. This was done by subplantar injection of 0.05 mL of 1% carrageenan in 0.9% of normal saline solution (NSS) (Winter *et al*., 1962). Using a Vernier caliper, the paw thickness was measured 1 hr prior to and after the carrageenan injection at 1-hr intervals for 6 hr. The percentage of inhibition was estimated using the formula below:

$$\% \text{ of inhibition} = [(PT-PO) \text{ treated} / (PT-PO) \text{ control}] *100$$

where PT = Thickness of the paws at various time intervals and PO= Initial paw thickness.

2.2.13.2.2. Formalin induced chronic inflammation

The female Swiss albino mice (25-30g) were separated into 7 groups of 6 mice each, and the following treatments were carried out on the groups of mice

Group I - Control

Group II - Vehicle control (Propylene glycol)

Group III- Standard- Diclofenac (10 mg/kg b. wt)

Group IV - *S. asoca* low dose (SALD - 250 mg/kg b. wt)

Group V - *S. asoca* high dose (SAHD - 500 mg/kg b. wt)

Group VI - *K. pinnatum* low dose (KPLD - 250 mg/kg b. wt)

Group VII - *K. pinnatum* high dose (KPHD - 500 mg/kg b. wt)

The animals were administered with plant extracts or diclofenac as pre-treatment for 7 days, followed by further 7 days of treatment. After extract or diclofenac administration on the eighth day, chronic inflammation was generated by sub-planar injection in the right hind paw of mice in all groups by freshly prepared 0.05 mL of 1% formalin (Chau, 1989). The thickness of the paw was determined 1 hr earlier and every day for the following 6 days after formalin injection using a Vernier caliper. The percentage of inhibition was estimated using the formula below.

$$\% \text{ of inhibition} = [(PT-PO) \text{ treated} / (PT-PO) \text{ control}] * 100$$

where PT = Thickness of the paws at various time intervals and PO = Initial paw thickness

2.2.14. *In vivo* antitumour activity

2.2.14.1. DLA induced solid tumour model

The female Swiss albino mice, weighing between 25-30 g, were separated into seven groups, each comprising six animals. Subsequently, each group received the following treatments.

Group I - Control

Group II - Vehicle control (Propylene glycol)

Group III- Standard- Cyclophosphamide (10 mg/kg b.wt.)

Group IV - *S. asoca* low dose (SALD - 250 mg/kg b. wt.)

Group V - *S. asoca* high dose (SAHD - 500 mg/kg b. wt.)

Group VI - *K. pinnatum* low dose (KPLD - 250 mg/kg b. wt.)

Group VII - *K. pinnatum* high dose (KPHD - 500 mg/kg b. wt.)

The DLA cells were harvested from the tumour-bearing mice's peritoneal cavity, washed with PBS, and then injected intramuscularly into the right hind limb of each animal in 100 μL of cell suspension containing approximately 1×10^6 cells. The extracts were administered continuously for 10 days, starting 24 hr after the induction of the tumour. Diameter of the developed tumour was measured in two perpendicular planes with a Vernier caliper to determine the solid tumour development on the animal in each group. Up to the 30th day, the readings were recorded every three days. The formula used to find the tumour volume was $V = 4/3\, r_1^2\, r_2$, where r_1 indicates the minor radius and r_2 indicates the major radius (Ma *et al*., 1991). The formula used for calculating the percentage of tumour growth inhibition was % inhibition = [(C-T)/C] x 100, Where C represents control animals volume of tumour on 30th day and T represents treated animals volume of tumour on 30th day. Tumour weights of all groups were recorded.

2.2.14.2. EAC induced ascites tumour model

The mice were grouped together and the treatment plan was the same as it was for the solid tumour model. The following treatments were given to each group of seven groups of six female Swiss albino mice, each weighing between 25 and 30 g.

Group I - Control

Group II - Vehicle control (Propylene glycol)

Group III- Standard- Cyclophosphamide (10 mg/kg b.wt.)

Group IV - *S. asoca* low dose (SALD - 250 mg/kg b. wt.)

Group V - *S. asoca* high dose (SAHD - 500 mg/kg b. wt.)

Group VI - *K. pinnatum* low dose (KPLD - 250 mg/kg b. wt.)

Group VII - *K. pinnatum* high dose (KPHD - 500 mg/kg b. wt.)

In order to induce the tumour, EAC cells at 1×10^6 cells/mouse were injected intraperitoneally. A course of drug administration was initiated within 24 hr of tumour induction and carried on continuously for ten days in a row. To determine the extract's impact on ascites tumours, mice were observed daily for mortality over a period of 30 consecutive days. The mice's percentage increase in life span (% LS) was computed using the mortality data. In this case, the formula was as follows:

% LS = [(MS of drug treated group / MS of control group) - 1] x 100, in which MS refers to the mean survival time (Mazumdar *et al*., 1997).

2.2.15. Immature rodent uterotropic bioassay

Approval No: ACRC/IAEC/17(1)/P-05, dated 22-12-2017, was obtained from the Institutional animal ethical committee prior to the commencement of the study. The good laboratory practice and quality assurance guidelines proposed by the Organisation for Economic Co-operation and Development (OECD), were followed throughout the whole investigation for the test of estrogenicity or antiestrogenicity of compounds (OECD, 2007). Wistar pregnant rats were obtained from the Small Animal Breeding Station (SABS) at the Kerala Veterinary and Animal Sciences University (KVASU) in Thrissur, Kerala. Animals were sorted and housed separately in polypropylene casings with paddy husk utilized as bedding under standard laboratory conditions. All animals had complete access to purified water and regular rat feed. The temperature was kept stable at $22 \pm 3°C$ with a relative humidity of 50-60% and daily lighting sequence of 12 h light/dark cycles. The pregnant rats underwent daily observation and the day of delivery was designated as the first postnatal day. Initially, sex determination was made by locating areolae with or without nipple buds in the litters on postnatal day 12, and the sex was further verified through measurement of anogenital spacing on postnatal day 16. Female animals were identified by the presence of areolae and a decreased anogenital distance. The dams and the young animals were housed together until weaning. The animals were housed in

groups of up to three after weaning, since social group housing is advised by OECD due to the immature animal's young age. The animals were administered with single dose of plant extracts at a concentration of 2500 mg/kg/b.wt., via oral gavage and observed for fourteen days in order to determine the doses without toxicity or discomfort to animals thus safeguarding animal survival. The low dose and high dose for the experiment were taken as $1/10^{th}$ and $1/5^{th}$ of this dose, respectively.

For estrogenicity study, immature Wistar rats that were 16 days old and weighed between 25 and 35 g were sorted into 7 groups of 5 rats each as follows:

Group I - Control

Group II - Vehicle control (Propylene glycol)

Group III- Standard- 17β-estradiol (100 μg/kg b.wt., p.o.)

Group IV - *S. asoca* low dose (SALD - 250 mg/kg b. wt)

Group V - *S. asoca* high dose (SAHD - 500 mg/kg b. wt)

Group VI - *K. pinnatum* low dose (KPLD - 250 mg/kg b. wt)

Group VII - *K. pinnatum* high dose (KPHD - 500 mg/kg b. wt)

Plant extracts and 17β-estradiol were orally administered to the animals over the course of five days. On the final day of the study, young rats' body weights were measured (21st postnatal day) and after 24 hr of the last treatment animals were sacrificed. Since accumulation of fluid is an estrogen response, the uterus was carefully dissected to prevent fluid loss and maintain the structural integrity of both uterine horns. The fat tissues were trimmed off from the uterus, blotted on filter paper and promptly measured on a weighing balance to find the uterine wet weight. A 10% formalin solution was used to fix the tissues of the uterus and ovary, which were then dehydrated in ethanol solutions, washed in xylene and mounted in paraffin wax. To examine the histopathological alterations in the tissues, sections with a thickness ranging from 5–6 μm were sliced by means of a rotary microtome and dyed with hematoxylin and eosin stain. A cardiac puncture was used to collect blood and serum was separated. The radioimmunoassay (RIA) was employed to determine the serum estrogen level (Shahid *et al*., 2015).

For detection of antiestrogenicity (OECD, 2006c), 16 days old immature Wistar rats (25-35 g) were divided into 7 groups of 5 rats each as follows:

Group I – Control (17β-estradiol-100 μg/kg b.wt)

Group II - Vehicle control (Propylene glycol) +17β-estradiol-100 μg/kg b.wt

Group III- Standard- tamoxifen (20.0 mg/kg b. wt) +17β-estradiol (100 μg/kg b.wt)

Group IV - *S. asoca* low dose (SALD - 250 mg/kg b. wt) +17β-estradiol-100 μg/kg b.wt

Group V - *S. asoca* high dose (SAHD - 500 mg/kg b. wt) +17β-estradiol-100 μg/kg b.wt

Group VI - *K. pinnatum* low dose (KPLD - 250 mg/kg b. wt) +17β-estradiol-100 μg/kg b.wt

Group VII - *K. pinnatum* high dose (KPHD - 500 mg/kg b. wt) +17β-estradiol-100 μg/kg b.wt

The animals in all groups were administered with 17β-estradiol. Plants extracts and tamoxifen were given to respective groups for two weeks continuously along with 17β-estradiol. Animals were euthanized 24 hours following the final treatment. Uterus and ovaries were removed and weighed as mentioned above. As described above, histopathological analysis of the uterus and ovary were performed and serum estrogen levels were determined by radioimmunoassay (Shahid *et al*., 2015).

2.2.16. Cytotoxicity analysis

2.2.16.1. Murine cancer cells

Murine tumour cell lines like Ehrlich ascites carcinoma (EAC) and Dalton's lymphoma ascites (DLA) were collected from the animal house capacity of the Amala Cancer Research Centre, Thrissur, Kerala and transplanted into female Swiss albino mice. Two weeks after inoculation, aseptically harvested tumour cells were centrifuged at 1000 rpm for 3 min after being rinsed in PBS (pH 7.4). In order to conduct the cytotoxicity test, the procedure was repeated twice and the cell count was finally adjusted to 10^7 cells/mL.

2.2.16.2. Isolation of spleen and thymus cells

A filter paper was used to blot the spleen and thymus excised from mice after it was washed with saline. The thymus and spleen were carefully smashed through a nylon mesh with the plunger end of the syringe into a petridish containing PBS that had half of its volume filled. A 3 min centrifugation at 2000 rpm of suspended splenocytes and thymocytes was followed by two additional rounds of washing. After re-suspension of the pellet in DMEM medium, the cell count was standardized to 10^7 cells per mL. Splenocytes and thymocytes were used in order to test the toxicity of the extracts against normal cells.

2.2.16.3. Maintenance of cell lines

In Roswell Park Memorial Institute (RPMI 1640) medium, the cell lines HCT-15, Hep G2, PC-3, HeLa, Vero, HEK293T and IEC-6 have been maintained. DMEM (Dulbecco's modified Eagle medium) was used to maintain breast cancer cells (MDA-MB-231, SKBR-3, MCF 7, T-47D, MDA-MB-468) supplemented with Fetal Bovine Serum (100% v/v), penicillin and streptomycin (100 U/mL) and kept in an incubator with 5% CO_2 at 37 °C. Upon reaching 70-80% confluency, the cells were subcultured. Subculturing involves removing the spent medium from the culture flask, washing the cells three times in sterile PBS (pH-7.4), adding 1 mL of trypsin solution containing EDTA, and incubating the mixture for one minute at 37 °C. Fresh medium of 1 mL was added and the cells were gently pipetted into single cell suspensions before being evenly distributed into new flasks. The subculturing was performed by monitoring the level of confluence of the cells.

2.2.17. Determination of cell viability

2.2.17.1. Trypan blue dye exclusion assay

The dye trypan blue is an azo dye that cannot penetrate intact cell membranes. As a result, it only enters cells with compromised membranes. As soon as the dye is introduced into the cell, it binds to the intracellular proteins, enabling it to be used for the direct identification and enumeration of live (unstained) and dead (blue) cells (Moldéus *et al*., 1978). Following the method outlined in this chapter's section 2.2.9.2, cells (DLA, EAC, spleen, and thymus cells) were isolated and their cell count was adjusted. 1 mL of PBS was used to incubate 1×10^6 cells for 3 hr with various concentrations of extract. In the control group, cells were not treated with the extract. Following the incubation period, each tube containing cells received 100 μL of trypan blue dye added to it and the mixture was carefully stirred. A hemocytometer was used to count the cells, and the below formula was employed to calculate the viable or dead cell percentage

Percentage of viable/dead cells = [(Avg C – Avg V/D) / (Avg C) x 100]

The average number of control cells and the average number of viable/dead cells are represented by Avg C and Avg V/D, respectively.

2.2.17.2. MTT assay

Assays were conducted using 3-(4, 5-dimethylthiazol-2-yl)-2, 5-diphenyltetrazolium bromide (MTT) to assess the cytotoxic potential of the extracts (Mosmann, 1983). Tetrazolium dye (MTT), which is yellow in colour, enters the cells through the mitochondria, where it is converted by mitochondrial succinate dehydrogenase into a purple coloured formazan product. An organic solvent is used to solubilize the formazan product before it is measured spectrophotometrically. The level of activity indicates the viability of the cells because the reduction is possible only in metabolically active cells. In 12 well-plates with 1 mL of culture media, 1×10^5 cells were grown for 24 hr at 37 °C. Incubation at 37 °C for 48 hr was carried out with different concentrations of extracts added to the cells. The cells had been washed with PBS and fresh medium was added to all wells after the incubated period. Each well was incubated for 4 hr with 100 μL of MTT. A millilitre of solubilization reagent (5 mL of 10% Triton X-100, 0.43 mL of 0.1 N HCl and 50 mL of isopropanol) was used to dissolve the dark blue formazan crystals that had developed by continuous aspiration and re-suspension. The coloured product's absorbance was taken at 570 nm, and the percentage viability was calculated as follows:

$$\text{Percentage viability} = [(\text{Abs T/Abs C})] \times 100$$

Here Abs C represents controls absorbance and Abs T represents the absorbance of extract treated cells. The experiments were carried out in triplicate. The percentage survival versus extract concentration was plotted to calculate the IC_{50}.

2.2.17.3. Estrogen-screen assay

The breast cancer cell lines expressing ERα (MCF-7) and ERβ (MDA-MB-231) were cultured in DMEM (Dulbecco's Modified Eagle's Medium) with fetal bovine serum (FBS) and phenol red as a pH indicator under 37°C conditions with 5% CO_2 and 95% humidity. Cell count of 5×10^4 cells/mL were plated in 24-well culture plates and provided ample time to adhere. After 24 hr, the seeding medium was discarded and replaced with phenol red-free DMEM containing fetal bovine serum that had been treated with charcoal dextran (Han *et al*., 2002). The cells were exposed to various concentrations of extracts of both plants and 17β-estradiol (1–5 nM), before being incubated for three days at 37°C. The test had a blank that contained a complete culture devoid of cells. After

incubation, MTT was added on every well and kept for four hours. The solubilization reagent, which contained concentrated HCL, isopropanol and Triton X 100, was used to continuously aspirate and re-suspend the dark blue formazan crystals formed until they were completely dissolved. At 570 nm, the coloured product's absorbance was measured. The percentage of cell growth was calculated by analyzing the percentage of the treated cell population to the untreated control, determined by their relative absorbance measured with the MTT assay (Mosmann, 1983).

2.2.18. Staining of cellular morphological features

2.2.18.1. Crystal violet staining

The crystal violet assay involve using crystal violet to stain cells that are adhered to cell culture plates. The technique depends on adherent cells being detached from cell culture plates due to the effect of an agent and the living cells that are still attached staining with crystal violet. After reaching 90% confluency, MDA-MB-231 cells (0.5×10^5) were plated in 24 well culture plates consisting of media and maintained for 24 hours at 37 ℃. The cells were then exposed to various extract concentrations at 37 °C for 48 hr. The medium was discarded following incubation, and the wells were properly rinsed with PBS for fixation and staining. Afterwards, it was fixed with methanol and allowed to sit at room temperature for 5 min. After the fixation solution was removed, 0.5% crystal violet was added, and the mixture was let to remain for 1-2 min at room temperature. After gently removing the crystal violet, the plates were washed with tap water and air-dried at room temperature (Feoktistova *et al*., 2016). After the plates were air-dried, images were captured at various magnifications using an inverted phase contrast microscope coupled with a digital camera.

2.2.19. Evaluation of apoptosis using various methods

2.2.19.1. Acridine orange-ethidium bromide (AO-EB) staining

For the purpose of observing nuclear changes and the formation of apoptotic bodies, acridine orange-ethidium bromide staining was utilised. Both live and dead cells will be permeated with AO, which can cause the nuclei of both to appear green, while cells that have lost membrane integrity will be permeated with EB, which causes the nuclei to appear red. Therefore the live cell's nucleus will be a typical green colour, whereas the

early apoptotic cell's nucleus will have compacted chromatin with a bright shade of green. Late apoptotic cells will have fragmented, dense chromatin exhibiting orange to red nuclei. The necrotic cells will appear orange in colour but exhibit morphologies similar to viable cells without condensed chromatin. The MDA-MB-231 cells were seeded onto sterile coverslips for 24 hr at 37 °C, followed by 24 hr treatment with different concentrations of both the plant extracts. The cells were gently rinsed with PBS upon completion of the treatment and stained with 10 μL of solution which contains AO and EtBr in the concentration of 10 μg/mL each. With the aid of a blue excitation filter (470 nm), cells were visualized under a fluorescence microscope.

2.2.19.2. Apoptotic study using Caspase-3 activation analysis

Caspase-3 activation analysis was used to examine the cytotoxicity of crude methanolic extracts of *S. asoca* and *K. pinnatum* through the apoptotic pathway. Using a cell-based fluorescence resonance energy transfer (FRET) biosensor, the expression of caspase-3 was assessed. As part of the biosensor, there were caspase-3 recognition sequences (DEVD) that served as linkers between the FRET pair of cyan fluorescent protein (CFP) and yellow fluorescent protein (YFP) with nuclear localization signals (NLS) (Pillai *et al.*, 2018). The assay was conducted using MDA-MB-231 SCAT3 NLS cells expressing stable CFP-YFP FRET-based probes. These stable cells were developed at the laboratory of Dr. T.R Santhosh Kumar, Rajiv Gandhi Centre for Biotechnology (RGCB) in Kerala, India. The cells were plated onto 96 well plates and rinsed with PBS after 24 hr. This was followed by extract treatment at varying concentrations (50-200 μg/mL) in a 5 % CO_2 incubator at 37 °C. The cells were imaged after 24 hr of incubation under an EclipseTi2 inverted fluorescence microscope from Nikon (Japan) equipped with a Lumencore Spectra X light source. Two emission wavelengths were collected ranging from 450 to 470 nm for CFP and 520 to 550 nm for YFP for cells utilizing excitation at 440 nm. The CFP/YFP ratio was computed using the Nikon NIS element software. The CFP and YFP images gathered were subjected to analysis utilizing the ratiometric scale colour code, which has a range of 0 to 2 (Goyal *et al.*, 2021).

2.2.19.3. Analysis of the cell cycle using flow cytometry

The use of flow cytometry is to quantify the amount of nuclear DNA in a cell. The suspension of single cells has been dyed with a fluorescent dye which attaches to DNA. The basic concept behind this technique is that the amount of dye in the stained sample

is relative to the DNA amount. A fluorescent signal produced by stained material may therefore be regarded as an indication of cellular DNA content. A 6-well plate was plated with MDA-MB-231 cells at a density of 1 x 10^6 cells for 16 hrs and a dose of 100 μg/mL of each extract was treated for 24 hr. A trypsinization procedure with 300 μL of trypsin-EDTA was conducted and the cells were harvested and rinsed using ice-cold PBS. The cells were then centrifuged for five minutes at 5000 rpm followed by a second wash with ice-cold PBS. After resuspension, the pellets were fixed with 70% ice-cold ethanol and incubated for 2 hr on ice. After being washed again with ice-cold PBS, the cells were then suspended in 250 μL of PBS with RNase A (20 μg/mL) and Propidium Iodide (PI - 10 μg/mL) and incubated for 30 min in dark. Once the cells had been re-suspended in PBS they were examined by flow cytometry using the BD FACSAria III (BD Biosciences, USA) and the FACS Diva 7 program was used to interpret the data.

2.2.20. Molecular docking- *In silico* prediction

The Schrodinger Maestro software was used to perform molecular docking with the aim of potential interactions between specific compounds detected in *S. asoca* and *K. pinnatum* extracts, such as β-sitosterol, kaempferol and quercetin with the intended estrogen receptors, ERα and ERβ in breast cancer cell lines. From the protein data bank, the structures of the ERα and ERβ proteins with PDB IDs 3ERT and 3OLL, respectively, were downloaded. Prior to being used as a receptor for docking, the protein structures underwent processing. During the operation, hydrogen atoms were introduced, atomic charges were assigned, and water molecules not engaged in ligand binding were eliminated. The missing chains and loops were also inserted. The protein preparation wizard was used to prepare the proteins. The import and process tab was utilized for pre-processing while the review and modify tab was used to create the tautomeric states. Utilizing the refine tab, the structures were optimized and minimized, and the protein has been prepared for further studies.

The optimized structures of the compounds (β-sitosterol, kaempferol, quercetin) were used after they had been transformed into structures with .sdf extensions. The 2D sketcher feature in the Schrodinger Maestro was used for editing the imported structures. The ligands were then each prepared using the OPLS3 force field using the ligprep wizard. A complete set of tautomers for each structure has been generated. Then, a conformational change was applied to the molecules so that to create the stable conformer with the lowest

energy. In order to build a three-dimensional grid with 0.5 Å spacing and a maximum size of 20 Å × 20 Å × 20 Å, the glide receptor grid generating wizard was employed. Using the receptor grid generation wizard, any kind of constraint can be applied including accuracy constraints, H-bond constraints, and others. This docking procedure was performed using the XP (extra precision) method because it is the most powerful and discriminating procedure. As soon as the grid and ligands were configured, docking was performed with flexible molecules and protein molecules were used as rigid molecules (Hussan *et al*., 2020).

Chapter 3
Anti-proliferative, anti-tumour activity analysis and phytochemical profiling of *S. asoca* and *K. pinnatum*

3.1. Introduction

Medicinal plants have been used by mankind since prehistoric times. A sizable portion of the populace in developing nations relies upon herbal medicines and traditional practitioners for basic healthcare requirements. The use of herbal medicine for primary health care is estimated to be used by approximately 80% of the world's population (Kamboj, 2000). India has been recognized as one of the top 12 countries in the world with respect to diversity. Over 8,000 species of herbal plants make up our herbal wealth, representing approximately half of the higher flowering plants in India. Around 70 % of the medicinal plants are found in tropical forests in the Western Ghats region (Chandra, 2016). Plants synthesize a wide range of compounds and majority of these compounds are secondary metabolites with complex chemical compositions produced in response to various forms of stress and to perform important physiological functions (Ncube and Van Staden, 2015). These compounds are of scientific and industrial interest because of their pharmacological and toxicological effects on humans.

Saraca asoca (Asoka) is a tree commonly distributed in the middle section of the Western Ghats in the Indian subcontinent. The tree is considered auspicious and legendary throughout the Indian subcontinent. In Ayurveda, it is considered an important herbal medicine that can be used either alone or in a variety of formulations. The bark of *S. asoca* is considered to be the most medicinally valuable part of the plant. There are various substances known to be present in bark, such as tannins, steroids, volatile oils, glycosides, steroidal glycosides such as *β*-sitosterol, flavonoids such as catechin and epicatechin, as well as antioxidants such as polyphenolics, gallic acid, ellagic acid, among others (Borokar and Pansare, 2017). *Asokarishta*, an Ayurvedic tonic used to treat menstruation-related problems in women, is prepared from the stem bark. It is commonly referred to as the 'friend of women' due to its specific use in treating menorrhagia and female reproductive problems (Kauser *et al*., 2016). Since raw drugs are scarce, substitution of related raw drugs are common practices in the preparation of *Asokarishta*. Occasionally, *Kingiodendron pinnatum* (Roxb. ex DC.) Harms, a towering tree indigenous to the lush evergreen woods of the Western Ghats in India, is substituted for *Saraca asoca* in the preparation of *Asokarishta*. Despite its sparse presence in the wild, this species is extensively employed as a substitute due to its remarkable stature and the potential to harvest a significant volume of bark in comparison to Asoka trees. A similar pharmacological effect has been reported to be shared by *Kingiodendron pinnatum* and

Asoka and therefore the formulations containing *Kingiodendron pinnatum* is equally effective as the one containing *Saraca asoca* (Shahid *et al.*, 2018). Also the biological properties of *K. pinnatum* have not been fully explored except antioxidant, antibacterial and anti-inflammatory activities (Sheik and Chandrashekar, 2014, Shahid *et al.*, 2018).

Numerous studies have validated the ethnobotanical claims surrounding *Saraca asoca* and have revealed its diverse pharmacological properties. These include antioxidant, antibacterial, antihyperglycemic, antipyretic, anthelmintic, and anticancer activities (Biswas and Debnath, 1972, Seetharam *et al.*, 2003, Yadav *et al.*, 2015, Sasmal *et al.*, 2012, Kumar *et al.*, 2012). Notably, research has illustrated the cytotoxic effects of *S. asoca* on several cancer cell lines, such as cervical cancer, colon cancer, breast cancer, and lung cancer cell lines (Asokan and Thangavel, 2014, Dharshini *et al.*, 2021, Yadav *et al.*, 2015). Moreover, Asoka exhibits chemopreventive effects against acute myeloid leukemia (AML) and effectively inhibits DMBA/Croton oil-induced skin papilloma formation in mice (Mukhopadhyay *et al.*, 2017, Varghese *et al.*, 1993). These findings underscore the broad pharmacological potential of *Saraca asoca*, suggesting its possible utility in treating and preventing various diseases, notably cancer. Also, the limited research conducted on *K. pinnatum* has mostly concentrated on its antibacterial, anti-inflammatory, and antioxidant effects, leaving its biological characteristics largely unexplored. Subsequently, our study aimed to explore the anti-proliferative properties of *S. asoca* and *K. pinnatum* on different cancer cell lines, with specific emphasis on breast cancer, particularly triple-negative breast cancers. Furthermore, the extracts were analysed for their anti-tumour activities, in addition to their phytochemical screening.

3.2. Materials and methods

3.2.1. Preparation of extract

The stem bark from *Saraca asoca* and *Kingiodendron pinnatum* was used for the study. The extract was prepared in methanol by stirring at room temperature overnight using a magnetic stirrer and the resulting yield was subsequently calculated (section 2.2.2 of Chapter 2).

3.2.2. Chemicals

Dimethyl sulfoxide (DMSO), isopropanol, HCl, Triton X 100, trypan blue, MTT used for

the study were acquired as per the list in section 2.1.2 of Chapter 2. The solvents employed were all of analytical grades.

3.2.3. Animals

The animals were purchased from Kerala Veterinary and Animal Sciences University (KVASU) and maintained in accordance with chapter 2's section 2.1.4.

3.2.4. Cell lines

Ehrlich's Ascites Carcinoma (EAC) and Dalton's Lymphoma Ascites (DLA) cells were grown in peritoneal cavities of mice, which were housed at the animal facility of Amala Cancer Research centre. The isolation procedure followed for these cells is detailed in section 2.1.5 of Chapter 2. Spleen and thymus cells were isolated using the procedure outlined in Chapter 2's section 2.2.16.2. The breast cancer cell lines employed in the study (MDA-MB-231, MDA-MB-468, SK-BR-3, MCF-7, T-47D), other cancer cell lines (PC-3, Hep G2, HCT 116, HCT-15, HeLa), and normal cell lines (Vero, IEC-6, HEK293T), were procured from the National Centre for Cell Science in Pune, India, and maintained as detailed in section 2.2.16.3 of Chapter 2.

3.2.5. Cytotoxicity assays

To assess the cytotoxicity of extracts on DLA, EAC, splenocytes, and thymocytes, the trypan blue dye exclusion method was employed (section 2.2.17.1 of Chapter 2). The antiproliferative effect of extracts on different cancer cell lines, like PC-3, Hep G2, HCT-15, HCT 116, and HeLa, was assessed through the MTT assay. Various breast cancer cell lines such as MDA-MB-231, MCF-7, SK-BR-3, T-47D, MDA-MB-468 expressing distinct estrogen receptors, including ERα and ERβ, were utilized in the study. The effect of extracts on normal cell lines like Vero, IEC-6 and HEK293T were also used as stated in Chapter 2's section 2.2.17.2.

3.2.6. Anti-tumour activity

Acute toxicity of the crude methanol extract of *S. asoca* and *K. pinnatum* was evaluated by administrating 2500 mg/kg b.wt. of extracts to female Swiss albino mice in compliance with the process outlined in Chapter 2's section 2.2.4. The crude extracts have been tested for their anti-tumour effects using EAC-induced ascites and DLA-induced solid tumour

models. Swiss albino female mice were divided into control and treatment groups. DLA cells were injected into the right hind limb, while EAC cells were injected into the intraperitoneal cavity of the animals. Separate experiments were conducted for each of the animal models. The animals were then treated with low doses (SALD, KPLD) and high doses (SAHD, KPLD) of *S. asoca* and *K. pinnatum* respectively, as described in sections 2.2.14.1 and 2.2.14.2. of Chapter 2.

3.2.7. Phytochemical analysis of *S. asoca* and *K. pinnatum*

The crude extract was prepared using methanol and various fractions were prepared by employing solvents with distinct polarities, including petroleum ether, ethyl acetate, methanol and water.

3.2.7.1. Screening of *S. asoca* and *K. pinnatum* crude extract and fractions

The crude extracts has shown considerable cytotoxicity to various cell lines in the study. So to determine whether the various fractions of *S. asoca* and *K. pinnatum* exhibit higher activity than the crude extract, antioxidant and cytotoxicity assays were conducted. The antioxidant radical scavenging assays and cytotoxicity assays were performed according to sections 2.2.5. and 2.2.17.1 of Chapter 2.

3.2.7.2. Qualitative and quantitative estimation of compounds in the extracts of *S. asoca* and *K. pinnatum*

The crude extract of both plants were analyzed for the occurrence of alkaloids, phytosterols, flavonoids, terpenoids, saponins, phenols, tannins and compared with the methanol fraction of extracts (section 2.2.3.1 of Chapter 2). To determine the total phenolic content, crude and methanol fractions were quantified by Folin-Ciocalteau method (section 2.2.3.1.8. of Chapter 2) and aluminium chloride colorimetric method was used to quantify the flavonoids (section 2.2.3.1.9 of Chapter 2). The findings are presented as mean ± standard deviation (SD) after the test was carried out three times.

3.2.7.3. Ultraviolet-visible spectroscopy (UV-Vis) and Fourier-transform infrared spectroscopy (FT-IR) analysis

The samples were subjected to UV-Vis spectroscopy as mentioned in section 2.2.3.2 of chapter 2. The absorption spectrum of UV-spectrophotometric analysis was recorded. Using Fourier-transform infrared spectroscopy (FTIR), the organic functional groups

contained in the samples were identified (section 2.2.3.3 of chapter 2). The raw data obtained were used to generate spectra using OriginPro 9 software. The overall spectrum transmittance data at various wavelengths was then analyzed using "spectroscopic tools," and functional groups were analyzed (https://www.science-and-fun.de/tools/).

3.2.7.4. TLC and HPTLC profiling

Qualitative thin-layer chromatography (TLC) was performed using kaempferol as the standard. High performance thin-layer chromatography (HPTLC) was done using the standards β-sitosterol and quercetin (section 2.2.3.4 of Chapter 2). As a result of the analysis, the retention factor (Rf) values have been recorded.

3.2.7.5. HPLC and GCMS analysis

The crude and methanol fractions of bark extracts of *S. asoca* and *K. pinnatum* were analyzed through high-performance liquid chromatography (HPLC) and compared with the retention times of standard, β-sitosterol. The details of the procedure are provided in section 2.2.3.5 of Chapter 2. The volatile components existing in both plants were discerned utilizing Gas Chromatography-Mass Spectrometry (GC-MS) and protocol pertaining to this is narrated in section 2.2.3.6 of Chapter 2.

3.2.7.6. HR-LCMS

High Resolution-Liquid Chromatography/Mass Spectrometry was used to conduct the chemical profiling of crude and methanol fractions of bark extracts of both plants. Details are provided in the section 2.2.3.7 of Chapter 2.

3.2.8. *In silico* prediction by molecular docking

The Schrodinger Maestro program was used to perform molecular docking to investigate possible interactions among specific compounds identified in *S. asoca* and *K. pinnatum* extracts, with the targeted estrogen receptors, ERα and ERβ in breast cancer cell lines. Binding affinity of inbuilt ligand estradiol and tamoxifen were also studied. The comprehensive technique of the docking is laid out in detail in section 2.2.20 of Chapter 2.

3.2.9. Statistical analysis

For *in vitro* investigations, values were given as mean ± standard deviation (SD), derived from three distinct experiments, whereas for *in vivo* studies, data were based on six mice

per group. The data were analyzed using one-way ANOVA following Tukey's multiple comparison test and the Mantel-Cox test for the Kaplan-Meier survival curve in GraphPad Prism 8 software. The probability values, $p<0.01$**, $p<0.05$* were considered statistically significant, whereas $p>0.05$ was considered non-significant.

3.3. Results

3.3.1. Total yield of extracts

The crude extracts from *S. asoca* and *K. pinnatum* yielded an overall of 6.832 g and 5.602 g, respectively, per 20 g of bark powder.

3.3.2. Determination of cytotoxicity by Trypan blue exclusion method

The crude methanol extracts of *S. asoca* and *K. pinnatum* shown considerable cytotoxicity against DLA cells with IC_{50} values of 42.24 ± 3.65 and 50.09 ± 3.89 μg/mL respectively and on EAC cells with IC_{50} values of 51.58 ± 2.89 and 61.66 ± 3.68 μg/mL respectively (Figure 3.1). The exposure of normal murine splenocytes and thymocytes to the extracts at doses of up to 200 μg/mL revealed no toxicity (Figure 3.2).
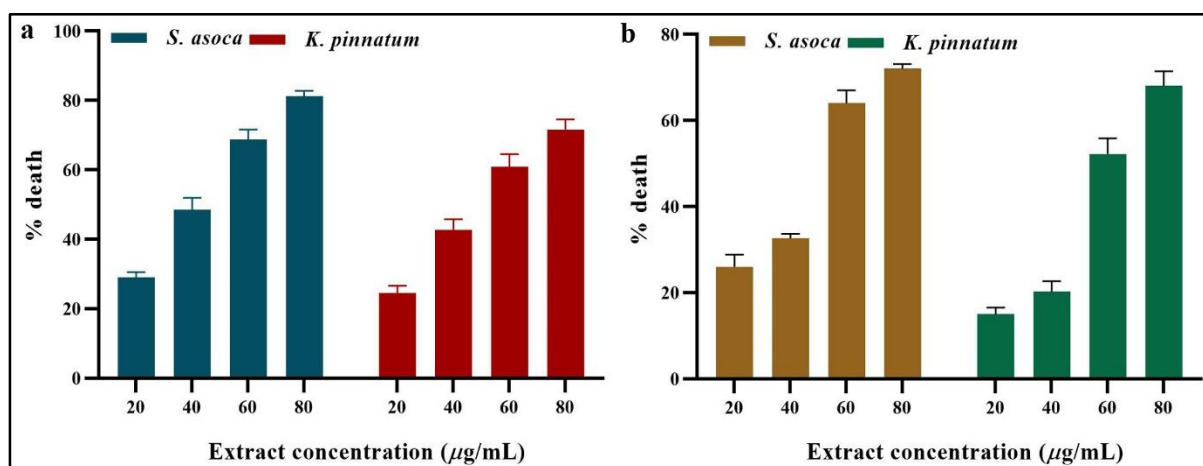
Figure 3.1. Cytotoxicity effect of plant extracts on DLA (a) and EAC (b) murine tumour cells determined by trypan blue exclusion assay. The values are presented as mean ± SD based on three separate evaluation
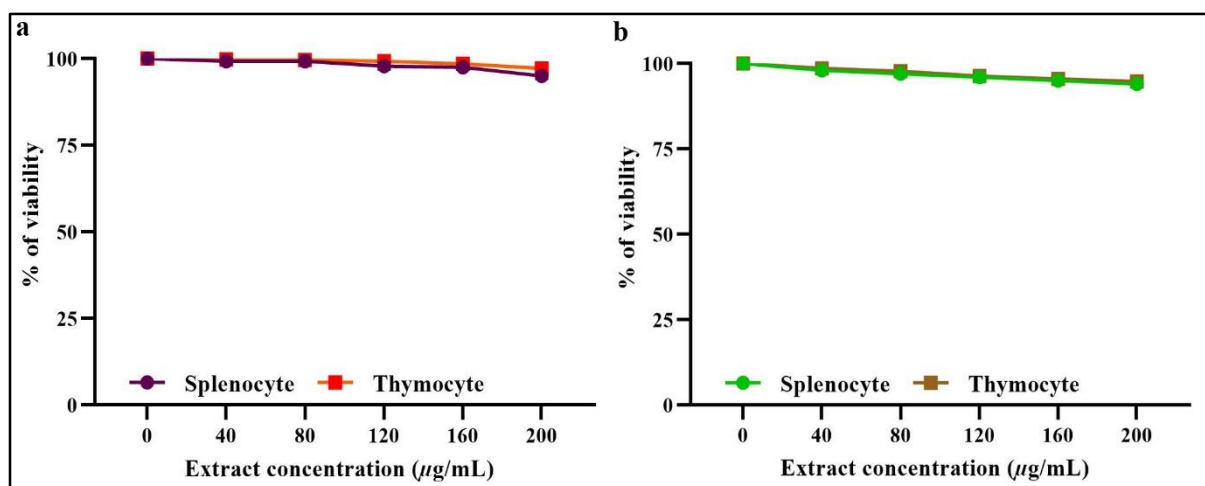
Figure 3.2. Percentage viability of normal murine cells after *S. asoca* (a) and *K. pinnatum* (b) treatment. The values are presented as mean ± SD based on three different determinations

3.3.3. Antitumour activities of extracts

3.3.3.1. Effect of extracts on DLA induced solid tumour

Animals administered with both plant crude extracts did not encounter any mortality and showed no signs of drug-related changes in behaviour, respiration, body weight, skin, intake of food and water etc. Therefore, the extracts were deemed safe at a dose level of 2500 mg/kg. In comparison to the normal group, no appreciable differences were found in the liver, heart, spleen, kidney, uterus and ovary's colour, texture, or relative organ weights. Table 3.1 shows the parameters that were observed following the administration of the plant extract compared to those the control group.

The size of the DLA-induced tumours in mice was significantly reduced when high doses of the plant extracts were given. Comparing with animals treated with SALD and KPLD (1.6 ± 0.35, 2.1 ± 0.20 g), a substantial reduction in tumour weight was observed in the SAHD and KPHD-treated animals (0.5 ± 0.25, 0.7 ± 0.15 g). The tumour weight of the control animals was determined to be 3.6 ± 0.24 g on the 30th day after tumour injection. Cyclophosphamide treated animals exhibits tumour weight of 0.9 ± 0.28 g (Fig. 3.3).

The tumour volume decreased in the extract treated groups in a dose-dependent manner. The control animal's tumour volume was determined to be 426.25 ± 37.61 cm^3 on the 30th day of the experiment (Figure 3.4). Tumour volume in the 250 and 500 mg/kg b. wt of *S.*

asoca treated groups decreased significantly (p<0.01) to 93.64 ± 10.42 cm³ (78.03% reduction) and 48.26 ± 10.7 cm³ (88.67% reduction), respectively. The tumour volume was significantly (p<0.01) reduced in the groups treated with *K. pinnatum* at doses of 250 and 500 mg/kg b. wt., reaching to 104.8 ± 20.2 cm³ (75.41% reduction) and 65.6 ± 18.1 cm³ (84.61% reduction), respectively. Tumour volume was considerably (p<0.01) reduced in cyclophosphamide-treated groups, dropping to 32.8 ± 1.6 cm³ (92.3% reduction) (Figure 3.5).

Table 3.1. Overall appearance and variations in behaviour of animals in normal and treated groups

Observations	Normal group	Treated group
Food consumption	Regular	Regular
Water consumption	Regular	Regular
Change in animal weight	None	None
Drowsiness	None	None
Alterations to skin	None	None
Looseness of bowels	None	None
Sedative effect	None	None
Overall physique	Usual	Usual
Mortality	None	None
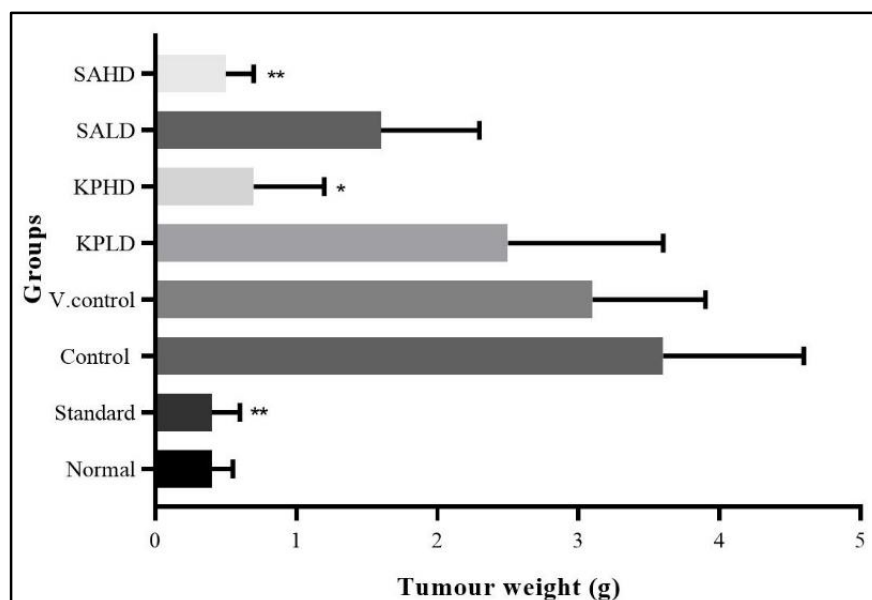
Figure 3.3. Tumour weight in grams of control and treated groups. Vehicle control – Propylene glycol, SALD – *S. asoca* 250 mg/kg b. wt, SAHD – *S. asoca* 500 mg/kg b. wt., KPLD – *K. pinnatum* 250 mg/kg b. wt, KPHD – *K. pinnatum* 500 mg/kg b. wt.
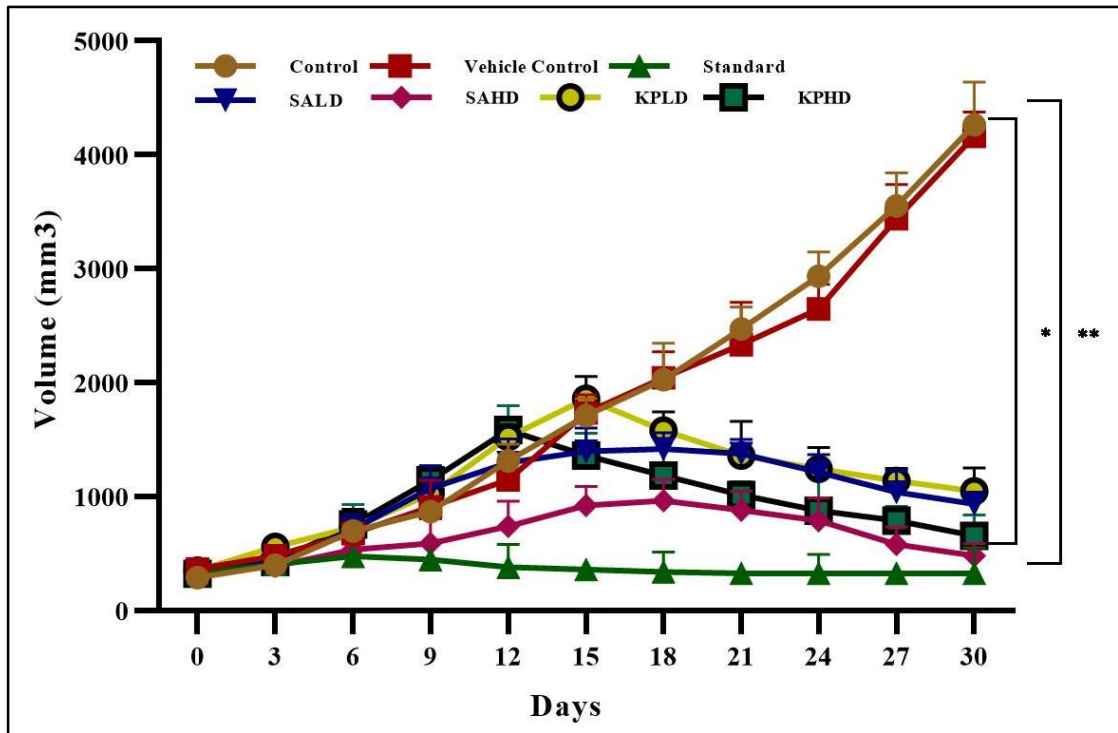
Figure 3.4. Effect of *S. asoca* and *K. pinnatum* extracts on the tumour volume of DLA solid tumour bearing mice. Vehicle control – Propylene glycol, SALD – *S. asoca* 250 mg/kg b. wt, SAHD – *S. asoca* 500 mg/kg b. wt., KPLD – *K. pinnatum* 250 mg/kg b. wt, KPHD – *K. pinnatum* 500 mg/kg b. wt. Each group contains 6 animals, and the values were calculated using the mean ± standard deviation (SD). *P<0.05 and **P<0.01 probability values are considered statistically significant

Figure 3.5. Tumour size of control and treated groups, A: Normal, B: Standard, C: Control, D: Vehicle control, E: *S. asoca* low dose (SALD), F: *K. pinnatum* low dose (KPLD), G: *S. asoca* high dose (SAHD), H: *K. pinnatum* high dose (KPHD)

3.3.3.2. Effect of extracts on EAC induced ascites tumour

The ascites tumours were developed in the mice in all groups. The body weight of EAC tumour-bearing mice increased due to a build-up in the volume of ascitic fluid. High doses of both plant extracts administered resulted in a considerable reduction in body weight and ascitic fluid accumulation (Figure 3.6). The mean survival time rate (MS) of tumour-bearing mice was substantially prolonged after treatment with *S. asoca* and *K. pinnatum* extracts. The mean survival rates for the animals in both the vehicle control and control groups are nearly identical, at 20.6 ± 4.77 and 20.3 ± 4.33 days, respectively. The animals subjected to a low dosage of *S. asoca* and *K. pinnatum* extract at 250 mg/kg b.wt exhibited survival rates of 25.2 ± 6.09 and 24 ± 7.34 days, leading to a percentage increase in life span (% LS) of 19.44 and 15.41 % LS, respectively. And animals received 500 mg/kg b.wt of *S. asoca* and *K. pinnatum* extract demonstrated elevated survival rates of 29.8 ± 7.88 (31.87 % LS) and 28.2 ± 8.72 (28.01 % LS) days, respectively. The animals administered the standard drug, cyclophosphamide, survived until 30.8 ± 7.52 days (34.09% LS), a duration similar to those that received *S. asoca* high doses (Figure 3.7).
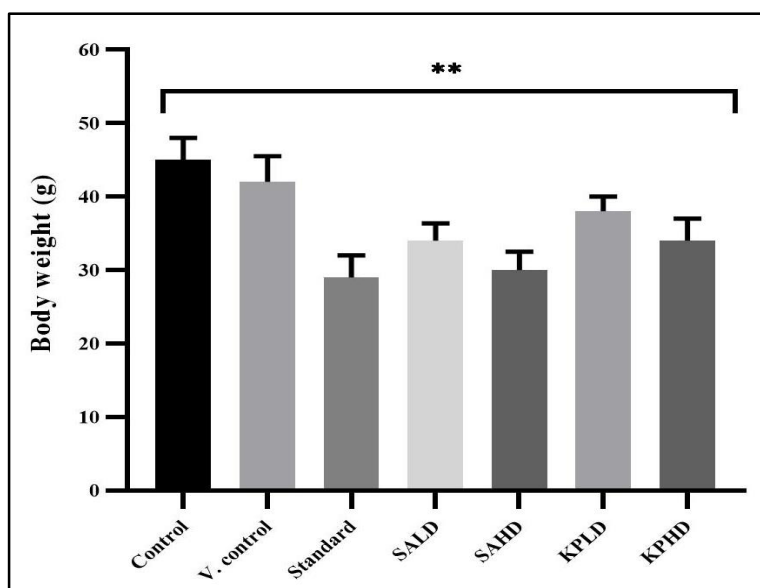
Figure 3.6. Comparison of body weight of EAC induced ascites tumour bearing mice treated with *S. asoca* and *K. pinnatum* extracts. Vehicle control – Propylene glycol, SALD – *S. asoca* 250 mg/kg b. wt, SAHD – *S. asoca* 500 mg/kg b. wt., KPLD – *K. pinnatum* 250 mg/kg b. wt, KPHD – *K. pinnatum* 500 mg/kg b. wt. Each group contains 6 animals and the values were calculated using the mean ± standard deviation (SD). **P<0.01 and *P<0.05 probability values are deemed statistically significant.
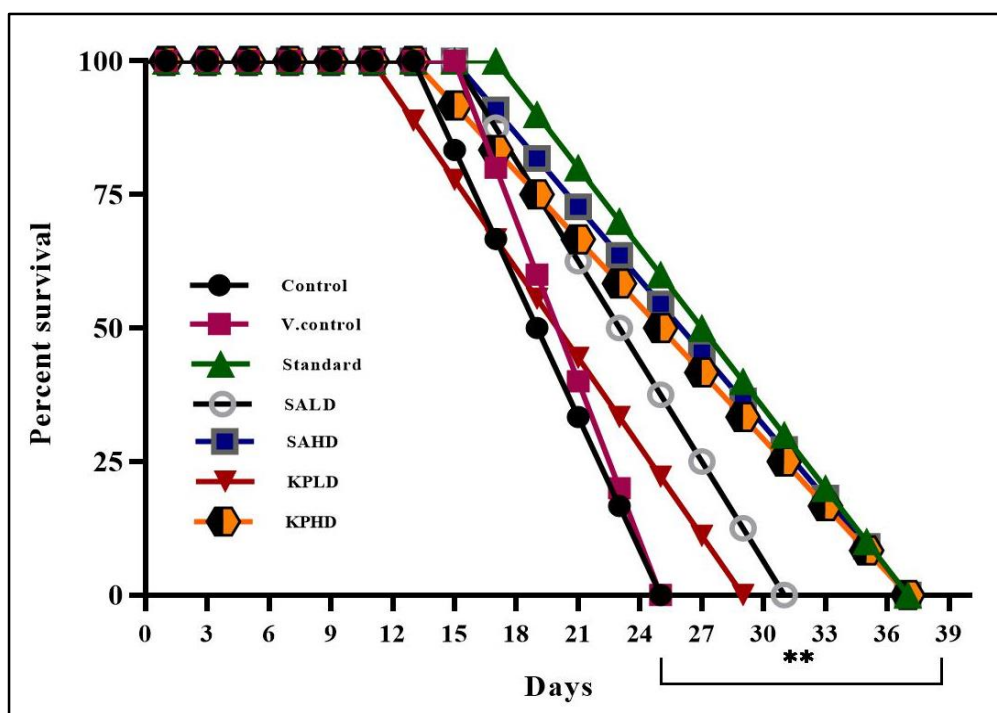
Figure 3.7. Effect of *S. asoca* and *K. pinnatum* extracts on the EAC induced ascites tumour bearing mice. Vehicle control – Propylene glycol, SALD – *S. asoca* 250 mg/kg b. wt, SAHD – *S. asoca* 500 mg/kg b. wt., KPLD – *K. pinnatum* 250 mg/kg b. wt, KPHD – *K. pinnatum* 500 mg/kg b. wt. Each group contains 6 animals and the values were calculated using the mean ± standard deviation (SD). **$P<0.01$ and *$P<0.05$ probability values are regarded as statistically significant.

3.3.4. Antiproliferative effect of extracts

The crude methanol extracts of *S. asoca* and *K. pinnatum* exhibited antiproliferative activity against a variety of cancer cell lines including PC-3, Hep G2, HCT-15, HCT 116 and HeLa (Figure 3.8). Concentration-dependent responses were shown by both plant extracts towards a range of breast cancer cells with different estrogen receptor statuses such as MDA-MB-231, MDA-MB-468, T-47D and SK-BR-3 (Figure 3.9). However, even at the highest concentration of 200 μg/mL, the extracts were unable to cause cytotoxicity in MCF-7 cell lines. The table 3.2 presents the IC$_{50}$ values for different cancer cell lines. No toxicity was shown by the extracts towards normal cells such as HEK293T, Vero and IEC-6 cell lines up to a concentration of 300 μg/mL (Figure 3.10). The morphological alterations brought about by the extracts on these cell lines were observed (Figure 3.11 to 3.16).
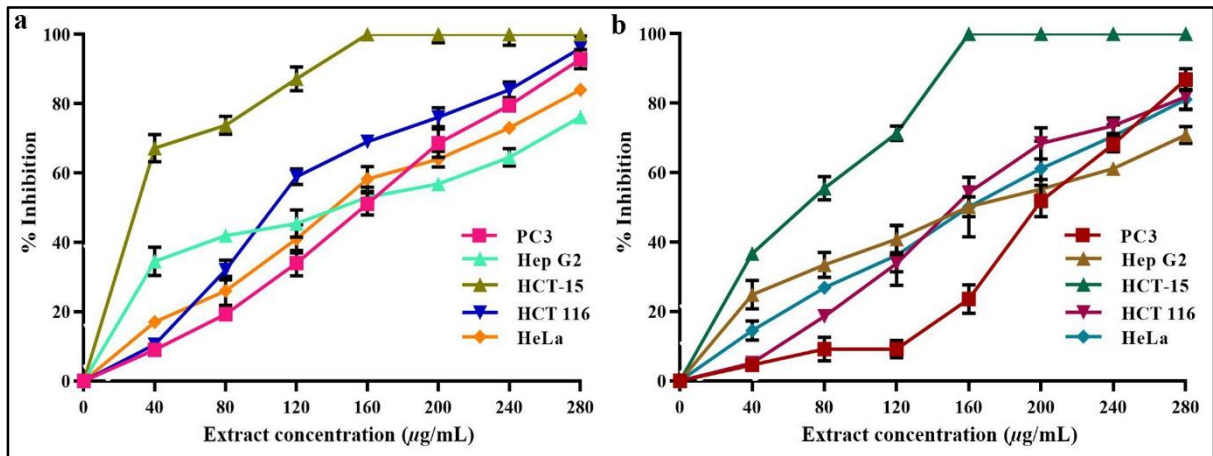
Figure 3.8. Antiproliferative effect of *S. asoca* (a) and *K. pinnatum* (b) extracts on different cancer cell lines. The values are presented as mean ± SD based on three different determinations
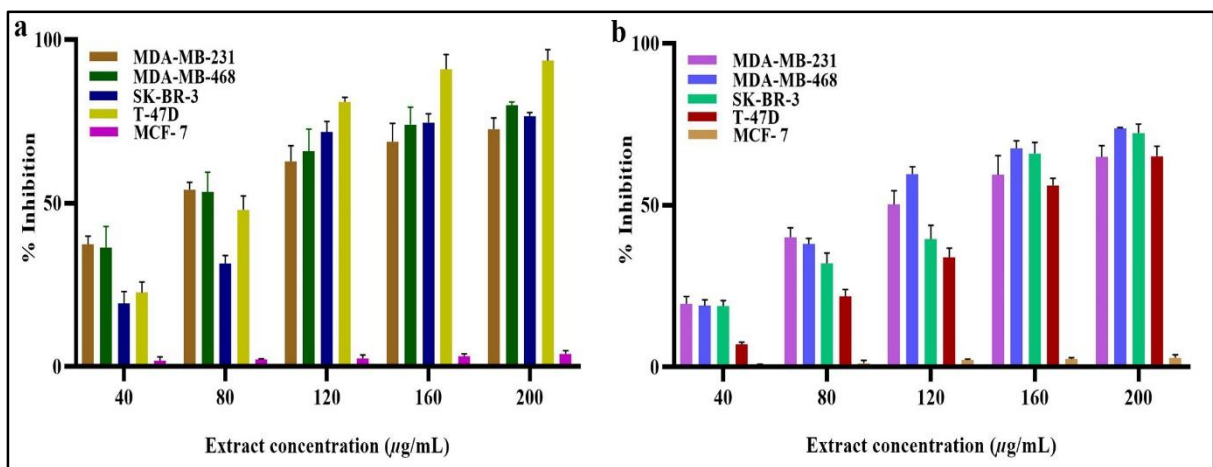
Figure 3.9. Antiproliferative effect of *S. asoca* (a) and *K. pinnatum* (b) extracts on different breast cancer cell lines. The values are presented as mean ± SD based on three separate evaluation
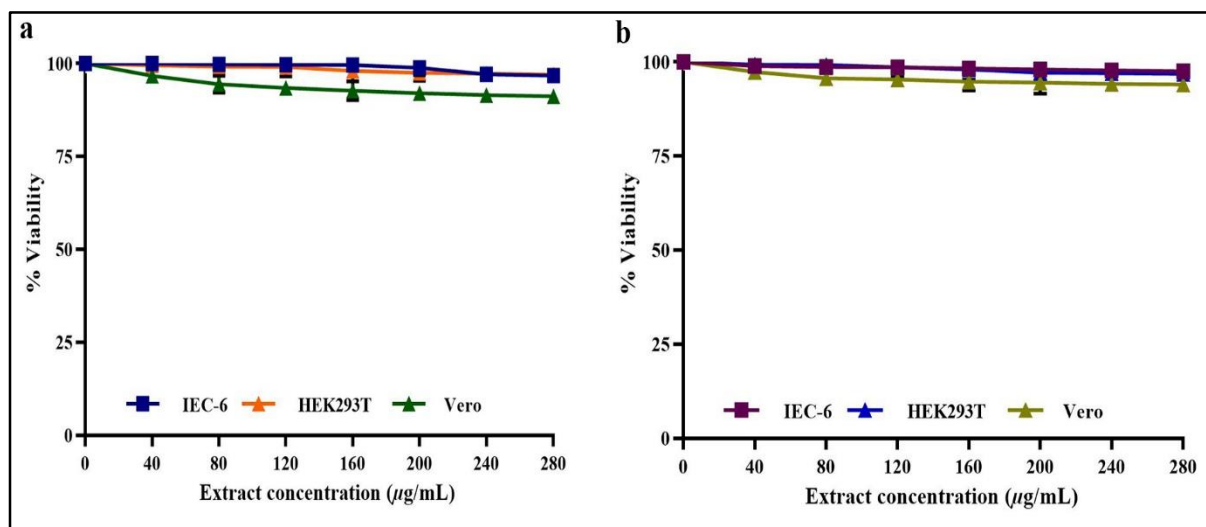
Figure 3.10. Percentage viability of various normal cells after *S. asoca* (a) and *K. pinnatum* (b) extract treatment. The values are presented as mean ± SD based on three different determinations

Table 3.2. Values of the inhibitory concentration (IC_{50}) of extracts on different cancer cell lines

Cell lines	*Saraca asoca*- IC_{50}	*Kingiodendron pinnatum*- IC_{50}
MDA-MB- 231	70.22 ± 1.89	119.22 ± 3.64
MDAMB-468	72.14 ± 2.16	102.2 ± 2.87
T47D	88.05 ± 2.62	149.04 ± 2.65
SKBR3	98.41 ± 2.31	132.79 ± 2.84
PC3	156.3 ± 2.87	197.5 ± 3.14
HCT-15	51.09 ± 3.51	78.99 ± 2.85
HeLa	155.4 ± 3.36	165.9 ± 3.48
HCT 116	121.3 ± 2.84	155.2 ± 3.09
Hep G2	155.6 ± 4.56	175.2 ± 4.46
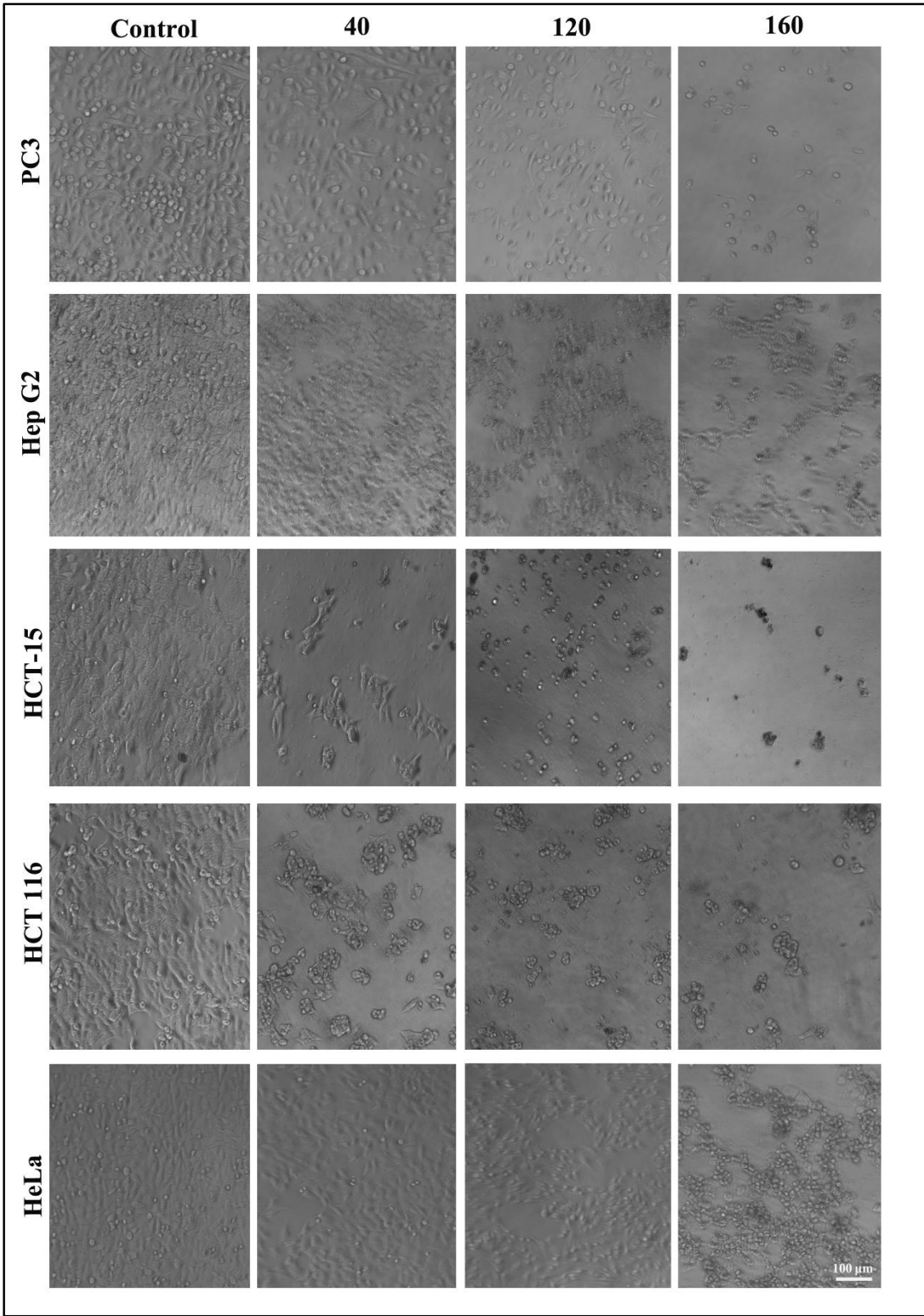
Figure 3.11. Morphological alterations induced by *S. asoca* extracts on various cancer cell lines observed using a phase contrast microscope (20X magnification, $100\,\mu$m scale bar applies to all images)
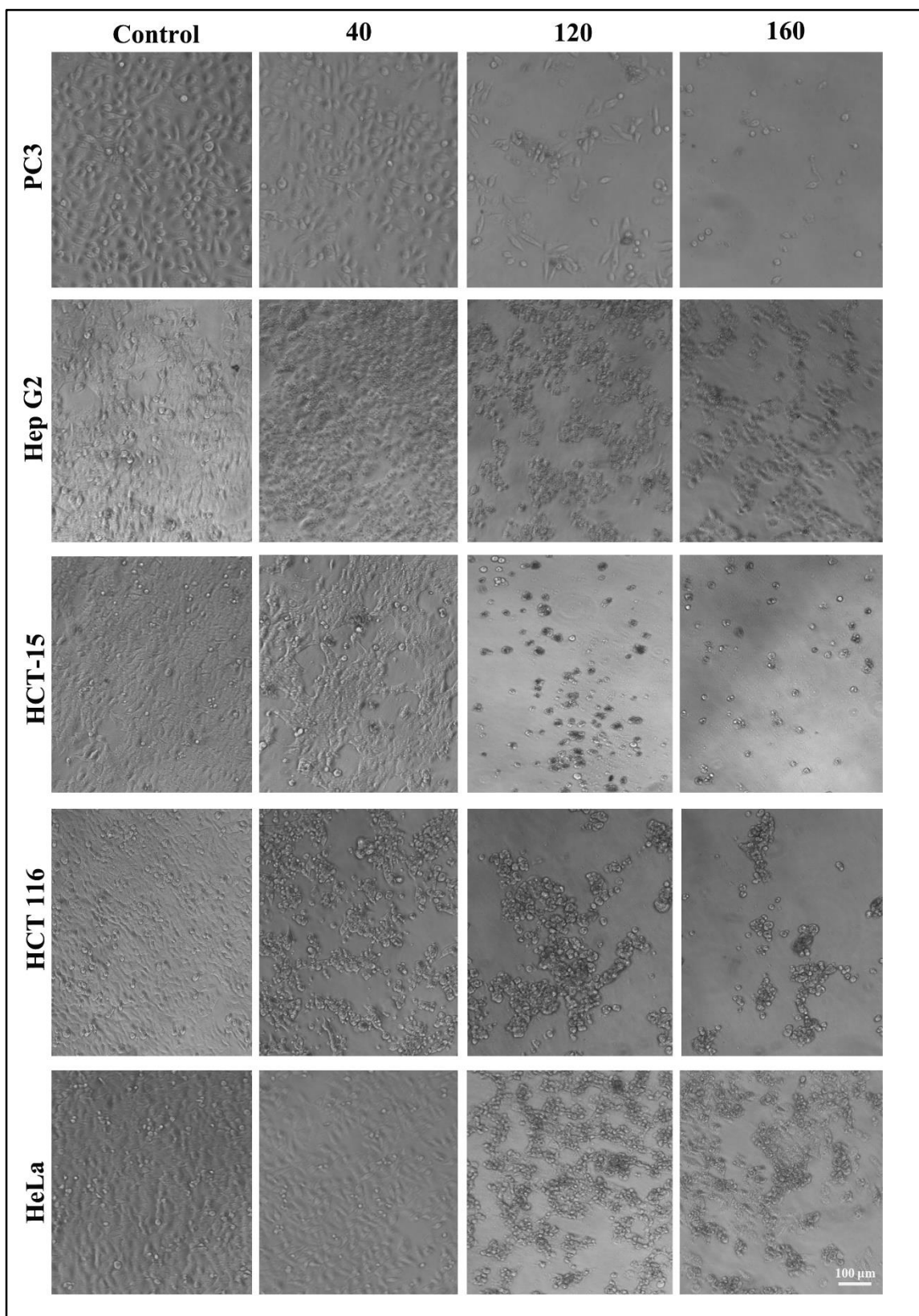
Figure 3.12. Morphological alterations induced by *K. pinnatum* extracts on various cancer cell lines observed using a phase contrast microscope (20X magnification, $100\,\mu$m scale bar applies to all images)
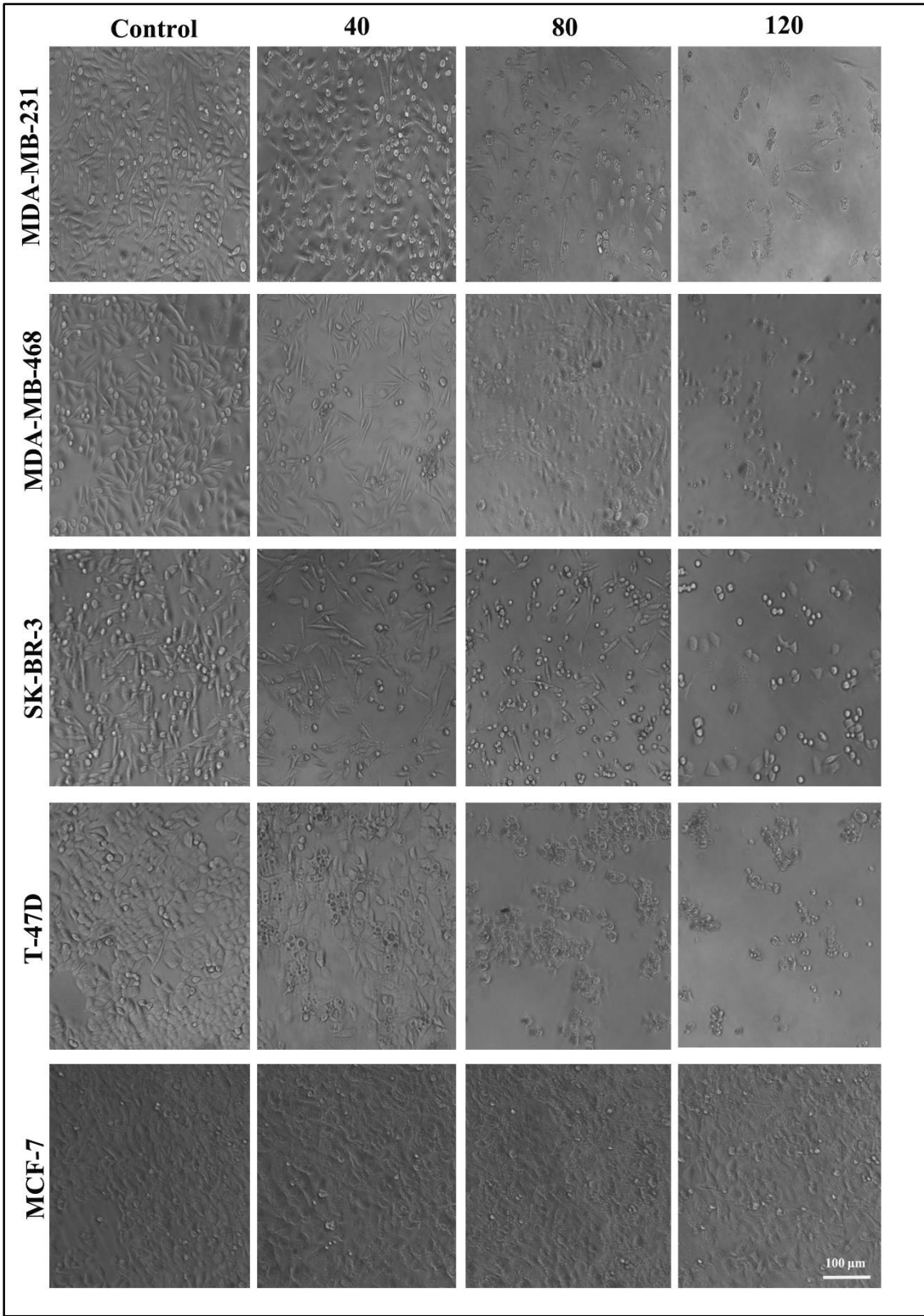
Figure 3.13. Morphological alterations induced by *S. asoca* extracts on various breast cancer cell lines observed using a phase contrast microscope (20X magnification, 100 μm scale bar applies to all images). No change in morphology was observed in case of MCF-7 cell lines
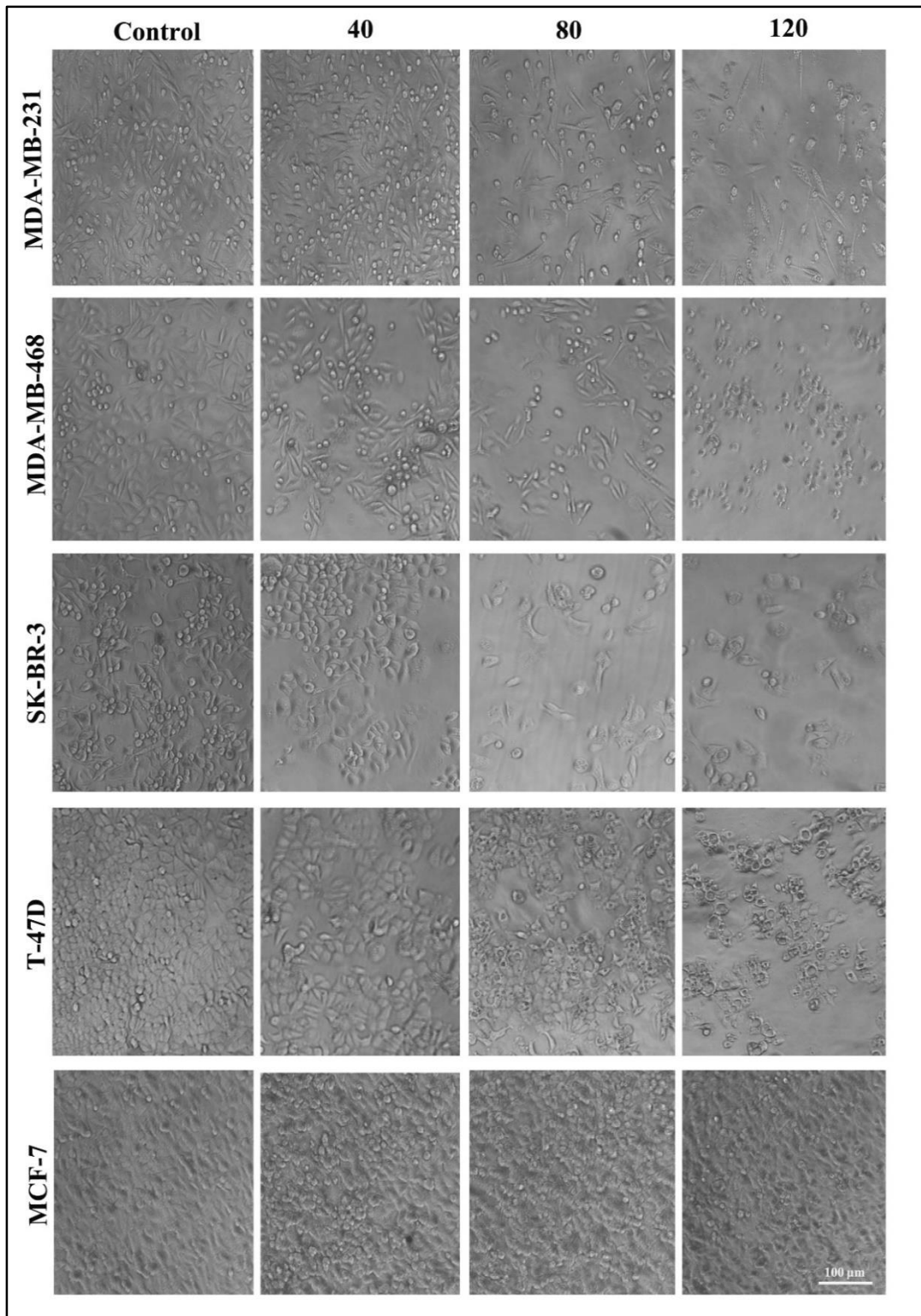
Figure 3.14. Morphological alterations induced by *K. pinnatum* extracts on various breast cancer cell lines observed using a phase contrast microscope (20X magnification, 100 μm scale bar applies to all images). No change in morphology was observed in case of MCF-7 cell lines.
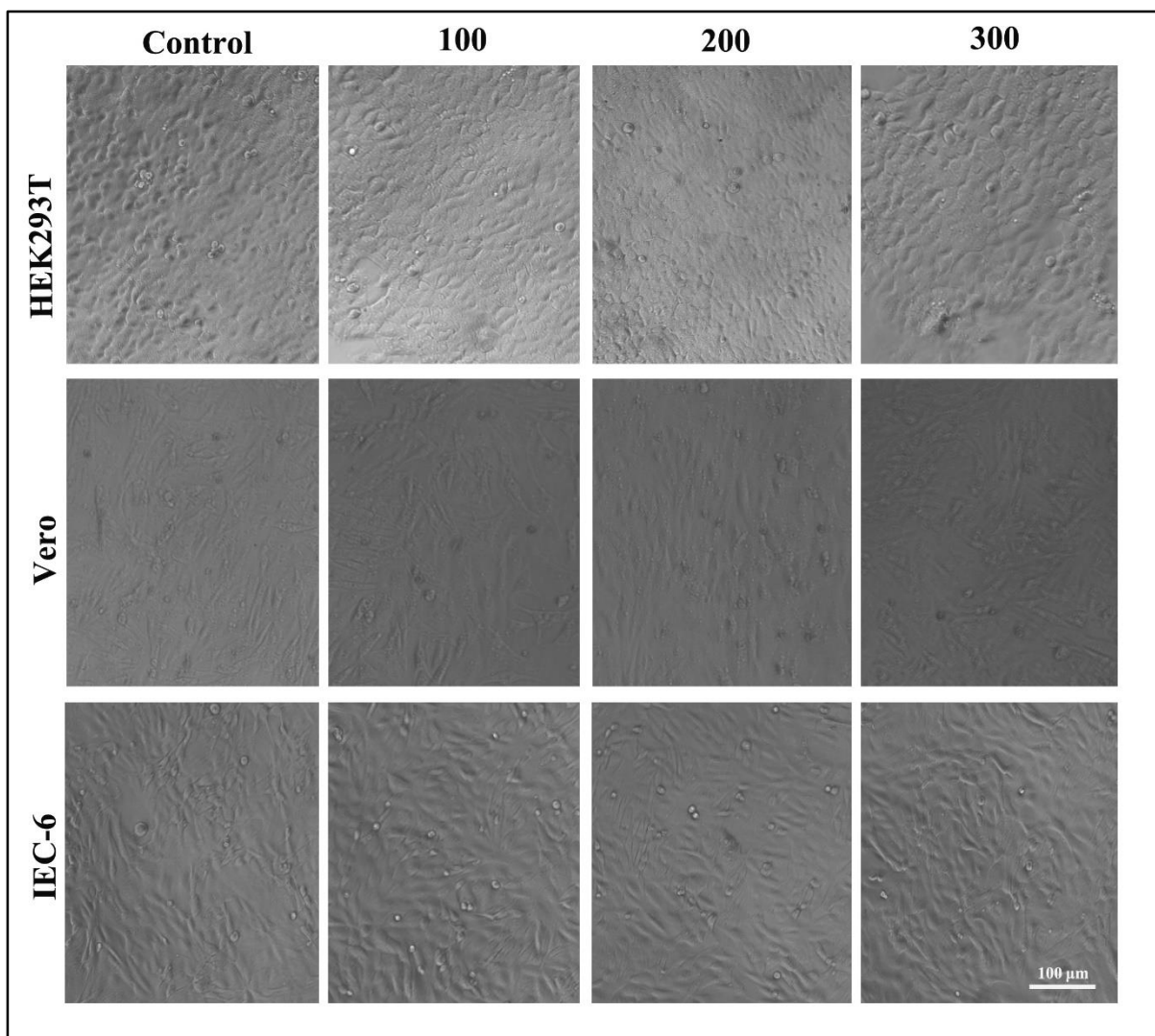
Figure 3.15. Morphology of normal cell lines treated with *S. asoca* extracts visualized using phase contrast microscope (20X magnification, 100 μm scale bar applies to all images)
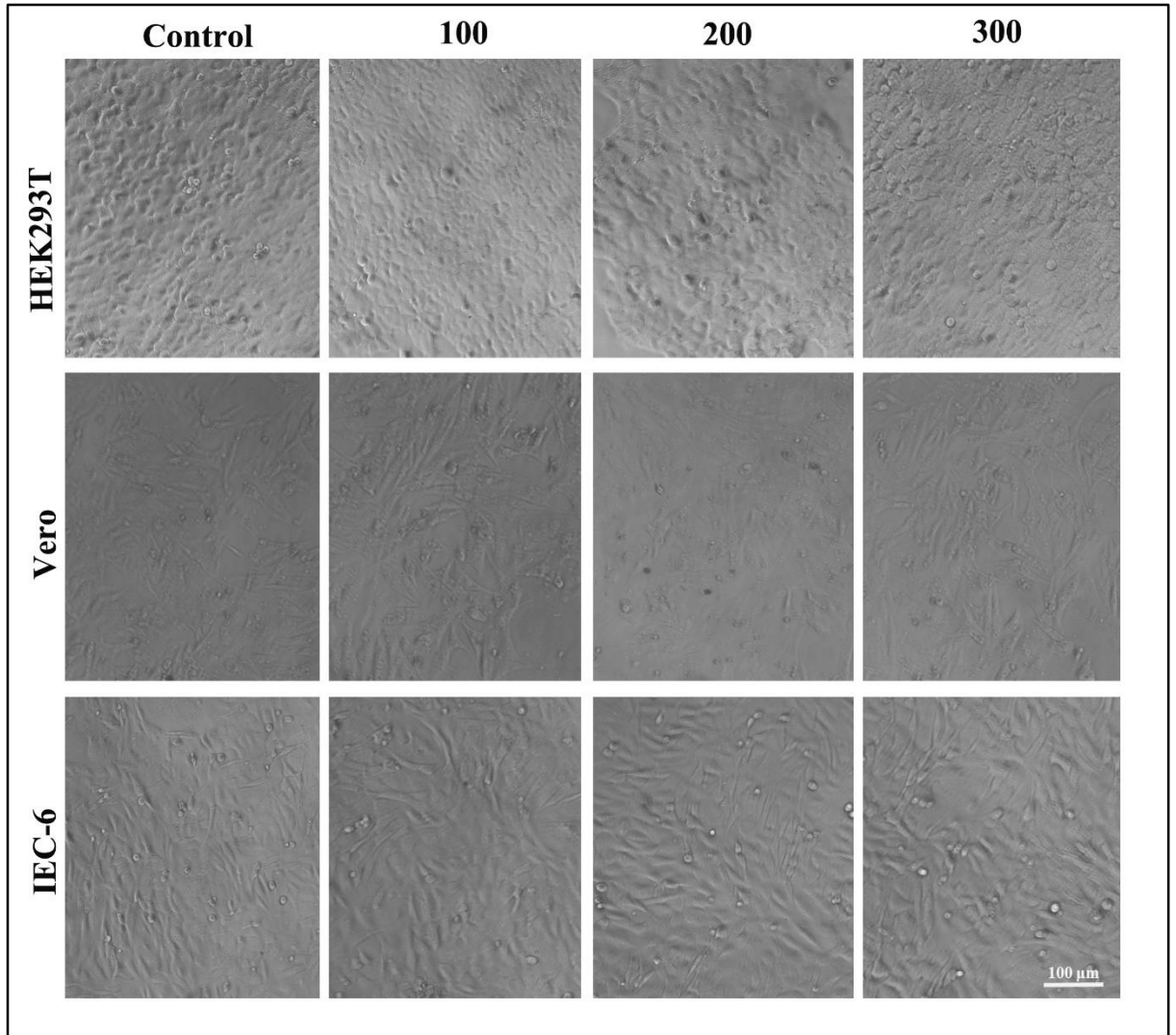
Figure 3.16. Morphology of normal cell lines treated with *K. pinnatum* extracts visualized using phase contrast microscope (20X magnification, 100 μm scale bar applies to all images)

3.3.5. Phytochemical analysis of *S. asoca* and *K. pinnatum* extracts

3.3.5.1. Preliminary screening

Initial screening study indicated that the crude extract displayed higher antioxidant and cytotoxic activity than other fractions, with the methanol fraction following closely in terms of activity. DPPH and superoxide radicals were most effectively scavenged by crude methanol extracts of both plants compared with petroleum benzene, ethyl acetate, methanol and water fractions. And the cytotoxicity study on DLA cells also revealed highest cytotoxicity of crude extract in comparison with the different solvent fractions of both plants. The IC_{50} values of the crude and fraction of extracts of both plants from the cytotoxicity and antioxidant studies are shown in tables 3.3 and 3.4, respectively. Consequently, the crude methanol bark extracts of both plants were selected for their phytoconstituent composition analysis along with the methanol fraction.

Table 3.3. DPPH and superoxide radical scavenging activity of different extracts of *S. asoca* and *K. pinnatum*

Plants	Extracts	IC_{50} value (μg/mL)	
		DPPH	**Superoxide radical**
S. asoca	Petroleum benzene fraction	-	-
	Ethyl acetate fraction	13.6 ± 1.56	84.3 ± 4.65
	Methanol fraction	4.58 ± 0.65	48.14 ± 4.31
	Water fraction	76.04 ± 5.58	118.8 ± 7.45
	Crude extract	2.86 ± 0.34	37.85 ± 2.96
K. pinnatum	Petroleum benzene fraction	-	-
	Ethyl acetate fraction	15.62 ± 1.18	99.5 ± 6.31
	Methanol fraction	6.23 ± 0.45	63.4 ± 4.22
	Water fraction	98.03 ± 7.12	130.63 ± 9.65
	Crude extract	4.72 ± 0.65	52.37 ± 3.20

Table 3.4. Cytotoxic activities of *S. asoca* and *K. pinnatum* extracts on DLA cells

Plants	Extracts	IC$_{50}$ value (μg/mL)
S. asoca	Petroleum benzene fraction	-
	Ethyl acetate fraction	83.44 ± 5.22
	Methanol fraction	60.56 ± 5.14
	Water fraction	176.67 ± 9.4
	Crude extract	42.24 ± 3.65
K. pinnatum	Petroleum benzene fraction	-
	Ethyl acetate fraction	95.74 ± 7.18
	Methanol fraction	72.48 ± 0.45
	Water fraction	188.03 ± 10.12
	Crude extract	50.09 ± 3.89

3.3.5.2. Qualitative and quantitative estimation of compounds in the extracts of *S. asoca* and *K. pinnatum*

The qualitative analysis revealed the existence of several compounds like phenols, alkaloids, saponins, flavonoids, terpenoids, phytosterols and tannins in the crude and methanol fractions of both plants (Table 3.5). The total polyphenolic content in crude and methanol fraction of *K. pinnatum* estimated from the calibration curve (R2= 0.998) was 155.25 ± 4.32 and 122.97 ± 6.14 mg of gallic acid equivalent (GAE)/g of dry extract respectively which was higher than that of *S. asoca* (120 ± 6.82 and 95.4 ± 5.16 mg of gallic acid equivalent (GAE)/g of dry extract respectively). The phenol content in extracts of *S. asoca* and *K. pinnatum* is given in table 3.5. The total flavonoid content in crude and methanol fraction of *S. asoca* determined from the calibration curve (R2= 0.999) was 61.54 ± 4.51 and 45.2 ± 3.12 mg of quercetin equivalent (QE)/g of dry extract respectively which was higher compared to *K. pinnatum* (39.6 ± 3.11 and 24.6 ± 2.87 mg of quercetin equivalent (QE)/g of dry extract respectively). The flavonoid content of both extracts are given in the table 3.6.

Table 3.5. Phytochemicals present in *S. asoca* and *K. pinnatum* extracts

Sl. No.	Phytochemicals	Present (Y)/Absent (N)			
		Crude *S. asoca*	*Methanol fraction S. asoca*	Crude *K. pinnatum*	*Methanol fraction K. pinnatum*
1.	Phenols	Y	Y	Y	Y
2.	Flavonoids	Y	Y	Y	Y
3.	Alkaloids	Y	Y	Y	Y
4.	Phytosterols	Y	Y	Y	Y
5.	Saponins	Y	Y	Y	Y
6.	Terpenoids	Y	Y	Y	Y
7.	Tannins	Y	Y	Y	Y

Table 3.6. Quantitative estimation of total phenols and flavonoids in extracts of *S. asoca* and *K. pinnatum*

Extracts	Flavonoids (mg QE/g of dry extract)		Phenols (mg GAE/g of dry extract)	
	Crude	Methanol fraction	Crude	Methanol fraction
S. asoca	61.54 ± 4.51	45.2 ± 3.12	120 ± 6.82	95.4 ± 5.16
K. pinnatum	39.6 ± 3.11	24.6 ± 2.87	155.25 ± 4.32	122.97 ± 6.14

-Data are expressed as mean $\pm$ standard deviation (SD). QE- quercetin equivalent, GAE-gallic acid equivalent

3.3.5.3. UV-Vis and FT-IR

UV-VIS spectrum of *Saraca asoca* and *Kingiodendron pinnatum* crude extracts and methanol fractions was determined. The peaks were observed at 280 nm with maximum absorption at 1.311 (Figure 3.17). In particular, these absorption bands are characteristic of flavonoids and their derivatives.

In the FTIR analysis, the functional groups identified in *S. asoca* and *K. pinnatum* crude extracts and methanol fractions are presented in tables 3.7 to 3.10 and the FTIR spectra are shown in figures 3.18 and 3.19. It was confirmed by the results that there were alkanes, alkenes, alcohols, aromatic amines, conjugated alkenes, carboxylic acids, esters, phenols and nitro compounds in the samples.
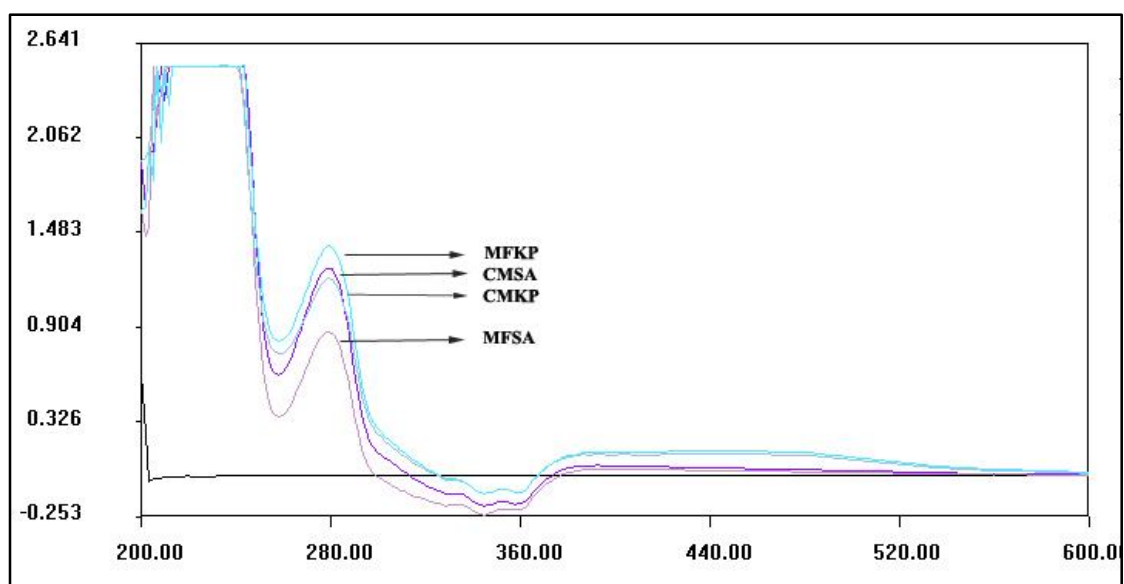
Figure 3.17. UV-Vis spectroscopy of *S. asoca* and *K. pinnatum* crude extracts and methanol fractions
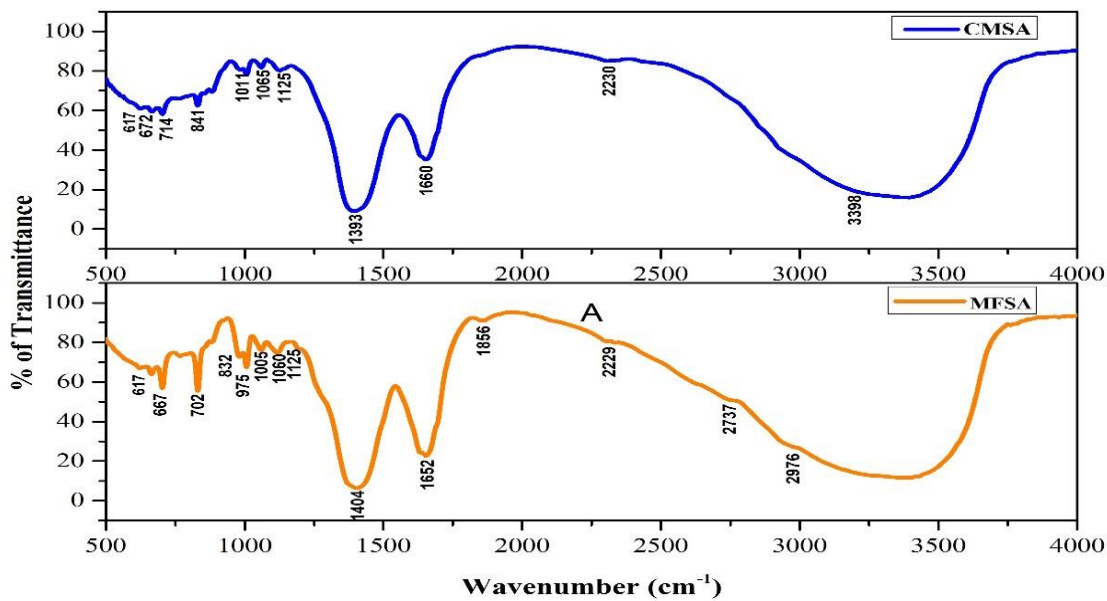
Figure 3.18. FT-IR spectrum of crude extract (CMSA) and methanol fraction (MFSA) of *S. asoca*
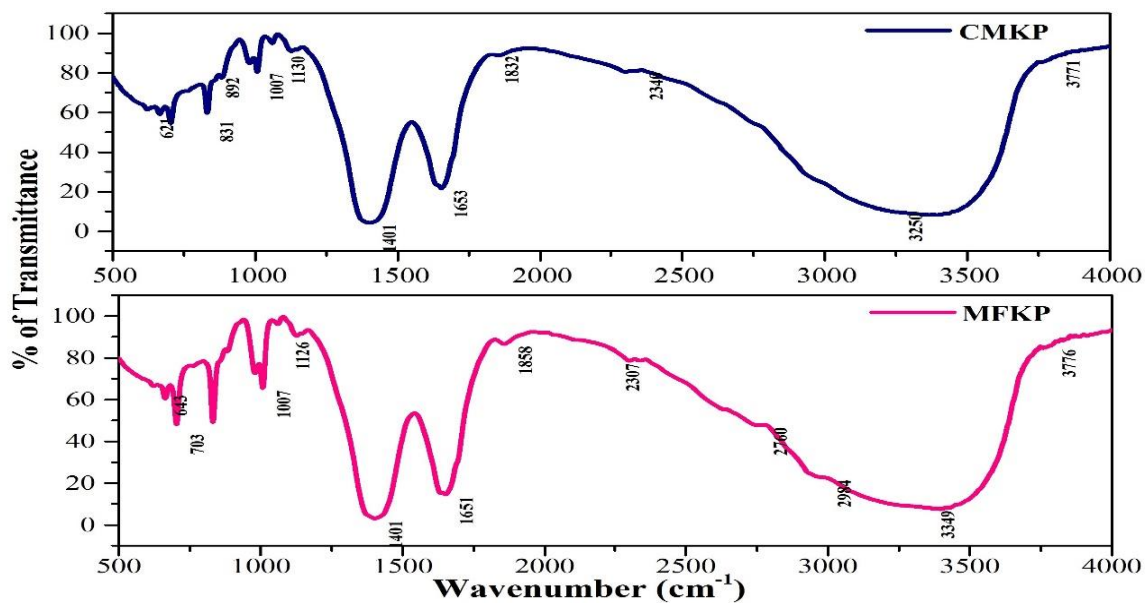
Figure 3.19. FT-IR spectrum of crude extract (CMKP) and methanol fraction (MFKP) of *K. pinnatum*

Table 3.7. FTIR interpretation of compounds of crude extract of *S. asoca*

Wave number cm^{-1}	Bond assigned	Functional groups
621	C=C bending	Alkenes
831	C=C bending, C−N stretching	Alkenes, amines
892	C=C bending, C−N stretching	Alkynes, amines
1007	O-H and C-O stretching	Alcohols, esters
1130	O-H and C-N stretching	Alcohols, amines
1401	O−H bending	Phenols
1653	N−O stretching	Nitro compounds
1832	C=O stretching	Carboxylic acids
2340	C=C bending	Conjugated alkenes
3250	O−H stretching	Carboxylic acids
3771	O−H stretching	Alcohols

Table 3.8. FTIR interpretation of compounds of methanol fraction of *S. asoca*

Wave number cm^{-1}	Bond assigned	Functional groups
617	C-H vibration	Alkanes, alkenes
672	C-H and C-C stretching	Alkenes, alcohols, phenols
714	C=C and N-H stretching	Alkenes, amines
841	C-C and C-H stretching	Amides, aldehydes
1011	C-O stretching	Alcohols
1065	C-O stretching	Alcohols, aromatics
1125	C-O stretching	Alcohols
1393	C-O and C-H stretching	Phenols, aldehydes
1660	C-C stretching	Phenols
2230	C=C stretching	Conjugated alkenes
3398	O-H stretching	Alcohols

Table 3.9. FTIR interpretation of compounds of crude extract of *K. pinnatum*

Wave number cm^{-1}	Bond assigned	Functional groups
617	C-H vibration	Alkanes, alkenes
667	C=C bending	Alkenes
702	O-H and N-H bending	Phenols, amines
832	C-O stretching	Esters
975	C-O and C≡C stretching	Esters, alkynes
1005	C-O stretching	Alcohols
1060	C-N stretching	Amines
1125	C-N and C-O stretching	Amines, esters
1404	C-H stretching	Aldehydes
1652	C-C stretching	Phenols
1856	C=C stretching	Conjugated alkenes
2737	O-H stretching	Carboxylic acids

Table 3.10. FTIR interpretation of compounds of methanol fraction of *K. pinnatum*

Wave number cm^{-1}	Bond assigned	Functional groups
643	C=C bending	Alkenes
703	C−N and O−H stretching	Alkenes, phenols
1007	O-H and C-O stretching	Alcohols, esters
1126	O-H and C-N stretching	Alcohols, amines
1401	O−H bending	Phenols
1651	N−O stretching	Nitro compounds
1858	C=O stretching	Carboxylic acids
2307	C−N stretching	Aromatic amines
2760	O-H stretching	Carboxylic acids
2984	N-H stretching	Aromatic amines
3349	N-H stretching	Amines
3706	O−H stretching	Alcohols

3.3.5.4. TLC and HPTLC profiling

The TLC analysis of crude extract and methanol fractions of both plants showed multiple bands at 254 and 366 nm (Figure 3.20). The Rf values of a band observed in the plant extracts were similar to those of kaempferol, the standard. The table 3.11 provides the Rf values for each component that has been separated. Thus, the results suggest that kaempferol might be one of the plants' biologically important constituents.
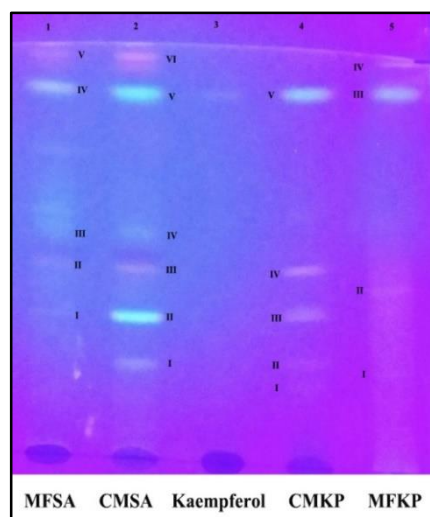
Figure 3.20. TLC profile of crude extract and methanol fractions of *S. asoca* and *K. pinnatum* obtained using a solvent mixture of toluene, ethyl acetate and formic acid in the ratio of 7:3:0.3, on pre-coated silica gel plate. Lane 1 – Methanol extract of *S. asoca*, Lane 2 - Crude extract of *S. asoca*, Lane 3 - Kaempferol, Lane 4 – Crude extract of *K. pinnatum*, Lane 5 – Methanol extract of *K. pinnatum*

Table 3.11. Rf values obtained in TLC analysis of crude extract and methanol fractions of *S. asoca* and *K. pinnatum* under UV transilluminator (365 nm)

Bands	Rf value		Rf value	
	Crude extract		Methanol fraction	
	S. asoca	*K. pinnatum*	*S. asoca*	*K. pinnatum*
I	0.22	0.18	0.33	0.23
II	0.33	0.23	0.47	0.42
III	0.45	0.35	0.56	0.89
IV	0.52	0.47	0.89	0.92
V	0.89	0.89	0.95	-
VI	0.94	-	-	-

HPTLC analysis was carried out using crude extract and methanol fractions of both plants along with standards of *β*-sitosterol (Figure 3.21) and quercetin (Figure 3.22). A series of bands were observed for quercetin at 254, 366 nm, while bands for *β*-sitosterol were obtained at 366 nm and after derivatization with spray reagent. A comparison of the Rf values for the separated components are presented in Tables 3.12 and 3.13. The Rf values of two different components present in the extracts of the plants were similar to those shown by the standards, namely *β*-sitosterol and quercetin. As a result of the findings, it seems that the plants may contain a number of biologically significant constituents, such as *β*-sitosterol and quercetin.
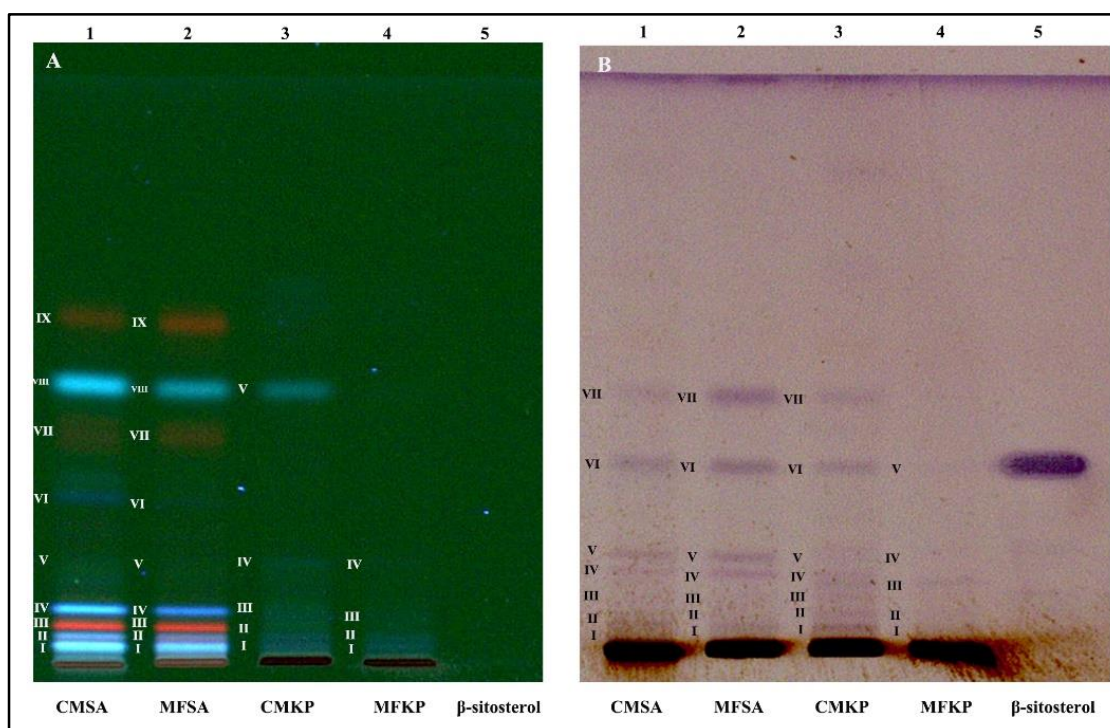
Figure 3.21. HPTLC profile of crude extract and methanol fractions of *S. asoca* and *K. pinnatum* obtained using a solvent mixture of toluene: chloroform: methanol in the ratio 8:3:1, on pre-coated silica gel plate. The plates scanned at 366 nm (A) and derivatized plate sprayed with reagent (B). Lane 1 – Crude extract of *S. asoca*, Lane 2 - Methanol fraction of *S. asoca*, Lane 3 - Crude extract of *K. pinnatum*, Lane 4 – Methanol fraction of *K. pinnatum,* Lane 5 – *β*-sitosterol
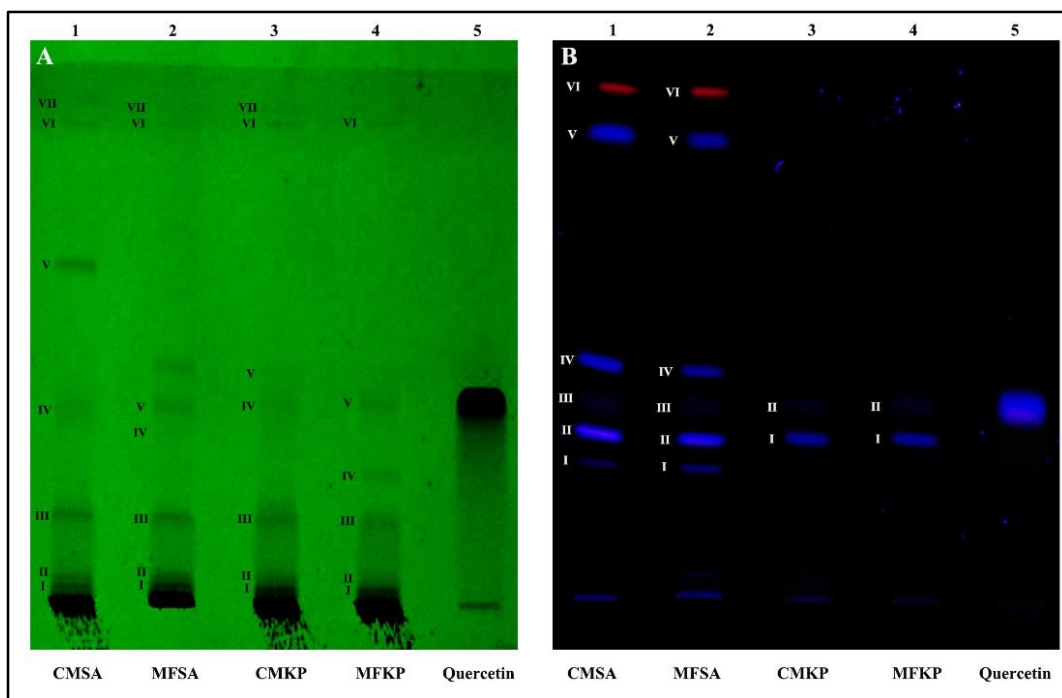
Figure 3.22. HPTLC profile of crude extract and methanol fractions of *S. asoca* and *K. pinnatum* obtained using a solvent mixture of toluene: chloroform: methanol in the ratio 8:3:1, on pre-coated silica gel plate. The plates scanned at 254 nm (A) and 366 nm (B). Lane 1 – Crude extract of *S. asoca*, Lane 2 - Methanol fraction of *S. asoca*, Lane 3 - Crude extract of *K. pinnatum*, Lane 4 – Methanol fraction of *K. pinnatum,* Lane 5 – Quercetin

Table 3.12. Rf values obtained in HPTLC analysis of crude extract and methanol fractions of *S. asoca* and *K. pinnatum* with standard *β*-sitosterol under UV transilluminator and from derivatized plate

Bands	Rf value (366 nm)				Rf value (derivatized plate)			
	CMSA	MFSA	CMKP	MFKP	CMSA	MFSA	CMKP	MFKP
I	0.03	0.02	0.02	0.02	0.02	0.02	0.02	0.02
II	0.05	0.04	0.05	0.04	0.05	0.05	0.06	0.06
III	0.07	0.06	0.1	0.08	0.1	0.09	0.09	0.11
IV	0.1	0.1	0.18	0.08	0.15	0.13	0.12	0.17
V	0.18	0.18	0.48	0.17	0.18	0.16	0.16	0.34
VI	0.28	0.28	-	-	0.34	0.34	0.34	-
VII	0.40	0.40	-	-	0.46	0.45	0.44	-
VIII	0.50	0.48	-	-	-	-	-	-
IX	0.61	0.60	-	-	-	-	-	-

Table 3.13. Rf values obtained in HPTLC analysis of crude extract and methanol fractions of *S. asoca* and *K. pinnatum* with standard quercetin under UV transilluminator

Bands	Rf value (254 nm)				Rf value (366 nm)			
	CMSA	**MFSA**	**CMKP**	**MFKP**	**CMSA**	**MFSA**	**CMKP**	**MFKP**
I	0.03	0.03	0.02	0.02	0.26	0.26	0.32	0.31
II	0.05	0.05	0.04	0.04	0.32	0.30	0.39	0.38
III	0.17	0.16	0.15	0.16	0.39	0.36	-	-
IV	0.34	0.32	0.34	0.25	0.45	0.86	-	-
V	0.62	0.35	0.42	0.39	0.86	0.94	-	-
VI	0.28	0.87	0.86	0.86	0.95	-	-	-
VII	0.87	0.91	0.90	-	-	-	-	-
VIII	0.92	-	-	-	-	-	-	-

3.3.5.5. HPLC and GCMS

The presence of β-sitosterol has been re-confirmed by HPLC analysis on the bark of *S. asoca* and *K. pinnatum*. The study demonstrated the presence of β-sitosterol in crude extract and methanol fractions of both plants. The β-sitosterol formed the detection peak at a retention time of 3.380 min. The HPLC chromatograms of the extracts and standard are given in figure 3.23 and 3.24.

The components present in the crude extract and methanol fractions of *S. asoca* and *K. pinnatum* were identified by GC-MS analysis. The retention time (RT), name of the compound and base M/Z detected are given in table 3.14 to 3.17. The compounds detected include polysaccharides such as mome inositol, antimicrobials such as octamethyl-3,5bis(trimethylsiloxy)tetrasiloxane, class of phenol such as phenol-2-propyl, plant metabolite such as tetradecane and antioxidant, antiproliferative compounds such as methyl orsellinate. The GC-MS spectra of components are given in figure 3.25.
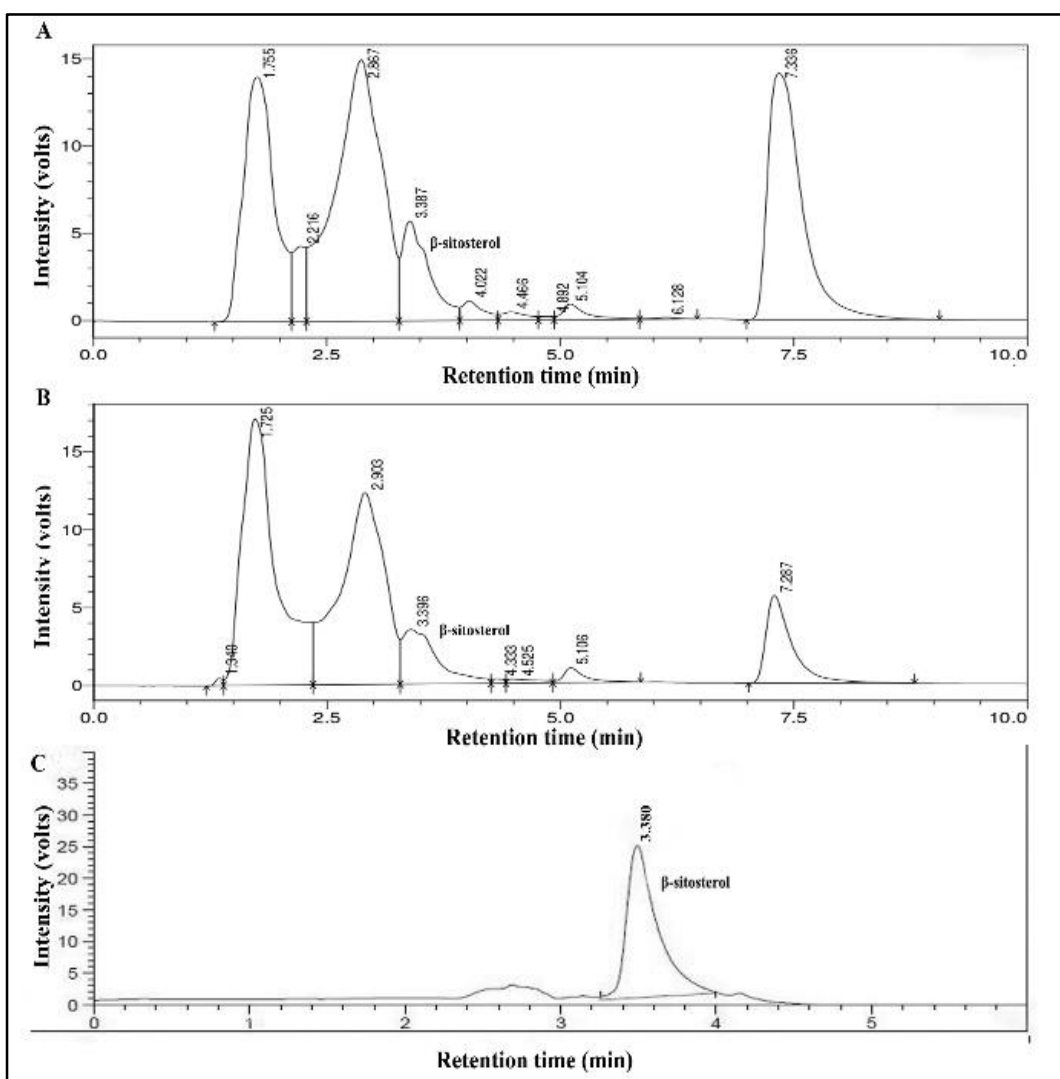
Figure 3.23. HPLC chromatograms of crude extract of *S. asoca* (A) and *K. pinnatum* (B). At a retention time of 3.380 minutes, the standard β-sitosterol (0.04 mg/mL) was detected. (C). Presence of β-sitosterol has been identified based on the standard compound's retention time
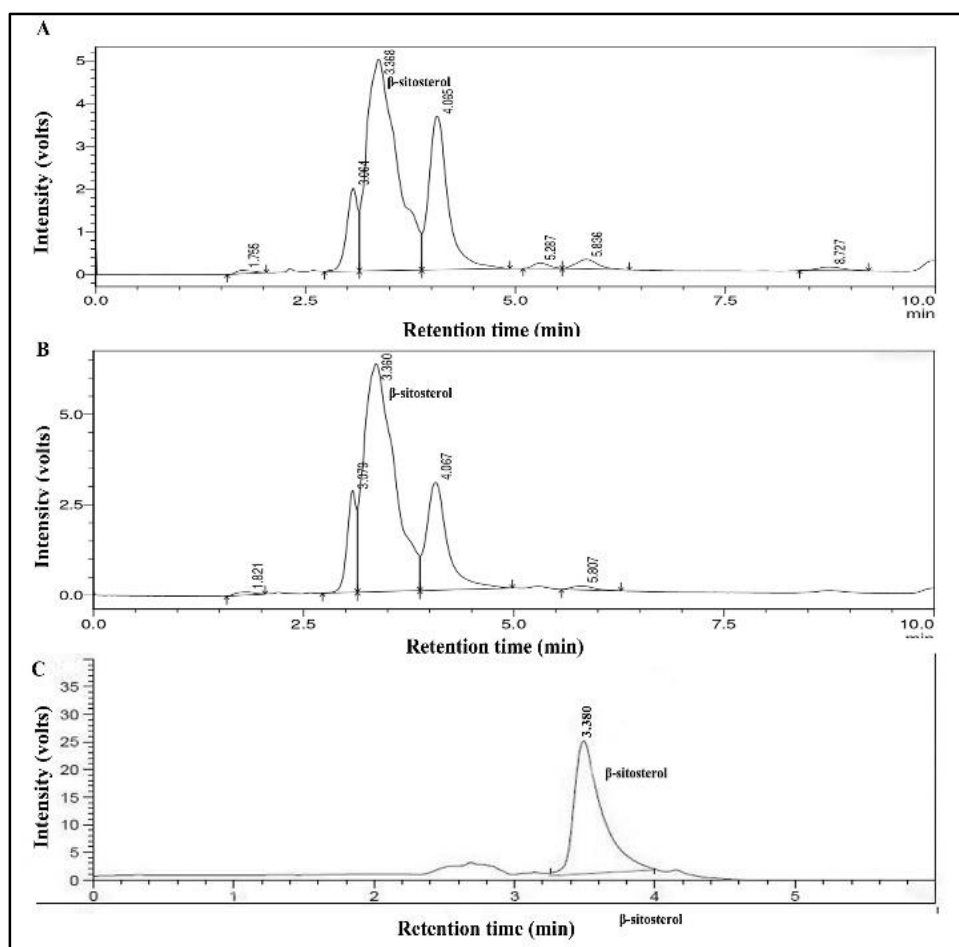
Figure 3.24. HPLC chromatograms of methanol fraction of *S. asoca* (A) and *K. pinnatum* (B). The standard β-sitosterol (0.04 mg/mL) was detected at a retention time of 3.380 min (C).

Table 3.14. Different constituents of crude extract of *S. asoca* identified by GC-MS

Retention time	Name of compound	Base m/z
4.482	3-methylcyclohexanol	96.00
7.117	Phenol,2-propyl	107.05
7.812	Guanosine	57.05
10.700	Methyl orsellinate	150.05
10.792	3-o-methyl-d-glucose	73.00
10.992	Mome inositol	87.05
22.574	1,2-benzenedicarboxylic acid	149.05
23.142	Tetradecane	71.10
23.275	1-bromo-4-bromomethyldecane	57.10
23.374	2,3,5-tri-tert-butyl-3-(4-oxo-2,5-cyclohexadien-1-yl)methylcyclopentanone	57.10
30.624	Undecane,6-cyclohexyl-	57.10
32.643	2-hexanone, 6-bromo-	71.05

138

Table 3.15. Different constituents of crude extract of *K. pinnatum* identified by GC-MS

Retention time	Name of compound	Base m/z
11.217	Hydroperoxide, 1,4-dioxan-2-yl	87.00
11.367	1,3-dioxolane, 2-methyl-	73.00
11.583	Hexane, 3-methoxy-	73.00
22.580	1,2-benzenedicarboxylic acid	149.00
26.117	Mome inositol	73.05
26.268	Inositol	73.05
26.483	5-bromo-n-valeric acid	73.00
26.558	1,3,4-trimethyl-2,6-anhydro-fructofuranose	82.95
27.507	1-methyl-1-n-pentyloxy-1-silacyclobutane	129.00

Table 3.16. Different constituents of methanol fraction of *S. asoca* identified by GC-MS

Retention time	Name of compound	Base m/z
32.243	Phthalamic acid	174.10
32.492	Methanamine, n-methyl-n-nitroso-	74.05
43.058	2-butanone, 1-(2-furanyl)-3-methyl-	81.00
44.384	1-iodo-4-hexyne	71.05
45.498	3-bromo-2-methoxycyclohexanone	207.00

Table 3.17. Different constituents of methanol fraction of *K. pinnatum* identified by GC-MS

Retention time	Name of compound	Base m/z
26.450	Mome inositol	87.05
26.567	2-methyl-1-thia-cyclopentane	87.05
28.592	Ethanol, 2,2'-(nitrosoimino)bis-	81.05
43.602	Hexasiloxane, tetradecamethyl-	73.05
45.384	1,1,1,3,5,7,7,7-octamethyl-3,5-bis(trimethylsiloxy)tetrasiloxane	355.00
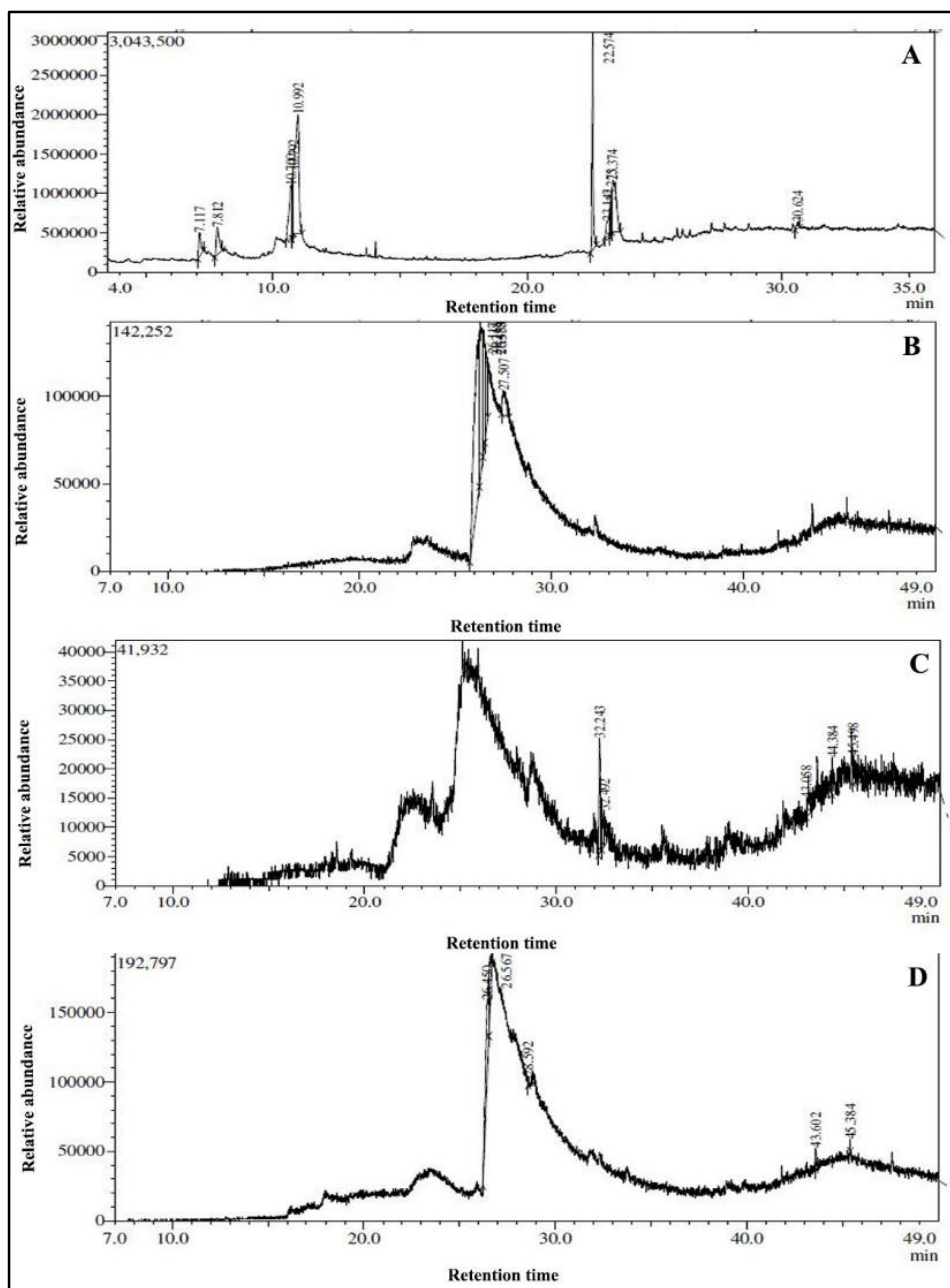
Figure 3.25. GC-MS chromatogram of crude extract (A- CMSA, B-CMKP) and methanol fractions (C-MFSA, D- MFKP) of *S. asoca* and *K. pinnatum*

140

3.3.5.6. HR-LCMS

Multiple biologically relevant components were identified in the crude extract and methanol fractions of *S. asoca* and *K. pinnatum* by HR-LCMS. The chromatogram of crude extracts and methanol fractions of both plants is shown in figure 3.26 and 3.27. The list of compounds tentatively identified in *S. asoca* and *K. pinnatum* crude samples and methanol fractions is presented in Tables 3.18 to 3.21. Some of the compounds identified in the extracts were phytoestrogens, may have been responsible for their selective cytotoxicity towards triple negative breast cancer cell lines.
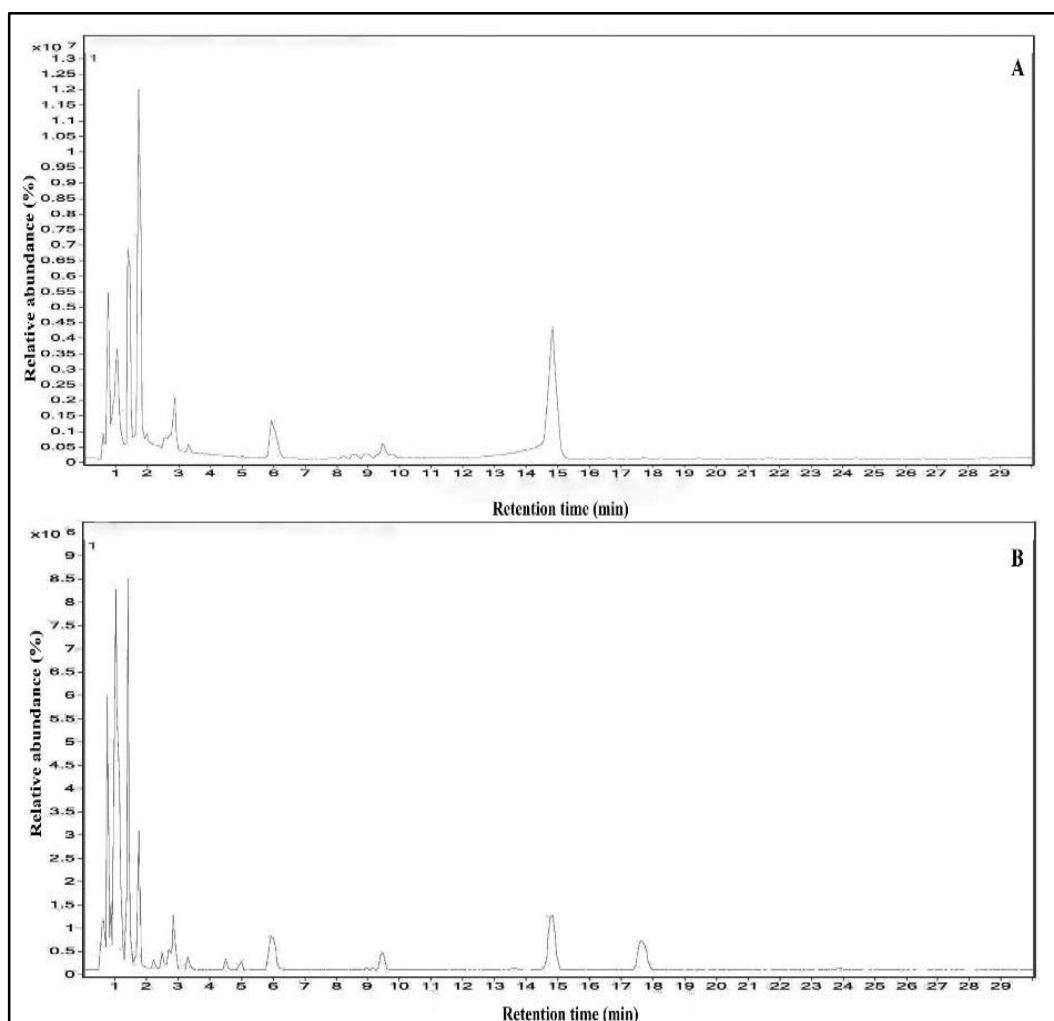
Figure 3.26. LCMS spectra of crude extract of *S. asoca* (A) and *K. pinnatum* (B)
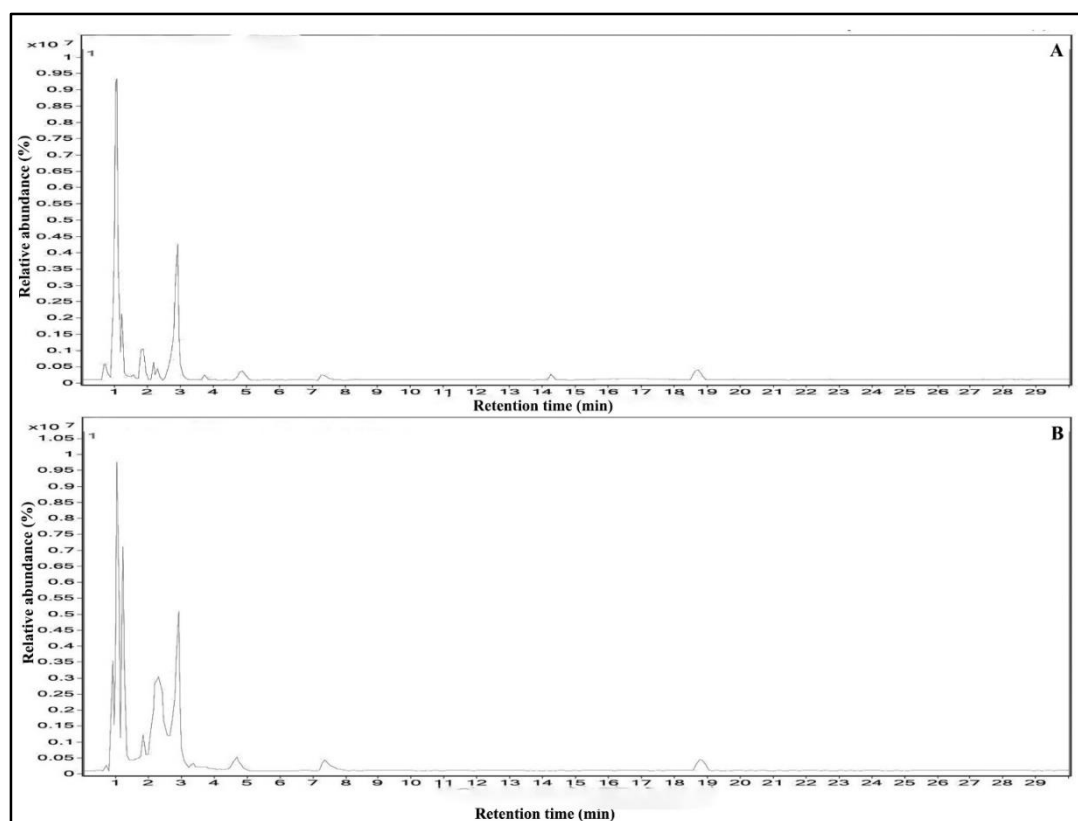
Figure 3.27. LCMS spectra of methanol fraction of *S. asoca* (A) and *K. pinnatum* (B)

Table 3.18. Compounds tentatively identified from *S. asoca* crude extract by HR-LCMS analysis

Name	RT	Mass	DB diff (ppm)
1-Phosphatidyl-1D-myoinositol 3-phosphate	0.803	470.0224	0.6
C16 Sphinganine	0.884	273.2652	5.73
6'beta-Hydroxylovastatin	1.087	420.2421	21.66
Cystamine	1.175	152.0453	-7.08
C16 Sphinganine	1.22	273.2658	3.67
7-Hydroxy-2'-methoxyisoflavone	1.542	268.0727	3.3
Arg Asp Pro	2.401	386.1831	21.54
Meperidine N-oxide	2.584	263.1529	-2.8
Tannic acid	2.945	282.0878	5.16
Gallic acid	3.355	170.0213	1.54
Caffeic acid	5.181	180.041	6.97
p-Coumaric acid	5.782	164.0475	-0.65
Rutin	5.782	610.1489	7.39
Quercetin	6.023	302.0406	6.67
Luteoline	7.036	286.046	5.9
Kaempferol	8.62	286.046	5.9

142

Catechin	9.564	278.1499	7.01
Phthalic acid Mono-2- ethylhexyl Ester	9.91	290.0796	-1.88
Epigallocatechin gallate	14.866	256.1212	-0.07
Beta-sitosterol	20.396	414.3822	9.47

Table 3.19. Compounds tentatively identified from *K. pinnatum* crude extract by HR-LCMS analysis

Name	RT	Mass	DB diff (ppm)
C16 Sphinganine	0.82	273.2649	6.83
Buddleoflavonoloside	0.939	592.187	-13.16
Sulfolithocholylglycine	1.056	513.2749	2.24
Tolbutamide	1.11	270.1064	-9.47
Docosatetraenoic acid	1.169	489.2905	-10.06
N-Acetylcystathionine	1.178	264.0808	-10.52
C16 Sphinganine	1.188	273.2651	-1.12
Gallic acid	2.046	170.0209	3.48
Theophylline	2.339	180.068	-17.94
Tannic acid	2.874	263.1527	-2.1
Gabapentin	3.189	171.127	-5.99
Catechin	4.8	290.0775	5.21
Rutin	5.477	610.1486	7.88
p-Coumaric acid	5.762	164.0472	0.94
Quercetin	5.984	302.0415	3.84
Caffeic acid	6.407	180.0412	5.7
Luteoline	8.985	286.0463	5.11
Kaempferol	8.985	286.0463	5.11
Hydroflumethiazide	9.498	330.9928	-5.83
Epigallocatechin gallate	14.884	458.0838	2.47
Myricetin O-glucoside	17.653	484.2784	3.55
Beta-sitosterol	20.95	263.1529	-2.78

Table 3.20. Compounds tentatively identified from methanol fraction of *S. asoca* by HR-LCMS analysis

Name	RT	Mass	DB diff (ppm)
Fendiline	0.763	315.2023	-11.27
Maltose	0.896	342.1134	8.23
1-Phosphatidyl-1D-myoinositol 3-phosphate	1.027	470.0219	1.63
Trp Trp Gln	1.032	518.2299	-4.18
Homovanillic acid	1.014	182.0575	2.12
p-Hydroxydextroamphetamine	1.18	151.0987	6.5
Gabapentin	1.594	171.1271	-6.77
Hydroflumethiazide	2.195	330.9933	-7.52

Pentanoic acid	2.319	353.9723	-2.91
Isorenieratene/ (Leprotene)	2.91	528.3624	25.02
Gallic acid	3.039	170.0208	4.48
Caffeic acid	4.983	180.0407	8.9
Rutin	5.786	610.1488	7.51
Catechin	6.453	290.0798	-2.48
Quercetin	6.663	302.0407	6.53
Luteoline	7.355	286.0462	5.21
Kaempferol	8.98	286.0462	5.21
Epigallocatechin gallate	14.235	458.0873	-5.25
Beta-sitosterol	18.762	414.3821	9.71

Table 3.21. Compounds tentatively identified from methanol fraction of *K. pinnatum* by HR-LCMS analysis

Name	RT	Mass	DB diff (ppm)
C16 Sphinganine	0.989	273.2644	8.62
1-Phosphatidyl-1D-myoinositol 3-phosphate	1.326	470.0218	1.92
Hydroflumethiazide	2.207	330.994	-9.54
Pentanoic acid	2.458	353.9719	-1.72
Gallic acid	3.016	3.016	1.17
BMPN-benzoic acid	3.315	256.1215	-1.35
Epigallocatechin gallate	3.878	458.0839	2.24
1-Phosphatidyl-1D-myoinositol 3-phosphate	4.776	470.0217	2.09
Caffeic acid	4.803	290.0773	6.13
Quercetin	5.299	302.0458	-10.46
Rutin	5.77	610.1448	14
p-Coumaric acid	5.77	164.0466	4.5
Catechin	6.449	180.0409	7.74
Luteoline	7.255	286.0463	4.97
Kaempferol	8.961	286.0463	4.97
Beta-sitosterol	18.8	414.385	2.91

3.3.6. *In silico* prediction by molecular docking

3.3.6.1. Interaction of phytoestrogens with ERα

The glide dock was used to dock the inbuilt ligand, estradiol into the 3D structure of ERα. The 3ERT's active site's amino acid residues are TRP383, LEU384, LEU387, MET388, GLY390, LBU391, VAL392, ARG394, MET342, MET343, LEU345, LEU346, THR347, ASN348, LEU349, ALA350, ASP351, GLU353, LEU354, LEU327, PHE404, LEU402, LEU428, PHE425, ILE424, VAL422, MET421, GLY420, GLU419, VAL418, MET517, SER518, LYS520, GLY521, MET522, GLU523, HIE524, LEU525, MET528, LYS529, CYS530, VAL533, LEU536, LEU539. Following docking into the active site region, interactions between the residues and the estradiol were established through hydrogen bonds with GLU353 and ARG394 and electrostatic bonds with ASP351. The inbuilt ligand exhibits a docking score of -12.17 and binding energy of -125.19 kcal/mol. By hydrogen bonding with ASP351, quercetin was docked into the active site region and made interactions with the residues. In comparison to kaempferol (-6.93), the docking score and binding energy of quercetin were found to be -6.945 and -47.026 kcal/mol, respectively. As a result of docking, tamoxifen has a score of -10.512, and β-sitosterol did not dock with the binding pocket of ERα. Therefore, among all the ligands, quercetin shows the most effective binding to the receptor. The 3D interaction between ligands and receptor is presented in figure 3.28 and the docking score and binding energy of the molecules are presented in table 3.22. The type of interaction between the ligands and amino acids at the estrogen receptor α active sites is shown in the 2D interaction picture (Figure 3.29). The ligand determines the number and kind of hydrogen bonds and therefore tamoxifen forms hydrogen bond with ASP 351 whereas estradiol, kaempferol and quercetin establish three hydrogen bonds with GLU 353, HIE 524 and ARG 394.
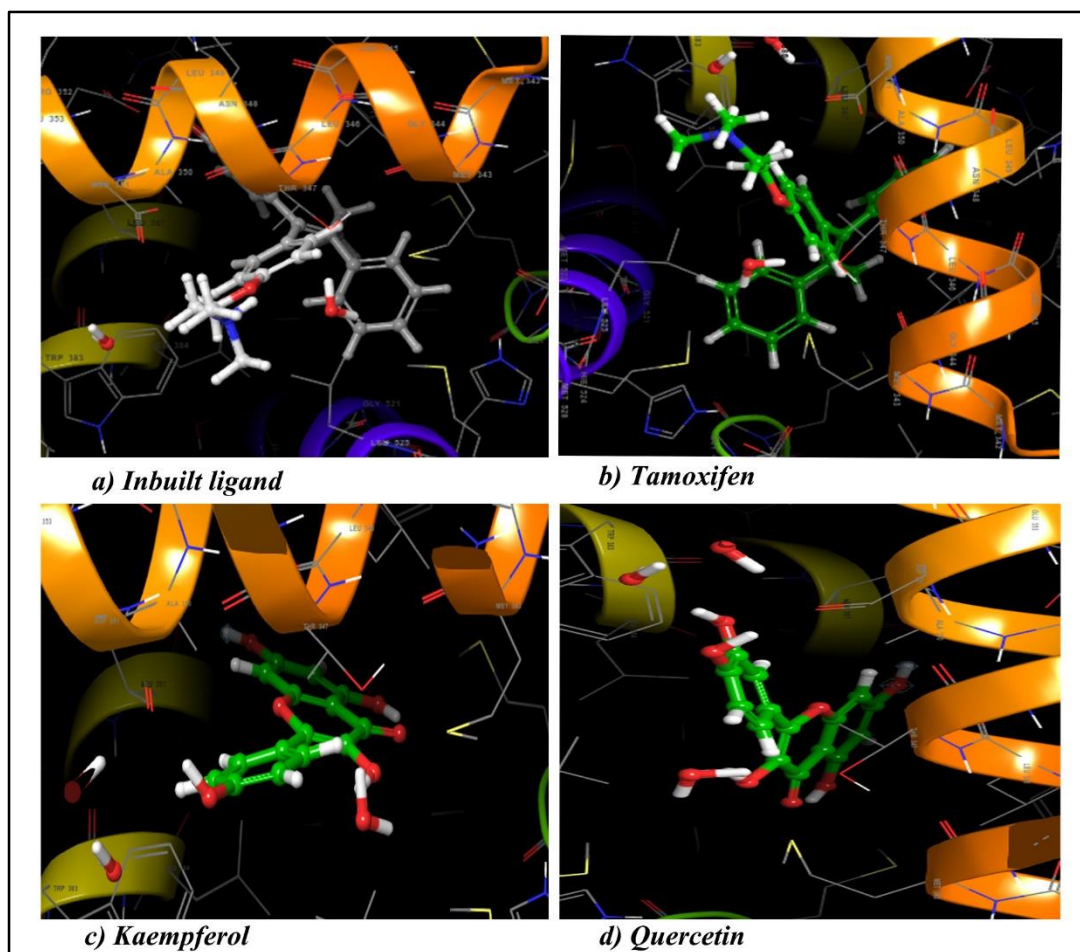
Figure 3.28. 3D interaction image of molecular docking between ERα and ligands

Table 3.22. Docking score and binding energy of estrogen receptors and ligands

Molecule	ERα		ERβ	
	Docking score	Binding energy (kcal/mol)	Docking score	Binding energy (kcal/mol)
Inbuilt ligand-Estradiol	-12.17	-125.19	-10.5	-85.248
Quercetin	-6.945	-47.026	-9.220	-66.945
Kaempferol	-6.93	-45.07	-8.478	-58.435
Tamoxifen	-10.512	-103.53	-8.023	-22.203

Figure 3.29. 2D interaction image of amino acid residues of ERα binding with ligands

3.3.6.2. Interaction of phytoestrogens with ERβ

The active site amino acid residues in estrogen receptor β (PDBID: 3OLL) are VAL280, GLU305, TRP335, MET295, SER297, LEU298, THR299, PHE377, LEU380, LEU301, ALA302, ASP303, MET336, LEU476, LEU339, MET340, GLY342, GLY472, LEU343, MET344, ARG346, LEU354, PHE356, VAL370, GLY372, ILE373, ILE376, ALA468, SER469, LYS471, MET473, HIE475, LEU477, MET479, VAL485, LEU491, LEU495. The inbuilt ligand was deeply positioned within the active site region, forming hydrogen bonding interactions with HIE475, ARG346, GLU305 and π-π stacking interactions with

147

PHE356. The inbuilt ligand displays a binding energy of -85.248 kcal/mol and a docking score of -10.5. The maximum docking score of -9.220 and binding energy of -66.945 kcal/mol were seen during the docking of ERβ with quercetin. With ARG346, GLU305 and HIE475, quercetin forms hydrogen bond interactions and with PHE356 forms π-π stacking. The quercetin shows the highest binding affinity towards ERβ followed by kaempferol (-8.478) and tamoxifen (8.023). In this instance also, β-sitosterol did not dock with the binding pocket of ERβ. The 3D interaction between ligands and receptor are given in figure 3.30 and the docking score and binding energy are given in Table 3.22. The type of interaction between the ligands and amino acids in the estrogen receptor β active sites is shown in the 2D interaction picture (Figure 3.31). The inbuilt ligand, estradiol, tamoxifen, kaempferol and quercetin create pi bonds from their aromatic rings to PHE 356. The number and nature of the hydrogen bonds vary depending on the ligand. With GLU 305, HID 475, and ARG 346, estradiol, kaempferol, and quercetin, respectively, make three hydrogen bonds whereas tamoxifen only forms one hydrogen bond with ASP 351. As a result, the findings demonstrate that phytoestrogens bind to the estrogen receptor (ER) β with greater affinity than ER alpha.
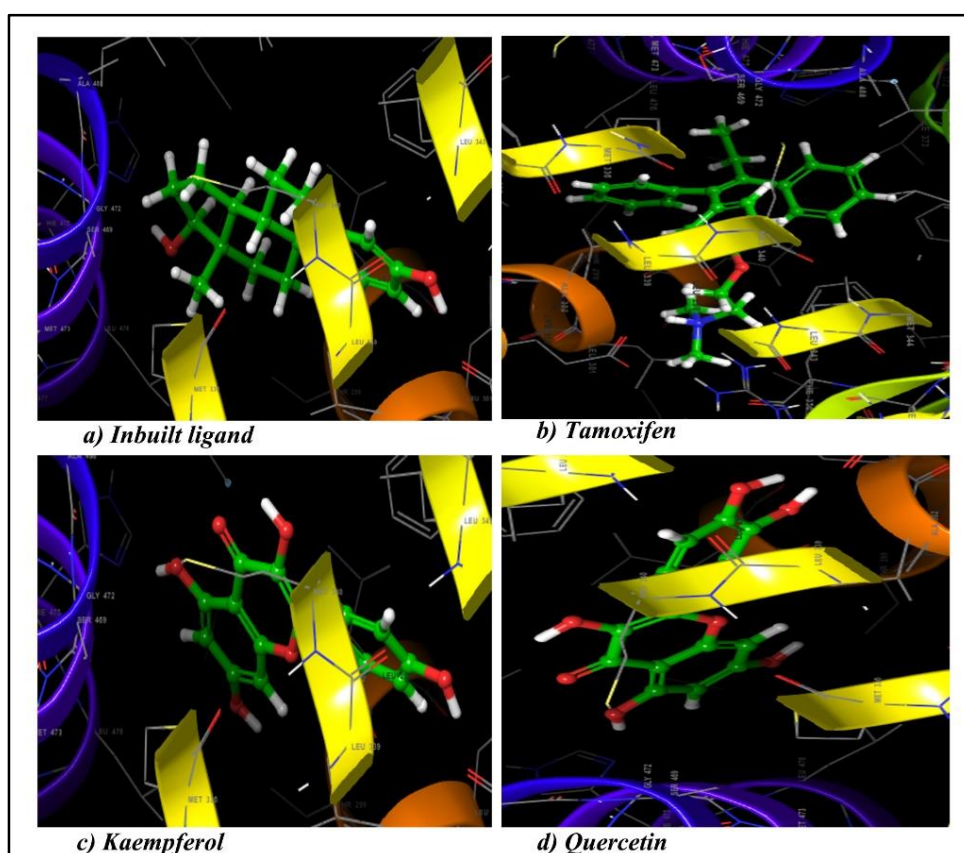
Figure 3.30. 3D interaction image of molecular docking between ERβ and ligands
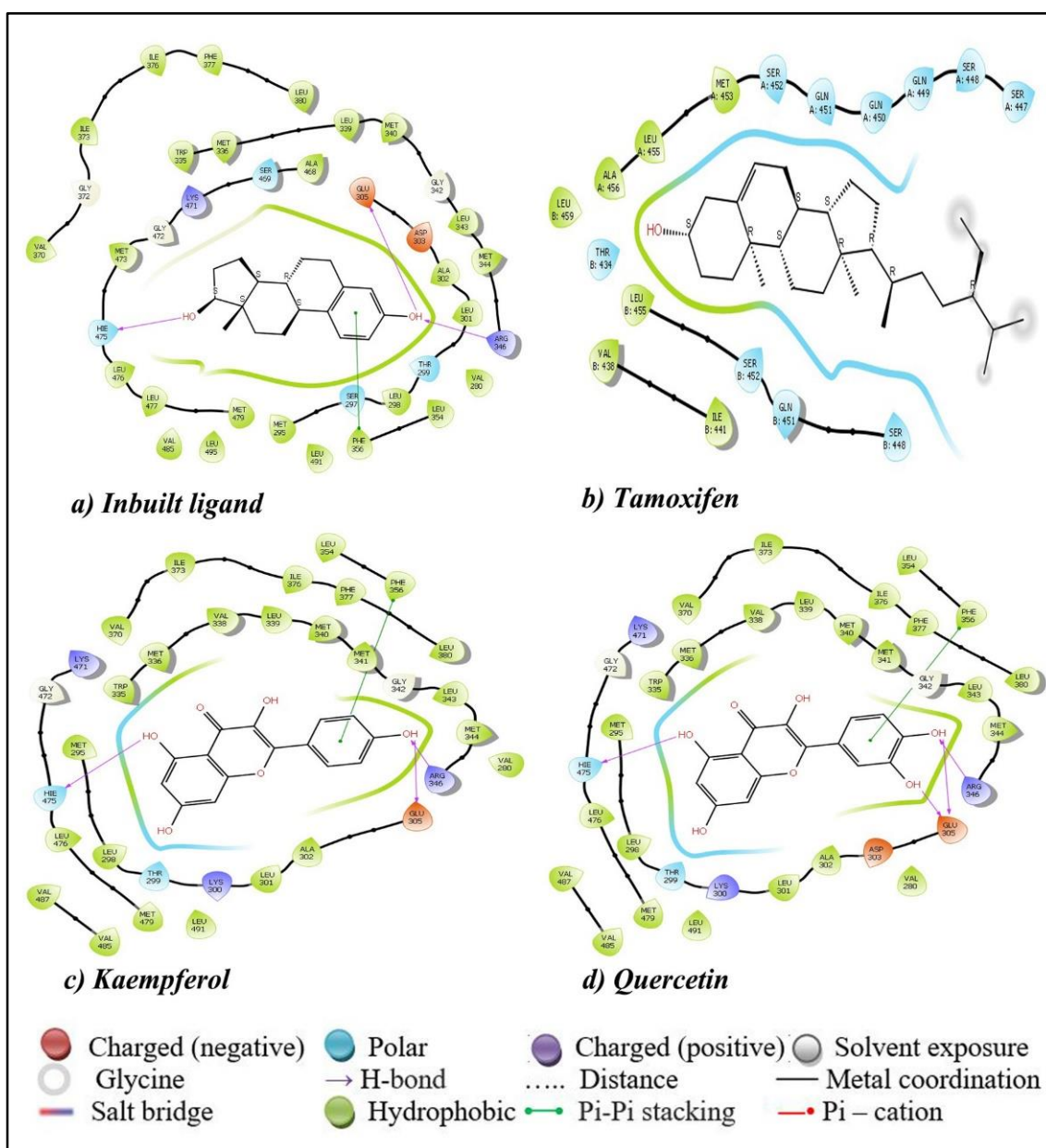
Figure 3.31. 2D interaction image of amino acid residues of ERβ binding with ligands

3.4. Discussion

Cytotoxicity assays are crucial methods in biological investigation, involving exposing cultured cells to a compound and observing resulting toxicity or cell damage (Aslantürk, 2018). There are various mechanisms through which the compounds may cause cell toxicity such as the breakdown of cell membranes, suppression of protein synthesis, irreversible interaction with receptors, enzymatic responses and inhibition of polydeoxynucleotide elongation (Ishiyama *et al*., 1996). In our current investigation, the trypan blue dye exclusion assay demonstrated cytotoxic effects of *S. asoca* and *K. pinnatum* extracts on murine tumour cells, DLA and EAC while the normal splenocytes and thymocytes were found to be unaffected by the extracts. This prompted us to assess the effects of the extracts on animals by using tumour models, including DLA-induced solid tumours and EAC-induced ascites tumours.

In the initial acute toxicity examination, administration of the crude extract to animals at a single dose of 2.5 g/kg b. wt. did not show mortality or toxicity throughout the 14-day evaluation period. As a result, the extract was deemed safe at 2.5 g/kg b. wt., and the LD_{50} (median lethal dose) calculated was higher than 2.5 g/kg b. wt. Therefore, for the *in vivo* studies, $1/10^{th}$ and $1/5^{th}$ of this dose was taken as the low dose and high dose respectively. Also other reports of acute and subacute toxicity study of *S. asoca* and *K. pinnatum* showed no death or toxicity (Mukhopadhyay and Nath, 2011, Shahid *et al*., 2018, Sasidharan and Padikkala, 2012). The crude extracts of both plants demonstrate significant antitumour properties against mice bearing solid and ascites tumours. Dalton lymphoma cells exhibit numerous favourable attributes, and immunological studies have indicated that these spontaneously arising tumours share greater similarities with human malignancies than experimentally induced ones (Ben-Efraim *et al*., 1999, Choudhury *et al*., 2016). Another often-used mouse model is the EAC tumour model, which may induce both solid and ascites tumours. It is a hormone-positive tumour that closely resembles breast cancer cells of human (Haldar *et al*., 2010, Radulski *et al*., 2023). In our study, considerable reduction in the DLA induced solid tumour and a noticeable decline in ascitic fluid accumulation as well as an extension of the lifespan of mice was observed in the EAC tumour model by the extract treatment. There are other reports of antitumour actions of *S. asoca* against Ehrlich ascites, Daltons lymphoma and S-180 tumour cell lines (Varghese *et al*., 1992, Varghese *et al*., 1993). As demonstrated in this study, extracts

were effective in preventing the growth and development of tumour cells in mice, thus providing evidence of their anti-tumour properties.

The considerable cytotoxicity exhibited by both plants led us to evaluate its antiproliferative action on various cancer cell lines using MTT assay. The extracts have shown cytotoxicity towards cancer cell lines of prostate, colorectal, cervical and breast cancers. In breast cancer cells the extracts exhibited remarkable cytotoxic effects on MDA-MB-231, SK-BR-3 and MDA-MB-468, which are ER-negative cell lines, in a dose-dependent manner. However, the extracts did not confer any anti-proliferative effects on ER-positive cell lines (MCF-7) despite high concentrations of extracts, expect T-47D cell lines. This specific cytotoxicity towards ER-negative cell lines is of prime importance as triple-negative breast cancer (TNBC), being the more prevalent and aggressive type of breast cancer, has no effective treatment approaches other than standard chemotherapy with limited success. As determined by protein expression and/or gene amplification, TNBCs are characterized by the absence of estrogen receptor α (ERα), progesterone receptor (PR), and human epidermal growth factor receptor 2 (HER 2) (Takano *et al*., 2023). However, recent studies on the immune profile of these cell lines confirm that 50 to 80% of TNBCs contain the estrogen receptor isoform ERβ (Yan *et al*., 2023).

Given the potent activities observed for *S. asoca* and *K. pinnatum*, we conducted phytochemical analysis of the crude extract and its various solvent fractions. A preliminary cytotoxicity and antioxidant assay was conducted on *S. asoca* and *K. pinnatum* bark extracts to determine the appropriate extract to use in the subsequent studies. Due to their superior activities in cytotoxicity and free radical scavenging, the crude methanol extracts of both plants were chosen for further studies. The ensuing studies also included methanol fractions, which closely corresponded with crude extract in terms of activity. The phytochemical analysis revealed phenols, alkaloids, saponins, flavonoids, terpenoids, phytosterols and tannins in extracts of both plants. Other authors also have reported similar compounds from the bark of Asoka (Bendigeri *et al*., 2019, Mukhopadhyay and Nath, 2011). Furthermore, extracts from *K. pinnatum* bark contain similar compounds as well reported by different authors (Sheik and Chandrashekar, 2014, Javarappa *et al*., 2016). The bioactive compound classes such as flavonoids and phenols detected were quantified in all the extracts from both plants and shown to have more

phenolic content in *K. pinnatum* than *S. asoca*. High phenolic content in the stem methanolic extract of *K. pinnatum* is reported (Sheik and Chandrashekar, 2014). In UV-visible spectroscopy, characteristic peaks were observed between 200 and 400 nm in all extracts. These peaks are likely indicative of phenolic compounds, since phenolic rings may absorb ultraviolet light and are known to exhibit colouration (Aleixandre-Tudo and Du Toit, 2018). The presence of one or more peaks in this region suggests the existence of unsaturated groups and O, N and S heteroatoms (Njokua *et al*., 2013). In a previous report, the absorption spectrum of *S. asoca* was observed to be dominated by peaks between 200 and 400 nm (Sharma *et al*., 2021). Any molecule's biological activity is affected by its functional groups, which contribute significantly to its overall physicochemical characteristics. The FTIR spectroscopy has proven to be a valuable method for characterizing and identifying the functional groups present in unidentified mixtures of plant extracts (Sasidharan *et al*., 2011). The results of FTIR analysis were found to contain terpenes attributed to C-H stretching, polyphenols and flavonoids from O-H stretching and alkaloids owing to N-H stretching, in all extracts of both plants. A number of functional groups have been identified within plants like amines, aldehydes, amides, alkenes, alcohols, anhydrides, aromatics, phenols, esters and carboxylic acids. As reported previously, the crude bark extract of *S. asoca* contained N-H stretching bonds, alkenes, aldehydes and carboxylic acids (Jyothi and Satyavati, 2016). Despite this, UV-Vis and FTIR spectroscopy has limitations as in UV-Vis it is challenging to identify specific constituents by their absorption peaks and in FTIR relative positions of the functional groups and molecular weight of the compound can't be determined (Njokua *et al*., 2013). Consequently, other analytical methods must be used in conjunction with these spectrometric findings to ensure that extracts are properly characterized and constituents are identified (Karpagasundari and Kulothungan, 2014). For that various chromatographic techniques were employed to enable accurate extract characterisation and constituent identification.

Chromatographic techniques such as TLC confirmed the presence of kaempferol and HPTLC revealed distinct bands of quercetin and *β*-sitosterol in both crude and methanol fraction of both plants. As a versatile separation technique, HPTLC can be used to evaluate the composition, purity, homogeneity, solubility, assay value, drug availability and interactions between drugs (Attimarad *et al*., 2011). *β*-sitosterol and quercetin identified by HPTLC are considered to be phytoestrogens due to their structural similarity

to estradiol (van Duursen, 2017). In the study HPLC analysis carried out also confirmed the presence of phytoestrogen, β-sitosterol in both the plants. In crude extract of *S. asoca* earlier studies have reported catechin, gallic acid, ellagic acid, quercetin by HPTLC analysis (Saha *et al*., 2013, Rathee *et al*., 2010) and ursolic acid, gallic acid, lupeol, epicatechin, epigallocatechin by HPLC analysis (Ahmad *et al*., 2016a, Ketkar *et al*., 2015). In GCMS the compounds detected include some polysaccharides, antimicrobials, class of phenolic compounds, plant metabolites, antioxidant and antiproliferative compounds in both plants. In another studies β-sitosterol, flavanpentol, catechin and other phenolic compounds were detected in *S. asoca* bark extracts using GCMS (Bangajavalli, 2019, Mukhopadhyay *et al*., 2017). Moreover, the existence of diterpene compounds in *K. pinnatum* was documented in a study, which was verified through TLC, HPTLC, FTIR, HPLC and LCMS screening of the compound obtained from the ethyl acetate extract of the plant (Javarappa *et al*., 2016). The LC-MS analysis of both plants identified some of the important and previously known compounds such as gallic acid, catechin, epigallocatechin gallate, caffeic acid, quercetin, kaempferol, luteoline, β-sitosterol, rutin, ursolic acid. In the previous reports of LCMS analysis of *S. asoca* crude bark methanolic extract, apigenin, catechin, caffeic acid, β-sitosterol, kaempferol, quercetin, gallic acid, tannic acid, vanillin and rutin were identified (Mittal *et al*., 2013b, Ghatak *et al*., 2015b, Gahlaut *et al*., 2013b).

Collectively, the findings of characterisation and phytochemical analysis of both plants shows important phytoestrogenic compounds. Various breast cancer cells we screened has different receptor statutes and expresses different isoform of estrogen receptors, ERα or ERβ. This suggests a possibility of phytoestrogens present in plants, which have structural similarities to natural estrogen, to act as agonists or antagonists to the estrogen receptors. Therefore we conducted molecular docking of phytoestrogens like β-sitosterol, quercetin and kaempferol present in both plants with targeted receptors, ERα and ERβ and compared the binding efficiency with that of estradiol and tamoxifen. The molecular docking technique predicts a ligand's binding affinity as well as its optimal position within a target's active site (Abdullahi and Adeniji, 2020). Generally, the ligands are small molecules, and algorithms for docking peptides with proteins and proteins with other proteins are currently under development (Agrawal *et al*., 2019). Docking studies have become more and more important in pharmaceutical research as different algorithms have been developed to perform molecular docking studies (Meng *et al*., 2011). The results of

the docking studies show that the phytoestrogens bind with ERβ with more affinity than ERα receptor. The docking score of quercetin was almost comparable to that of the inbuilt ligand, estradiol, and docking score and binding energy of quercetin and kaempferol were considerably higher than those of tamoxifen, the mainstream chemotherapy drug. Also, there are reports of high binding interaction of flavonoids in *S. asoca* with human estrogen receptors. The binding scores of *Saraca asoca* flavonoids in a molecular simulation study with estrogen receptors demonstrate their remarkable binding capability to the active site of estrogen receptors, and molecular orbital analyses and pharmacokinetic metrics confirm the effectiveness of the compounds (Sherin and Manojkumar, 2017). This binding affinity of flavonoids for estrogen receptors was greater than the values reported in another study on flavonoids (Suganya *et al*., 2014). According to our docking results, phytoestrogens like quercetin and kaempferol dock deeper into active amino acid binding pockets in estrogen receptor β than ERα. The high affinity of these phytoestrogens for ERβ is relevant because it indicates that the chemopreventive effects of these phytoestrogens are related to their interactions with estrogen receptors, particularly for ERβ, which may result in a variety of biological reactions (Kuiper *et al*., 1998).

Hence, this chapter highlights the antiproliferative properties of the crude extracts from both plants especially on triple negative breast cancers. Phytochemical analysis confirms the presence of phytoestrogens and molecular docking studies demonstrate their potential binding capabilities with estrogen receptors, particularly ERβ. Given that phytoestrogens modulate their effects through estrogen receptors, their estrogenic and anti-estrogenic effects warrant further investigation and is discussed in the subsequent chapter along with the anti- inflammatory properties.

Chapter 4
Anti-inflammatory and anti-estrogenic properties of extracts of *S. asoca* and *K. pinnatum*

4.1. Introduction

Saraca asoca has been used in traditional Indian medicine for many centuries. Within Ayurveda, it is employed for addressing a range of women's health issues, including excessive uterine bleeding, gynecological problems, and irregular menstruation, among others (Sivarajan and Balachandran, 1994). The plant *Kingiodendron pinnatum*, belonging to the same family as Asoka, is utilized by tribes to treat conditions such as gonorrhoea, various respiratory tract ailments, genitourinary issues, and joint pains (Kumar *et al*., 2011). A study has demonstrated the pharmacological effectiveness of *K. pinnatum* in Ayurvedic formulations as an alternative to *S. asoca* (Shahid *et al*., 2018). Based on the findings presented in previous chapter, both plants have been demonstrated to contain phytoestrogens, including *β*-sitosterol, quercetin, kaempferol, and others. The strong cytotoxic properties observed in both plants are believed to stem from the potential binding of these phytoestrogens to the estrogen receptors, resulting in the inhibition of cell growth. Thus, in this chapter, both *in vitro* and *in vivo* tests were undertaken to evaluate the estrogenicity/antiestrogeneicity of plant extracts.

The chosen *in vivo* screen for the testing for the estrogenic/antiestrogenic potential of plant extracts was determined to be the rodent uterotropic response assay, which has long been regarded as the gold standard for assessing estrogenicity/antiestrogenicity of compounds (Padilla-Banks *et al*., 2001). We limited our analysis to the use of immature animals rather than adult ovariectomized animals since developing tissues are particularly sensitive to hormonal interruptions (McLachlan, 1993). Estrogen elicits two responses in the uterus. The initial response involves an increase in uterus weight due to water intake, followed by subsequent weight gain attributed to tissue growth (Jones and Edgren, 1973). Rats are commonly utilized in toxicological testing, and in this study, we employed immature rats to assess the sensitivity to various doses of plant extracts. We compared the increase in uterine wet weight and morphological endpoints, which are acknowledged as estrogenic responses (Newbold *et al*., 1997). Estrogen agonists and antagonists function as substrates for estrogen receptors *α* and *β* and can either stimulate or hinder the receptors' ability to regulate transcription (Owens and Ashby, 2002). When estrogens are stimulated, uterine tissues grow quickly and vigorously, especially in laboratory rodents where the estrous cycle persists for around 4 days. Therefore for the *in vivo* assessment of estrogen agonists and antagonists, the rat uterus is a suitable target organ

(Oecd/Ocde, 2007). Consequently, in this study, we compared uterine responses of *S. asoca* and *K. pinnatum* extracts in immature Wistar rats for its estrogenic/antiestrogenic activity.

Estrogen has a vital role in reproductive processes and also has an important influence on inflammation in the body. The impact of estrogen is mediated by estrogen receptors (ERs), which are found in a variety of cell types and are essential for both modulating the cellular response to estrogen and controlling inflammation (Fuentes and Silveyra, 2019). Depending on the circumstances and physiological conditions involved, estrogen has both pro-inflammatory and anti-inflammatory effects (Straub, 2007). By activating NF-κB, estrogen can upregulate pro-inflammatory gene expression, exacerbating inflammation in diverse tissues such as in endometrium (Zhang *et al*., 2023). Additionally, estrogen can modulate immune cell function, influencing the initiation and progression of inflammatory responses by B cells, T cells and dendritic cells (Fan *et al*., 2019). However, estrogen also exhibits anti-inflammatory properties by inhibiting the production of pro-inflammatory cytokines like TNF-α, IL-1, and IL-6 (Brown *et al*., 2010). The improper regulation of estrogen signaling has been linked to a variety of inflammatory ailments, including metabolic disorders, autoimmune diseases, cardiovascular diseases, and neuroinflammatory syndromes (Villa *et al*., 2016). As a result, the body's inflammatory processes are greatly influenced by an imbalance in estrogen. Phytoestrogens are natural compounds structurally similar to estrogen and are found in both *S. asoca* and *K. pinnatum*. These compounds have the ability to bind to estrogen receptors and can elicit different biological effects. Therefore, the anti-inflammatory properties of crude extracts of *S. asoca* and *K. pinnatum* were investigated in the current study utilizing various *in vitro* and *in vivo* assays. The nitric oxide scavenging assay, 5-lipoxygenase inhibition assay, and assay for measurement of nitric oxide in the LPS activated RAW 264.7 cultured cells were used for *in vitro* anti-inflammatory evaluation. The plants *in vivo* anti-inflammatory abilities were assessed using experimental models of inflammation, including formalin and carrageenan-induced chronic and acute paw edema respectively.

4.2. Materials and methods

4.2.1. Preparation of extract

The crude methanolic bark extracts of *S. asoca and K. pinnatum* were prepared as per the method detailed in section 2.2.1 of Chapter 2.

4.2.2. Animals

The animals were acquired from Kerala Veterinary and Animal Sciences University (KVASU) and were handled in accordance with Chapter 2's section 2.1.4.

4.2.3. Cell lines

Using the method outlined in Chapter 2's section 2.1.5, murine macrophage cell line, RAW 264.7 cells were maintained.

4.2.4. Evaluation of the anti-inflammatory properties of the extracts

The *in vitro* anti-inflammatory properties of *S. asoca* and *K. pinnatum* extracts was determined using nitric oxide (NO) scavenging assay, 5-Lipoxygenase inhibition assay and *in vitro* measurement of NO levels in LPS activated RAW 264.7 cells.

4.2.4.1. *In-vitro* anti-inflammatory activities

4.2.4.1.1. Nitric oxide (NO) scavenging assay

Both plant's crude methanol extracts potential to scavenge NO was analysed using the protocol outlined in Chapter 2's section 2.2.13.1.1.

4.2.4.1.2. 5-Lipoxygenase inhibition assay

The inhibition of the activity of 5-Lipoxygenase (5-LO) enzyme by *S. asoca* and *K. pinnatum* extracts were determined as outlined in the section 2.2.13.1.2. of Chapter 2.

4.2.4.1.3. Inhibition of nitric oxide formation in LPS-induced RAW264.7 cells

The prevention of NO generation in lipopolysaccharide (LPS) activated RAW 264.7 cells by both the crude methanol extracts of plants were assessed in accordance with section 2.2.13.1.3. of chapter 2.

4.2.4.2. *In-vivo* anti-inflammatory activities

The anti-inflammatory properties of *S. asoca* and *K. pinnatum* extracts have been evaluated in experimental models of inflammation, such as formalin-induced chronic paw edema and carrageenan-induced acute paw edema.

4.2.4.2.1. Carrageenan induced acute paw edema

In the acute model, carrageenan was injected into the paw of mice followed by treatment with the plant extracts as detailed in the section 2.2.13.2.1. of Chapter 2.

4.2.4.2.2. Formalin induced chronic inflammation

A chronic paw edema model was developed by injecting formalin into the paws of mice followed by subsequent treatment with the plant extracts as detailed in Chapter 2's section 2.2.13.2.2.

4.2.5. Estrogen- screen assay

The breast cancer cell lines expressing ERα (MCF-7) and ERβ (MDA-MB-231) were cultured in standard growth media (DMEM) and incubated for 24 hr. The growth media was subsequently replaced by phenol red-free DMEM with charcoal-stripped FBS containing similar ingredients as the growth media. Both plant extracts (0-200 μg/mL) and 17β-estradiol (1-5 nM) were added and allowed to incubate at 37 °C for three days. The MTT test was used to determine the rate of proliferation of cells (section 2.2.17.2 of Chapter 2) and the process is described in detail in Chapter 2's section 2.2.17.3.

4.2.6. Immature rodent uterotropic bioassay

Estrogenicity/antiestrogenicity of *S. asoca* and *K. pinnatum* extracts was evaluated following the recommendations provided by the OECD. The female immature rats were supplied by the Kerala Veterinary and Animal Sciences University, located in Thrissur, Kerala. Initial toxicity testing of plant extracts was done after weaning. Plant extracts and 17β-estradiol were given orally to the animals over the course of five days for the estrogenicity study, while plant extracts and tamoxifen were provided continuously for two weeks for the antiestrogenicity study. The detailed procedure of both the studies are given in section 2.2.15 of Chapter 2.

4.2.7. Statistical analysis

The values were expressed as mean ± standard deviation (SD) based on six animals per group for *in vivo* studies. The data were evaluated using one-way ANOVA following Tukey's multiple comparison test in GraphPad Prism 8. P-values at these levels were only regarded statistically significant at $p<0.01$**, $p<0.05$* and $p>0.05$ was deemed non-significant.

4.3. Results

4.3.1. Determination of *in-vitro* anti-inflammatory activities

The nitric oxide (NO) scavenging activity of the crude methanolic extracts of *S. asoca* and *K. pinnatum* shows considerable ability of extracts to scavenge nitric oxide radical in a concentration dependent manner (Figure 4.1). The IC_{50} value of *S. asoca* and *K. pinnatum* were found to be 38.47 ± 2.44 and 48 ± 5.21 μg/mL respectively. The potential of extracts for inhibiting NO production in LPS-activated RAW 264.7 were also carried out and nitric oxide generation was assessed as the nitrite concentration in the culture medium. Both plant extracts have been found to significantly scavenge nitric oxide free radicals with IC_{50} values of 67.42 ± 3.89 μg/mL for *S. asoca* and 82.21 ± 6.33 μg/mL for *K. pinnatum* respectively (Figure 4.2). The plant extracts also reversed the morphological alterations brought on by the LPS (Figure 4.3). RAW 264.7 cell viability was assessed utilizing MTT assay in the presence of extracts and shown to have no major change in cell viability in LPS stimulated extract treated groups and unstimulated control cells (Figure 4.4). In the 5-lipoxygenase enzyme inhibition assay, 41.55 μg/mL of *S. asoca* and 78.65 μg/mL of *K. pinnatum* extract were found to be effective in inhibiting 50 % of 5-lipoxygenase enzyme activity (Figure 4.5).
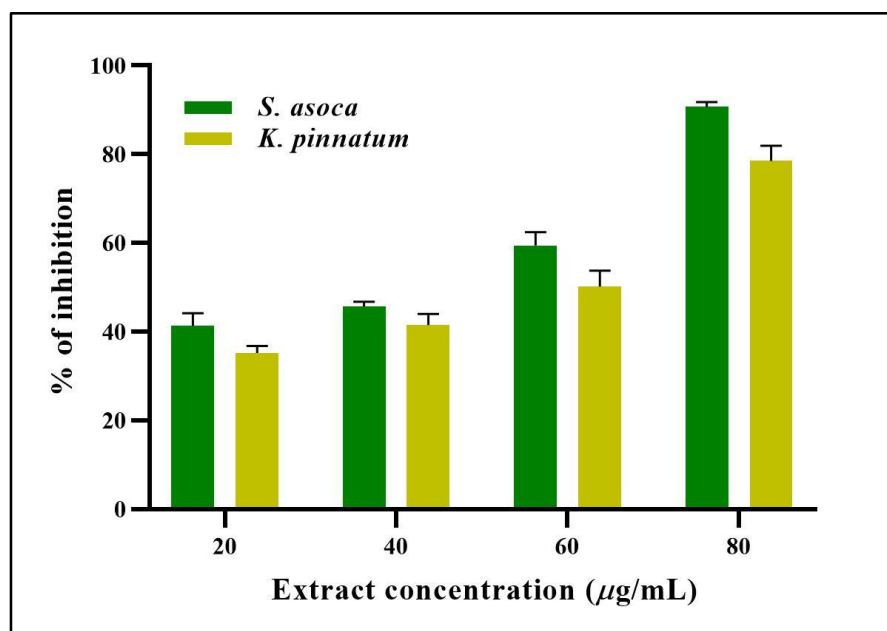
Figure 4.1. Percentage inhibition of nitric oxide radicals by *S. asoca* and *K. pinnatum* extracts. The values are presented as mean $\pm$ SD based on three different determinations

160
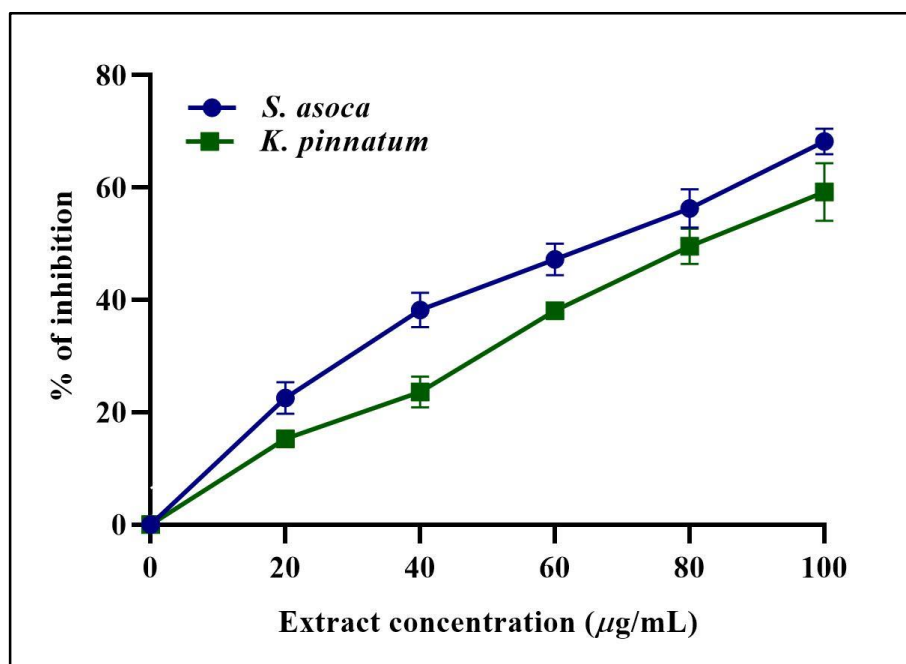
Figure 4.2. Nitric oxide production inhibition in LPS-stimulated RAW 264.7 by *S. asoca* and *K. pinnatum* extracts. The values are presented as mean ± SD based on three separate evaluation
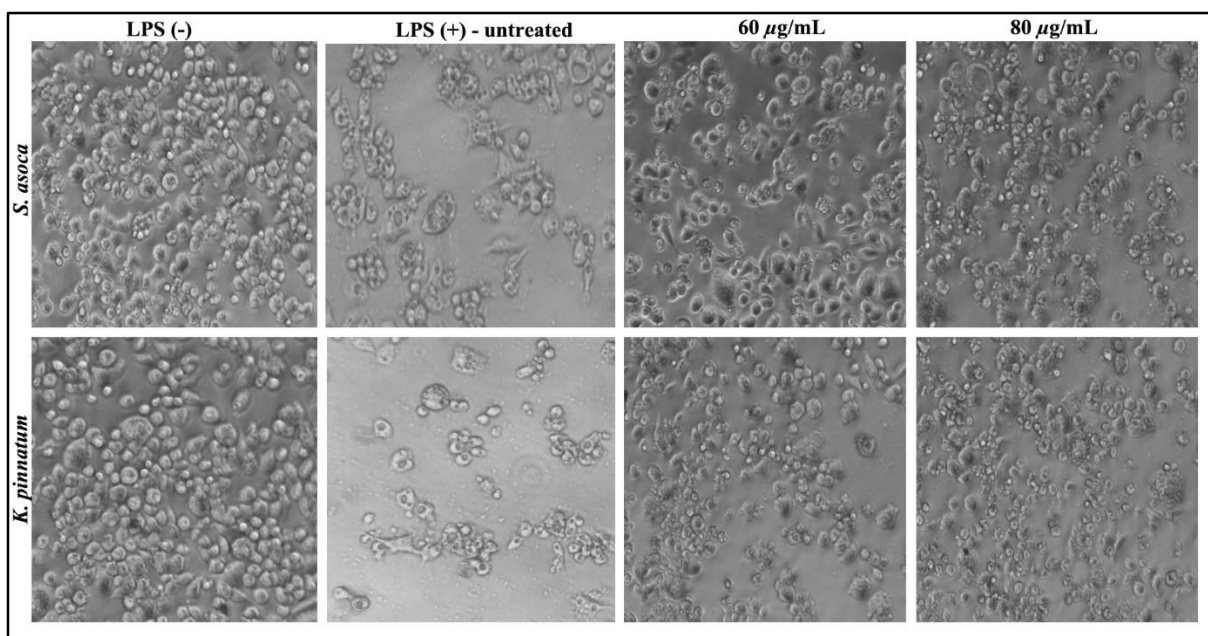
Figure 4.3. Inhibition of morphological alterations in LPS stimulated RAW 264.7 macrophages cells by extracts visualized by phase contrast microscopy (20X magnification)
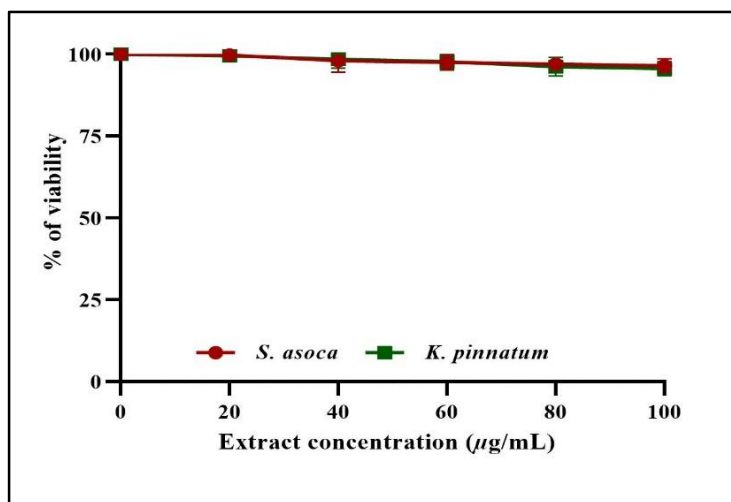
Figure 4.4. Percentage viability of macrophage RAW 264.7 cells after extracts treatment. The values are presented as mean ± SD based on three different determinations
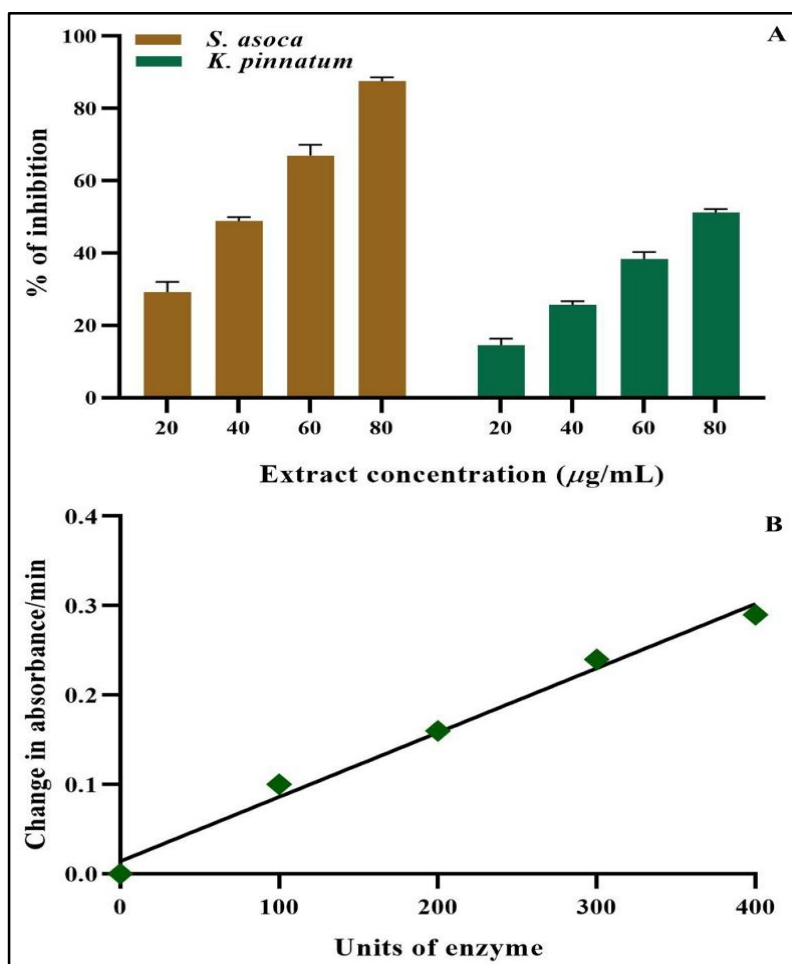
Figure 4.5. 5- Lipoxygenase enzyme inhibition by extracts of *S. asoca* and *K. pinnatum* (A), Calibration curve of 5- lipoxygenase enzyme (B). The values are presented as mean ± SD based on three different determinations

Table 4.1. Percentage inhibition of acute and chronic inflammation by *S. asoca* and *K. pinnatum* extracts

Treatments	% inhibition of inflammation caused by carrageenan	% inhibition of inflammation caused by formalin
S. asoca low dose (SALD - 250 mg/kg b. wt)	54.43 %	51.85 %
S. asoca high dose (SAHD - 500 mg/kg b. wt)	70.88 %	60.18 %
K. pinnatum low dose (KPLD - 250 mg/kg b. wt)	46.83 %	40.86 %
K. pinnatum high dose (KPHD - 500 mg/kg b. wt)	60.75 %	53.76 %
Standard- Diclofenac (10 mg/kg b. wt)	77.21 %	66.66 %

4.3.2. Assesment of *in-vivo* anti-inflammatory activities

4.3.2.1. Effect of extracts on acute inflammation induced by carrageenan

The edema caused by carrageenan injection increased gradually over three hours. The paw edema in the extract-treated mice was significantly reduced compared to the control group. In comparison to control, *S. asoca* extract showed 54.1 and 70.88% decline in inflammation at 250 and 500 mg/kg b.wt. dosages correspondingly, while *K. pinnatum* extract exhibited 46.83 and 60.75% reduction at the same doses (Table 4.1). Diclofenac, the standard drug used was able to reduce paw edema by 77.21% compared to control (Figure 4.6 and 4.7).

4.3.2.2. Effect of extracts on chronic inflammation induced by formalin

The *S. asoca* extract treated animals with low (SALD) and high (SAHD) doses were observed to reduce paw edema volume by 51.85 % and 60.18 % respectively in animals induced with chronic paw edema using formalin. Whereas the decrease in inflammation by KPLD and KPHD was 40.86 % and 53.76 % respectively for *K. pinnatum* extract. In comparison with the control group, diclofenac reduced paw edema by 66.66 % (Table 4.1). The effects of *S. asoca* and *K. pinnatum* extracts on the chronic paw edema of animals injected with formalin are shown in figure 4.8 and 4.9.
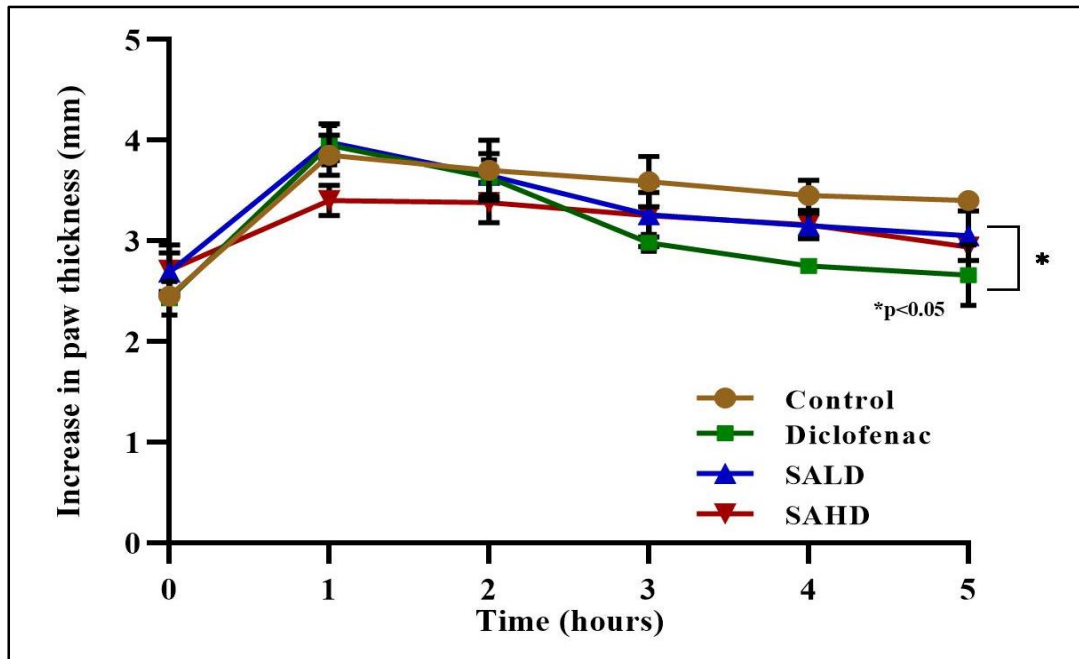
Figure 4.6. Influence of *S. asoca* extract administration on acute paw edema induced by carrageenan. A total of 6 animals are included in each group and the values are based on the mean ± standard deviation (SD). *P<0.05 and **P<0.01 probability values are regarded as statistically significant
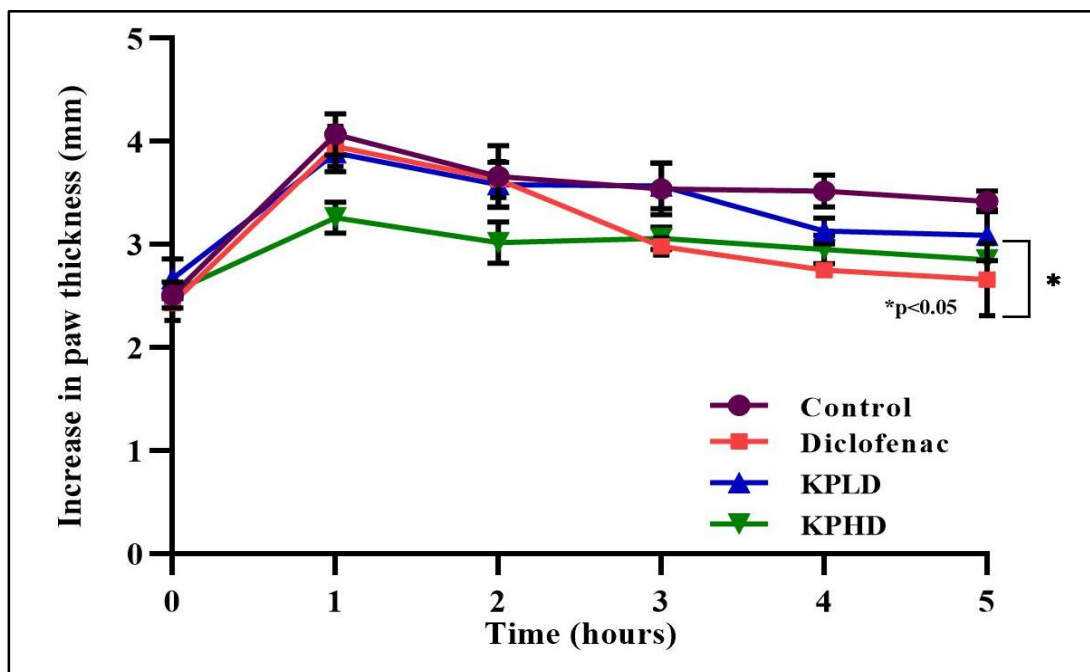
Figure 4.7. Influence of *K. pinnatum* extract administration on acute paw edema induced by carrageenan. A total of 6 animals are included in each group and the values are based on the mean ± standard deviation (SD). *P<0.05 and **P<0.01 probability values are regarded as statistically significant
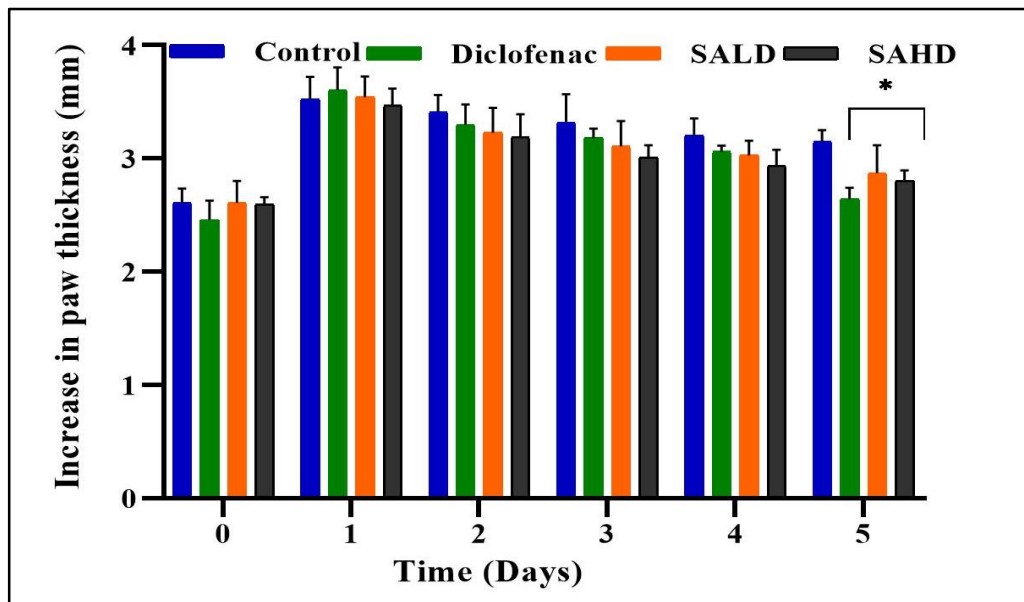
Figure 4.8. Effect of *S. asoca* extract administration on chronic paw edema induced by formalin. A total of 6 animals are included in each group and the values are based on the mean ± standard deviation (SD). *P<0.05 and **P<0.01 probability values are deemed statistically significant
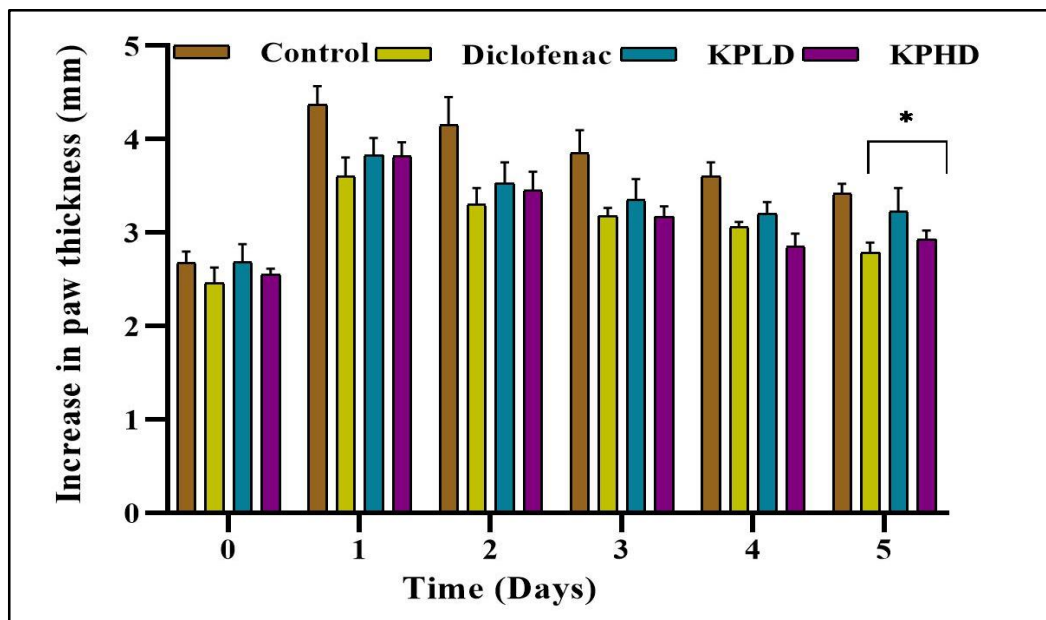
Figure 4.9. Effect of *K. pinnatum* extract administration on chronic paw edema induced by formalin. A total of 6 animals are included in each group and the values are based on the mean ± standard deviation (SD). *P<0.05 and **P<0.01 probability values are regarded as statistically significant

165

4.3.3. Estrogen-screen assay

The MCF-7 cells exhibit induction of cell proliferation when cultured in phenol red-free DMEM culture media with 17β-estradiol (1-5 nM). The proportion of viable cells varies depending on the dose, and at 5 nM, the viability of the cells was 30% higher than control (Figure 4.10). MCF-7 cells treated with various doses of both plant extracts (0-200 μg/mL) also exhibited cell growth. At a concentration of 200 μg/mL of *S. asoca* and *K. pinnatum* extracts, no reduction in cell growth was observed instead the cell growth was found to be 7 and 8% respectively, greater than control. A slight reduction of 10% in cell volume was seen in MDA-MB-231 cells treated with 5 nM 17β-estradiol, but there was no significant decrease in the rate of cell proliferation (Figure 4.11). When MDA-MB-231 cells were exposed to SA and KP extracts at concentrations of 100 and 120 μg/mL, the number of cells were drastically reduced to half.
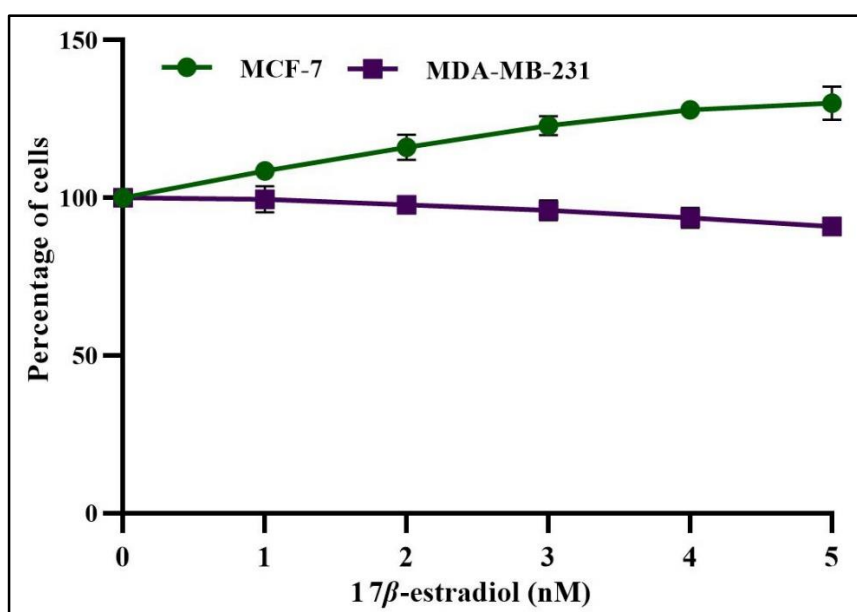
Figure 4.10. Effect of 17β-estradiol on proliferation of MDA-MB-231 and MCF-7 cells in phenol red-free DMEM
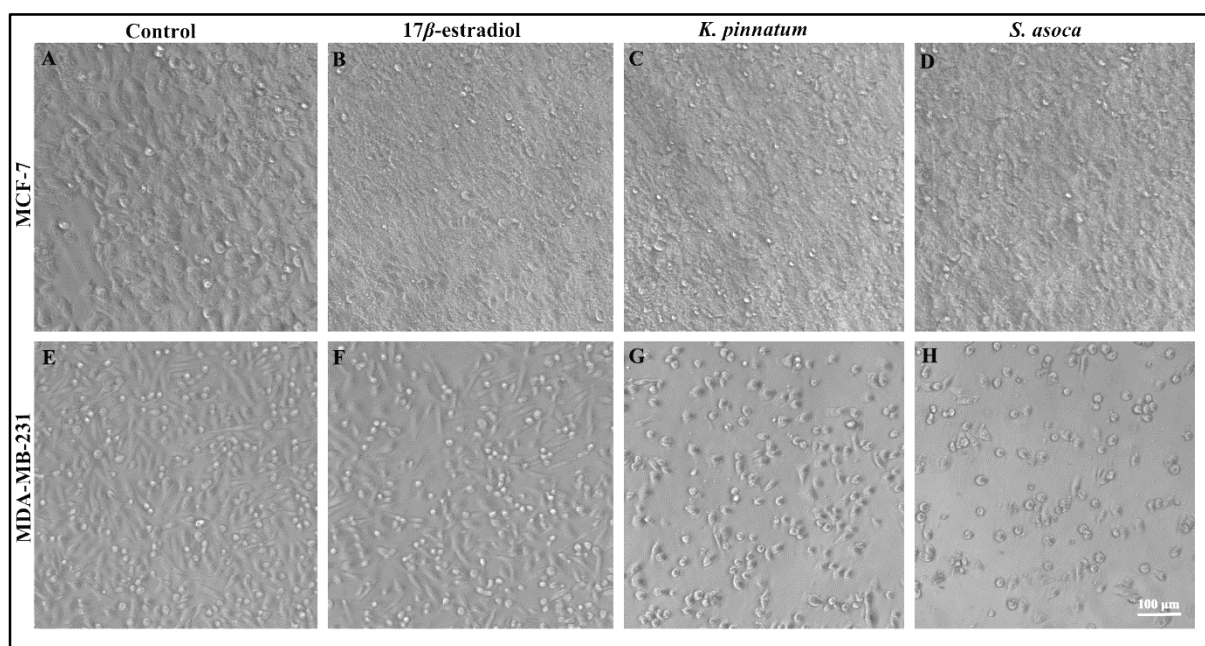
Figure 4.11. Morphology of MDA-MB-231 and MCF-7 cells exposed to 17β-estradiol and extracts visualized using phase contrast microscope (20 X magnification, 100 μm scale bar is applicable to all images). A, E- Control; B, F- 17β-estradiol (5 nM); C- *K. pinnatum* (200 μg/mL); D- *S. asoca* (200 μg/mL); G- *K. pinnatum* (120 μg/mL); H- *S. asoca* (100 μg/mL)

4.3.4. Immature rodent uterotropic bioassay

4.3.4.1. Evaluation of estrogenic actions of *S. asoca* and *K. pinnatum* extracts on immature rats

The initial toxicity testing of plant extracts shows no sign of toxicity to animals up to 2.5 g/kg b.wt. None of the animals showed any observable changes when they were checked for death, sickness, and overall clinical symptoms like altered behaviour, skin, fur, eyes, odd breathing patterns, or occurrence of excretions and secretions. The animals administered with low and high doses of *S. asoca* and *K. pinnatum* extracts showed no significant differences in body weight from untreated animals. The uterus in the extract-treated animals appeared normal in shape whereas 17β-estradiol treated group exhibited uterine water imbibition in response to estrogen (Figure 4.12). A statistically significant ($p < 0.05$) 3.62-fold increase in uterine wet weight was induced by the 17β-estradiol treated group (Figure 4.13). Radioimmunoassay (RIA) analysis of estrogen levels in

167

extract-treated animals did not indicate an estrogenic effect, since the levels of estrogen were below 10 pg/mL. In contrast, the level of estrogen was 95.75 pg/mL in animals treated with 100 μg/mL of 17β-estradiol.

From the histopathological observations of the uterus, the 17β-estradiol treated group induces proliferative changes in the endometrium as evidenced by loose stroma, an increase in gland number and an increase in luminal epithelium height. When compared to the normal group, the histopathological analysis of the uterus of the immature rats administrated with *S. asoca* and *K. pinnatum* extracts did not reveal any significant differences (Figure 4.14). The usual ovoid shape with follicles in the primary and secondary stages of development and a dense cellular stroma was seen in the ovarian histoarchitecture of the normal and extract-treated groups. The treatment of immature female rats with 17β-estradiol triggered the progress of their puberty characterized by an increase in tertiary developing follicles in the ovary (Figure 4.15).
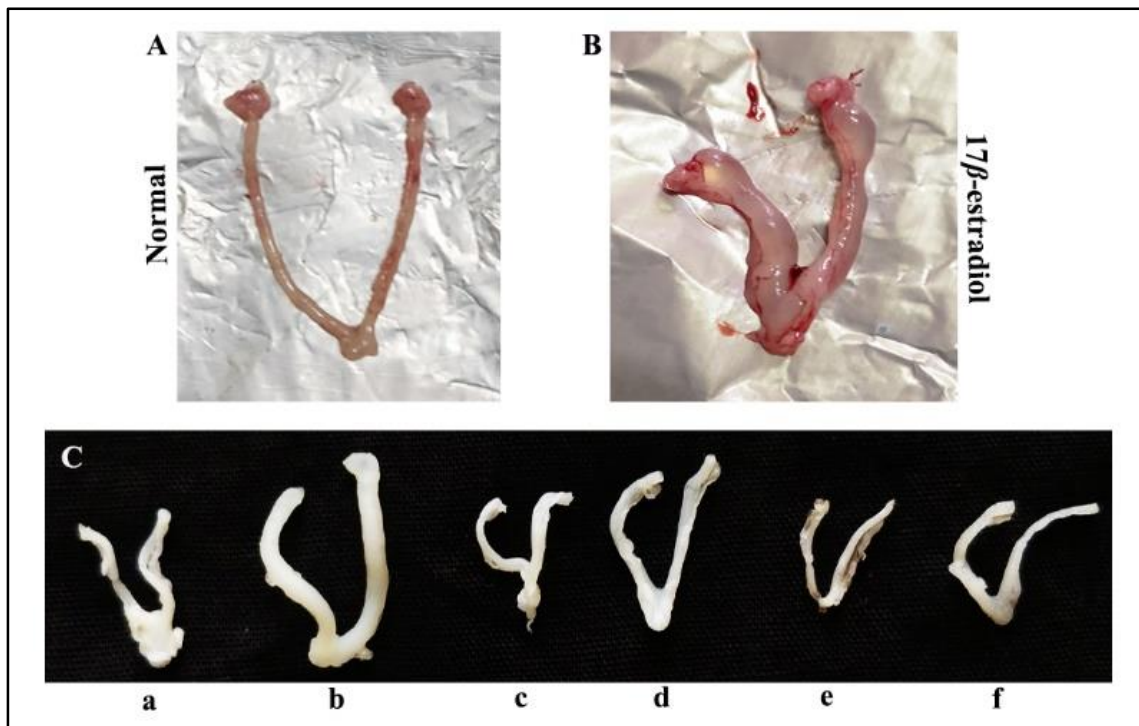
Figure 4.12. Size of uterus after different treatment. A and B- uterus of normal and 17β-estradiol treated group; C- dry uterus of different treatment groups, a- normal, b- control, c- SAHD, d- SALD, e- KPHD, f- KPLD
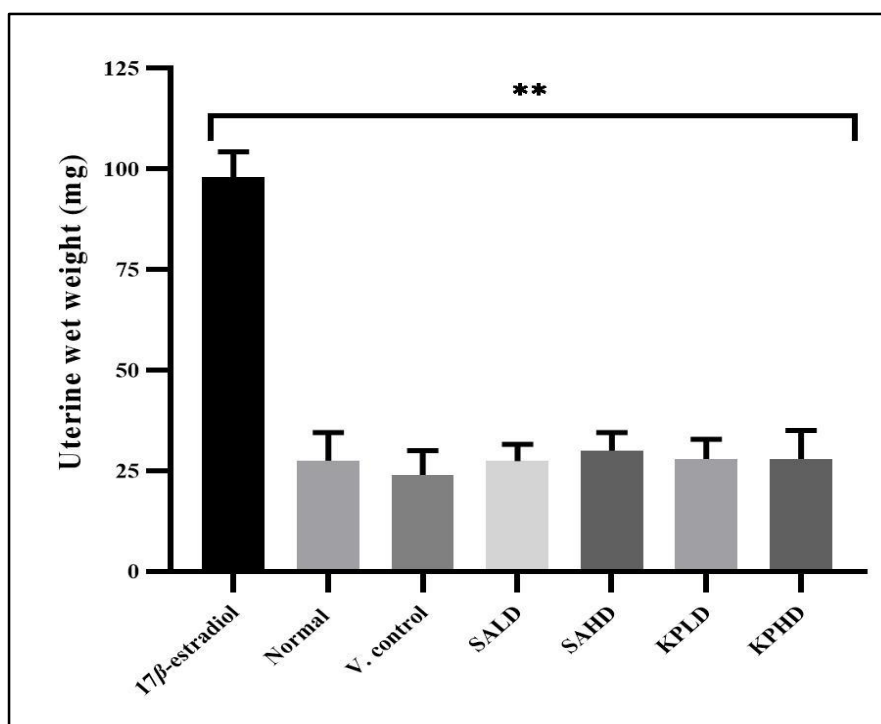
Figure 4.13. Weight of uterus after different treatment. Vehicle control – Propylene glycol, SALD – *S. asoca* 250 mg/kg b. wt, SAHD – *S. asoca* 500 mg/kg b. wt., KPLD – *K. pinnatum* 250 mg/kg b. wt, KPHD – *K. pinnatum* 500 mg/kg b. wt. Each group contains 5 animals and the values were calculated using the mean ± standard deviation (SD). *P<0.05 and **P<0.01 probability values are regarded as statistically significant
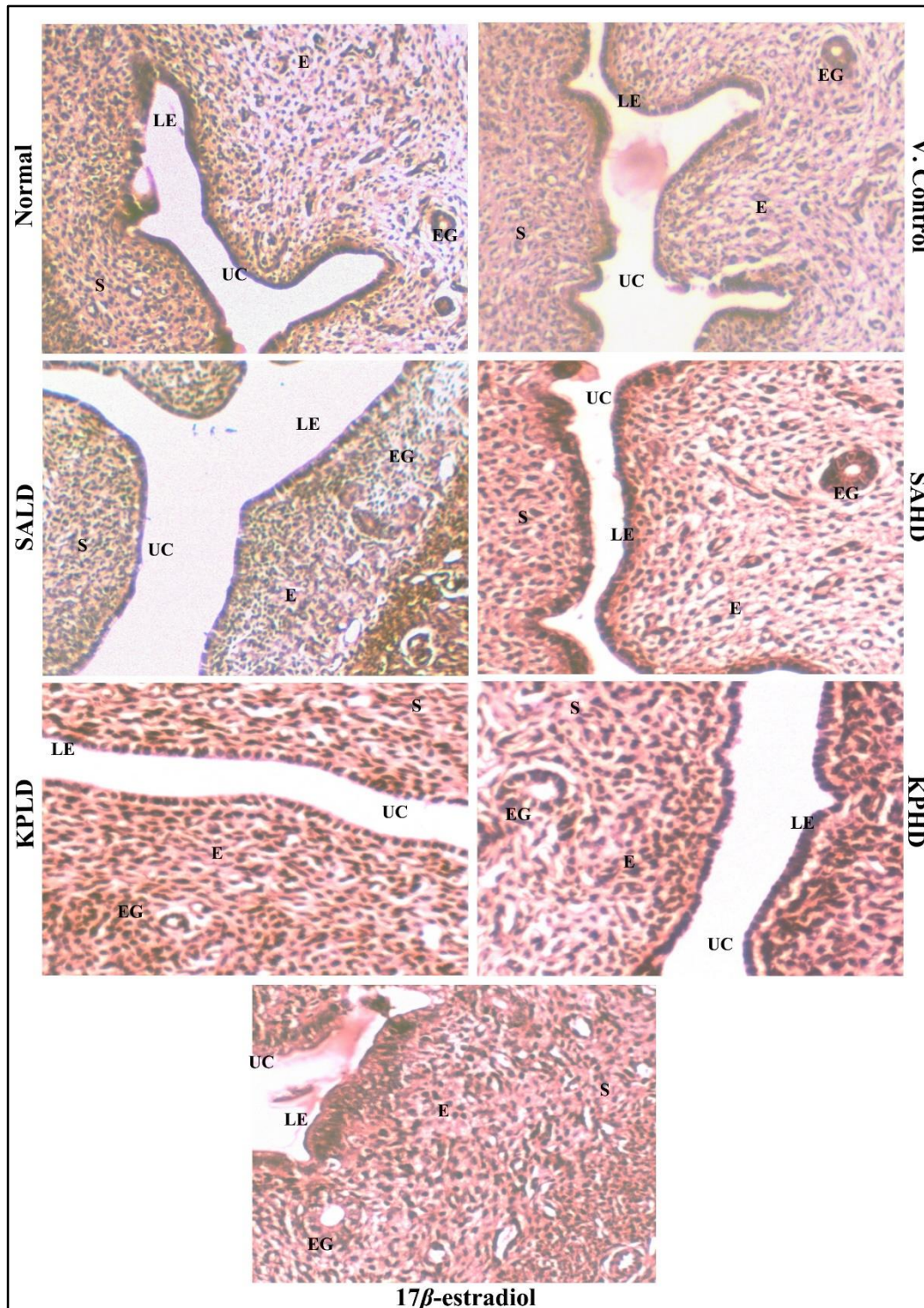
Figure 4.14. Histology of uterus of different groups. Vehicle control – Propylene glycol, SALD – *S. asoca* 250 mg/kg b. wt, SAHD – *S. asoca* 500 mg/kg b. wt., KPLD – *K. pinnatum* 250 mg/kg b. wt, KPHD – *K. pinnatum* 500 mg/kg b. wt. E- endometrium, S- stroma, UC- uterine cavity, EG- endometrial gland, LE- luminal epithelium
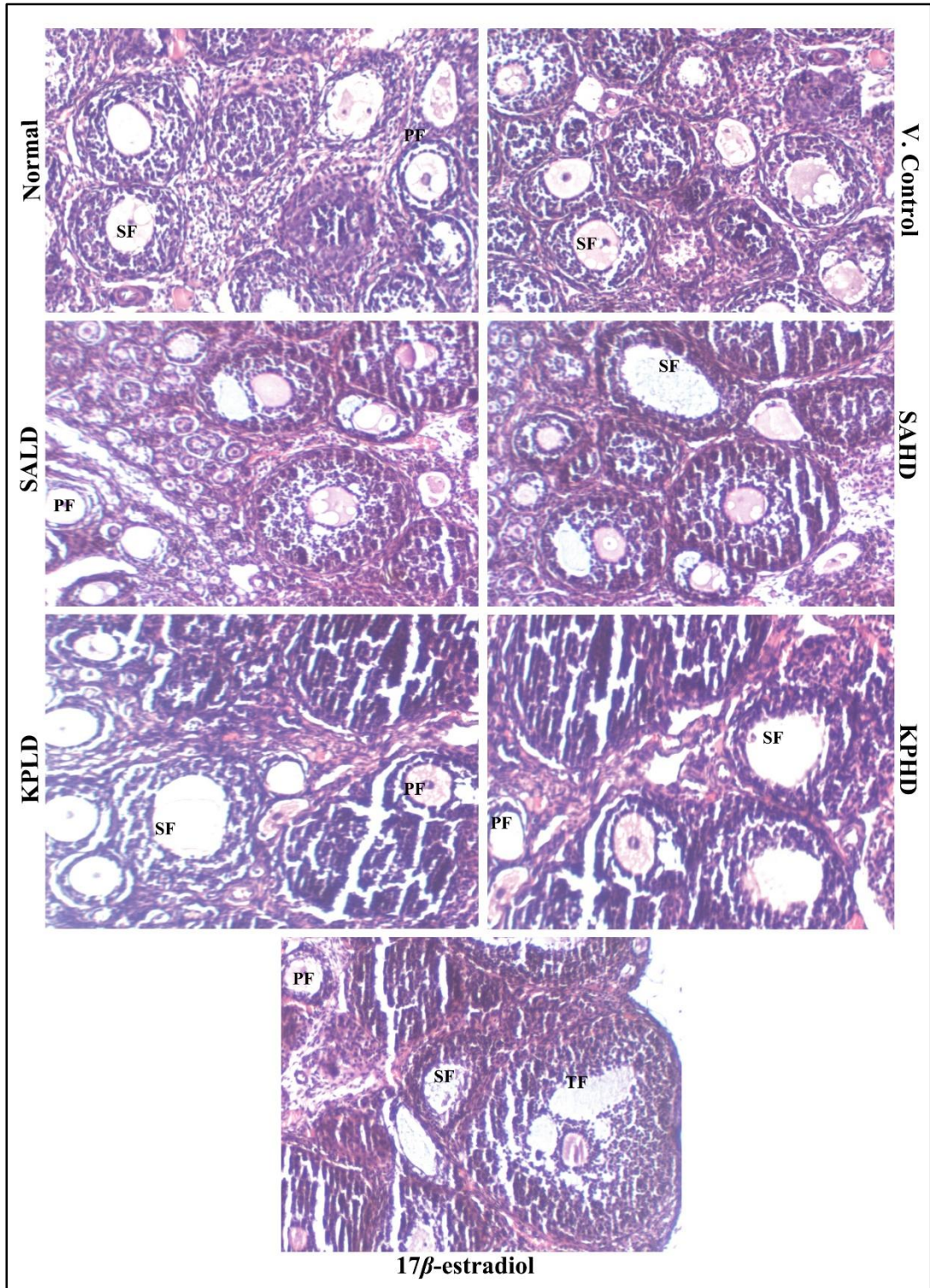
Figure 4.15. Histology of mice ovaries of different groups. Vehicle control – Propylene glycol, SALD – *S. asoca* 250 mg/kg b. wt, SAHD – *S. asoca* 500 mg/kg b. wt., KPLD – *K. pinnatum* 250 mg/kg b. wt, KPHD – *K. pinnatum* 500 mg/kg b. wt. PF- primary follicle, SF- secondary follicle, TF- tertiary follicle

4.3.4.2. Evaluation of anti-estrogenic effects of *S. asoca* and *K. pinnatum* extracts on immature rats

In immature rats, *S. asoca* and *K. pinnatum* extract administration had an antiestrogenic effect as shown by decreased water imbibition, reduced uterine wet weight, variations in estrogen levels and histological modifications in the uterus and ovaries. The body weight of the animals in the various treatment groups showed no clear differences. In response to estrogen, water is imbibed into uterine tissue, however, this process was greatly diminished in groups that received high doses of SA and KP extracts (Figure 4.16). The uterine wet weight was found to be 101.5±7 mg in the 17β-estradiol-treated group, while it significantly (p<0.01) decreased in SA and KP high-dose groups to 38±6 and 47±6 mg, respectively. Additionally, the uterine wet weight (33±5 mg) was reduced in the tamoxifen-treated group (Figure 4.17). The estrogen levels dropped considerably from 204.5±15 pg/mL in the 17β-estradiol-treated group to 31.16±5.5 and 39.02±4.8 pg/mL in the SA and KP treatment groups, respectively. Also in tamoxifen-treated group it was reduced to 26±5 pg/mL. A substantial decrease in estrogen levels of 6.57 and 5.24 fold in the extract-treated groups thus indicates the antiestrogenic effect of *S. asoca* and *K. pinnatum* extracts (Figure 4.18).

The histological analysis of the SA and KP administrated groups presented uterine histology different from that observed in the control groups. In comparison to 17β-estradiol and vehicle control groups, the thickness of the luminal epithelium was reduced, there was a dense cellular stroma and there were fewer endometrial glands seen in the extract-treated groups. On the other hand, the endometrium of the 17β-estradiol-treated group exhibits proliferative alterations as shown by thickening of the luminal epithelium, loose stroma, and an increase in the number of endometrial glands (Figure 4.19). The ovaries of the immature female rats in the control groups displayed graffian follicle development and follicles in various levels of maturation. In control groups, 17β-estradiol induced early maturation of follicles. The ovaries of the immature female rats that received extract treatment lacked graffian follicle and seemed to have more secondary follicles (Figure 4.20).
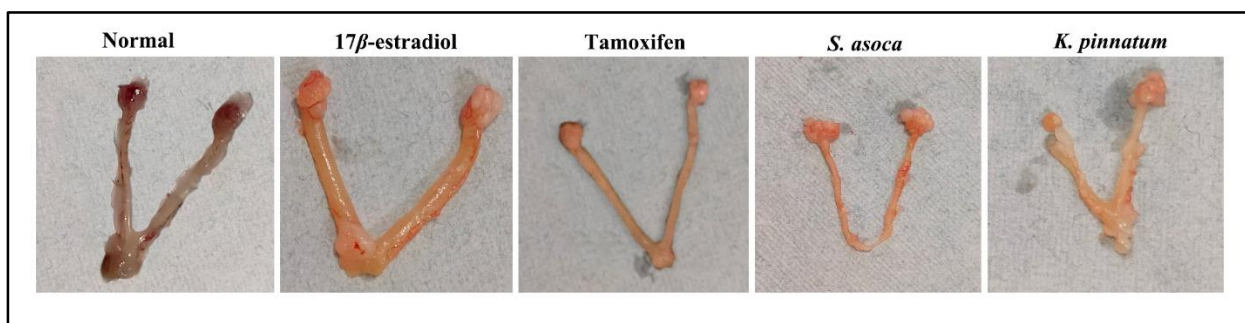
Figure 4.16. Uterus of immature female rats from various groups
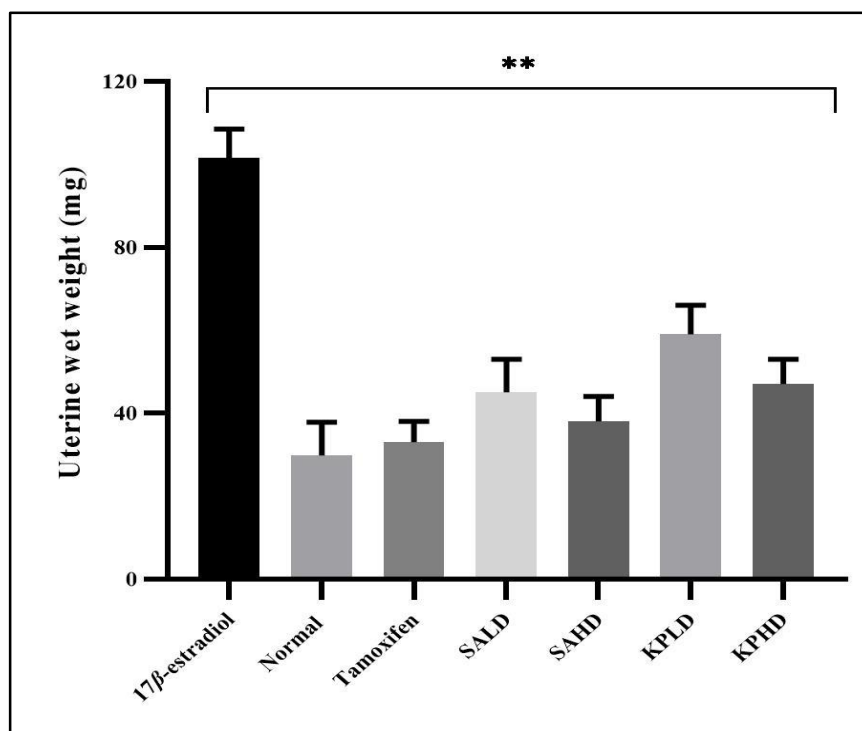
Figure 4.17. Uterine weight after different treatment. SALD – *S. asoca* 250 mg/kg b. wt, SAHD – *S. asoca* 500 mg/kg b. wt., KPLD – *K. pinnatum* 250 mg/kg b. wt, KPHD – *K. pinnatum* 500 mg/kg b. wt. Each group contains 5 animals and the values were calculated using the mean ± standard deviation (SD). *P<0.05 and **P<0.01 probability values are regarded as statistically significant
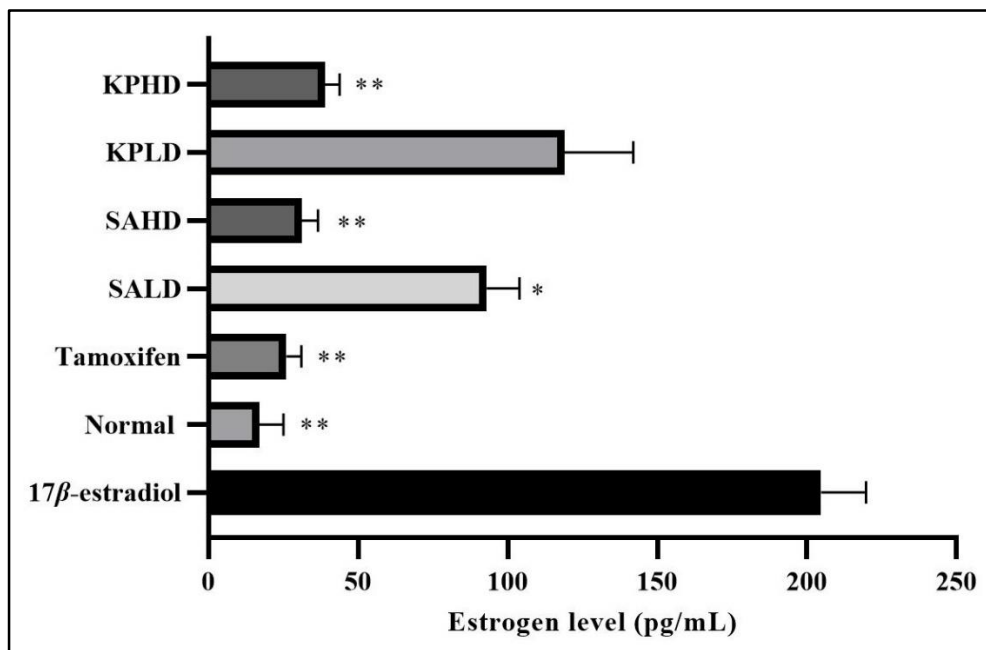
Figure 4.18. Estrogen levels of animals of different treatment groups. SALD – *S. asoca* 250 mg/kg b. wt, SAHD – *S. asoca* 500 mg/kg b. wt., KPLD – *K. pinnatum* 250 mg/kg b. wt, KPHD – *K. pinnatum* 500 mg/kg b. wt. Each group contains 5 animals and the values were calculated using the mean ± standard deviation (SD). *P<0.05 and **P<0.01 probability values are regarded as statistically significant
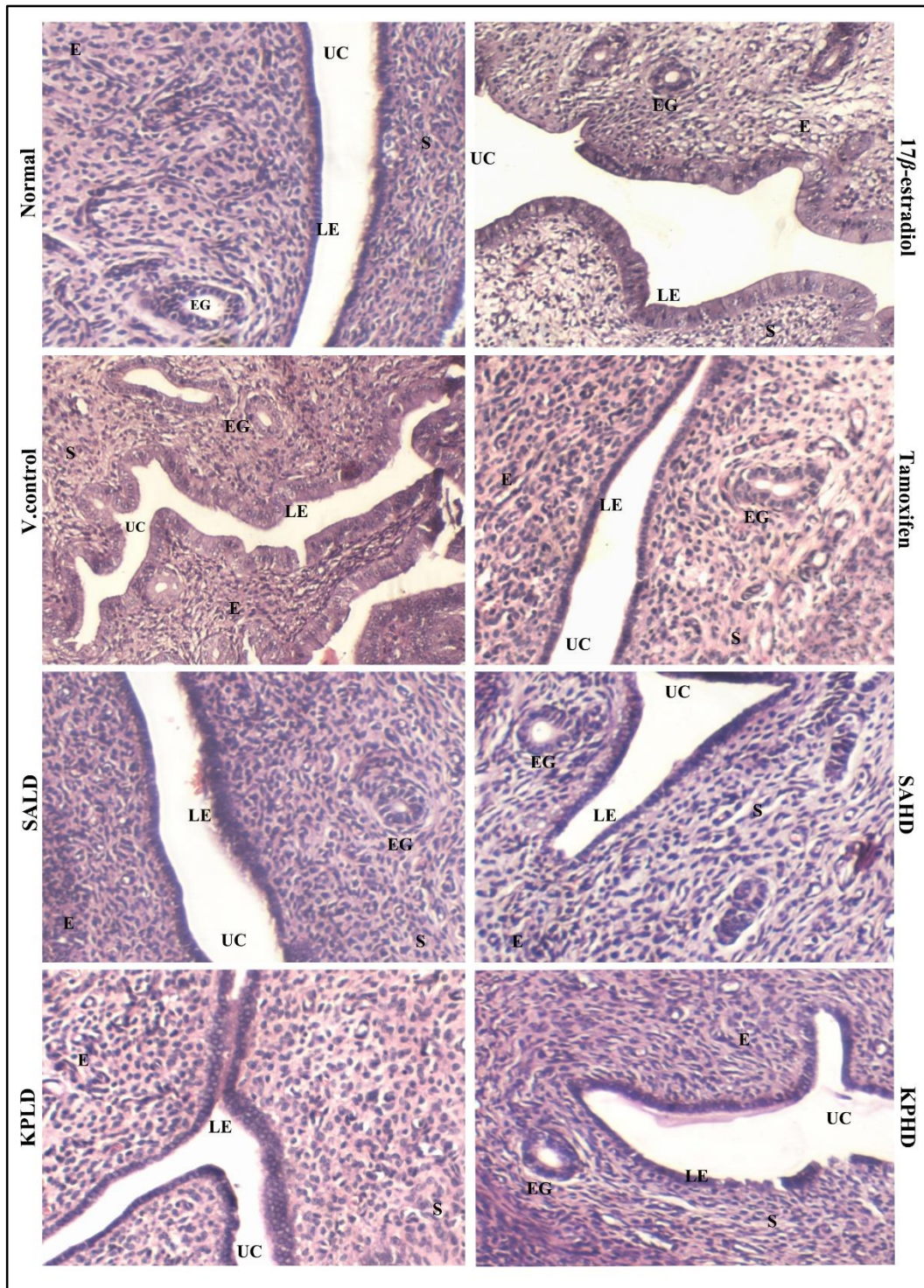
Figure 4.19. Histology of mice uterus of different treatment groups. Vehicle control – Propylene glycol, SALD – *S. asoca* 250 mg/kg b. wt, SAHD – *S. asoca* 500 mg/kg b. wt., KPLD – *K. pinnatum* 250 mg/kg b. wt, KPHD – *K. pinnatum* 500 mg/kg b. wt. E-endometrium, S- stroma, UC- uterine cavity, EG- endometrial gland, LE- luminal epithelium
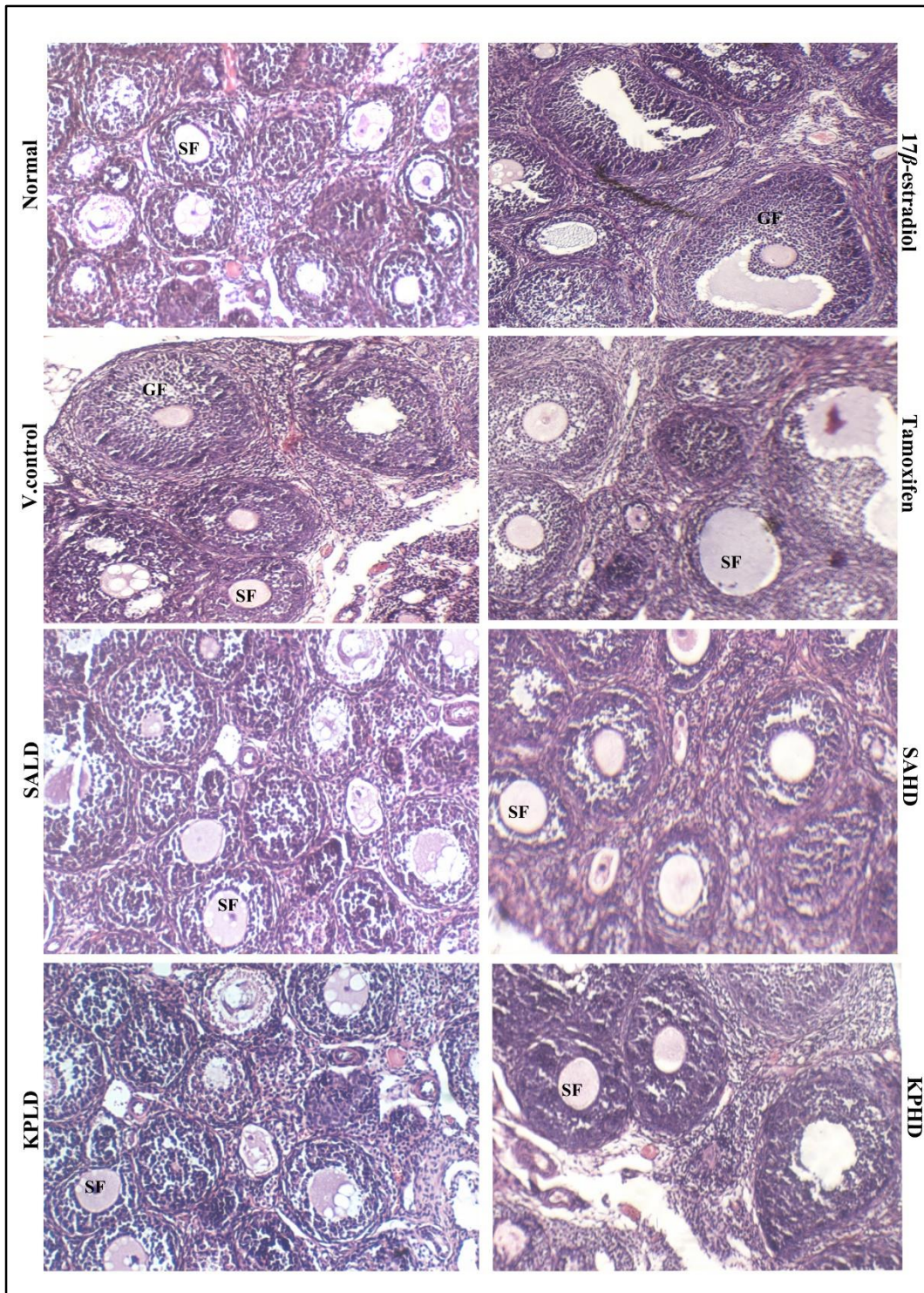
Figure 4.20. Histological of mouse ovaries across different treatment groups. Vehicle control – Propylene glycol, SALD – *S. asoca* 250 mg/kg b. wt, SAHD – *S. asoca* 500 mg/kg b. wt., KPLD – *K. pinnatum* 250 mg/kg b. wt, KPHD – *K. pinnatum* 500 mg/kg b. wt. SF- secondary follicle, GF- graafian follicle

4.4. Discussion

A bioassay serves as a valuable tool for screening different compounds. The estrogen-screen assay is a well-characterized bioassay used to evaluate the estrogenicity or antiestrogenicity by assessing the proliferative or antiproliferative action of estrogen on the cells they are targeting (Soto *et al*., 1995). This bioassay estimates the number of cells that become more or less active in response to estrogen, which is biologically similar to an increase/decrease in mitotic activity within the tissues of the reproductive tract (Soto and Sonnenschein, 1985). In our study both plant extracts exhibit proliferative action on ERα expressing breast cancer cell line, MCF-7 and a slight antiproliferative effect on ERβ expressing TNBC cell line, MDA-MB-231. Both plants contain phytoestrogens such as quercetin, kaempferol, β-sitosterol, etc., as revealed by LCMS analysis (discussed in Chapter 3). Phytoestrogens are of focus because of their purportedly advantageous effects on a variety of human diseases, such as cancer, cardiovascular disease, diabetes and neurodegeneration (Resende *et al*., 2013). Additionally, there is an ongoing search for substances that can mitigate some of adverse effects of estrogen such as the increased risk of breast cancer. There are reports of flavonoids like quercetin, chrysin and 3-hydroxyflavone having antiestrogenic properties (Resende *et al*., 2013). These phytoestrogens have the ability to inhibit estrogen binding to ERα and restrict estrogen-stimulated gene expression which is beneficial respective to the prevention and treatment of breast cancer (Liu *et al*., 2013). Therefore the initial *in vitro* indication of antiestrogenic properties of plant extracts was confirmed by the *in vivo* immature rodent uterotrophic assay.

The rodent uterotropic assay is an excellent model for determining the estrogenicity or antiestrogenicity of a compound (Gray Jr *et al*., 2004). In this study the reliability of the uterotrophic assay for detecting estrogenic/antiestrogenic activity of *S. asoca* and *K. pinnatum* bark extracts was evaluated and both plants couldn't exert any estrogenic action. Whereas the extracts hindered the growth of the endometrial lining and reduced estrogen levels in serum indicating its antiestrogenic potential. Asoka is mainly used in Ayurveda for managing feminine reproductive issues like dysfunctional uterine bleeding, irregular menstruation etc (Sulaiman *et al*., 2020). According to reports, *K. pinnatum* has the same pharmacological effectiveness as *S. asoca* and can be used to treat gynecological problems (Shahid *et al*., 2018, Sasidharan and Padikkala, 2012). Dysfunctional uterine bleeding is caused from an overexposure to estrogen which may

result in rupturing of the keratinized endometrium, whereas an underexposure of estrogen may cause a condition known as menorrhagia (Severino, 2011). As a result, estrogen augmentation is suggested for menorrhagia, while anti-estrogenic drugs are employed for dysfunctional uterine bleeding (Micks and Jensen, 2013, Dhananjay and Nanda, 2013). Our findings are in conformity with prior reports of antiestrogenic activity of *S. asoca* and *K. pinnatum* bark extracts (Shahid *et al*., 2015, Shahid *et al*., 2018, Sasidharan and Padikkala, 2012). Another study has also shown that *S. asoca* bark extracts were unable to exert estrogenic activity in the immature rat model (Kamat *et al*., 2015). However, Asoka has also been reported to have estrogenic effects by a number of authors (Sulaiman *et al*., 2020, Swar *et al*., 2017, Deka *et al*., 2012). This raises concerns about its mode of action. While there are uncertainties about the estrogenic or antiestrogenic properties of both plants, it is evident that endogenous factors/hormones contribute significantly to the majority of cancer-causing factors.

Estrogen, primarily recognized as the female sex hormone, has a complex function in regulating inflammation in the body. There can be significant differences in the way estrogen affects inflammation depending on the particular tissues involved, the amount of estrogen present, the level of other hormones, and the overall physiological environment (Straub, 2007). Estrogen plays a major role in controlling endometrial inflammation, and high estrogen levels promote endometrial development and proliferation, which in turn causes the generation of cytokines and chemokines that promote inflammation. These molecules cause an inflammatory response by attracting immune cells to the endometrium (García-Gómez *et al*., 2020). In our study, *S. asoca* and *K. pinnatum* extracts revealed significant anti-inflammatory effects both *in vitro* and *in vivo*. Nitric oxide regulates a wide range of pathophysiological processes including neurotoxicity, neural transmission and vasodilation (Nakagawa and Yokozawa, 2002). However, chronic and acute inflammation-related tissue damage is brought on by NO overproduction (Taira *et al*., 2009). The extracts of both plants have a substantial scavenging effect on NO radicals *in vitro* in a concentration-dependent manner. In the mammalian immune system, macrophages serve a crucial function by acting as an immediate line of defense against foreign invaders before leukocyte migration and generation of numerous pro-inflammatory mediators, such as NO free radical (Moncada *et al*., 1991). One of the most potent macrophage activators, lipopolysaccharide (LPS), found in the cell walls of gram-negative bacteria, causes the generation of

cytokines that promote inflammation (Nicholas *et al*., 2007). Therefore, one potential method of screening various anti-inflammatory drugs is to inhibit NO generation in LPS-stimulated RAW 264.7 cells. The plant extracts have significantly decreased nitric oxide generation in LPS-stimulated RAW 264.7 and also reversed the morphological alterations brought on by the LPS. Other authors have also reported the NO scavenging of *S. asoca* plant extracts (Yadav *et al*., 2015). The human body's lipoxygenase enzyme plays a major role in inducing inflammatory responses. Excessive production of free radicals may cause inflammation, which in turn may cause cytokines to be released and LOXs to be activated, which are necessary for the synthesis of prostaglandins and leukotrienes. They are linked to the emergence of diseases, and preventing them is viewed as a key step in disease prevention (Srivastava *et al*., 2016, Lončarić *et al*., 2021). In our study, *S. asoca* and *K. pinnatum* extracts were found to be effective in inhibiting 5-lipoxygenase enzyme activity in a dose dependent manner. The remarkable *in vitro* anti-inflammatory activities were complemented by *in vivo* anti-inflammatory ability of extracts. Both the plant extracts exhibited appreciable anti-inflammatory activity against carrageenan and formalin induced acute and chronic paw edema models in mice.

Carrageenan-induced paw edema model is the frequently used model to assess the anti-inflammatory effects of various compounds (Patil *et al*., 2019). The cyclooxygenase pathway is often associated with the carrageenan model (Boominathan *et al*., 2004). Carrageenan-induced edema is depicted as a biphasic curve. The injection trauma and histamine and serotonin release are partially attributed to the initial phase of carrageenan-triggered inflammation. The second phase, which begins roughly three hours after the injection of carrageenan, is mainly brought on by the release of cyclooxygenase and prostaglandins (Perianayagam *et al*., 2006, Patil and Patil, 2017). In our investigation, the administration of extracts led to a decrease in paw oedema after the third hour which may be due to the inhibition of cyclooxygenase and thus prostaglandin generation by the extracts. The formalin-induced chronic paw edema model is quite similar to human arthritis and is regarded as the most suitable experimental model to assess how effectively different agents reduce chronic inflammation (Alhadidi *et al*., 2009). It has two phases: the early neurogenic phase is mediated by substance P and bradykinin, while the later inflammatory phase is mediated by prostaglandins, nitric oxide, serotonin and histamine (Segawa *et al*., 2007). In our study, the inflammation began to subside on the second day and became noticeably less on the fifth day. By observing the inflammatory trend, the

extracts may have suppressed the second phase of inflammation. The *in vivo* anti-inflammatory effects of *S. asoca* and *K. pinnatum* have also been documented by other authors as well (Suhail *et al*., 2019, Sharif *et al*., 2011).

Inflammation has a close connection to cancer and is crucial to the growth and development of tumours. Chronic inflammation encourages the development of cancer by triggering proliferation, angiogenesis and metastasis as well as by lowering the immune system and chemotherapeutic drug responses (Balkwill and Mantovani, 2001). It is widely acknowledged that estrogen has a crucial part in development of malignancies in the reproductive system (Shahid *et al*., 2015). Consequently, drugs capable of inhibiting the action of estrogen would be effective in preventing or treating hormone-related malignancies. Building on this concept, the development of antiestrogenic drugs is essential to block estrogen's action, thereby impeding the growth of cancers. Based on the findings in our study, the observed decrease in endometrial thickening and lower estrogen levels in the extract-treated experimental animals implies potential antiestrogenic activity of the crude bark extract of *S. asoca* and *K. pinnatum.* Simultaneously, both plant extracts have demonstrated substantial anti-inflammatory activity *in vitro* and have been shown to attenuate acute and chronic inflammations *in vivo.* These plants have a tremendous amount of potential and thorough investigation may result in the discovery of drugs that possess different biological characteristics.

Chapter 5
Protective effect of *S. asoca* and *K. pinnatum* on sodium fluoride induced oxidative stress

5.1. Introduction

Free radicals have received considerable attention in the realms of biology and medicine due to their critical role in various pathophysiological conditions and their implications in a broad spectrum of diseases (Martemucci *et al*., 2022). The production of free radicals stems from numerous endogenous and exogenous processes. Endogenous sources include the endoplasmic reticulum, mitochondria, phagocytic cells, peroxisomes, reactive oxygen species (ROS), and reactive nitrogen species (RNS). Exogenous sources encompass alcohol, industrial solvents, smoke, heavy metals, pesticides, pollution, transition metals, tobacco and certain drugs like halothane and paracetamol (Phaniendra *et al*., 2015). The overproduction of free radicals is associated with various chronic and degenerative diseases, resulting in the deterioration of macromolecules like lipids, proteins, and nucleic acids.

Antioxidants serve as the body's protective system, safeguarding biomolecules and the organism from the detrimental effects of free radicals. The antioxidant defense mechanism involves mitigating or repairing the damage inflicted on a target molecule by reactive oxygen species (ROS) (Kıran *et al*., 2023). These compounds, characterized by their low molecular weight, possess the stability required to donate an electron to an unstable free radical. This action interrupts the chain reaction, preventing damage to essential elements. Some of these antioxidants are naturally produced by the body during regular metabolism, including glutathione, ubiquinol, and uric acid. Furthermore, the body acquires additional antioxidants from dietary sources, such as α-tocopherol, ascorbic acid and beta-carotene. Given that the body cannot synthesize these micronutrients, they must be obtained through dietary intake (Lobo *et al*., 2010). Both food and medicinal plants contains a plethora of antioxidants, with notable examples being polyphenols and carotenoids. These antioxidants exhibit diverse biological effects, encompassing anti-inflammatory, anti-aging, anti-atherosclerotic, and anticancer properties (Xu *et al*., 2017). Certain plants known for their anticancer properties also produce compounds with exceptionally potent antioxidative capabilities. Hence, the aim of the study was to evaluate the antioxidant capabilities of extracts obtained from *S. asoca* and *K. pinnatum* using both *in vitro* and *in vivo* assays.

Antioxidant activities of compounds found in medicinal plants have been evaluated using a variety of methods. Among free radical assays one of the most frequently employed methods for assessing *in vitro* antioxidant capacity is ABTS [2,2-azinobis (3-

ethylbenzothiazoline-6-sulfonic acid)] assay. This assay gauges an antioxidant's relative capacity to scavenge the ABTS radicals produced by a strong oxidizing agent and the ABTS salt. The spectrophotometric reduction of blue-green ABTS radical colored solution by hydrogen-donating antioxidants is measured (Shalaby and Shanab, 2013). The FRAP assay evaluates antioxidant power in terms of the ability to reduce ferric ions in an acidic medium by electron-donating antioxidants by reducing yellow ferric tripyridyltriazine complexes (Fe(III)-TPTZ) to ferrous complexes (Fe(II)-TPTZ) (Benzie and Strain, 1996). Moreover, human RBCs subjected to compound 2,2′-azobis(2-amidinopropane) hydrochloride (AAPH) induces haemolysis, is an excellent model for studying free radical mediated oxidative damage to membranes and evaluating the antioxidant properties of novel compounds (Banerjee *et al*., 2008). Therefore, the current study monitors haemolysis by assessing lipid peroxidation, and scavenging of AAPH peroxyl radicals by *S. asoca* and *K. pinnatum* extracts.

Oxidative stress induced models in Wistar rats were used to assess the *in vivo* antioxidant activity of *S. asoca* and *K. pinnatum* extracts. One of such oxidative stress induced model is the sodium fluoride (NaF)-induced antioxidant model. Sodium fluoride is potentially harmful to the organism if excessively exposed and can alter enzyme activity by creating complexes with the metal portion of enzyme molecules, which can impede the metabolism of proteins, lipids, and carbohydrates (Abdel-Wahab, 2013). One of the key mechanisms of fluoride toxicity is the production of free radicals. Several studies have demonstrated an increase in oxidative stress in the liver and serum of animals exposed to fluoride (Grucka-Mamczar *et al*., 2009). Furthermore, fluoride affects the activity of enzymes involved in the antioxidant system of the cell such as superoxide dismutase, catalase and decreases the glutathione content, which protects the cell from free radicals (Strunecka *et al*., 2007). Therefore the study evaluated the ability of plants to restore antioxidant defenses in animals that were administrated with sodium fluoride.

Multiple studies by different authors have documented the antioxidant activities of both Asoka and *K. pinnatum* (Mohan *et al*., 2016, Yadav *et al*., 2015, Sheik and Chandrashekar, 2014). The research conducted on the antioxidant activity of both plants lays a rational foundation for conducting further research. Consequently, the antioxidant capacity of the crude methanolic extracts of *S. asoca* and *K. pinnatum* was further investigated through various *in vitro* and *in vivo* experiments.

5.2. Materials and methods

5.2.1. Preparation of extract

The stem barks of both plants has been chopped into small fragments and dried for seven to ten days at 45 to 50 °C after being thoroughly washed with distilled water. The dry bark was pulverized into fine powder using a grinder. Subsequently, 250 mL of methanol were mixed with 20 g of the powder to extract it by stirring it for an extended period of time at room temperature using a magnetic stirrer. After centrifugation of the solutions for 10 min at 2000 rpm, the supernatant was gathered and strained through filter paper (Whatman No. 1). After repeating the process three times, the filtrate was evaporated until dry. For *in vitro* antioxidant analysis, the residue obtained was dissolved in ethanol, whereas for *in vivo* experiments, it was dissolved in propylene glycol.

5.2.2. Chemicals

The chemicals employed in the antioxidant tests, 2,2′-azobis(2-amidinopropane) hydrochloride (AAPH), 2,2-azinobis (3-ethylbenzothiazoline-6-sulfonic acid) (ABTS), ascorbic acid, 2,2-diphenyl-1-picrylhydrazyl (DPPH), ammonium molybdate, 5-5'dithiobis (2-nitrobenzoic acid) (DTNB), deoxyribose, ferric chloride ($FeCl_3$), hydrogen peroxide (H_2O_2), nitro blue tetrazolium (NBT), ethylenediamine tetra-acetic acid, potassium dihydrogen phosphate, riboflavin, sodium fluoride (NaF), sodium nitroprusside, sodium dodecyl sulphate (SDS), sulphanilamide, naphthylethylene diamine dihydrochloride (NEDD), tripyridyltriazine (TPTZ), thiobarbituric acid (TBA) were acquired in accordance with the list in Section 2.1.2 of Chapter 2. All additional chemicals utilized in the experiments were of analytical quality.

5.2.3. Animals

The animals were purchased from Kerala Veterinary and animal Sciences University (KVASU) and maintained as described in section 2.1.4 of chapter 2.

5.2.4. *In vitro* antioxidant assays
5.2.4.1. ABTS radical scavenging assay

According to the method outlined in section 2.2.5.1 of Chapter 2, ABTS radical scavenging activity of crude extract of *S. asoca* and *K. pinnatum* at concentrations of 2.5-10 μg/mL was determined.

5.2.4.2. Ferric reducing antioxidant power activity

In accordance with section 2.2.5.4 of Chapter 2, the ferric reducing antioxidant activity of the different extracts of *S. asoca* and *K. pinnatum* (2.5-12.5 μg/mL) was determined.

5.2.4.3. Hydroxyl radical scavenging assay

The crude extracts *S. asoca* and *K. pinnatum* at concentrations ranging from 2.5-15 μg/mL was used to determine the inhibition of the formation of hydroxyl radicals *in vitro*, using the methods as stated in Chapter 2's section 2.2.5.5.

5.2.5. AAPH induced erythrocyte haemolysis

5.2.5.1. Erythrocyte haemolysis inhibition assay

The red blood cell suspension was prepared according to section 2.2.5.6.1. of Chapter 2. The crude extract of *S. asoca* and *K. pinnatum* was used to determine the efficacy of the extracts (5-25 μg/mL) in preventing erythrocyte hemolysis using the method as specified in Chapter 2's section 2.2.5.6.2.

5.2.5.2. AAPH induced lipid peroxidation

As explained in Chapter 2's section 2.2.5.6.3, the crude extract of both plants have been assessed for their protective effects against AAPH-induced lipid peroxidation on the erythrocyte membrane.

5.2.6. *In vivo* antioxidant activity of extracts

Mice in each group (aside from the normal group) were pretreated with the appropriate dose for the first seven days, after which NaF (600 ppm) was administered through drinking water for the following seven days, along with extracts (section 2.2.6, chapter 2). After the study mice were sacrificed with anesthesia with ether. Through cardiac puncture, the blood was drawn from the heart and stored into heparinized vials. Following its removal, the liver was kept in buffered formalin (10 %) solution for histological analysis after it was rinsed with physiological saline. Hemolysate and tissue homogenate (10%) have been prepared in accordance with sections 2.2.6.1 and 2.2.6.2 of Chapter 2. Lowry's method was used to calculate the tissue's total protein content (Chapter 2, section 2.2.9.6). In the hemolysate and tissue homogenate, antioxidants (superoxide dismutase, catalase, and reduced glutathione) were measured (sections 2.2.8.1, 2.2.8.2, and 2.2.8.3, respectively, of Chapter 2). Malondialdehyde (MDA) concentration in the liver

homogenate was measured to estimate the degree of lipid peroxidation (section 2.2.8.4 of Chapter 2). Additionally, liver tissue was subjected to histological analysis in accordance with the method outlined in Chapter 2, section 2.2.6.3.

5.2.7. Statistical analysis

For *in vitro* investigations, values were given as mean ± standard deviation (SD), derived from three distinct experiments, whereas for *in vivo* studies, data were based on six mice per group. The data were analyzed using Two-way ANOVA following Tukey's multiple comparison test in GraphPad Prism 8. P-values at these levels were considered statistically significant only at $p < 0.01**$, $p < 0.05*$ and $p > 0.05$ was deemed non-significant.

5.3. Results

5.3.1. *In vitro* antioxidant property of *S. asoca* and *K. pinnatum* extracts

In the *in vitro* antioxidant assays, the crude extract of *S. asoca* and *K. pinnatum* demonstrated efficient and concentration-dependent inhibition of free radicals. The table 5.1 provides the inhibitory concentration (IC_{50}) values of *S. asoca* and *K. pinnatum* crude methanol extracts for ABTS and hydroxyl radicals. The figures 5.1 and 5.2 illustrate the percentage inhibition by the extracts at various concentrations. In the FRAP assay, it was observed that the reducing power of the extract increased as its concentration increased (Figure 5.3).

Table 5.1. IC_{50} values of *S. asoca* and *K. pinnatum* extracts on ABTS and hydroxyl radicals

Plants	Extracts	IC_{50} value (μg/mL)	
		ABTS	**Hydroxyl**
S. asoca	Crude	2.78 ± 0.56	3.507 ± 2.36
K. pinnatum	Crude	3.15 ± 0.87	5.43 ± 3.33
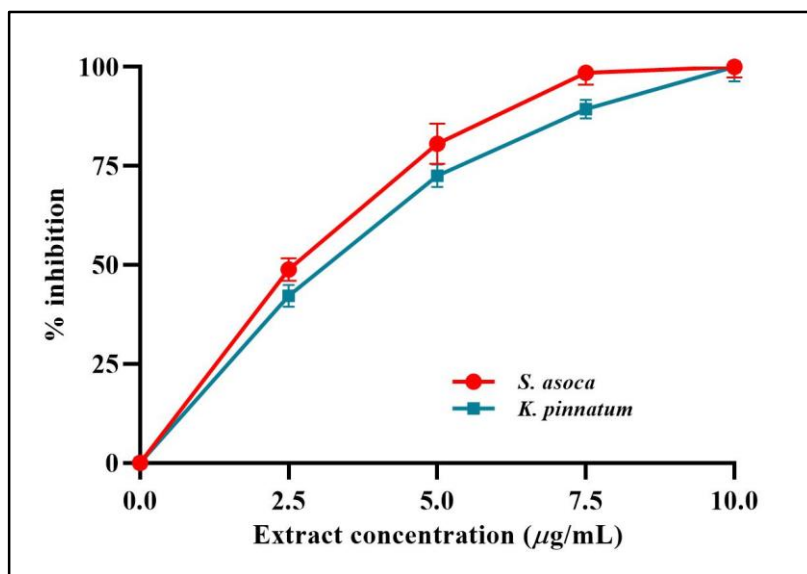
Figure 5.1. Percentage inhibition of ABTS radicals by *S. asoca* and *K. pinnatum* extracts
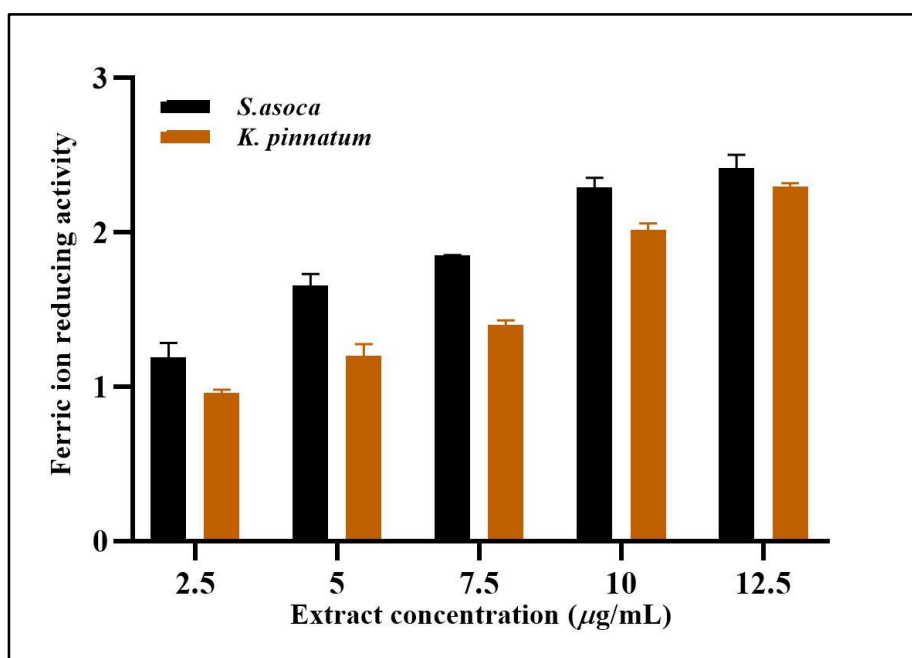
Figure 5.2. Reducing power of *S. asoca* and *K. pinnatum* extracts by FRAP assay
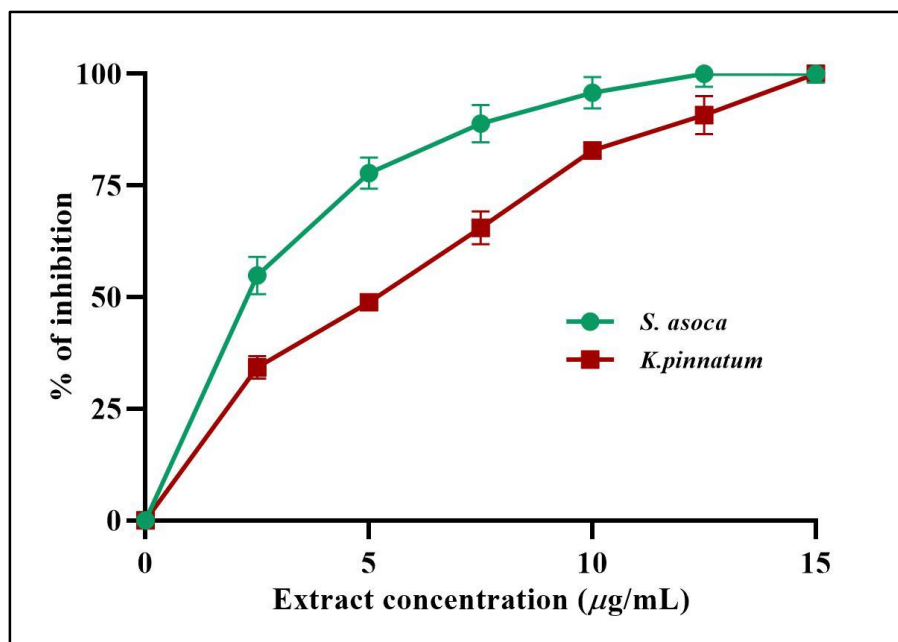
Figure 5.3. Percentage inhibition of hydroxyl radicals by *S. asoca* and *K. pinnatum* extracts

5.3.2. Effect of extracts in preventing AAPH-induced hemolysis and lipid peroxidation

The crude methanol extract of *S. asoca* and *K. pinnatum* reduced AAPH-induced hemolysis in erythrocytes in a concentration-dependent manner. The plants exhibited protective effects on erythrocytes against oxidative damage, with IC_{50} values of 16.8 and 17.5 μg/mL, respectively for *S. asoca* and *K. pinnatum*. A comparison of the inhibition of hemolysis by *S. asoca* and *K. pinnatum* at various concentrations is presented in figure 5.4. Various concentrations (20-100 μg/mL) of both extracts were added to determine whether AAPH-induced lipid peroxidation was inhibited. It was found that both the crude methanolic plant extracts inhibited the rate of peroxidation of AAPH-treated RBCs. A comparison of the absorbance values of the control and test was used to calculate the percentage inhibition. The IC_{50} value obtained for *S. asoca* and *K. pinnatum* was found to be 83.76 and 92.80 μg/mL (Figure 5.5). As a result, this study has demonstrated that extracts are protective against AAPH-induced oxidative hemolysis.
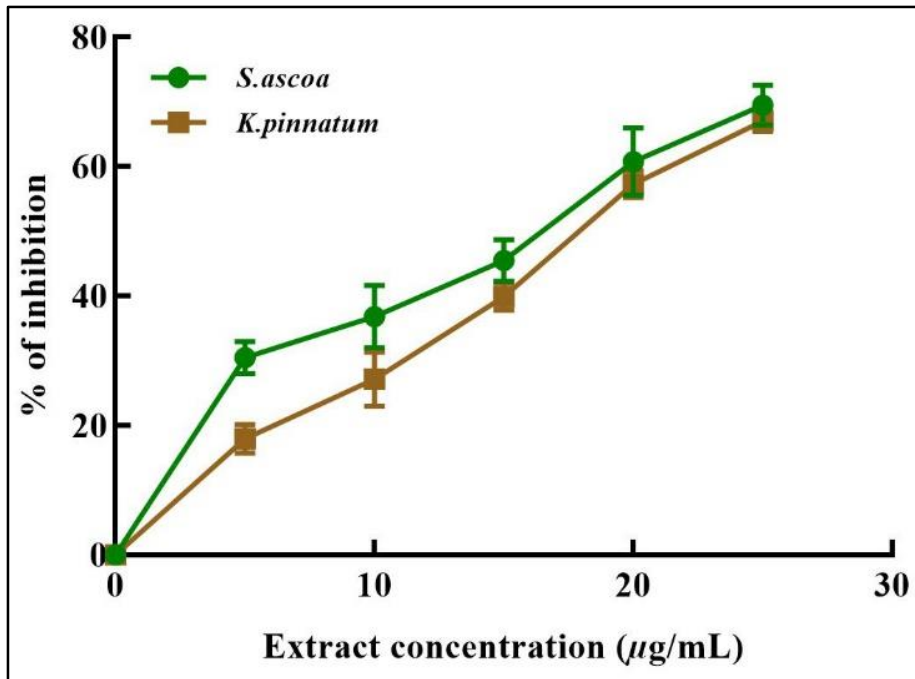
Figure 5.4. Effect on *S. asoca* and *K. pinnatum* extracts on AAPH induced erythrocyte hemolysis
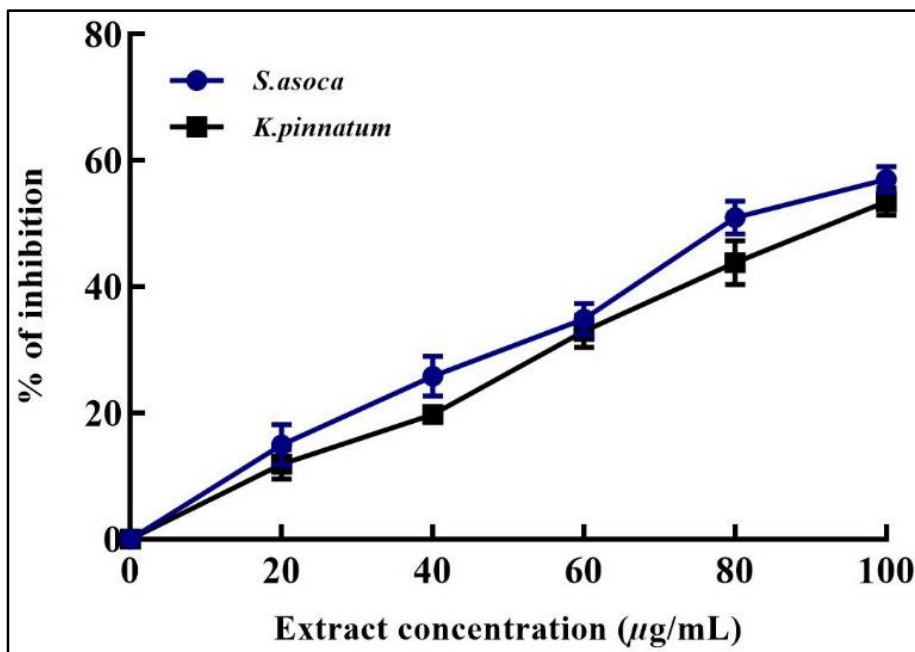
Figure 5.5. Effect on *S. asoca* and *K. pinnatum* extracts on AAPH induced lipid peroxidation in erythrocyte membrane

5.3.3. Protective effects of extracts against sodium fluoride induced oxidative stress

No significant changes were observed in the hematological parameters analyzed across different groups of animals, except for the white blood cell (WBC) count when compared with normal group. Table 5.2 presents the various hematological parameters examined. Compared to the normal group, which exhibited an SGPT level of 55±3.5 U/L, administration of NaF resulted in an elevation of SGPT to 101±2.4 U/L in the control group. Improved levels were observed in the high dose treatment groups of *S. asoca* and *K. pinnatum*. There were no significant alterations noted in other parameters across the various groups. Table 5.3 displays the change in values of serum marker levels caused due to administration of NaF.

Sodium fluoride exposure was associated with the decrease of SOD and CAT activity along with decline in GSH content in both blood and liver tissues of the mice. These findings indicate an impaired functioning of the hepatic antioxidant defense system which was reverted by the plant extracts.

5.3.3.1. Effect of SA and KP extracts on blood antioxidant enzymes

The figure 5.6 shows the status of blood antioxidant enzymes in animals treated with *S. asoca* and *K. pinnatum* extracts. It was found that the level of SOD, CAT and GSH activity was reduced in the control group than in the normal group. The activity of SOD and CAT was returned to normal levels following the administration of 500 mg/kg of SAHD (0.72 ± 0.05 and 46.2 ± 0.8) and KPHD (0.68 ± 0.09 and 44.3 ± 1.2) for 30 days compared to the control group. The levels of GSH were also reduced in control (1.28 ± 0.33) and vehicle control (1.54 ± 0.82) groups, but they were significantly ($p<0.01$) increased in high dosage extract treated groups (SAHD- 4.4 ± 0.5, KPHD - 4.3 ± 0.72) (Table 5.4).

Table 5.2. Hematological parameters of NaF induced mice and treated groups

	Normal	Control	V. control	Standard	KPLD	KPHD	SALD	SAHD
Haemoglobin (g/dl)	14.3±0.2	11.7±0.2	12.3±0.2	15±0.1	12.7±0.2	12.5±0.2	13.4±0.3	16.4±0.2
Total RBC count (millions/cu mm)	8.0±0.1	6.5±0.2	7.1±0.2	8.8±0.2	6.6±0.2	6.4±0.1	6.8±0.2	8.8±0.3
Platelet count (lakhs/cu mm)	10.9±0.2	7.1±0.2	7.5±0.2	11.1±0.2	9.5±0.2	10±0.1	7.2±0.2	10.1±0.2
Total WBC count (cells/cu mm)	5600±205	5600±270	5900±190*	6000±230*	5900±510*	6000±550*	6100±350*	6000±300*
Neutrophils (%)	8±3	40±2.8	25±2.5	12±4.5	22±1.5	24±2.1	23±2.8	16±1.8
Lymphocytes (%)	55±2.5	82±2.2	80±1.7	60±3.2	81±3.1	77±4.2	70±3	58±2.2
Eosinophils (%)	5±0.1	6±0.1	8±0.2	5±0.2	6±0.1	6±0.1	7±0.2	6±0.3

†Vehicle control – propylene glycol, standard – vitamin C (15 mg/kg.b.wt), SALD – *S. asoca* 250 mg/kg b. wt, SAHD – *S. asoca* 500 mg/kg b. wt, KPLD – *K. pinnatum* 250 mg/kg b. wt, KPHD – *K. pinnatum* 500 mg/kg b. wt. Values for each group of six animals are shown as the mean ± standard deviation (SD). *P<0.05 probability values are regarded as statistically significant

Table 5.3. Liver function test of control and treated groups

Parameters	Normal	Control	V. Control	Standard	KPLD	KPHD	SALD	SAHD
SGOT (U/L)	98±5.3	105±4.8*	101±3	98±3.5	103±8.9	98±4.3	102±4.5	96±2.5
SGPT (U/L)	55±3.5	101±2.4**	110±2.8**	72±1.8**	70±3.2*	71±3.5**	73±2.4**	61±3.5*
Alkaline phosphatase (U/L)	350±2.5	360±2.1*	355±2.4	345±7.8	345±8.5	350±7.5	350±4.5	355±3.2
Totalprotein (g/dl)	7±0.5	7.6±0.9	8.3±0.8	7.3±2.5	8±1.5	6.4±0.5	7.2±0.9	7.6±0.3
Albumin (g/dl)	3.6±0.2	3.5±0.2	3±0.2	2.5±0.1	2.8±0.1	3.2±0.2	2.8±0.2	3.1±0.2
Globulin (g/dl)	3.3±0.2	3.3±0.1	3.2±0.2	3.3±0.2	4.1±0.1	3±0.3	3.9±0.1	3.7±0.3
Total Bilirubin (mg/dl)	0.3±0.1	0.2±0.1	0.2±0.1	0.3±0.1	0.2±0.1	0.2±0.1	0.3±0.2	0.2±0.1

†Vehicle control – propylene glycol, standard – vitamin C (15 mg/kg.b.wt), SALD – *S. asoca* 250 mg/kg b. wt, SAHD – *S. asoca* 500 mg/kg b. wt, KPLD – *K. pinnatum* 250 mg/kg b. wt, KPHD – *K. pinnatum* 500 mg/kg b. wt. Values for each group of six animals are shown as the mean ± standard deviation (SD). *P<0.05 and **P<0.01 probability values are regarded as statistically significant
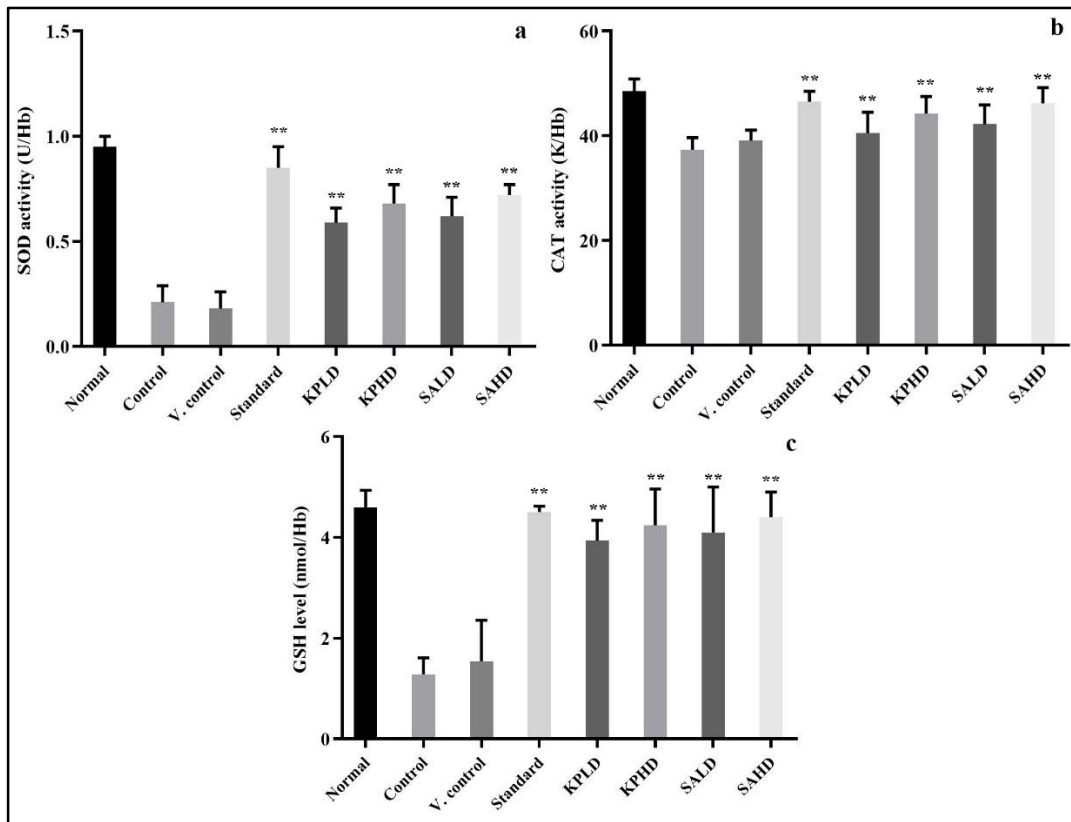
Figure 5.6. Blood antioxidant enzyme levels in response to administration of *S. asoca* and *K. pinnatum* extracts - (a) SOD, (b) CAT and (c) GSH (standard-vitamin C-15 mg/kg b.wt.; KPLD: SALD- 250 mg/kg b.wt.; KPHD: SAHD- 500 mg/kg.b.wt.). Data are presented as mean ± SD for 6 animals per group. *$P<0.05$ and **$P<0.01$ probability values are deemed statistically significant

Table 5.4. Effect of *S. asoca and K. pinnatum* extract on blood antioxidant enzymes activity changes in NaF treated mice

	Normal	Control	V. control	Standard	KPLD	KPHD	SALD	SAHD
SOD (U/Hb)	0.95±0.05	0.21±0.08	0.18±0.08	0.85±0.1**	0.59±0.07**	0.68±0.09**	0.62±0.09**	0.72±0.05**
CAT (K/Hb)	48.5±2.40	37.4±2.3	39.1±2	46.5±2**	40.5±4**	44.3±3.2*	42.2±3.7**	46.2±3**
GSH (nmol/Hb)	4.6±0.34	1.28±0.33	1.54±0.82	4.51±0.11**	3.94±0.4**	4.24±0.72**	4.1±0.9**	4.4±0.5**

5.3.3.2. Influence of SA and KP extracts on hepatic antioxidant enzymes

An illustration of the hepatic antioxidant status of the animals treated with *S. asoca* and *K. pinnatum* is provided in figure 5.7. The activity of SOD was significantly ($p < 0.01$) reduced in the NaF-treated group (0.51 ± 0.03) compared to the normal group (1.45 ± 0.08) animals. The administration of SAHD (1.24 ± 0.03) and KPHD (1.1 ± 0.08) significantly ($p < 0.01$) increased the levels of SOD in extract treated groups. When administered at 500 mg/kg of body weight, SAHD and KPHD enhanced catalase activity by 22.2 ± 2.6 and 20.7 ± 1.3 respectively, compared to control (13.2 ± 2.2) group of animals. Similarly the GSH levels were also reduced in the control and vehicle control groups which was significantly ($p < 0.01$) elevated in extract treated groups (Table 5.5).

Table 5.5. Effect of *S. asoca and K. pinnatum* extract treatment on antioxidant profile of liver in NaF induced animals

	Normal	Control	V. control	Standard	KPLD	KPHD	SALD	SAHD
SOD (U/Hb)	1.45±0.08	0.51±0.05	0.6±0.1	1.2±0.08**	0.89±0.07**	1.1±0.08**	0.95±0.1**	1.24±0.09**
CAT (K/Hb)	25.8±1.4	13±2.2	14.6±1.8	23.4±1.9**	18.9±1.2**	20.7±1.3**	19.6±1.7**	22.2±2.6**
GSH (nmol/Hb)	22.4±3.4	12.74±3.33	11.98±4.82	21.5±2.11**	19.35±2.5**	20.5±2.7**	18±3.5**	21.3±2.5**
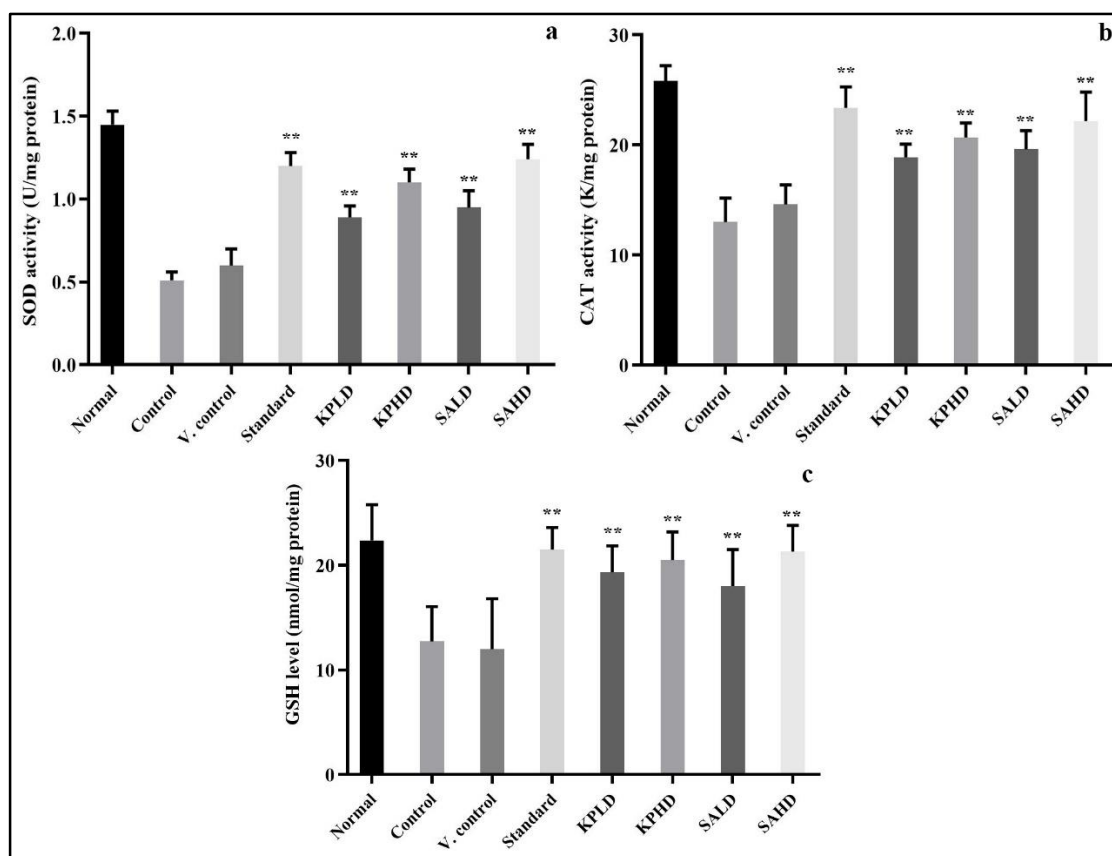
Figure 5.7. Effect of *S. asoca* and *K. pinnatum* extract administration on hepatic antioxidant enzymes - (a) SOD, (b) CAT and (c) GSH (standard-vitamin C-15 mg/kg b.wt.; KPLD: SALD- 250 mg/kg b.wt.; KPHD: SAHD- 500 mg/kg.b.wt.). Data are presented as mean ± SD for 6 animals per group. *P<0.05 and **P<0.01 probability values are deemed statistically significant

5.3.3.3. Effect of SA and KP extracts on lipid peroxidation in liver

The level of MDA, a marker of lipid peroxidation that had been observed to be elevated in NaF alone groups was reduced in extract treated groups (Table 5.6). The standard vitamin C-treated group (2.54 ± 0.45) exhibited the maximum reduction in lipid peroxidation (nmol MDA/mg protein) as compared to the control group (6.33 ± 0.54) animals. The animals administrated with KP at dosages of 250 and 500 mg/kg b.wt. had levels of lipid peroxidation of 4.12 ± 0.33 and 3.45 ± 0.86, respectively. The estimated MDA content was 3.69 ± 0.21 and 3.25 ± 0.72, respectively, in the SALD and SAHD groups (Figure 5.8.).

Table 5.6. Effect of *S. asoca* and *K. pinnatum* extract on lipid peroxidation

Groups	TBARS (nmol of MDA/mg protein)
Normal	2.15±0.35
Control	6.33±0.54
V. control	5.95±0.75
Standard	2.54±0.45**
KPLD	4.12±0.33**
KPHD	3.45±0.86**
SALD	3.69±0.21**
SAHD	3.25±0.72**
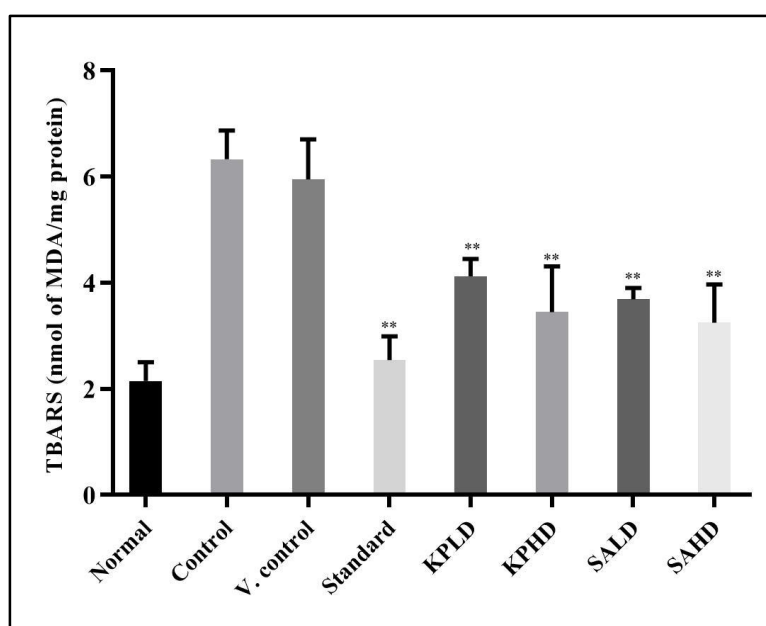
Figure 5.8. Effect of *S. asoca* and *K. pinnatum* extract administration on lipid peroxidation- (standard-vitamin C-15 mg/kg b.wt.; KPLD: SALD- 250 mg/kg b.wt.; KPHD: SAHD- 500 mg/kg.b.wt.). Data are presented as mean ± SD for 6 animals per group. *P<0.05 and **P<0.01 probability values are deemed statistically significant

5.3.3.4. Histopathological analysis of liver

Histopathological analysis of liver of NaF intoxicated mice showed structural abnormalities and severely damaged hepatic tissue architecture. As a result of fluoride toxicity, the liver tissue exhibits degeneration of hepatocytes (blue arrows), necrosis, cytoplasmic vacuolization in hepatic lobules (black arrows), and loss of tissue architecture (Figure 5.9). In the group receiving standard vitamin C, the altered tissue architecture was shown to be reversed. The damages incited by NaF were reverted by treatment with extracts of *S. asoca* and *K. pinnatum.*
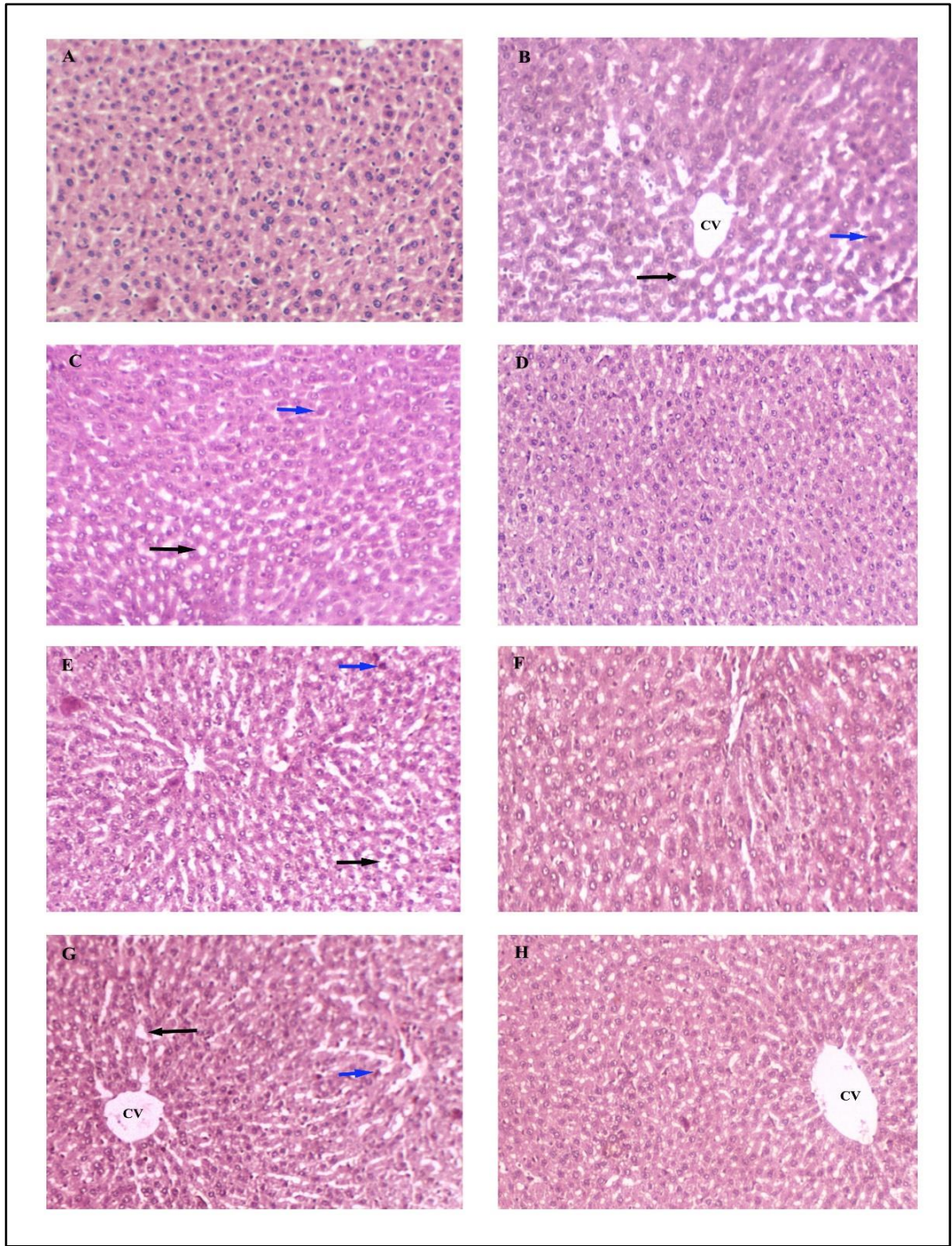
Figure 5.9. Hepatic tissue sections stained with haematoxylin and eosin (20X magnification)- (**A**) Normal, (**B**) Control (NaF 600 ppm/L/day), (**C**) Vehicle control-propylene glycol+ NaF., (**D**) Vitamin C-15 mg/kg b.wt. + NaF, (**E**) KPLD-250 mg/kg b.wt. + NaF, (**F**) KPHD-500 mg/kg b.wt. + NaF, (**G**) SALD- 250 mg/kg b.wt. + NaF, (**H**) SAHD- 500 mg/kg b.wt. + NaF. Administration of NaF, resulted in severe damages including degeneration of hepatocytes (blue arrows), cytoplasmic vacuolization in hepatic lobules (black arrows)

5.4. Discussion

Excessive generation of free radicals leads to oxidative stress, a factor implicated in various pathophysiological conditions. Conditions such as cardiovascular disease, inflammatory diseases, cancer, and other chronic health issues are linked to oxidative stress. Antioxidants can reduce oxidative stress by restricting radical formation, directly scavenging free radicals or accelerating their decomposition. Therefore, in recent years there has been an intensified search for natural compounds with antioxidative properties (Lobo *et al*., 2010). Furthermore, due to the fact that traditional medicine is based on centuries of therapeutic skill and is practiced by more than 85% of the world's population, it has regained favour in today's medical world (Cengiz, 2019). The scientific examination has revealed that numerous plants utilized in traditional medicine serve as reservoirs of valuable pharmacological compounds, possessing anti-inflammatory, antioxidant, cytotoxic, anticancer and organoprotective properties. *Saraca asoca* is an important plant used in Ayurveda to treat a variety of health conditions. *Kingiodendron pinnatum* is often used as an alternative to *S. asoca* in Ayurvedic formulations but has not been adequately investigated from a pharmacological standpoint. As a result, a detailed evaluation of the *in vitro* and *in vivo* antioxidant capacity of *S. asoca* and *K. pinnatum* have been determined in this chapter. Since numerous processes are known to be involved in antioxidant activity, the results provided by a single approach could not accurately reflect the true antioxidant capacity of a given compound or extract. Therefore, it would be helpful to confirm the antioxidant activity of the extracts by using several assays. In light of this, several *in vitro* and *in vivo* investigations were performed to assess the antioxidant capacity of *S. asoca* and *K. pinnatum*.

The findings of this study indicate that the crude methanolic extract from *S. asoca* and *K. pinnatum* effectively inhibited or scavenged free radicals such as ABTS, superoxide and hydroxyl *in vitro*, exhibiting a concentration-dependent response. The FRAP assay further demonstrated that the plant extract reduced ferric ions into ferrous ions, again in a concentration-dependent manner. Similar findings regarding the antioxidant properties of the methanol bark of *S. asoca* have been documented, demonstrating its highest efficacy in scavenging DPPH and superoxide radicals (Ghatak *et al*., 2015a). A number

of other studies have also examined the free radical scavenging ability of the methanol extract of *S. asoca* (Yadav *et al*., 2015, Mohan *et al*., 2016). *Kingiodendron pinnatum* has also been previously reported to possess antioxidant properties (Sheik and Chandrashekar, 2014, Kumar *et al*., 2011). The methods for evaluating antioxidants are divided into two categories: those that measure the potential to scavenge free radicals and those that measure lipid peroxidation (Alves *et al*., 2010). In this study the lipid peroxidation was induced on the erythrocyte membrane by AAPH, a peroxyl radical generator. The extend of peroxidation was measured by the quantification of malondialdehyde (MDA), an aldehyde generated during the lipid peroxidation reaction that gives information on the redox state. The high reactivity of MDA makes it one of the most studied biomarkers for lipid peroxidation (França *et al*., 2013). Both the plant extracts considerably inhibited the lipid peroxidation on human erythrocytes induced by AAPH. Haemolysis of human RBCs is an excellent model in order to examine the oxidative damage caused by free radicals to membranes and to assess the antioxidant activity of novel substances (Banerjee *et al*., 2008). In the study of the protective impact of extracts against haemolysis of the erythrocytes induced by AAPH, extracts from both plants substantially reduced haemolysis. Therefore the present findings have significance because free radicals including hydroxyl, superoxide, nitric oxide radicals and others are capable of damaging biologically important molecules. As *in vitro* studies demonstrated the potent antioxidant activities of both plants, it led to the evaluation of the protective effects against sodium fluoride-induced oxidative stress *in vivo*.

The antioxidant activity of both plants was further confirmed *in vivo* because biological systems have both enzymatic and non-enzymatic defense mechanisms built in to counteract the negative effects of reactive oxygen species. A number of antioxidant enzymes including catalase, superoxide dismutase and glutathione are vital to the antioxidant protection of biological systems from free radical damage (Ighodaro and Akinloye, 2018). In the study, untreated animals exposed to sodium fluoride (NaF), displayed decreased antioxidant profiles in the liver tissue and blood, but treatment with *S. asoca* and *K. pinnatum* bark extract greatly improved their ability to survive stress. The levels of MDA in mice liver tissue increased, however the activities of catalase, SOD and GSH were lowered in fluoride-intoxicated group. In the extract-treated group, a considerable enhancement of the endogenous antioxidant system has been observed as

evidenced by elevated levels of catalase, SOD and GSH, together with a decrease in lipid peroxidation. Similar results of enhanced activity of antioxidant enzymes by the administration of extracts prepared with *S. asoca* and *K. pinnatum* are reported (Suhail, 2019). Also the lipid peroxidation inhibition activity by the *S. asoca* bark extract is described in a study (Yadav *et al*., 2015). As seen during histological evaluation, fluoride exposure caused structural changes in liver tissue. These changes included cytoplasmic vacuolization in hepatic lobules, degeneration of hepatocytes, impairment of tissue architecture, etc. The treatment with both extracts significantly reduced tissue damage, indicating the antioxidant capacity of both plant extracts.

Fluoride damages soft tissues including the blood, brain, and liver by penetrating the cell membrane. Due to its active metabolism, the liver is especially vulnerable to fluoride poisoning and leads to lipid peroxidation and may alter the function of liver antioxidant enzymes (Nabavi *et al*., 2012, Nabavi *et al*., 2013). In the current study, an increase in TBARS levels along with a decrease in hepatic antioxidant enzymes suggests the oxidative stress in hepatic tissue. Extracts of *S. asoca* and *K. pinnatum* appear to counteract the negative effects of experimentally induced oxidative stress, which may be attributable to the presence of antioxidant components, particularly polyphenols. Therefore, the study emphasizes the antioxidant properties of *S. asoca* and *K. pinnatum* extract as well as its role in ameliorating oxidative stress both *in vitro* and *in vivo*.

Chapter 6
Evaluation of the effect of *S. asoca* and *K. pinnatum* extracts on DMBA induced mammary carcinogenesis and 4T1 induced TNBC model

6.1 Introduction

Breast cancer is one of the most common neoplastic disease among women and its incidence and mortality rates have been increasing steadily around the world. Its aggressive nature has resulted in increased younger age distribution, high death rates, advanced stage distribution and an increased prevalence of high-grade tumours (Minari *et al*., 2016). Breast cancer develops and progresses in a complex manner, with aberrant differentiation, uncontrolled proliferation and resistance to apoptosis (Hanahan and Weinberg, 2011). Currently available treatments have substantial safety and effectiveness flaws. Therefore, preventive, and innovative therapeutic techniques play a crucial role in the fight against this disease. In addition, as advanced metastasized breast cancer remains incurable, further research into safer and more efficient chemoprevention and treatment methods is required to enhance its effectiveness (Minari *et al*., 2016). Chemoprevention has proven to be one of the effective approach toward achieving this goal.

Chemoprevention aims to reduce the risk of cancer or slow its progression in individuals already at high risk. This involves the use of synthetic or natural products, including medications, dietary supplements, vitamins, minerals, and lifestyle adjustments, to hinder or halt the development, promotion, or advancement of cancer. Chemopreventive drugs can work in a number of ways, including preventing DNA damage, reducing inflammation, encouraging apoptosis, and impeding the development and spread of cancer cells (Swetha *et al*., 2022). Populations of premalignant cells may acquire early indications of cancer due to the absence of cellular repair processes that would normally repair DNA damage and enable proper chromosomal segregation during mitosis. Chemoprevention activity frequently arises from the combination of multiple diverse intracellular interactions rather than from a single biological response. Antioxidant, anti-inflammatory, and apoptosis-inducing activities, as well as monitoring cell cycle progression at certain points, are some of the more crucial mechanisms (Mukhopadhyay *et al*., 2017). The process of developing new chemopreventive agents has undergone a significant change over the past years and today the agents are thoroughly examined in preclinical studies before clinical trials are launched (Steward and Brown, 2013).

The development of mammary tumours occurs spontaneously in a few animal species, such as dogs, rats and mice. The majority of studies regarding experimental breast carcinogenesis are conducted in rodents for practical reasons (Barros *et al*., 2004). Several

mouse strains' mammary glands are susceptible to transformation induced by chemical carcinogens. The 7,12-dimethylbenz(a)anthracene (DMBA) is the most potent and often used active chemical inducer of mammary cancer. It is important to note that the response of mice to DMBA is strain dependent and multiple doses of DMBA are required to trigger the response (Medina, 2010). The breast tissue is particularly susceptible to carcinogenesis induced by DMBA and the metabolized products of DMBA induce DNA damage. These metabolites produce DNA-adducts, which encourage tumour growth by modulating gene expression, as well as contributing to genomic instability, thereby promoting tumour progression. There is a close parallel between this multi-step process and breast cancer in humans (Plante, 2021). The efficacy of antioxidants to inhibit carcinogenesis is strongly linked towards their capability to hinder the metabolism of DMBA. *Saraca asoca* and *Kingiodendron pinnatum* are reported to contain phytochemicals with strong antioxidant properties. Numerous preclinical studies have supported the use of phytochemicals as chemopreventive agents, which make up a significant fraction of currently used anticancer medications. Furthermore, the protective effect of *Saraca asoca* extract against chemically induced cell carcinogenesis was reported (Cibin *et al*., 2012, Mukhopadhyay *et al*., 2017).

The 4T1 induced breast cancer model is an ideal model to study triple negative breast cancers (TNBC). The 4T1 mammary carcinoma is a transplantable tumour cell line known for its elevated tumourigenicity, high invasiveness and significant potential for spontaneous metastasis. A number of characteristics of the 4T1 tumour make it a suitable experimental animal model for human TNBC (Pulaski and Ostrand-Rosenberg, 2001). The growth of 4T1 cells and their metastatic spread are efficient in BALB/c mice, and that they closely mimic the type of breast cancer found in humans. Subcutaneous injection of 4T1 cells into the mammary pad results in highly metastatic tumours of 4T1. It is noteworthy that this TNBC animal tumour mimics the condition of human mammary carcinomas, particularly stage IV triple-negative breast cancer (Rajaratinam *et al*., 2022). In most cases, BALB/c mice are used, which are validated by Organization for Economic Co-operation and Development (OECD). Therefore, the purpose of the study was to examine the protective effects of the crude methanol extracts of *Saraca asoca* and *Kingiodendron pinnatum* against DMBA induced mammary carcinoma and 4T1 cell induced TNBC model in mice.

6.2 Materials and methods

6.2.1. Preparation of extracts

Using the method described in chapter 5, section 5.2.1, the crude methanol bark extracts of *Saraca asoca* and *Kingiodendron pinnatum* were prepared.

6.2.2. Chemicals

The carcinogen, 7,12-dimethylbenz[a]anthracene (DMBA), for inducing breast cancer was procured as per the list in Section 2.1.2 of Chapter 2. RevertAid first strand cDNA synthesis kit (ThermoFisher) was used for cDNA synthesis and SsoADV Univer SYBR GRN SMX 500 kit (Biorad) for qRT-PCR. The primers were purchased from Integrated DNA Technologies (IDT). The additional chemicals employed in the experiment were all of analytical standard.

6.2.3. Animals

The animals were acquired from Kerala Veterinary and Animal Sciences University (KVASU) and were handled and cared for in accordance with section 2.1.4 of chapter 2.

6.2.4. MTT assay

The 4T1 cells were cultured overnight in well plates at a cell density of 5×10^4 cells per well and the plant extracts were applied at a concentration of 0-200 μg/mL. The method is laid out in detail in Chapter 2's section 2.2.17.2.

6.2.5. Establishment of DMBA-induced murine breast tumours

The induction of mammary tumours in female Swiss albino mice (25-30g) was accomplished using DMBA. The details of the study are described in section 2.2.10 of chapter 2. Animals were euthanized at the conclusion of the study, and blood serum was gathered and analysed for haematological parameters (section 2.2.7 of chapter 2), liver function test and renal function test (section 2.2.9 of chapter 2). The mammary gland whole mount preparation and analysis were also done (section 2.2.10 of chapter 2). The tissues from the breast and liver were histopathologically examined (section 2.2.6.3. of chapter 2).

6.2.5.1. Gene expression studies

From the mammary pad of animals of different groups, total RNA was extracted using TRIZOL reagent. The first-strand cDNA was synthesized utilising the cDNA synthesis

kit (ThermoFisher's RevertAid) with RNA isolated from the mouse mammary pad. A qRT-PCR was conducted using Biorad's SsoADV Universal SYBR Green Supermix on a StepOnePlusTM Real-Time PCR system. StepOne version 2.2.2 was used as the software (section 2.2.11 of chapter 2).

6.2.6. Induction of mouse TNBC by 4T1 cells

The five weeks old BALB/c female mice were given injection of murine 4T1 cells into their mammary fat pads (fourth), for the induction of triple negative breast cancer (TNBC). A pre-treatment period of ten days preceded the administration of plant extracts daily to BALB/c mice for 20 days following the challenge with 4T1 breast cancer cells. The detailed procedure of the study is given in section 2.2.12 of chapter 2. All animals were euthanized after twenty days. Blood was drawn from heart to conduct hematological examination (section 2.2.7 of chapter 2). Mammary pad and lungs were sliced out for histological analysis.

6.2.7. Statistical analysis

For *in vitro* investigations, values were given as mean ± standard deviation (SD), derived from three distinct experiments, whereas for *in vivo* studies, data were based on six mice per group. The data were analyzed using one way and two-way ANOVA following Tukey's multiple comparison test in GraphPad Prism 8. P-values at these levels were considered statistically significant only at $p < 0.01$**, $p < 0.05$* and $p > 0.05$ was deemed non-significant.

6.3. Results

6.3.1. Chemopreventive effect of *S. asoca* and *K. pinnatum* extract

The *S. asoca* and *K. pinnatum* plant extracts reduced the DMBA-induced tumourigenesis and lowered the prevalence of breast tumours in mice. Throughout the whole 6 week experiment, there were no deaths reported in the control or treatment groups. The mice in the control and vehicle control group shows significantly lower final body weights. All of the other groups' animals displayed a steady rise in body weight throughout the experiment. When compared to the tumour induced control groups, no appreciable changes were found in the mice's diet or water intake in any of the groups.

6.3.1.1. DMBA impact on haematological indicators

The decreased haemoglobin level (8.1 ± 0.45 g/dL) and RBC count (4.3 ± 0.1 millions/mm^3) of the control group with respect to the normal ((Hb: 12.5 ± 0.37 g/dL; RBC: 6.8 ± 0.2 millions/mm^3) demonstrate that DMBA-induced modifications in the erythropoietic parameters. At doses of 500 mg/kg b.wt of *S. asoca* and *K. pinnatum* extracts, the drop in the level of Hb caused by the administration of DMBA was reinstated to 12.4 ± 0.45 and 12.1 ± 0.2 g/dL, respectively. Likewise, treatment with plant extracts considerably enhanced the RBC count to 6.3 ± 0.2 and 5.7 ± 0.1 millions/mm^3, respectively, which is approximately equal to standard, tamoxifen (6.6 ± 0.2 millions/mm^3). Table 6.1 displays changes in other haematological indicators.

Table 6.1. Hematological parameters of DMBA induced mammary tumour mice and normal group

	Normal	Control	V. Control	Standard	SALD	SAHD	KPLD	KPHD
Haemoglobin (g/dl)	12.5±0.3	8.1±0.45	9.2±0.2ns	12.8±0.4**	11.9±0.3**	12.4±0.2*	11.4±0.4*	12.1±0.2**
Total RBC count (millions/cu mm)	6.8±0.2	4.3±0.1	4.9±0.2ns	6.6±0.2**	5.5±0.2**	6.3±0.2**	5.2±0.2**	5.7±0.1**
Platelet count (lakhs/cu mm)	4.5±0.3	2.6±0.2	3±0.5ns	4.3±0.2**	3.58±0.4**	4±0.2**	3.6±0.1**	3.9±0.1**
Total WBC count (cells/cu mm)	6900±520	8800±205	9100±270ns	7000±190**	8100±230**	7500±510**	8400±450**	7800±550**
Neutrophils (%)	26±2.2	43±3	45±2.8ns	29±2.5**	35±0.8**	32±1.5**	36±0.9**	34±2.1**
Lymphocytes (%)	52±2.6	75±2.5	78±2.2ns	59±1.7**	67±3.2**	63±3.1**	69±1.5**	66±4.2**
Eosinophils (%)	2±0.4	4±0.25	4±0.3ns	3±0.2*	3±0.2*	2±0.1**	3±0.2*	2±0.1**

†Vehicle control – Propylene glycol, SALD – *S. asoca* 250 mg/kg b. wt, SAHD – *S. asoca* 500 mg/kg b. wt, KPLD – *K. pinnatum* 250 mg/kg b. wt, KPHD – *K. pinnatum* 500 mg/kg b. wt,, standard – Tamoxifen 20 mg/kg b. wt. Values for each group of six animals are presented as mean ± SD. *P<0.05 and **P<0.01 probability values are deemed statistically significant; ns – non significant ^{ns}p>0.05

6.3.1.2. Effect of DMBA on liver and renal enzymes

In comparison to the normal group, which had SGOT (55 ± 3.3 U/L), SGPT (42 ± 3.1 U/L), and ALP (128±2.5 U/L), DMBA administration caused an increase in SGOT (84 ± 1.8 U/L), SGPT (70 ± 1.5 U/L) and ALP (178 ± 2.1 U/L) in the control group. Table 6.2 displays alterations in serum marker levels brought on by the administration of plant extracts and standard. LDH levels were elevated in control and vehicle control groups compared to normal groups indicating that concentration of the enzyme closely follows the growth of the tumour. In renal function test, the treated group's values for urea and creatinine were non-significant when compared to the normal group (Table 6.3).

Table 6.2. Liver function test and LDH levels of control and treated groups

Parameters	Normal	Control	V. Control	Standard	SALD	SAHD	KPHD	KPHD
SGOT (U/L)	55 ± 3.3	84 ± 1.8	87 ±1.1^{ns}	63 ± 3.5**	68 ± 1.9**	64 ± 4.3**	74 ± 2.5**	68 ± 6.3**
SGPT (U/L)	42 ± 3.1	70 ± 1.5	74 ± 2.2 ^{ns}	51 ±1.5**	57 ± 4.2**	55 ± 2.5**	64 ± 4.4**	59 ± 2.5**
ALP (U/L)	128±2.5	178 ± 2.1	175 ±4.4 ^{ns}	154 ±2.8**	160 ± 2.5**	144±2.4**	164 ±5.8**	149 ±3.5**
Total protein (g/dL)	6.9±0.4	6.8±0.9	6.5±0.8 ^{ns}	6.3±2.5	5.8±1.5	6.4±0.5	5.7±0.9	6.5±0.3
Albumin (g/dL)	3.6±0.2	3.5±0.2	3±0.2 ^{ns}	2.5±0.1	2.8±0.1	3.2±0.2	2.8±0.2	3.1±0.2
Globulin (g/dL)	3.3±0.2	3.3±0.1	3.2±0.2 ^{ns}	3.3±0.2	3±0.1	3.2±0.3	2.9±0.1	3.4±0.3
Total Bilirubin (mg/dL)	0.3±0.1	0.3±0.1	0.3±0.1 ^{ns}	0.4±0.1	0.3±0.1	0.5±0.1	0.4±0.2	0.5±0.1
LDH (Units/mg protein)	1341±104	2512±235	2498±205 ^{ns}	1255±128**	1912±210**	1374±96*	1872±260**	1448±130**

†Vehicle control – Propylene glycol, SALD – *S. asoca* 250 mg/kg b. wt, SAHD – *S. asoca* 500 mg/kg b. wt, KPLD – *K. pinnatum* 250 mg/kg b. wt, KPHD – *K. pinnatum* 500 mg/kg b. wt,, standard – Tamoxifen 20 mg/kg b. wt. Values for each group of six animals are presented as mean ± SD. *P<0.05 and **P<0.01 probability values are deemed statistically significant; ns – non significant ^{ns}p>0.05

Table 6.3. Influence of extracts on serum indicators for renal function

Biochemical parameters	Normal	Control	V. Control	Standard	SALD	SAHD	KPLD	KPHD
Urea (mg/dL)	35 ± 1.25	36 ±0.9	37 ± 0.5	36 ± 0.7	37 ± 0.4	35 ± 0.3	37 ± 0.3	35 ± 0.5
Creatinine (mg/dL)	1.3 ± 0.13	1.25 ±0.28	1.38 ± 0.3	1.3 ±0.02	1.44±0.5	1.32 ±0.2	1.4 ±0.3	1.38 ±0.2

†Vehicle control – Propylene glycol, SALD – *S. asoca* 250 mg/kg b. wt, SAHD – *S. asoca* 500 mg/kg b. wt, KPLD – *K. pinnatum* 250 mg/kg b. wt, KPHD – *K. pinnatum* 500 mg/kg b. wt,, standard – Tamoxifen 20 mg/kg b. wt. Values for each group of six animals are presented as mean ± SD. *P<0.05 and **P<0.01 probability values are deemed statistically significant; ns – non significant [ns]p>0.05

6.3.1.3. Antioxidant status and degree of lipid peroxidation of DMBA-induced breast tumours

The antioxidant enzyme, CAT (U/g Hb), SOD (U/g Hb) and GSH (nmol/g Hb) levels in breast tissue was found to be lowered in the control and vehicle control groups. Treatment with both the extracts nearly restored the enzyme status to normal levels (Figure 6.1). In contrast to the normal group (0.18 ± 0.03 nmol MDA/mg protein) of animals, the level of lipid peroxidation in the control group was found to be higher (0.55 ± 0.07 nmol MDA/mg protein). The extracts of *S. asoca* and *K. pinnatum* at doses of 500 mg/kg b.wt., markedly decreased levels of lipid peroxidation to 0.33 ± 0.06 and 0.36 ± 0.04 nmol MDA/mg protein, respectively (Figure 6.1).
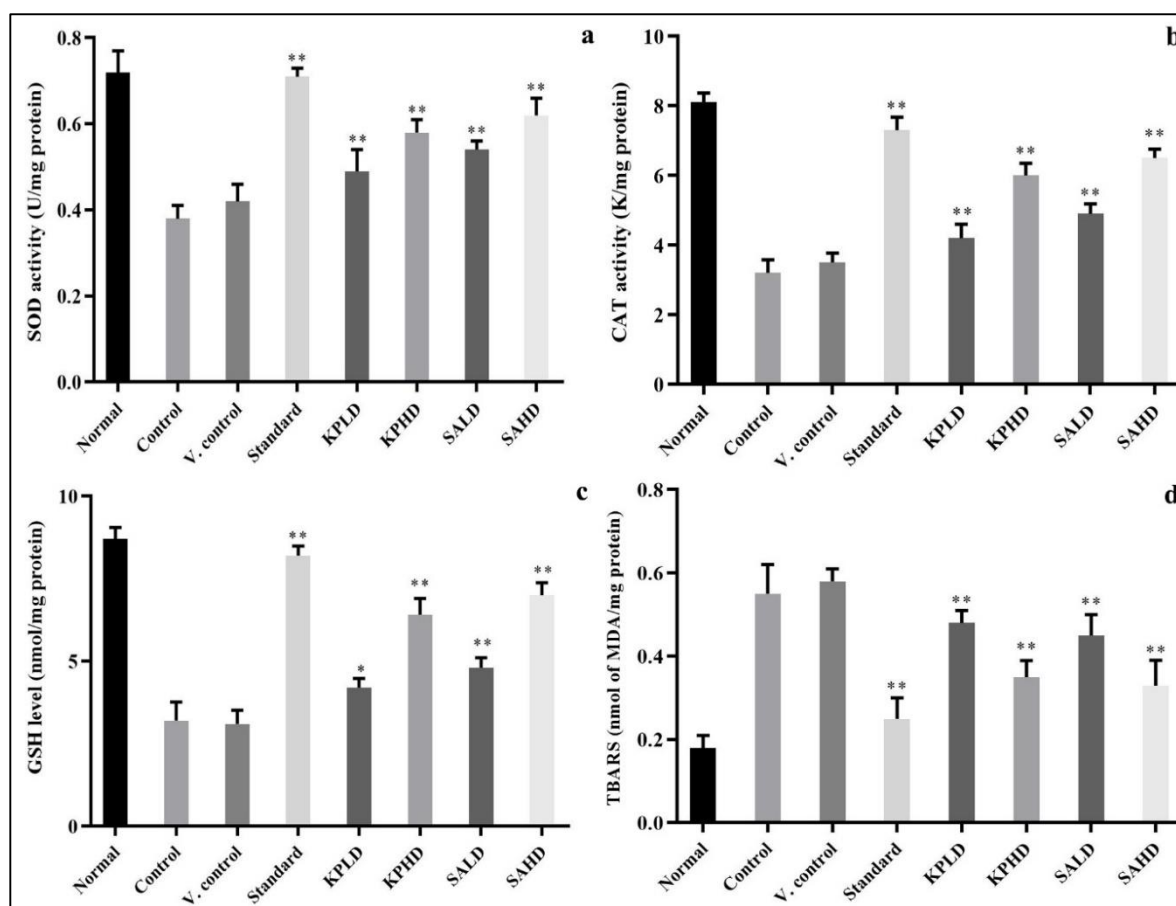
Figure 6.1. Antioxidant enzyme and lipid peroxidation levels in breast tissue of DMBA induced mice - (a) SOD, (b) CAT and (c) GSH (d) TBARS (standard-tamoxifen 20 mg/kg b. wt., KPLD: SALD- 250 mg/kg b.wt.; KPHD: SAHD- 500 mg/kg.b.wt.). Data are presented as mean ± SD for 6 animals per group. *P<0.05 and **P<0.01 probability values are deemed statistically significant

6.3.1.4. Animal necropsy

As evidenced by the necropsy of animals treated with DMBA the abdominal mammary glands of mice have been seen to enlarge relative to normal groups. The mammary glands in these animals have a red appearance due to increased vascularization (Figure 6.2). During the experimental period, palpable breast tumour was noted in the control and vehicle control groups. The inside body walls of DMBA treated animals contain more blood vessels than normal group animals. There was extensive vascularization around the mammary gland and the ovaries. The animals given high dosages of SAHD and KPHD showed a marked reduction in the number of blood vessels, as compared to the control group. The tumour size was comparatively smaller and the rate of tumour initiation and

progression was lowered in the extract-treated groups when compared to the control groups.
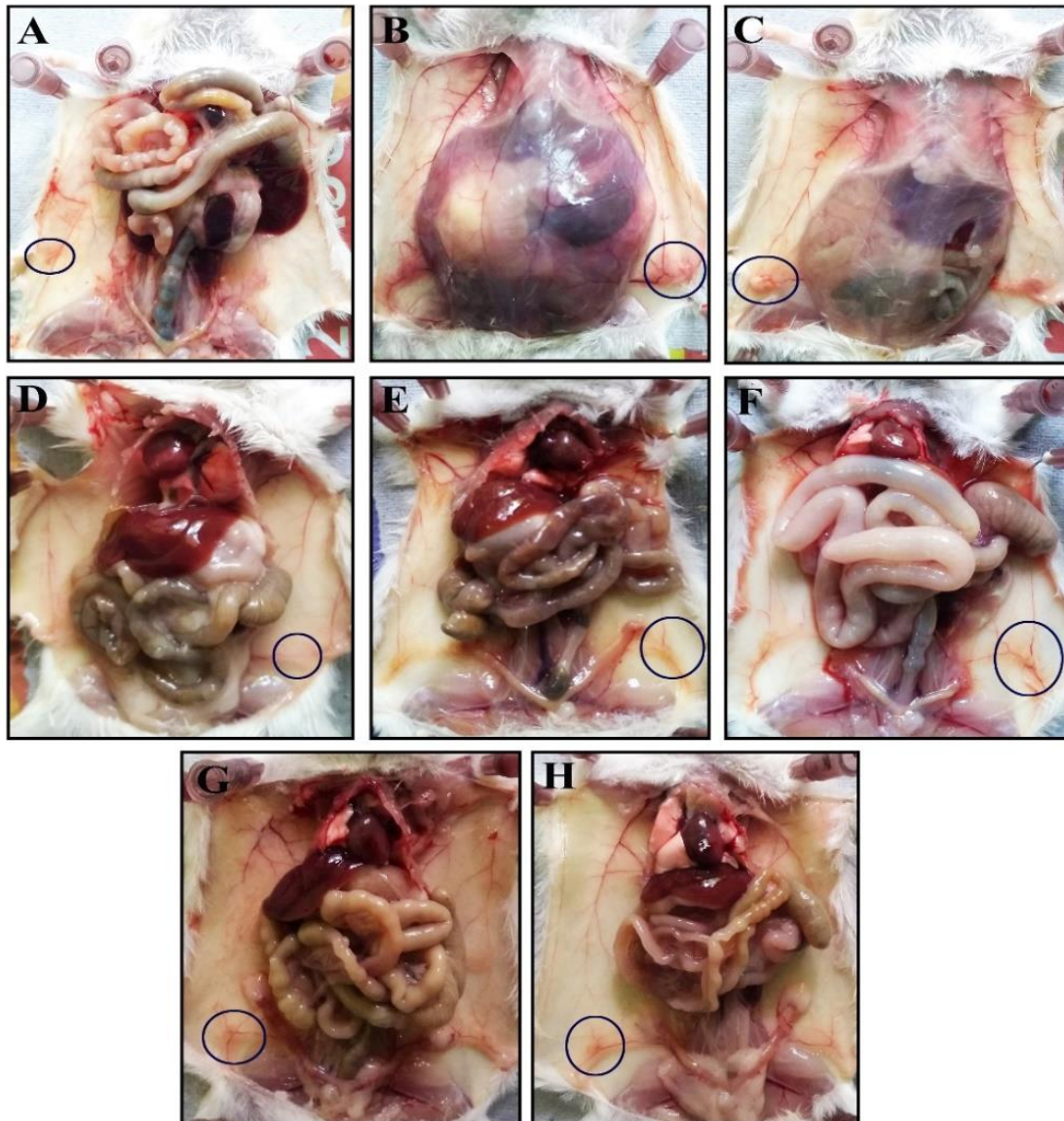
Figure 6.2. Anatomy of DMBA-treated and untreated mice after six weeks. A-normal, B- control, C- v.control, D- tamoxifen 20 mg/kg b. wt, E- SALD – *S. asoca* 250 mg/kg b. wt, F- SAHD - *S. asoca* 500 mg/kg b. wt, G- KPLD – *K. pinnatum* 250 mg/kg b. wt, H-KPHD - *K. pinnatum* 500 mg/kg b. wt.

6.3.1.5. Mammary pad staining and histological analysis

Mammary pad staining with carmine alum revealed the branching complexity of epithelial structures and its changes. Staining intensity was increased in hyperplasic areas

in control and vehicle control groups whereas in treated groups intensity was comparatively lower (Figure 6.3). The histological section of breast tissues from the untreated groups shows normal stromal tissue, adipose tissue and mammary duct. In control group the stroma in most areas show carcinomatous growth composed of pleomorphic polyhedral or oval cells having hyperchromatic nuclei. In addition to hyperplastic areas, the ducts and lobes were enlarged. Mice treated with the extracts and the standard drug tamoxifen had less breast tissue with hyperplasia of the ducts. In treated groups, section shows breast tissue with lobules of acini and dialted ducts all of them lined by cuboidal cells. There was a decrease in proliferative lesions in the extract treated groups (Figure 6.4). Histopathological examination of liver tissues from control showed necrosis, intrusion of inflammatory cells and moderate sinusoidal inflammation. Normal group shows typical hepatic architecture whereas standard group shows hepatocellular damage (Figure 6.5). The central vein and nearby tissues of mice in the extract-treated groups displayed a little infiltration of inflammatory cells.
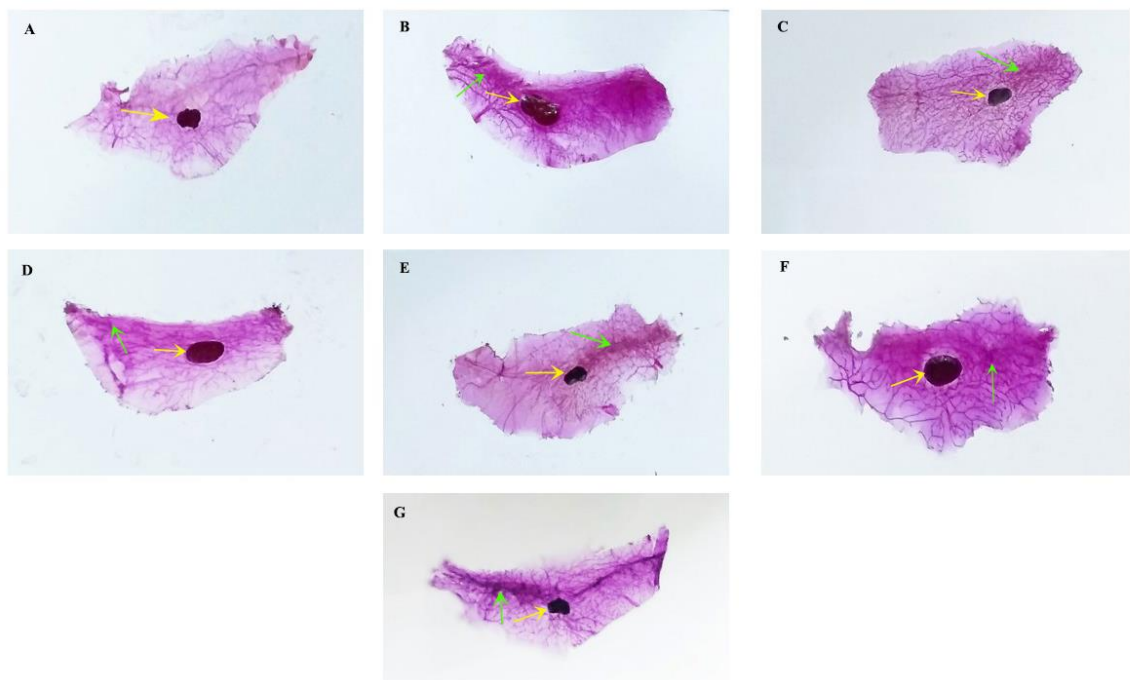
Figure 6.3. Whole mount of mammary gland A: normal, B: control, C: standard, D: SAHD, E: SALD, F: KPHD, G: KPLD, Yellow arrow: Lymph node, Green arrow: Hyperplastic areas
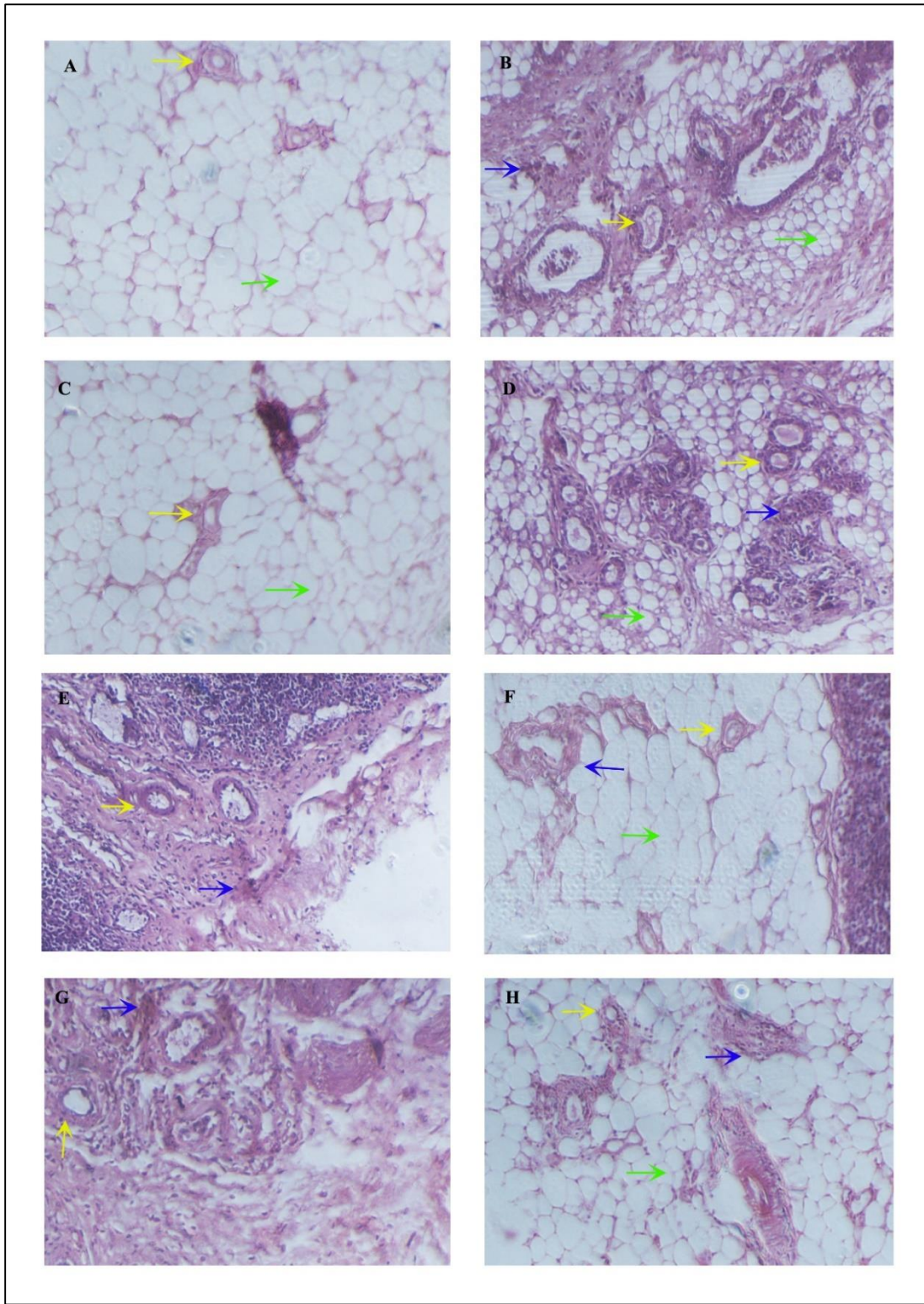
Figure 6.4. Mammary gland histology of mice across different groups - A: normal, B: control, C: standard, D: v. control, E: SALD, F: SAHD, G: KPLD, H: KPHD, blue arrow- hyperplastic areas, green arrow- adipose tissue, yellow arrow- duct
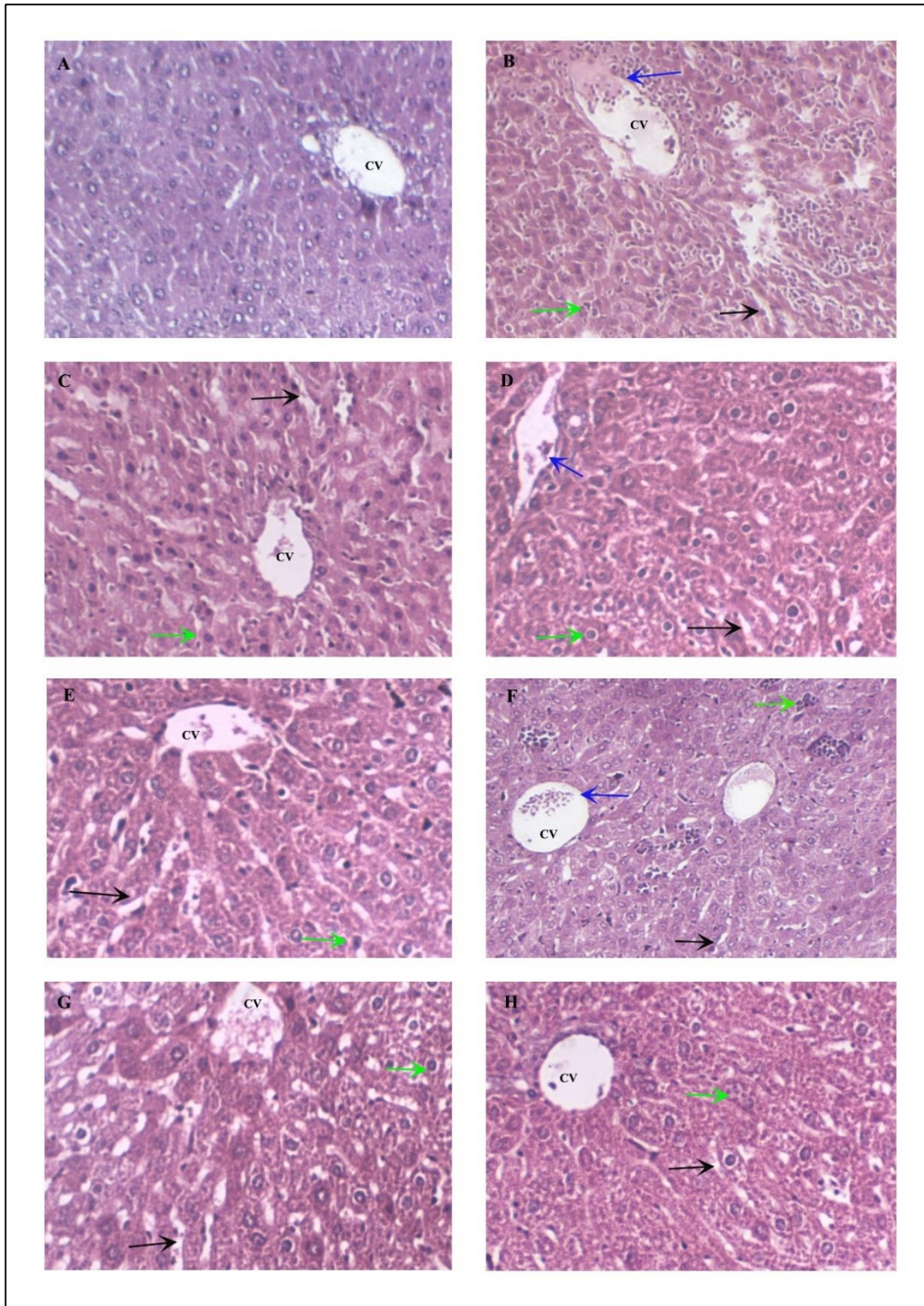
Figure 6.5. Hepatic histology of mice among different groups - A: normal, B: control, C: standard, D: v. control, E: SALD, F: SAHD, G: KPLD, H: KPHD, Black arrow- Duct, Green arrow- necrosis, Blue arrow- infiltration of inflammatory cells, CV- central vein

6.3.1.6. Gene expression analysis

DMBA-induced mammary tumours displayed enhanced levels of the ER-α1, BCL2, PIN1 and c-MYC mRNA expression when compared to normal mammary glands. PIN1 mRNA levels in control and extract treated tumours did not differ significantly (Figure 6.6). The upregulation of mRNA expression levels of BCL2 in DMBA induced tumours were downregulated by the extracts of *S. asoca* and *K. pinnatum* by 2.01 and 3.04 fold, respectively. Meanwhile, treatment with SA and KP extracts downregulated ERα1 expression levels by 2.33 and 1.75 fold, respectively and c-MYC mRNA expression levels by 2.22 and 2 fold, correspondingly, in comparison with the DMBA-treated group.
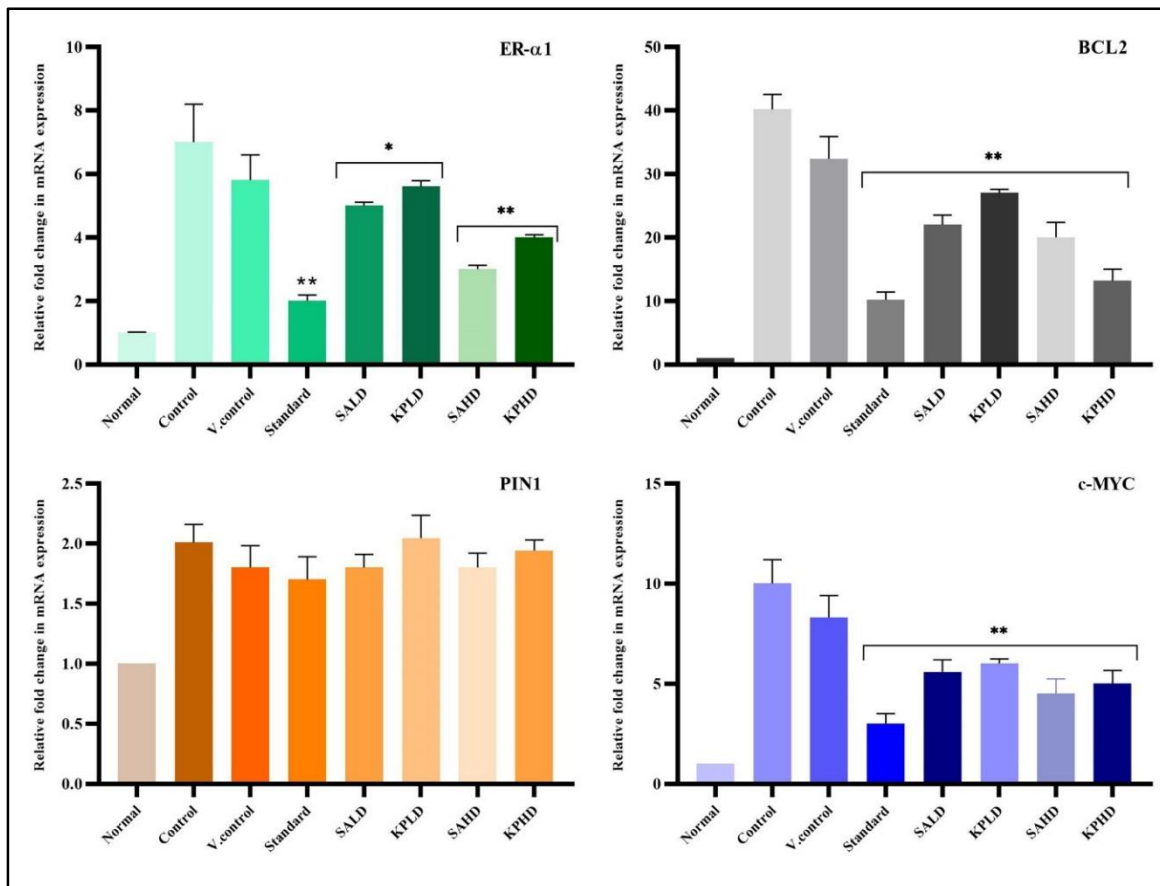
Figure 6.6. Comparison of mRNA expression levels of BCL2, ER-α1, c-MYC and PIN1 in the DMBA control and extract treated groups of animals (standard-tamoxifen 20 mg/kg b. wt., KPLD: SALD- 250 mg/kg b.wt.; KPHD: SAHD- 500 mg/kg.b.wt.). Data is presented as mean ± SD. *P<0.05 and **P<0.01 probability values are deemed statistically significant

6.3.2. Protective effect of extracts against 4T1 induced TNBC in mouse

6.3.2.1. *In vitro* cytotoxicity analysis

The MTT analysis shows significant dose-dependent antiproliferative effect against the 4T1 cells, with IC_{50} values of 132.2 and 152.4 μg/mL, respectively. Figures 6.7 and 6.8 depict the dose-dependent cytotoxicity and the morphological alterations of extracts respectively, towards 4T1 cell line.
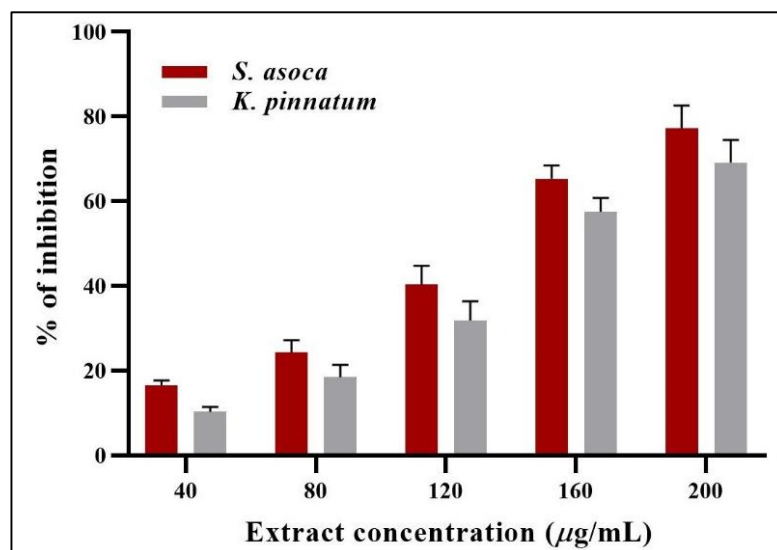
Figure 6.7. Percentage of inhibition of 4T1 cell line by the plant extracts
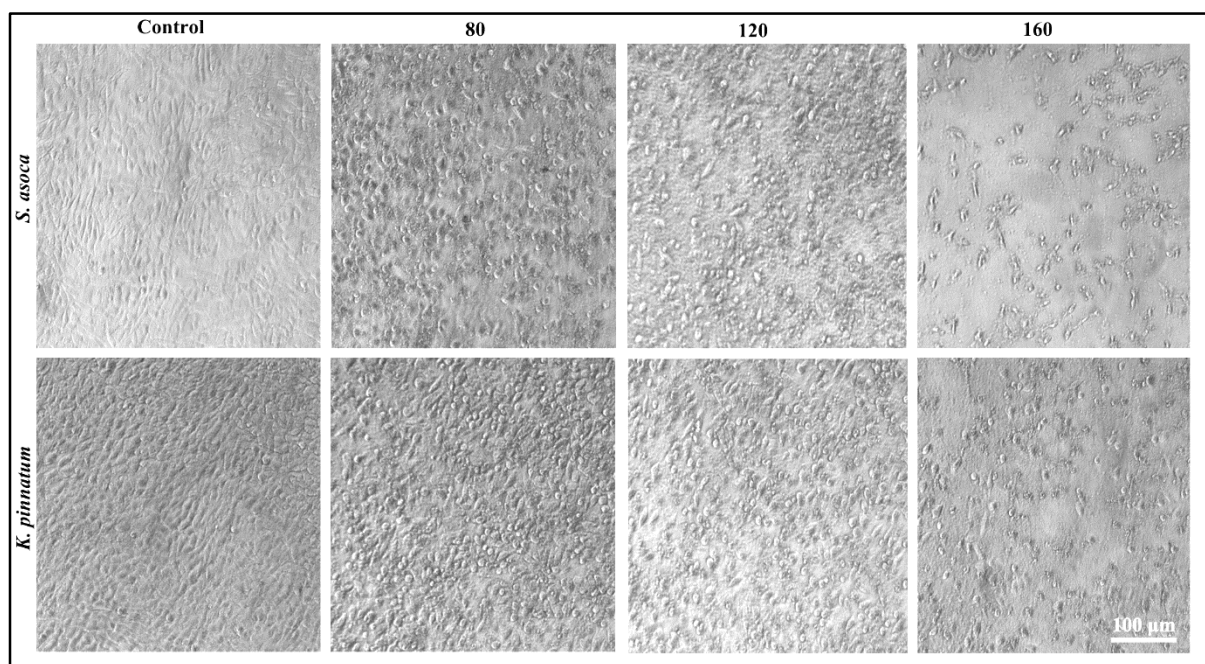
Figure 6.8. Morphological alterations caused by *S. asoca* and *K. pinnatum* extracts on 4T1 cells visualised using a phase contrast microscope at 20X magnification

6.3.2.2. 4T1 induced TNBC model

The 4T1 induced animals in various treatment groups and the control group did not significantly alter in terms of body weight or food and water intake during the course of the experiment. There were also no death recorded in control and treated groups throughout the experiment. Additionally, no change in hematological indices among different groups were observed except for total white blood cell (WBC) count. The elevated WBC levels observed in the control group was considerably reduced ($P<0.05$) in the groups received 500 mg/kg b.wt. of the extracts. This suggests a notable impact on WBC levels due to the administered extracts (Figure 6.9).
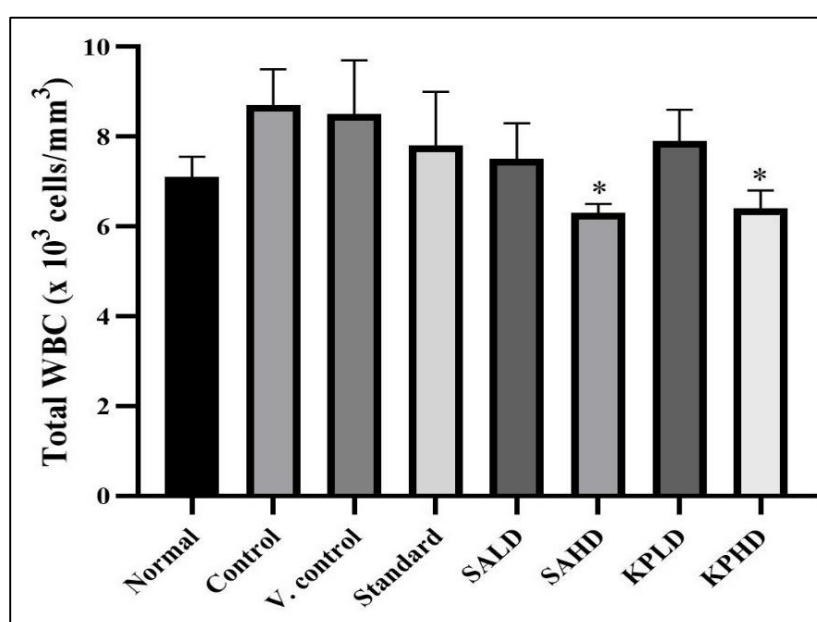
Figure 6.9. Impact of extracts on total WBC count in 4T1 induced breast cancer mice (standard-doxorubicin 10 mg/kg b. wt., KPLD: SALD- 250 mg/kg b.wt.; KPHD: SAHD-500 mg/kg.b.wt.). Data is presented as mean ± SD. *$P<0.05$ and **$P<0.01$ probability values are deemed statistically significant

6.3.2.3. Necropsy of animals

The plant extracts of *S. asoca* and *K. pinnatum* hindered tumour growth in mice. The tumour size in extract treated animals were reduced as compared to control group especially at high doses of plant extract (500 mg/kg b.wt.) (Figure 6.10). The tumour volume in the control group (0.74 ± 0.1 mm^3) was reduced to 0.66 ± 0.14 and 0.34 ± 0.11 mm^3 in the high dose groups of *S. asoca* and *K. pinnatum* respectively. The standard shows a tumour volume of 0.31 ± 0.1 mm^3 (Figure 6.11).

216
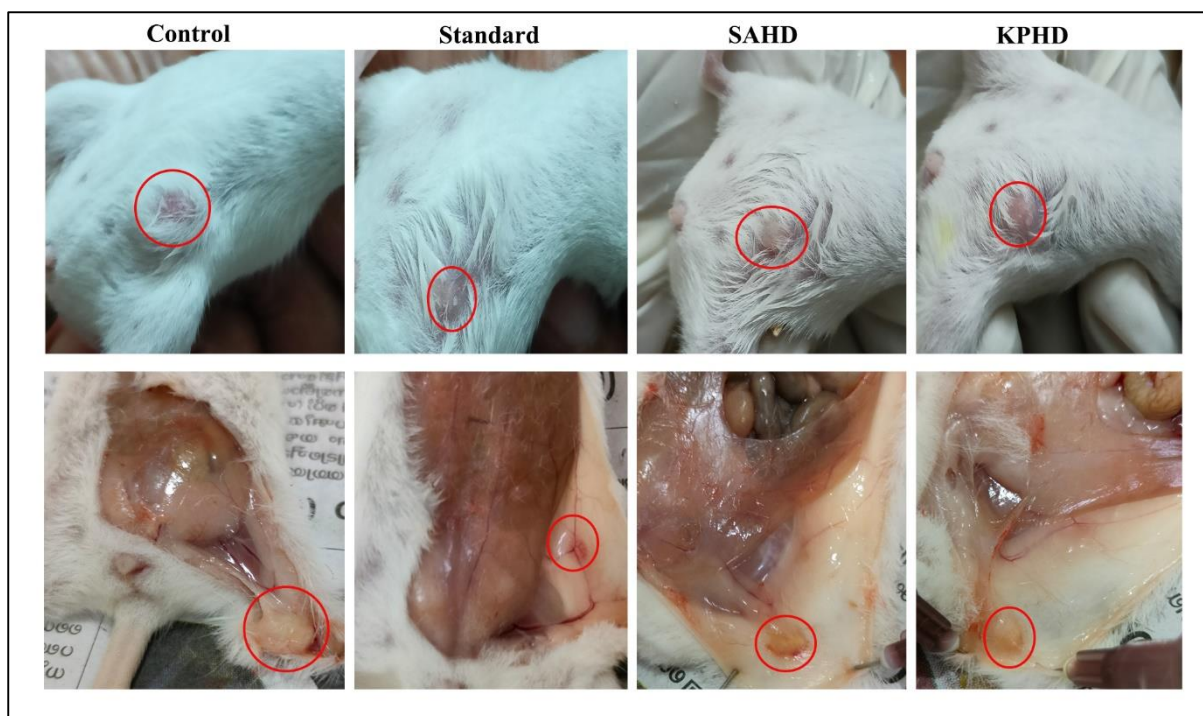
Figure 6.10. Representative tumours from different groups of 4T1 induced BALB/c mice 20 days after subcutaneous injection. Tumour size regression observed in extract-treated group compared to control group
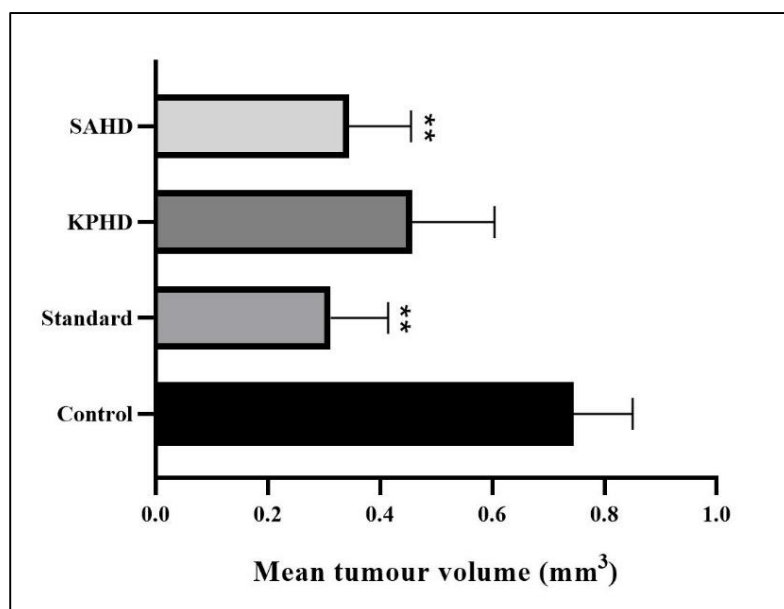
Figure 6.11. Comparison of tumour volume among different groups. Data is presented as mean ± SD. Statistical comparisons were performed using one-way ANOVA, followed by Tukey's multiple comparisons test. *P<0.05 and **P<0.01 probability values are deemed statistically significant

6.3.2.4. Histopathological analysis

Hematoxylin/eosin staining of mammary pad in control group shows carcinomatous growth composed of tumour cells having hyper chromatic nuclei whereas treated group shows better architecture with less tumour cell infiltration (Figure 6.12). Necrotic areas seen in control and vehicle control group were greatly reduced in extract treated groups. The histology of lung tissues of 4T1-injected control and vehicle control group shows extensive malignant infiltration of cells indicating metastatic spread. The lungs harvested from *S. asoca* and *K. pinnatum* extract treated group mice shows congested lung tissue with minimal tumour spread of 4T1 cells (Figure 6.13). The data were obtained from five fields per slide from 3 tumours examined from each group. The histology of liver didn't show any metastatic tumour colonies in control and extract treated groups (Figure 6.14).
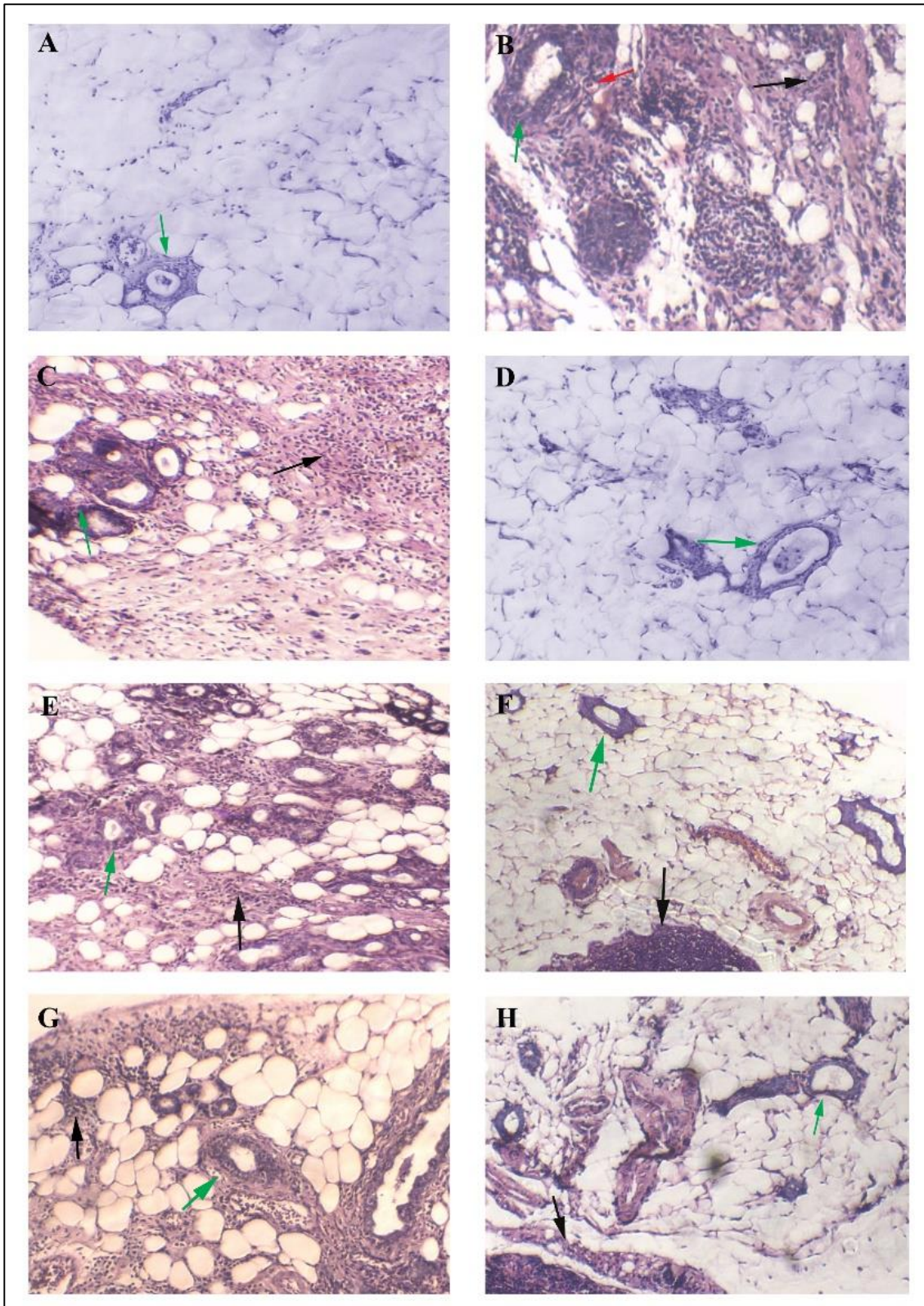
Figure 6.12. Hematoxylin and eosin staining of mice mammary pad of 4T1-induced tumours. A: normal, B: control, C: vehicle control, D: standard, E: SALD, F: SAHD, G: KPLD, H: KPHD, green arrow- mammary gland, red arrow- oval cells having hyperchromatic nuclei, black arrow- infiltration of malignant cells
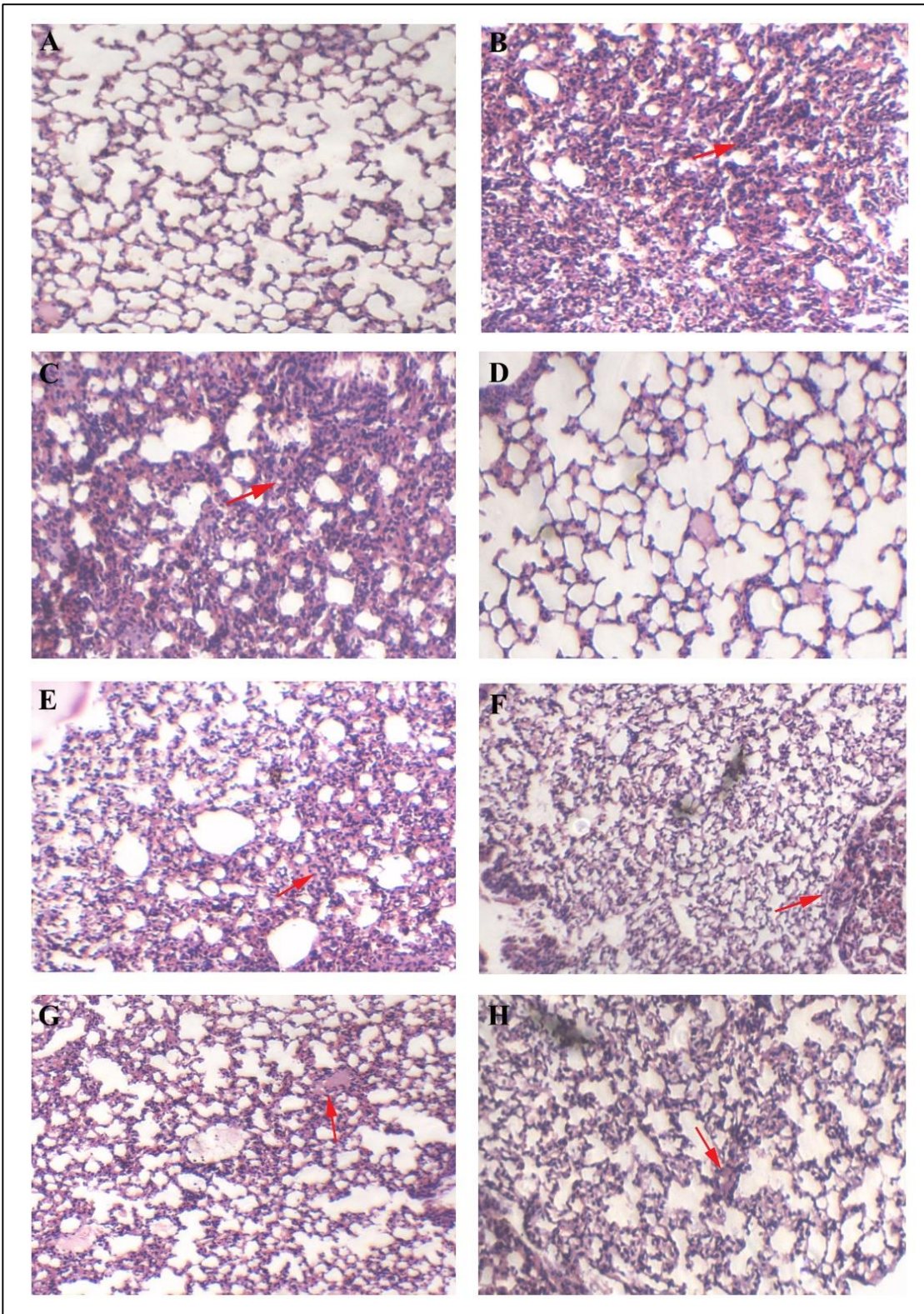
Figure 6.13. Hematoxylin and eosin staining of lung tissue in mice induced with 4T1 cells. A: normal, B: control, C: vehicle control, D: standard, E: SALD, F: SAHD, G: KPLD, H: KPHD. Red arrow indicates 4T1 cells infiltration
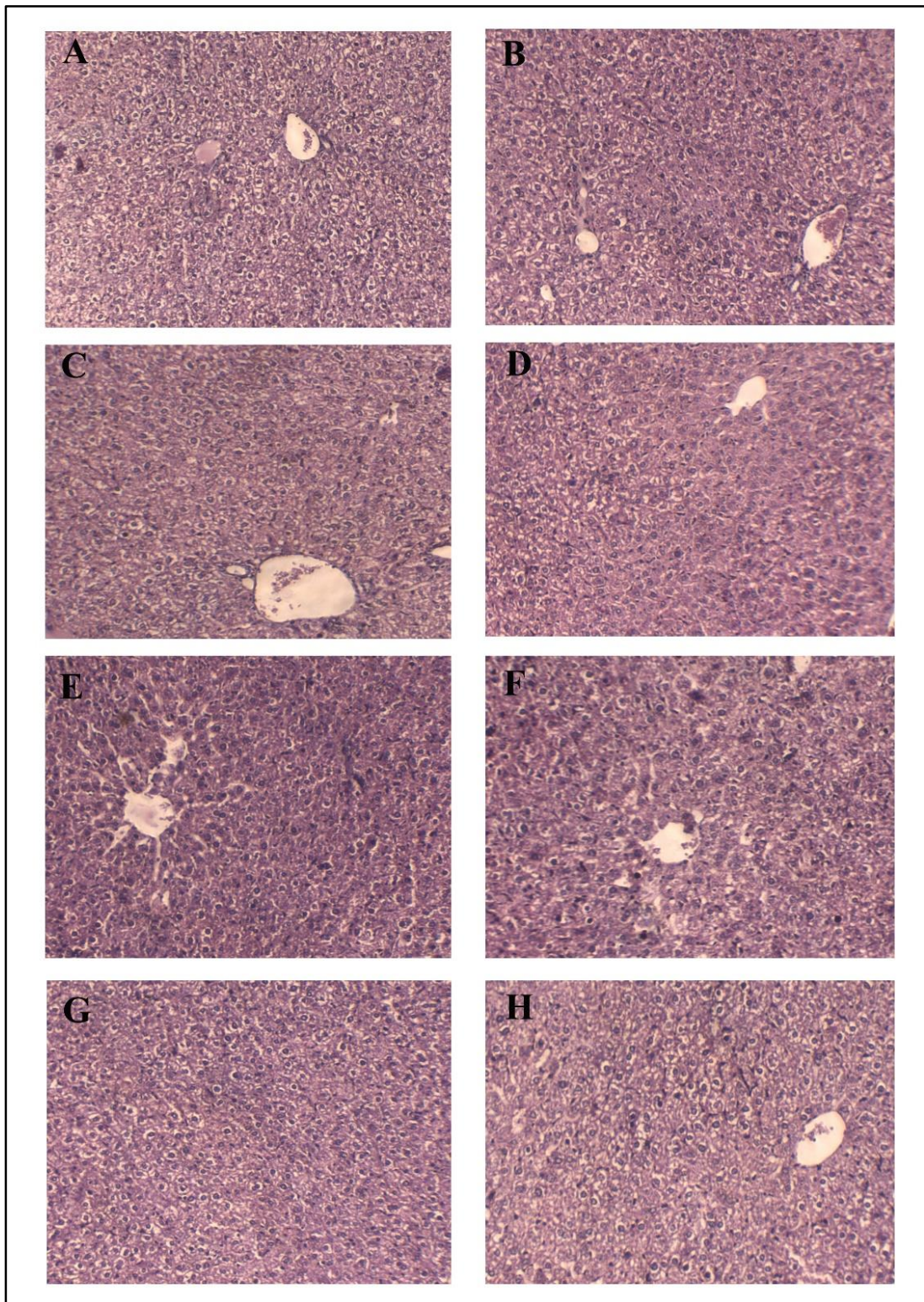
Figure 6.14. Hematoxylin and eosin staining of liver tissue in mice induced with 4T1 cells. A: normal, B: control, C: vehicle control, D: standard, E: SALD, F: SAHD, G: KPLD, H: KPHD

6.4. Discussion

The crude extracts of *S. asoca* and *K. pinnatum* have demonstrated notable antioxidant, anti-inflammatory and antiproliferative properties, as elucidated in previous chapters. These properties are linked to the presence of various phenolic compounds in the plants, believed to possess diverse biological characteristics, such as anti-inflammatory and anti-cancer effects (Xu *et al*., 2017). Recognizing the significant biological potential of these plant extracts, it became imperative to delve into their anticancer properties *in vivo*. The present study demonstrated an exploration of the anticancer potential, especially against breast cancer by *S. asoca* and *K. pinnatum* extracts and focused on two distinct models: firstly, the examination of their effects against chemically induced mammary carcinogenesis in Swiss albino mice, and secondly, the assessment of their impact on cell line induced Triple-negative breast cancer (TNBC) model in BALB/c mice. Through this analysis, we aimed to shed light on the promising anticancer properties of these plant extracts, potentially covering the way for novel therapeutic strategies in the battle against breast cancer.

DMBA (7,12-dimethylbenz[a]anthracene), belonging to the anthracene class of polycyclic aromatic hydrocarbons, is a potent carcinogen. Generally, it is considered safe to use and, because it closely mimics breast cancer in humans, it is often employed in animal experiments as an inducing agent for breast cancer (Zhao *et al*., 2011). Although the liver is the main organ where carcinogens are biologically deposited and activated, DMBA is deposited in extrahepatic tissues, such as the mammary glands. Through a series of events, the cytochrome p450 enzyme transforms this carcinogenic material to DMBA-3,4-diol-1,2-epoxide (DMBA-DE). And the resulting carcinogen interacts with DNA to produce adducts (Akhouri *et al*., 2020). In turn, this upsets and interrupts the tissue's redox balance, causing oxidative stress. Resulting reactive oxygen species can damage DNA or a protein cell cycle, causing unregulated cell division and growth (Hamza *et al*., 2022).

In the DMBA-induced mammary tumourigenesis model, no fatalities were observed among the animals in either the control or treatment groups over the entire six-week experimental period. Furthermore, no noticeable variations in the dietary habits or water

consumption were noticed between untreated and the extract treated groups. However, there were significant alterations in the body weight of the animals in the tumour-induced control and vehicle control groups when compared to the other experimental groups. The body weight of the normal and extract-treated groups increased progressively during the course of the study. DMBA causes the aryl hydrocarbon receptor (AHR) to downregulate and proto-oncogenes to transform into oncogenes, which produced cancer cells and slowed down cellular metabolism, impairing normal cellular proliferation (Ma *et al*., 2018). As a result, DMBA-induced breast cancer model animals had lower body weights. A similar conclusion was made in a study where the normal group animals weight was higher than that of the DMBA-treated group (Tran *et al*., 2018). Also the level of erythrocytes were reduced in DMBA induced animals. Erythrocytes play a significant part in the transport of O_2 and CO_2, maintaining blood viscosity and preserving the acid-base balance (Tran *et al*., 2018). Therefore the covalent bond formation of DMBA with DNA leads to disruption of DNA replication and repair mechanisms and destruction of DNA structure leading to hematopoietic stem cells in the bone marrow to perish which resulted in reduced erythrocyte numbers (Chen *et al*., 2017, Ghandehari and Fatemi, 2018). These results demonstrated that DMBA altered hematological indices in addition to reduced body weight of animals.

An important indicator of malignant disorders is the level of liver marker enzymes. There was a notable increase observed in the liver marker enzyme levels including ALP, AST, ALT, and LDH, in the serum of the DMBA group. However, the upsurge was significantly reduced in animals treated with plant extracts. In another study, liver marker enzymes were observed to be increased as a result of exposure to DMBA (Wang and Zhang, 2017). Moreover, reactive oxygen species damage a cell's membrane integrity when they react with polyunsaturated fatty acids (PUFA), which ultimately results in the formation of malondialdehyde (MDA) (Akhouri *et al*., 2020). MDA levels have long been recognised as a sign of antioxidant status and oxidative stress (Grawel *et al*., 2004). DMBA treated groups showed a significant decrease in MDA levels, which was restored in extract treated groups. This decrease in MDA levels suggests that lipid peroxidation (LPO) has been inhibited and that oxidative stress has been reduced. DMBA led to the depletion of endogenous antioxidants like SOD, CAT and GSH in breast tissues which

was resorted with administration of extracts. Other authors have also reported the DMBA induced change in MDA levels and endogenous antioxidants (Wang and Zhang, 2017, Hamza *et al.*, 2022). The histopathological analysis of mammary pad and liver further confirms the protective effect of *S. asoca* and *K. pinnatum* extracts which are evident from the differences in degree of severity of the tissue architecture between the extract treated group and DMBA treated group. Mammary glands of extract treated group revealed fewer invasive cancer cells, more organized adipose tissue and decreased cell proliferation. Chemopreventive activity of methanolic bark extract of *S. asoca* was previously reported by authors using benzene induced secondary AML model and DMBA induced two-stage skin carcinogenesis (Mukhopadhyay *et al.*, 2017, Cibin *et al.*, 2012).

Gene expression analysis sheds light on the networks and pathways that cancer disrupts. The mRNA expression of the genes ER-α1, BCL2, PIN 1 and c-MYC was enhanced in the control groups when compared to mammary glands of treated groups. A significant correlation has been found between the expression of these oncogenes and the risk of breast cancer. The transcription of estrogen-responsive genes is activated by estrogen binding to ERα and ERβ, which speeds up the proliferation of tumour cells (Korach *et al.*, 1996). Therefore, one of the main mechanisms to prevent mammary gland carcinogenesis may be the regulation of ERα and ERβ (Leygue *et al.*, 1998). BCL2 has anti-apoptotic functions, in addition to oncogenic properties. In the absence of normal expression of BCL2, the balance between cell proliferation and cell death is shifted toward growth (Akl *et al.*, 2014). The c-MYC oncogene has been hypothesised to play a role in transcriptional activation of growth-related genes. There is an association between c-MYC deregulation and breast cancer development and progression (Xu *et al.*, 2010). Also PIN1 expression has been found to be increased in human mammary tumours. PIN1 ability to maintain or enable oncoproteins and destabilise or inactivate tumour suppressors accounts for its oncogenic activity (Liou *et al.*, 2011, Lu and Hunter, 2014). The DMBA upregulated the expression of these oncogenes which was reduced by the plant extracts of SA and KP, expect for PIN1 mRNA expression.

Triple-negative breast cancer (TNBC) has few therapeutic choices available for the treatment such as chemotherapy due to the absence of target receptors. The 4T1 induced TNBC mouse model is an excellent approach since it closely mimics stage IV human

breast cancer (McCarthy *et al*., 2014). In the present study, *in vitro* cytotoxic analysis shows considerable cytotoxic action exerted by both the plants on murine TNBC 4T1 cells in a dose dependent manner. In the animal study the plant extracts did not manifest any toxicity to animals evident from the body weight at the end of the experiment. The control groups develop palpable tumours within 10 days of receiving the 4T1 orthotopic injection. The tumours developed in the extract treated group were significantly smaller than those in the control groups. The size of tumours in the 4T1-challenged mice shown to have decreased 2.4 times in the doxorubicin-treated group, 2.1 times in the SAHD group, and 1.6 times in the KPHD group of animals respectively. Also the WBC levels in control animals were found to have risen above normal levels, whereas the levels in the extract-treated groups considerably decreased compared to control group. A rise in WBC count has also been reported by other authors in 4T1 challenged TNBC studies (Fakhroueian *et al*., 2022, Xiang *et al*., 2015). The histology of the mammary tumours exhibits better architecture with less tumour cell infiltration and fewer necrotic regions in the animals administered with extracts, as compared to the animals in the control group. The primary tumour in the mammary gland of this extremely tumourigenic and intrusive cancer can rapidly spread to a number of distant locations in the body including the lung and liver (Nigjeh *et al*., 2019). The histopathology of the extract treated (500 mg/kg b.wt) mice lungs showed that oral treatment for 30 days either decreased the proliferation of 4T1 cells or prevented their metastasis to the lungs to a great extent in contrast with the control groups of animals. There was no evidence of metastatic spread to liver of control groups and mice treated with the extracts. The protective action of extracts may be due to the phenolic compounds present which was discussed in Chapter 3. Other authors have described the effectiveness of certain phenolic and non-phenolic compounds found in plants against 4T1-induced tumours (Bove *et al*., 2002, Nigjeh *et al*., 2019, Abd Razak *et al*., 2020).

The findings outlined in this chapter support the hypothesis that the crude methanolic extracts from *S. asoca* and *K. pinnatum* exhibit considerable protective effects against breast cancer particularly, triple-negative breast cancer (TNBC). These effects are primarily achieved through the inhibition of cell proliferation and the prevention of metastatic spread. The compounds identified in both plant extracts, such as *β*-sitosterol, quercetin, kaempferol, catechin, and others, as determined in Chapter 3 using LC-MS analysis, possess notable antioxidant and anti-inflammatory properties. It is reasonable to

infer that these compounds serves an essential part in the observed anticancer activities of the plants. To sum up, the results of this study provide promising evidence that both plants hold potential in the fight against breast cancer, particularly TNBC. The protective effects, combined with the antioxidant and anti-inflammatory capabilities of the identified compounds, offer hope for the development of novel therapies or preventive strategies for individuals at risk of or diagnosed with triple-negative breast cancer. Further research and clinical studies are warranted to explore the plants full therapeutic potential in breast cancer management.

Chapter 7
Elucidation of possible mechanism of action of *S. asoca* and *K. pinnatum* extracts on TNBC cells by cell death pattern analysis

7.1. Introduction

The prevalence of breast cancer in women is high, ranking as the second leading reason for mortality among women globally. Although surgery, radiation, and chemotherapy are the most commonly used forms of treatment for breast cancer, they have generally been found to be less effective. Concerning factors include the harmful side effects and several health problems brought on by the cytotoxic nature of the chemotherapy medications (Khan *et al*., 2022). These medications are exceedingly expensive, and in many cases the tumour builds resistance to a specific medication, necessitating the use of a pharmaceutical combination instead. Tamoxifen, which is used to treat hormone-dependent breast tumours at all stages, has a number of adverse effects, including renal and liver damage (Khan *et al*., 2022). Hormone-independent breast cancer, such as triple negative breast cancer is one of the hardest forms of breast cancer to treat since there are no effective treatment strategies available. Thus, it is crucial to develop innovative therapeutic drugs that specifically target key checkpoints to effectively battle breast cancer. There is little question that new, effective anti-cancer medications with fewer side effects are desperately needed, and compounds originating from plants are a promising source. It is estimated that over 60% of anti-cancer medications are obtained directly or indirectly from plants owing to the significance of battling cancer and the range of possible compounds that plants can provide (Graziose *et al*., 2010, Fridlender *et al*., 2015). These compounds fall under various chemical categories, including alkaloids, flavonoids, phenolic acids and terpenoids (Khan *et al*., 2022). Asoka and *K. pinnatum* are reported to have phytoestrogens such as *β*-sitosterol, kaempferol, quercetin identified through LCMS analysis (discussed in Chapter 3).

The bi-faceted function of phytoestrogen and the entire class of flavonoids is linked to the structural similarity to human estrogens. One of the targets in treatment for breast cancer is the estrogen receptor. Medicinal plant flavonoids are regarded as phytoestrogens due to their ability to bind the estrogen receptor and mimic the effects of estrogen (Levitsky and Dembitsky, 2015). The analysis of epidemiological data and *in vitro* research on ER*α* and ER*β* expressing breast cell lines allowed for the hypothesis that phytoestrogens may have opposite effects according to their amounts in blood and experimental dosages (Rice and Whitehead, 2006). Some phytoestrogens promote the proliferation of ER*α* expressing breast cell lines while others inhibit the growth of breast cell lines that express ER*β*. After binding with ER*α*, phytoestrogens activate metabolic

pathways that contribute to enhancing cell proliferation, particularly the progression of the cell cycle by regulating activities in both the S and G2/M phases of the cell cycle (JavanMoghadam *et al*., 2016). The binding of phytoestrogens to ERβ is reported to be associated with decreased cell proliferation, reduced metastatic potential, and enhanced late apoptosis, indicating ERβ mediated inhibition of the PI3K/AKT pathway through PTEN (Anestis *et al*., 2018). Moreover, since the plant extracts exhibited preferential cytotoxicity towards ERβ expressing breast cancer cells and not to ERα expressing cells, it raises a notion of phytoestrogens in the plants being agonistic to ERβ. The molecular docking between specific compounds identified (β-sitosterol, kaempferol, quercetin) in *S. asoca* and *K. pinnatum* extracts with the targeted estrogen receptors, ERα and ERβ revealed strong binding of the phytoestrogens particularly towards ERβ (discussed in chapter 3).

Research has demonstrated that specific phytoestrogens like genistein, resveratrol and quercetin exhibit apoptotic effects in diverse cancer cell lines (Singh *et al*., 2017, Hsiao *et al*., 2019, Nguyen *et al*., 2017). These compounds can trigger apoptosis by modulating crucial apoptotic proteins such as caspases, p53 and those belonging to the BCL2 family, thereby facilitating the removal of cancerous cells (Seo *et al*., 2011). The absence of apoptosis is one of the causes of malignancies, autoimmune illnesses, and many other diseases, making the study of apoptosis a significant area of biological research. In order to combat cancer effectively and limit concurrent death of normal cells, the majority of cancer research is devoted to the development of new drugs that induce apoptosis in cancer cells (Gerl and Vaux, 2005). Also, a quick and simple assay for apoptosis measurement would be very beneficial for many biological researchers (Ribble *et al*., 2005). Different morphological staining techniques, such as those using ethidium bromide and acridine orange (Coligan *et al*., 1998), caspase-3 activation (Goyal *et al*., 2021) and cell cycle analysis are presently employed for detecting apoptosis *in vitro*. Although current methods can identify a variety of characteristics of apoptotic cells, chromatin condensation and nuclear fragmentation continue to be the distinguishing features of apoptotic cells (Stewart, 1994). In general, it has been advised that morphological analysis should always be combined with at least one other assay in the classification of cell death in a given model (Renvoize *et al*., 1998). Therefore the present study has combined morphological staining techniques like crystal violet staining and ethidium bromide and acridine orange (EB/AO) staining along with caspase-3 activation

assay and cell cycle analysis by flow cytometry, to study the apoptotic effect of *S. asoca* and *K. pinnatum* extracts on MDA-MB-231 breast cancer cells.

7.2. Materials and methods

7.2.1. Preparation of extract

The crude methanol bark extracts of *S. asoca* and *K. pinnatum* were prepared using the procedure described in Chapter 2's section 2.2.1.

7.2.2. Chemicals

The chemicals utilised in the experiment like acridine orange, crystal violet, ethidium bromide, ethylenediaminetetraacetic acid (EDTA), propidium iodide, NaCl, Tris, Triton X-100 were purchased according to the list in section 2.1.2 of Chapter 2. The other compounds and solvents utilized were all of analytical standard.

7.2.3. Cell lines

MDA-MB-231 SCAT3 NLS cells was procured from the laboratory of Dr. T.R Santhosh Kumar, Rajiv Gandhi Centre for Biotechnology, Trivandrum, Kerala. MDA-MB-231 cell line was purchased from National Centre for Cell Science, Pune, India. The cell lines were cultured as described in section 2.2.16.3 of Chapter 2.

7.2.4. Crystal violet staining

The 24 well culture plate was seeded with MDA-MB-231 cells and treated with various concentrations of *S. asoca* and *K. pinnatum* crude methanolic extracts for 48 hr at 37 °C. In the subsequent process 0.5% crystal violet was used to stain the cells. The detailed procedure of the staining method is given in section 2.2.18.1 of Chapter 2.

7.2.5. Acridine orange-ethidium bromide (AO-EB) staining

MDA-MB-231 cells were plated onto sterile coverslips for 24 hr followed by treatment with *S. asoca* and *K. pinnatum* crude methanolic extracts for another 24 hr. After the treatment period the cells were stained with ethidium bromide and acridine orange stain. The specifics of the method are provided in Chapter 2's section 2.2.19.1.

7.2.6. Apoptotic study using Caspase-3 activation analysis

MDA-MB-231 SCAT3 NLS cells expressing stable CFP-YFP FRET-based probes were used to investigate the cytotoxicity of various concentrations (50-200 μg/mL) of crude

methanolic extracts of *S. asoca* and *K. pinnatum* via Caspase-3 activation. After the treatment with extracts at varying concentrations the cells were imaged. The details of the methodology are described in section 2.2.19.2. of Chapter 2.

7.2.7. Analysis of the cell cycle using flow cytometry

The single suspension of MDA-MB-231 cells has been dyed with propidium iodide dye after the subsequent treatment with the *S. asoca* and *K. pinnatum* crude methanolic extracts for 24 hr. The cells were analyzed by flow cytometry and plot diagrams were generated. The complete procedure is outlined in the section 2.2.19.3. of Chapter 2.

7.3. Results

7.3.1. Crystal violet staining

The crude methanol extract of *S. asoca* and *K. pinnatum* caused cytotoxicity and altered the morphology of MDA-MB-231 cells following 48 hours of treatment. The amount of crystal violet staining decreased as a result of cell death because the cells lost their adhesion and were eliminated from the cell population. At a magnification of 40X, it was possible to clearly identify the morphological differences between treated and control cells. The preparation shows cells with nuclear condensation, nuclear fragmentation and the presence of vacuoles. The figure 7.1 and 7.2 show treated cells and control cells at various doses of *S. asoca* and *K. pinnatum* extracts at various magnifications.
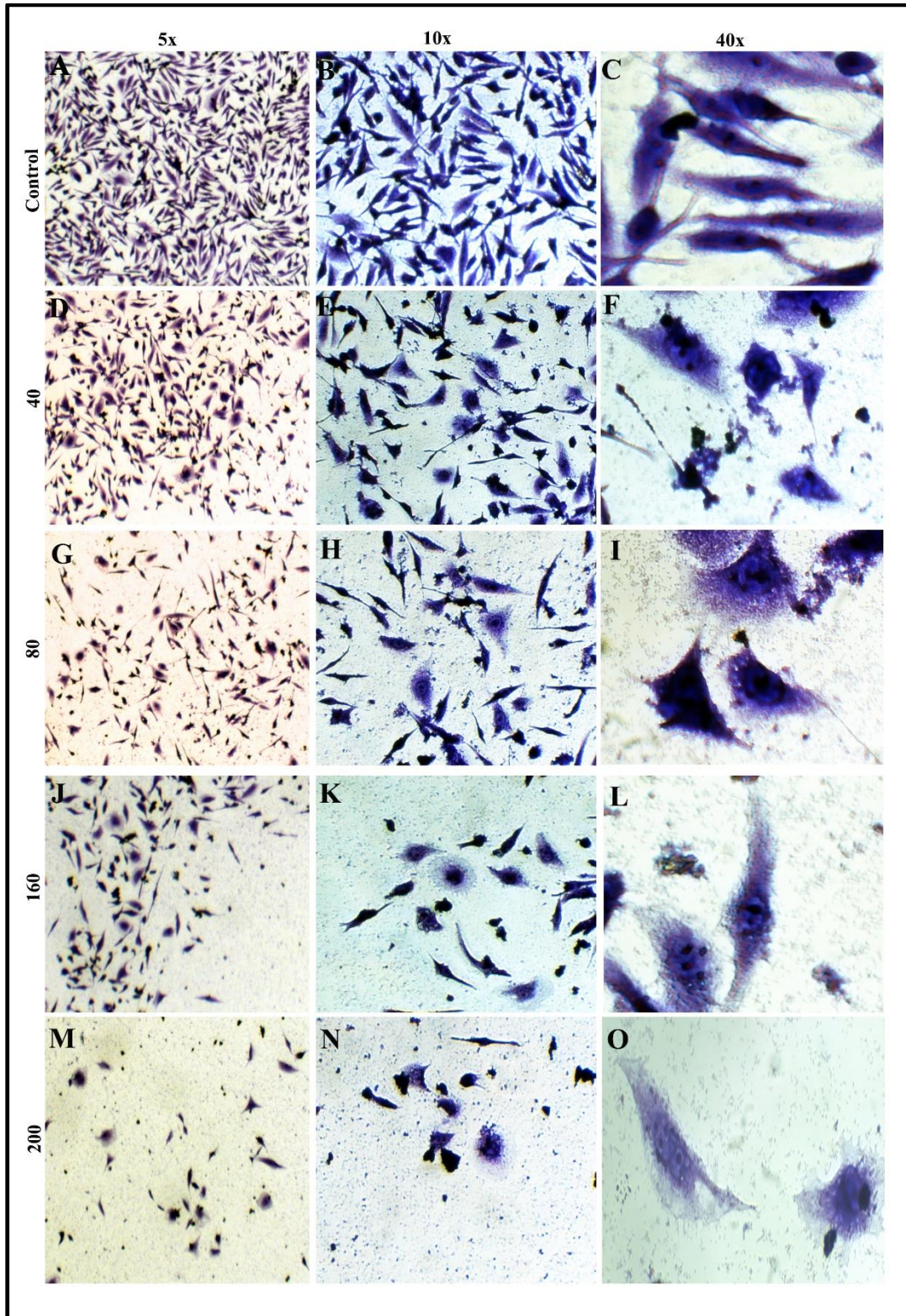
Figure 7.1. Morphology of MDA-MB-231 cells treated with *S. asoca* extract under different magnifications after crystal violet staining. Preparation shows distorted cells with nuclear condensation, (I) nuclear fragmentation (L)
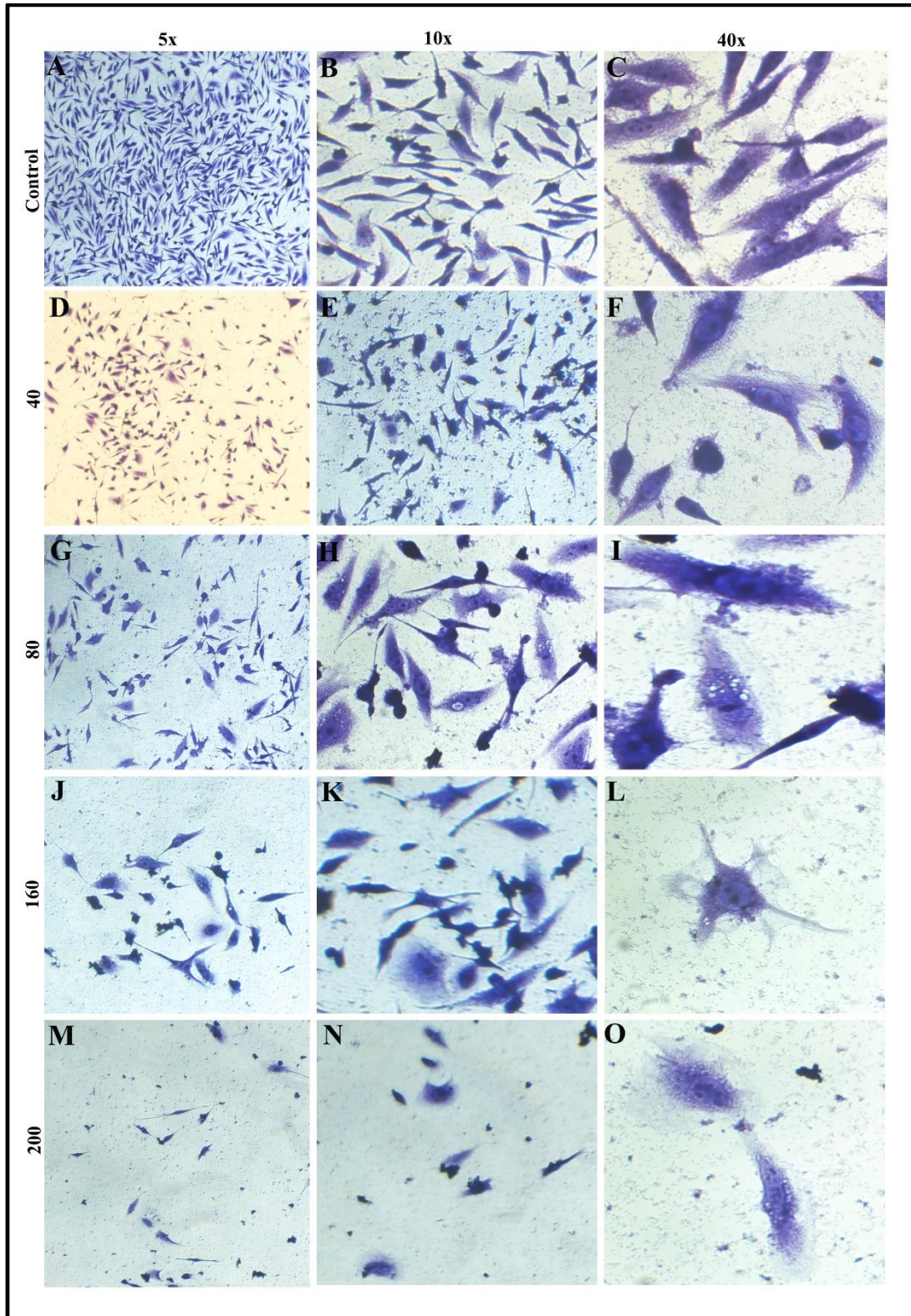
Figure 7.2. Morphology of MDA-MB-231 cells treated with *K. pinnatum* extract under different magnifications after crystal violet staining. Preparation shows distorted cells with nuclear fragmentation and presence of vacuoles (I, L)

7.3.2. Acridine orange-ethidium bromide (AO-EB) dual staining

The MDA-MB-231 cells were subjected to treatment with varying concentrations of *S. asoca* and *K. pinnatum* extracts for 24 hr before being stained with acridine orange-ethidium bromide to determine the underlying cause of the rise in cell death. The viable control cells with equally distributed AO stains appeared green under a fluorescent microscope, had normal nuclear morphology, and did not show red fluorescence. Dead cells' nuclei were stained red with ethidium bromide. MDA-MB-231 cells that were in the early apoptotic stage were stained greenish-yellow, whereas those that were in the late stage were stained orange. The necrotic cells had an indistinct shape and unsteady orange-red fluorescence. Therefore, the outcome of the study demonstrated that higher extract concentrations caused an increase in orange and red staining, and a decrease in green staining, indicating the destruction or apoptosis of cells. Membrane blebbing and cytoplasmic vacuolation were observed in extract treated cells. The figure 7.3 and 7.4 show cell in different stages of apoptosis when treated with *S. asoca* and *K. pinnatum* extracts, respectively.
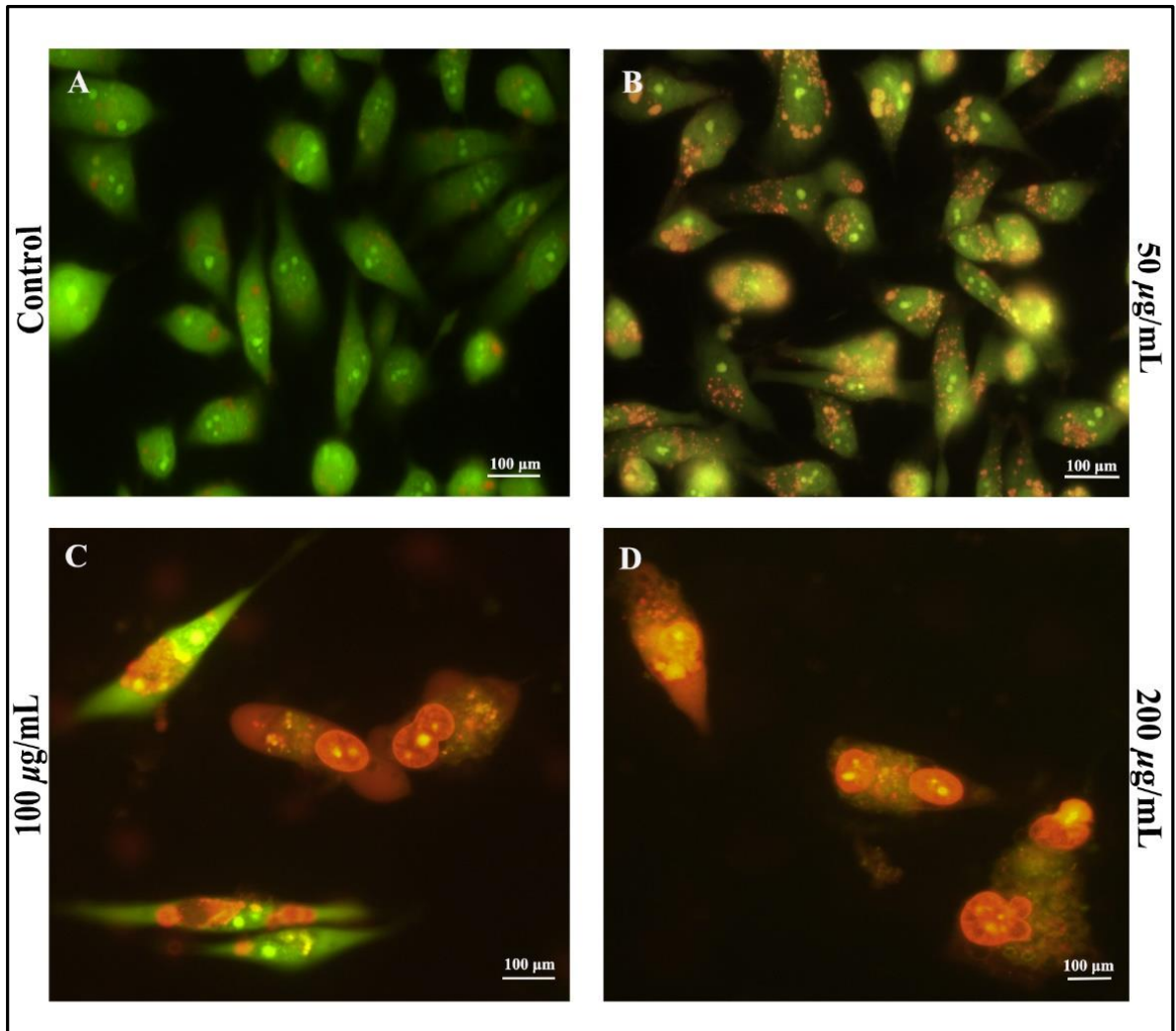
Figure 7.3. Fluorescent microphotograph of *S. asoca* treated MDA-MB-231 cells as assessed by dual AO/EB staining
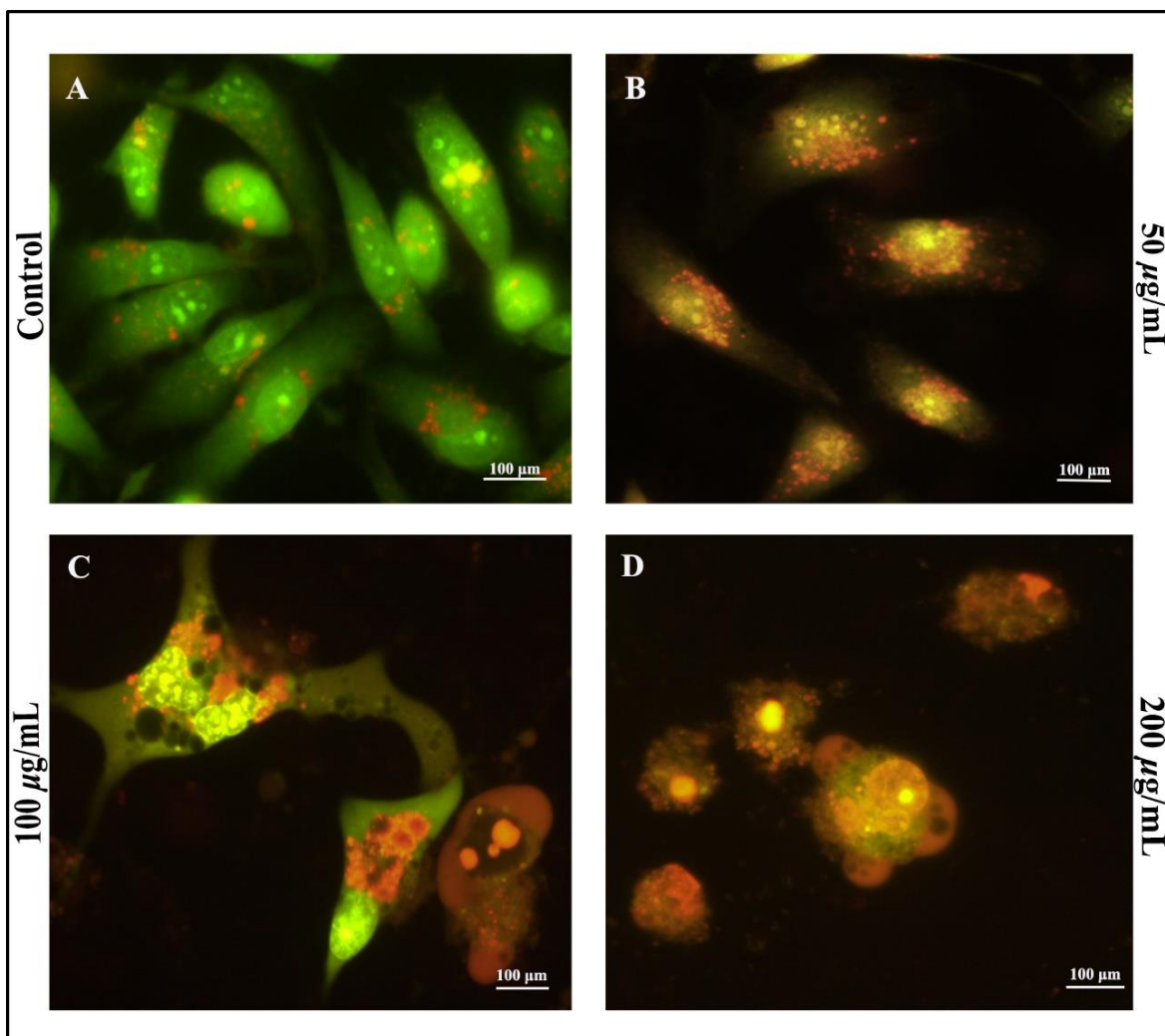
Figure 7.4. Fluorescent microphotograph of *K. pinnatum* treated MDA-MB-231 cells as assessed by dual AO/EB staining

8.3.5. Apoptotic study using Caspase-3 activation analysis

The MDA-MB-231 cells used in this experiment had a stable expression of the FRET-based CFP-YFP probe. The linker peptide sequence in this probe connects two fluorescent proteins- cyan fluorescent protein (CFP) and yellow fluorescent protein (YFP), by a Caspase-3 cleavage site (DEVD). In the study, MDA-MB-231 cells treated with plant extract at a dose of 200 μg/mL had higher CFP/YFP percentages than the control cells, and cleavage of CFP-DEVD-YFP suggests lower FRET. On the ratio scale, the shade changed from blue to green-yellow when the CFP/YFP ratio was altered (Figure 7.5 and 7.6). The data point to a decrease in FRET, and it is deduced that the caspase-3 pathway has been activated.
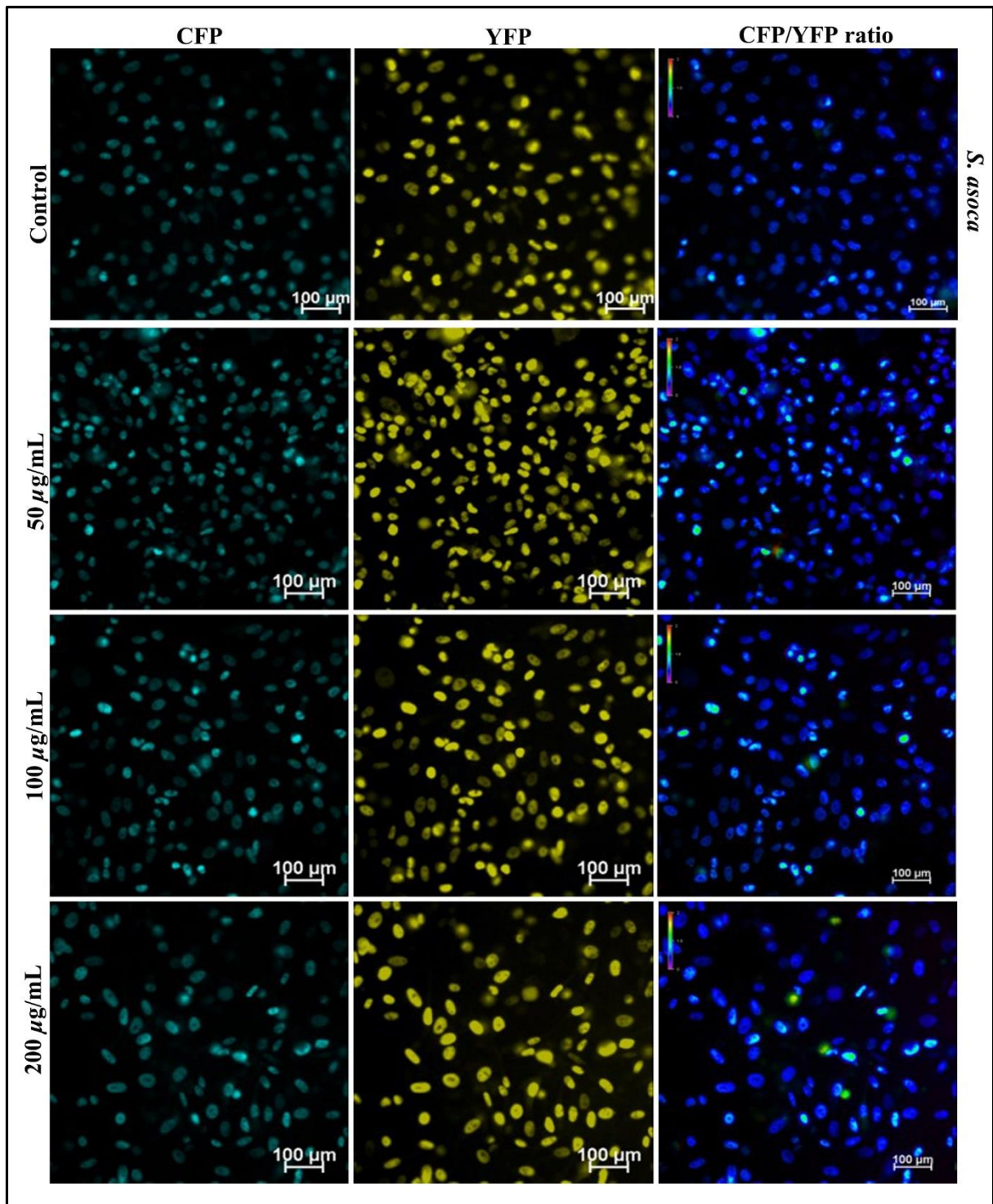
Figure 7.5. Representative pictures of control and various concentrations of *S. asoca* extract-treated MDA-MB-231 cells illustrating the blue-to-green-yellow shift in the CFP/YFP ratio
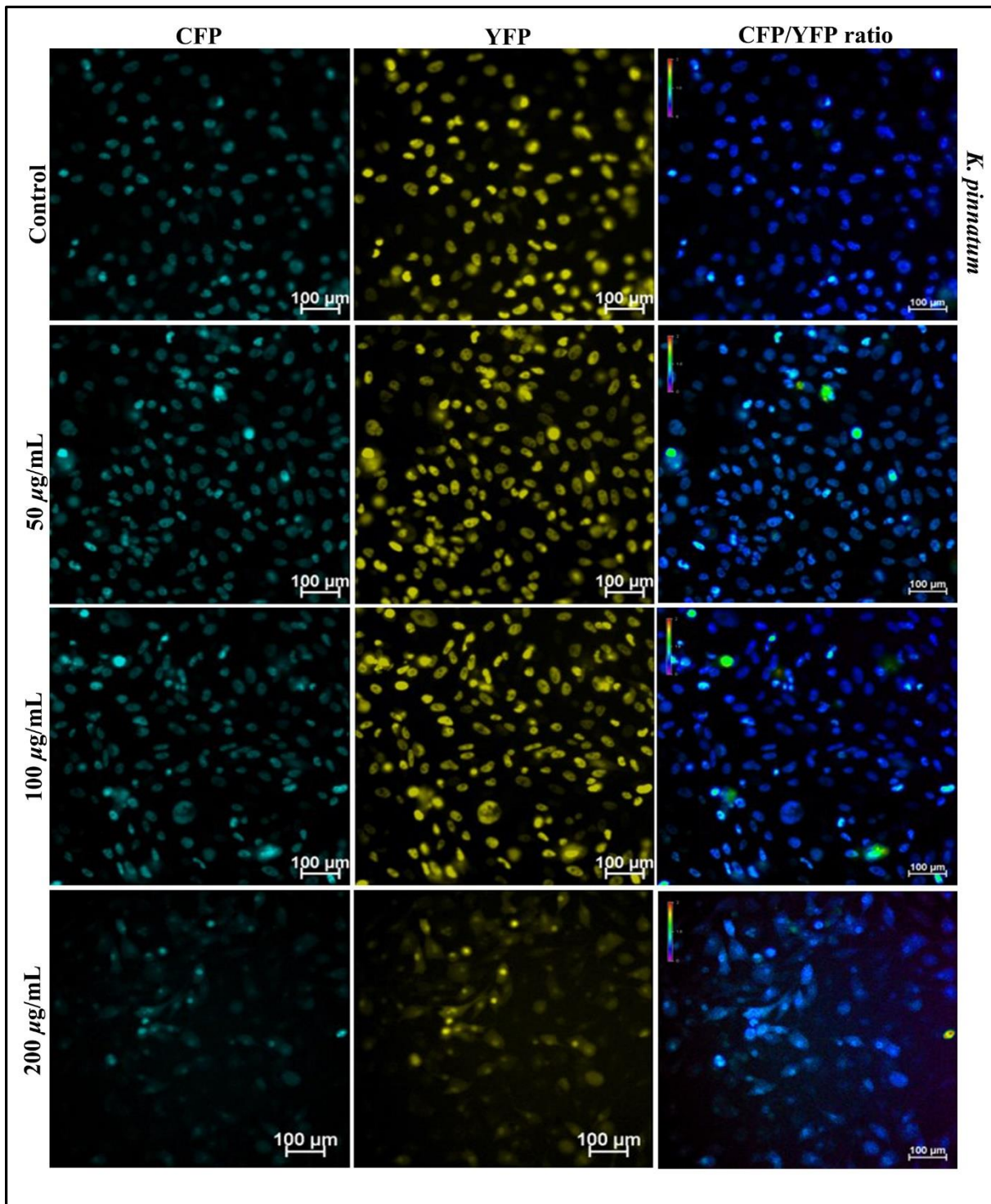
Figure 7.6. Representative pictures of control and various concentrations of *K. pinnatum* extract-treated MDA-MB-231 cells illustrating the blue-to-green-yellow shift in the CFP/YFP ratio

7.3.6. Cell cycle analysis using flow cytometry

Flow cytometry was employed to analyse the cell cycle of MDA-MB-231 cells treated with *S. asoca* and *K. pinnatum.* The MDA-MB-231 cell count in the sub-G0/G1 phase that represent apoptotic cells increased to 57.2% when *S. asoca* extract was added to the cells as opposed to the untreated cell population in sub-G0/G1 phase. The *K. pinnatum* extract (100 μg/mL) treated cells exhibited an 8.5% increase in the cell count in the sub-G0/G1 phase, when compared to the cells untreated. Therefore, both plant extracts increased the cell count in the sub-G0/G1 phase, suggesting the activation of apoptosis by the extracts. Figures 7.7 and 7.8 depict the proportion of cells in each phase of the cell cycle following treatment with *S. asoca* and *K. pinnatum* extracts.
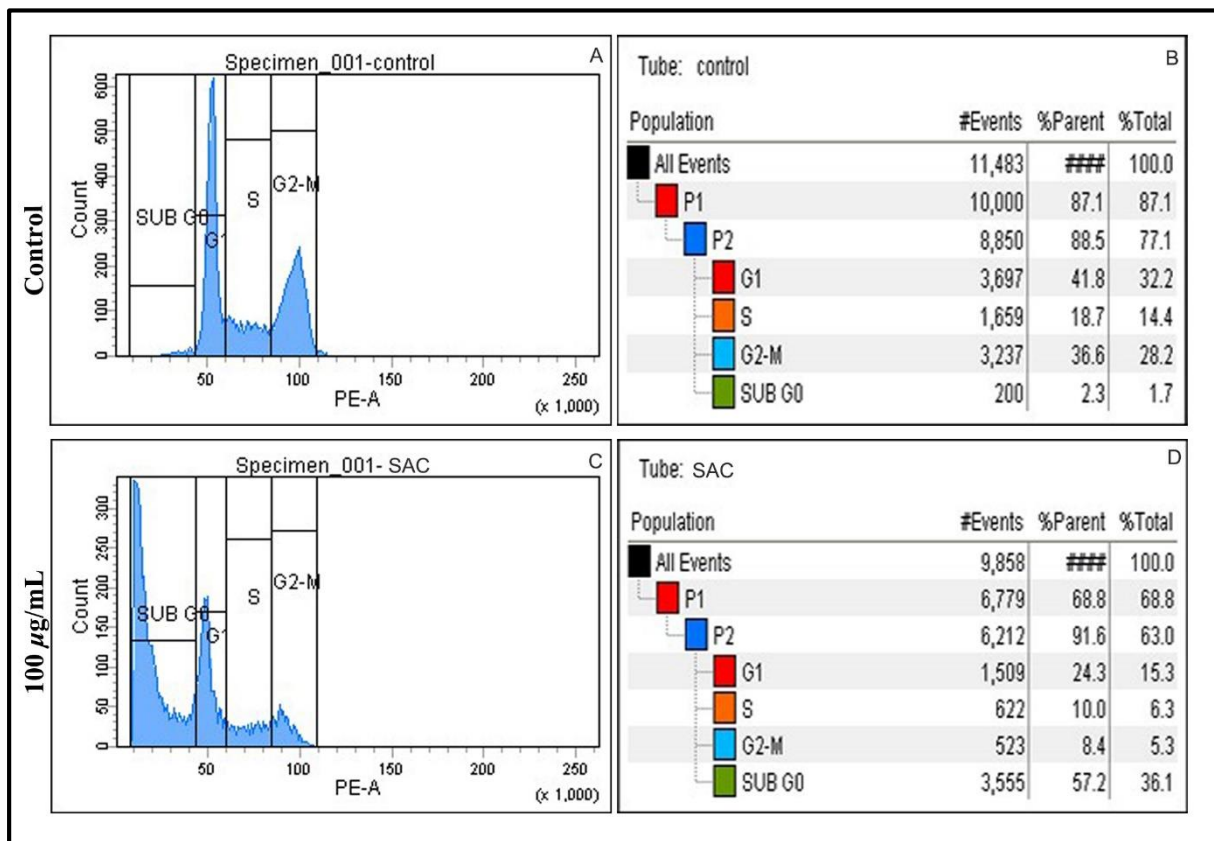
Figure 7.7. Flow cytometry plot diagrams (A, C) and cell population in each phase of cell cycle (B, D) of *S. asoca* extract treated MDA-MB-231 cells
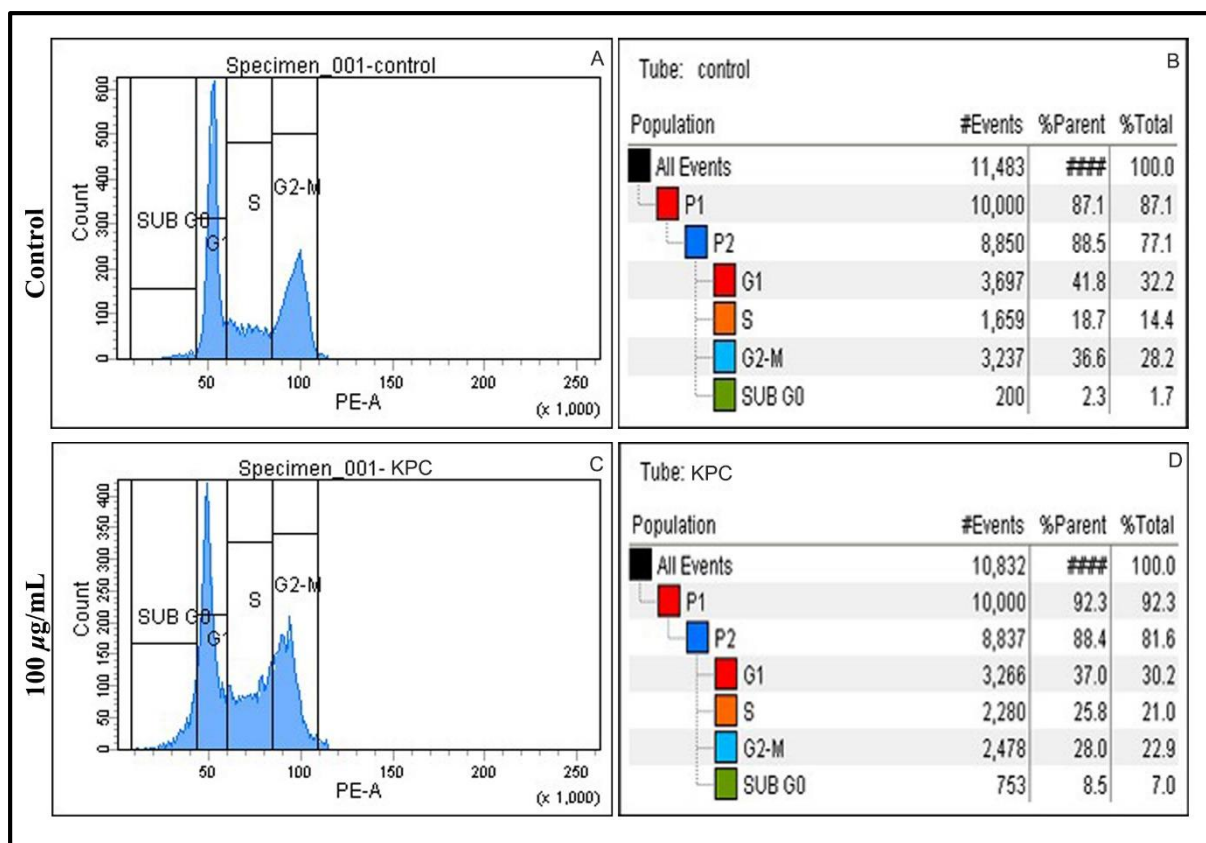
Figure 7.8. Flow cytometry plot diagrams (A, C) and cell population in each phase of cell cycle (B, D) of *K. pinnatum* extract treated MDA-MB-231 cells

7.4. Discussion

In this study, the possible mechanism of action of *S. asoca* and *K. pinnatum* extracts on TNBC cells was analysed *in vitro* by assessing cell death patterns and the results indicates apoptotic mediated cell death. Apoptosis is an intricate process involving pathways that trigger a chain of events leading to the breakdown of the nuclear membrane and chromatin. Cancer develops when this physiological mechanism starts to be dysregulated, resulting in many pathological alterations (Koff *et al*., 2015). Apoptosis dysregulation can result in unregulated cell division, altered cellular differentiation, and cell death signal evasion, all of which are factors in the initiation and spread of cancer (Jan and Chaudhry, 2019). Comprehending the intricate nature of dysregulated apoptosis is essential in order to discover new therapeutic targets and create efficient cancer treatments. Therefore, finding a mechanism to trigger this process in cancer cells may

help to prevent the spread and growth of the disease. The findings of the current study indicated that the *S. asoca* and *K. pinnatum* extracts exerted their anticancer effects on triple negative breast cancer cells by causing DNA damage and inducing apoptosis.

Phytoestrogens, naturally occurring compounds with structural resemblance to natural estrogen, are found in *S. asoca* and *K. pinnatum.* They possess the ability to engage in interactions with the estrogen receptor beta (ERβ) and alpha (ERα), the primary receptors for estrogen in the body. Upon binding to ERα and ERβ, phytoestrogens can induce a spectrum of effects, ranging from agonistic to antagonistic, which are influenced by factors like the specific phytoestrogen type, concentration and the type of tissue (Anandhi Senthilkumar *et al*., 2018). Recent studies have reported the presence of ERβ in triple-negative breast cancers, which are generally classified as lacking receptors (Wisinski *et al*., 2016). The results of our study shown considerable antiproliferative effect on ERβ expressing breast cancer such as TNBCs whereas no cytotoxicity was exerted on ERα expressing breast cancer cells (discussed in chapter 3). Given the documented reports of estrogen binding to ERα promoting cell proliferation (Paterni *et al*., 2014), and to ERβ triggering anti-proliferative effects (Zhou and Liu, 2020), the selective cytotoxicity of extracts towards ERβ-expressing cells, rather than ERα-expressing cells, suggests a potential agonistic role of phytoestrogens on ERβ. This implies that the observed cytotoxicity may be mediated through ERβ. Therefore in this study the mechanism of action of the extracts of *S. asoca* and *K. pinnatum* plant extracts was investigated through *in vitro* morphological and biochemical assays.

Staining of cells with crystal violet offers greater sensitivity in staining proteins and DNA compared to other dyes, making it a suitable method for visualizing cell morphology due to its capacity to effectively stain all macromolecules (Krause and Goldring, 2019, Yang *et al*., 2001). For its ease of use, pace and precision, fluorescence light microscopy with variable absorption of fluorescent DNA-binding dyes like EB/AO staining is a preferred technique for morphological analysis of cells (Renvoize *et al*., 1998). While ethidium bromide only penetrates cells when the integrity of the cytoplasmic membrane is compromised and colours the nucleus red, acridine orange penetrates all cells and turns the nuclei green (Ribble *et al*., 2005). The results of morphological studies using both staining methods indicated structural changes in the cells. In crystal violet staining, as a consequence of nuclear condensation, cell shrinkage, and other abnormalities, which are

features of apoptotic cells, the cells have changed the shape from spindle-like to round, as well as lose their attachment to the surface. In EB/AO staining the nucleus of living cells appeared green; that of early apoptotic cells were greenish-yellow with condensed or damaged chromatin; that of late apoptotic cells were orange with perforated cells and scattered chromatin; and that of cells that died directly from necrosis appeared orange-red. The event of apoptosis was further confirmed by additional methods that can detect an increase in apoptotic signals like FRET based caspase-3 activation assay followed by flow cytometry analysis.

Caspases are essential parts of the apoptosis-inducing machinery and are a varied member of the cysteine protease family (Asong *et al*., 2022). Vital structural proteins, cell cycle proteins, and DNase proteins will be broken down by executional caspases like caspase 3 once they are activated, causing blebbing and condensing of cells that eventually results in cell death (Thomsen *et al*., 2013). As a result, we assessed the mode of cell death through assessing the activation of caspase 3, and the results demonstrate that treatment of MDA-MB-231 cells with both plant extracts activates caspase 3 as determined through a FRET- based bio sensor. Cell cycle refers to multiple stages of cell division that involve numerous biological changes, including the amount of DNA. According to cell cycle analysis, the population of cells is indicative of a healthy or damaged cell cycle based on the variation in DNA content inside the cells (Asong *et al*., 2022). A large cell population may be quickly examined using flow cytometry, and analysis of the light scatter signals from the cells offers an additional way for identifying apoptotic cells based on their physical characteristics (Plesca *et al*., 2008). Consequently, we treated MDA-MB-231 cells with both plant extracts and conducted the cell cycle analysis to determine the proportion of cells in each phase. The results revealed that both extracts cause an arrest in the cell cycle at the G0/G1 phase, which is evident from the MDA-MB-231 cell population in the sub-G0/G1 phase representing apoptotic cells. Therefore from the morphological and biochemical assays we determined that the cytotoxicity exerted by *S. asoca* and *K. pinnatum* crude methanolic extracts is through apoptotic mechanism.

Natural compounds generated from plants and plant extracts are attractive prospects for utilization as anticancer therapies. *Saraca asoca* is a legendary plant used in Ayurveda contains phytoestrogens which can bind to estrogens receptors like human estrogen and can trigger a cascade of reactions. And *Kingiodendron pinnatum* which is used as a substitute also contains phytoestrogens. Our investigation reveals that the strong binding

affinity of phytoestrogens in plants towards the ERβ receptor is likely to have played a substantial part in the antiproliferative effects of both plant extracts on TNBC cells by inducing apoptosis. ERβ mediated activation of caspase 3 by phytoestrogens such as genistein and apigenin is also reported (Mak *et al*., 2006). In conclusion, the *Saraca asoca* and *Kingiodendron pinnatum* plant extracts may have exerted cytotoxicity towards triple negative breast cancers by triggering the ERβ mediated activation of apoptosis.

Summary and conclusion

Plants have a long and varied history of application to treat a diversity of health conditions with roots spanning centuries and embracing a range of traditional medical systems across multiple cultures. Traditional healing systems such as Ayurveda, indigenous healing practices have utilized a wide range of plants based on their perceived therapeutic properties (Jaiswal and Williams, 2017). The utilization of plants for medicinal purposes, encompassing the management of cancer, is based on the acknowledgment of different chemical compounds found in plants, which exhibit therapeutic properties. Bioactive substances present in plants such as alkaloids, flavonoids, terpenoids, and polyphenols have demonstrated antioxidant, cytotoxic, anti-inflammatory and many other properties (Vidal-Casanella *et al.*, 2021). Progress in scientific research has resulted in the isolation and identification of distinct plant compounds with anti-cancer potential. Certain of these compounds have become foundational in the development of chemotherapy drugs, illustrating the link between the use of plants in traditional medicine and modern drugs.

India stands as one of the most affluent countries globally in terms of the diversity of its flora with numerous species still unused and underexplored (Wells, 2006). In the current study, we have chosen *Saraca asoca* and *Kingiodendron pinnatum* to examine their anticancer properties. Asoka is a renowned plant utilized in Ayurveda for various ailments. The bark of Asoka is a crucial component in a polyherbal formulation called *Asokarishta*, employed in the treatment of diverse gynecological issues in women (Kauser *et al.*, 2016). Occasionally, the bark of *K. pinnatum* serves as a substitute for Asoka in polyherbal preparations. Due to its potential anti-estrogenic properties, a formulation made using *K. pinnatum* were as effective as *S. asoca* in a prior study carried out by the Kerala Forest Research Institute (KFRI), Thrissur, Kerala (Sasidharan and Padikkala, 2012). Estrogen receptors affect the growth of tumours in hormone-dependent breast cancer and estrogen is a key growth-promoting agent in these tumours (Dickson and Lippman, 1987). Anti-estrogens are a class of medications designed primarily to oppose the effects of estrogen and are essential for treating and preventing hormone-dependent breast cancer (Sola and Renoir, 2006).

Anti-estrogens, including aromatase inhibitors and tamoxifen operate by binding to estrogen receptors on the surface of cancer cells (Begam *et al.*, 2017). Tamoxifen, for instance, competes with estrogen for receptor binding by acting like a selective estrogen receptor modulator (SERM). Anti-estrogens obstruct the signaling pathways activated by

estrogen through attaching with estrogen receptors. This interference prevents the stimulatory impact of estrogen on cancer cell growth (Renoir *et al*., 2013). Estrogen is essential to the growth and spread of hormone-dependent breast cancers. Anti-estrogens disrupt this dependence, resulting in a deceleration or inhibition of tumour cell division. Aromatase inhibitors, another category of anti-estrogens, diminish estrogen production in postmenopausal women. By inhibiting the enzyme aromatase, responsible for converting androgens to estrogen, these medications reduce circulating estrogen levels (Miller, 2003). In summary, anti-estrogens are essential in the prevention and management of hormone-dependent breast cancer as they interfere with estrogen signaling and impede the proliferation of cancer cells (Ikeda *et al*., 2015). Their application is personalized based on individual circumstances, and ongoing research is refining and enhancing these treatment strategies.

In our study, crude extracts of *S. asoca* and *K. pinnatum* displayed potent cytotoxic effects on ERβ expressing breast cancer cell lines (MDA-MB-231, SK-BR-3, MDA-MB-468). Conversely, on ERα expressing breast cancer cells (MCF-7), the extracts exhibited no anti-proliferative effects even at high concentrations. The notable cytotoxicity observed against triple-negative breast cancer cells holds particular importance, given the challenges associated with conventional chemotherapy in addressing this specific type of breast cancer. Furthermore, both extracts were found to activate caspase 3 and arrest the cell cycle at the G0/G1 phase, indicating the induction of apoptosis. Studies have reported that approximately 50 to 80% of TNBCs contain the estrogen receptor isoform ERβ. Phytoestrogens, recognized as natural agonists for ERβ, are actively pursued as potential therapeutic options. They demonstrate a beneficial affinity for ERβ and have the ability to hinder the transcriptional growth promoted by ERα. Through the E-screen assay, we observed a proliferative effect of both plant extracts on the ERα-expressing breast cancer cell line and a modest antiproliferative effect on the ERβ-expressing triple-negative breast cancer cell line. Additionally, the *in vivo* rodent uterotropic assay demonstrates the antiestrogenic effects of the extracts, as evidenced by the suppressed growth of the endometrial lining and decreased serum estrogen levels. Many well-known phytoestrogens including catechin, quercetin, kaempferol, β-sitosterol, were identified in our study using chemical characterisation and phytochemical analysis of *S. asoca* and *K.*

pinnatum crude extracts. Therefore, the specific cytotoxicity towards TNBCs is believed to result from the interaction of these phytoestrogens with ERβ leading to activation of apoptotic mechanism.

Docking studies reveal that phytoestrogens such as quercetin and kaempferol exhibit deeper binding into active amino acid pockets in ERβ compared to ERα. This high affinity for ERβ suggests a significant role in the chemopreventive effects of these phytoestrogens, indicating potential biological reactions through interactions with estrogen receptors. The relationship between phytoestrogens and breast cancer is intricate and continually evolving in research. Studies investigating this connection have produced diverse outcomes, and the precise mechanisms of phytoestrogen action remain incompletely understood (Mense *et al*., 2008). Phytoestrogens exhibit dual roles as both estrogen agonists and antagonists, influenced by several factors (Harini *et al*., 2018). Through their interactions with estrogen receptors, especially ERα and ERβ, phytoestrogens can either mimic the effects of estrogen or block or inhibit estrogen receptors (Basu and Maier, 2018). The effects of phytoestrogens on cell proliferation, apoptotic induction, and angiogenesis are dependent on a number of variables, including the particular phytoestrogen type, the cellular environment, intrinsic estrogenic state, metabolism, exposure duration, and dose (Moutsatsou, 2007). According to some research, certain phytoestrogens may have chemopreventive qualities that could reduce the incidence of breast cancer (Sakamoto *et al*., 2010). This is believed to be related to their capacity to control estrogen activity and produce antioxidant and anti-inflammatory benefits. Nonetheless, there are contradictory data in the literature with certain research points to the potential preventive benefits of phytoestrogens, while other studies raise questions about their ability to worsen hormone-sensitive malignancies (Kirk *et al*., 2001). In summary, the impact of phytoestrogens on breast cancer is a complex subject necessitating further exploration. Ongoing research aims to unravel the intricacies of these compounds, understand their diverse effects and determine their potential role in the prevention and treatment of breast cancer. Furthermore, strong anti-inflammatory, antioxidant, anti-tumour and anti-carcinogenic properties were noted for the crude extracts of *S. asoca* and *K. pinnatum*. Both plant extracts had a substantial protective effect against 4T1 challenged triple-negative breast cancer (TNBC) model as evidenced by the decreased tumour size and prevention of organ metastasis.

In conclusion, the study identified the presence of phytoestrogens in both plant extracts, showcasing distinct actions on breast cancer cell lines. The notable cytotoxicity against triple-negative breast cancers (TNBCs) is particularly significant, given the limited treatment options for this aggressive cancer type. The findings present a promising avenue for further investigations targeting TNBCs. Moreover, the impact of phytoestrogens on ERβ-expressing cancers warrants additional exploration. Compounds with the ability to bind to ERβ hold potential for preventing or treating malignancies like TNBCs. Therefore, the development of antiestrogenic drugs is crucial for inhibiting the growth of such cancers.

Recommendations

Saraca asoca and *Kingiodendron pinnatum* have demonstrated distinctive biological properties, including antioxidant, anti-inflammatory, anti-estrogenic, anti-tumour effects, and potent anti-cancer effects, particularly against triple negative breast cancers (TNBCs). However, the study faced several constraints and shortcomings. The diverse array of bioactive components with varying polarities in plant extracts posed a significant challenge in isolating single compounds, hindering the identification and characterization of active components. Consequently, the study was limited by the inability to isolate pure bioactive compounds from the extracts. Furthermore, as the crude methanolic extract from both plants demonstrated superior activities compared to the various fractions in our study, we chose to proceed with the crude extract.

In our study, potent anticancer effects were exerted by both plants against TNBCs, as validated by the findings from *in silico, in vitro,* and *in vivo* studies. Different phytoestrogens have been identified in both plant extracts in our investigation, and the attributed anticancer activities against TNBCs were hypothesized to result from the interaction of these phytoestrogens with the estrogen receptor *β*. Considering the limited treatment options available for TNBCs, our reports recommend to explore the use of *S. asoca* and *K. pinnatum* against this aggressive type of cancer. Therefore, looking ahead, it is crucial to focus on the identification and characterization of the specific phytoestrogens in both plants exhibiting agonistic properties towards ER*β*. Future efforts should also involve assessing the downstream signalling events resulting from ER*β* activation.

Furthermore, in our study, we have only conducted molecular docking analysis of the phytoestrogens found in the plants with the designated estrogen receptors. However molecular dynamics simulation studies must be considered in the future investigations as they can shed light on the flexibility, structural alterations, energetics, and stability of the ligand-receptor complex and are a useful tool for understanding biological processes at the atomic level, finding new drugs and studying protein-ligand interaction. In conclusion, delving deeper into the ER*β* activation by phytoestrogen binding and exploring the subsequent downstream signalling events, holds significant promise for future research in the quest to develop a potential drug candidate against TNBCs

.

Bibliography

ABD RAZAK, N., YEAP, S. K., ALITHEEN, N. B., HO, W. Y., YONG, C. Y., TAN, S. W., TAN, W. S. & LONG, K. 2020. Eupatorin suppressed tumor progression and enhanced immunity in a 4T1 murine breast cancer model. *Integrative cancer therapies,* 19**,** 1534735420935625.

ABDEL-MAGID, A. F. 2017. Selective estrogen receptor degraders (SERDs): a promising treatment to overcome resistance to endocrine therapy in ERα-positive breast cancer. ACS Publications.

ABDEL-WAHAB, W. M. 2013. Protective effect of thymoquinone on sodium fluoride-induced hepatotoxicity and oxidative stress in rats. *The Journal of Basic & Applied Zoology,* 66**,** 263-270.

ABDULLAHI, M. & ADENIJI, S. E. 2020. In-silico molecular docking and ADME/pharmacokinetic prediction studies of some novel carboxamide derivatives as anti-tubercular agents. *Chemistry Africa,* 3**,** 989-1000.

AEBI, H. 1984. [13] Catalase in vitro. *Methods in enzymology.* Elsevier.

AGGARWAL, B. B. & SHISHODIA, S. 2006. Molecular targets of dietary agents for prevention and therapy of cancer. *Biochemical Pharmacology,* 71**,** 1397-1421.

AGRAWAL, P., SINGH, H., SRIVASTAVA, H. K., SINGH, S., KISHORE, G. & RAGHAVA, G. P. S. 2019. Benchmarking of different molecular docking methods for protein-peptide docking. *BMC bioinformatics,* 19**,** 105-124.

AHMAD, F., MISRA, L., TEWARI, R., GUPTA, P., GUPTA, V. K. & DAROKAR, M. P. 2016a. Isolation and HPLC profiling of chemical constituents of Saraca asoca stem bark.

AHMAD, F., MISRA, L., TEWARI, R., GUPTA, P., MISHRA, P. & SHUKLA, R. 2016b. Anti-inflammatory flavanol glycosides from Saraca asoca bark. *Natural product research,* 30**,** 489-492.

AJILA, C. & RAO, U. P. 2008. Protection against hydrogen peroxide induced oxidative damage in rat erythrocytes by Mangifera indica L. peel extract. *Food and Chemical Toxicology,* 46**,** 303-309.

AKHOURI, V., KUMARI, M. & KUMAR, A. 2020. Therapeutic effect of Aegle marmelos fruit extract against DMBA induced breast cancer in rats. *Scientific reports,* 10**,** 18016.

AKL, H., VERVLOESSEM, T., KIVILUOTO, S., BITTREMIEUX, M., PARYS, J. B., DE SMEDT, H. & BULTYNCK, G. 2014. A dual role for the anti-apoptotic Bcl-2 protein in cancer: Mitochondria versus endoplasmic reticulum. *Biochimica et Biophysica Acta (BBA) - Molecular Cell Research,* 1843**,** 2240-2252.

ALEIXANDRE-TUDO, J. L. & DU TOIT, W. 2018. The role of UV-visible spectroscopy for phenolic compounds quantification in winemaking. *Frontiers and new trends in the science of fermented food and beverages***,** 200-204.

ALFAKEEH, A. & BREZDEN-MASLEY, C. 2018. Overcoming endocrine resistance in hormone receptor–positive breast cancer. *Current oncology,* 25**,** 18-27.

ALHADIDI, Q., AHMED, Z., T. NUMAN, I. & HUSSAIN, S. 2009. Dose-dependent anti-inflammatory effect of silymarin in experimental animal model of chronic inflammation. *African journal of pharmacy and pharmacology,* 3**,** 242-247.

ALVES, C. Q., DAVID, J. M., DAVID, J. P., BAHIA, M. V. & AGUIAR, R. M. 2010. Métodos para determinação de atividade antioxidante in vitro em substratos orgânicos. *Química Nova,* 33**,** 2202-2210.

AMIN, M. B., GREENE, F. L., EDGE, S. B., COMPTON, C. C., GERSHENWALD, J. E., BROOKLAND, R. K., MEYER, L., GRESS, D. M., BYRD, D. R. & WINCHESTER, D. P. 2017. The eighth edition AJCC cancer staging manual: continuing to build a bridge from a population-based to a more "personalized" approach to cancer staging. *CA: a cancer journal for clinicians,* 67**,** 93-99.

ANANDHI SENTHILKUMAR, H., FATA, J. E. & KENNELLY, E. J. 2018. Phytoestrogens: The current state of research emphasizing breast pathophysiology. *Phytotherapy Research,* 32**,** 1707-1719.

ANESTIS, A., MIHAILIDOU, C., THEOCHARIS, S., TRYFONOPOULOS, D., KOROGIANNOS, A., KOUMARIANOU, A., XINGI, E., KONTOS, M., PAPAVASSILIOU, A. G. & KARAMOUZIS, M. V. 2018. The predictive role of

estrogen receptor beta (ER-β) in androgen receptor (AR)-positive triple-negative breast cancer (TNBC). *Annals of Oncology,* 29**,** iii32.

ANGELI, D., SALVI, S. & TEDALDI, G. 2020. Genetic predisposition to breast and ovarian cancers: how many and which genes to test? *International journal of molecular sciences,* 21**,** 1128.

ANYWAR, G., KAKUDIDI, E., BYAMUKAMA, R., MUKONZO, J., SCHUBERT, A., ORYEM-ORIGA, H. & JASSOY, C. 2021. A Review of the Toxicity and Phytochemistry of Medicinal Plant Species Used by Herbalists in Treating People Living With HIV/AIDS in Uganda. *Front Pharmacol,* 12**,** 615147.

AQUINO, R., MORELLI, S., LAURO, M. R., ABDO, S., SAIJA, A. & TOMAINO, A. 2001. Phenolic constituents and antioxidant activity of an extract of *Anthurium versicolor* leaves. *Journal of Natural Products,* 64**,** 1019-1023.

ARNOLD, M., MORGAN, E., RUMGAY, H., MAFRA, A., SINGH, D., LAVERSANNE, M., VIGNAT, J., GRALOW, J. R., CARDOSO, F. & SIESLING, S. 2022. Current and future burden of breast cancer: Global statistics for 2020 and 2040. *J The Breast,* 66**,** 15-23.

ASLANTÜRK, Ö. S. 2018. In vitro cytotoxicity and cell viability assays: principles, advantages, and disadvantages. *Genotoxicity-A predictable risk to our actual world,* 2**,** 64-80.

ASOKAN, A. & THANGAVEL, M. 2014. In vitro cytotoxic studies of crude methanolic extract of Saraca indica bark extract. *IOSR Journal of Pharmacy and Biological Sciences,* 9**,** 26-30.

ASONG, G. M., VOSHAVAR, C., AMISSAH, F., BRICKER, B., LAMANGO, N. S. & ABLORDEPPEY, S. Y. 2022. An Evaluation of the Anticancer Properties of SYA014, a Homopiperazine-Oxime Analog of Haloperidol in Triple Negative Breast Cancer Cells. *Cancers,* 14**,** 6047.

ATHIRALAKSHMY, T., DIVYAMOL, A. & NISHA, P. 2016. Phytochemical screening of *Saraca asoca* and antimicrobial activity against bacterial species. *Asian Journal of Plant Science and Research,* 6**,** 30-36.

ATTIMARAD, M., AHMED, K. K., ALDHUBAIB, B. E. & HARSHA, S. 2011. High-performance thin layer chromatography: A powerful analytical technique in pharmaceutical drug discovery. *Pharm Methods,* 2**,** 71-5.

BAFFORD, A. C., BURSTEIN, H. J., BARKLEY, C. R., SMITH, B. L., LIPSITZ, S., IGLEHART, J. D., WINER, E. P. & GOLSHAN, M. 2009. Breast surgery in stage IV breast cancer: impact of staging and patient selection on overall survival. *Breast cancer research and treatment,* 115**,** 7-12.

BALKWILL, F. & MANTOVANI, A. 2001. Inflammation and cancer: back to Virchow? *The lancet,* 357**,** 539-545.

BANDARUPALLI, D., THAAKUR, S., PUTTUGUNTA, S. B. & SASIDHAR, R. L. C. 2014. WOUND HEALING AND ANTIOXIDANT POTENTIAL OF CHLOROFORM EXTRACT OF SARACA ASOCA (ROXB.). *International Journal of Pharmaceutical Sciences and Research,* 5**,** 2285.

BANERJEE, A., KUNWAR, A., MISHRA, B. & PRIYADARSINI, K. I. 2008. Concentration dependent antioxidant/pro-oxidant activity of curcumin: Studies from AAPH induced hemolysis of RBCs. *Chemico-biological interactions,* 174**,** 134-139.

BANGAJAVALLI, S. 2019. GC-MS analysis of bioactive componenets of bark of *Saraca asoca. European journal of pharmaceutical and medical research,* 6**,** 258-261.

BARNES, S. 1998. 2Phytoestrogens and breast cancer. *Bailliere's clinical endocrinology and metabolism,* 12**,** 559-579.

BARRIGA, F., RAMÍREZ, P., WIETSTRUCK, A. & ROJAS, N. 2012. Hematopoietic stem cell transplantation: clinical use and perspectives. *Biological research,* 45**,** 307-316.

BARROS, A. C. S. D., MURANAKA, E. N. K., MORI, L. J., PELIZON, C. H. T., IRIYA, K., GIOCONDO, G. & PINOTTI, J. A. 2004. Induction of experimental mammary carcinogenesis in rats with 7, 12-dimethylbenz (a) anthracene. *Revista do Hospital das Clínicas,* 59**,** 257-261.

BASU, P. & MAIER, C. 2018. Phytoestrogens and breast cancer: In vitro anticancer activities of isoflavones, lignans, coumestans, stilbenes and their analogs and derivatives. *Biomedicine & Pharmacotherapy,* 107**,** 1648-1666.

BEENA, C. & RADHAKRISHNAN, V. V. 2010. Haemagglutination as a rapid tool to differentiate Saraca asoca bark from the adulterant Polyalthia longifolia. *Journal of Progressive Agriculture,* 1**,** 1-3.

BEERS, R. F. & SIZER, I. W. 1952. A spectrophotometric method for measuring the breakdown of hydrogen peroxide by catalase. *J Biol chem,* 195**,** 133-140.

BEGAM, A. J., JUBIE, S. & NANJAN, M. J. 2017. Estrogen receptor agonists/antagonists in breast cancer therapy: A critical review. *Bioorganic chemistry,* 71**,** 257-274.

BEGUM, S. N., RAVIKUMAR, K. & VED, D. K. 2014. 'Asoka'–an important medicinal plant, its market scenario and conservation measures in India. *Current Science,* 107**,** 26-28.

BEHAN, L. A., AMIR, E. & CASPER, R. F. 2015. Aromatase inhibitors for prevention of breast cancer in postmenopausal women: a narrative review. *Menopause,* 22**,** 342-350.

BEN-NASR, S., AAZZA, S., MNIF, W. & MIGUEL, M. D. G. C. 2015. Antioxidant and anti-lipoxygenase activities of extracts from different parts of Lavatera cretica L. grown in Algarve (Portugal). *Pharmacognosy magazine,* 11**,** 48.

BENDIGERI, S., DAS, G., SHRMAN, K., KUMAR, S., KHARE, R. K., SACHAN, S. & SAIYAM, R. 2019. Phytochemical analysis of Saraca asoca bark and Azadirachta indica seeds. *Internation Journal of Chemical Studies***,** 126-131.

BENGALURU, I. 2020. Report of national cancer Registry programme (ICMR-NCDIR); c2020. *Available on: https://www. ncdirindia. org/All_Reports/Report_2020/default. aspx. Accessed September,* 10.

BENZIE, I. F. & STRAIN, J. 1999. Ferric reducing/anti-oxidantpower assay: directmeasure of total antioxidant activity of biological fluids and modified version for simultaneous of totalantioxidant power and ascorbic acid concentration. *Methods; in Enzymology,* 299**,** 15.

BENZIE, I. F. F. & STRAIN, J. J. 1996. The ferric reducing ability of plasma (FRAP) as a measure of "antioxidant power": the FRAP assay. *Analytical biochemistry,* 239**,** 70-76.

BERNSTEIN, L., HENDERSON, B. E., HANISCH, R., SULLIVAN-HALLEY, J. & ROSS, R. K. 1994. Physical exercise and reduced risk of breast cancer in young women. *JNCI: Journal of the National Cancer Institute,* 86**,** 1403-1408.

BINASCHI, M., BIGIONI, M., CIPOLLONE, A., ROSSI, C., GOSO, C., MAGGI, C. A., CAPRANICO, G. & ANIMATI, F. 2001. Anthracyclines: selected new developments. *Current Medicinal Chemistry-Anti-Cancer Agents,* 1**,** 113-130.

BISWAS, T. K. & DEBNATH, P. K. 1972. Aśoka (Saraca Indica Linn)-a cultural and scientific evaluation. *Indian journal of history of science,* 7**,** 99-114.

BONES, R. W. & TAUSKY, H. H. 1945. Colorimetric determination of creatinine by the Jaffe reaction. *Journal of Biological Chemistry***,** 581-591.

BOOMINATHAN, R., PARIMALADEVI, B., MANDAL, S. C. & GHOSHAL, S. K. 2004. Anti-inflammatory evaluation of Ionidium suffruticosam Ging. in rats. *Journal of ethnopharmacology,* 91**,** 367-370.

BOROKAR, A. A. & PANSARE, T. A. 2017. Plant profile, phytochemistry and pharmacology of Ashoka (Saraca asoca (Roxb.), De. Wilde)-A comprehensive review. *Int. J. Ayurvedic Herb. Med,* 7**,** 2524-2541.

BOSCH, A., EROLES, P., ZARAGOZA, R., VIÑA, J. R. & LLUCH, A. 2010. Triple-negative breast cancer: molecular features, pathogenesis, treatment and current lines of research. *Cancer treatment reviews,* 36**,** 206-215.

BOVE, K., LINCOLN, D. W. & TSAN, M.-F. 2002. Effect of resveratrol on growth of 4T1 breast cancer cells in vitro and in vivo. *Biochemical and biophysical research communications,* 291**,** 1001-1005.

BOYD, N. F., LOCKWOOD, G. A., BYNG, J. W., TRITCHLER, D. L. & YAFFE, M. J. 1998. Mammographic densities and breast cancer risk. *Cancer epidemiology, biomarkers & prevention: a publication of the American Association for Cancer Research, cosponsored by the American Society of Preventive Oncology,* 7**,** 1133-1144.

BROOKS, P. C. 1996. Cell adhesion molecules in angiogenesis. *Cancer and Metastasis Reviews,* 15**,** 187-194.

BROWN, C. M., MULCAHEY, T. A., FILIPEK, N. C. & WISE, P. M. 2010. Production of proinflammatory cytokines and chemokines during neuroinflammation: novel roles for estrogen receptors alpha and beta. *Endocrinology,* 151**,** 4916-25.

BROWN, S. B. & HANKINSON, S. E. 2015. Endogenous estrogens and the risk of breast, endometrial, and ovarian cancers. *Steroids,* 99**,** 8-10.

CANDELA, J. L. 2016. Cardiotoxicity and breast cancer as late effects of pediatric and adolescent Hodgkin lymphoma treatment. *The American Journal of Nursing,* 116**,** 32-42.

CAO, R., FOMINA, A. & MCGUIGAN, A. P. 2022. Tissue-engineered Cancer Models in Drug Screening. *Biomaterial Based Approaches to Study the Tumour Microenvironment.* The Royal Society of Chemistry.

CELLA, D. & FALLOWFIELD, L. J. 2008. Recognition and management of treatment-related side effects for breast cancer patients receiving adjuvant endocrine therapy. *Breast cancer research and treatment,* 107**,** 167-180.

CENGIZ, M. 2019. Introductory Chapter: Traditional and Complementary Medicine. *In:* CENGIZ, M. (ed.) *Traditional and Complementary Medicine.* Rijeka: IntechOpen.

CHANDRA, L. D. 2016. Bio-diversity and conservation of medicinal and aromatic plants. *Adv Plants Agric Res,* 5**,** 00186.

CHANG, C. C., YANG, M. H., WEN, H. M. & CHERN, J. C. 2002. Estimation of total flavonoid content in propolis by two complementary colorimetric methods. *Journal of food and drug analysis,* 10.

CHAU, T. 1989. Pharmacology methods in the control of inflammation. *Modern methods in pharmacology***,** 195-212.

CHEN, C.-H., WU, S.-H., TSENG, Y.-M., LIAO, J.-B., FU, H.-T., TSAI, S.-M. & TSAI, L.-Y. 2017. Suppressive effects of Puerariae Radix on the breast tumor incidence in rats treated with DMBA. *Journal of Agricultural Science,* 9**,** 68-79.

CHEN, P., LI, B. & OU-YANG, L. 2022. Role of estrogen receptors in health and disease. *Frontiers in Endocrinology,* 13**,** 839005.

CHEN, Y., CLEGG, N. J. & SCHER, H. I. 2009. Anti-androgens and androgen-depleting therapies in prostate cancer: new agents for an established target. *The lancet oncology,* 10**,** 981-991.

CHESBROUGH, M. A. & ARTHUR, M. 1972. Determination of RBC and WBC count. *Laboratory Manual of Rural Tropical Hospitals,* 145.

CHLEBOWSKI, R. T., CHEN, Z., ANDERSON, G. L., ROHAN, T., ARAGAKI, A., LANE, D., DOLAN, N. C., PASKETT, E. D., MCTIERNAN, A. & HUBBELL, F. A. 2005. Ethnicity and breast cancer: factors influencing differences in incidence and outcome. *Journal of the National Cancer Institute,* 97**,** 439-448.

CHOUDHARY, A., ELUMALAI, P., RAGHUNANDHAKUMAR, S., LAKSHMI, T. & ROY, A. 2021. Anti-Cancer Effects of Saraca asoca Flower Extract on Prostate Cancer Cell Line.

CHOW, A. Y. 2010. Cell cycle control by oncogenes and tumor suppressors: driving the transformation of normal cells into cancerous cells. *Nature Education,* 3**,** 7.

CHUBAK, J., KAMINENI, A., BUIST, D. S. M., ANDERSON, M. L. & WHITLOCK, E. P. 2015. Aspirin use for the prevention of colorectal cancer: an updated systematic evidence review for the US Preventive Services Task Force.

CIBIN, T. R., DEVI, D. G. & ABRAHAM, A. 2012. Chemoprevention of two-stage skin cancer in vivo by Saraca asoca. *Integrative cancer therapies,* 11**,** 279-286.

CLAIR, R. S. 1998. Cardiovascular effects of soybean phytoestrogens. *American Journal of Cardiology,* 82**,** 40S-42S.

COATES, J. 2000. Interpretation of infrared spectra, a practical approach. Encyclopedia of analytical chemistry. *US: John Wiley Sons, Ltd*.

COLIGAN, J. E., KRUISBEEK, A. M., MARGULIES, D. H., SHEVACH, E. M. & STROBER, W. 1998. Current Protocols in Immunology John Wiley & Sons. *vol.-, No.-*.

COOPER, G. M. & ADAMS, K. 2023. *The cell: a molecular approach*, Oxford University Press.

CRAGG, G. M. & PEZZUTO, J. M. 2016. Natural products as a vital source for the discovery of cancer chemotherapeutic and chemopreventive agents. *Medical Principles and Practice,* 25**,** 41-59.

DABUR, R., GUPTA, A., MANDAL, T. K., SINGH, D. D., BAJPAI, V., GURAV, A. M. & LAVEKAR, G. S. 2007. Antimicrobial activity of some Indian medicinal plants. *African Journal of Traditional, Complementary and Alternative Medicines,* 4**,** 313-318.

DAS, P., NATH, V., GODE, K. & SANYAL, A. 1964. Preliminary phytochemical and pharmacological studies on cocculus hirsutus, linn. *J The Indian journal of medical research,* 52**,** 300-307.

DASARI, S. & TCHOUNWOU, P. B. 2014. Cisplatin in cancer therapy: molecular mechanisms of action. *European journal of pharmacology,* 740**,** 364-378.

DE MAGALHÃES, J. P. 2013. How ageing processes influence cancer. *Nature Reviews Cancer,* 13**,** 357-365.

DEAN-COLOMB, W. & ESTEVA, F. J. 2008. Her2-positive breast cancer: herceptin and beyond. *European Journal of Cancer,* 44**,** 2806-2812.

DEEPTI, B., SANTH RANI, T. & SRINIVASA, B. P. 2012. Evaluation of anti-helmintic and wound healing potential of Saraca asoca (Roxb) bark. *Pharmacognosy Journal,* 4**,** 40-45.

DEKA, A., KALITA, J. C., SINGH, Y. R. & DEKA, M. 2012. Determination of estrogenicity of Asoca plant (Saraca asoca Linn.) in adult female ovariectomized mice. *Int J Recent Sci Res,* 6**,** 7661-4.

DHANANJAY, B. S. & NANDA, S. K. 2013. The role of sevista in the management of dysfunctional uterine bleeding. *Journal of clinical and diagnostic research: JCDR,* 7**,** 132.

DHARSHINI, A. D., ELUMALAI, P., RAGHUNANDHAKUMAR, S., LAKSHMI, T. & ROY, A. 2021. Evaluation of Anti-Cancer Activity of Saraca asoca Flower Extract against Lung Cancer Cell Line.

DIAS, K., DVORKIN-GHEVA, A., HALLETT, R. M., WU, Y., HASSELL, J., POND, G. R., LEVINE, M., WHELAN, T. & BANE, A. L. 2017. Claudin-low breast cancer; clinical & pathological characteristics. *PloS one,* 12**,** e0168669.

DICKSON, R. B. & LIPPMAN, M. E. 1987. Estrogenic regulation of growth and polypeptide growth factor secretion in human breast carcinoma. *Endocrine Reviews,* 8**,** 29-43.

DRABKIN, D. L. & AUSTIN, J. H. J. J. O. B. C. 1935. Spectrophotometric studies: II. Preparations from washed blood cells; nitric oxide hemoglobin and sulfhemoglobin. 112**,** 51-65.

DZUTSEV, A., BADGER, J. H., PEREZ-CHANONA, E., ROY, S., SALCEDO, R., SMITH, C. K. & TRINCHIERI, G. 2017. Microbes and cancer. *Annual review of immunology,* 35**,** 199-228.

EBRAHIMZADEH, M. A., NABAVI, S. M., NABAVI, S. F., BAHRAMIAN, F. & BEKHRADNIA, A. R. 2010. Antioxidant and free radical scavenging activity of H. officinalis L. var. angustifolius, V. odorata, B. hyrcana and C. speciosum. *Pak J Pharm Sci,* 23**,** 29-34.

EISEN, A., TRUDEAU, M., SHELLEY, W., MESSERSMITH, H. & PRITCHARD, K. I. 2008. Aromatase inhibitors in adjuvant therapy for hormone receptor positive breast cancer: a systematic review. *Cancer treatment reviews,* 34**,** 157-174.

EKOR, M. 2014. The growing use of herbal medicines: issues relating to adverse reactions and challenges in monitoring safety. *Front Pharmacol,* 4**,** 177.

FAKHROUEIAN, Z., MASSIHA, A., ESMAEILZADEH, P., ASSMAR, M., ZAHEDI, A., ESMAEILZADEH, P., REZAEI, S. & LALEHDASHT, S. R. 2022. In Vivo Animal Model Evaluation of a Powerful Oral Nanomedicine for Treating Breast Cancer in BALB/c Mice Using 4T1 Cell Lines without Chemotherapy. *Advances in Nanoparticles,* 11**,** 73-109.

FAN, X. Q. & GUO, Y. J. 2001. Apoptosis in oncology. *Cell Research,* 11**,** 1-7.

FAN, Z., CHE, H., YANG, S. & CHEN, C. 2019. Estrogen and estrogen receptor signaling promotes allergic immune responses: Effects on immune cells, cytokines, and inflammatory factors involved in allergy. *Allergol Immunopathol (Madr),* 47**,** 506-512.

FENG, Y., SPEZIA, M., HUANG, S., YUAN, C., ZENG, Z., ZHANG, L., JI, X., LIU, W., HUANG, B. & LUO, W. 2018. Breast cancer development and progression: Risk factors, cancer stem cells, signaling pathways, genomics, and molecular pathogenesis. *Genes & diseases,* 5**,** 77-106.

FEOKTISTOVA, M., GESERICK, P. & LEVERKUS, M. 2016. Crystal violet assay for determining viability of cultured cells. *Cold Spring Harb Protoc,* 2016**,** 343-6.

FERLAY, J., COLOMBET, M., SOERJOMATARAM, I., PARKIN, D. M., PIÑEROS, M., ZNAOR, A. & BRAY, F. 2021. Cancer statistics for the year 2020: An overview. *International journal of cancer,* 149**,** 778-789.

FIGUEROA-MAGALHÃES, M. C., JELOVAC, D., CONNOLLY, R. M. & WOLFF, A. C. 2014. Treatment of HER2-positive breast cancer. *The Breast,* 23**,** 128-136.

FOLKMAN, J. 1992. shing Y. *Angiogenesis. J Biol Chem,* 267**,** 10931-10934.

FRANÇA, B. K., ALVES, M. R. M., SOUTO, F. M. S., TIZIANE, L., BOAVENTURA, R. F., GUIMARÃES, A. & ALVES JR, A. 2013. Peroxidação lipídica e obesidade: Métodos para aferição do estresse oxidativo em obesos. *GE jornal português de gastrenterologia,* 20**,** 199-206.

FRIDLENDER, M., KAPULNIK, Y. & KOLTAI, H. 2015. Plant derived substances with anti-cancer activity: from folklore to practice. *Frontiers in plant science,* 6**,** 799.

FUENTES, N. & SILVEYRA, P. 2019. Estrogen receptor signaling mechanisms. *Adv Protein Chem Struct Biol,* 116**,** 135-170.

GAHLAUT, A., SHIROLKAR, A., HOODA, V. & DABUR, R. 2013a. A rapid and simple approach to discriminate various extracts of Saraca asoca [Roxb.], De. Wild using UPLC-QTOFMS and multivariate analysis. *journal of pharmacy research,* 7**,** 143-149.

GAHLAUT, A., SHIROLKAR, A., HOODA, V., DABUR, R. J. J. O. A. P. T. & RESEARCH 2013b. β-sitosterol in different parts of Saraca asoca and herbal drug ashokarista: Quali-quantitative analysis by liquid chromatography-mass spectrometry. 4**,** 146.

GARCÍA-GÓMEZ, E., VÁZQUEZ-MARTÍNEZ, E. R., REYES-MAYORAL, C., CRUZ-OROZCO, O. P., CAMACHO-ARROYO, I. & CERBÓN, M. 2020. Regulation of inflammation pathways and inflammasome by sex steroid hormones in endometriosis. *Frontiers in endocrinology,* 10**,** 935.

GARDNER, T., ELZEY, B. & HAHN, N. M. 2012. Sipuleucel-T (Provenge) autologous vaccine approved for treatment of men with asymptomatic or minimally symptomatic castrate-resistant metastatic prostate cancer. *Human vaccines & immunotherapeutics,* 8**,** 534-539.

GERL, R. & VAUX, D. L. 2005. Apoptosis in the development and treatment of cancer. *Carcinogenesis,* 26**,** 263-270.

GHANDEHARI, F. & FATEMI, M. 2018. The effect of Ficus carica latex on 7, 12-dimethylbenz (a) anthracene-induced breast cancer in rats. *Avicenna journal of phytomedicine,* 8**,** 286.

GHATAK, A., NAIR, S., VAJPAYEE, A., CHATURVEDI, P., SAMANT, S., SOLEY, K., KUDALE, S. & DESAI, N. 2015a. Evaluation of antioxidant activity, total phenolic content, total flavonoids, and LC-MS characterization of Saraca asoca (Roxb.) De. Wilde. *Int J Adv Res,* 3**,** 318-27.

GHATAK, A., NAIR, S., VAJPAYEE, A., CHATURVEDI, P., SAMANT, S., SOLEY, K., KUDALE, S. & DESAI, N. J. I. J. A. R. 2015b. Evaluation of antioxidant activity, total phenolic content, total flavonoids, and LC-MS characterization of Saraca asoca (Roxb.) De. Wilde. 3**,** 318-27.

GHOSH, S., MAJUMDER, M., MAJUMDER, S., GANGULY, N. K. & CHATTERJEE, B. P. 1999. Saracin: a lectin from Saraca indica seed integument induces apoptosis in human T-lymphocytes. *Archives of Biochemistry and Biophysics,* 371**,** 163-168.

GONZÁLEZ-VALLINAS, M., GONZÁLEZ-CASTEJÓN, M., RODRÍGUEZ-CASADO, A. & RAMÍREZ DE MOLINA, A. 2013. Dietary phytochemicals in cancer prevention and therapy: a complementary approach with promising perspectives. *Nutrition reviews,* 71**,** 585-599.

GOYAL, R., JERATH, G., AKHIL, R., CHANDRASEKHARAN, A., PUPPALA, E. R., PONNEGANTI, S., SARMA, A., NAIDU, V. G. M., SANTHOSHKUMAR, T. R. &

RAMAKRISHNAN, V. 2021. Geometry encoded functional programming of tumor homing peptides for targeted drug delivery. *Journal of controlled release,* 333**,** 16-27.

GRAVENA, A. A. F., LOPES, T. C. R., DE OLIVEIRA DEMITTO, M., BORGHESAN, D. H. P., DELL'AGNOLO, C. M., BRISCHILIARI, S. C. R., DE BARROS CARVALHO, M. D. & PELLOSO, S. M. 2018. The obesity and the risk of breast cancer among pre and postmenopausal women. *Asian Pacific journal of cancer prevention: APJCP,* 19**,** 2429.

GRAWEL, S., WARDAS, M. & NIEDWOROK, E. 2004. Malondialdehyde (MDA) as a lipid peroxidation marker. *Wiad Lek,* 57**,** 453-455.

GRAY JR, L. E., WILSON, V., NORIEGA, N., LAMBRIGHT, C., FURR, J., STOKER, T. E., LAWS, S. C., GOLDMAN, J., COOPER, R. L. & FOSTER, P. M. D. 2004. Use of the laboratory rat as a model in endocrine disruptor screening and testing. *Ilar Journal,* 45**,** 425-437.

GRAZIOSE, R., ANN LILA, M. & RASKIN, I. 2010. Merging traditional Chinese medicine with modern drug discovery technologies to find novel drugs and functional foods. *Current drug discovery technologies,* 7**,** 2-12.

GRUCKA-MAMCZAR, E., BIRKNER, E., BLASZCZYK, I., KASPERCZYK, S., WIELKOSZYHSKI, T., SWIETOCHOWSKA, E. & STAWIARSKA-PIETA, B. 2009. The influence of sodium fluoride and antioxidants on the concentration of malondialdehyde in rat blood plasma. *Fluoride,* 42**,** 101.

GÜRSEL, Ö. K. 2018. Recent Technological Advances in Radiotherapy. *Eur Arch Med Res,* 34**,** 55-60.

HADDAD, S. A., DIZON, D. S. & GRAFF, S. L. 2023. Sequencing systemic therapy in hormone-receptor positive metastatic breast cancer: a modern paradigm. *Chinese Clinical Oncology,* 12**,** 42-42.

HALL, J. 2005. The Ataxia-telangiectasia mutated gene and breast cancer: gene expression profiles and sequence variants. *Cancer letters,* 227**,** 105-114.

HAMZA, A. A., KHASAWNEH, M. A., ELWY, H. M., HASSANIN, S. O., ELHABAL, S. F. & FAWZI, N. M. 2022. Salvadora persica attenuates DMBA-induced mammary cancer through downregulation oxidative stress, estrogen receptor expression and proliferation and augmenting apoptosis. *Biomedicine & Pharmacotherapy,* 147**,** 112666.

HAN, D.-H., DENISON, M. S., TACHIBANA, H. & YAMADA, K. 2002. Relationship between estrogen receptor-binding and estrogenic activities of environmental estrogens and suppression by flavonoids. *Bioscience, biotechnology, and biochemistry,* 66**,** 1479-1487.

HAN, Y., LIU, D. & LI, L. 2020. PD-1/PD-L1 pathway: current researches in cancer. *Am J Cancer Res,* 10**,** 727-742.

HANAHAN, D. 2022. Hallmarks of cancer: new dimensions. *Cancer discovery,* 12**,** 31-46.

HANAHAN, D. & WEINBERG, R. A. 2000. The hallmarks of cancer. *cell,* 100**,** 57-70.

HANAHAN, D. & WEINBERG, R. A. 2011. Hallmarks of cancer: the next generation. *cell,* 144**,** 646-674.

HANDY, D. E., CASTRO, R. & LOSCALZO, J. 2011. Epigenetic modifications: basic mechanisms and role in cardiovascular disease. *Circulation,* 123**,** 2145-56.

HARBORNE, A. 1998. *Phytochemical methods a guide to modern techniques of plant analysis,* springer science & business media.

HARINI, A. S., FATA, J. E. & KENNELLY, E. J. 2018. Phytoestrogens: The current state of research emphasizing breast pathophysiology. *Phytotherapy Research,* 32**,** 1707-1719.

HELMINK, B. A., KHAN, M. A. W., HERMANN, A., GOPALAKRISHNAN, V. & WARGO, J. A. 2019. The microbiome, cancer, and cancer therapy. *Nature medicine,* 25**,** 377-388.

HEMMINKI, K., FÖRSTI, A., KHYATTI, M., ANWAR, W. A. & MOUSAVI, M. 2014. Cancer in immigrants as a pointer to the causes of cancer. *The European Journal of Public Health,* 24**,** 64-71.

HENDRIKS, H. F. J. 2020. Alcohol and human health: what is the evidence? *Annual review of food science and technology,* 11**,** 1-21.

HIGGINS, M. J. & STEARNS, V. 2009. Understanding Resistance to Tamoxifen in Hormone Receptor–Positive Breast Cancer. *Clinical chemistry,* 55**,** 1453-1455.

HOEIJMAKERS, J. H. 2001. Genome maintenance mechanisms for preventing cancer. *Nature,* 411**,** 366-74.

HOLLIDAY, D. L. & SPEIRS, V. 2011. Choosing the right cell line for breast cancer research. *Breast Cancer Research,* 13**,** 215.

HOLMBERG, L., IVERSEN, O.-E., RUDENSTAM, C. M., HAMMAR, M., KUMPULAINEN, E., JASKIEWICZ, J., JASSEM, J., DOBACZEWSKA, D., FJOSNE, H. E. & PERALTA, O. 2008. Increased risk of recurrence after hormone replacement therapy in breast cancer survivors. *Journal of the National Cancer Institute,* 100**,** 475-482.

HONG, J.-M., KWON, O.-K., SHIN, I.-S., JEON, C.-M., SHIN, N.-R., LEE, J., PARK, S.-H., HAI, D. V., OH, S.-R. & HAN, S.-B. 2015. Anti-inflammatory effects of methanol extract of Canarium lyi CD Dai & Yakovlev in RAW 264.7 macrophages and a murine model of lipopolysaccharide-induced lung injury. *International Journal of Molecular Medicine,* 35**,** 1403-1410.

HSIAO, Y. C., PENG, S. F., LAI, K. C., LIAO, C. L., HUANG, Y. P., LIN, C. C., LIN, M. L., LIU, K. C., TSAI, C. C., MA, Y. S. & CHUNG, J. G. 2019. Genistein induces apoptosis in vitro and has antitumor activity against human leukemia HL-60 cancer cell xenograft growth in vivo. *Environ Toxicol,* 34**,** 443-456.

HUANG, W., HICKSON, L. J., EIRIN, A., KIRKLAND, J. L. & LERMAN, L. O. 2022. Cellular senescence: the good, the bad and the unknown. *Nature Reviews Nephrology,* 18**,** 611-627.

HUSSAN, K. P. S., THAYYIL, M. S., AHAMED, T. S. & MURALEEDHARAN, K. 2020. Biological evaluation and molecular docking studies of benzalkonium ibuprofenate. *Computational Biology and Chemistry.* IntechOpen.

HUYNH, M.-M., PAMBID, M. R., JAYANTHAN, A., DORR, A., LOS, G. & DUNN, S. E. 2020. The dawn of targeted therapies for triple negative breast cancer (TNBC): A snapshot of investigational drugs in phase I and II trials. *Expert opinion on investigational drugs,* 29**,** 1199-1208.

IGHODARO, O. M. & AKINLOYE, O. A. 2018. First line defence antioxidants-superoxide dismutase (SOD), catalase (CAT) and glutathione peroxidase (GPX): Their fundamental role in the entire antioxidant defence grid. *Alexandria Journal of Medicine,* 54**,** 287-293.

IKEDA, K., HORIE-INOUE, K. & INOUE, S. 2015. Identification of estrogen-responsive genes based on the DNA binding properties of estrogen receptors using high-throughput sequencing technology. *Acta Pharmacologica Sinica,* 36**,** 24-31.

INSTITUTE, N. C. 2007. Defining Cancer.

ISHIYAMA, M., TOMINAGA, H., SHIGA, M., SASAMOTO, K., OHKURA, Y. & UENO, K. 1996. A combined assay of cell vability and in vitro cytotoxicity with a highly water-soluble tetrazolium salt, neutral red and crystal violet. *Biological and Pharmaceutical Bulletin,* 19**,** 1518-1520.

JAIN, A., JASMINE, S. S. & SAINI, V. 2013. Hypolipidemic, hypoglycemic and antioxidant potential of Saraca asoca ethanolic leaves extract in streptozotocin induced-experimental diabetes. *Int J Pharm Pharm Sci,* 5**,** 302-305.

JAIN, N., SHARMA, V. & RAMAWAT, K. G. 2011. Therapeutic potentials of medicinal plants traditionally used during postpartum period and their molecular targets. *Journal of Ecobiotechnology,* 3.

JAISWAL, Y. S. & WILLIAMS, L. L. 2017. A glimpse of Ayurveda–The forgotten history and principles of Indian traditional medicine. *Journal of traditional and complementary medicine,* 7**,** 50-53.

JAN, R. & CHAUDHRY, G. E. 2019. Understanding Apoptosis and Apoptotic Pathways Targeted Cancer Therapeutics. *Adv Pharm Bull,* 9**,** 205-218.

JAVANMOGHADAM, S., WEIHUA, Z., HUNT, K. K. & KEYOMARSI, K. 2016. Estrogen receptor alpha is cell cycle-regulated and regulates the cell cycle in a ligand-dependent fashion. *Cell Cycle,* 15**,** 1579-90.

JAVARAPPA, K. K., PRASAD, A. G. D., PRASAD, A. J. M. & MANE, C. 2016. Bioactivity of diterpens from the ethyl acetate extract of Kingiodendron pinnatum rox. hams. *Pharmacognosy Research,* 8**,** 287.

JIA, H., TRUICA, C. I., WANG, B., WANG, Y., REN, X., HARVEY, H. A., SONG, J. & YANG, J.-M. 2017. Immunotherapy for triple-negative breast cancer: Existing challenges and exciting prospects. *Drug resistance updates,* 32**,** 1-15.

JONES, R. C. & EDGREN, R. A. 1973. The effects of various steroids on the vaginal histology in the rat. *Fertility and sterility,* 24**,** 284-291.

JYOTHI, A. & SATYAVATI, D. 2016. FT-IR studies of ethanolic extract of Saraca asoka. *INDO AMERICAN JOURNAL OF PHARMACEUTICAL SCIENCES,* 3**,** 187-190.

KAMAT, S. K., BARDE, P. J. & RAUT, S. B. 2015. Evaluation of the estrogenic activity of Indian medicinal plants in immature rats. *Ancient Science of Life,* 35**,** 90.

KAMBOJ, V. P. 2000. Herbal medicine. *Current Science,* 78**,** 35-39.

KARIMI, B., ASHRAFI, M. & MASOUDIAN, M. 2020. Effect of simvastatin on c-myc, cyclin D1 and p53 expression in DMBA-induced breast cancer in mice. *Physiology and Pharmacology,* 24**,** 152-158.

KARPAGASUNDARI, C. & KULOTHUNGAN, S. 2014. Analysis of bioactive compounds in Physalis minima leaves using GC MS, HPLC, UV-VIS and FTIR techniques. *Journal of Pharmacognosy and Phytochemistry,* 3**,** 196-201.

KATZENELLENBOGEN, J. A. 2011. The 2010 Philip S. Portoghese Medicinal Chemistry Lectureship: Addressing the "Core Issue" in the Design of Estrogen Receptor Ligands: Award Address. *Journal of medicinal chemistry,* 54**,** 5271-5282.

KAUR, C. & KAPOOR, H. C. 2002. Anti-oxidant activity and total phenolic content of some Asian vegetables. *International Journal of Food Science,* 37**,** 153-161.

KAUSER, A. S., HASAN, A., PARREY, S. A. & AHMAD, W. 2016. Ethnobotanical, phytochemical and pharmacological properties of Saraca asoca bark: A Review. *European Journal of Pharmaceutical and Medical Research,* 3**,** 274-279.

KETKAR, P. M., NAYAK, S. U., PAI, S. R., JOSHI, R. K. J. J. O. A. & MEDICINE, I. 2015. Monitoring seasonal variation of epicatechin and gallic acid in the bark of Saraca asoca using reverse phase high performance liquid chromatography (RP-HPLC) method. 6**,** 29.

KHAN, M. I., BOUYAHYA, A., HACHLAFI, N. E. L., MENYIY, N. E., AKRAM, M., SULTANA, S., ZENGIN, G., PONOMAREVA, L., SHARIATI, M. A. & OJO, O. A. 2022. Anticancer properties of medicinal plants and their bioactive compounds against breast cancer: a review on recent investigations. *Environmental Science and Pollution Research,* 29**,** 24411-24444.

KIND, P. & KING, E. 1954. Estimation of plasma phosphatase by determination of hydrolysed phenol with amino-antipyrine. *Journal of clinical Pathology,* 7**,** 322.

KıRAN, T. R., OTLU, O. & KARABULUT, A. B. 2023. Oxidative stress and antioxidants in health and disease. *Journal of Laboratory Medicine,* 47**,** 1-11.

KIRK, C. J., HARRIS, R. M., WOOD, D. M., WARING, R. H. & HUGHES, P. J. 2001. Do dietary phytoestrogens influence susceptibility to hormone-dependent cancer by disrupting the metabolism of endogenous oestrogens? : Portland Press Ltd.

KOBAYASHI, S., SUGIURA, H., ANDO, Y., SHIRAKI, N., YANAGI, T., YAMASHITA, H. & TOYAMA, T. 2012. Reproductive history and breast cancer risk. *Breast cancer,* 19**,** 302-308.

KOFF, J. L., RAMACHANDIRAN, S. & BERNAL-MIZRACHI, L. 2015. A time to kill: targeting apoptosis in cancer. *International journal of molecular sciences,* 16**,** 2942-2955.

KORACH, K. S., COUSE, J. F., CURTIS, S. W., WASHBURN, T. F., LINDZEY, J., KIMBRO, K. S., EDDY, E. M., MIGLIACCIO, S., SNEDEKER, S. M. & LUBAHN, D. B. 1996. Estrogen receptor gene disruption: molecular characterization and experimental and clinical phenotypes. *Recent progress in hormone research,* 51**,** 159-86.

KRAUSE, R. G. E. & GOLDRING, J. P. D. 2019. Crystal violet stains proteins in SDS-PAGE gels and zymograms. *Analytical biochemistry,* 566**,** 107-115.

KUIPER, G. G. J. M., LEMMEN, J. G., CARLSSON, B. O., CORTON, J. C., SAFE, S. H., VAN DER SAAG, P. T., VAN DER BURG, B. & GUSTAFSSON, J.-A. K. 1998. Interaction of estrogenic chemicals and phytoestrogens with estrogen receptor β. *Endocrinology,* 139**,** 4252-4263.

KUMAR, A. & JNANESHA, A. C. 2017. Genetic diversity and conservation of medicinal plants in Deccan plateau region in India. *Journal of Medicinal Plants,* 5**,** 27-30.

KUMAR, J. K., PRASAD, A. G. D. & CHATURVEDI, V. 2014. Phytochemical screening of five medicinal legumes and their evaluation for in vitro anti-tubercular activity. *Ayu,* 35**,** 98.

KUMAR, J. K., PRASAD, A. G. D. & RICHARD, S. A. 2011. Biochemical activity of endangered medicinal plant Kingiodendron pinnatum. *Asian Journal of Plant Science and Research,* 1**,** 70-75.

KUMAR, S., NARWAL, S., KUMAR, D., SINGH, G., NARWAL, S. & ARYA, R. 2012. Evaluation of antihyperglycemic and antioxidant activities of Saraca asoca (Roxb.) De Wild leaves in streptozotocin induced diabetic mice. *Asian Pacific Journal of Tropical Disease,* 2**,** 170-176.

KUNCHANDY, E. & RAO, M. 1990. Oxygen radical scavenging activity of curcumin. *International journal of pharmaceutics,* 58**,** 237-240.

LABRIE, F., DUPONT, A., BELANGER, A., ST-ARNAUD, R., GIGUERE, M., LACOURCIERE, Y., EMOND, J. & MONFETTE, G. 1986. Treatment of prostate cancer with gonadotropin-releasing hormone agonists. *Endocrine reviews,* 7**,** 67-74.

LAFC1, O., CELEPLI, P., ÖZTEKIN, P. S. & KOŞAR, P. N. 2023. DCE-MRI Radiomics analysis in differentiating luminal a and luminal B breast cancer molecular subtypes. *Academic Radiology,* 30**,** 22-29.

LAKSHMI, M. 2020. Plant-Based Drugs as an Adjuvant to Cancer Chemotherapy. *In:* MUHAMMAD, A. (ed.) *Alternative Medicine.* Rijeka: IntechOpen.

LANS, C. 2007. Ethnomedicines used in Trinidad and Tobago for reproductive problems. *Journal of ethnobiology and ethnomedicine,* 3**,** 1-12.

LEVITSKY, D. O. & DEMBITSKY, V. M. 2015. Anti-breast cancer agents derived from plants. *Natural products and bioprospecting,* 5**,** 1-16.

LEYGUE, E., DOTZLAW, H., WATSON, P. H. & MURPHY, L. C. 1998. Altered estrogen receptor α and β messenger RNA expression during human breast tumorigenesis. *Cancer research,* 58**,** 3197-3201.

LIBERTI, M. V. & LOCASALE, J. W. 2016. The Warburg Effect: How Does it Benefit Cancer Cells? *Trends Biochem Sci,* 41**,** 211-218.

LIN, S. R., CHANG, C. H., HSU, C. F., TSAI, M. J., CHENG, H., LEONG, M. K., SUNG, P. J., CHEN, J. C. & WENG, C. F. 2020. Natural compounds as potential adjuvants to cancer therapy: Preclinical evidence. *Br J Pharmacol,* 177**,** 1409-1423.

LINDNER, P., PAUL, S., ECKSTEIN, M., HAMPEL, C., MUENZNER, J. K., ERLENBACH-WUENSCH, K., AHMED, H. P., MAHADEVAN, V., BRABLETZ, T., HARTMANN, A., VERA, J. & SCHNEIDER-STOCK, R. 2020. EMT transcription factor ZEB1 alters the epigenetic landscape of colorectal cancer cells. *Cell Death Dis,* 11**,** 147.

LIOU, Y.-C., ZHOU, X. Z. & LU, K. P. 2011. Prolyl isomerase Pin1 as a molecular switch to determine the fate of phosphoproteins. *Trends in biochemical sciences,* 36**,** 501-514.

LIU, S., HAN, S. J. & SMITH, C. L. 2013. Cooperative activation of gene expression by agonists and antagonists mediated by estrogen receptor heteroligand dimer complexes. *Molecular pharmacology,* 83**,** 1066-1077.

LIU, X.-L., DING, J. & MENG, L.-H. 2018. Oncogene-induced senescence: a double edged sword in cancer. *Acta Pharmacologica Sinica,* 39**,** 1553-1558.

LOBB, R., AYANIAN, J. Z., ALLEN, J. D. & EMMONS, K. M. 2010. Stage of breast cancer at diagnosis among low-income women with access to mammography. *Cancer,* 116**,** 5487-96.

LOBO, V., PATIL, A., PHATAK, A. & CHANDRA, N. 2010. Free radicals, antioxidants and functional foods: Impact on human health. *Pharmacogn Rev,* 4**,** 118-26.

LONČARIĆ, M., STRELEC, I., MOSLAVAC, T., ŠUBARIĆ, D., PAVIĆ, V. & MOLNAR, M. 2021. Lipoxygenase Inhibition by Plant Extracts. *Biomolecules,* 11.

LOPES-PACIENCIA, S., SAINT-GERMAIN, E., ROWELL, M.-C., RUIZ, A. F., KALEGARI, P. & FERBEYRE, G. 2019. The senescence-associated secretory phenotype and its regulation. *Cytokine,* 117**,** 15-22.

LOW, Y.-L., DOWSETT, M., DUNNING, A. & BINGHAM, S. 2005. Phytoestrogen exposure, polymorphisms in COMT, CYP17, CYP19, EDH17B2, ESR1 and SHBG genes and sex hormone levels among postmenopausal women in EPIC-Norfolk. *Cancer Research,* 65**,** 599-599.

LOWRY, O. H., ROSEBROUGH, N. J., FARR, A. L. & RANDALL, R. J. 1951. Protein measurement with the Folin phenol reagent. *J Biol Chem,* 193**,** 265-75.

LU, Z. & HUNTER, T. 2014. Prolyl isomerase Pin1 in cancer. *Cell research,* 24**,** 1033-1049.

LYNCH, E. D., OSTERMEYER, E. A., LEE, M. K., ARENA, J. F., JI, H., DANN, J., SWISSHELM, K., SUCHARD, D., MACLEOD, P. M. & KVINNSLAND, S. 1997. Inherited mutations in PTEN that are associated with breast cancer, cowden disease, and juvenile polyposis. *The American Journal of Human Genetics,* 61**,** 1254-1260.

LYNCH, H. T., SILVA, E., SNYDER, C. & LYNCH, J. F. 2008. Hereditary breast cancer: part I. Diagnosing hereditary breast cancer syndromes. *The breast journal,* 14**,** 3-13.

MA, Y., MIZINO, T. & ITO, H. 1991. Antitumor activity of some polysaccharides isolated from a Chinese mushroom,"Huangmo", the fruiting body of Hohenbuehelia serotina. *Agricultural and biological chemistry,* 55**,** 2701-2710.

MA, Z., KIM, Y. M., HOWARD, E. W., FENG, X., KOSANKE, S. D., YANG, S., JIANG, Y., PARRIS, A. B., CAO, X., LI, S. & YANG, X. 2018. DMBA promotes ErbB2-mediated carcinogenesis via ErbB2 and estrogen receptor pathway activation and genomic instability. *Oncol Rep,* 40**,** 1632-1640.

MAK, P., LEUNG, Y.-K., TANG, W.-Y., HARWOOD, C. & HO, S.-M. 2006. Apigenin suppresses cancer cell growth through ERβ. *Neoplasia,* 8**,** 896-904.

MARCHBANKS, P. A., MCDONALD, J. A., WILSON, H. G., FOLGER, S. G., MANDEL, M. G., DALING, J. R., BERNSTEIN, L., MALONE, K. E., URSIN, G. & STROM, B. L. 2002. Oral contraceptives and the risk of breast cancer. *New England journal of medicine,* 346**,** 2025-2032.

MARTEMUCCI, G., COSTAGLIOLA, C., MARIANO, M., D'ANDREA, L., NAPOLITANO, P. & D'ALESSANDRO, A. G. 2022. Free Radical Properties, Source and Targets, Antioxidant Consumption and Health. *Oxygen* [Online], 2.

MARTIN, S. A. 2016. The DNA mismatch repair pathway. *DNA Repair in Cancer Therapy.* Elsevier.

MARTIN, T. A., YE, L., SANDERS, A. J., LANE, J. & JIANG, W. G. 2013. Cancer invasion and metastasis: molecular and cellular perspective. *Madame Curie Bioscience Database [Internet].* Landes Bioscience.

MARUSYK, A. & POLYAK, K. 2010. Tumor heterogeneity: causes and consequences. *Biochim Biophys Acta,* 1805**,** 105-17.

MASCIARI, S., DILLON, D. A., RATH, M., ROBSON, M., WEITZEL, J. N., BALMANA, J., GRUBER, S. B., FORD, J. M., EUHUS, D. & LEBENSOHN, A. 2012. Breast cancer phenotype in women with TP53 germline mutations: a Li-Fraumeni syndrome consortium effort. *Breast cancer research and treatment,* 133**,** 1125-1130.

MATHEW, A., RAJAGOPAL, P. S., VILLGRAN, V., SANDHU, G. S., JANKOWITZ, R. C., JACOB, M., ROSENZWEIG, M., OESTERREICH, S. & BRUFSKY, A. 2017. Distinct Pattern of Metastases in Patients with Invasive Lobular Carcinoma of the Breast. *Geburtshilfe Frauenheilkd,* 77**,** 660-666.

MATHEW, N., ANITHA, M. G., BALA, T. S. L., SIVAKUMAR, S. M., NARMADHA, R. & KALYANASUNDARAM, M. 2009. Larvicidal activity of Saraca indica, Nyctanthes arbor-tristis, and Clitoria ternatea extracts against three mosquito vector species. *Parasitology research,* 104**,** 1017-1025.

MATHUR, P., SATHISHKUMAR, K., CHATURVEDI, M., DAS, P., SUDARSHAN, K. L., SANTHAPPAN, S., NALLASAMY, V., JOHN, A., NARASIMHAN, S. & ROSELIND, F. S. J. J. G. O. 2020. Cancer statistics, 2020: report from national cancer registry programme, India. 6**,** 1063-1075.

MAZUMDAR, U. K., GUPTA, M., MAITI, S. & MUKHERJEE, D. 1997. Antitumor activity of Hygrophila spinosa on Ehrlich ascites carcinoma and sarcoma-180 induced mice. *Indian Journal of Experimental Biology,* 35**,** 473-477.

MCCARTHY, M., AUDA, G., AGRAWAL, S., TAYLOR, A., BACKSTROM, Z., MONDAL, D., MOROZ, K. & DASH, S. 2014. In vivo anticancer synergy mechanism of doxorubicin and verapamil combination treatment is impaired in BALB/c mice with metastatic breast cancer. *Experimental and molecular pathology,* 97**,** 6-15.

MCCORD, J. M. & FRIDOVICH, I. 1969. Superoxide dismutase: an enzymic function for erythrocuprein (hemocuprein). *Journal of Biological chemistry,* 244**,** 6049-6055.

MCLACHLAN, J. A. 1993. Functional toxicology: a new approach to detect biologically active xenobiotics. *Environmental Health Perspectives,* 101**,** 386-387.

MCQUEEN, M. 1975. True Arrhenius relationships of human lactate dehydrogenase. *Zeitschrift für Klinische Chemie und Klinische Biochemie***,** 17-20.

MEDINA, D. 2010. Of mice and women: A short history of mouse mammary cancer research with an emphasis on the paradigms inspired by the transplantation method. *Cold Spring Harbor perspectives in biology,* 2**,** a004523.

MENG, X. Y., ZHANG, H. X., MEZEI, M. & CUI, M. 2011. Molecular docking: a powerful approach for structure-based drug discovery. *Curr Comput Aided Drug Des,* 7**,** 146-57.

MENSE, S. M., HEI, T. K., GANJU, R. K. & BHAT, H. K. 2008. Phytoestrogens and breast cancer prevention: possible mechanisms of action. *Environmental health perspectives,* 116**,** 426-433.

MENTA, A., FOUAD, T. M., LUCCI, A., LE-PETROSS, H., STAUDER, M. C., WOODWARD, W. A., UENO, N. T. & LIM, B. 2018. Inflammatory breast cancer: what to know about this unique, aggressive breast cancer. *Surgical Clinics,* 98**,** 787-800.

MICKS, E. A. & JENSEN, J. T. 2013. Treatment of heavy menstrual bleeding with the estradiol valerate and dienogest oral contraceptive pill. *Advances in therapy,* 30**,** 1-13.

MILLER, K., WANG, M., GRALOW, J., DICKLER, M., COBLEIGH, M., PEREZ, E. A., SHENKIER, T., CELLA, D. & DAVIDSON, N. E. 2007. Paclitaxel plus bevacizumab versus paclitaxel alone for metastatic breast cancer. *New England journal of medicine,* 357**,** 2666-2676.

MILLER, W. R. Aromatase inhibitors: mechanism of action and role in the treatment of breast cancer. 2003 2003. Elsevier, 3-11.

MINARI, J. B., OGAR, G. O. & BELLO, A. J. 2016. Antiproliferative potential of aqueous leaf extract of Mucuna pruriens on DMBA-induced breast cancer in female albino rats. *Egyptian Journal of Medical Human Genetics,* 17**,** 331-343.

MITTAL, A., KADYAN, P., GAHLAUT, A. & DABUR, R. 2013a. Nontargeted identification of the phenolic and other compounds of Saraca asoca by high performance liquid chromatography-positive electrospray ionization and quadrupole time-of-flight mass spectrometry. *International Scholarly Research Notices,* 2013.

MITTAL, A., KADYAN, P., GAHLAUT, A. & DABUR, R. J. I. S. R. N. 2013b. Nontargeted identification of the phenolic and other compounds of Saraca asoca by high performance liquid chromatography-positive electrospray ionization and quadrupole time-of-flight mass spectrometry. 2013.

MOHAN, C., KISTAMMA, S., VANI, P. & NARSHIMHA REDDY, A. 2016. Biological activities of different parts of Saraca asoca an endangered valuable medicinal plant. *Int. J. Curr. Microbiol. App. Sci,* 5**,** 300-308.

MOLDÉUS, P., HÖGBERG, J. & ORRENIUS, S. 1978. [4] Isolation and use of liver cells. *Methods in enzymology.* Elsevier.

MONCADA, S., PALMER, R. M. L. & HIGGS, E. A. 1991. Nitric oxide: physiology, pathophysiology, and pharmacology. *Pharmacological reviews,* 43**,** 109-142.

MORON, M. S., DEPIERRE, J. W. & MANNERVIK, B. 1979. Levels of glutathione, glutathione reductase and glutathione S-transferase activities in rat lung and liver. *J Biochimica et biophysica acta -general subjects,* 582**,** 67-78.

MOSMANN, T. 1983. Rapid colorimetric assay for cellular growth and survival: application to proliferation and cytotoxicity assays. *Journal of immunological methods,* 65**,** 55-63.

MOUTSATSOU, P. 2007. The spectrum of phytoestrogens in nature: our knowledge is expanding. *HORMONES-ATHENS-,* 6**,** 173.

MUGGERUD, A. A., HALLETT, M., JOHNSEN, H., KLEIVI, K., ZHOU, W., TAHMASEBPOOR, S., AMINI, R.-M., BOTLING, J., BØRRESEN-DALE, A.-L. & SØRLIE, T. 2010. Molecular diversity in ductal carcinoma *in situ* (DCIS) and early invasive breast cancer. *Molecular oncology,* 4**,** 357-368.

MUKHOPADHYAY, M. K. & NATH, D. 2011. Phytochemical screening and toxicity study of Saraca asoca bark methanolic extract. *Int J Phytomed,* 3**,** 498.

MUKHOPADHYAY, M. K., SHAW, M. & NATH, D. 2017. Chemopreventive potential of major flavonoid compound of methanolic bark extract of Saraca asoca (Roxb.) in benzene-induced toxicity of acute myeloid leukemia mice. *Pharmacognosy Magazine,* 13**,** S216.

NABAVI, S. F., NABAVI, S. M., HABTEMARIAM, S., MOGHADDAM, A. H., SUREDA, A., JAFARI, M. & LATIFI, A. M. 2013. Hepatoprotective effect of gallic acid isolated from Peltiphyllum peltatum against sodium fluoride-induced oxidative stress. *Industrial Crops and Products,* 44**,** 50-55.

NABAVI, S. M., NABAVI, S. F., ESLAMI, S. & MOGHADDAM, A. H. 2012. In vivo protective effects of quercetin against sodium fluoride-induced oxidative stress in the hepatic tissue. *Food Chemistry,* 132**,** 931-935.

NAITHANI, N., SINHA, S., MISRA, P., VASUDEVAN, B. & SAHU, R. 2021. Precision medicine: Concept and tools. *Med J Armed Forces India,* 77**,** 249-257.

NAKAGAWA, T. & YOKOZAWA, T. 2002. Direct scavenging of nitric oxide and superoxide by green tea. *Food and chemical Toxicology,* 40**,** 1745-1750.

NAKANISHI, C., YAMAGUCHI, T., IIJIMA, T., SAJI, S., TOI, M., MORI, T. & MIYAKI, M. 2005. Germline mutation of the LKB1/STK11 gene with loss of the normal allele in an aggressive breast cancer of Peutz-Jeghers syndrome. *Oncology,* 67**,** 476-479.

NCUBE, B. & VAN STADEN, J. 2015. Tilting plant metabolism for improved metabolite biosynthesis and enhanced human benefit. *Molecules,* 20**,** 12698-12731.

NEWBOLD, R. R., HANSON, R. B. & JEFFERSON, W. N. 1997. Ontogeny of lactoferrin in the developing mouse uterus: a marker of early hormone response. *Biology of reproduction,* 56**,** 1147-1157.

NGUYEN, L. T., LEE, Y. H., SHARMA, A. R., PARK, J. B., JAGGA, S., SHARMA, G., LEE, S. S. & NAM, J. S. 2017. Quercetin induces apoptosis and cell cycle arrest in triple-negative breast cancer cells through modulation of Foxo3a activity. *Korean J Physiol Pharmacol,* 21**,** 205-213.

NICHOLAS, C., BATRA, S., VARGO, M. A., VOSS, O. H., GAVRILIN, M. A., WEWERS, M. D., GUTTRIDGE, D. C., GROTEWOLD, E. & DOSEFF, A. I. 2007. Apigenin blocks lipopolysaccharide-induced lethality in vivo and proinflammatory cytokines expression by inactivating NF-κB through the suppression of p65 phosphorylation. *The Journal of Immunology,* 179**,** 7121-7127.

NIGJEH, S. E., YEAP, S. K., NORDIN, N., RAHMAN, H. & ROSLI, R. 2019. In vivo anti-tumor effects of citral on 4T1 breast cancer cells via induction of apoptosis and downregulation of aldehyde dehydrogenase activity. *Molecules,* 24**,** 3241.

NISHIDA, N., YANO, H., NISHIDA, T., KAMURA, T. & KOJIRO, M. 2006. Angiogenesis in cancer. *Vasc Health Risk Manag,* 2**,** 213-9.

NJOKUA, D. I., CHIDIEBERE, M. A., OGUZIE, K. L., OGUKWE, C. E. & OGUZIE, E. E. 2013. Corrosion inhibition of mild steel in hydrochloric acid solution by the leaf extract of Nicotiana tabacum. *Advances in Materials and Corrosion,* 2**,** 54-61.

NOBILI, S., LIPPI, D., WITORT, E., DONNINI, M., BAUSI, L., MINI, E. & CAPACCIOLI, S. 2009. Natural compounds for cancer treatment and prevention. *Pharmacological research,* 59**,** 365-378.

NOWAK, M. A. & WACLAW, B. 2017. Genes, environment, and "bad luck". *Science,* 355**,** 1266-1267.

O'CONNELL, J. 2002. Fas ligand and the fate of antitumour cytotoxic T lymphocytes. *Immunology,* 105**,** 263-6.

ODEY, M., IWARA, I., UDIBA, U., JOHNSON, J., INEKWE, U., ASENYE, M., VICTOR, O. J. I. J. O. S. & TECHNOLOGY 2012. Preparation of plant extracts from indigenous medicinal plants. 1**,** 688-692.

OECD 2006c. OECD Report of the Validation of the Rodent Uterotrophic Bioassay: Phase 2 - Testing of Potent and Weak Oestrogen Agonists by Multiple Laboratories No. 66OECD (2007a). Guidance Document on the Uterotrophic Bioassay - Procedure to Test for Antioestrogenicity. *OECD Series on Testing and Assessment* No. 71.

OECD 2007. *Additional data supporting the Test Guideline on the Uterotrophic Bioassay in rodents*, OECD Environmental Health and Safety Publication Series on Testing and Assessment.

OECD 2008. Guideline for testing of chemicals: acute oral toxicity–up-and-down procedure. *Organization for Economic Cooperation and Development*.

OECD/OCDE 2007. OECD GUIDELINE FOR THE TESTING OF CHEMICALS; Uterotrophic Bioassay in Rodents: A short-term screening test for oestrogenic properties.

OHKAWA, H., OHISHI, N. & YAGI, K. 1979. Assay for lipid peroxides in animal tissues by thiobarbituric acid reaction. *Anal Biochem,* 95**,** 351-8.

OKUMURA, S., KONISHI, Y., NARUKAWA, M., SUGIURA, Y., YOSHIMOTO, S., ARAI, Y., SATO, S., YOSHIDA, Y., TSUJI, S. & UEMURA, K. 2021. Gut bacteria identified in colorectal cancer patients promote tumourigenesis via butyrate secretion. *Nature communications,* 12**,** 5674.

OMOTO, Y. & IWASE, H. 2015. Clinical significance of estrogen receptor β in breast and prostate cancer from biological aspects. *Cancer science,* 106**,** 337-343.

ONO, M., TORISU, H., FUKUSHI, J.-I., NISHIE, A. & KUWANO, M. 1999. Biological implications of macrophage infiltration in human tumor angiogenesis. *Cancer chemotherapy and pharmacology,* 43**,** S69-S71.

OWENS, J. W. & ASHBY, J. 2002. Critical review and evaluation of the uterotrophic bioassay for the identification of possible estrogen agonists and antagonists: in support of the validation of the OECD uterotrophic protocols for the laboratory rodent. *Critical reviews in toxicology,* 32**,** 445-520.

PADILLA-BANKS, E., JEFFERSON, W. N. & NEWBOLD, R. R. 2001. The immature mouse is a suitable model for detection of estrogenicity in the uterotropic bioassay. *Environmental health perspectives,* 109**,** 821-826.

PALMER, J. R., WISE, L. A., HORTON, N. J., ADAMS-CAMPBELL, L. L. & ROSENBERG, L. 2003. Dual effect of parity on breast cancer risk in African-American women. *Journal of the National Cancer Institute,* 95**,** 478-483.

PANCHAWAT, S., GAUTAM, R. K. & GOYAL, S. 2022. ANTI-ULCER ACTIVITY OF HYDRO-ALCOHOLIC EXTRACT OF SARACA ASOCA STEM BARK IN RATS. *Indian Drugs,* 59.

PARSA, N. 2012. Environmental factors inducing human cancers. *Iran J Public Health,* 41**,** 1-9.

PATERNI, I., GRANCHI, C., KATZENELLENBOGEN, J. A. & MINUTOLO, F. 2014. Estrogen receptors alpha (ERα) and beta (ERβ): subtype-selective ligands and clinical potential. *Steroids,* 90**,** 13-29.

PATIL, K. R., MAHAJAN, U. B., UNGER, B. S., GOYAL, S. N., BELEMKAR, S., SURANA, S. J., OJHA, S. & PATIL, C. R. 2019. Animal models of inflammation for screening of anti-inflammatory drugs: implications for the discovery and development of phytopharmaceuticals. *International journal of molecular sciences,* 20**,** 4367.

PATIL, K. R. & PATIL, C. R. 2017. Anti-inflammatory activity of bartogenic acid containing fraction of fruits of Barringtonia racemosa Roxb. in acute and chronic animal models of inflammation. *Journal of Traditional and Complementary Medicine,* 7**,** 86-93.

PATISAUL, H. B. & JEFFERSON, W. 2010. The pros and cons of phytoestrogens. *Frontiers in neuroendocrinology,* 31**,** 400-419.

PEDDI, P. F., ELLIS, M. J. & MA, C. 2012. Molecular basis of triple negative breast cancer and implications for therapy. *International journal of breast cancer,* 2012.

PERIANAYAGAM, J. B., SHARMA, S. K. & PILLAI, K. K. 2006. Anti-inflammatory activity of Trichodesma indicum root extract in experimental animals. *Journal of ethnopharmacology,* 104**,** 410-414.

PHANIENDRA, A., JESTADI, D. B. & PERIYASAMY, L. 2015. Free radicals: properties, sources, targets, and their implication in various diseases. *Indian J Clin Biochem,* 30**,** 11-26.

PHAROAH, P. D. P., GUILFORD, P., CALDAS, C. & INTERNATIONAL GASTRIC CANCER LINKAGE, C. 2001. Incidence of gastric cancer and breast cancer in CDH1 (E-cadherin) mutation carriers from hereditary diffuse gastric cancer families. *Gastroenterology,* 121**,** 1348-1353.

PILLAI, L. S., REGIDI, S., VARGHESE, S. D., RAVINDRAN, S., MAYA, V., VARGHESE, J., RAMASWAMI, K., GOPIMOHAN, R. & GOPI, M. 2018. Nonhormonal selective estrogen receptor modulator 1-(2-[4-{(3R, 4S)-7-Methoxy-2, 2-dimethyl-3-phenyl-chroman-4yl} phenoxy] ethyl) pyrrolidine hydrochloride (ormeloxifene hydrochloride) for the treatment of breast cancer. *Drug development research,* 79**,** 275-286.

PLANTE, I. 2021. Chapter 2 - Dimethylbenz(a)anthracene-induced mammary tumorigenesis in mice. *In:* GALLUZZI, L. & BUQUÉ, A. (eds.) *Methods in Cell Biology.* Academic Press.

PLESCA, D., MAZUMDER, S. & ALMASAN, A. 2008. DNA damage response and apoptosis. *Methods in enzymology,* 446**,** 107-122.

PORTAL, K. P. D. H. S.-I. B. 2021. India Biodiversity Portal.

PRADHAN, P., JOSEPH, L., GUPTA, V., CHULET, R., ARYA, H., VERMA, R. & BAJPAI, A. 2009. Saraca asoca (Ashoka): a review. *Journal of chemical and pharmaceutical research,* 1**,** 62-71.

PRAY, L. A. 2008. Gleevec: the breakthrough in cancer treatment. *Nature Education,* 1**,** 37.

PULASKI, B. A. & OSTRAND-ROSENBERG, S. 2001. Mouse 4T1 breast tumor model. Curr Protoc Immunol Chapter 20. *Unit 20.2.*

RAHMAN, N. & SCOTT, R. H. 2007. Cancer genes associated with phenotypes in monoallelic and biallelic mutation carriers: new lessons from old players. *Human molecular genetics,* 16**,** R60-R66.

RAJAN, S., JOHNSON, J. & SELVICHRISTY, J. 2008. Antibacterial activity and preliminary screening of the extracts of the bark of Saraca asoca. *J. Sci. Trans. Environ,* 1**,** 149-151.

RAJARATINAM, H., RASUDIN, N. S., SAFUAN, S., ABDULLAH, N. A., MOKHTAR, N. F. & MOHD FUAD, W. E. 2022. Passage Number of 4T1 Cells Influences the Development of Tumour and the Progression of Metastasis in 4T1 Orthotopic Mice. *Malays J Med Sci,* 29**,** 30-42.

RAKHA, E. A. & ELLIS, I. O. 2009. Triple-negative/basal-like breast cancer. *Pathology,* 41**,** 40-47.

RALHAN, R. & KAUR, J. 2007. Alkylating agents and cancer therapy. *Expert Opinion on Therapeutic Patents,* 17**,** 1061-1075.

RANGANATHAN, P., SENGAR, M., CHINNASWAMY, G., AGRAWAL, G., ARUMUGHAM, R., BHATT, R., BILIMAGGA, R., CHAKRABARTI, J., CHANDRASEKHARAN, A. & CHATURVEDI, H. K. J. T. L. O. 2021. Impact of COVID-19 on cancer care in India: a cohort study. 22**,** 970-976.

RATHEE, P., RATHEE, S., RATHEE, D. & RATHEE, D. J. D. P. C. 2010. Quantitative estimation of (+)-Catechin in stem bark of Saraca asoka Linn using HPTLC. 2**,** 306-314.

REINLI, K. & BLOCK, G. 1996. Phytoestrogen content of foods—a compendium of literature values. *Nutrition and cancer,* 26**,** 123-148.

REITMAN, S. & FRANKEL, S. 1957. A colorimetric method for the determination of serum glutamic oxalacetic and glutamic pyruvic transaminases. *American journal of clinical pathology,* 28**,** 56-63.

RENOIR, J.-M., MARSAUD, V. & LAZENNEC, G. 2013. Estrogen receptor signaling as a target for novel breast cancer therapeutics. *Biochemical pharmacology,* 85**,** 449-465.

RENVOIZE, C., BIOLA, A., PALLARDY, M. & BREARD, J. 1998. Apoptosis: identification of dying cells. *Cell biology and toxicology,* 14**,** 111-120.

RESENDE, F. A., DE OLIVEIRA, A. P. S., DE CAMARGO, M. S., VILEGAS, W. & VARANDA, E. A. 2013. Evaluation of estrogenic potential of flavonoids using a recombinant yeast strain and MCF7/BUS cell proliferation assay. *Plos one,* 8**,** e74881.

RIBBLE, D., GOLDSTEIN, N. B., NORRIS, D. A. & SHELLMAN, Y. G. 2005. A simple technique for quantifying apoptosis in 96-well plates. *BMC biotechnology,* 5**,** 1-7.

RICE, S. & WHITEHEAD, S. A. 2006. Phytoestrogens and breast cancer–promoters or protectors? *Endocrine-Related Cancer,* 13**,** 995-1015.

ROBERTS, M. E., JACKSON, S. A., SUSSWEIN, L. R., ZEINOMAR, N., MA, X., MARSHALL, M. L., STETTNER, A. R., MILEWSKI, B., XU, Z. & SOLOMON, B. D. 2018. MSH6 and PMS2 germ-line pathogenic variants implicated in Lynch syndrome are associated with breast cancer. *Genetics in Medicine,* 20**,** 1167-1174.

RUSSNES, H. G., LINGJÆRDE, O. C., BØRRESEN-DALE, A.-L. & CALDAS, C. 2017. Breast Cancer Molecular Stratification: From Intrinsic Subtypes to Integrative Clusters. *The American Journal of Pathology,* 187**,** 2152-2162.

RUSSO, J. & RUSSO, I. H. 2006. The role of estrogen in the initiation of breast cancer. *J Steroid Biochem Mol Biol,* 102**,** 89-96.

SAHA, J., MITRA, T., GUPTA, K. & MUKHERJEE, S. 2012. Phytoconstituents and HPTLC analysis in Saraca asoca (Roxb.) Wilde. *International Journal of Pharmacy and Pharmaceutical Sciences,* 4**,** 96-99.

SAHA, J., MUKHERJEE, S., GUPTA, K. & GUPTA, B. J. J. O. P. R. 2013. High-performance thin-layer chromatographic analysis of antioxidants present in different parts of Saraca asoca (Roxb.) de Wilde. 7**,** 798-803.

SAK, K. 2012. Chemotherapy and dietary phytochemical agents. *Chemotherapy research and practice,* 2012.

SAKAMOTO, T., HORIGUCHI, H., OGUMA, E. & KAYAMA, F. 2010. Effects of diverse dietary phytoestrogens on cell growth, cell cycle and apoptosis in estrogen-receptor-positive breast cancer cells. *The Journal of nutritional biochemistry,* 21**,** 856-864.

SANDHU, G. S., ERQOU, S., PATTERSON, H. & MATHEW, A. 2016. Prevalence of triple-negative breast cancer in India: systematic review and meta-analysis. *Journal of global oncology,* 2**,** 412-421.

SARACA ASOCA, T. W. 2023.

SARKAR, S. & MANDAL, M. 2011. Breast cancer: classification based on molecular etiology influencing prognosis and prediction. *Breast Cancer-Focusing Tumor Microenvironment, Stem cells and Metastasis.*

SASIDHARAN, N. & PADIKKALA, J. 2012. Evaluation of Saraca asoca, Kaempferia rotunda, their substitutes and medicinal preparations with respect to phytochemical and biological properties. *Kerala Forest Research Institute Research Report,* No.424: 83,84

SASIDHARAN, S., CHEN, Y., SARAVANAN, D., SUNDRAM, K. M. & YOGA LATHA, L. 2011. Extraction, isolation and characterization of bioactive compounds from plants' extracts. *Afr J Tradit Complement Altern Med,* 8**,** 1-10.

SASMAL, S., MAJUMDAR, S., GUPTA, M., MUKHERJEE, A. & MUKHERJEE, P. K. 2012. Pharmacognostical, phytochemical and pharmacological evaluation for the antipyretic effect of the seeds of Saraca asoca Roxb. *Asian Pacific journal of tropical biomedicine,* 2**,** 782-786.

SCHMITTGEN, T. D. & LIVAK, K. J. 2008. Analyzing real-time PCR data by the comparative C(T) method. *Nat Protoc,* 3**,** 1101-8.

SEETHARAM, Y. N., SUJEETH, H., JYOTHISHWARAN, G., BARAD, A., SHARANABASAPPA, G. & PARVEEN, S. 2003. Antibacterial activity of Saraca asoca bark.

SEGAWA, S., TAKATA, Y., KANEDA, H. & WATARI, J. 2007. Effects of a hop water extract on the compound 48/80-stimulated vascular permeability in ICR mice and histamine release from OVA-sensitized BALB/c mice. *Bioscience, biotechnology, and biochemistry,* 71**,** 1577-1581.

SEO, H.-S., JU, J.-H., JANG, K. & SHIN, I. 2011. Induction of apoptotic cell death by phytoestrogens by up-regulating the levels of phospho-p53 and p21 in normal and malignant estrogen receptor α–negative breast cells. *Nutrition research,* 31**,** 139-146.

SEVERINO, M. 2011. Dysfunctional Uterine Bleeding. *Glob. libr. women's med*.

SEYFRIED, T. N. & HUYSENTRUYT, L. C. 2013. On the origin of cancer metastasis. *Crit Rev Oncog,* 18**,** 43-73.

SHAHID, A. P., SALINI, S., SASIDHARAN, N., PADIKKALA, J., RAGHAVAMENON, A. C. & BABU, T. D. 2015. Effect of Saraca asoca (Asoka) on estradiol-induced keratinizing metaplasia in rat uterus. *Journal of Basic and Clinical Physiology and Pharmacology,* 26**,** 509-515.

SHAHID, A. P., SASIDHARAN, N., SALINI, S., PADIKKALA, J., MEERA, N., RAGHAVAMENON, A. C. & BABU, T. D. 2018. Kingiodendron pinnatum, a pharmacologically effective alternative for Saraca asoca in an Ayurvedic preparation, *Asokarishta. Journal of Traditional and Complementary Medicine,* 8**,** 244-250.

SHALABY, E. A. & SHANAB, S. M. M. 2013. Comparison of DPPH and ABTS assays for determining antioxidant potential of water and methanol extracts of Spirulina platensis.

SHARIF, M. K., HOSSAIN, M., UDDIN, M. E., FAROOQ, A. T. M. O., ISLAM, M. A. & SHARIF, M. M. 2011. Studies on the anti-inflammatory and analgesic efficacy of Saraca asoca in laboratory animals. *Archives of Pharmacy Practice,* 2**,** 16-22.

SHARMA, G. N., DAVE, R., SANADYA, J., SHARMA, P. & SHARMA, K. K. 2010. Various types and management of breast cancer: an overview. *Journal of advanced pharmaceutical technology & research,* 1**,** 109.

SHARMA, L., BAHGA, H. & SRIVASTAVA, P. 1971. In vitro anthelmintic screening of indigenous medicinal plants against Haemonchus contortus (Rudolphi, 1803) Cobbold, 1898 of sheep and goats. *J Indian Journal of Animal Research,* 5**,** 33-38.

SHARMA, S., TIWARI, G. & TIWARI, R. 2021. Development and Validation of UV-Spectrophotometric method for the Estimation of Saraca asoca, Bauhinia variegata Linn, and Commiphora mukul in standardized Polyherbal Formulation. *Journal of Pharmaceutical Sciences and Research,* 13**,** 525-528.

SHEIK, S. & CHANDRASHEKAR, K. R. 2014. Antimicrobial and antioxidant activities of Kingiodendron pinnatum (DC.) Harms and Humboldtia brunonis Wallich: endemic plants of the Western Ghats of India. *Journal of the National Science Foundation of Sri Lanka,* 42.

SHERIN, D. R. & MANOJKUMAR, T. K. 2017. Flavanoids from Saraca asoca-Ideal Medication for Breast Cancer-A Molecular Simulation Approach. *Biomedical Journal of Scientific & Technical Research,* 1**,** 1761-1763.

SHERR, C. J. 2004. Principles of tumor suppression. *Cell,* 116**,** 235-246.

SHIRAVAND, Y., KHODADADI, F., KASHANI, S. M. A., HOSSEINI-FARD, S. R., HOSSEINI, S., SADEGHIRAD, H., LADWA, R., O'BYRNE, K. & KULASINGHE, A. 2022. Immune Checkpoint Inhibitors in Cancer Therapy. *Curr Oncol,* 29**,** 3044-3060.

SHIROLKAR, A., GAHLAUT, A., CHHILLAR, A. K. & DABUR, R. 2013. Quantitative analysis of catechins in Saraca asoca and correlation with antimicrobial activity. *Journal of pharmaceutical analysis,* 3**,** 421-428.

SHUEN, A. Y. & FOULKES, W. D. 2011. Inherited mutations in breast cancer genes—risk and response. *Journal of mammary gland biology and neoplasia,* 16**,** 3-15.

SINGH, A. K., SINGH, A. K., SINGH, M., YADAV, V. K. & SINGH, N. 2014. In-vitro anthelmintic activity of stem bark extracts of Saraca indica Roxb. against Pheretima posthuma. *Asian Journal of Research in Chemistry,* 7**,** 141-143.

SINGH, S., KRISHNA, T. H. A., KAMALRAJ, S., KURIAKOSE, G. C., VALAYIL, J. M. & JAYABASKARAN, C. 2015. Phytomedicinal importance of Saraca asoca (Ashoka): an exciting past, an emerging present and a promising future. *Current Science***,** 1790-1801.

SINGH, S. K., BANERJEE, S., ACOSTA, E. P., LILLARD, J. W. & SINGH, R. 2017. Resveratrol induces cell cycle arrest and apoptosis with docetaxel in prostate cancer cells via a p53/p21WAF1/CIP1 and p27KIP1 pathway. *Oncotarget,* 8**,** 17216.

SIVARAJAN, V. V. & BALACHANDRAN, I. 1994. Ayurvedic Drugs and their Plant Sources Oxford and IBH Publishing Co. *Pvt. Ltd***,** 374-376.

SOLA, B. & RENOIR, J.-M. 2006. Antiestrogenic therapies in solid cancers and multiple myeloma. *Current Molecular Medicine,* 6**,** 359-368.

SOLANKI, P. A., KO, N. Y., QATO, D. M. & CALIP, G. S. 2016. Risk of cancer-specific, cardiovascular, and all-cause mortality among Asian and Pacific Islander breast cancer survivors in the United States, 1991–2011. *Springerplus,* 5**,** 1-12.

SONG, Q., MERAJVER, S. D. & LI, J. Z. 2015. Cancer classification in the genomic era: five contemporary problems. *Human Genomics,* 9**,** 27.

SOTO, A. M. & SONNENSCHEIN, C. 1985. The role of estrogens on the proliferation of human breast tumor cells (MCF-7). *Journal of steroid biochemistry,* 23**,** 87-94.

SOTO, A. M., SONNENSCHEIN, C., CHUNG, K. L., FERNANDEZ, M. F., OLEA, N. & SERRANO, F. O. 1995. The E-SCREEN assay as a tool to identify estrogens: an update on estrogenic environmental pollutants. *Environ Health Perspect,* 103 Suppl 7**,** 113-22.

SRIVASTAVA, P., VYAS, V. K., VARIYA, B., PATEL, P., QURESHI, G. & GHATE, M. 2016. Synthesis, anti-inflammatory, analgesic, 5-lipoxygenase (5-LOX) inhibition activities, and molecular docking study of 7-substituted coumarin derivatives. *Bioorganic chemistry,* 67**,** 130-138.

ŚRUTEK, E., NOWIKIEWICZ, T. & ZEGARSKI, W. 2017. Current guidelines on the diagnosis and management of lobular carcinoma *in situ*. *Current Gynecologic Oncology,* 15**,** 87-90.

STEWARD, W. P. & BROWN, K. 2013. Cancer chemoprevention: a rapidly evolving field. *Br J Cancer,* 109**,** 1-7.

STEWART, B. W. 1994. Mechanisms of apoptosis: integration of genetic, biochemical, and cellular indicators. *JNCI: Journal of the National Cancer Institute,* 86**,** 1286-1296.

STRAUB, R. H. 2007. The complex role of estrogens in inflammation. *Endocrine reviews,* 28**,** 521-574.

STRUNECKA, A., PATOCKA, J., BLAYLOCK, R. L. & CHINOY, N. J. 2007. Fluoride interactions: from molecules to disease. *Current Signal Transduction Therapy,* 2**,** 190-213.

SUGANYA, J., RADHA, M., NAOREM, D. L. & NISHANDHINI, M. 2014. In silico docking studies of selected flavonoids-natural healing agents against breast cancer. *Asian Pacific Journal of Cancer Prevention,* 15**,** 8155-8159.

SUHAIL, P. T. 2019. Comparative evaluation of antioxidant activity of methanolic extract of Saraca asoca and its commonly used substitute plants. *Int. J. Res. Rev,* 6**,** 37-43.

SUHAIL, P. T., BALASUBRAMANIAN, T., ROSHINI, K. V. & ANIL, K. 2019. A Comparative Evaluation Study of Anti-inflammatory Activity of Saraca asoca and its Commonly used Substitute Plants. *Asian Journal of Pharmaceutical and Health Sciences,* 9.

SULAIMAN, C. T., JYOTHI, C. K., PRABHUKUMAR, K. M. & BALACHANDRAN, I. 2020. Identification of validated substitute for Asoka (Saraca asoca (Roxb.) Willd.) by phytochemical and pharmacological evaluations. *Future Journal of Pharmaceutical Sciences,* 6.

SUMANGALA, R. C., ROSARIO, S., CHARLES, B., GANESH, D. & RAVIKANTH, G. 2017. Identifying conservation priority sites for Saraca asoca: an important medicinal plant using ecological Niche models. *Indian Forester,* 143**,** 531-536.

SUNG, H., FERLAY, J., SIEGEL, R. L., LAVERSANNE, M., SOERJOMATARAM, I., JEMAL, A. & BRAY, F. 2021. Global cancer statistics 2020: GLOBOCAN estimates of incidence and mortality worldwide for 36 cancers in 185 countries. *CA: a cancer journal for clinicians,* 71**,** 209-249.

SUNG, J. J. Y., LAU, J. Y. W., GOH, K. L. & LEUNG, W. K. 2005. Increasing incidence of colorectal cancer in Asia: implications for screening. *The lancet oncology,* 6**,** 871-876.

SUTHA, S., MOHAN, V. R., KUMARESAN, S., MURUGAN, C. & ATHIPERUMALSAMI, T. 2010. Ethnomedicinal plants used by the tribals of Kalakad-Mundanthurai Tiger Reserve (KMTR), Western Ghats, Tamil Nadu for the treatment of rheumatism.

SWAR, G., SHAILAJAN, S. & MENON, S. 2017. Activity based evaluation of a traditional Ayurvedic medicinal plant: Saraca asoca (Roxb.) de Wilde flowers as estrogenic agents using ovariectomized rat model. *Journal of ethnopharmacology,* 195**,** 324-333.

SWEET, M. G., SCHMIDT-DALTON, T. A., WEISS, P. M. & MADSEN, K. P. 2012. Evaluation and management of abnormal uterine bleeding in premenopausal women. *American family physician,* 85**,** 35-43.

SWETHA, M., KEERTHANA, C. K., RAYGINIA, T. P. & ANTO, R. J. 2022. Cancer chemoprevention: A strategic approach using phytochemicals. *Frontiers in Pharmacology,* 12**,** 809308.

TAIRA, J., NANBU, H. & UEDA, K. 2009. Nitric oxide-scavenging compounds in Agrimonia pilosa Ledeb on LPS-induced RAW264. 7 macrophages. *Food chemistry,* 115**,** 1221-1227.

TAKANO, E. A., YOUNES, M. M., MEEHAN, K., SPALDING, L., YAN, M., ALLAN, P., FOX, S. B., REDFERN, A., CLOUSTON, D., GILES, G. G., CHRISTIE, E. L., ANDERSON, R. L., ZETHOVEN, M., PHILLIPS, K.-A., GORRINGE, K. & BRITT, K. L. 2023. Estrogen receptor beta expression in triple negative breast cancers is not associated with recurrence or survival. *BMC Cancer,* 23**,** 459.

THEFELD, W., HOFFMEISTER, H., BUSCH, E., KOLLER, P. & VOLLMAR, J. 1974. Reference values for the determination of GOT, GPT, and alkaline phosphatase in serum with optimal standard methods (author's transl). *Deutsche Medizinische Wochenschrift,* 99**,** 343-4 passim.

THILAGAM, E., CHIDAMBARAM, K., RAVITEJA, C., VAHANA, T., VASUDEVAN, P. & GARRIDO, G. 2021. Anti-hyperglycemic and hypolipidemic effects of Saraca asoca (Roxb.) Wild. flowers in alloxan-treated diabetic rats. *J Pharm Pharmacogn Res,* 9**,** 58-68.

THOMSEN, N. D., KOERBER, J. T. & WELLS, J. A. 2013. Structural snapshots reveal distinct mechanisms of procaspase-3 and-7 activation. *Proceedings of the National Academy of Sciences,* 110**,** 8477-8482.

TODORIC, J., ANTONUCCI, L. & KARIN, M. 2016. Targeting inflammation in cancer prevention and therapy. *Cancer Prevention Research,* 9**,** 895-905.

TOLG, C., COWMAN, M. & TURLEY, E. A. 2018. Mouse mammary gland whole mount preparation and analysis. *Bio-protocol,* 8**,** e2915-e2915.

TOMASETTI, C. & VOGELSTEIN, B. 2015. Variation in cancer risk among tissues can be explained by the number of stem cell divisions. *Science,* 347**,** 78-81.

TOMLINSON-HANSEN, S., KHAN, M. & CASSARO, S. 2023. Atypical Ductal Hyperplasia. *StatPearls.* Treasure Island (FL) with ineligible companies. Disclosure: Myra Khan declares no relevant financial relationships with ineligible companies. Disclosure: Sebastiano Cassaro declares no relevant financial relationships with ineligible companies.: StatPearls Publishing Copyright © 2023, StatPearls Publishing LLC.

TORO, G. & ACKERMANN, P. G. 1975. *Practical clinical chemistry*, Little Brown & Company.

TRABERT, B., SHERMAN, M. E., KANNAN, N. & STANCZYK, F. Z. 2020. Progesterone and breast cancer. *Endocrine reviews,* 41**,** 320-344.

TRAN, G. B., TRAN, T. P. N. & NGUYEN, T. T. 2018. Characterization of Crilin and Nanocurcumin's Synergistic Effect on Treatment for 7.12-Dimethylbenz [a] anthracene (DMBA)-Induced Breast Cancer Mice. *VNU Journal of Science: Medical and Pharmaceutical Sciences,* 34.

URSIN, G., ROSS, R. K., SULLIVAN-HALLEY, J., HANISCH, R., HENDERSON, B. & BERNSTEIN, L. 1998. Use of oral contraceptives and risk of breast cancer in young women. *Breast Cancer Res Treat,* 50**,** 175-84.

VAN DUURSEN, M. B. M. 2017. Modulation of estrogen synthesis and metabolism by phytoestrogens in vitro and the implications for women's health. *Toxicol Res (Camb),* 6**,** 772-794.

VAN ZIJL, F., KRUPITZA, G. & MIKULITS, W. 2011. Initial steps of metastasis: cell invasion and endothelial transmigration. *Mutat Res,* 728**,** 23-34.

VARAPRASAD, N., SURESH, A., SURESH, V., KUMAR, S. N., RAJENDAR, A. & MADESHWARAN, M. 2011. Antipyretic activity of methanolic extract of Saraca asoca (roxb.) de Wild leaves. *IJPRD,* 3**,** 202-207.

VARGHESE, C. D., NAIR, C. & PANIKKAR, K. R. 1992. Potential anticancer activity of saraca asoca extracts towards transplantable tumours in mice. *Indian Journal of Pharmaceutical Sciences,* 54**,** 37-40.

VARGHESE, C. D., NAIR, S. C., PANIKKAR, B. & PANIKKAR, K. R. 1993. Effect of asoka on the intracellular glutathione levels and skin tumour promotion in mice. *Cancer letters,* 69**,** 45-50.

VARRICCHIO, C. G. 2004. *A cancer source book for nurses*, Jones & Bartlett Learning.

VIDAL-CASANELLA, O., NÚÑEZ, O., GRANADOS, M., SAURINA, J. & SENTELLAS, S. 2021. Analytical methods for exploring nutraceuticals based on phenolic acids and polyphenols. *Applied Sciences,* 11**,** 8276.

VILLA, A., VEGETO, E., POLETTI, A. & MAGGI, A. 2016. Estrogens, Neuroinflammation, and Neurodegeneration. *Endocr Rev,* 37**,** 372-402.

VISVADER, J. E. 2011. Cells of origin in cancer. *Nature,* 469**,** 314-322.

WALTERS, M. I. & GERARDE, H. 1970. An ultramicromethod for the determination of conjugated and total bilirubin in serum or plasma. *Microchemical Journal,* 15**,** 231-243.

WALZ, C. & SATTLER, M. 2006. Novel targeted therapies to overcome imatinib mesylate resistance in chronic myeloid leukemia (CML). *Critical reviews in oncology/hematology,* 57**,** 145-164.

WANG, J. & XU, B. 2019. Targeted therapeutic options and future perspectives for HER2-positive breast cancer. *Signal Transduction and Targeted Therapy,* 4**,** 34.

WANG, T., LIU, Z., SHI, F. & WANG, J. 2016. Pin1 modulates chemo-resistance by up-regulating FoxM1 and the involvements of Wnt/β-catenin signaling pathway in cervical cancer. *Molecular and cellular biochemistry,* 413**,** 179-187.

WANG, T. H., WANG, H. S. & SOONG, Y. K. 2000. Paclitaxel-induced cell death: where the cell cycle and apoptosis come together. *Cancer: Interdisciplinary International Journal of the American Cancer Society,* 88**,** 2619-2628.

WANG, Y., SHI, J., CHAI, K., YING, X. & ZHOU, B. P. 2013. The Role of Snail in EMT and Tumorigenesis. *Curr Cancer Drug Targets,* 13**,** 963-972.

WANG, Z. & ZHANG, X. 2017. Chemopreventive activity of honokiol against 7, 12-dimethylbenz [a] anthracene-induced mammary cancer in female Sprague Dawley rats. *Frontiers in Pharmacology,* 8**,** 320.

WEITZEL, J. N., NEUHAUSEN, S. L., ADAMSON, A., TAO, S., RICKER, C., MAOZ, A., ROSENBLATT, M., NEHORAY, B., SAND, S. & STEELE, L. 2019. Pathogenic and likely pathogenic variants in PALB2, CHEK2, and other known breast cancer susceptibility genes among 1054 BRCA-negative Hispanics with breast cancer. *Cancer,* 125**,** 2829-2836.

WELCH, C. R., WU, Q. & SIMON, J. E. 2008. Recent Advances in Anthocyanin Analysis and Characterization. *Curr Anal Chem,* 4**,** 75-101.

WELLS, D. A. 2006. India: A pharmacist's medical mission. *American Journal of Health-System Pharmacy,* 63**,** 2048-2050.

WILLIAMS, C., EDVARDSSON, K., LEWANDOWSKI, S. A., STRÖM, A. & GUSTAFSSON, J. Å. 2008. A genome-wide study of the repressive effects of estrogen receptor beta on estrogen receptor alpha signaling in breast cancer cells. *Oncogene,* 27**,** 1019-1032.

WILLIAMS, M. T. & HORD, N. G. 2005. The role of dietary factors in cancer prevention: beyond fruits and vegetables. *Nutrition in clinical practice,* 20**,** 451-459.

WINTER, C. A., RISLEY, E. A. & NUSS, G. W. 1962. Carrageenin-induced edema in hind paw of the rat as an assay for antiinflammatory drugs. *Proceedings of the society for experimental biology and medicine,* 111**,** 544-547.

WINTROBE, M., GREER, J. & PARASKEVAS, F. 2009. Lymphocytes and lymphatic organs. *Wintrobe's clinical hematology, 12th edn. Wolters Kluwer Health/Lippincott Williams Wilkins, Philadelphia 300-325*

WISINSKI, K. B., XU, W., TEVAARWERK, A. J., SAHA, S., KIM, K., TRAYNOR, A., DIETRICH, L., HEGEMAN, R., PATEL, D., BLANK, J., HARTER, J. & BURKARD, M. E. 2016. Targeting Estrogen Receptor Beta in a Phase 2 Study of High-Dose Estradiol in Metastatic Triple-Negative Breast Cancer: A Wisconsin Oncology Network Study. *Clinical Breast Cancer,* 16**,** 256-261.

WORLD HEALTH, O. 2002. *The world health report 2002: reducing risks, promoting healthy life*, World Health Organization.

WU, S., ZHU, W., THOMPSON, P. & HANNUN, Y. A. 2018. Evaluating intrinsic and non-intrinsic cancer risk factors. *Nature communications,* 9**,** 3490.

XIANG, J., HURCHLA, M. A., FONTANA, F., SU, X., AMEND, S. R., ESSER, A. K., DOUGLAS, G. J., MUDALAGIRIYAPPA, C., LUKER, K. E. & PLUARD, T. 2015. CXCR4 protein epitope mimetic antagonist POL5551 disrupts metastasis and enhances chemotherapy effect in triple-negative breast cancer. *Molecular cancer therapeutics,* 14**,** 2473-2485.

XIAO, W., MOHSENY, A. B., HOGENDOORN, P. C. W. & CLETON-JANSEN, A.-M. 2013. Mesenchymal stem cell transformation and sarcoma genesis. *Clinical Sarcoma Research,* 3**,** 10.

XU, D. P., LI, Y., MENG, X., ZHOU, T., ZHOU, Y., ZHENG, J., ZHANG, J. J. & LI, H. B. 2017. Natural Antioxidants in Foods and Medicinal Plants: Extraction, Assessment and Resources. *Int J Mol Sci,* 18.

XU, F., SAMAD, N. A. & ANSOR, N. M. Targeting Microtubules by Phytoestrogens for the Treatment of Cancer: An Overview.

XU, J., CHEN, Y. & OLOPADE, O. I. 2010. MYC and Breast Cancer. *Genes Cancer,* 1**,** 629-40.

YADAV, N. K., SAINI, K. S., HOSSAIN, Z., OMER, A., SHARMA, C., GAYEN, J. R., SINGH, P., ARYA, K. R. & SINGH, R. K. 2015. Saraca indica bark extract shows in vitro antioxidant, antibreast cancer activity and does not exhibit toxicological effects. *Oxid Med Cell Longev,* 2015**,** 205360.

YAN, S., WANG, J., CHEN, H., ZHANG, D. & IMAM, M. 2023. Divergent features of ERβ isoforms in triple negative breast cancer: progress and implications for further research. *Frontiers in Cell and Developmental Biology,* 11.

YANG, J., VISSCHER, P. M. & WRAY, N. R. 2010. Sporadic cases are the norm for complex disease. *European Journal of Human Genetics,* 18**,** 1039-1043.

YANG, Y. I., JUNG, D. W., BAI, D. G., YOO, G. S. & CHOI, J. K. 2001. Counterion-dye staining method for DNA in agarose gels using crystal violet and methyl orange. *Electrophoresis,* 22**,** 855-859.

YERSAL, O. & BARUTCA, S. 2014. Biological subtypes of breast cancer: Prognostic and therapeutic implications. *World J Clin Oncol,* 5**,** 412-24.

YOUNG, D. S., PESTANER, L. & GIBBERMAN, V. 1975. Effects of drugs on clinical laboratory tests. *Clinical chemistry,* 21**,** 1D-432D.

YUAN, S., NORGARD, R. J. & STANGER, B. Z. 2019. Cellular plasticity in cancer. *Cancer discovery,* 9**,** 837-851.

ZARDAVAS, D., PUGLIANO, L. & PICCART, M. 2013. Personalized therapy for breast cancer: a dream or a reality? *Future Oncology,* 9**,** 1105-1119.

ZENG, J., EDELWEISS, M., ROSS, D. S., XU, B., MOO, T. A., BROGI, E. & D'ALFONSO, T. M. 2021. Triple-Positive Breast Carcinoma: Histopathologic Features and Response to Neoadjuvant Chemotherapy. *Arch Pathol Lab Med,* 145**,** 728-735.

ZEWEIL, M. M., SADEK, K. M., TAHA, N. M., EL-SAYED, Y. & MENSHAWY, S. 2019. Graviola attenuates DMBA-induced breast cancer possibly through augmenting apoptosis and antioxidant pathway and downregulating estrogen receptors. *Environmental Science and Pollution Research,* 26**,** 15209-15217.

ZHANG, H., SHENG, S., PAN, Z., ZHAO, L., YANG, C., LI, C. & WANG, F. 2023. Immune and Endocrine Regulation in Endometriosis: What We Know. *Journal of Endometriosis and Uterine Disorders***,** 100049.

ZHAO, J. A., CHEN, J. J., JU, Y. C., WU, J. H., GENG, C. Z. & YANG, H. C. 2011. The effect of childbirth on carcinogenesis of DMBA-induced breast cancer in female SD rats. *Chin J Cancer,* 30**,** 779-85.

ZHOU, Y. & LIU, X. 2020. The role of estrogen receptor beta in breast cancer. *Biomarker Research,* 8**,** 39.

Publications

- ➤ Peer reviewed publications
    1. Analysis of anticancer potential of *Kingiodendron pinnatum* (DC.) Harms, published in Clinical Phytoscience journal
    2. Antiproliferative effect of *Saraca asoca* methanol bark extract on triple negative breast cancer (TNBC), published in Future Journal of Pharmaceutical Sciences

- ➤ Non-peer reviewed publications
    1. Effect of *Saraca asoca* and *Kingiodendron pinnatum* bark extracts on DMBA-induced mammary tumorigenesis in mice, oral presentation delivered at National seminar on recent trends in disease prevention and health management held at CSIR- National Institute for Interdisciplinary Science and Technology, Thiruvananthapuram during 14th & 15th December 2022

    2. *Saraca asoca* and *Kingiodendron pinnatum* bark extracts suppress growth and metastasis of 4T1- induced mammary tumours in BALB/c mice, poster presented at 42nd annual conference of the Indian association of cancer research held at Advanced centre for treatment research and education in cancer, Tata memorial centre, Navi Mumbai during 12th-16th January 2023

ORIGINAL CONTRIBUTION

Open Access

Analysis of anticancer potential of *Kingiodendron pinnatum* (DC.) Harms

Chennattu M. Pareeth[1], Nair Meera[1], Prabha Silpa[1], Kannoor M. Thara[2], Achuthan C. Raghavamenon[1] and Thekkekara D. Babu[1*]

Abstract

Background The plant *Kingiodendron pinnatum* (DC.) Harms, belonging to the family Fabaceae is endemic to the Western Ghats of India and is commonly used for various ailments, especially by the tribes. *K. pinnatum* is occasionally used as a substitute for *Saraca asoca* in *Asokarishta*, a well-known uterine tonic in Ayurveda. Recent studies revealed a pharmacological similarity between the plants. *S. asoca* is reported to have anti-cancer properties, but there are no reports on *K. pinnatum* except for antioxidant and antimicrobial activities. Therefore, the study is aimed to investigate the anticancer potential of the plant.

Methods Cytotoxicity of methanolic bark extract of the plant was analysed on different cancer cell lines by 3-(4, 5-dimethylthiazol-2-yl)-2, 5-diphenyltetrazolium bromide (MTT) assay. Dalton's lymphoma ascites (DLA) cell-induced solid and Ehrlich ascites carcinoma (EAC) cell-induced ascites tumour models in mice were used to study the antitumor potential. Phytochemical screening of the extract was also performed.

Results The extract was found cytotoxic to DLA, EAC, HCT15, MDA-MB-231, T47D and PC3 with inhibitory concentration (IC_{50}) values of 50.09, 74.74, 67.02, 119.22, 149.04 and 194.5 μg/mL, respectively. In the solid tumour model, a significant ($P < 0.001$) reduction in tumour weight of 0.7 ± 0.15 g was observed in 500 mg/kg b.wt. extract treated group compared to the control group (3.6 ± 0.24 g) by oral administration for 30 days. In the ascites tumour model, a high survival rate of 28.2 ± 8.72 days ($P < 0.01$) was found by the extract treatment compared to the control animals. Phytochemicals like alkaloids, flavonoids, phenols, phytosterols, saponins, tannins, steroids and terpenoids were detected in the extract.

Conclusion Results obtained by the cytotoxic and anti-tumour studies revealed the anticancer potential of *K. pinnatum*. The plant exhibits more cytotoxicity towards cancer cell lines of the reproductive system such as the breast and prostate.

Keywords *Kingiodendron pinnatum*, *Saraca asoca*, Asoka, Cytotoxicity, Anti-tumour, Reproductive cancer, Phytoestrogen

Introduction

Cancer is one of the leading causes of death globally and the number of cases is mounting gradually. According to the International Agency for Research on Cancer (IARC), 18.1 million new cancer cases and 9.6 million cancer deaths were accounted for in 2018. The incidence rate of commonly diagnosed cancer types such as lung (2.09 million), breast (2.08 million), colorectal (1.8 million), prostrate (1.3 million) and stomach cancer (1 million) are

*Correspondence:
Thekkekara D. Babu
babutd@amalaims.org
[1] Department of Biochemistry, Amala Cancer Research Centre (Recognized Research Centre, University of Calicut), Amala Nagar, Thrissur 680 555, Kerala, India
[2] Department of Biotechnology, University of Calicut, Thenhipalam P O, Malappuram 673 636, Kerala, India

Pareeth *et al. Clinical Phytoscience*   (2023) 9:4

Page 2 of 9

increased [1]. Currently, there are many drugs available on market for different cancers but they are not completely effective and safe. Present treatment modalities like chemotherapy and radiotherapy have serious side effects affecting some vital organs. Hence, the studies are more focused on plant-derived products as they have shown to be effective and have fewer side effects. Many natural products and their analogues including camptothecin, resveratrol, taxol, vinblastine and sulforaphane have been recognised as anti-cancer drugs and various plants with anticancer potential are being identified day by day [2, 3]. Biologically active compounds are often characterized by unique structures, making natural product research an effective method for discovering new compounds with distinct mechanisms of action. Despite the advances that have enabled the use of natural products in the discovery of new therapeutic agents, there are still challenges to be addressed. In most cases, bioactive natural products must be produced at a large scale to meet the manufacturing requirements, which constitutes a major hurdle before they are eventually available for clinical use. For these issues to be resolved, it will be necessary to develop innovative therapeutic concepts and new technologies, thereby advancing the transformation of the field [4].

Kingiodendron pinnatum, the plant belonging to the family Fabaceae is endemic to the Western Ghats of India and is mainly distributed in the evergreen hill and deciduous forests of Karnataka, Kerala and Tamil Nadu states. Traditionally, an oleo-gum-resin extracted from the tree is being used by tribes for gonorrhoea, catarrhal conditions of genitourinary and respiratory tracts and curing sores in elephants [5]. The resin obtained by piercing the trunk has been used for joint pains and to get relief for the fissured foot by *Kanikkar*, a predominant tribal community of Kalakad-Mundanthurai of Western Ghats, Tirunelveli, Tamil Nadu, India [6]. Phytochemicals such as phenols, flavonoids, tannins, glycosides and terpenes were reported from the plant [7]. The plant is reported to have antioxidant, antifungal and antibacterial activities [5]. *K. pinnatum* is occasionally used as a substitute for *Saraca asoca* (Asoka), which is the prime raw material in the preparation of *Asokarishta*, a fermented formulation, commonly used to treat gynaecological ailments especially abnormal uterine bleeding (menorrhagia). The population of the tree is less in wild but is generally used as a substitute due to its massive size and the chance of getting a good amount of bark compared to the Asoka tree [8]. A previous study revealed the pharmacological efficacy of *K. pinnatum* as an alternative for *S. asoca* in *Asokarishta* by demonstrating the inhibitory effect of estrogen-induced uterus endometrial thickening in immature female rats, giving scientific validation for its use in polyherbal formulations [8]. *S. asoca* is reported to have anticancer properties [9], but there are no reports on *K. pinnatum*. Therefore, the present study is intended to analyse the cytotoxic effect of the plant on reproductive cancers such as breast and prostate and its antitumour potential using mouse solid and ascites tumour models. The study is expected to provide insights into the anticancer potential of *K. pinnatum.*

Materials and methods

Chemical and reagents

Dulbecco's Modified Eagle Medium (DMEM), Fetal Bovine Serum (FBS) was procured from Thermo Fisher Scientific Inc., USA. Streptomycin, penicillin was purchased from Sigma Aldrich, USA. MTT, trypan blue dye, phosphate buffer saline were procured from Sisco Research Laboratory Pvt. Ltd., India and methanol, isopropanol, HCl, Triton X 100 from Merck, India.

Collection of the plant sample

The stem bark of *K. pinnatum* was collected from the Wayanad region of Western Ghats, Kerala, India. The plant was authenticated by Dr. N. Sasidharan, Taxonomist, Kerala Forest Research Institute (KFRI), Thrissur, Kerala (India). The voucher specimen of *K. pinnatum* (No. KFRI 4725) was deposited in the Herbarium of KFRI. The collected stem bark was shade dried, powdered and stored in air-tight containers until use.

Preparation of the extract

About 20 g of the powder was extracted with 250 mL methanol by stirring overnight. The extract was filtered using Whatman no. 1 filter paper and evaporated to dryness. It was weighed to determine the percentage yield of the soluble constituents using the formula.

$$\% \text{ Yield } = (\text{weight of dry extract/weight taken for extraction}) \times 100$$

The residue thus obtained was stored at 4 °C until use.

Phytochemical analysis

The extract obtained was dissolved in methanol and subjected to various analysis to find out the presence of different phytochemicals. The total phenolic and flavonoid contents of *K. pinnatum* extract was determined by Folin–Ciocalteu colorimetric reagent (FCR) [10] and aluminium chloride colorimetric methods [11], respectively. Dragendorff's, Hagers and Mayer's tests were used to detect the presence of alkaloids. Shinoda's, ferric chloride, Froth formation, Salkowski and Liebermann-Burchard tests, lead acetate and Salkowski

Pareeth *et al. Clinical Phytoscience*   (2023) 9:4

Page 3 of 9

tests were used to detect the presence of flavonoids, phenols, saponins, sterols, tannins and terpenoids [12], respectively.

Animals

Female Swiss albino mice (25–30 g) were purchased from the Small Animal Breeding Station (SABS), College of Veterinary, KVASU, Thrissur, Kerala. The animals were kept in the animal house facility of Amala Cancer Research Centre following standard conditions of 24–28 °C, 60–70% humidity, 12 h dark/light cycle and fed with standard rat feed bought from Sai Durga Feeds, Bangalore, India and water ad libitum. All the animal experiments were carried out with the prior permission of the Institutional Animal Ethics Committee (IAEC) and were conducted strictly according to the guidelines of the Committee for the Purpose of Control and Supervision of Experiments on Animals (CPCSEA) constituted by the Ministry of Environment and Forest, Government of India.

Cell lines

Breast cancer cell lines (MDA-MB-231, T47D), colorectal cancer cell line (HCT-15), prostate cancer cell line (PC3) and normal African green monkey kidney epithelial cells (Vero) obtained from National Centre for Cell Science (NCCS), Pune (India) were cultured in DMEM medium supplemented with FBS (10% v/v), streptomycin (100 μg/mL) and penicillin (100 U/mL). All cells were maintained at 37 °C, 5% CO_2, 95% air and 100% relative humidity. Daltons Lymphoma Ascites (DLA) and Ehrlich's Ascites Carcinoma (EAC) cell lines were obtained from Amala Cancer Research Centre's animal house facility. The cells were maintained in the intra-peritoneal cavity of mice.

In vitro cytotoxicity by trypan blue dye exclusion method

The short-term cytotoxic activity of the extract was evaluated by determining the percentage viability of murine tumour cells like DLA and EAC using the trypan blue exclusion method [13]. Crude methanolic extract of the plant was used for the study. The cells were grown in the peritoneal cavity of female mice (8 weeks old, 25–30 g) by injecting 1×10^6 cells/mL intra-peritoneally. Cells were aspirated aseptically from the cavity of mice after 15 days of inoculation, washed with PBS and centrifuged at 1000 rpm for 5 min. Pellets were resuspended in PBS and the cell count was adjusted to 1×10^6 cells/mL. The cells were pipetted out and added into each tube having PBS with different concentrations of the drug. It was then incubated for 3 h at 37ºC. After incubation, trypan blue dye was added and left for 3 min before observation. It was then observed under a light microscope using a haemocytometer. The experiments were performed in triplicate and the percentage of cytotoxicity was determined by counting the number of dead cells to that of live cells and substituting in the equation:

$$\% \text{ of cytotoxicity} = \frac{\text{No. of dead cells}}{\text{Total no. of cells}} \times 100$$

The graph was plotted and the half-maximal inhibitory concentration (IC_{50}) was calculated.

In vitro cytotoxic analysis by MTT assay

MDA-MB-231, T47D, HCT-15, PC3 and Vero cell lines were used to study the cytotoxic activity of crude methanolic extract of *K. pinnatum* using MTT assay [14]. Approximately, 1×10^5 cells were seeded in a 12-well plate containing medium and incubated at 37 °C for 24 h. The cells were incubated with different concentrations of the extract at 37 °C for 24 h. After incubation, 100 μL of 3-(4, 5-dimethylthiazol-2-yl)-2, 5-diphenyltetrazolium bromide (MTT) was added to each well and incubated for 4 h. The dark blue formazan crystals were dissolved in a 1 mL solubilization solution containing isopropanol, HCl and Triton X 100 by continuous aspiration and resuspension. The absorbance of the coloured product was measured at 570 nm. Three experiments with comparable outcomes were carried out in duplicate and the cytotoxicity was determined by comparing the percentage of death of the treated cell population with the untreated control indicated by their respective absorbance assessed with the MTT assay.

Acute toxicity studies

The extract of *K. pinnatum*, at the concentration 2500 mg/kg b.wt. was administrated to 3 male and 3 female Swiss albino mice (25–30 g) orally according to the Organization of Economic Co-operation and Development (OECD) guideline for testing chemicals [15]. The animals were monitored for 14 successive days for any visible changes in behaviour, body weight, water and food intake, hair loss etc. At the end of the experimental period, the animals were sacrificed and the internal organs were examined for any sign of change by conducting a necropsy. The experiment was repeated with another set of animals.

Anti-tumour analysis in mouse models

For the study, Swiss albino mice were grouped into 5 groups comprising 6 animals. Group I: control-untreated; group II: vehicle control (propylene glycol); group III: KPLD—*K. pinnatum* (KP) low dose (250 mg/kg b.wt.); group IV: KPHD—KP high dose (500 mg/kg b.wt.); group V: standard—cyclophosphamide (10 mg/kg b.wt.). DLA and EAC cells were aspirated from the peritoneal cavity

Pareeth *et al. Clinical Phytoscience* (2023) 9:4

Page 4 of 9

of the tumour-bearing mice and washed with PBS. DLA cell suspension (100 μL) containing approximately 1×10^6 cells was injected intramuscularly into the right hind limb for the development of solid tumour and EAC cells into the peritoneal cavity of the animals for the ascites tumour development. The extracts were administered 24 h after the induction of the tumour and continued for 10 consecutive days. Solid tumour development was determined by measuring the diameter of the tumour growth in two perpendicular planes using a Vernier calliper. The readings were taken at a 3 days interval basis up to the 30th day [16]. The tumour volume was calculated according to the following formula,

$$V = 4/3\pi \ r_1^2 \ r_2$$

where, r_1 is the minor radius and r_2 is the major radius.

The percentage inhibition of tumour growth was calculated according to the formula,

$$\% \text{ inhibition} = [(C - T)/C] \times 100$$

Where C is the tumour volume of control animals on the 30th day and T is the tumour volume of treated animals on the 30th day. The tumours excised from the animal were weighed. In EAC model, the number of survival days of animals was recorded.

Statistical analysis

Data were presented as mean $\pm$ standard deviation. Data analysis was performed by one-way ANOVA method followed by Dunnett's multiple comparison test and Kaplan–Meier survival curve by Mantel-Cox test in Graphpad Prism 7. The level of significance was considered as $p < 0.05^*$, $p < 0.01^{**}$ and $p < 0.001^{***}$.

Results

Phytochemicals present in the extract

The total yield of the extract from 20 g of powdered bark using 250 mL methanol was 5.6022 g. Preliminary phytochemical screening revealed the presence of alkaloids, flavonoids, phenols, phytosterols, saponins, tannins and terpenoids in the methanolic extract (Tab. 1). The total phenol and flavonoid contents were found to be 2.297 mg GAE/g extract and 0.246 mg QE/g extract, respectively.

Cytotoxic effect of the extract on cancer cells

The extract was shown to have cytotoxicity against murine tumour cells like DLA and EAC cells in a dose-dependent manner with IC$_{50}$ values of 50.09 and 74.74 µg/mL, respectively (Fig. 1). In the MTT assay, the extract was found to be cytotoxic on breast cancer cell

Table 1 Phytochemicals present in *K. pinnatum*

Phytochemicals	Presence
Alkaloids	+
Flavonoids	+
Phenols	+
Phytosterols	+
Saponins	+
Tannins	+
Terpenoids	+

lines MDA-MB-231 and T47D with IC$_{50}$ of 70.22 and 149.04 µg/mL, respectively. It also showed cytotoxicity towards a colorectal cancer cell line, HCT-15 in a dose-dependent manner with an IC$_{50}$ value of 67.02 µg/mL and prostate cancer cell line, PC3 with an IC$_{50}$ of 198 µg/mL. The extract shows less cytotoxicity in the normal African green monkey kidney epithelial cell line, Vero even at the concentration of 280 µg/mL (Figs. 2 and 3).

Acute toxicity

The animals treated with the extract appeared healthy and no mortality was observed. There was no significant change in the behaviour of animals including, breathing, skin effects, water and food consumption, body weight etc. No changes in colour, texture and relative organ weights of the liver, heart, spleen, kidney, uterus and ovary were observed. Therefore, the extract seems to be safe up to a dose level of 2500 mg/kg. The parameters observed after the administration of the extract are represented in (Table 2).

Anti-tumour potential of the extract

The methanolic extract of *K. pinnatum* was found to inhibit the DLA-induced solid tumour in mice. The tumour weight in the control and vehicle group of animals was found to be 3.6 ± 0.24 and 3.1 ± 0.3 g, respectively on day 30th of tumour inoculation. High dose of *K. pinnatum* treated animals shows a significant reduction in tumour weight (0.7 ± 0.15 g, $P < 0.001$) compared to the control group animals (3.6 ± 0.24 g). The high dose of the extract reduced the tumour volume to 65.69 ± 18.1 cm^3 from 426.25 ± 36.61 cm^3 in the control group animals (Fig. 4). The tumour size and weight of control and treatment group animals are represented in Fig. 5.

K. pinnatum also shows a significant anti-tumour effect in the ascites tumour model. Animals in the control and vehicle control groups show almost the same mean survival rate with values of 20.4 ± 4.33 and 20.4 ± 4.77 days, respectively. The animals administrated with 500 mg/kg. b.wt. dose *K. pinnatum* extract showed a high survival

Pareeth *et al. Clinical Phytoscience*   (2023) 9:4

Page 5 of 9
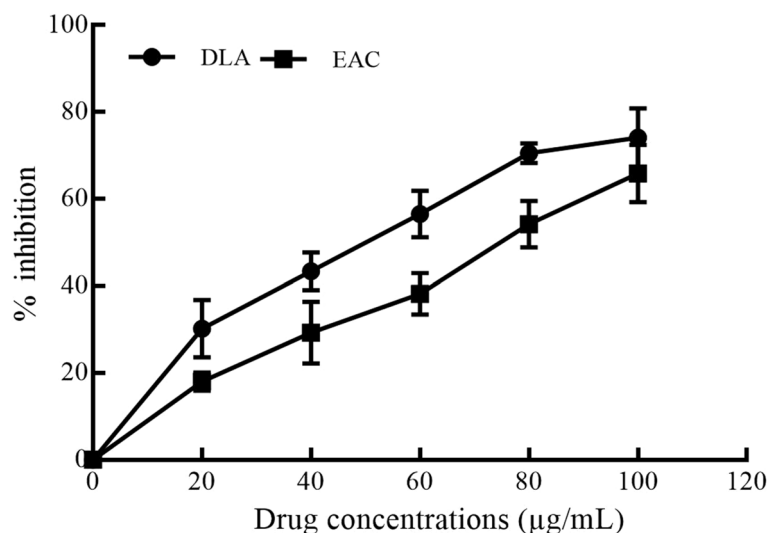
Fig. 1 Short-term cytotoxicity of *K. pinnatum* on murine tumour cells using trypan blue dye exclusion method
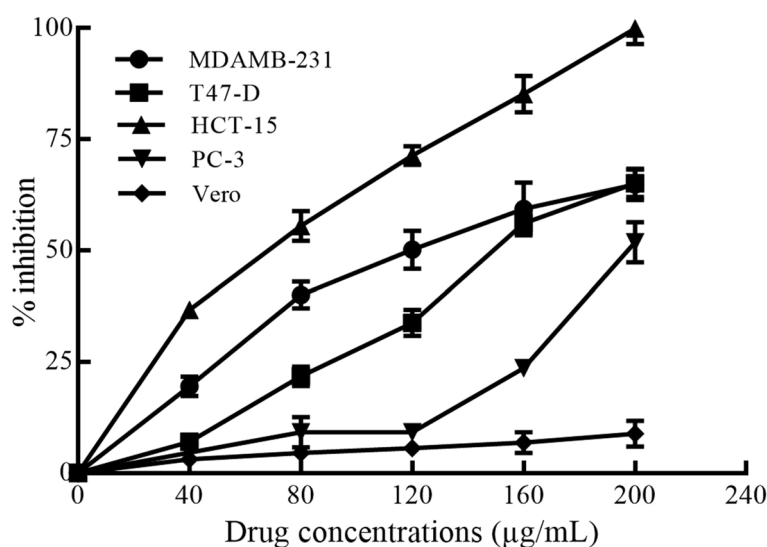
Fig. 2 Cytotoxicity of *K. pinnatum* on different cancer cell lines by MTT assay

rate of 28.2 ± 8.72 days ($P < 0.01$) compared to the control group animals (20.4 ± 4.33 days). Animals treated with the standard drug cyclophosphamide survived up to 30.8 ± 7.52 days, which was close to animals administrated with a high dose of *K. pinnatum* extract (Fig. 6).

Discussion

It has been reported that *Kingiodendron pinnatum* has a pharmacological similarity to that of *S. asoca* and can be used as a substitute in Ayurvedic preparations [8]. There are reports of cytotoxic and anticancer activities of *S. asoca* against different cancer cell lines [9, 17] and mouse tumour models [18], but no reports on *K. pinnatum* even

though the plant is reported to have antioxidant, antifungal and antibacterial activities [5]. In our study, the plant *K. pinnatum* shows a cytotoxic and anti-proliferative effect on different types of cancer cell lines such as breast, colorectal, prostate and murine tumour cells and inhibits the development of mouse solid and ascites tumours suggesting its anticancer potential. *K. pinnatum* exhibited considerable in vitro cytotoxicity towards reproductive cancers such as breast and prostate cancer cell lines. In DLA induced solid tumour model, the extract treated group showed a decrease of the tumour growth. The mean tumour weight of the control was comparable to other groups except for the standard group. In the EAC

Pareeth *et al. Clinical Phytoscience* (2023) 9:4

Page 6 of 9
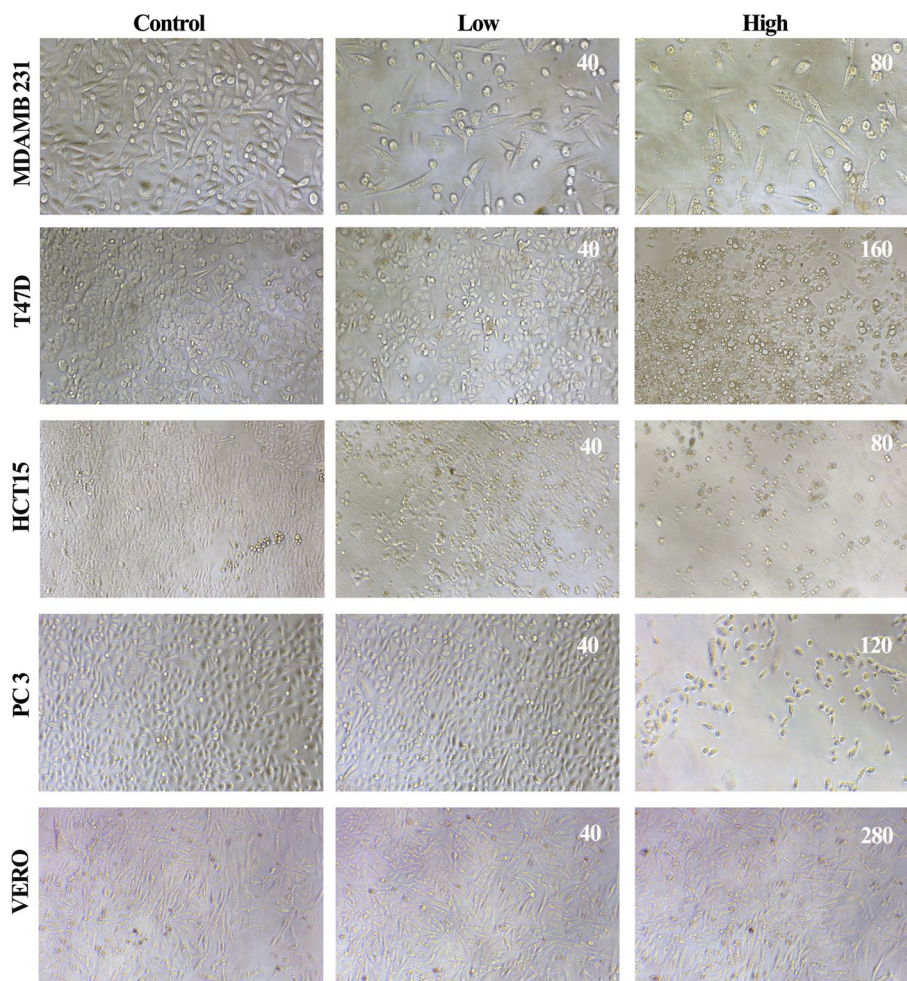
Fig. 3 Morphology of different cancer cell lines treated with *K. pinnatum* at different concentrations

Table 2 General appearance and behavioral observations of control and treated animals

Observations	Normal group	Treated groups
Food intake	Normal	Normal
Water intake	Normal	Normal
Body weight	Normal	No change
Fatigue	Not present	Not present
Changes in skin	No change	No change
Diarrhoea	Not present	Not present
Sedation	No effect	No effect
General physique	Normal	Normal
Death	Alive	Alive

ascites model, the survival curves were statistically significant for the high extract treated group and standard, compared to other groups.

S. asoca is reported to have phytoestrogens such as quercetin, kaempferol, *β*-sitosterol and luteolin [18] with anticancer potential. The mechanisms of action of these are suggested to be the modulation of estrogen receptors. Many studies have stated a connection between phytoestrogens and their possible role in cancer therapy or prevention [17, 19]. Phytoestrogens are reported to induce apoptosis in breast cancer cells and inhibit prostate and ovarian cancer growth [20–22]. They can interact and modulate different growth factors and activate/inhibit cytokine signalling pathways. genistein, a phytoestrogen, induced apoptosis in MCF-7 breast cancer cells through the down-regulation of the Akt signalling pathway [23]. Also, it inhibits triple-negative breast cancer cell, MDA-MB-231 growth by inhibiting NF-kB activity *via* the Notch-1 pathway [24]. In prostate cancer cells, it inhibits the activation of NF kB *via* the Akt signalling pathway [25].

Pareeth *et al. Clinical Phytoscience*   (2023) 9:4

Page 7 of 9
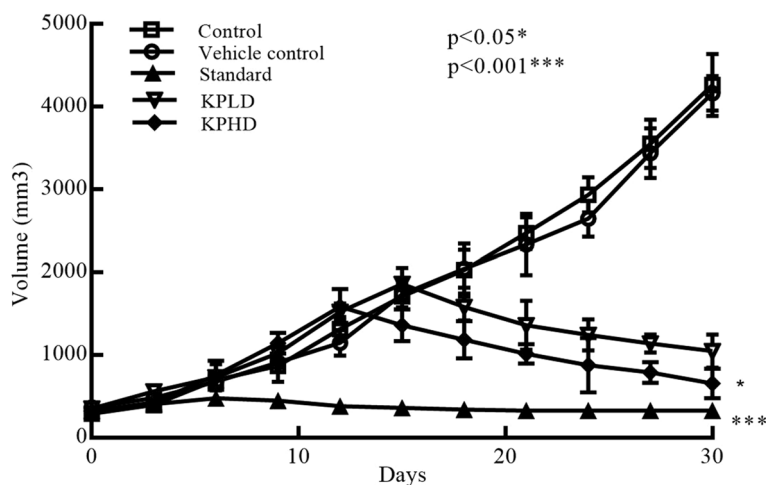
Fig. 4 Effect of *K. pinnatum* extract on DLA induced mouse solid tumor. Results are presented as mean ± SD, n = 5. One-way ANOVA was used to determine the statistical comparison followed by Dunnett's multiple comparison test. *$P < 0.05$, **$P < 0.01$, ***$P < 0.001$, statistically significant as compared to the control group
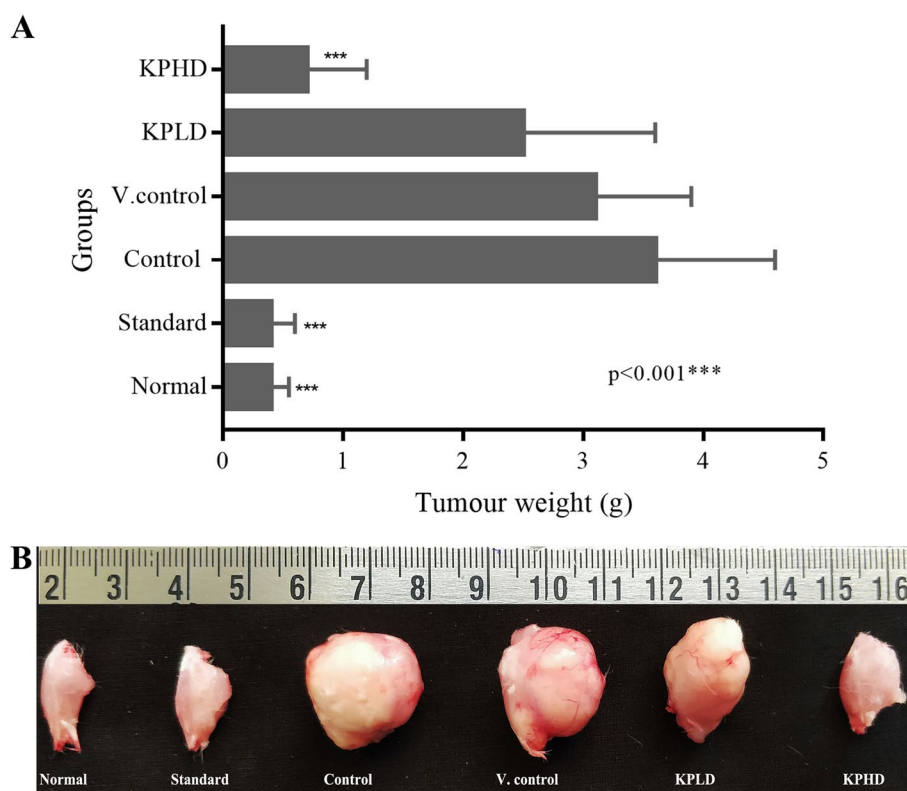
Fig. 5 **A** Comparison of tumour weight (in grams) (**B**) tumour size. Results are presented as mean ± SD, *n* = 5. One-way ANOVA was used to determine the statistical comparison followed by Dunnett's multiple comparison test. *$P < 0.05$, **$P < 0.01$, ***$P < 0.001$, statistically significant as compared to the control group

The phytochemical screening of *K. pinnatum* has shown the presence of important phytoestrogens and revealed a similar phytochemical profile as that of *S.* *asoca*. In a pharmacological study on estradiol-induced keratinization, *K. pinnatum* was found to reduce cornification in immature rat uterus. The elevated level of
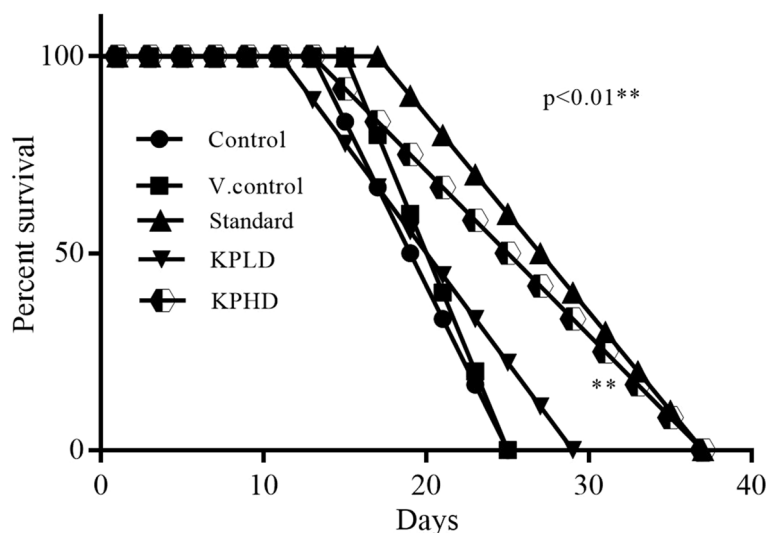
Fig. 6 Effect of *K. pinnatum* extract on the survival of ascites bearing animals. Results are presented as mean $\pm$ SD, $n = 5$. Kaplan–Meier survival curve was used to analyse the statistical comparison followed by Mantel-Cox test. *$P < 0.05$, **$P < 0.01$, ***$P < 0.001$, statistically significant as compared to the control group

estrogen in estradiol-administered animals has reduced and inhibited acute as well as chronic inflammations in mice [8]. This study gives a scientific validation for the use of *K. pinnatum* in polyherbal uterine tonic, *Asokarishta* as a substitute for *S. asoca*. In the present study, *K. pinnatum* exhibits more inhibitory effects toward reproductive cancers such as breast and prostate cancers. Thus, the activity of *K. pinnatum* may be due to the presence of similar phytoestrogens seen in *S. asoca* as they are pharmacologically related.

Conclusion

The results obtained by the cytotoxic and antitumour studies indicate the anticancer potential of the plant *K. pinnatum,* especially on reproductive cancers. The study also suggests the presence of phytoestrogens which are reported to have a variety of biological activities. The phytoestrogens can bind to reproductive cancer cells with estrogen receptors and can be a possible target of some phytoestrogens. This modulation of estrogen receptors may be the reason for the cytotoxic properties of some phytoestrogens against breast cancer cells. Thus, to comprehend the subsequent mechanism, it is necessary to analyse how phytoestrogens of *K. pinnatum* interact with estrogen receptors.

Abbreviations

BWT	Body weight
DLA	Dalton's lymphoma ascites
EAC	Ehlich ascites carcinoma
IC$_{50}$	Half maximal inhibitory concentration
KP	*Kingiodendron pinnatum*
KPLD	*Kingiodendron pinnatum* Low dose
KPHD	*Kingiodendron pinnatum* High dose
MTT	(3-(4,5-Dimethylthiazol-2-yl)-2,5-diphenyltetrazolium bromide

Authors' contributions
All authors have read and approved the final manuscript.

Availability of data and materials
Data supporting the findings of this study are available on request from the corresponding author

Declarations

Ethics of approval and consent to participate
All the animal experiments were carried out with the prior permission of the Institutional Animal Ethics Committee (IAEC) (Approval No: ACRC/IAEC/17(l)/P-05 dt: 22–07-2017) and were conducted strictly according to the guidelines of the Committee for the Purpose of Control and Supervision of Experiments on Animals (CPCSEA) constituted by Ministry of Environment and Forest, Government India.

Consent for publication
All authors agreed to the publication of the research.

Competing interests
The authors declare that they have no competing interest.

Pareeth *et al. Clinical Phytoscience*　(2023) 9:4

Page 9 of 9

References

1. Bray F, Ferlay J, Soerjomataram I, Siegel RL, Torre LA, Jemal A. Global cancer statistics 2018: GLOBOCAN estimates of incidence and mortality worldwide for 36 cancers in 185 countries. CA Cancer J Clin. 2018;68(6):394–424.
2. Prakash O, Kumar A, Kumar P. Anticancer potential of plants and natural products. J Am J Pharmacol Sci. 2013;1(6):104–15.
3. Cragg GM, Pezzuto JM. Natural products as a vital source for the discovery of cancer chemotherapeutic and chemopreventive agents. Med Princ Pract. 2016;25(Suppl. 2):41–59.
4. Huang M, Lu J-J, Ding J. Natural products in cancer therapy: past, present and future. Nat prod bioprospect. 2021;11(1):5–13.
5. Kumar KJ, Prasad AGD, Richard SA. Biochemical activity of endangered medicinal plant *Kingiodendron pinnatum*. Asian J Plant Sci. 2011;1(4):70–5.
6. Sutha S, Mohan VR, Kumaresan SS, Murugan C, Athiperumalsami T. Ethnomedicinal plants used by the tribals of Kalakad-Mundanthurai Tiger Reserve (KMTR), Western Ghats, Tamil Nadu for the treatment of rheumatism. Indian J Tradit Knowl. 2010;9:502–9.
7. Sheik S, Chandrashekar KR. Antimicrobial and antioxidant activities of *Kingiodendron pinnatum* (DC.) Harms and *Humboldtia brunonis* Wallich: endemic plants of the Western Ghats of India. J Natl Sci Found. 2014;42(4):307.
8. Shahid AP, Sasidharan N, Salini S, Padikkala J, Meera N, Raghavamenon AC, et al. *Kingiodendron pinnatum*, a pharmacologically effective alternative for *Saraca asoca* in an Ayurvedic preparation, *Asokarishta* J Tradit Complement Med. 2017;8(1):244–50.
9. Yadav NK, Saini KS, Hossain Z, Omer A, Sharma C, Gayen JR, et al. *Saraca indica* bark extract shows *in vitro* antioxidant, antibreast cancer activity and does not exhibit toxicological effects. Oxid Med Cell Longev. 2015;205360(10):16.
10. Kaur C, Kapoor HC. Anti-oxidant activity and total phenolic content of some Asian vegetables. Int J Food Sci Technol. 2002;37(2):153–61.
11. Chang C-C, Yang M-H, Wen H-M, Chern J-C. Estimation of total flavonoid content in propolis by two complementary colorimetric methods. J Food Drug Anal. 2002;10:3.
12. Dey PM. Oligosaccharides. Methods in plant biochemistry (ed), Vol. 2. London: Academic Press; 1990. p. 189–218
13. Moldeus P, Hogberg J, Orrenius S, Fleischer S, Packer L. Methods in enzymology. Academic Press, New York. 1978;52:60–71.
14. Mosmann T. Rapid colorimetric assay for cellular growth and survival: application to proliferation and cytotoxicity assays. J Immunol Methods. 1983;65(1–2):55–63.
15. OECD. OECD guideline for testing of chemicals. 2001. https://www.oecd.org/chemicalsafety/risk-assessment/1948378.pdf. Accessed 17 Dec 2001
16. Ma Y, Mizino T, Ito H. Antitumor activity of some polysaccharides isolated from a Chinese mushroom, Huangmo, the fruiting body of *Hohenbuehelia serotina*. Agric Biol Chem. 1991;55(11):2701–10.
17. Virk-Baker MK, Nagy TR, Barnes S. Role of phytoestrogens in cancer therapy. Planta Med. 2010;76(11):1132–42.
18. Swar G, Shailajan S, Menon S. Activity based evaluation of a traditional Ayurvedic medicinal plant: *Saraca asoca* (Roxb.) de Wilde flowers as estrogenic agents using ovariectomized rat model. J Ethnopharmacol. 2017;195:324–33. https://doi.org/10.1016/j.jep.2016.11.038.
19. Basu P, Maier C. Phytoestrogens and breast cancer: *In vitro* anticancer activities of isoflavones, lignans, coumestans, stilbenes and their analogs and derivatives. Biomed Pharmacother. 2018;107:1648–66.
20. Cotterchio M, Boucher BA, Manno M, Gallinger S, Okey A, Harper P. Dietary phytoestrogen intake is associated with reduced colorectal cancer risk. J Nutr. 2006;136(12):3046–53.
21. Raffoul JJ, Banerjee S, Che M, Knoll ZE, Doerge DR, Abrams J, et al. Soy isoflavones enhance radiotherapy in a metastatic prostate cancer model. Int J Cancer. 2007;120(11):2491–8.
22. Obiorah IE, Fan P, Jordan VC. Breast cancer cell apoptosis with phytoestrogens is dependent on an estrogen-deprived state. Cancer Prev Res. 2014;7(9):939–49. https://doi.org/10.1158/1940-6207.capr-14-0061.
23. Anastasius N, Boston S, Lacey M, Storing N, Whitehead SA. Evidence that low-dose, long-term genistein treatment inhibits oestradiol-stimulated growth in MCF-7 cells by down-regulation of the PI3-kinase/Akt signalling pathway. J Steroid Biochem Mol Biol. 2009;116(1–2):50–5. https://doi.org/10.1016/j.jsbmb.2009.04.009.
24. Pan H, Zhou W, He W, Liu X, Ding Q, Ling L, et al. Genistein inhibits MDA-MB-231 triple-negative breast cancer cell growth by inhibiting NF-κB activity *via* the Notch-1 pathway. Int J Mol Med. 2012;30(2):337–43.
25. Li Y, Sarkar FH. Inhibition of nuclear factor kappa B activation in PC3 cells by genistein is mediated *via* Akt signaling pathway. Clin Cancer Res. 2002;8(7):2369–77.

Publisher's Note

RESEARCH

Antiproliferative effect of *Saraca asoca* methanol bark extract on triple negative breast cancer (TNBC)

Chennattu M. Pareeth[1], K. P. Safna Hussan[1], Davis Anu[1], Nair Meera[1], Deepu Mathew[2], Ravishankar Valsalan[2], Mohamed Shahin Thayyil[3], Kannoor M. Thara[4], Achuthan C. Raghavamenon[1] and Thekkekara D. Babu[1]*

Abstract

Background *Saraca asoca* (Asoka) is reported to possess phytoestrogenic components with anticancer properties. The phytoestrogens are recognized as natural agonists for ERβ, which acts as an antagonist to ERa. Despite the absence of ERa, studies have identified ERβ in 50–80% of triple negative breast cancers (TNBC). Thus, the present study is intended to reveal the role of phytoestrogens of Asoka on TNBC. The cytotoxic effect of Asoka methanol bark extract was analyzed on different breast cancer cell lines by MTT assay. Estrogen-screen assay was employed to determine the proliferative/antiproliferative effect. Identification of phytoestrogens in Asoka was accomplished using LC-MS analysis and in silico docking studies were performed to investigate possible interactions of phytoestrogens with ERa and β.

Results The extract of Asoka was found to be cytotoxic against TNBC cell line, MDAMB-231 with IC$_{50}$ of 70.22 ± 1.89 µg/mL and towards HER$^+$ breast cancer cell line, SKBR3 with IC$_{50}$ of 98.41 ± 2.31 µg/mL, respectively. Whereas the extract did not show any cytotoxicity towards ERa cell line, MCF-7 even up to the concentration 300 µg/mL. Estrogen-screen assay emphasized an estrogenic effect of the extract on MCF-7 and an anti-estrogenic/antiproliferative effect on MDAMB-231 cells. LC–MS analysis identified phytoestrogens such as β-sitosterol, quercetin, kaempferol and others. The docking results revealed good binding efficacy of phytoestrogens with ERβ than ERa and quercetin shows more affinity with the highest docking score of -9.220. Strikingly, it was found that the *S. asoca* methanol extract was preferentially cytotoxic to TNBC cells.

Conclusion The study demonstrates selective anticancer properties of *S. asoca* methanol extract on TNBC, which indicates a selective impact on ER subtypes. The identification of phytoestrogens, such as β-sitosterol, quercetin and kaempferol, in the Asoka methanol bark extract provides a molecular basis for its observed effects. In silico studies further support the view that these phytoestrogens may preferentially interact with ERβ rather than ERa. Quercetin, in particular, demonstrated the highest binding efficacy with ERβ, suggesting its potential role in mediating the anticancer effects observed in TNBC cells. Further research is warranted to explore the full therapeutic potential of phytoestrogens in breast cancer treatment.

Keywords Asoka, Anticancer, Phytoestrogen, Estrogen receptor, Molecular docking, TNBC

*Correspondence:
Thekkekara D. Babu
babutharakan@gmail.com
Full list of author information is available at the end of the article

Springer Open

Pareeth *et al. Future Journal of Pharmaceutical Sciences*   (2024) 10:52

Page 2 of 13

Background

Saraca asoca (Roxb.) De Wilde, commonly known as Asoka, belonging to the family Fabaceae is considered one of the most ancient and holistic trees in India. Various ethnopharmacological uses of Asoka in different treatment aspects are well documented in Indian old classical Ayurvedic treatises, *Charaka Samhita* (1000 BC), *Susruta* (500 BC) *Vaghbatta* (sixth century) *Dhanvantari Nighantu* (ninth century) and *Chakradatta*, (eleventh century) etc. In Ayurveda, the stem bark of Asoka is used to make *Asokarishta*, a polyherbal decoction used to manage various gynecological complications, especially menorrhagia [1]. This traditional practice reflects the significance of Asoka especially in women's health, as emphasized in the traditional healing systems of India. Inspired by these treatises, several studies have validated the ethnobotanical claims and unveiled novel pharmacological properties [2] like antibacterial [3], antioxidant [4], antipyretic [5] antihyperglycemic [6], anthelmintic [7] and anticancer [8] activities. The cytotoxic activity of *S. asoca* on the breast (MDAMB-231, MCF-7), cervical (HeLa), colon (HT-29), and lung (A549) cancer cell lines were reported [9–11]. *Saraca asoca* exhibits chemopreventive activity against acute myeloid leukemia (AML) and DMBA/croton oil-induced skin papilloma formation in mice [12, 13]. The phytochemical analysis of the stem bark revealed the presence of alkaloids, flavonoids, phenols, phytosterols, saponins, tannins, steroids and terpenoids [14]. The phytoestrogens in this plant β-sitosterol, quercetin, kaempferol and catechin are reported to show anticancer properties including breast cancers.

Breast cancer is closely dependent on estrogen in its initiation and progression. Thus, estrogen receptors ERα/β plays a pivotal role in maintaining the homeostasis of the normal mammary gland [15]. ERα, the primary receptor of estrogen activates the cell cycle and stimulates proliferation, but ERβ functions as a counterbalance to ERα, actively inhibiting cellular proliferation and providing a regulatory mechanism to the proliferative effect of ERα [16]. This intrinsic counteraction creates a dynamic interplay between ERα and ERβ, influencing the delicate equilibrium of mammary gland homeostasis. Although ERα serves as the primary receptor for estrogen and is vital for the homeostasis of the normal mammary gland, its activation promotes cell cycle and stimulates proliferation, potentially leading to the initiation and development of cancer. Conversely, ERβ functions as a counterbalance to ERα, actively inhibiting cellular proliferation and consequently, offering potential therapeutic avenues for breast cancer [17, 18]. Various reports indicate that ERβ is expressed in triple-negative breast cancer (TNBC), accounting 50–80 % [19]. By leveraging the inhibitory properties of ERβ, researchers and clinicians can explore targeted interventions to modulate hormonal signaling and disrupt the uncontrolled cell growth characteristic of breast cancer [20]. Several consistent findings have shown that ERβ expression decreases in precancerous and cancerous breast lesions [21].

Currently, the predominant focus lies in the identification of novel selective ERβ agonists, with numerous synthetic and natural molecules demonstrating high efficacy in breast cancer prevention and treatment. Notably, recent studies indicate that phytoestrogens exhibit a heightened affinity for ERβ compared to ERα [22]. The potential for phytoestrogens to accumulate in breast tissue suggests significant clinical implications [23]. Among ERβ agonists, phytoestrogens offer a distinctive therapeutic avenue for targeting ERβ [24]. Liquiritigenin [25] and genistein [26] are notable examples, forming stable complexes with ERβ, recruiting selective co-activators, and interacting with chromatin regulatory elements in estrogen-responsive genes [27]. Both liquiritigenin and genistein have been reported as protective factors against breast cancer, demonstrating the capacity to reduce invasiveness and growth of triple-negative breast cancer (TNBC) through pathway modulation [28, 29]. Another phytoestrogen kaempferol specifically inhibits the migration and invasion of TNBC cells by blocking RhoA and Rac1 signaling pathways. Given these findings, the present study aims to investigate the role of phytoconstituents in Asoka in inhibiting breast cancer cell growth, employing MCF-7, MDAMB-231, and SKBR3 cell lines through estrogen-screen and MTT assays. Additionally, the binding efficacy of phytoestrogens on estrogen receptors will be explored through in silico molecular docking.

Methods

Collection and preparation of extract

The stem bark of *S. asoca* was collected from the Thrissur district of Kerala, India, and its authenticity was confirmed by Dr. N. Sasidharan, Taxonomist, Kerala Forest Research Institute (KFRI), Thrissur, Kerala, India. The collected specimens have been deposited in the Herbarium of KFRI, assigned the voucher specimen number KFRI 4725. The plant sample underwent thorough washing with distilled water, followed by cutting into small pieces and subsequent drying at 45–50 °C for one week. The dried bark was then powdered using a grinder and stored in light-resistant, airtight containers. About 20 g of the powdered sample was subjected to extraction with 200 mL of methanol at room temperature through overnight stirring. The resulting Asoka crude methanol extract was filtered using Whatman No.1 filter paper. The extraction process was repeated 2–3 times, and the residue was evaporated to dryness utilizing a vacuum concentrator. The weight of the dried extract was measured

to determine the percentage yield of the soluble constituents [30].

Cell lines and animals

The triple-negative breast cancer cell line, MDAMB-231, the HER-2 expressed breast cancer cell line, SKBR3, and the hormone-positive breast cancer cell line, MCF-7, were procured from National Center for Cell Science (NCCS), Pune, India. These cell lines were cultured in DMEM medium supplemented with fetal bovine serum (FBS) at a concentration of 10% v/v. For the estrogen-screen assay, phenol red-free DMEM supplemented with charcoal–dextran-treated FBS was employed. Both media were also supplemented with streptomycin (100 μg/mL) and penicillin (100 U/mL). The cell lines were incubated at 37 °C in an incubator with 5% CO_2. Murine tumor cells, including Daltons Lymphoma Ascites (DLA) and Ehrlich's Ascites Carcinoma (EAC) cell lines, were grown in the intraperitoneal cavity of Swiss albino mice and were maintained in the animal house facility at Amala Cancer Research Center. Prior approval was obtained from the Institutional Animal Ethics Committee for the use of experimental animals with Approval No: ACRC/IAEC/17(1)/P-05 dt: 22-12-2017.

Phytochemical analysis

The crude methanol extract obtained from *S. asoca* was dissolved in methanol and underwent qualitative and quantitative analysis to identify the presence and concentrations of various phytochemicals. Different standard tests were employed for qualitative assessment to identify the presence of various compounds. Flavonoids were detected using Shinoda's test, phenols with the ferric chloride test, saponins with the Froth formation test, sterols with Salkowski and Liebermann-Burchard tests, tannins with the lead acetate test, and terpenoids with Salkowski tests [31, 32]. Additionally, the *S. asoca* crude extract was quantitatively analyzed using the Folin–Ciocalteau method to determine the total phenolic content using gallic acid as standard and expressed as mg of gallic acid equivalent (GAE)/g of dry extract [33]. For the quantification of flavonoids, the aluminium chloride colorimetric method was employed utilizing standard quercetin and expressed as milligrams of quercetin equivalent (QE) per gram of dry extract [34]. The experiments were meticulously conducted in triplicates to ensure accuracy and reliability, and the results are reported as the mean ± standard deviation (SD).

Cytotoxicity assay

The short-term cytotoxic activity of the Asoka crude extract was assessed by determining the percentage viability of murine tumor cells such as DLA and EAC, employing the trypan blue exclusion method [35]. The murine tumor cells were cultivated in the peritoneal cavity of female Swiss albino mice (25–30 g, 2 months old) through intraperitoneal injection of 1×10^6 cells/mL. Cells were aspirated aseptically from the cavity of mice after 15 days of inoculation; washed with PBS and centrifuged at 1000 rpm for 5 min. Pellets were resuspended in PBS and the cell count was adjusted to 1×10^6 cells/mL. Cells were pipetted out and added into each tube having PBS with different concentrations of the extract. It was then incubated for 3 h at 37 °C. After incubation, trypan blue dye was added and observed under the light microscope using a haemocytometer. The experiments were replicated in triplicates, and the percentage of cytotoxicity was assessed by enumerating the number of dead cells relative to that of live cells and substituting in the equation:

$$\% \text{ of cytotoxicity} = \frac{\text{No. of dead cells}}{\text{Total no of cells}} \times 100$$

The dose–response curve was fitted with the Hill equation using data analysis and graphing software, OriginPro 9 software [36].

Breast cancer cell lines such as MDAMB-231, SKBR3 and MCF-7, were employed to assess the antiproliferative activity of the extract using the MTT assay [37]. Approximately, 1×10^5 cells were seeded in 12 well plates containing medium and incubated at 37 °C for 24 h. Cells were then incubated with different concentrations of extract at 37 °C for 24 h. The test also included a blank containing a complete culture without cells. After incubation, 100 μL of 3-(4, 5-dimethylthiazol-2-yl)-2, 5-diphenyltetrazolium bromide (MTT) was added to each well and incubated for 4 h. The dark blue formazan crystals were dissolved in 1 mL solubilization solution containing isopropanol, concentrated HCl and Triton X 100 by continuous aspiration and re-suspension. The absorbance of the colored product was measured at 570 nm. The cytotoxicity was determined by comparing the percentage death of the treated cell population with the untreated control, indicated by their respective absorbance assessed with the MTT assay. The dose–response curve was fitted with the Hill equation [36].

$$\frac{E}{E_{\max}} = \frac{1}{1 + \left(\frac{EC_{50}}{|A|}\right)^n}$$

where the maximum percentage of inhibition is $E_{\max}$, the half-maximal effective concentration is EC_{50}, the Hill coefficient is '*n*' and the extract concentration is '*A*'. The Hill equation was computed using OriginPro 9. The assays were performed in triplicates, and statistical analysis was carried out using one-way ANOVA followed by

Pareeth *et al. Future Journal of Pharmaceutical Sciences*   (2024) 10:52

Page 4 of 13

Tukey's multiple comparison test in GraphPad Prism 8 software.

Estrogen-screen assay

Breast cancer cell lines expressing ERβ, including MDAMB-231 and cell lines expressing ERα, such as MCF-7, were used for the study. The cell lines were cultivated in Dulbecco's Modified Eagle's Medium (DMEM) with FBS and phenol red as pH indicators with culture conditions of 5% CO_2 and 95% humidity at 37 °C. The cells were plated in well culture plates and allowed to attach. After 24 h, the seeding medium was removed and replaced with phenol red-free DMEM containing charcoal dextran treated FBS [38]. The cells were treated with different concentrations of 17 β-estradiol (0.1–1000 pM) and incubated at 37 °C for 3 days. After incubation, 100 μL of MTT was added to each well and incubated for 4 h. The dark blue formazan crystals were dissolved in 1 mL solubilization solution by continuous aspiration and re-suspension. The absorbance of the colored product was measured at 570 nm and the cytotoxicity was determined by comparing the percentage death of the treated cell population with the untreated control, indicated by their respective absorbance assessed with the MTT assay [37].

UV–visible spectroscopy

The *S. asoca* crude extract underwent centrifugation at 3000 rpm for 10 min and were subsequently filtered through the Whatman No.1 filter paper. The resulting samples were diluted with the same solvent employed for extraction, achieving a final concentration of 1 mg/mL. Standard solutions of quercetin, kaempferol, and β-sitosterol were also prepared at a concentration of 1 mg/mL of ethanol. Utilizing a UV–Vis spectrophotometer (PG Instruments, UK), the extract and standards were scanned across a wavelength range of 200 to 900 nm, and characteristic peaks were identified.

Fourier transform infrared spectroscopy (FTIR)

To characterize the functional group present in the sample, FTIR spectroscopy was conducted. A translucent sample disk was created by encapsulating 10 mg of *S. asoca* crude powder in 100 mg of potassium bromide (KBr) pellets. The FTIR spectroscopy analysis was performed using a Shimadzu IR Affinity 1 (Kyoto, Japan) within the range of 500 to 4000 cm^{-1} [39]. The obtained raw data was employed to generate FTIR spectra using OriginPro 9 software. The 'spectroscopic tools' were utilized for the analysis of the FTIR spectra (https://www.science-and-fun.de/tools/).

LC–MS analysis

The chemical profiling of the Asoka crude extract was done using High Resolution-Liquid Chromatography/Mass Spectrometry. The analysis was performed on an Agilent 6550 iFunnel Q-TOF LC/MS system (G6550A) equipped with an Agilent 1290 Infinity Autosampler (G4226A), an Agilent 1290 Infinity Binary Pump VL (G4220B), and an Agilent 1200 series thermostatted column compartment. A reverse-phase analytical column (Zorbax SB-C18, 100×2.1 mm i.d., 1.8 μm particle size) was used for separation at a flow rate of 0.3 mL/min for a total of 30 min. Sample injection involved 5 μL of the sample. The mobile phases comprised aqueous 0.1% formic acid (A) and 90% acetonitrile in 0.1% aqueous formic acid (B). Mass spectroscopy utilized a dual ion source system with full scan mode, covering a mass range of 50 to 500 m/z. Mass Hunter Qualitative Analysis software was employed for data analysis.

Molecular docking

Molecular docking was done using Schrodinger Maestro software to investigate the possible interactions between β-sitosterol, kaempferol and quercetin which are specific compounds identified in *S. asoca* extract with the targeted receptors, ERα and ERβ. Also, inbuilt ligand estradiol and the classical chemotherapy drug, tamoxifen was used to find out the binding affinity of estrogen receptors towards them. The structures of proteins with PDB IDs 3ERT and 3OLL were downloaded from the protein data bank for ERα and ERβ, respectively. The protein structures were processed before being used as a receptor for docking. Hydrogen atoms were added, atomic charges were assigned and water molecules that were not involved in ligand binding were removed during the operation. Chains and loops that were missing were also inserted. Protein preparation was done by using the protein preparation wizard. The pre-processing was done with the use of the import and process tab, while the review and modify tab was used for the generation of tautomeric states. The structures were optimized and minimized using the refine tab and protein was prepared for further studies. The optimized structures of the standards β-sitosterol, kaempferol and quercetin were used after converting them to structures with.sdf extension. The imported structures were edited using the 2D sketcher option in the Schrodinger Maestro. Then the ligprep wizard was employed to prepare each ligand using the OPLS3 force field. All tautomers of the structures were generated. Then the molecules were subjected to conformational change to form a stable conformer with the lowest energy. The glide receptor grid generating wizard was used to create a three-dimensional grid with

0.5 Å spacing and a maximum size of 20 Å × 20 Å × 20 Å. Any type of constraint, such as accuracy constraints, H-bond constraints, and so on, can be applied using the receptor grid generation wizard. The XP (extra precision) method was used for docking as it is the most powerful and discriminating procedure. After setting the location of the grid and ligands, docking was done with flexible molecules, and the proteins were used as rigid molecules [40].

Statistical analysis

The data from in vitro studies were presented as mean ± standard deviation (SD), derived from three distinct experiments. Statistical analysis was conducted using one-way ANOVA, followed by Tukey's multiple comparison test in GraphPad Prism 8 software. Statistical significance was assigned to p values $< 0.05^*$, $< 0.01^{**}$, and $< 0.001^{***}$, while $p > 0.05$ was considered non-significant.

Results

Phytochemical analysis

The qualitative analysis of the *S. asoca* crude methanol extract indicated positive results for the presence of flavonoids, alkaloids, phytosterols, phenols, saponins, tannins and terpenoids. The quantification of polyphenolic content in the *S. asoca* crude extract, determined from the calibration curve ($R2 = 0.998$), revealed a concentration of 120 ± 6.82 mg of gallic acid equivalent (GAE) per gram of dry extract. Additionally, the total flavonoid content in the crude extract, estimated from the calibration curve ($R2 = 0.999$), was found to be 61.54 ± 4.51 mg of quercetin equivalent (QE) per gram of dry extract. These results provide a comprehensive insight into the chemical composition of *S. asoca* crude methanol extract, highlighting its rich polyphenolic and flavonoid content.

Anticancer properties

The cytotoxic effect of *S. asoca* crude methanol extract was assessed using the trypan blue assay and demonstrated considerable cytotoxic effects on DLA and EAC cells. The concentrations required to achieve 50% cytotoxicity were 42.24 ± 3.65 and 65.44 ± 2.89 μg/mL for DLA and EAC cells, respectively (Fig. 1). In MTT assay, the efficacy of *S. asoca* extract was evident against triple-negative breast cancer cell lines, MDAMB-231, with an IC_{50} of 70.22 ± 1.89 μg/mL, and HER-2 positive breast cancer cell line, SKBR3, with an IC_{50} of 98.41 ± 2.31 μg/mL (Fig. 1). A statistically significant ($p < 0.05$) decrease in cell numbers was observed in both MDAMB-231 and SKBR3 following extract treatment. Treated cells exhibited a noticeable difference in morphology compared to control cells, characterized by cell shrinkage and shift in morphology from epithelial-like to round in both
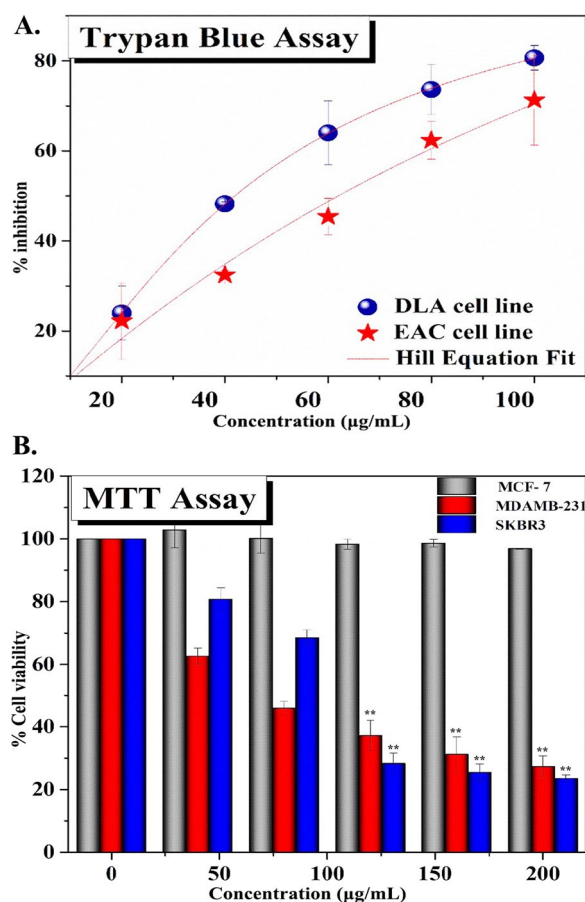
Fig. 1 A Cytotoxic effect of *S. asoca* crude methanol extract on murine tumor cells by trypan blue assay, **B** Antiproliferative effect of *S. asoca* on different breast cancer cells by MTT assay. The results are expressed as mean ± SD, with $n = 3$. Statistical comparisons were conducted using one-way ANOVA, followed by Tukey's multiple comparison test. Statistically significant probabilities are denoted as $^*p < 0.05$ and $^{**}p < 0.01$

MDAMB-231 and SKBR3 (Fig. 2). However, the extract did not exhibit any cytotoxicity towards MCF-7, even at a concentration of 300 μg/mL.

Estrogen-screen assay

In this study, the ERα expressing MCF-7 cells exhibited a proliferative response to 17 β-estradiol (1000 pM), showing a 30% increase in cell count and a 7% increase in response to crude extract within a 72-h timeframe. Along with 17 β-estradiol, the crude extract exhibited a mild estrogenic effect. Conversely, ERβ expressing MDAMB-231 cells demonstrated a 10% decrease in proliferation with 17 β-estradiol treatment, and the cell population was halved when treated with the crude extract at a concentration of 100 μg/mL (Fig. 3). Notably, the crude extract did not induce cytotoxicity in MCF-7 cell lines even at higher concentrations, while they decreased the

Pareeth *et al. Future Journal of Pharmaceutical Sciences*   (2024) 10:52

Page 6 of 13
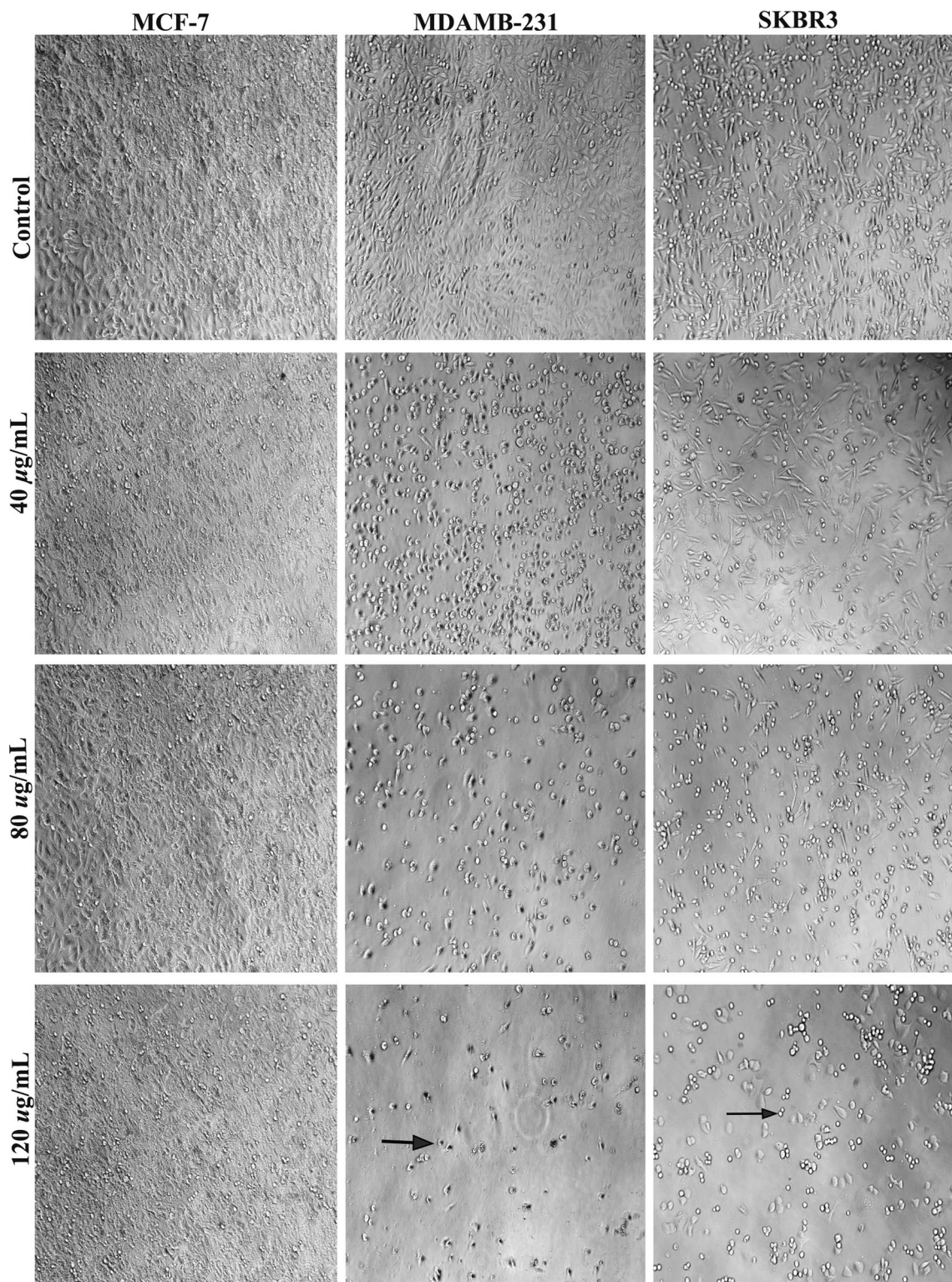
Fig. 2 Morphology of different breast cancer cells after exposure to varying concentrations of *S. asoca* crude extract (20× magnification). The black arrow indicates altered morphology from epithelial-like to round

Pareeth *et al. Future Journal of Pharmaceutical Sciences*   *(2024) 10:52*

Page 7 of 13
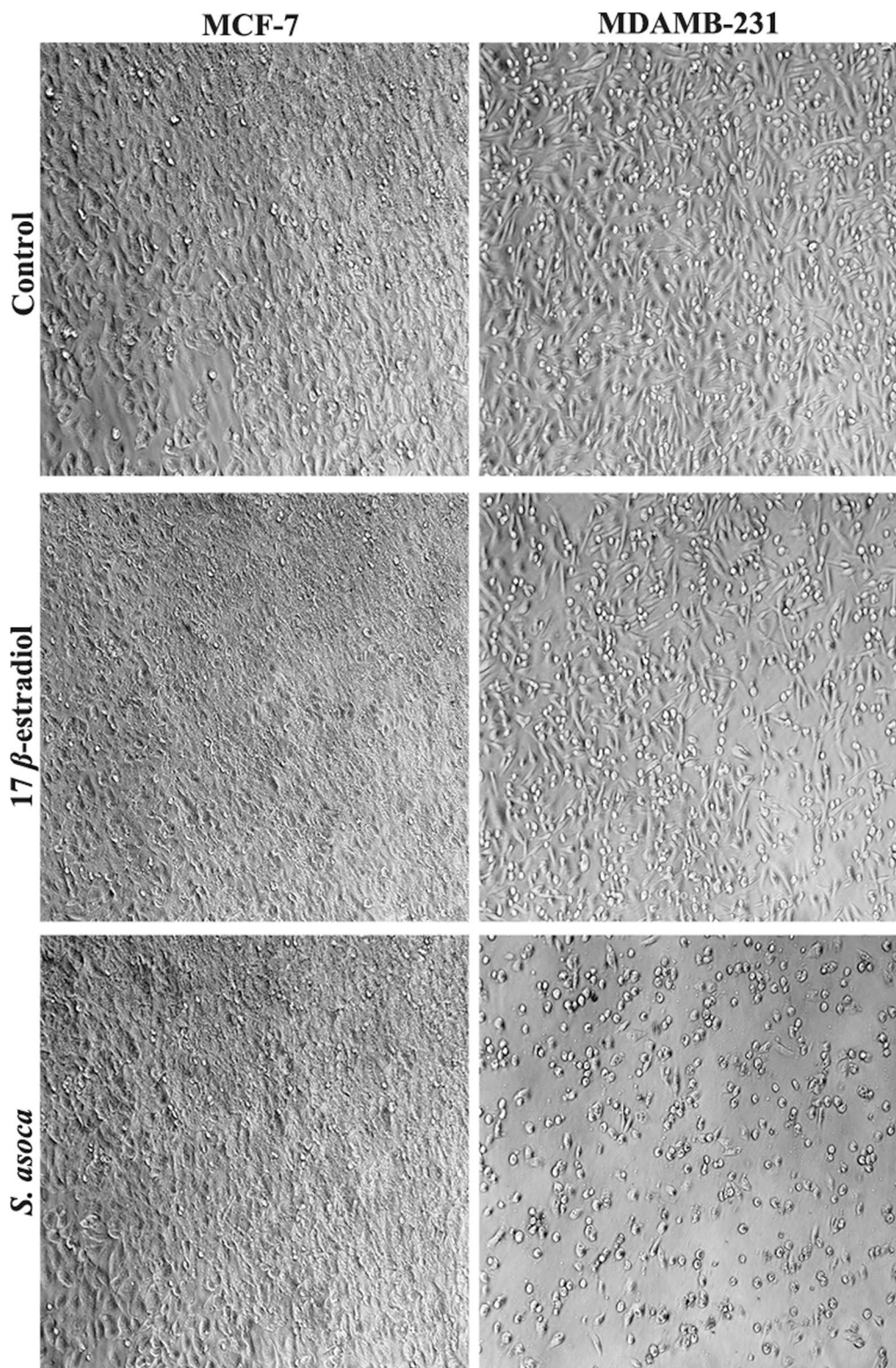
Fig. 3 Change in cell volume of MCF-7 and MDAMB-231 breast cancer cells following exposure to extract and 17 β-estradiol (1000 pM) in the estrogen-screen assay

cell viability of MDAMB-231 cells in a concentration-dependent manner. Consequently, the estrogen-screen assay highlights the estrogenic impact of *S. asoca* crude extract on MCF-7 and its anti-estrogenic/antiproliferative effect on MDAMB-231 cells.

Chemical profiling

Various techniques like UV–Vis spectroscopy, fourier-transform infrared spectroscopy (FTIR) and LC–MS were employed to evaluate the chemical profile of *S. asoca*. The absorption spectrum of UV-Spectrophotometric analysis of *S. asoca*, showed prominent peaks at 232, 275 and 449 nm which is in good correlation with the reported data [41]. These prominent peaks may have arisen from the phytoestrogens. Henceforth, the UV-spectra of standards (quercetin, kaempferol, β-sitosterol) were cross-checked and found that all of the suspected phytoestrogens have three peaks between 230 and 290 nm in the UV range and a single

peak in a visible area (387–390 nm) (Fig. 4A). Accordingly, there is a likelihood of superpositioning of these distinct peaks in the *S. asoca* crude extract. The biological activity of any molecule is influenced by its functional groups which play a key role in determining the overall physicochemical properties. In FTIR, the results show functional groups such as alcohol, phenol, ester, alkane, aromatic and alkene in the extract. The functional groups identified in the extract are shown in Fig. 4B and Table 1.

The LC–MS analysis identified some of the important compounds such as caffeic acid, catechin, quercetin, kaempferol, gallic acid, rutin, β-sitosterol, p-coumaric acid, luteolin etc. (Fig. 5). Phytoestrogenic compounds like β-sitosterol, kaempferol, and quercetin present in the extract are presumed to contribute to the proliferative/antiproliferative effects of the *S. asoca* crude methanol extract on MCF-7, MDAMB-231, and SKBR3 cancer cell lines.
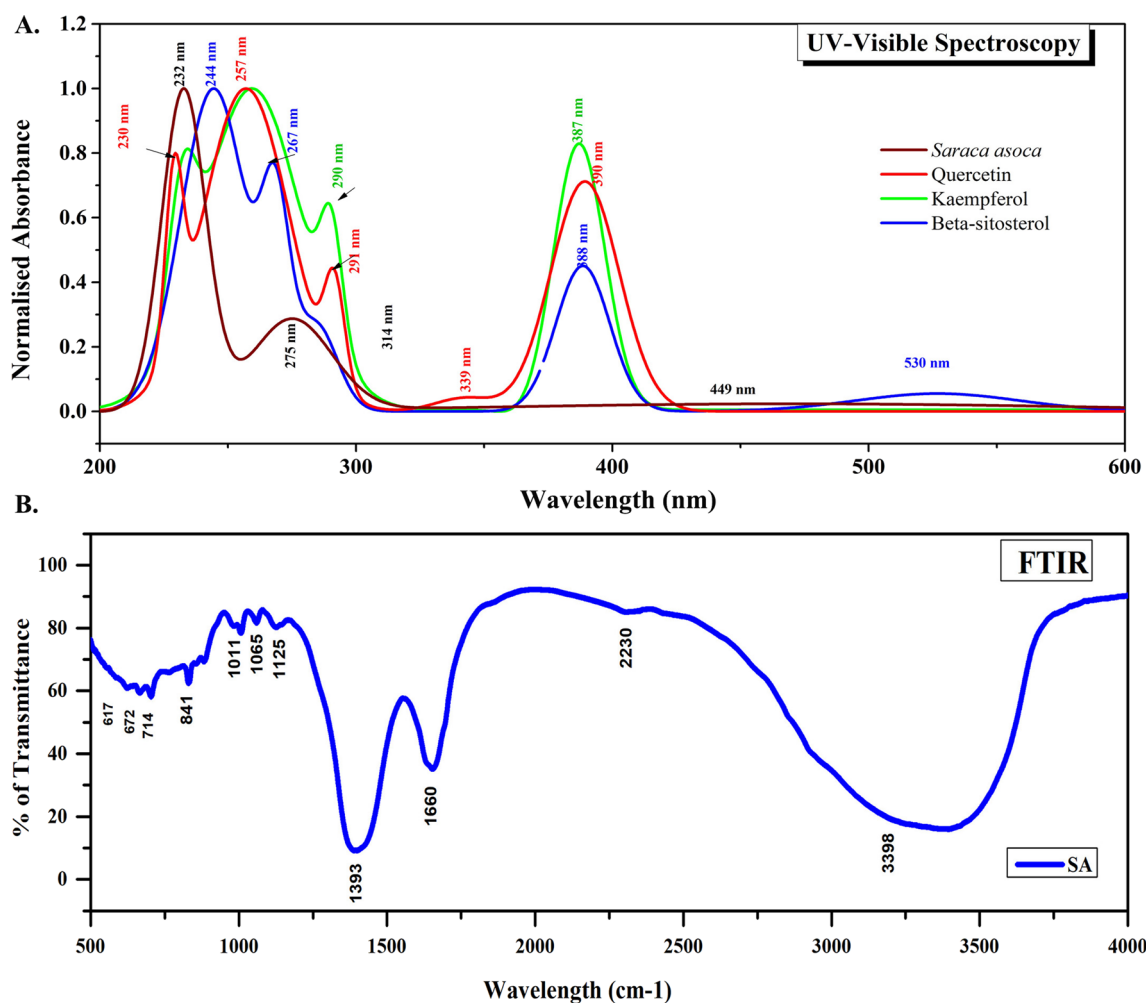

Fig. 4 **A** UV–visible spectrum of *S. asoca* crude methanol extract and phytoestrogen standards, **B** FTIR spectrum of *S. asoca* crude extract

Pareeth *et al. Future Journal of Pharmaceutical Sciences*   (2024) 10:52

Page 9 of 13

Table 1 FTIR interpretation of compounds of *S. asoca* crude extract

Wave number cm^{-1}	Bond assigned	Functional groups
617	C–H vibration	Alkanes, alkenes
672	C–H and C–C stretching	Alkenes, alcohol, phenol
714	C=C and N–H stretching	Alkenes, amines
841	C–C and C–H stretching	Amides, aldehydes
1011	C–O stretching	Alcohol
1065	C–O stretching	Alcohol, aromatic
1125	C–O stretching	Alcohol
1393	C–O and C–H stretching	Phenol, aldehydes
1660	C–C stretching	Phenols
2230	C=C stretching	Conjugated alkene
3398	O–H stretching	Alcohol

Molecular docking

The studies suggest that certain phytoestrogens act as natural agonists for ERβ, making them promising drug candidates for their ability to modulate the cell cycle, influence epigenetic events, and induce apoptosis. Interestingly, in the current investigation, the extract exhibits specific cytotoxicity towards ERβ expressing cells, not affecting ERα. This raises the intriguing possibility that the phytoestrogens in the plant may act as agonists for ERβ. To explore potential interactions between phytoestrogens and ERα/β, molecular docking was performed using Schrodinger Maestro software.

Interaction of phytoestrogens with ERα

The docking of the inbuilt ligand, estradiol into the 3D structure of ERα was done using a glide dock. The amino acid residues in the active site of 3ERT are Trp383, Leu384, Leu387, Met388, Gly390, Lbu391, Val392, Arg394, Met342, Met343, Leu345, Leu346, Thr347, Asn348, Leu349, Ala350, Asp351, Glu353, Leu354, Leu327, Phe404, Leu402, Leu428, Phe425, Ile424, Val422, Met421, Gly420, Glu419, Val418, Met517, Ser518, Lys520, Gly521, Met522, Glu523, Hie524, Leu525, Met528, Lys529, Cys530, Val533, Leu536, Leu539. The estradiol was docked into the active site region and interactions were made with the residues by hydrogen bonding with GLU353 and ARG394 and electrostatic bonding with ASP351. The inbuilt ligand shows a docking score of -12.17 and binding energy of -125.19 kcal/mol. The quercetin was docked into the active site region making interactions with the residues by hydrogen bonding with ASP351. The docking score and binding energy were found to be -6.945 and -47.026 kcal/mol which was more compared to kaempferol (-6.93). Tamoxifen shows

Compound label	RT	Mass	DB diff (ppm)
Meperidine N-oxide	2.584	263.1529	-2.8
Tannic acid	2.945	282.0878	5.16
Gallic acid	3.355	170.0213	1.54
Caffeic acid	5.181	180.041	6.97
p-Coumaric acid	5.782	164.0475	-0.65
Rutin	5.782	610.1489	7.39
Quercetin	6.023	302.0406	6.67
Luteoline	7.036	286.046	5.9
Kaempferol	8.62	286.046	5.9
Catechin	9.564	278.1499	7.01
Phthalic acid Mono-2-ethylhexyl Ester	9.91	290.0796	-1.88
Epigallocatechin gallate	14.866	256.1212	-0.07
β-sitosterol	20.396	414.3822	9.47

Fig. 5 LC–MS spectrum of *S. asoca* crude methanol extract

Pareeth *et al. Future Journal of Pharmaceutical Sciences*   (2024) 10:52

Page 10 of 13

a docking score of −10.512 and *β*-sitosterol did not dock with the binding pocket of ER*α*. The 3D interaction picture of the study is shown in Fig. 6A and their docking score and binding energy are tabulated in Table 2.

The 2D image (Fig. 6A) reveals the type of interaction between the ligands and amino acids in the active sites of ER*α*. The inbuilt ligands estradiol, tamoxifen, kaempferol and quercetin form p bonds from their aromatic ring to Phe 404 but the number and nature of hydrogen bonds vary with ligands. Estradiol, kaempferol and quercetin form three hydrogen bonds with Glu353, Hie524 and Arg394, and tamoxifen only once with Asp351.

Interaction of phytoestrogens with ER*β*

The amino acid residues in the active site of ER*β* (PDBID: 3OLL) are Val280, Met295, Ser297, Leu298, Thr299, Leu301, Ala302, Asp303, Glu305, Trp335, Met336, Leu339, Met340, Gly342, Leu343, Met344, Arg346,
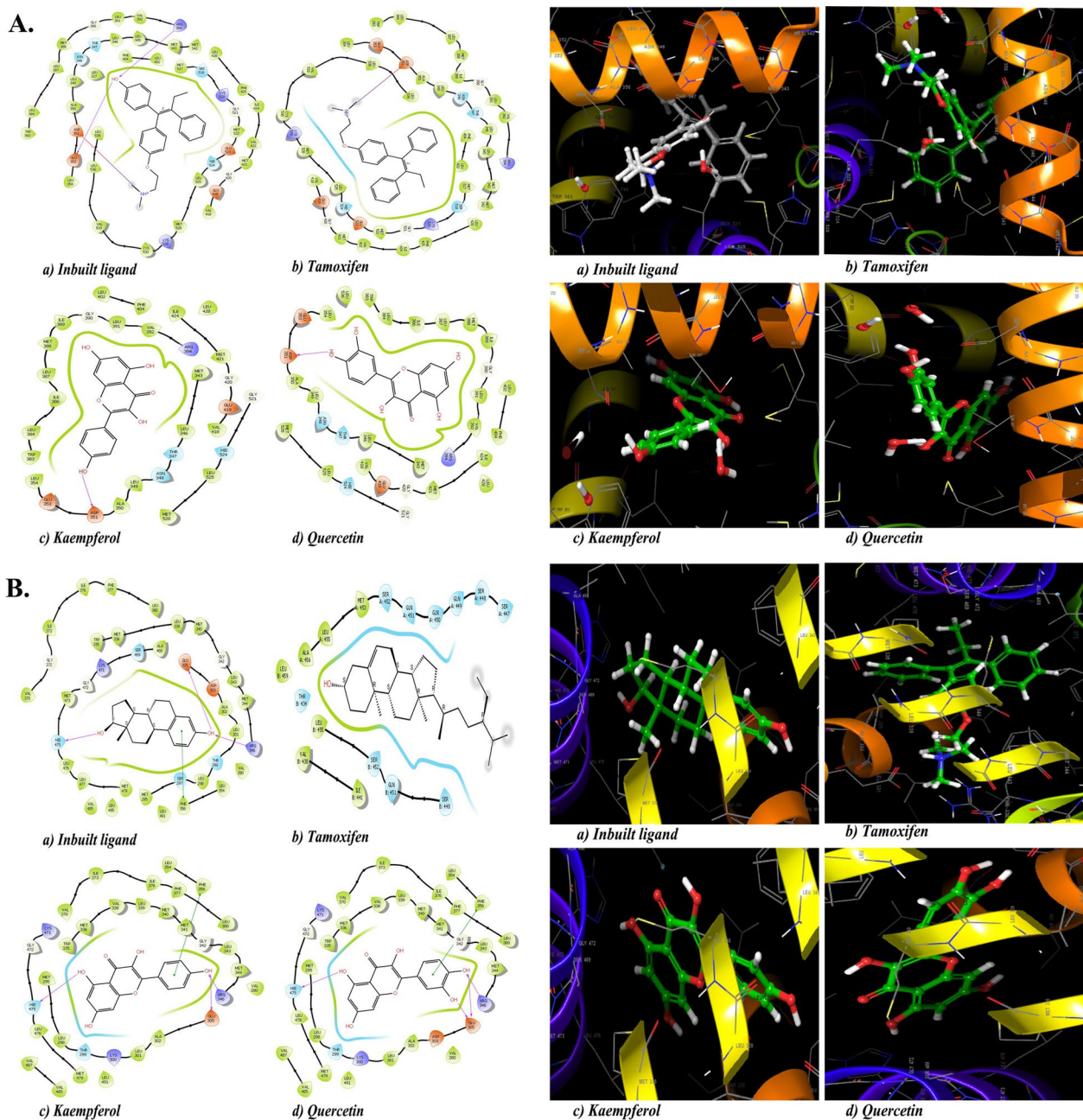

Fig. 6 **A** 2D and 3D image of the interaction between ER*α* and ligands, **B** 2D and 3D image of the interaction between ER*β* and ligands

Pareeth *et al. Future Journal of Pharmaceutical Sciences*   (2024) 10:52

Page 11 of 13

Table 2 Docking score and binding energy of estrogen receptors and ligands

Molecule	ERα		ERβ	
	Docking score	Binding energy (kcal/mol)	Docking score	Binding energy (kcal/mol)
Inbuilt ligand-Estradiol	− 12.17	− 125.19	− 10.5	− 85.248
Quercetin	− 6.945	− 47.026	− 9.220	− 66.945
Kaempferol	− 6.93	− 45.07	− 8.478	− 58.435
Tamoxifen	− 10.512	− 103.53	− 8.023	− 22.203

Leu354, Phe356, Val370, Gly372, Ile373, Ile376, Phe377, Leu380, Ala468, Ser469, Lys471, Gly472, Met473, Hie475, Leu476, Leu477, Met479, Val485, Leu491, Leu495.

The inbuilt ligand was bound deep into the active site area, making hydrogen bonding interactions with Hie475, Arg346, Glu305 and π–π stacking interactions with Phe356. The inbuilt ligand shows a docking score of − 10.5 and binding energy of − 85.248 kcal/mol. The docking of ERβ with quercetin showed the highest docking score of − 9.220 and binding energy of − 66.945 kcal/mol. Quercetin makes hydrogen bond interactions with Arg346, Glu305, Hie475 and π–π stacking with Phe356. Quercetin shows the highest affinity followed by kaempferol (− 8.478) and tamoxifen (− 8.023). Here also, β-sitosterol did not dock with the binding pocket of ERβ. The 3D and 2D figures of other ligands are given in Fig. 6B. The docking score and binding energy of other ligands are given in Table 2.

The 2D image (Fig. 6B) reveals the type of interaction between the ligands and amino acids in the active sites of ERβ. The inbuilt ligands estradiol, tamoxifen, kaempferol and quercetin form p bonds from their aromatic ring to Phe 356 but the number and nature of hydrogen bonds vary with ligands. Estradiol, kaempferol and quercetin form three hydrogen bonds with Glu305, Hid475 and Arg346, and tamoxifen only once with Asp351.

Discussion

The study emphasizes the considerable antiproliferative potential of crude extract from *Saraca asoca* against breast cancer cells, particularly targeting triple negative breast cancers. Specifically, the plant demonstrated selective cytotoxicity towards breast cancer cells expressing ERβ, while sparing those expressing ERα. The estrogen-screen assay conducted on MDAMB-231 breast cancer cells revealed a pronounced antiproliferative effect, in contrast to MCF-7 cells, which exhibited a proliferative response to estrogen and the extract. The LC-MS analysis identified phytoestrogens such as β-sitosterol, quercetin, kaempferol, and others in the plant. In in-silico docking analysis, these phytoestrogens showed higher binding affinity towards ERβ compared to ERα receptors, except

for β-sitosterol. Therefore, the observed preferential cytotoxicity of *S. asoca* towards ERβ expressing breast cancers holds significant clinical relevance, given that triple negative breast cancers represent the most aggressive form of cancer with limited treatment options.

Triple-negative breast cancer (TNBC) is characterized by the absence of expression of ERα, progesterone receptor (PR), and human epidermal growth factor receptor-2 (HER-2) [42]. In recent research on the immunological profile of these TNBC cell lines, the presence of estrogen receptor isoform ERβ, which acts as an opponent of ERα, in 50–80% of TNBCs was found [19]. In cytotoxic assays conducted in this study, Asoka exhibited significant cytotoxicity towards various cancer cells of both murine and human origin. This was evidenced by a concentration-dependent increase in the percentage of dead cells, particularly in DLA and EAC murine cancer cells. Notably, previous research has already reported comparable cytotoxic effects against mouse tumor cells [43]. Interestingly, despite the use of high concentrations, the extract did not induce cytotoxic effects on breast cancer cells expressing ERα, such as MCF-7, as observed in the MTT assay. However, the extract did exhibit cytotoxic effects on breast cancer cell lines expressing ERβ, such as MDAMB-231 and SKBR3. Prior investigations have suggested the antiproliferative effects of *S. asoca* on MDAMB-231 and also on MCF-7 cell lines [11]. However, in our study, MCF-7 cell lines did not exhibit any cytotoxicity even at higher concentrations of the extract. This interesting contrast in cytotoxicity between ERα and ERβ expressing breast cancer cells in our study corresponds with earlier findings which mention ERα activation leading to cell proliferation, while ERβ activation exhibiting an antiproliferative effect [15, 18].

The proliferative/anti-proliferative effect of the *S. asoca* crude extract was evaluated through an estrogen-screen assay on various breast cancer cell lines, with 17β-estradiol as a reference. This bioassay determines the increase or decrease in cell number in response to estrogen, resembling an increase in mitotic activity within reproductive system-associated tissues [44]. Our investigation revealed that Asoka demonstrates a moderate

Pareeth *et al. Future Journal of Pharmaceutical Sciences*   (2024) 10:52

Page 12 of 13

anti-proliferative effect on the MDAMB-231 cell line expressing ERβ, while it induces proliferation in the MCF-7 cell line expressing ERα. The presence of phytoestrogens such as quercetin, kaempferol, and β-sitosterol, among others, was reported in Asoka by LC-MS. Additionally, there are reports of flavonoids like quercetin, chrysin, and 3-hydroxyflavone with known anti-proliferative properties [45]. Therefore, it is likely that the phytoestrogens in Asoka may act as agonists for ERβ due to their specific affinity for ERβ expressing cells.

The results of our docking experiments also have demonstrated the potent affinity of phytoestrogens towards ERβ in comparison to the ERα. Both quercetin and kaempferol exhibited significantly higher docking scores and binding energies than tamoxifen, a commonly used chemotherapeutic medication. Remarkably, quercetin's docking score was close to that of estradiol, the endogenous ligand for estrogen receptors. Furthermore, there have been reports highlighting the robust binding affinity of *S. asoca* flavonoids to human estrogen receptors. In a molecular simulation research involving Asoka flavonoids and estrogen receptors, the binding scores indicate their exceptional ability to form strong interactions with these receptors. Molecular orbital analysis and pharmacokinetic parameters further support their efficacy [46]. Notably, our study revealed high binding affinity values of phytoestrogens binding with estrogen receptors which surpassed that reported in a previous investigation on Asoka flavonoids [47]. This increased affinity of phytoestrogens, particularly for ERβ, holds significant implications, as it appears to underpin their antiproliferative effects. This interaction with estrogen receptors, notably ERβ, may give rise to a wide array of biological responses [22].

Conclusion
The study highlights the preferential cytotoxicity of the *S. asoca* crude methanol extract towards ERβ expressing cells, particularly to triple negative breast cancers, a highly aggressive and therapeutically challenging type. The observed antiproliferative effects on breast cancer cells may be attributed to the action and interaction of phytoestrogens present in Asoka with ERβ. Notably, quercetin and kaempferol among the identified phytoestrogens exhibit high docking into the binding sites of active amino acids in the ERβ. These findings suggest that the phytoestrogens in Asoka may act as agonists to ERβ, offering promising prospects for the development of targeted therapies for triple negative breast cancer, thereby opening new avenues in the currently limited treatment landscape.

Abbreviations
MTT   3-(4, 5-Dimethylthiazol-2-yl)-2, 5-diphenyltetrazolium bromide
ERβ Estrogen Receptor β
DLA   Daltons Lymphoma Ascites
EAC   Ehrlich's Ascites Carcinoma

Author contributions
Chennattu M Pareeth has done experiments and wrote the paper, K P Safna Hussan, Davis Anu, Nair Meera discussed and designed experiments and done dry lab calculations. Deepu Mathew, Ravishankar Valsalan, Mohamed Shahin Thayyil—Resources, Software, and Supervision of the in-silico (molecular docking) works. Kannoor M Thara, Achuthan C Raghavamenon, Thekkekara D Babu—Supervision, finalize the design, experiments and corrections.

Availability of data and material
Available upon request to the corresponding author.

Declarations

Ethics approval and consent to participate
Not applicable.

Consent for publication
All the authors have no objection to publishing the data.

Competing interests
The authors declare that they have no competing interests.

Author details
[1]Department of Biochemistry, Amala Cancer Research Center (Recognized Research Center, University of Calicut), Thrissur 680 555, Kerala, India. [2]Bioinformatics Center, Kerala Agricultural University, Vellanikkara 680 656, Kerala, India. [3]Department of Physics, University of Calicut, Malappuram 673 635, Kerala, India. [4]Department of Biotechnology, University of Calicut, Malappuram 673 635, Kerala, India.
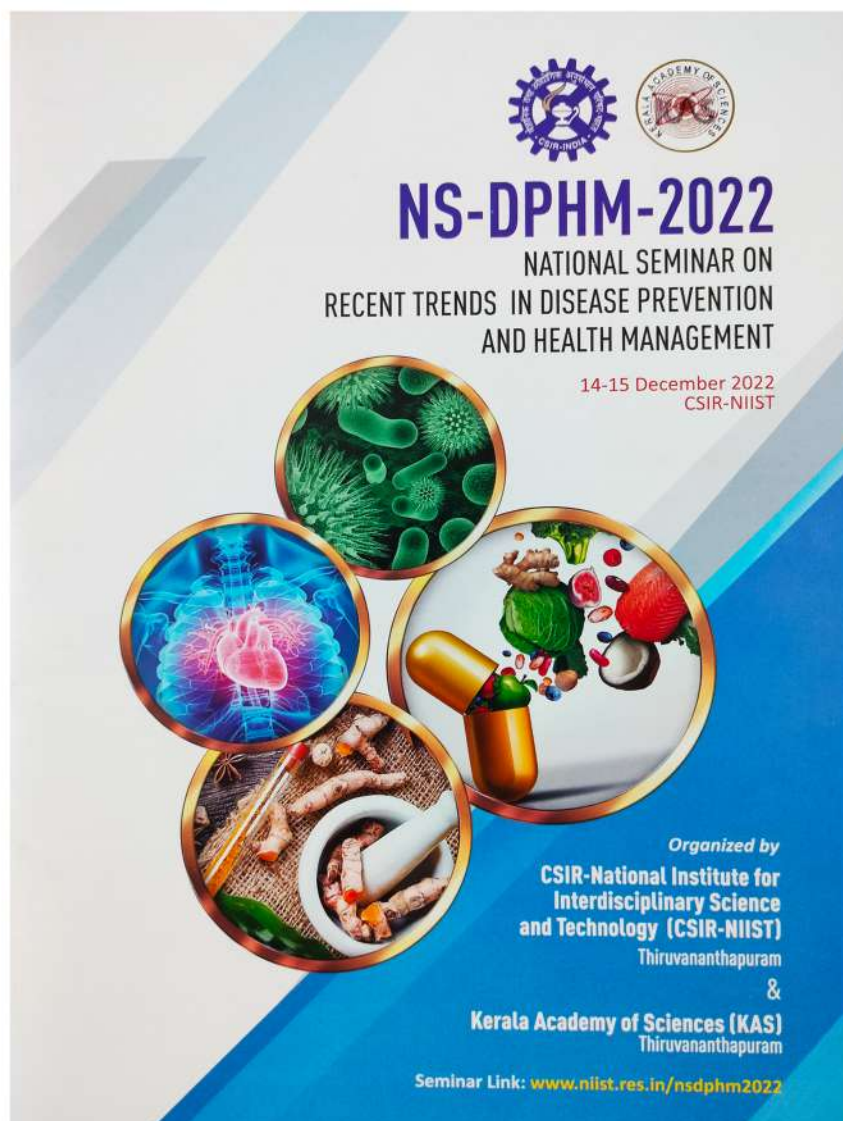
References
1. Pradhan PK, Joseph LS, Gupta V, Chulet R, Arya H, Verma R, Bajpai A (2009) *Saraca asoca* (Ashoka): A review. J Chem Pharm Res 1:62–71
2. Biswas TK, Debnath PK (1972) Aśoka (*Saraca indica* Linn)—A cultural and scientific evaluation. Indian J Hist Sci 7:99–114
3. Seetharam YN, Sujeeth H, Jyothishwaran G, Barad A, Sharanabasappa G, Parveen S (2003) Antibacterial activity of *Saraca asoca* bark. Indian J Pharm Sci 65:658–659
4. Yadav NK, Saini KS, Hossain Z, Omer A, Sharma C, Gayen JR, Singh P, Arya K, Singh R (2015) *Saraca indica* bark extract shows *in vitro* antioxidant, antibreast cancer activity and does not exhibit toxicological effects. Oxid Med Cell Longev 2015(2015):205360
5. Sasmal S, Majumdar S, Gupta M, Mukherjee A, Mukherjee PK (2012) Pharmacognostical, phytochemical and pharmacological evaluation for the antipyretic effect of the seeds of *Saraca asoca* Roxb. Asian Pac J Trop Biomed 2:782–786
6. Kumar S, Narwal S, Kumar D, Singh G, Narwal S, Arya R (2012) Evaluation of antihyperglycemic and antioxidant activities of *Saraca asoca* (Roxb.) De Wild leaves in streptozotocin induced diabetic mice. Asian Pac J Trop Dis 2:170–176
7. Nayak S, Sahoo AM, Chakraborti CK (2011) Anthelmintic activity study of *Saraca indica* leaves extracts. Int J Appl Biol Pharm Technol 2:37
8. Varghese CD, Satish, Nair CPR, Panikkar KR (1992) Potential anticancer activity of *Saraca asoca* extracts toward transplantable tumors in mice. Indian J Pharm Sci 54:37

Pareeth *et al. Future Journal of Pharmaceutical Sciences*   (2024) 10:52

Page 13 of 13

9.   Asokan A, Thangavel M (2014) *In vitro* cytotoxic studies of crude metha-nolic extract of *Saraca indica* bark extract. IOSR J Pharm Biol Sci 9:26–30

10. Dharshini AD, Elumalai P, Raghunandhakumar S, Lakshmi T, Roy A (2021) Evaluation of anti-cancer activity of *Saraca asoca* flower extract against lung cancer cell line. J Pharm Res Int 33:423–431

11. Yadav NK, Saini KS, Hossain Z, Omer A, Sharma C, Gayen JR, Singh P, Arya KR, Singh RK (2015) *Saraca indica* bark extract shows *in vitro* antioxidant, antibreast cancer activity and does not exhibit toxicological effects. Oxid Med Cell Longev 2015(2015):205360

12. Mukhopadhyay MK, Shaw M, Nath D (2017) Chemopreventive potential of major flavonoid compound of methanolic bark extract of *Saraca asoca* (Roxb.) in benzene-induced toxicity of acute myeloid leukemia mice. Pharmacogn Mag 13:S216

13. Varghese CD, Nair SC, Panikkar B, Panikkar KR (1993) Effect of Asoka on the intracellular glutathione levels and skin tumor promotion in mice. Cancer Lett 69:45–50

14. Bendigeri S, Das G, Shrman K, Kumar S, Khare R, Sachan S, Saiyam R (2019) Phytochemical analysis of *Saraca asoca* bark and *Azadirachta indica* seeds. Int J Chem Stud 7:126–131

15. Paterni I, Granchi C, Katzenellenbogen JA, Minutolo F (2014) Estrogen receptors alpha (ERα) and beta (ERβ): subtype-selective ligands and clini-cal potential. Steroids 90:13–29

16. Song D, He H, Indukuri R, Huang Z, Stepanauskaite L, Sinha I, Haldosén L-A, Zhao C, Williams C (2022) ERα and ERβ homodimers in the same cellular context regulate distinct transcriptomes and functions. Front Endocrinol 13:930227

17. Sellitto A, D'Agostino Y, Alexandrova E, Lamberti J, Pecoraro G, Memoli D, Rocco D, Coviello E, Giurato G, Nassa G (2020) Insights into the role of estrogen receptor β in triple-negative breast cancer. Cancers 12:1477

18. Zhou Y, Liu X (2020) The role of estrogen receptor beta in breast cancer. Biomark Res 8:39

19. Wisinski KB, Xu W, Tevaarwerk AJ, Saha S, Kim K, Traynor A, Dietrich L, Hegeman R, Patel D, Blank J, Harter J, Burkard ME (2016) Targeting estro-gen receptor beta in a phase 2 study of high-dose estradiol in metastatic triple-negative breast cancer: A Wisconsin Oncology Network Study. Clin Breast Cancer 16:256–261

20. Saha Roy S, Vadlamudi RK (2012) Role of estrogen receptor signaling in breast cancer metastasis. Int J Breast Cancer 2012(2012):654698

21. Chantzi NI, Palaiologou M, Stylianidou A, Goutas N, Vassilaros S, Kourea HP, Dhimolea E, Mitsiou DJ, Tiniakos DG, Alexis MN (2014) Estrogen recep-tor β2 is inversely correlated with Ki-67 in hyperplastic and noninvasive neoplastic breast lesions. J Cancer Res Clin Oncol 140:1057–1066

22. Kuiper GGJM, Lemmen JG, Carlsson BO, Corton JC, Safe SH, Van Der Saag PT, Van Der Burg B, Gustafsson J-AK (1998) Interaction of estrogenic chemicals and phytoestrogens with estrogen receptor β. Endocrinology 139:4252–4263

23. Bilal I, Chowdhury A, Davidson J, Whitehead S (2014) Phytoestrogens and prevention of breast cancer: The contentious debate. World J Clin Oncol 5:705–712

24. Harris DM, Besselink E, Henning SM, Go VLW, Heber D (2005) Phytoes-trogens induce differential estrogen receptor alpha- or beta-mediated responses in transfected breast cancer cells. Exp Biol Med 230:558–568

25. Mersereau JE, Levy N, Staub RE, Baggett S, Zogric T, Chow S, Ricke WA, Tagliaferri M, Cohen I, Bjeldanes LF (2008) Liquiritigenin is a plant-derived highly selective estrogen receptor β agonist. Mol Cell Endocrinol 283:49–57

26. Middleton E, Kandaswami C, Theoharides TC (2000) The effects of plant flavonoids on mammalian cells: Implications for inflammation, heart disease, and cancer. Pharmacol Rev 52:673–751

27. Sareddy GR, Vadlamudi RK (2015) Cancer therapy using natural ligands that target estrogen receptor beta. Chin J Nat Med 13:801–807

28. Schüler-Toprak S, Häring J, Inwald EC, Moehle C, Ortmann O, Treeck O (2016) Agonists and knockdown of estrogen receptor β differentially affect invasion of triple-negative breast cancer cells *in vitro*. BMC Cancer 16:1–13

29. Hinsche O, Girgert R, Emons G, Gründker C (2015) Estrogen receptor β selective agonists reduce invasiveness of triple-negative breast cancer cells. Int J Oncol 46:878–884

30. Meera N, Divya MK, Silpa P, Pareeth CM, Raghavamenon AC, Babu TD (2021) Amelioration of sodium fluoride induced oxidative stress by *Cyn-ometra travancorica* Bedd in mice. J Complement Integr Med 19:243–249

31. Harborne AJ (1998) Phytochemical methods a guide to modern tech-niques of plant analysis. Springer, Dordrecht

32. Das PK, Nath V, Gode KD, Sanyal AK (1964) Preliminary phytochemical and pharmacological studies on *Cocculus hirsutus*, Linn. Indian J Med Res 52:300–307

33. Kaur C, Kapoor HC (2002) Anti-oxidant activity and total phenolic content of some Asian vegetables. Int J Food Sci Technol 37:153–161

34. Chang C-C, Yang M-H, Wen H-M, Chern J-C (2002) Estimation of total flavonoid content in propolis by two complementary colorimetric meth-ods. J Food Drug Anal 10:178

35. Moldeus P, Hogberg J, Orrenius S, Fleischer S, Packer L (1978) Methods in enzymology, vol 52. Academic Press, New York, pp 60–71

36. Prinz H (2010) Hill coefficients, dose–response curves and allosteric mechanisms. J Chem Biol 3:37–44

37. Mosmann T (1983) Rapid colorimetric assay for cellular growth and survival: Application to proliferation and cytotoxicity assays. J Immunol Methods 65:55–63

38. Han D-H, Denison MS, Tachibana H, Yamada K (2002) Relationship between estrogen receptor-binding and estrogenic activities of envi-ronmental estrogens and suppression by flavonoids. Biosci Biotechnol Biochem 66:1479–1487

39. Coates J (2000) Interpretation of infrared spectra, a practical approach. Encycl Anal Chem 12:10815

40. Hussan KPS, Thayyil MS, Ahamed TS, Muraleedharan K (2020) Biological evaluation and molecular docking studies of benzalkonium ibuprofenate. In: Computational Biology and Chemistry. IntechOpen

41. Sharma S, Tiwari G, Tiwari R (2021) Development and validation of UV-Spectrophotometric method for the estimation of *Saraca asoca*, *Bauhinia variegata* Linn, and *Commiphora mukul* in standardized polyherbal formu-lation. J Pharm Sci Res 13:525–528

42. Takano EA, Younes MM, Meehan K, Spalding L, Yan M, Allan P, Fox SB, Redfern A, Clouston D, Giles GG (2023) Estrogen receptor beta expression in triple negative breast cancers is not associated with recurrence or survival. BMC Cancer 23:1–12

43. Varghese CD, Nair C, Panikkar KR (1992) Potential anticancer activity of *Saraca asoca* extracts toward transplantable tumors in mice. Indian J Pharm Sci 54:37–40

44. Soto AM, Sonnenschein C (1985) The role of estrogens on the prolifera-tion of human breast tumor cells (MCF-7). J Steroid Biochem 23:87–94

45. Resende FA, de Oliveira APS, de Camargo MS, Vilegas W, Varanda EA (2013) Evaluation of estrogenic potential of flavonoids using a recom-binant yeast strain and MCF7/BUS cell proliferation assay. PLoS ONE 8:e74881

46. Sherin DR, Manojkumar TK (2017) Flavonoids from *Saraca asoca*-ideal medication for breast cancer-A molecular simulation approach. Biomed J Sci Tech Res 1:1761–1763

47. Suganya J, Radha M, Naorem DL, Nishandhini M (2014) *In silico* docking studies of selected flavonoids-natural healing agents against breast cancer. Asian Pac J Cancer Prev 15:8155–8159

Publisher's Note

Springer Nature remains neutral with regard to jurisdictional claims in pub-lished maps and institutional affiliations.

National Seminar on Recent Trends in Disease Prevention and Health Management

NS-DPHM-2022

National Seminar on Recent Trends in Disease Prevention and Health Management

14-15 December 2022
CSIR-NIIST

Organized by
CSIR-National Institute for Interdisciplinary Science and Technology (CSIR-NIIST)
Thiruvananthapuram
&
Kerala Academy of Sciences (KAS)
Thiruvananthapuram

Seminar Link: www.niist.res.in/nsdphm2022

| NC-OP 11 | Effect of Saraca asoca and Kingiodendron pinnatum bark extracts on DMBA-induced mammary tumorigenesis in mice | Chennattu M Pareeth[1], Nair Meera[1], Praba Silpa[1], Edappilly M Shaji[1], Kannoor M Thara[2] and Thekkekara D Babu[1]*
[1]Department of Biochemistry, Amala Cancer Research Centre (Recognized Research Centre, University of Calicut), Amalanagar P O, Thrissur - 680 555, Kerala, India
[2]Department of Biotechnology, University of Calicut, Thenhipalam P O, Malappuram - 673 636, Kerala, India |

40

***Saraca asoca* and *Kingiodendron pinnatum* bark extracts suppress growth and metastasis of 4T1-induced mammary tumours in BALB/c mice**

Chennattu M Pareeth[1], Chandrasekhar Leena[2], Davis Anu[1], Kannoor M Thara[3] and Thekkekara D Babu[1]*
[1]*Department of Biochemistry, Amala Cancer Research Centre Society, Amala Nagar P O, Thrissur - 680 555, Kerala, India*
[2]*Department of Veterinary Anatomy, College of veterinary and animal Sciences, Madakkathara P O, Thrissur – 680 651, Kerala, India*
[3]*Department of Biotechnology, University of Calicut, Thenhipalam P O, Malappuram - 673 636, Kerala, India*

The bark of *Saraca asoca* (Asoka) is a prime ingredient of *Asokarishta*, a well-known formulation in Ayurveda for gynecological disorders in women. *Kingiodendron pinnatum*, morphologically similar to Asoka is occasionally used as a substitute. Our previous study shows that the phytoestrogenic components of the plants exert specific cytotoxic effect on cancer cells possessing the estrogen receptor β (ERβ). Hence the present study is aimed to find out the potential of *S. asoca* (SA) and *K. pinnatum* (KP) bark extracts on TNBC. 4T1, a murine triple negative breast cancer (TNBC) cell line is used to induce TNBC in mice. In MTT assay, a significant decrease in the proliferation of 4T1 cells was shown by the SA and KP with an IC_{50} of 132.5 and 155 μg/mL, respectively. The LC-MS analysis revealed the phytoestrogens such as β-sitosterol, kaempferol and quercetin. The *in silico* docking of ERβ with phytoestrogens, quercetin showed the highest score of -9.220 and binding energy of -66.945 kcal/mol. The growth and metastasis of mammary tumours were found reduced significantly ($P<0.01$) by the treatment of SA and KP. Histological analysis of the mammary pad and lung tissue of the treated animals shows normal architecture without any signs of tumour formation except large areas of necrosis, whereas the control group shows malignant infiltration of cells both in mammary and lung. Overall, the results suggest the possibility of using *S. asoca* and *K. pinnatum* bark extracts for effective anticancer drug development in the treatment of TNBCs.

Key words: Asoka, TNBC, 4T1